SODIUM-NaK ENGINEERING HANDBOOK

Volume I

SODIUM-NaK ENGINEERING HANDBOOK

VOLUME I SODIUM CHEMISTRY and PHYSICAL PROPERTIES

Chap. 1 Physical Properties
Chap. 2 Chemistry

VOLUME II SODIUM FLOW, HEAT TRANSFER, INTERMEDIATE HEAT EXCHANGERS, and STEAM GENERATORS

Chap. 1 Fluid Mechanics of Liquid Metals
Chap. 2 Liquid-Metal Heat Transfer
Chap. 3 Intermediate Heat Exchangers (IHX's)
Chap. 4 Steam Generators

VOLUME III SODIUM SYSTEMS, SAFETY, HANDLING, and INSTRUMENTATION

Chap. 1 Sodium and NaK Systems
Chap. 2 Safety
Chap. 3 Handling
Chap. 4 Instruments

VOLUME IV SODIUM PUMPS, VALVES, PIPING, and AUXILIARY EQUIPMENT

Chap. 1 Pumps
Chap. 2 Bearings and Seals
Chap. 3 Valves
Chap. 4 Vessels and Piping
Chap. 5 Auxiliary Equipment and System Accessories

VOLUME V SODIUM PURIFICATION, MATERIAL, HEATERS, COOLERS, and RADIATORS

Chap. 1 Purification
Chap. 2 Effects on Materials
Chap. 3 Heaters and Coolers
Chap. 4 Radiators, Condensers, and Boilers
Chap. 5 Applications

Each volume includes an index for that volume.

SODIUM-NaK ENGINEERING HANDBOOK

Volume I

Sodium Chemistry and Physical Properties

by

O. J. FOUST, Editor
Director, Engineering
Liquid Metal Engineering Center

Prepared under the auspices of the
Division of Reactor Development and Technology
United States Atomic Energy Commission

GORDON AND BREACH, SCIENCE PUBLISHERS, INC.
New York London Paris

440 Park Avenue South, New York, N. Y. 100016

Editorial office for Great Britain:
Gordon and Breach, Science Publishers Ltd.
12 Bloomsbury Way
London W.C.1, England

Editorial office for France:
Gordon & Breach
7–9 rue Emile Dubois
Paris 14^{e}

ISBN 0 677 03020 4

Library of Congress catalog card number: 70-129473

Printed in the United States of America

Foreword

On June 4, 1971, President Nixon sent to the U. S. Congress a comprehensive energy message proposing a program to ensure an adequate supply of clean energy for the years ahead.

The Presidential message conveyed the theme that national energy study efforts have converged to the conclusions that actions had to be taken to ensure the United States a sufficient supply of clean energy in the years ahead. The message stated that "Our best hope today for meeting the Nation's growing demand for economical clean energy lies with the fast breeder reactor." To realize the immense potential of the fast breeder, the President provided for an augmented Liquid Metals Fast Breeder Reactor (LMFBR) program and a charter for establishing a commitment to complete the successful demonstration of the LMFBR by 1980. There has been a highly favorable supporting concensus by the Congress, the industry, and the utilities for the LMFBR program. All these participants are fully committed to meeting the tremendous challenges implicit in the LMFBR program objectives.

Sodium has been chosen as the coolant for the LMFBR because of its good technical characteristics, including its excellent nuclear and heat-transfer properties, large heat capacity, low vapor pressure, and freedom from corrosion in the absence of air and water. The experience gained in over 20 years of use of sodium as a reactor coolant has provided the base for the present extensive research and development programs now under way in this country.

To provide for high nuclear plant reliability requires that each of the component parts be extremely reliable since the overall reliability is a product of the individual component reliabilities. The reactor heat-transfer and -removal agent, sodium, is an important and a vital component in the LMFBR system, and its reliability as well as the reliability of sodium components and sodium systems should be unquestionable. Sodium must—at all times—be compatible with the materials it contacts, retain its heat-transfer characteristics, and remain free of impurities to the extent necessary to prevent blocking of flow passages, prevent corrosion, and allow for free movement of mechanisms in sodium or in the cover gas. The impurities content of sodium (including fission products) can be maintained within predetermined levels based on:

1. Knowledge of impurity levels required for each of the operating temperatures.
2. Means for detecting and/or measuring the impurities.
3. Means for removing impurities to within the set levels.

In addition, it is vital for personnel to be able to live with sodium on a routine basis. The LMFBR operations and maintenance crews must handle it, store it, clean it off equipment, keep it liquid when needed, and prevent it from contacting air and water. If inadvertent leakages occur, they must be able to minimize the reactions and control the subsequent events. Experiences to date have confirmed that sodium systems and components must and can be designed for ease of accessibility, inspection, replacement, and repair.

The many complex problems involved in the development and use of sodium and sodium components and systems require a disciplined engineering approach and the application of strong quality-assurance measures to resolve them. In this connection, strong quality-assurance measures for the sodium coolant are as vital as for sodium components. Fundamental to this approach to the development of components, systems, and sodium technology is the application of first engineering principles. One of the tools in this application is to have available and in hand all those experiences—good and bad—which have been the precursors of where we now stand. These experiences should be made available to each and every member of the LMFBR nuclear community.

The *Sodium–NaK Engineering Handbook* is one of the methods for centralizing the knowledge gained and for providing guidelines and information useful for the design, engineering, and development of sodium systems and their components and development of sodium technology. Further, it contains pertinent references to other technical sources for more detailed information. This handbook, designed to be a major extension to the Liquid Metals Handbooks initiated by the U. S. Naval Reactors Program in the early 1950's, which have served a very useful purpose in the interim period, has extended the state of the art which has progressed through experiences gained in the Experimental Breeder Reactor No. 2, the Enrico Fermi Fast-Breeder Reactor, the Southwest Experimental Fast Oxide Reactor, the Hallam Reactor, the Sodium Reactor Experiment, the many sodium test facilities, and the many sodium-cooled reactors and test facilities in other countries.

It is hoped that this book, in a worthwhile manner, will assist the scientists and engineers participating in the LMFBR program who have dedicated themselves to meeting the challenge of providing reliable, safe, and economical LMFBR nuclear power plants and have accepted the tremendous responsibilities inherent in this challenge.

The U. S. nuclear community is now convinced more than ever that nuclear power by way of the LMFBR is a decisive way to provide the United States and the world a means of meeting the growing demands for abundant, relatively inexpensive energy with acceptable effects on the environment.

Milton Shaw, Director
Division of Reactor Development
and Technology

Preface

Since publication of the *Sodium—NaK Supplement* to the *Liquid Metals Handbook* in 1955, liquid metal technology has expanded in depth, in spectra, and in the size of equipment that has been developed. Even so, further expansion is needed to satisfy the requirements of the Liquid Metals Fast Breeder Program. Reliable components, with engineering capabilities up to an order of magnitude greater than those developed to date, are required, an expansion of capability beyond the mere extrapolation of laboratory devices.

The capability increase now demanded renders the admonition contained in the Foreword to the 1955 supplement that only test will demonstrate satisfactory performance of a component constructed for an advanced technology as vital now as it was in 1955. Testing alone can demonstrate that all facets of sound engineering have been incorporated into the design and manufacture of the final product.

Through the technology described in this *Sodium—NaK Engineering Handbook,* it is hoped that designers will have a basis for freeing their imaginations from the bonds of small-scale experience and create systems and components which incorporate the lessons of the past into the industrial requirements of the future.

Robert W. Dickinson, Director
Liquid Metal Engineering Center

Editor's Preface

This handbook, comprised of five volumes, is intended for use by present and future designers in the Liquid Metals Fast Breeder Reactor (LMFBR) Program and by the engineering and scientific community performing other type investigation and experimentation requiring high-temperature sodium and NaK technology. The arrangement of subject matter progresses from a technological discussion of sodium and sodium—potassium alloy (NaK) to discussions of various categories and uses of hardware in sodium and NaK systems.

Emphasis is placed on sodium and NaK as heat-transport media; other applications of these metals are treated in the final volume. Several thousand documents were reviewed in accumulating and compiling information; those believed to be most valuable are cited as references.

Sufficient detail is included for basic understanding of sodium and NaK technology and of technical aspects of sodium and NaK components and instrument systems. Information presented is considered adequate for use in feasibility studies and conceptual design, sizing components and systems, developing preliminary component and system descriptions, identifying technological limitations and problem areas, and defining basic constraints and parameters. Preparation of a finished design, however, will require more extensive research into the reference literature.

The handbook includes the work of some 50 contributors; the efforts of each were coordinated to facilitate an end product with a common theme, each part consistent in perspective with the whole, but considerable individual license was permitted in presentation of that material. Therefore each volume and chapter reflects the style of its author and, to this extent, differs from other volumes and chapters.

In many instances, the data from various sources were in conflict and the authors had no basis for selecting those which were most valid. In such instances explanations and references are supplied in sufficient detail to permit the reader to perform independent research. Attention is invited to the existence of the Liquid Metals Information Center, located at the Liquid Metal Engineering Center, as a continuing source of current information.

O. J. Foust

Contents

Chapter 1 Physical Properties

APPENDIXES

Chapter 2 Chemistry

CONTENTS

APPENDIX

Chapter 1

Physical Properties

Principal Authors: H.J. BOMELBURG and C.R.F. SMITH

Contributing Authors: H.N. ROYDEN, V.A. SWANSON, A.W. THIELE and R.J. TUTTLE

1-1 INTRODUCTION

Interest and research in the physical properties of liquid sodium and potassium date back over a century; however, only in the last two decades has the interest reached a relatively high level. This is due mainly to the feasibility of using liquid metals (in particular, liquid sodium) in practical engineering applications. Presently, liquid metals are used or considered primarily as heat-transfer fluids in nuclear reactors or as working fluids for power cycles in space power-generating systems.

The physical properties of sodium (and to a lesser extent those of potassium also) have been compiled before. The earlier editions of the Liquid Metals Handbook [1-3] contain the first collection of property data specifically gathered for engineering application purposes. Subsequent important general compilations have been prepared by Thomson and Garelis [4], Weatherford, Tyler and Ku [5], Weatherford [6], Spiller [7, 8], Kutateladze *et al.* [9], Achener *et al.* [10] and others [11-17].

Several compilations have specialized merely on thermophysical properties of sodium [18-21]. In particular, the recent work by Golden and Tokar [19] critically evaluates the newer thermophysical data that have become available during the last decade. A significant part of the material in this chapter is based on this extensive compilation.

The data collections and reviews for potassium and NaK are generally less comprehensive with the exception of thermodynamic data on potassium vapor, which recently has been investigated extensively [22-24]. Properties of liquid potassium have been compiled previously in Refs. 5, 7, 9, and 24; however there is no equivalent critical survey available on potassium that matches the thoroughness of Ref. 19 on sodium.

A brief survey of various U.S. research projects conducted to determine sodium and potassium properties is presented. The oldest effort (extending back, with some interruptions, for more than two decades) is a Naval

Research Laboratory (NRL) project (under C.T. Ewing, J.P. Stone and others) to investigate the properties of liquid metals. Their recent work on vapor properties of sodium and potassium is used extensively in this handbook [25-29].

A group at MSA Research Corporation [30] and a group at Southwest Research Institute [5] have investigated liquid-metal properties for the Air Force Systems Command.

The National Aeronautics and Space Administration (NASA) has sponsored several investigations of potassium properties, especially at high temperatures [31]. A group at Battelle Memorial Institute has measured most of the important engineering properties of potassium. Several in-house studies [22, 24] on potassium properties have been performed at the NASA Lewis Research Center.

The U.S. Atomic Energy Commission has repeatedly sponsored efforts to investigate liquid-metal properties [11, 19, 32-35]. A group at Aerojet-General Corp. [10] has been measuring selected liquid-metal properties since 1958. Another group at Columbia University [36] is presently engaged in measuring the transport properties of liquid metals and their vapors. Furthermore, there have been many minor research projects (sponsored and nonsponsored) concerned with particular aspects of liquid-metal properties.

The data and references quoted in this chapter are mainly from the more recent literature (since 1955). References 13 and 14 contain additional background material and an extensive guide to the older literature. Reference 37 is a general nonannotated bibliography on liquid metals covering the unclassified literature since 1958. References 38 to 41 are additional less extensive bibliographies specializing in liquid metals and their applications. Gmelins Handbook [13] doubtlessly contains the most comprehensive general review on sodium* properties ever assembled, not only on chemical properties and reactions but also on physical properties. It covers the literature thoroughly to the end of 1960, with occasional additional references as late as 1964. Other handbooks (such as Refs. 12 and 42-47) usually contain only brief specialized sections on liquid-metal properties.

Extensive research has also been conducted on the theoretical foundation of liquid-metal behavior. This has grown by now into a large specialized field by itself, which for obvious reasons cannot be surveyed in this engineering handbook. For interested readers, Refs. 48-58 may serve as a guide to this interesting, however complicated subject. At this time, unfortunately, the theory is not sufficiently advanced that accurate property data could be predicted on a purely analytical basis. Therefore most of the data in this handbook are based on experimental measurements. Only in a few isolated cases where no such data are available have predictions on a theoretical basis been made and the resulting data included. It is to be expected that, with a better future theoretical understanding, the bulk of available experimental data can more easily be fitted into a consistent and accurate overall picture of the liquid metals.

Certain liquid-metal properties can be affected by impurities present in the sample that was used for a particular measurement. In most cases the samples were extremely pure so that any potential deviations could be neglected. The original literature frequently lists an exact chemical analysis of the samples. Thus far, however, no systematic investigation is known

---

*The corresponding new supplementary volumes of Gmelins 8th edition for potassium have not appeared at the time of this writing.

which deals specifically with the influence of impurities on liquid-metal properties. Hence the physical properties described in this chapter are, in general, those of pure sodium and potassium and of their eutectic alloy, NaK. Because of their higher practical importance for the Liquid Metal Fast Breeder Reactor (LMFBR) program [59], the properties of sodium will generally be treated at greater length than those of potassium and NaK. Although the emphasis is clearly on the liquid state, a certain amount of data on the solid and the vapor states is included. Since alkali metals also have recently been considered as working fluids in space power systems [60], the thermodynamic properties of the vapors are treated rather thoroughly.

Although at times it may appear somewhat arbitrary to treat a certain property in a particular section, this chapter is divided into the following three major sections:

1. Mechanical properties.
2. Thermophysical properties.
3. Electrical, nuclear and miscellaneous properties.

A synopsis of the physical properties of sodium, potassium and eutectic NaK is given in Sec. 1-2.3 for quick reference to values at useful temperatures. Where practical, each topic is subordered in a consistent sequence: the property of the sodium metal is discussed first, followed by that of potassium and the NaK alloy. If information on the properties of a particular state or composition has been sought but not found, this fact is so stated. Among the many possible NaK alloys, this handbook will concentrate on eutectic NaK (NaK-77.8) only. However, since experimental data on eutectic NaK found in the literature are not all based on the exact weight proportions, data based on weight proportions from 75 to 80% potassium generally will be considered sufficiently close to the eutectic condition and will be included. In each case the exact proportion, if quoted in the original literature, will be cited in the text.

In a search of the literature, it is inevitable that contradictory reports will be found on almost any physical property. In this chapter all major reports will be cited, and the preferred or recommended data, equations, etc., will be indicated. In some instances new graphs and equations have been generated as a best fit to the existing data. As much as possible, an attempt has been made to state the errors inherent in all values, equations, and graphs.

Dimensional units from different systems are used in this chapter. Normally the most convenient or most commonly used units have been chosen. Equations and formulas are presented mostly in centimeter-gram-second (cgs) units,* whereas tables and graphs usually also carry other units that are more familiar to engineers in the field. Some of the more important equations are given both for cgs and engineering units. A standard conversion table is included in Sec. 1-2 for a convenient conversion of the various units. Additional conversion factors can be found in Ref. 61.

Frequently the equations cited in this chapter carry coefficients with four and even more significant figures.† This might induce a false impression in regard to the accuracy

---

*In the original literature the physical properties have usually been reported in these units.

†In some cases the appearance of so many significant figures can be traced

of the results from such equations. Most of the cited equations are actually mere curve fits to experimentally measured data as they have been copied from the literature. An error estimate given with such an equation usually represents the standard deviation of the data points from the main curve. Such an estimate obviously results only from the normal "scatter" of the measured data and does not include any systematic errors of the particular experimental method used. Therefore such error quotations should not be construed as the absolute accuracy limits of the quoted data.

The absolute accuracy of the data presented in this handbook varies with the properties; generally it is of the order of 1%. Some property data (e.g. density, melting points, sonic velocity, etc.) are more accurate (in the 0.1% range), whereas others, such as vapor transport properties, may actually be known only within some 10%. Generally, therefore, the accuracy of the data can be considered quite adequate for engineering purposes. Also, it is not likely that the quality of the presented data will be significantly improved in the near future. If improvements come, they will be spotty and relatively minor, although improved data for one property (e.g., the specific heat) might affect a number of other properties (e.g., enthalpy, entropy, etc.) as well. This is particularly true for the vapor state with its rather complicated thermodynamic relations.

1-2 CONVERSION FACTORS, NOMENCLATURE AND SYNOPSIS

1-2.1 *Conversion Factors*

Density Equivalents

Convert to Given	g/cm^3	lb/in^3	lb/ft^3
g/cm^3		0.036127	62.428
lb/in^3	27.680	1	1728.0
lb/ft^3	0.016018	5.7870×10^{-4}	1

---

to manipulation of the original data in secondary reports. For example, Stone *et al.* [25] list four significant figures for the virial coefficients in their original report, whereas Golden and Tokar [19] list six significant figures for these same coefficients after some manipulation.

Energy Equivalents*

Convert to Given	abs. joules (10^7 ergs)	g-cal	Btu	kW-hr
abs. joules (10^7 ergs)	1	0.23901	9.4845×10^{-4}	2.7778×10^{-7}
g-cal	4.1840	1	3.9683×10^{-3}	1.1622×10^{-8}
Btu	1054.35	251.9958	1	2.9288×10^{-4}
kW-hr	3.6×10^{6}	8.6042×10^{5}	3414.4	1

Heat Capacity-Entropy Equivalents*

1 cal/g mole-°C = 1 Btu/lb mole-°F

1 cal/g-°C = 1 Btu/lb-°F

Enthalpy per Unit Mass Equivalents*

Convert to Given	cal/g	Btu/lb	joules/ kg
cal/g	1	1.8	4184
Btu/lb	0.5556	1	2324.4
joules/kg	2.3901×10^{-4}	4.3021×10^{-4}	1

Pressure Equivalents

Convert to Given	dynes/cm^2	kg/m^2	atm	mm Hg at 0°C (torrs)	lb/in.^{2}
dynes/cm^2	1	0.010197	9.8692×10^{-7}	7.5006×10^{-4}	1.4504×10^{-5}
kg/m^2	98.0665	1	9.6784×10^{-5}	0.073556	1.4223×10^{-3}
atm	1.01325×10^{6}	10332.3	1	760	14.696
mm Hg at 0°C (torrs)	1.33322×10^{3}	13.5951	1.3158×10^{-3}	1	0.019337
lb/in.^{2}	6.8948×10^{4}	703.07	0.068046	51.715	1

---

*See note at end of this section.

Thermal-Conductivity Equivalents*

Convert to Given	cal/sec-cm-°C	W/cm-°C	Btu/hr-ft-°F	Btu/sec-ft-°F
cal/sec-cm-°C	1	4.1840	241.91	0.067197
W/cm-°C	0.23901	1	57.818	0.016060
Btu/hr-ft-°F	4.1338×10^{-3}	0.017296	1	2.7778×10^{-4}
Btu/sec-ft-°F	14.882	62.265	3600	1

Thermal-Diffusivity Equivalents

Convert to Given	cm^2/sec	m^2/sec	ft^2/sec	ft^2/hr
cm^2/sec	1	10^{-4}	1.0764×10^{-3}	3.8750
m^2/sec	10^{4}	1	10.764	3.8750×10^{4}
ft^2/sec	929.03	0.092903	1	3600
ft^2/hr	0.25806	2.5806×10^{-5}	2.7778×10^{-4}	1

Coefficient of Heat-Transfer Equivalents*

Convert to Given	g-cal/sec-cm^2-°C	W/cm^2-°C	kcal/hr-m^2-°C	Btu/hr-ft^2-°F
g-cal/sec-cm^2-°C	1	4.1840	36000	7373.4
W/cm^2-°C	0.23901	1	8604.2	1762.3
kcal/hr-m^2-°C	2.7778×10^{-5}	1.1622×10^{-4}	1	0.20482
Btu/hr-ft^2-°F	1.3562×10^{-4}	5.6745×10^{-4}	4.8824	1

Heat-Flux Equivalents*

Convert to Given	g-cal/sec-cm^2	W/cm^2	kcal/hr-m^2	Btu/hr-ft^2
g-cal/sec-cm^2	1	4.184	36000	13272
W/cm^2	0.23901	1	8604.2	3172.1
kcal/hr-m^2	2.7778×10^{-5}	1.1622×10^{-4}	1	0.36867
Btu/hr-ft^2	7.5346×10^{-5}	3.1525×10^{-4}	2.7125	1

*See note at end of this section.

Dynamic or Absolute Viscosity Equivalents

Convert to Given	centipoises (10^{-2}g/cm-sec)	lb/ft-sec	lb/ft-hr
centipoises	1	6.7197×10^{-4}	2.4191
lb/ft-sec	1.4882×10^{3}	1	3600
lb/ft-hr	0.41338	2.7778×10^{-4}	1

Kinematic Viscosity Equivalents

Convert to Given	centistokes (or mm^2/sec)	m^2/sec	ft^2/sec	ft^2/hr
centistoke	1	10^{-6}	1.07×10^{-5}	3.85×10^{-2}
m^2/sec	10^{6}	1	1.07×10	3.85×10^{4}
ft^2/sec	9.35×10^{4}	9.35×10^{-2}	1	3.60×10^{3}
ft^2/hr	2.60×10	2.60×10^{-5}	2.78×10^{-4}	1

Surface-Tension Equivalents

Convert to Given	dynes/cm	kg/m	lb/ft
dyne/cm	1	1.0197×10^{-4}	6.8522×10^{-5}
kg/m	9806.65	1	0.67197
lb/ft	1.4594×10^{4}	1.4882	1

Temperature

°F = 9/5 (°C + 32)

°C = 5/9 (°F - 32)

°K = °C + 273.15

°R = °F + 459.67

Gas Constant

R = 1.98717 cal/mole-°K
= 8.31432 joules/mole-°K
= 82.0560 cm^3-atm/mole-°K
= 1.98717 Btu-lb/mole-°R
= 1545.32 lb-ft^2/mole-°R

Note: In these tables energy is expressed in terms of the gram-calorie [also referred to as the cal (TC) or thermochemical calorie], which is defined in terms of the more fundamental unit, the absolute joule, as follows (other definitions differ by less than 0.2%):

1 gram-calorie = 4.1840 absolute joules exactly. Similarly, the British thermal unit (Btu) referred to is the thermochemical Btu, which is equal to 251.9958 gram-calories (not exactly).

1-2.2 *Nomenclature*

The following symbols are used in this chapter. Because some symbols have a traditional and accepted use in certain fields, duplication was unavoidable. In all cases the meaning should be clear from the context. A small number of additional symbols are explained in the text. Their significance is limited to only the one equation (or paragraph) in which they are used.

A	Area
A_w	Atomic weight
Å	Angstrom unit (10^{-8} cm)
B	Magnetic induction; second virial coefficient
barn	Barn (10^{-24}cm^2)
C	Third virial coefficient
c	Sonic velocity
c_p	Heat capacity at constant pressure
c_v	Heat capacity at constant volume
D	Heat of dimerization; fourth virial coefficient
d	Self-diffusion coefficient
E_H	Electric Hall field
F	Free energy
f	Frequency
g	Gravity constant
g	Gram
H	Enthalpy; magnetic-field intensity
J	Electric current
k	Thermal conductivity; equilibrium constant
k_0	Boltzmann constant
k_S	Adiabatic compressibility
k_T	Isothermal compressibility
L	Lorenz number
L_f	Heat of fusion
L_v	Heat of vaporization
ℓ	Length
log	Common logarithm
ln	Natural logarithm
M	Molecular weight
N	Mole fraction
p	Pressure
Pr	Prandtl number
q	Time rate of heat conduction
R	Ideal gas constant
r	Electrical resistivity; radius of curvature
r'	Specific electrical resistivity
S	Entropy
T	Absolute temperature (in °K or °R)
t	Temperature (in °C or °F)
V	Volume; volt
v	Specific volume ($1/\rho$)
W	Watt
X	Weight fraction
χ	Specific magnetic susceptibility
α	Thermal diffusivity
β	Volume-expansion coefficient
γ	Adiabatic exponent ($=c_p/c_v$); specific weight (ρ/g)
Δh_v	Enthalpy change for vaporization
ΔS_f	Entropy change of fusion
ΔS_v	Entropy change for vaporization
κ_m	Magnetic susceptibility
η	Dynamic (absolute) viscosity
η_β	Bulk viscosity
μ	Absolute magnetic permeability
$\mu\Omega$	Microohm
ν	Kinematic viscosity
ρ	Density
σ	Surface tension; atomic diameter
ϕ	Fluidity ($1/\eta$)

Subscripts

1	Monomer
2	Dimer
4	Tetramer
a	Average
c	Solid phase
$c\ell$	Pertaining to solid and liquid
cr	At critical point
K	Pertaining to potassium
ℓ	Liquid phase
m.p.	At melting point
Na	Pertaining to sodium
o	Total, or reference value
oc	Reference value for solid phase
p	At constant pressure
s	At saturation conditions
T	At constant temperature
v	At constant volume

Superscripts

g	Gas phase
ℓ	Liquid phase
$\rightarrow$	Vector
o	Reference value
*	Reduced variable

1-2.3 *Synopsis of Physical Properties*

(a) *Sodium*

Atomic number	11	
Atomic weight (based on C = 12)	22.9898	
Natural isotopes (mass number)	23	
Isotopic abundance	100%	
Absorption cross section to 0.025-ev (thermal) neutrons	0.53 barn	
Total cross section to 0.025-ev neutrons	3.9 barns	
Ionization potential	5.12 volts	
Melting point	97.82°C (208.1°F)	
Boiling point	881.4°C (1618°F)	
Volume increase on melting	2.7%	
Latent heat of fusion	27.0 cal/g	
Latent heat of vaporization at the boiling point	926 cal/g	
Critical temperature	2733°K(estimate)	
Critical pressure	408 atm (estimate)	
Critical volume	0.128 cm^3/gram-mole (estimate)	
Density (solid)	20°C	0.968 g/cm^3
	m.p.	0.951 g/cm^3(estimate)
Density (liquid)	m.p.	0.927 g/cm^3
	400°C	0.856 g/cm^3
	550°C	0.820 g/cm^3
	b.p.	0.740 g/cm^3
Specific volume (saturated vapor)	400°C	3.8 × 10^6 cm^3/g
	550°C	2.3 × 10^5 cm^3/g
	b.p.	3.7 × 10^3 cm^3/g
Viscosity (liquid)	100°C	0.680 centipoise
	400°C	0.284 centipoise
	550°C	0.225 centipoise
	b.p.	0.149 centipoise
Surface tension	m.p.	192 dynes/cm
	400°C	161 dynes/cm
	550°C	146 dynes/cm
	b.p.	113 dynes/cm
Electrical resistivity (solid)	20°C	4.69 μΩcm
	m.p.	6.6 (μΩcm (estimate)
Electrical resistivity (liquid)	m.p.	9.64 μΩcm
	400°C	22.14 μΩcm
	550°C	29.91 μΩcm
	b.p.	52.87 μΩcm
Thermal conductivity (solid)	20°C	1.323 W/cm-°C
	m.p.	1.193 W/cm-°C (estimate)

Thermal conductivity (liquid)	m.p.	0.870 W/cm-°C	
	400°C	0.722 W/cm-°C	
	550°	0.648 W/cm-°C	
	b.p.	0.486 W/cm-°C	
Specific heat (solid)	20°C	0.480 cal/g-°C	
	m.p.	0.515 cal/g-°C	
Specific heat (liquid)	m.p.	0.331 cal/g-°C	
	400°C	0.305 cal/g-°C	
	550°C	0.300 cal/g-°C	
	b.p.	0.307 cal/g-°C	
Specific heat (vapor)	b.p.	0.65 cal/g-°C	

(b) *Potassium*

Atomic number	19		
Atomic weight (based on C = 12)	39.102		
Natural isotopes (mass number)	39	40	41
Isotopic abundance	93.10%	0.012%	6.88%
Absorption cross section to 0.025-ev (thermal) neutrons	2.1 barns		
Total cross section to 0.025-ev neutrons	4.3 barns		
Ionization potential	4.318 volts		
Melting point	63.2°C (146°F)		
Boiling point	756.5°C (1394°F)		
Volume increase on melting	2.4%		
Latent heat of fusion	14.2 cal/g		
Latent heat of vaporization at the boiling point	474 cal/g		
Critical temperature	2287°K (estimate)		
Critical pressure	167 atm (estimate)		
Critical volume	0.216 cm^3/gram-mole (estimate)		
Density (solid)	20°C	0.855 g/cm^3	
	m.p.	0.848 g/cm^3	
Density (liquid)	m.p.	0.828 g/cm^3	
	100°C	0.819 g/cm^3	
	400°C	0.750 g/cm^3	
	550°C	0.715 g/cm^3	
	b.p.	0.664 g/cm^3	
Specific volume (saturated vapor)	400°C	1.7×10^5 cm^3/g	
	550°C	2.2×10^4 cm^3/g	
	b.p.	1.8×10^3 cm^3/g	
Viscosity (liquid)	100°C	0.472 centipoise	
	400°C	0.216 centipoise	
	550°C	0.167 centipoise	
	b.p.	0.130 centipoise	
Surface tension	m.p.	111 dynes/cm	
	100°C	109 dynes/cm	
	400°C	90 dynes/cm	
	550°C	80 dynes/cm	
	b.p.	67 dynes/cm	

Electrical resistivity (solid)	20°C	4.7 μΩcm
	m.p.	6.5 μΩcm (estimate)
Electrical resistivity (liquid)	m.p.	12.0 μΩcm
	100°C	14.3 μΩcm
	400°C	34.5 μΩcm
	550°C	47.3 μΩcm
	b.p.	70.5 μΩcm
Thermal conductivity (solid)	20°C	1.08 W/cm-°C (estimate)
	m.p.	1.05 W/cm-°C (estimate)
Thermal conductivity (liquid)	m.p.	0.540 W/cm-°C
	100°C	0.522 W/cm-°C
	400°C	0.408 W/cm-°C
	550°C	0.364 W/cm-°C
	b.p.	0.307 W/cm-°C
Specific heat (solid)	20°C	0.184 cal/g-°C
	m.p.	0.193 cal/g-°C
Specific heat (liquid)	m.p.	0.197 cal/g-°C
	100°C	0.194 cal/g-°C
	400°C	0.182 cal/g-°C
	550°C	0.182 cal/g-°C
	b.p.	0.187 cal/g-°C

(c) *Eutectic NaK*

Eutectic composition	77.8 wt.% potassium	
Melting point	-12.6°C	
Boiling point	785°C (estimate)	
Volume increase on melting	2.5%	
Density (liquid)	m.p.	0.875 g/cm^3(estimate)
	20°C	0.867 g/cm^3
	100°C	0.855 g/cm^3
	550°C	0.749 g/cm^3
Viscosity (liquid)	m.p.	1.3 centipoises (estimate)
	20°C	0.94 centipoise
	100°C	0.505 centipoise
	550°C	0.176 centipoise
Electrical resistivity (liquid)	m.p.	33.5 μΩcm (estimate)
	20°C	38.0 μΩcm (estimate)
	100°C	40.7 μΩcm (estimate)
	550°C	72.0 μΩcm (estimate)
Thermal conductivity (liquid NaK, 77.7)	20°C	0.218 W/cm-°C
	100°C	0.232 W/cm-°C
	550°C	0.262 W/cm-°C
Specific heat (liquid)	m.p.	0.233 cal/g-°C
	20°C	0.232 cal/g-°C
	100°C	0.224 cal/g-°C
	550°C	0.208 cal/g-°C

1-3 GENERAL DISCUSSION OF SODIUM, POTASSIUM, AND NaK

1-3.1 *Sodium*

Sodium is the sixth most abundant metal on earth and the most abundant of the alkali metals. Sodium metal is manufactured commercially by the electrolysis of a eutectic mixture of $NaCl-CaCl_2$. Commercial sodium is typically about 99.95% pure, the principal impurities being calcium and potassium. It is a silvery metal, soft and ductile and having a density slightly less than that of water, with which it reacts vigorously. It melts at about 98°C (208°F) to form a silvery liquid having about 0.7 the viscosity of water at 20°C. Its volume change on melting is +2.7% at 1 atm. Its normal boiling point is 881°C (1618°F), and thus it exhibits a conveniently long liquidus over a useful range of temperatures. This and its high thermal conductivity make it an excellent heat-transfer fluid. Sodium vapor in heavy layers appears bluish. At higher temperature this color turns to yellow [62]. In the saturated-vapor state, sodium monomer and dimer are in equilibrium, the dimer being favored by increasing temperature [25]. The proportion of dimer in the superheated vapor decreases with temperature. According to Feldman [63] dimerization occurs after vaporization. Thermodynamic considerations based on pressure-volume-temperature (PVT) data by Stone *et al.* [25] imply the presence of a tetramer in the saturated vapor in small but appreciable amounts. The concentration of the tetramer also appears to be favored by increasing temperature. Unlike the dimer, the tetramer has not yet been identified spectroscopically.

1-3.2 *Potassium*

Potassium, in many respects, shows a behavior very similar to that of sodium. Potassium has but limited uses, and its manufacture has accordingly been restricted to a comparatively small scale. The established method of manufacture is a thermal process [64], in contrast to the predominant electrolytic routes used for sodium. The approximate price of commercial potassium is about $4 per pound vs. only about $0.20 per pound for sodium. Potassium is a silvery-white metal that is ductile and soft, although less so than sodium. Its density at room temperature is 86% of that of water, with which it reacts slightly more violently than does sodium. Its normal melting point is around 63°C (146°F). In liquid form it is slightly less viscous than sodium. It normally boils at 756°C (1393°F). The heat conductivity of the liquid is only about one-half that of sodium, and this clearly makes the latter the superior heat-transfer fluid. Potassium vapor in the vicinity of the boiling point appears greenish in heavy layers. At high temperatures the color reverses to violet according to Kirchhoff's law. The vapor undergoes dimerization similar to that of sodium vapor.

1-3.3 *NaK*

Sodium-potassium alloy is generally referred to as NaK (pronounced "Nak"). In the liquid state sodium and potassium metals are miscible in all proportions. Conventionally the alloy composition is given in weight percent of potassium following "NaK." Thus NaK-78 is sodium-potassium alloy containing 78 wt.% potassium. The melting point of NaK ranges downward from the melting point of sodium (98°C) [20] and the melting point of potassium (63°C) [20] to the melting point of the eutectic mixture, NaK-77.8 (67.3 at. % potassium) at -12.6°C [65]. The single advantage of NaK over sodium as a heat-transfer fluid is the fact that it has a lower melting point. Over the composition range NaK-46 to NaK-89, the alloy is liquid at or below room temperature. On the other hand, it is chemically more reactive than sodium and has lower thermal conductivity than either sodium or potassium. Liquid NaK is similar to mercury in appearance. The density and viscosity of eutectic NaK at 20°C are 0.87 g/cm^3 and 0.9 centipoise, respectively, compared to 1.000 g/cm^3 and 1.00 centipoise, respectively, for water at 20°C.

1-4 MECHANICAL PROPERTIES

1-4.1 *Density*

(a) *Density of Sodium*

(1) *Solid Sodium.* Best values for the density of sodium from absolute zero to its melting point are given in Table 1.1 and are plotted in Fig. 1.1. The sources for these values are an empirical equation derived by Thomson and Garelis [4] and a table of densities calculated by Martin [66].

The equation of Thomson and Garelis,

$$\rho\ (g/cm^3) = 0.9725 - 20.11 \times 10^{-5}t - 1.5 \times 10^{-7}t^2 \qquad (1.1)$$

was obtained by a best fit to the old density measurements of Hagen [67]. It is valid to ±0.0003 g/cm^3 over the temperature range $0°C \leq t \leq 96.6°C$, and its extrapolation from -30°C to the melting point of sodium (97.82°C) is considered reasonably exact.

Martin [66] developed an equation relating ρ_T to ρ_0, where ρ_T is the density at temperature T (°K) and ρ_0 is the density at absolute zero. This is a generalized equation containing three terms that represent the effect on density from latent thermal expansion, electronic thermal expansion, and thermally generated lattice vacancies. Martin calculated the values of the constants in the equation by fitting it to the experimental data determined by other investigators from 20 to 293°K. Thereby he arrived at $\rho_0 = 1.011\ g/cm^3$, which is in reasonable agreement with measurements of the density of sodium at 5°K by Barrett [68]. His equation is in excellent agreement with the equation of Thomson and Garelis above 0°C.

(2) *Liquid Sodium.* Many investigators have studied the variation in density of liquid sodium with temperature. These studies are generally in good agreement below 260°C, but at higher temperatures density data by different investigators tend to diverge. Graphs of these collective data suggest the presence of systematic errors.

The density equation of Stone *et al.* [25] is recommended* here because it is based on measurements at higher temperatures than the others and because the slope of very-high-temperature (normalized) measurements by Dillon *et al.* [69] tends to confirm it. The recent work of Goltsova [70] over the temperature range 100 to 1450°C also supports this relation within less than 0.4% even in the high-temperature regime. Stone's equation is:

$$\rho\ (lb/ft^3) = 59.566 - 7.9504 \times 10^{-3}t - 0.2872 \times 10^{-6}t^2 + 0.0603 \times 10^{-9}t^3 \qquad (1.2)$$

with t in °F for $208 \leq t \lesssim 2500°F$. If converted to cgs units, it reads

$$\rho\ (g/cm^3) = 0.9501 - 2.2976 \times 10^{-4}t - 1.460 \times 10^{-8}t^2 + 5.638 \times 10^{-12}t^3 \qquad (1.3)$$

with t in °C for $98 \leq t \lesssim 1370°C$.

The values in Table 1.2 were obtained from this equation. Figure 1.2 shows a graph of this equation.

The constants of Stone's equation (Eq. 1.2) are obtained from a fit to his data, which extend to 1366°C (2491°F), and to the data of

---

*This equation was also the recommended choice of Golden and Tokar [19].

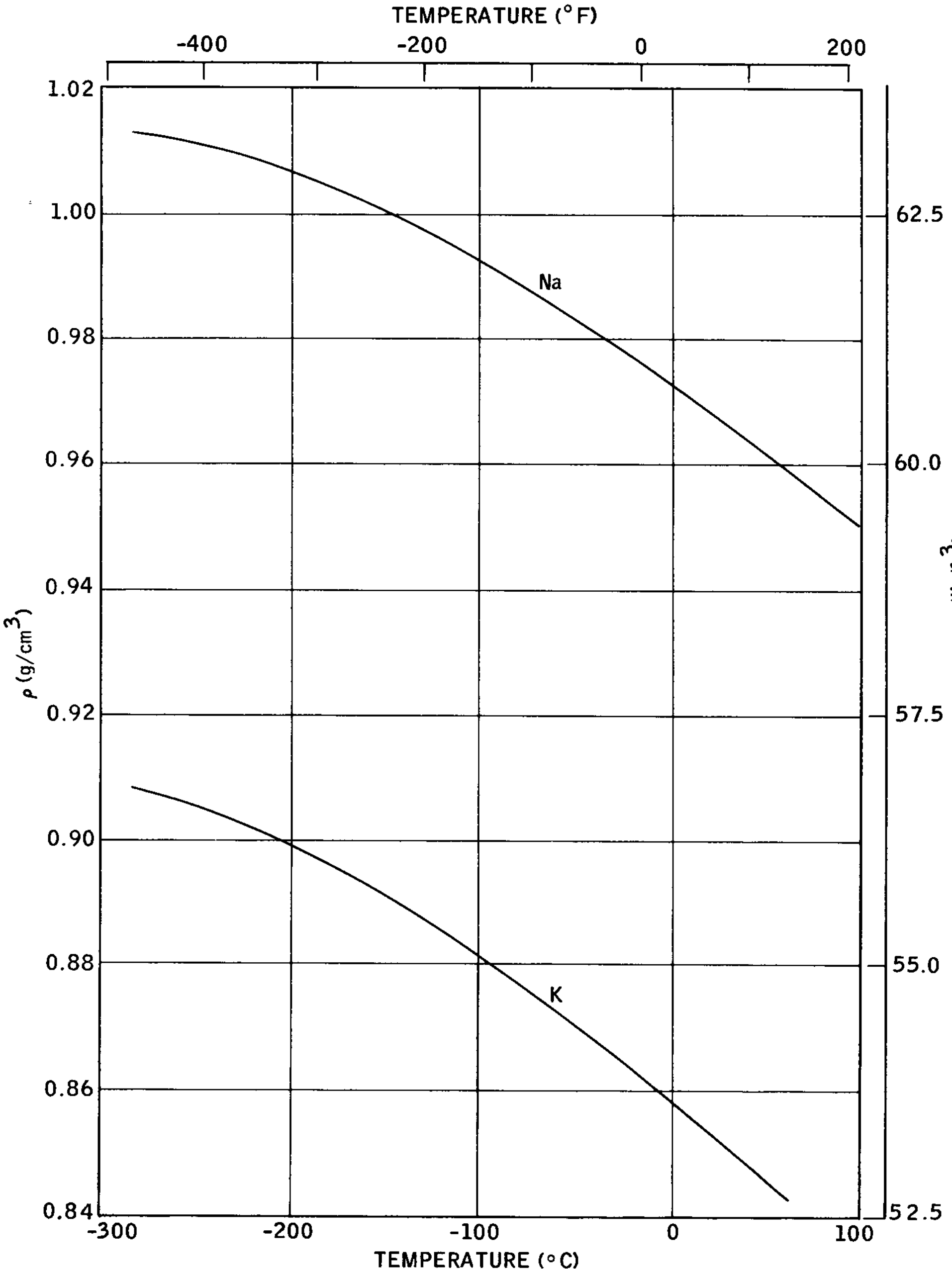

Fig. 1.1 Density (ρ) of solid sodium and potassium.

others [71-74] at lower temperatures. Stone assigns to his equation an accuracy of 0.3% from the melting point to 593°C (208 to 1100°F) and of 0.4% over the range 593 to 1371°C (1100 to 2500°F). Values above 1350°C in Table 1.2 were obtained by extrapolating his equation beyond its limitation. This extrapolation was made to allow comparison with the work of Dillon *et al.* [69] at high temperature. However, according to Goltsova [70], such almost linearly extrapolated data must be considered with caution. This temperature regime therefore needs further experimental investigation.

TABLE 1.1 - Density of Solid Sodium and Potassium

Temp., °C	Na density g/cm³		K density g/cm³
	Martin [66]	Thomson and Garelis [4]	Martin [66]
-273	1.011		0.909
-193	1.007		0.899
-173	1.004		0.894
-73	0.9867		0.873
-30		(0.9784)*	
-20		(0.9765)*	
-10		(0.9745)*	0.859
0	0.9725	0.9725	
10		0.9705	
20	0.9684	0.9684	0.855
30		0.9663	
40		0.9642	
50		0.9621	
60		0.9599	
70		0.9577	
80		0.9555	
90		0.9532	
97.82		(0.9514)*	

*Values in parentheses are extrapolated beyond experimental data.

Thomson and Garelis [4] evaluated liquid-sodium density data reported in the literature from 1883 to 1948. From a field of seven sets of investigators, they selected the three whose data were most compatible. To the data of these investigators, they fitted the following empirical equation:

$$\rho\ (\mathrm{g/cm^3}) = 0.9490 - 22.3 \times 10^{-5}t - 1.75 \times 10^{-8}t^2 \quad (t \text{ in } °\mathrm{C}) \qquad (1.4)$$

They considered this equation valid to ±0.2% up to 640°C (1184°F).

More or less simultaneously with the work of Stone, Tepper *et al.* [75] reported density measurements made on liquid sodium. Their measurements consisted of 36 points over the temperature range 210 to 1110°C (411 to 2031°F). From these data they obtained a linear equation that is converted here to cgs units:

$$\rho\ (\mathrm{g/cm^3}) = 0.9453 - 2.2473 \times 10^{-4}t \quad (t \text{ in } °\mathrm{C}) \qquad (1.5)$$

The standard deviation of their data from this equation was 0.0013 g/cm³, which is equivalent to ±0.14% near the melting point and to ±0.18% at 1100°C.

Dillon *et al.* [69] in the course of determining critical constants of the alkali metals, developed a novel method for measuring the relative densities of liquid metals and their equilibrium vapors. A capsule containing a measured quantity of the

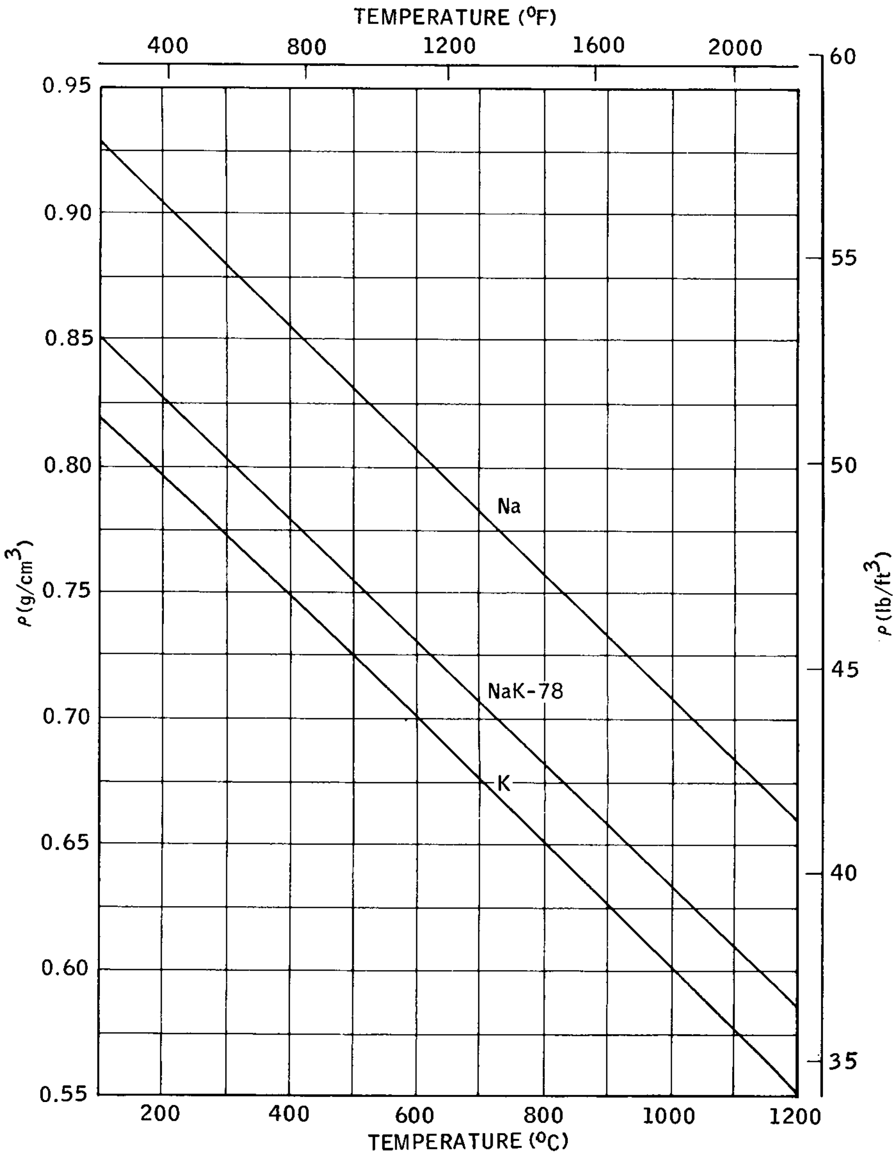

Fig. 1.2 Density (ρ) of liquid sodium, potassium, and NaK-78.

metal was activated by thermal neutrons. The capsule was then heated to such temperatures that significant quantities of the metal vapor were in equilibrium with the metal liquid. The gamma-ray activity emanating from the liquid and vapor phases, respectively, was collimated and measured. Although this method is less exact than more conventional methods, it is particularly adaptable to measurements at high temperature. With this technique Dillon *et al.* extended the measurement of the density of liquid sodium to 1927°C (3500°F). Their method was, however, a comparative one because absolute values depended on at least one well-established density measurement made by some absolute method. The point of normalization chosen for their calculations was the density of sodium at 1190°C (2174°F) taken from an earlier density equation by Stone [76], which was subsequently reported in error and superseded by Eq. 1.2. If the densities reported by

TABLE 1.2 - Density (ρ) of Liquid Sodium, Potassium, and Eutectic NaK

Temperature		Liquid sodium		Liquid potassium		Eutectic NaK	
°C	°F	g/cm^3	lb/ft^3	g/cm^3	lb/ft^3	g/cm^3	lb/ft^3
50	122					0.8669	54.12
100	212	0.9269	57.87	0.8195	51.16	0.8556	53.42
150	302	0.9153	57.14	0.8083	50.46	0.8442	52.71
200	392	0.9036	56.41	0.7970	49.75	0.8327	51.99
250	482	0.8918	55.68	0.7855	49.04	0.8211	51.26
300	572	0.8800	54.94	0.7740	48.32	0.8094	50.53
350	662	0.8681	54.20	0.7623	47.59	0.7976	49.79
400	752	0.8562	53.45	0.7506	46.86	0.7857	49.05
450	842	0.8442	52.71	0.7387	46.11	0.7737	48.30
500	932	0.8322	51.96	0.7267	45.37	0.7616	47.55
550	1022	0.8202	51.21	0.7146	44.61	0.7495	46.79
600	1112	0.8082	50.45	0.7024	43.85	0.7372	46.02
650	1202	0.7961	49.70	0.6902	43.09	0.7249	45.24
700	1292	0.7840	48.95	0.6778	42.31	0.7125	44.48
750	1382	0.7719	48.19	0.6654	41.54	0.7001	43.71
800	1472	0.7598	47.43	0.6529	40.76	0.6875	42.92
850	1562	0.7477	46.68	0.6403	39.97	0.6750	42.14
900	1652	0.7356	45.17	0.6276	39.18	0.6623	41.35
950	1742	0.7234	45.17	0.6148	38.38	0.6496	40.56
1000	1832	0.7113	44.41	0.6020	37.58	0.6369	39.76
1050	1922	0.6992	43.65	0.5891	36.78	0.6241	38.96
1100	2012	0.6872	42.90	0.5762	35.97	0.6112	38.16
1150	2102	0.6751	42.15	0.5632	35.16	0.5983	37.36
1200	2192	0.6631	41.40	0.5502	34.35	0.5854	36.55
1250	2282	0.6511	40.64				
1300	2372	0.6391	39.90				
1350	2462	0.6272	39.15				
1500	2732	0.5916	36.93	Extrapolated			
1700	3092	0.5450	34.02				
1900	3452	0.4996	31.19				
2000	3812	0.4773	29.80				

Dillon *et al.* are normalized to the density 0.6655 g/cm^3 at 1190°C (obtained from Eq. 1.3), they agree with those from Stone's equation within about ±3% over the range from about 900 to 2000°C.

The agreement between the equations of Stone and Tepper is generally within stated limits of accuracy. Above 700°C, however, they diverge from these limits; Tepper's equation gives the higher densities. Additional high-temperature density data are required before a definite choice can be made between the two equations. However, as indicated by the slope of the data by Dillon *et al.* from the point of normalization, the equation by Stone is favored over that by Tepper. In view of the scatter of the density data, used in generating Eq. 1.2, a first-order equation should be entirely adequate.

(3) *Sodium Vapor*. This subject is covered in Sec. 1-5.8(d).

(b) *Density of Potassium*

(1) *Solid Potassium*. Comparatively few data on the density of solid potassium are available [66]; they are shown in Table 1.1 and Fig. 1.1. According to Ref. 10, the density of solid potassium can be expressed in the form

$$\rho\ (\text{g/cm}^3) = 0.864 - 2.4162 \times 10^{-4}t \quad (t \text{ in } ^\circ\text{C}) \tag{1.6}$$

The standard deviation is said to be 0.006 g/cm from the melting point down to -269°C. It should be noted, however, that for temperatures below 0°C this equation depends solely on the data by Swenson [77], which are in variance with those by Martin [66].

(2) *Liquid Potassium*. Recently, Coe [24] has critically evaluated the density data of liquid potassium as reported by various investigators [Refs. 3, 5, 26, 75 and 78]. The agreement among them appears to be surprisingly good, particularly in the lower temperature range. Achener *et al.* [10] also find very good agreement with several other investigators. Recommended here is the density equation as proposed by Ewing *et al.* [26]

$$\rho\ (\text{lb/ft}^3) = 52.768 - 7.4975 \times 10^{-3}t - 0.5255 \times 10^{-6}t^2 + 0.0498 \times 10^{-9}t^3 \quad (t \text{ in } ^\circ\text{F}) \tag{1.7}$$

If converted to cgs units, this equation becomes

$$\rho\ (\text{g/cm}^3) = 0.8415 - 2.172 \times 10^{-4}t - 2.70 \times 10^{-8}t^2 + 4.77 \times 10^{-12}t^3 \quad (t \text{ in } ^\circ\text{C}) \tag{1.8}$$

This equation is said to be valid from the melting point to about 1250°C (2290°F) with an average deviation of less than ±0.25%. It is also supported by recently reported data by Goltsova [70]. Recent measurements by Liu [79] for temperatures up to 300°C also agree well within the experimental scatter (0.3%) with the data recommended here. The smoothed data agree excellently (within 0.1%). The density of liquid potassium is shown in Fig. 1.2 and Table 1.2.

(3) *Potassium Vapor*. This subject is covered in Sec. 1-5.8(d).

(c) *Density of NaK*

(1) *Solid NaK*. No data found in the literature referred specifically to the density of solid NaK.

(2) *Liquid NaK*. The most comprehensive study of the liquid NaK system is that by Ewing *et al.* [80] published in 1948. Fig. 1.3 is a graph of NaK composition-density isotherms taken from that report. From these the density of any NaK alloy from its melting point to 400°C can be obtained with less than ±0.4% error and from 400 to 700°C with less than ±0.8% error.

Ewing also developed the following empirical equation from which the density of any liquid NaK alloy can be calculated:

$$v_{\text{NaK}} = N_{\text{K}}v_{\text{K}} + N_{\text{Na}}v_{\text{Na}} \tag{1.9}$$

where

$v_{\text{NaK}} \equiv$ specific volume of alloy $= 1/\rho_{\text{NaK}}$

$v_{\text{K}}, v_{\text{Na}} \equiv$ specific volumes of K and Na, respectively

$N_{\text{K}}, N_{\text{Na}} \equiv$ mole fractions of K and Na, respectively

The densities of NaK alloy calculated from this equation tend to be slightly higher than the experimental measurements in the middle ranges of composition. Thus, from 30 to 90 wt.% potassium, the right-hand side of Eq. 1.9 should be multiplied by the

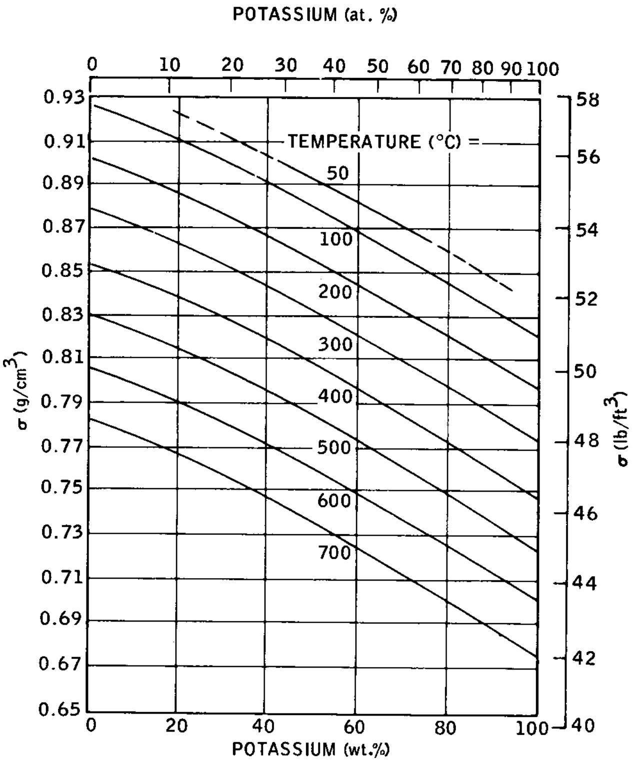

Fig. 1.3 Density (ρ) of sodium-potassium alloys for various temperatures.

correction factor 1.003. Densities so calculated will agree with the density-composition isotherms in Fig. 1.3 within ±0.4%. According to Ref. 81, the reason for this small discrepancy can be found in the neglection of the Na_2K and NaK_2 components in the composition. The slightly negative deviation of the actual molar volume indicates that the liquid contracts somewhat on alloying. However, no direct measurements of the volume change on mixing NaK alloys have been reported in the literature [82].

Densities for NaK-75 reported by Kutateladze *et al.* [9] are in good agreement with the isotherms by Ewing *et al.*, as are experimental values reported by Liu [79], which are about 1% lower. Kanda and Maxwell [83] determined a composition-density isotherm for NaK at 48°C over the composition range 30 to 56 wt.% potassium. Their densities are about 1% higher than should be expected by extrapolation from the isotherms by Ewing *et al.* Essentially, the same results (higher by about 0.5%) were obtained by Faxon [84], who extended the measurements up to approximately 80 at.% potassium.

(3) *NaK Vapor.* This subject is covered in Sec. 1-5.8(d).

(d) *NaK Relations and Equilibrium Diagram*

Because of the difference in the atomic weights, A_w, of sodium and potassium, the relation of the mole fraction N to the weight fraction X in NaK is not linear. This relation is shown graphically in Fig. 1.4; the underlying formula is also shown in the figure.

The phase equilibrium diagram for the sodium-potassium system is given in Fig. 1.5. It was obtained by MacDonald *et al.* [85] by measuring

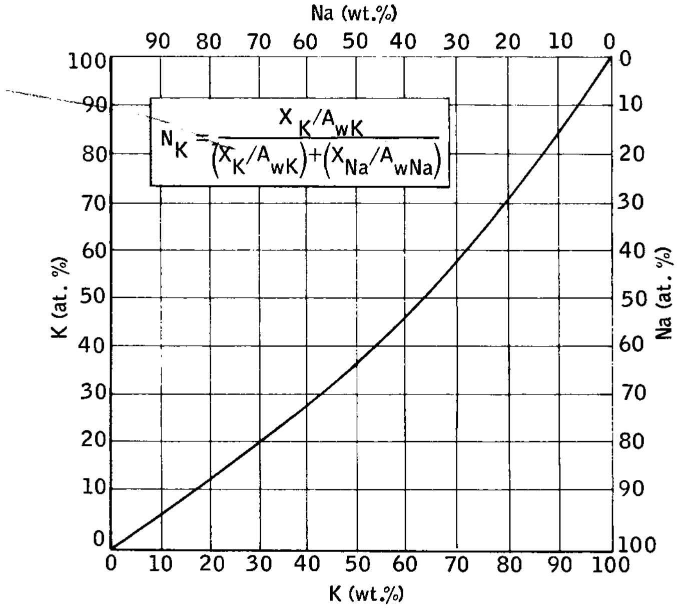

Fig. 1.4 Atomic percent and weight percent relations for sodium-potassium alloys.

changes in the electrical resistivity of samples of known composition. Their technique consisted in measuring the electrical resistance across a glass capillary tube filled with a sample of NaK alloy. The temperature of the cell was raised in steps; resistance measurements were made only after the alloy attained equilibrium at the holding temperature. Discontinuities in the change of resistivity with temperature were used to indicate change-of-phase boundaries.

With this technique MacDonald claims to have identified two solid-solid phases heretofore unreported, namely, a region of up to 3 at.% solid potassium dissolved in sodium and a region of up to 4.5 at.% sodium dissolved in solid potassium. Other than these two phases, the diagram established by MacDonald is in good agreement with the diagram established by Rinck [86].

MacDonald found the peritectic temperature [the temperature at which Na_2K (solid) dissociates into its component elements] to be 7.3 ± 1°C and the eutectic temperature (at about 66.6 at.% potassium) to be -12 ± 1°C.

The most accurate measurements of the peritectic and eutectic temperature in the NaK system, 6.90 ± 0.00 °C and -12.65 ± 0.01°C, respectively, were made by Krier *et al.* [65]. Measurements of the peritectic temperature by Van Bleiswijk [87] and Rinck [86] were 6.9 and 6.6°C, and measurements of the eutectic temperature by Van Bleiswijk [87], Rinck [86] and Miller *et al.* [88] were -12.6, -12.5 and -12.3°C, respectively. Recently, Cafasso *et al.* [89] have questioned the existence of Na_2K molecules in NaK alloys.

1-4.2 *Viscosity*

The viscosity of a fluid is a measure of its resistance to shear or angular deformation. For incompressible flows (like that of liquid metals), only the regular "shear viscosity," η, is important. Only in very few special cases (such as in the propagation of ultrasonic waves) will the "bulk viscosity," η_β, of the liquid metals [see Sec. 1-4.3(c)]

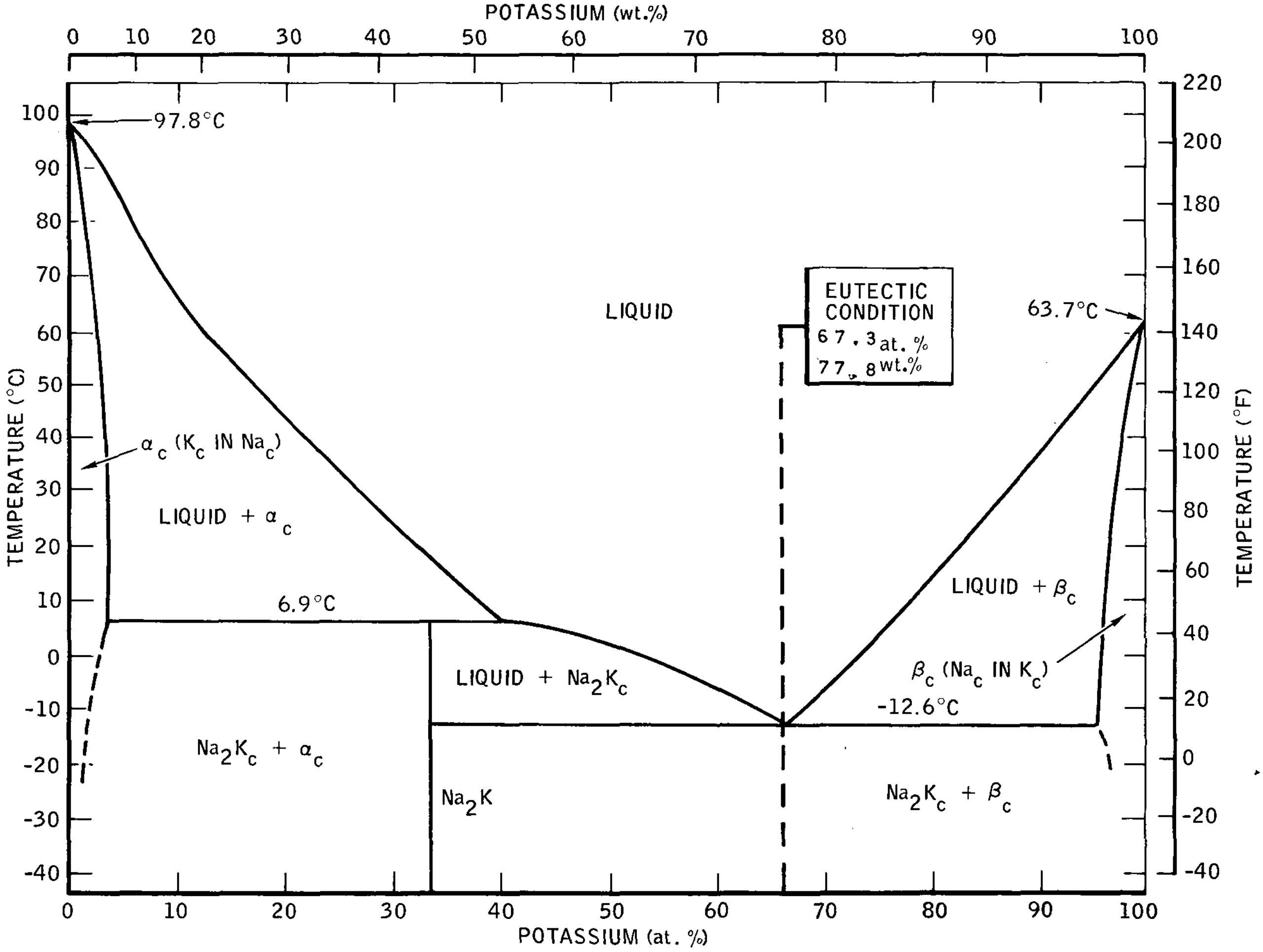

Fig. 1.5 Sodium-potassium equilibrium diagram.

play a role. Various names, such as shear viscosity, absolute viscosity, dynamic viscosity, Newtonian viscosity, etc., are used for η. In this chapter, η will be called the coefficient of "dynamic viscosity" since this expression seems to be the most commonly used. The ratio of the dynamic viscosity, η, to density, ρ, is usually termed the "kinematic viscosity," $\nu(\nu = \eta/\rho)$.

For almost all practical purposes of liquid-metal flows, the dynamic viscosity of liquid metals can be considered to be independent of pressure. It is therefore only the temperature dependence of η and ν that is being presented here. The preferred units are the centipoise for η and the centistoke for ν. Section 1-2 lists conversion factors for various other units that are also being used for η and ν.

(a) *Liquid Sodium*

The viscosity of liquid sodium has been measured by Chiong [90] and Godfrey [91] using the oscillating-sphere method and by Novikov *et al.* [92], Nikolskiy *et al.* [93] Shpil'rain *et al.* [94] and Achener and Fisher [95] using oscillating-cylinder method. Ewing *et al.* [96, 97] have used the capillary-flow method. Values tabulated in Ref. 9

are taken from the data by Nikolskiy. Although the original data by Nikolskiy were not available, the tabulated values are in excellent agreement with the results of Novikov. Chiong's measurements were in the temperature range 98 to 355°C, Godfrey's in the range 327 to 879°C, Novikov's in the range 100 to 800°C, Shpil'rain's in the range 160 to 800°C, Achener's in the range 133 to 1040°C, and Ewing's in the range 103 to 193°C when he used a pyrex capillary and 143 to 686°C when he used a nickel capillary. All the measurements are in good agreement with the exception of those made by Godfrey, which, although in general agreement with the others, have large internal scatter.

Andrade *et al.* [98] proposed the following equation for expressing the variation of viscosity with temperature:

$$\eta v^{1/3} = Ae^{C/vT} \tag{1.10}$$

where v is the specific volume at the absolute temperature, T, and A and C are constants characteristic of the substance.

This equation derives from the fact that viscosity should be inversely proportional to the number of molecules or ions having sufficient energy to cause the configurational change required to relieve the shearing stress. If $\ln \eta v^{1/3}$ is plotted against $1/vT$, a straight line should result with the slope equal to C and intercept equal to A at $1/vT = 0$. The data in Fig. 1.6 show a slight break at about 500°C, with the data above the break lying on one straight line and those below the break on another straight line. This type of anomaly has been observed by Ward [99] in lithium nitrate and also by Hall and Blocher [100] and Rigney, Kapelner and Cleary [101] in potassium. The measurements made by Novikov *et al.* in lithium, potassium, and NaK-75 also show this anomaly. Ewing *et al.* [80] noted the same behavior in their work on sodium and potassium alloys but were reluctant to attribute it to the physical properties of the metals themselves. No explanation for this puzzling behavior has been put forward so far (except that the degree of coordination between atoms may be changing), and it might even ultimately turn out that this "break" in the curve is not real.

A least-squares fit to the equation by Andrade *et al.* was made for the data above 500°C and for the data below 500°C. The resulting constants (for η in centipoises) are:

	Below 500°C	Above 500°C
A	0.1235 ± 0.0018	0.0851 ± 0.003
C	697 ± 9	1040 ± 19

It should be noted that all data were given equal weight. Data near the melting point (below 110°C) were not used in the preceding fit because of the apparent rapid increase in viscosity in that region. The results by Shpil'rain were given only in the form of an equation and therefore could not be used in the least-squares fit. His equation,

$$\log \eta = -1.6814 - 0.4296 \log T + 234.65/T \tag{1.11}$$

agrees well at low temperatures but gives higher values than the above fit for temperatures above 500°C. The data by Achener [95] were ignored because of certain deviations as pointed out in Ref. 10. The data of Godfrey were also not used in the preceding fit because of the large scatter. If his data are included, the values of the constants become:

	Below 500°C	Above 500°C
A	0.1185 ± 0.0028	0.0853 ± 0.0042
C	718 ± 18	1057 ± 60

The first set of constants is recommended. If it is used with Andrade's equation (Eq. 1.10), the following formulas for the temperature dependence of

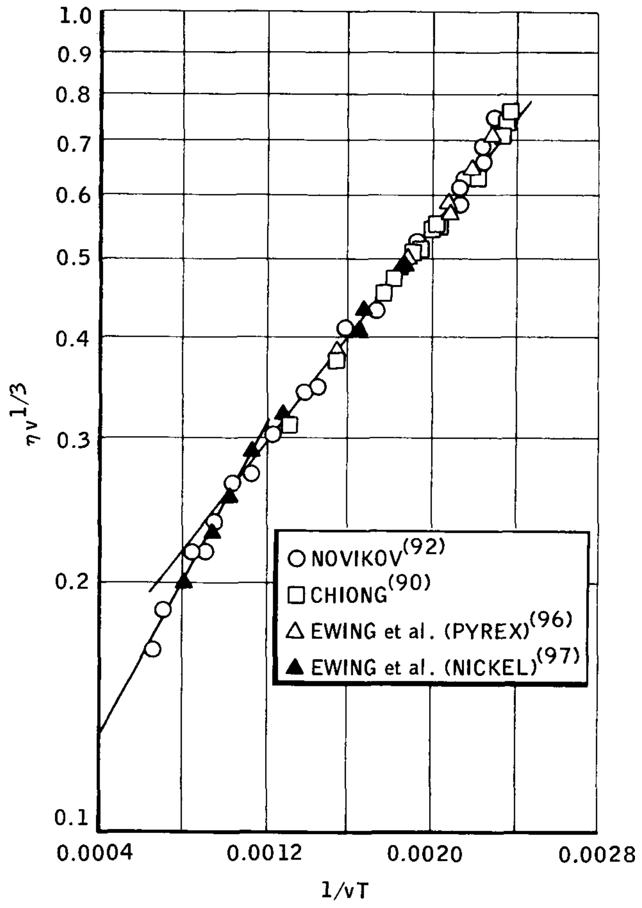

Fig. 1.6 Andrade plot for liquid sodium.

liquid-sodium viscosity result:

$$\eta = (0.1235 \pm 0.0018)\rho^{1/3} \exp\left[\frac{(697 \pm 9)\rho}{T}\right] \quad \text{(below 500° C, standard deviation } \sigma = 0.0065 \text{ centipoise)} \tag{1.12}$$

$$\eta = (0.0851 \pm 0.0013)\rho^{1/3} \exp\left[\frac{(1040 \pm 19)\rho}{T}\right] \quad \text{(above 500°C, standard deviation } \sigma = 0.0035 \text{ centipoise)} \tag{1.13}$$

where η is in centipoise, ρ is in g/cm^3, and T is in °K. Tables 1.3 and 1.4 list the viscosity values of η and ν for sodium as obtained from these equations. The recommended density values given in Sec. 1-4.1(a) were used in these calculations. The viscosity values are presented in a convenient graphical form in Figs. 1.7 and 1.8. Up to 700°C, these values are in close agreement (within ±1%) with those recommended by Golden and Tokar [19]. Data in the extrapolated region (>800°C) tend to differ by wider margins.

Recently Grosse [102, 103] proposed a scheme to extrapolate the absolute and kinematic viscosity data of sodium and potassium all the way up to the critical point. On the opposite end of the liquid range, it is permissible, according to Cavalier [104], to extrapolate the viscosity curve (straight line in Andrade plot) into the region of the subcooled liquid below the melting point.

(b) *Liquid Potassium*

The viscosity of potassium has been measured by Sauerwald [105], Gering and Sauerwald [106] and Ewing *et al.* [96, 97], using capillary viscometers, by Chiong [90] using the oscillating-sphere method, and by Novikov *et al.* [92], Nikolskiy *et al.* [93], Hall and Blocher [100], and Rigney, Kapelner and Cleary [101] using the oscillating-cylinder method. Although the measurements by Ewing *et al.* show excellent internal agreement, they are consistently lower than the results of the other investigators.

If a plot of the Andrade equation is made, as discussed in the section on sodium, it is apparent that the viscosity of potassium also shows an anomaly. The slight break in the potassium curve occurs at about 380°C. A least-squares fit to the data of Novikov *et al.*, Hall and Blocher, and Rigney, Kapelner and Cleary, gives the following equations:

$$\eta=(0.1131\pm0.0060)\rho^{\frac{1}{3}}\ \exp\left[\frac{(680\pm40)\rho}{T}\right]$$

(below 380°C , standard deviation σ=0.017 centipoise) (1.14)

$$\eta=(0.0799\pm0.0032)\rho^{\frac{1}{3}}\ \exp\left[\frac{(978\pm59)\rho}{T}\right]$$

(above 380°C, standard deviation σ=0.007 centipoise) (1.15)

The numerical results from these equations are presented in Tables 1.3 and 1.4 and in Figs. 1.7 and 1.8. A viscosity curve very recently published by Achener *et al.* [10] (based on a fit to a different set of measurements of various experimenters) is practically identical within the stated accuracy limits.

(c) *Liquid Eutectic NaK*

Very little experimental information is available on the viscosity of eutectic NaK. Ewing *et al.* [96, 97] have made measurements on various NaK alloys, including an alloy of 78.6 wt.%. Their measurements , which employed a capillary viscometer, were made in the limited temperature range of 58.3 to 192.7°C. Novikov *et al.* [92] and Nikolskiy *et al.* [93] have made measurements on a 75 wt.% potassium alloy using an oscillating-cylinder technique in the temperature range 65 to 725°C. Macur *et al.* [107] have made measurements on various alloys of NaK in the close vicinity of 78.5 wt.% potassium. They used a capillary viscometer to investigate viscosities in the low-temperature range of -6.1 to 148.9°C. Pingi and Tien [108] reported on viscosity measurement for three types of NaK alloys (NaK-49, NaK-51, and NaK-74) for temperatures up to 300°C.

Since the amount of viscosity data available on sodium and potassium is much greater than that of the alloys, a mixture equation will be used here to obtain the viscosity of eutectic NaK.

Ewing *et al.* [96] give the following equation for the viscosity of a mixture of liquids, which was in good agreement with their measurements:

$$\phi = X_1\phi_1 + X_2\phi_2 \qquad (1.16)$$

where the fluidity ϕ is equal to $1/\eta$, X_1 and X_2 are the weight fractions of the two liquids, and ϕ_1 and ϕ_2 are the fluidities of the two pure liquids. If mole fractions are used in place of weight fractions, better agreement is obtained with the results of Novikov and of Nikolskiy for NaK-75. Because Ewing's data on the viscosity of potassium are in doubt, Eq. 1.17 is used subsequently. Thus

$$\phi = N_1\phi_1 + N_2\phi_2 \qquad (1.17)$$

The viscosity of sodium and potassium has been discussed in the previous sections. The viscosity values obtained with the pertinent equations (Eqs. 1.12 - 1.15) were then used with Eq. 1.17 for mixtures to obtain the viscosity of eutectic NaK:

$$\eta=0.116\rho^{\frac{1}{3}}\ \exp\left[\frac{688\rho}{T}\right]$$ (for temperatures below 400°C) (1.18)

$$\eta=0.082\rho^{\frac{1}{3}}\ \exp\left[\frac{979\rho}{T}\right]$$ (for temperatures above 400°C (1.19)

where again η is measured in centipoise, ρ in g/cm^3, and T in °k.

Numerical results of these equations are presented in Tables 1.3 and 1.4 and in Figs. 1.7 and 1.8. Since the melting point of eutectic NaK is lower than that of sodium or potassium, it is not clear whether the mixture equation is

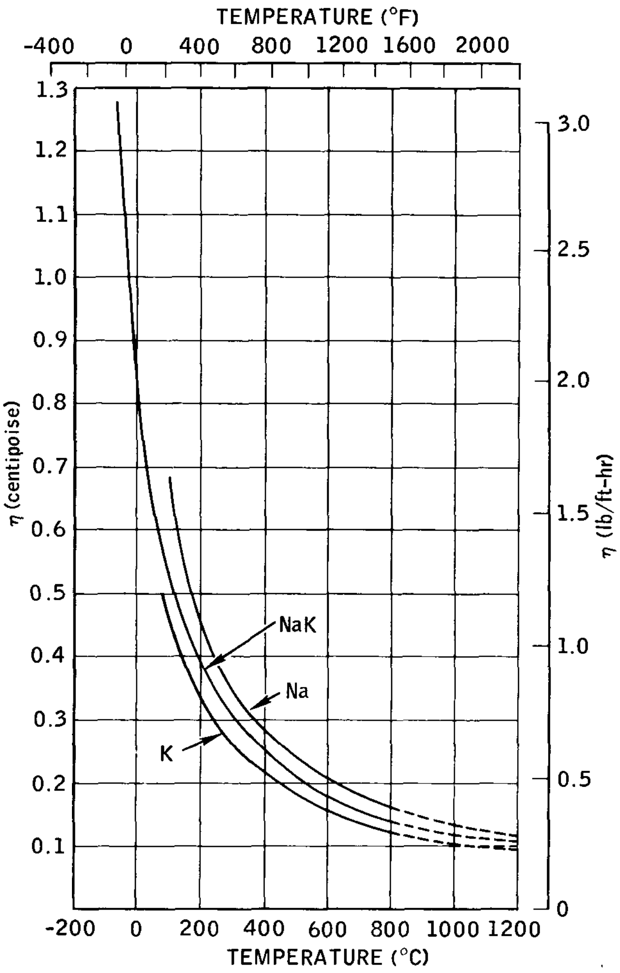

Fig. 1.7 Absolute viscosity (η) for liquid sodium, potassium, and NaK-78.

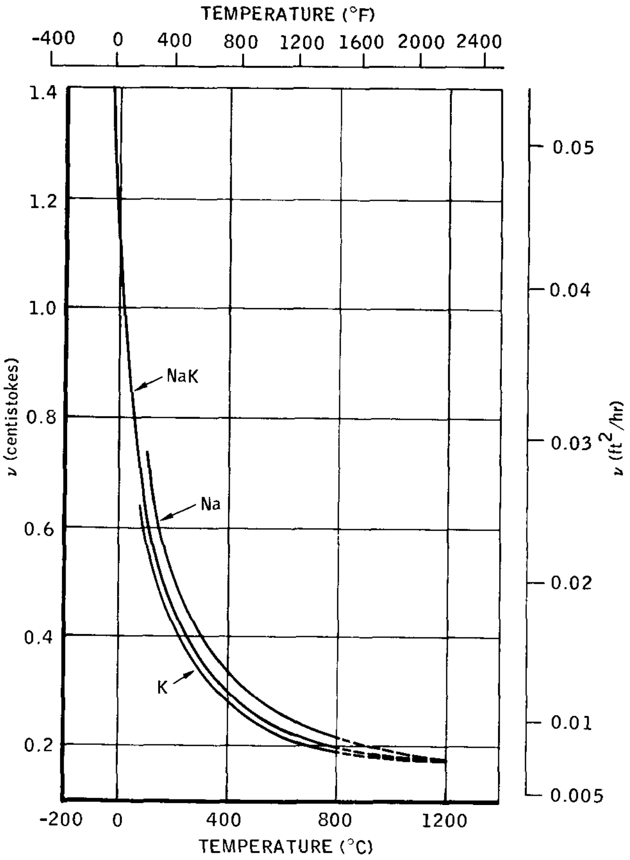

Fig. 1.8 Kinematic viscosity (ν) of liquid sodium, potassium, and NaK-78.

valid at temperatures below 100°C. Therefore the data of Macur *et al.* [107] were used to extend the graph down to the melting point of eutectic NaK.

(d) *Sodium and Potassium Vapor*

Information on the viscosity of these vapors is very scarce. Because of the great experimental difficulties involved, measurements have been reported only very recently [109, 110]. The work of Stefanov *et al.* [109], which has been reported only in brief summary form with viscosity values given at regular intervals of temperature and pressure, indicates that the tabulated values are probably taken from curves drawn through data points. In addition, their tabulated values are given for the temperature range of 700 to 1500°K and the pressure range of 0.001 to 5 atm, whereas their stated experimental range was only 959 to 1143°K and 0.055 to 0.398 atm. A falling-weight method was employed which gave results with an estimated maximum error of 3%. Lee and Bonilla [111] have measured alkali-vapor viscosities with a coiled capillary viscometer over similar temperature and pressure ranges.* Their method

---

*Due to a breakdown of the apparatus, so far only a very limited amount of sodium data over a narrow temperature range is available [110]. However, additional runs on sodium are planned.

TABLE 1.3 - Absolute Viscosity (η)

Temperature		Liquid sodium		Liquid potassium		Eutectic NaK	
°C	°F	Centipoise	Lb/ft-hr	Centipoise	Lb/ft-hr	Centipoise	Lb/ft-hr
50	122					0.7004	1.6944
100	212	0.6802	1.6454	0.4715	1.1411	0.5333	1.2902
150	302	0.5415	1.3099	0.3863	0.9350	0.4326	1.0464
200	392	0.4519	1.0932	0.3297	0.7981	0.3663	0.8861
250	482	0.3900	0.9435	0.2898	0.7013	0.3198	0.7736
300	572	0.3450	0.8347	0.2602	0.6297	0.2856	0.6909
350	662	0.3110	0.7525	0.2374	0.5746	0.2595	0.6277
400	752	0.2845	0.6884	0.2161	0.5230	0.2389	0.5780
450	842	0.2633	0.6370	0.1961	0.4747	0.2145	0.5190
500	932	0.2460	0.5950	0.1801	0.4359	0.1964	0.4752
550	1022	0.2245	0.5431	0.1670	0.4041	0.1816	0.4393
600	1112	0.2075	0.5021	0.1560	0.3775	0.1693	0.4095
650	1202	0.1933	0.4678	0.1467	0.3550	0.1589	0.3843
700	1292	0.1813	0.4387	0.1387	0.3357	0.1499	0.3628
750	1382	0.1710	0.4138	0.1317	0.3189	0.1422	0.3441
800	1472	0.1621	0.3922	0.1256	0.3041	0.1355	0.3278
850	1562	0.1543	0.3733	0.1202	0.2910	0.1295	0.3133
900	1652	0.1474	0.3567	0.1154	0.2793	0.1242	0.3005
950	1742	0.1413	0.3418	0.1110	0.2688	0.1194	0.2889
1000	1832	0.1358	0.3285	0.1071	0.2592	0.1151	0.2785
1050	1922	0.1308	0.3165	0.1035	0.2505	0.1112	0.2690
1100	2012	0.1263	0.3057	0.1002	0.2425	0.1076	0.2602
1150	2102	0.1222	0.2957	0.0972	0.2351	0.1042	0.2522
1200	2192	0.1185	0.2866	0.0943	0.2283	0.1012	0.2448

(described in Ref. 111) uses a theoretical analysis to extrapolate the experimental data into pressure-temperature regions not covered by direct measurements. Lemmon *et al.* [31] have attempted unsuccessfully to measure the viscosity of potassium vapor between 900 and 2100°F.

Lee and Bonilla, as well as others before, have also attempted to calculate the viscosity of alkali-metal vapors. It appears quite important to treat these vapors as a mixture of the various molecular species, which obviously increases the theoretical difficulties. By use of a scaling procedure [112], Lee [110] and Lee and Bonilla [111] determined interaction potentials for the various alkali species, from which they then calculated the collision integrals and finally the transport properties. Thus, like Stefanov, they have extrapolated their scant experimental data over a much wider range of pressures and temperatures.

The data by Stefanov and by Lee are generally only in fair agreement, as can be seen from Figs. 1.9 and 1.10, which show the various viscosity data obtained for sodium and potassium vapor. It appears that the agreement for potassium vapor is somewhat better than that for sodium vapor. Since there are no valid reasons so far for recommending one set over the other, both data sets

TABLE 1.4 - Kinematic Viscosity (ν)

Temperature		Liquid sodium		Liquid potassium		Eutectic NaK	
°C	°F	Centistoke	Ft^2/hr	Centistoke	Ft^2/hr	Centistoke	Ft^2/hr
50	122					0.8079	0.0313
100	212	0.7338	0.02843	0.5753	0.02215	0.6233	0.02415
150	302	0.5916	0.02292	0.4779	0.01840	0.5124	0.01985
200	392	0.5001	0.01937	0.4137	0.01593	0.4398	0.01704
250	482	0.4373	0.01694	0.3689	0.01420	0.3894	0.01507
300	572	0.3921	0.01519	0.3361	0.01294	0.3528	0.01367
350	662	0.3583	0.01388	0.3114	0.01199	0.3253	0.01261
400	752	0.3323	0.01287	0.2879	0.01108	0.3041	0.01178
450	842	0.3119	0.01208	0.2655	0.01022	0.2773	0.01074
500	932	0.2955	0.01145	0.2479	0.00954	0.2579	0.00999
550	1022	0.2737	0.01060	0.2336	0.00900	0.2423	0.00939
600	1112	0.2568	0.00995	0.2221	0.00855	0.2296	0.00890
650	1202	0.2429	0.00941	0.2125	0.00818	0.2191	0.00849
700	1292	0.2313	0.00896	0.2046	0.00788	0.2104	0.00815
750	1382	0.2216	0.00859	0.1980	0.00762	0.2032	0.00787
800	1472	0.2134	0.00827	0.1925	0.00741	0.1970	0.00763
850	1562	0.2064	0.00800	0.1878	0.00723	0.1919	0.00744
900	1652	0.2004	0.00776	0.1839	0.00708	0.1875	0.00727
950	1742	0.1953	0.00756	0.1806	0.00695	0.1838	0.00712
1000	1832	0.1909	0.00740	0.1779	0.00685	0.1807	0.00700
1050	1922	0.1871	0.00725	0.1757	0.00676	0.1781	0.00690
1100	2012	0.1838	0.00712	0.1739	0.00669	0.1760	0.00682
1150	2102	0.1811	0.00702	0.1725	0.00664	0.1742	0.00675
1200	2192	0.1787	0.00692	0.1714	0.00660	0.1728	0.00670

are reproduced in their entirety in Tables 1.5 and 1.6.

In a different analytical attempt, Dunning [21] uses an empirical equation by Johnson, Huong and Kemp [113], which admittedly does not work for all materials, to obtain the viscosities of sodium monomer and dimer. An equation by Wilke [114] for the viscosity of a mixture of gases was then used to arrive at the viscosity of the saturated-sodium vapor. Values obtained by this method are generally about a factor of 2 lower than the values obtained by Stefanov and by Lee. It should be noted, however, that the equation of Johnson, Huong and Kemp involves the critical temperatures and pressures that are not well known for sodium.

Grosse [102] uses the following ideal dilute gas equation [115] for the viscosity of sodium vapor

$$\eta \text{ (poise)} = 2.6693 \times 10^{-5} \frac{\sqrt{A_w T}}{\sigma^2} \qquad (1.20)$$

where A_w is the atomic weight, T is in °K, and σ is the atomic diameter in Å. Grosse used 3.46 Å for σ, which is the diameter of a sodium atom having a ligandcy of 12 as given by Pauling [116]. This method, which ignores dimerization, gives values that are almost a factor of 2 higher than those of Stefanov.

If σ^2 in Eq. 1.20 is replaced by sodium collision integrals for

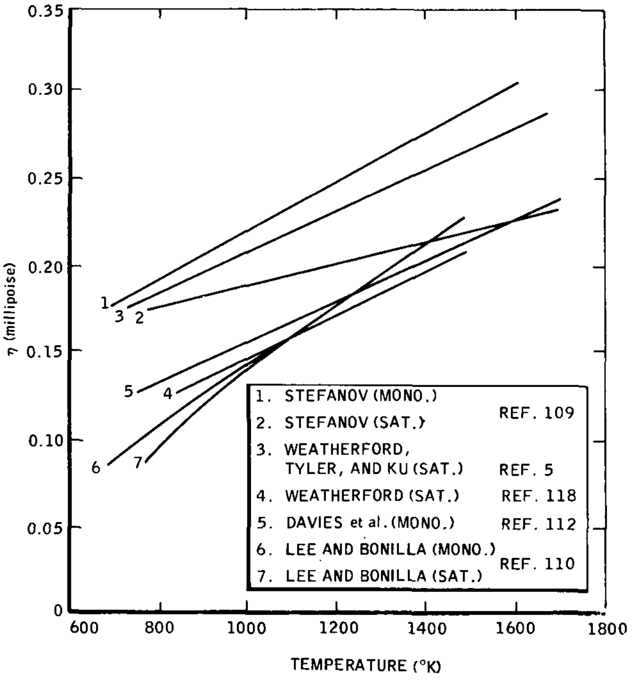

Fig. 1.9 Viscosity (η) of sodium vapor.

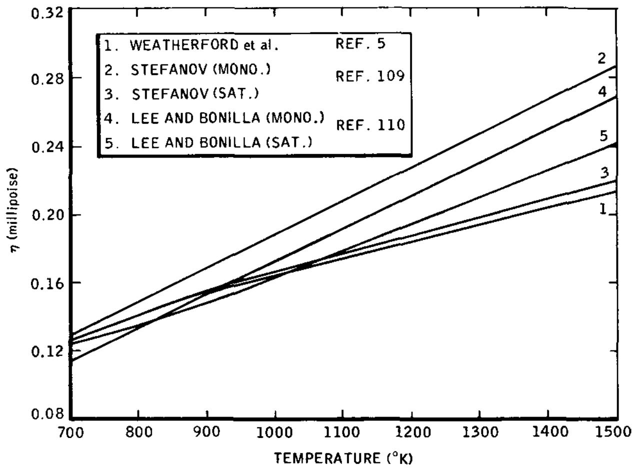

Fig. 1.10 Viscosity (η) of potassium vapor.

viscosity, $[\overline{\Omega}^{(2,2)}]$, as calculated by Davies *et al.* [112], then viscosity values in better agreement with those of Stefanov are obtained. This method is based on monomer only and gives values about 30% below Stefanov's monomer curve.

Weatherford *et al.* [5] calculated viscosity values (for saturated vapor only) that are in fair agreement with those of Stefanov (generally higher by about 10 to 20%). Their method supposedly takes dimerization into account. Another attempt by Weatherford [117] predicts viscosity values that are consistently much lower (roughly by a factor of 2) than Stefanov's data. However, in his latest attempt based on molecular kinetic theory, Weatherford [118] comes much closer to measured values [109, 110]. His predictions are generally 10 to 20% low, which actually is a quite good agreement considering the accuracy of the experimental measurements and the simplifying assumptions in the theory. Estimated viscosity values by Svehla [119] are generally 5 to 40% below the data by Stefanov.

It can be expected that in the near future further experimental data on the viscosity of alkali vapors will become available from Bonilla's group at Columbia University [36] and from Achener's group at Aerojet-General [120].

(e) *Eutectic NaK*

No measurements on the viscosity of NaK vapors have been made. However, since Stefanov *et al.* [109] as well as Lee [110] have measured the viscosities of both sodium and potassium vapors, the viscosity of NaK of any composition can be calculated from the values for sodium and potassium by using the mixture equation given by Wilke [114]:

$$\eta_{NaK} = \frac{\eta_{Na}}{1 + \dfrac{(N_K/N_{Na})\left[1+(\eta_{Na}/\eta_K)^{\frac{1}{2}}(M_K/M_{Na})^{\frac{1}{4}}\right]^2}{(4/\sqrt{2})\left[1+(M_{Na}/M_K)\right]^{\frac{1}{2}}}}$$

$$+ \frac{\eta_K}{1 + \dfrac{(N_{Na}/N_K)\left[1+(\eta_K/\eta_{Na})^{\frac{1}{2}}(M_{Na}/M_K)^{\frac{1}{4}}\right]^2}{(4/\sqrt{2})\left[1 + (M_K/M_{Na})\right]^{\frac{1}{2}}}} \qquad (1.21)$$

where N_K and N_{Na} are the mole fractions and M_K and M_{Na} are molecular weights of potassium and sodium, respectively. (No allowance was made in M and N for dimerization.) The result of this method for the saturated vapor is shown in Fig. 1.11. (Because of the somewhat questionable basis for determining the curve in Fig. 1.11, it should be used with caution.)

1-4.3 *Compressibility and Sonic Velocity*

(a) *Isothermal and Adiabatic Compressibilities*

(1) *Sodium.* The isothermal compressibility of sodium has been measured over a range of pressures and temperatures. For the solid phase, the compressibility is given by the following equation [121], on the basis of extensive experiments:

$$k_T = -\frac{1}{V}\left(\frac{\partial V}{\partial P}\right)_T = -3.09 \times 10^{-5}\left(1 - \frac{V}{15.61}\right)$$

$$(\text{in atm}^{-1}) \qquad (1.22)$$

where V is the molar volume in cubic centimeters. The molar volume is the ratio of the molecular weight to the density, the latter being temperature dependent. This equation is valid to within about 10% from 0 to 20,000 atm and from 20 to 359°K. For higher pressures (up to about 3×10^5 atm), the pressure-volume relation of alkali metals has been investigated by shock-wave measurements [122], in which case the shock-waves were generated by explosives.

The adiabatic compressibility, k_S, of the liquid as determined from sonic-velocity measurements at 1 atm is given in Table 1.7 according to the equation:

$$k_S = \frac{1}{\rho c^2} \qquad (1.23)$$

where the density, ρ, and the sonic velocity, c, were obtained from Secs. 1-4.1 (b) and 1-4.3 (b).

The adiabatic compressibility is related to the isothermal compressibility by the equation

$$k_T - k_S = \frac{T\beta^2}{\rho c_p} \qquad (1.24)$$

where k_T = isothermal compressibility (cm^2/dyne)
k_S = adiabatic compressibility (cm^2/dyne)
T = absolute temperature (°K)
β = volume coefficient of expansion* (1/°K)
ρ = density (g/cm^3)
c_p = heat capacity at constant pressure† (ergs/g°K)

This equation is equivalent to $k_T/k_S = c_p/c_v$, where c_v is the heat capacity at constant volume.

(2) *Potassium.* For solid potassium the compressibility has been determined by Bridgman [123] up to 10^5 atm. At 45°C the initial isothermal compressibility of potassium has been given as 35.6×10^{-12}cm^2/dyne. More recently, more general PVT relations for solid potassium have been determined experimentally by Monford and Swenson [124]. The compressibility of liquid potassium has been determined indirectly from

---

*β can be obtained from Eqs. 1.38 and 1.39.

†c_p can be obtained from Sec. 1-5.8 (b).

TABLE 1.5 - Viscosity of Sodium Vapor

T, °K	Viscosity, millipoise [110]							
	Monomer	0.5 atm	1.0 atm	2.0 atm	3.0 atm	4.0 atm	5.0 atm	Saturated vapor
700	0.88							0.1005
800	0.105							0.1110
900	0.122							0.1240
1000	0.128							0.1400
1100	0.156	0.1563						0.1570
1200	0.174	0.1750	0.1760					0.1763
1300	0.192	0.1925	0.1935	0.1945	0.1955	0.1960		0.1960
1400	0.209	0.2095	0.2100	0.2107	0.2112	0.2117	0.2121	0.2130
1500	0.226	0.2260	0.2262	0.2265	0.2268	0.2270	0.2272	0.2285

T, °K	Viscosity, millipoise [109]						
	Monatomic vapor	0.001 atm	0.01 atm	0.1 atm	1.0 atm	5.0 atm	On saturated curve
700	0.1784						0.1685
800	0.1920	0.1896					0.1751
900	0.2056	0.2048	0.1989				0.1810
1000	0.2192	0.2190	0.2166	0.1984			0.1868
1100	0.2328	0.2327	0.2316	0.2219			0.1926
1200	0.2464	0.2464	0.2458	0.2404	0.2074		0.1987
1300	0.2600	0.2600	0.2596	0.2562	0.2326		0.2050
1400	0.2736	0.2736	0.2733	0.2712	0.2544	0.2173	0.2117
1500	0.2872	0.2872	0.2856	0.2734	0.2408	0.2193	

sound-velocity measurements [125] by using Eq. 1.23. Data are listed in Table 1.8.

The compressibility of sodium and potassium vapor is treated in detail in Sec. 1-5.8 (d). As long as the vapor can be considered an ideal gas, the normal PVT relations for ideal gases can be applied (compressibility factor Z = 1). For nonideal (real) gas behavior, compressibility factors less than 1 have to be applied. These factors are listed in Appendix D as functions of pressure and temperature.

(3) *Eutectic NaK.* The adiabatic compressibility of eutectic NaK was calculated from Eq. 1.23, and the isothermal compressibility was calculated by using Eq. 1.24. The results are given in Table 1.9. For other than the eutectic ratios, the compressibility of NaK alloys has been determined by Abowitz and Gordon [125].

(b) *Sonic Velocity*

(1) *Sodium.* Since sonic velocities can be measured by inherently very accurate methods, the velocity data as reported by various investigators [125 - 132]* differ only within 0.15% from their mean value. The velocity at the

---

*The relatively old values reported by Kleppa [133] are being disregarded since they are significantly lower than the rest.

TABLE 1.6 - Viscosity of Potassium Vapor

T, °K	Viscosity, millipoise [110]							
	Monomer	0.5 atm	1.0 atm	2.0 atm	3.0 atm	4.0 atm	5.0 atm	Saturated vapor
700	0.114							0.1240
800	0.134							0.1342
900	0.154							0.1480
1000	0.173	0.1660						0.1630
1100	0.192	0.1870	0.1835					0.1780
1200	0.212	0.2095	0.2070	0.2030	0.1990			0.1960
1300	0.232	0.230	0.2285	0.2255	0.2225	0.2195	0.2175	0.2120
1400	0.251	0.2500	0.2485	0.2460	0.2440	0.2420	0.2405	0.2275
1500	0.270	0.2695	0.2685	0.2665	0.2650	0.2630	0.2615	0.2420

T, °K	Viscosity, millipoise [109]						
	Monatomic vapor	0.001 atm	0.01 atm	0.1 atm	1.0 atm	5.0 atm	On saturated curve
700	0.1296	0.1293					0.1256
800	0.1493	0.1492	0.1478				0.1410
900	0.1690	0.1689	0.1682	0.1620			0.1546
1000	0.1887	0.1886	0.1883	0.1848			0.1667
1100	0.2084	0.2084	0.2081	0.2059	0.1880		0.1780
1200	0.2281	0.2291	0.2279	0.2269	0.2135		0.1885
1300	0.2479	0.2479	0.2478	0.2468	0.2367	0.2074	0.1991
1400	0.2676	0.2676	0.2675	0.2667	0.2589	0.2385	0.2033
1500	0.2873	0.2873	0.2872	0.2865	0.2807	0.2609	0.2202

melting point is 2527 ± 5 m/sec.[†] The temperature coefficient of -0.52 m/sec°C is practically constant up to at least 800°C. Thus the recommended equation for the sonic velocity in liquid sodium is

$$c\ (\text{cm/sec}) = 2578 - 0.52t \qquad (t \text{ in } °\text{C}) \qquad (1.25)$$

Numerical values are given in Table 1.10.

Because of the relatively high compressibility of sodium, the sound velocity in liquid sodium is also affected by absolute pressure. The pressure coefficient $(\partial c/\partial p)_T$ for liquid sodium has been determined to be 6.2 cm/sec-atm [135, 136].

No experimental data were found on the sound velocity in solid sodium. Indirectly it can be determined from Eqs. 1.22 to 1.24.

(2) *Potassium.* The sound velocity in liquid potassium is given as [128]

[†] A recent theoretical prediction [134] of the sound velocity of sodium based on the "hard sphere model of liquid metals" has come surprisingly close (within about 1%) to the measured value.

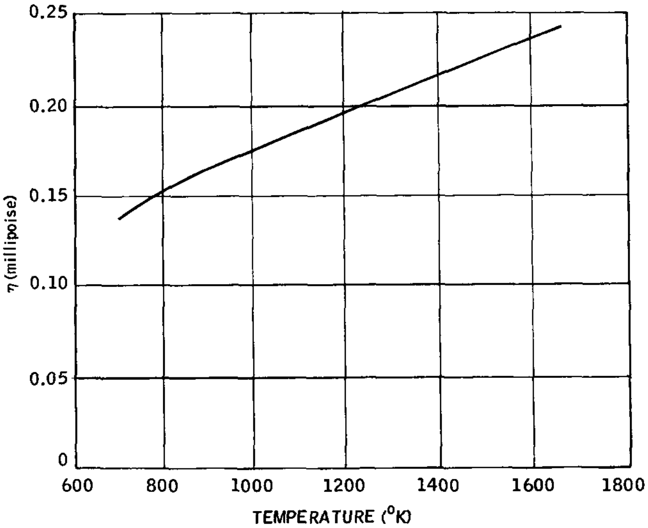

Fig. 1.11 Viscosity (η) of eutectic NaK vapor under saturation conditions.

TABLE 1.7 - Compressibility of Sodium

Temperature		k_S, 10^{-12}	k_T, 10^{-12}
°C	°F	cm^2/dyne	cm^2/dyne
100	212	16.90	18.61
200	392	18.08	21.72
300	572	19.37	24.65
400	752	20.79	27.59
500	932	22.37	30.69
600	1112	24.10	33.97
700	1292	26.02	37.24

$$c \text{ (m/sec)} = 1922 - 0.54t \quad (t \text{ in °C}) \qquad (1.26)$$

Scattering of the underlying experimental data was reported to be ±0.6%. The agreement at 100°C with the data of Abowitz and Gordon [125] is excellent (within 0.1%). Numerical values are given in Table 1.10.

No data were found on the sound velocity in solid potassium. It can be computed from compressibility data by using Eqs. 1.22 to 1.24. The sound velocity in sodium, NaK, and potassium vapor apparently has never been measured. Theoretically it can be determined from the equation

$$c = \sqrt{\gamma\left(\frac{\partial p}{\partial \rho}\right)_T} \qquad (1.27)$$

where $\gamma = c_p/c_v$ is not yet well known for alkali vapors (see Sec. 1-8.5).

TABLE 1.8 - Compressibility of Potassium

Temperature		k_S, 10^{-12}	k_T, 10^{-12}
°C	°F	cm^2/dyne	cm^2/dyne
100	212	35.02	38.60
200	392	38.12	44.32
300	572	41.70	50.27
400	752	45.79	56.45
500	932	50.43	62.63
600	1112	55.74	69.07
700	1292	61.88	75.75

TABLE 1.9 - Compressibility of NaK

Temperature		k_S, 10^{-12}	k_T, 10^{-12}
°C	°F	cm^2/dyne	cm^2/dyne
100	212	28.98	32.57
200	392	31.50	36.36
300	572	34.32	40.52
400	752	37.50	45.10
500	932	41.07	50.11
600	1112	45.12	55.65
700	1292	49.70	61.75

(3) *Eutectic NaK.* No data are available on the true eutectic mixture. Therefore an equation will be quoted for NaK-72 [128], valid at least from 50 to 800°C.

$$c \text{ (m/sec)} = 2088 - 0.53t \quad (t \text{ in °C}) \qquad (1.28)$$

From a linear interpolation of the experimental data [128], the sound velocity for NaK-78 would be

TABLE 1.10 - Sonic Velocity

Temperature		Liquid sodium		Liquid potassium		Eutectic NaK	
°C	°F	m/sec	ft/sec	m/sec	ft/sec	m/sec	ft/sec
50	122					2024	6642
100	212	2526	8287	1868	6128	1998	6555
150	302	2500	8202	1841	6040	1971	6468
200	392	2474	8117	1814	5951	1945	6381
250	482	2448	8031	1787	5863	1918	6294
300	572	2422	7946	1760	5774	1892	6207
350	662	2396	7861	1733	5685	1865	6120
400	752	2370	7775	1706	5597	1839	6033
450	842	2344	7690	1679	5508	1812	5946
500	932	2318	7605	1652	5420	1786	5859
550	1022	2292	7520	1625	5331	1759	5772
600	1112	2266	7434	1598	5243	1733	5685
650	1202	2240	7349	1571	5154	1706	5599
700	1292	2214	7264	1544	5065	1680	5512
750	1382	2188	7178	1517	4977	1653	5425
800	1472	2162	7093	1490	4888	1627	5338
850	1562	2136	7008	1463	4800	1600	5251
900	1652	2110	6922	1436	4711	1574	5164
950	1742	2084	6837	1409	4622	1547	5077
1000	1832	2058	6752	1382	4534	1521	4990
1050	1922	2032	6666	1355	4445	1494	4903
1100	2012	2006	6581	1328	4357	1468	4816
1150	2102	1980	6496	1301	4368	1441	4729
1200	2192	1954	6411	1274	4179	1415	4642

$$c\ (\text{m/sec}) = 2051 - 0.53t \quad (t \text{ in } ^\circ\text{C}) \tag{1.29}$$

Scattering of data was reported to be ±15 m/sec, which is equivalent to 0.6%. These data are in good agreement with earlier data obtained by Abowitz and Gordon [125]. According to Trelin *et al.* [128], the velocity of sound in liquid NaK is approximately connected with the sound velocities in pure sodium and potassium by the following "additivity law":

$$c_{\text{NaK}} = c_{\text{Na}}X_{\text{Na}} + c_{\text{K}}(1 - X_{\text{Na}}) \tag{1.30}$$

where X_{Na} is the weight percentage of sodium in the alloy. Numerical values are given in Table 1.10.

(c) *Acoustic Absorption Coefficients*

In liquid metals, the normal shear viscosity, η, and the thermal conductivity, k, normally contribute the major part to "classical" sound absorption. ($\alpha_{cl} = \alpha_s + \alpha_T$, where α_s and α_T are the absorption coefficients due to η and k, respectively). For liquid sodium, however, the bulk viscosity, η_β, contributes another relatively small fraction [129] (signified by α_β). In liquid potassium the small bulk-viscosity contribution is practically concealed by the large thermal-conductivity contribution.* In NaK the sonic absorption phenomenon appears to be further complicated by a second relaxation process [129].

The sound absorption coefficients α_0, α_s, and α_T, for liquid sodium, potassium, and NaK are presented in Table 1.11 as a function of temperature. (The total absorption coefficient, α_0, is defined as $\alpha_0 = \alpha_s + \alpha_\beta$.) It is customary to present these coefficients in the form α/f^2 (sec^2/cm), where f is the frequency of the sound waves. In this form they are practically independent of f (sec^{-1}). The more recent measurements (up to 600°F) by Ying and Scott [131] are in surprisingly good agreement ($\sim$ 5%) with those by Jarzynski and Litovitz [129]. The bulk viscosity, η_β, can then be determined from the equation [129]

$$\eta_\beta = \frac{\rho c^3}{2\pi^2}\,\frac{\alpha_\beta}{f^2} \qquad (1.31)$$

where ρ and c are the density and the sound velocity, respectively, of the liquid metal.

It can be expected that $\alpha_{c\ell}$ is known with an accuracy of 5 to 10% and that α_β is merely accurate to ±50[Ref. 130]; this difference is due mainly to the fact that α_β is obtained indirectly as the small difference between the two quantities α_0 and $\alpha_{c\ell}$. It should be kept in mind that the absorption coefficients quoted here are valid only for small-amplitude waves. Generally, they increase with increasing amplitude [137]. Furthermore, it should be emphasized here that sonic absorption is usually quite small and therefore frequently altogether negligible for sound waves in the audio range, becoming significant only at ultrasonic frequencies. It has been shown also that sound-wave dispersion and absorption in liquid metals is affected slightly by the presence of a magnetic field [138]. This effect is particularly evident for NaK alloys, as shown in Ref. 139.

Webber and Stephens [135] have recently published a thorough, up-to-date review of the whole field of sound propagation in liquid metals. A similar review article by Gitis and Mikhailov [140] places particular emphasis on the relations between the molecular structure, compressibility, and sound velocity in liquid metals.

1-4.4 *Surface Tension and Wetting Characteristics*

(a) *Definitions*

All liquids (including liquid metals) have properties such as cohesion and adhesion, both of which are forms of molecular attraction. Cohesion enables a liquid to resist tensile stress,* whereas adhesion enables it to adhere to another body. Surface tension is caused by cohesion between fluid particles at the surface of a liquid. Capillarity is the depression or rise of a liquid surface on a solid wall, e.g., within a capillary tube by means of a meniscus, and is caused by both cohesion and adhesion. When cohesion is of less effect than adhesion, the liquid will wet a solid surface with which it is in contact and rise at the point of contact. If cohesion predominates, the liquid surface will be depressed at the point of contact. Thus capillarity causes water to rise in a glass tube while mercury at room temperature is depressed below the true level (Fig. 1.12). Liquid sodium can be either wetting or nonwetting, depending on temperature and wall material. The capillary rise or depression, h, as shown in Fig. 1.12, is determined by the equation

---

*Corresponding conclusions from Ref. 130 are in some disagreement with these statements, however.

*The tensile strength of liquid sodium and potassium (contrary to liquid mercury) has apparently never been measured [141].

TABLE 1.11 - Absorption, Velocity, and Bulk-Viscosity Data*

Temp., °C	Sonic Velocity, m/sec	α_0/f^2, 10^{-17} sec^2/cm	α_S/f^2, 10^{-17} sec^2/cm	α_T/f^2, 10^{-17} sec^2/cm	η_β, centipoises	η_β/η
			Sodium			
104	2523	11.7	1.21	8.11	1.79	2.6
118	2516	12.2	1.13	8.59	1.85	2.9
130	2513	12.8	1.07	9.05	1.98	3.3
147	2501	13.2	1.01	9.70	1.81	3.3
154	2498	13.4	0.98	9.96	1.77	3.3
			Potassium			
74	1887	29.9	2.39	26.7	<0.95	<1.9
108	1867	33.5	2.08	30.6	<0.91	<2.2
116	1863	33.3	2.02	31.7	<0.59	<1.5
150	1843	37.6	1.83	36.0	<0.72	<2.1
			Na-68 At.%*K* Alloy (∿ Eutectic NaK)			
20	2046	11.1	2.94	5.22	1.10	1.3
65	2022	10.6	2.20	7.16	0.45	0.8
100	2003	11.7	1.86	8.85	0.34	0.7

*From J. Jarzynski and T.A. Litovitz, *Journal of Chemical Physics*, 41:1291 (1964).

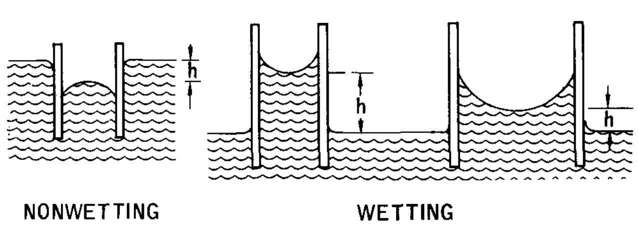

Fig. 1.12 Capillarity in circular tubes.

$$h = \frac{2\sigma}{(\gamma_1 - \gamma_2)r} \qquad (1.32)$$

where σ = surface tension
r = radius of curvature (at the bottom or top of meniscus)
γ_1= specific weight of liquid below meniscus
γ_2= specific weight of fluid above meniscus (can be a gas or another liquid)

The physical chemistry of surfaces constitutes a vast discipline by itself [127], and numerous variations of surface-tension measurements have been developed. Of particular importance is the presence of any impurities on the liquid surface; they can significantly change the value of the surface tension [142, 143].

The most commonly used dimension for the surface tension is dynes per centimeter. This is dimensionally identical to ergs per square centimeter, which is also being used, particularly if one wants to stress that σ also signifies surface energy. One dyne/cm = 1 erg/cm^2 is equivalent to 0.686 × 10^{-4}lb/ft.

(b) *Surface Tension of Liquid Sodium*

The surface tension of liquid sodium has been measured repeatedly over the last 100 years. Although the results lie within a range of ±5% of the mean value, most of the workers considered their own results to have been within ±1% of the true value [144].

Measurements of the surface tension of sodium have been made by Poindexter and Kernaghan [145] at 103 to 243°C using a sessile-drop technique and by Addison *et al.* [146, 147] at 128 to 180°C using a vertical-plate technique and at 110 to 220°C using a drop-volume technique. The maximum-bubble-pressure method has been employed by Taylor [148] at 98 to 450°C, by Tepper and Roehlich [30] at 141 to 992°C, and by Bohdansky and Schins [149] at 430 to 930°C. Recently an improved version of the vertical-plate method was also used by Jordan and Lane [144] at 130 to 245°C. In the USSR, Solov'ev and Makarova [150] used the plate method up to 1000°C*.

Because of the moderately good agreement between most of the correlations, the task of choosing a best fit is difficult. Several of the referenced authors put forth various arguments as to why their data should be treated as being accurate and as to why results obtained from other investigations should be subject to some doubt. In our estimation most of these arguments were circumstantial and relied heavily on strings of deductions; therefore little credence was given to them.

It appears, therefore, that the method used by Golden and Tokar [19] in pooling the various sources and averaging both their melting-point surface-tension values and their temperature coefficients represents the most sensible way in arriving at the most credible relation for the surface tension. In this way the average melting-point surface tension comes to 196.9 dynes/cm, with a temperature coefficient† of -0.10 dyne/cm-°C, and the recommended relation for the surface tension of liquid sodium is

$$\sigma \text{ (dynes/cm)} = 206.7 - 0.10t \quad (t \text{ in °C}) \qquad (1.33)$$

or

$$\sigma \text{ (lb/ft)} = 0.01429 - 3.81 \times 10^{-6}t \quad (t \text{ in °F}) \qquad (1.34)$$

Values obtained from the recommended equation are given in Fig. 1.13. An approximate theoretical equation, derived by Solov'ev and Caplun [151], shows surprisingly good agreement with this formula.

Longson and Thorley [152] found recently that the temperature coefficient increases from 0.08 to 0.11 dyne/cm-°C with increasing oxygen content of the sodium.

(c) *Surface Tension of Liquid Potassium*

Recent data on the surface tension of liquid potassium are available in sufficient quantities. However, their accuracy is generally not quite so high as that of the sodium data.

Measurements of the surface tension of potassium have been made by Chung [153-155], Cooke [156], Taylor [157, 158], Bohdansky and Schins [149], and Tepper and Roehlich [30], all of whom used the maximum-bubble-pressure method. Very recent measurements reported by Solov'ev and Makarova [150] in Russia and by Jordan and Lane [144] in Australia have been made by use of the vertical-plate method.

Older measurements, such as those by Quaterman and Primak [160], Zhivov [161], and Quincke [162], are not being considered here because they are not at all in agreement with newer data.

---

*Additional sources of sodium surface-tension measurements are listed in Ref. 19.

†The recommended temperature coefficient of -0.10 dyne/cm-°C has very recently been verified experimentally by new measurements in an ultrahigh vacuum under extremely clean conditions [159].

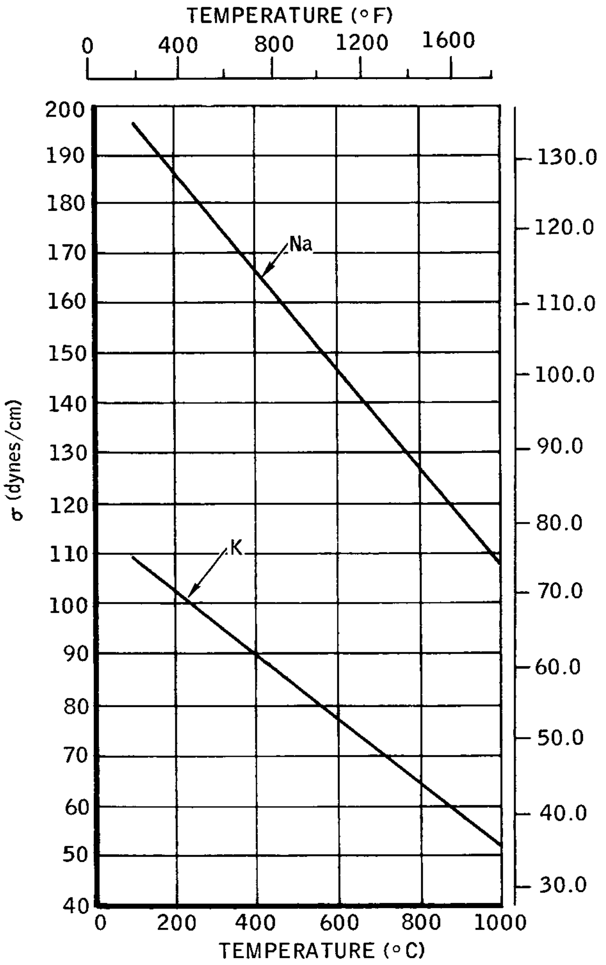

Fig. 1.13 Surface tension (σ) of liquid sodium and potassium.

With the use of a method equivalent to that used for sodium [19], the recommended surface-tension relation for liquid potassium is

$$\sigma \text{ (dynes/cm)} = 115.7 - 0.064t \quad (t \text{ in } ^\circ\text{C}) \qquad (1.35)$$

Values obtained from this equation are plotted in Fig. 1.13. The data of Cooke [156] come very close to this equation.

(d) *Surface Tension of Eutectic NaK*

The literature contains little information on the surface tension of NaK. Ewing *et al.* [80] measured the surface tension of various NaK alloys using the capillary-rise method from the melting point to 200°C. Their results are of little value because of the large error associated with them and because their values for pure sodium and potassium are far below presently accepted values. Weatherford *et al.* [5] give a value of 108 dynes/cm at the melting point based on measurements made at MSA Research Corporation. A similar value of 110 dynes/cm at the melting point has been reported by Bradhurst and Buchanan [163] (at 200 and 250°C, their values are 103 and 99 dynes/cm, respectively). These values are said to be coincident with unpublished NRL data of 1955 (see Ref. 3).

(e) *Parachor*

Computed from the surface tension, the parachor of sodium is 92 and that of potassium is about 150 [15].

(f) *Wetting Characteristics*

Numerous metals are said to show a critical temperature of wetting by liquid sodium [14]. Above this critical temperature, wetting by sodium is a ready process; below it, wetting occurs slowly and only with difficulty, if at all. Graphite is wetted already slightly above the melting point of sodium [164]. Sodium is even drawn into the pores of the graphite [165]. Glass is wetted above 306°C. Wetting characteristics are affected by the presence of an oxide film and by impurities in the sodium [152, 163].

The wetting behavior (such as the wetting rate) of liquid metals is, on the whole, very complex, and no general rules or theories have been successfully established [166, 167]. There is an abundance of literature [166, 168-174] dealing with special wetting problems of liquid sodium which obviously cannot be reviewed here in detail. Wetting by NaK alloys has been studied to a lesser degree only [163, 174], and only a few references dealing with the wetting characteristics of potassium were found [173]. In many respects the wetting behavior of NaK is very similar to that of pure sodium [174].

It was found experimentally that surface roughness and oxidation increase the wetting temperatures on materials such as stainless steel, uranium, and thorium. Previous wetting lowers the wetting temperatures.

Although the fundamental principles governing wetting are generally fairly well understood [166, 167, 175], the wetting of solids by liquid metals cannot be considered an exact science at the present stage owing mainly to practical difficulties associated with obtaining solid and liquid surfaces in known and reproducible states of roughness and cleanliness. For these reasons, empirical data are often merely qualitative and contradictory in nature [166, 167].

1-4.5 *Self-Diffusion*

The temperature dependence of the relatively large self-diffusion coefficient, d, of liquid sodium and potassium* can be expressed [58, 176] by an exponential function that contains two constants, a frequency factor, d_0, and the activation energy, Q:

$$d = d_0 e^{-Q/RT} \tag{1.36}$$

The numerical values of these constants are shown in Table 1.12. The self-diffusion coefficient is usually measured [177] by tracing radioactive isotopes (e.g., ^{42}K). In the presence of electrical currents, the self-diffusion coefficient in many liquid metals is increased significantly [178-180] (Haeffner effect). Isotope diffusion has also been observed as a result of temperature gradients in liquid potassium [181]. The light isotope always wanders toward the hot end.

Contrary to amalgam alloys, no diffusion experiments have been reported for NaK alloys [58].

For solid sodium (0 to 95°C), the self-diffusion coefficient [184] is d (cm^2/sec) = 0.242 exp $(-10450/RT)$. It decreases slightly with increasing pressure [184].

Diffusion of sodium vapor in nitrogen and other gases has been studied [14, 185]. At 1 atm, the diffusion coefficient in N_2 is 0.68 ± 0.03 cm^2/sec at 253°C and 0.91 cm^2/sec at 382°C. Other diffusion constants at approximately 380°C and 1 atm are 3.14 cm^2/sec in H_2, 2.17 cm^2/sec in helium, and 0.88 cm^2/sec in argon.

1-5 THERMOPHYSICAL PROPERTIES

1-5.1 *Melting Points*

The recommended values for the melting points of sodium and potassium at atmospheric pressure, 97.82°C (208.1°F) and 63.2°C (145.8°F), respectively, are the "selected" values of Evans *et al.* [20], who evaluated the work of many investigators. Recently the selected value for the melting point of sodium has been reconfirmed [186] as being 97.83 ± 0.02°C. The best value for the melting point of eutectic NaK is -12.65 ± 0.01°C, determined by Krier *et al.* [65] by calorimetric techniques. Krier *et al.* also established the incongruent melting point, or peritectic point, of Na_2K at 6.90 ± 0.00°C. The temperatures of other solid-liquid phase changes in the sodium-potassium system can be obtained from the equilibrium diagram [85] in Sec. 1-4.1 (d). The melting points of sodium, NaK, and potassium increase monotonically with pressure [123, 187-189] (see Fig. 1.14). For 50,000 atm (730,000 psi), the melting point of sodium reaches 294°C. Recently measurements have been extended to 80,000 atm [190].

The triple point of sodium, 97.81°C, is practically identical with its melting point [191]. The same is true for potassium, which has a triple point

---

*For a definition of d and its significance, see Ref. 182.

TABLE 1.12 - Self-Diffusion Coefficients for Liquid Sodium and Potassium

Metal	d_0, 10^{-3} cm^2/sec	Q, kcal/mole	Temp. range, °C
Sodium [183]	1.10 ± 0.37	2.43 ± 0.2	98.5 to 226.5
Potassium [177]	1.67 ± 0.55	2.55 ± 0.27	67 to 217

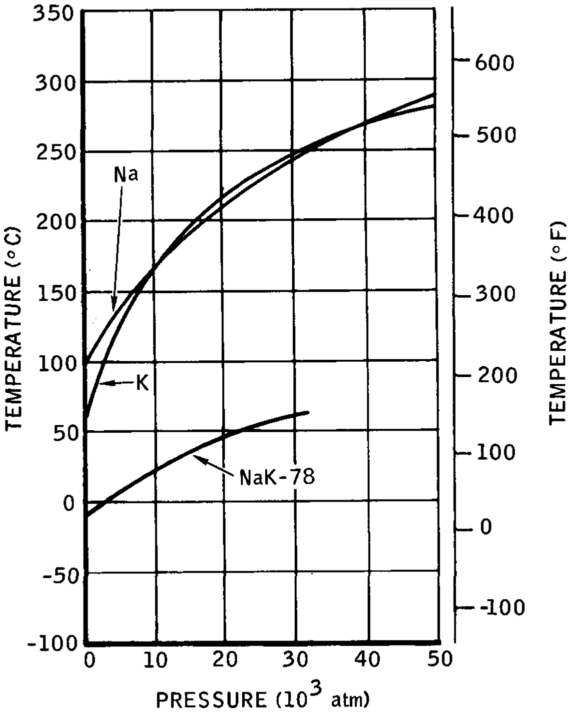

Fig. 1.14 Melting temperature as a function of pressure for sodium, potassium, and NaK-78.

0.02°C below its melting point [15].

(a) *Volume Change at the Melting Point*

(1) *Sodium.* Bridgman [123], in measuring volume change as a function of pressure, determined that the volume change of sodium upon melting at 1 atm pressure was +2.71%. When the recommended density values for liquid and solid sodium very close to the melting point are used, the volume change amounts to 2.63%.

(2) *Potassium.* The reported [15] volume change for potassium upon melting varies between 2.41 and 2.81%.

(3) *NaK*-78. Hluchan [192] gives the volume change of NaK-78 at its melting point as +2.5%. The source for this value is not stated.

(b) *Heats of Fusion*

The recommended values for heats of fusion, L_f, of sodium and potassium at their normal melting points are:

Sodium: L_f = 27.05 cal/g
= 621.8 cal/mole
Potassium: L_f = 14.17 cal/g
= 553.8 cal/mole

These values were obtained by Evans *et al.* [20] by difference from the heat-content curves for the metals in their liquid and solid states. Other reported values for potassium (as reviewed in Ref. 193) range from 12.80 to 14.52 cal/g.

No value was found for the heat of fusion of eutectic NaK. However, Krier *et al.* [65] measured the heat of dissociation of the solid compound Na_2K at its incongruent melting point (29.23 cal/g).

Reported data on the entropy of fusion, ΔS_f, differ widely [13]. It appears that $\Delta S_f = R/2$ [R (gas constant) is equal to 1.98 cal/mole-°K] is correct [194].

1-5.2 *Normal Boiling Points*

(a) *Sodium*

The normal boiling point of sodium has been determined by many investigators by interpolation from saturated-vapor-pressure curves. The values recommended here are those of Stone *et* *al.* [25] and Makansi *et al.* [195], who reported boiling points at 881.4 ± 0.6°C (1618.6 ± 1°F) (standard deviation, 0.52%) and 881.3 ± 1.0°C (1618.4 ± 1.8°F) (standard deviation, 0.9%), respectively, from independent measurements. Within experimental errors these values are equivalent. Boiling points for sodium reported by other investigators [5, 196-198] range from 877 to 892°C. An excellent critical review of these investigations is given by Golden and Tokar [19], who also favor the values of Stone *et al.* and Makansi *et al.*

(b) *Potassium*

The recommended value for potassium is 756.5 ± 0.5°C (1393.7 ± 1°F) (standard deviation, 0.43%), obtained by Ewing [26] from vapor-pressure data. Other reported [197, 199] values range from 753.8 to 761.5°C.

(c) *NaK*

The normal boiling point of NaK alloys as a function of composition [200] is shown in Fig. 1.15. Within the limits of experimental error, the sodium-potassium alloys evidently obey a simple linear relation. The boiling point of the eutectic alloy is interpolated at 785°C.

(d) *Heats of Vaporization at the Normal Boiling Point* *

The heat of vaporization, L_v, is that quantity of heat necessary to change 1 mole (or gram) of liquid to vapor without change of temperature. The standard unit is kilocalories per mole (or kilocalories per gram). If British thermal units per pound is the desired unit, multiply the value in kilocalories per gram by 1800.

(1) *Sodium.* In a survey by Stull and Sinke [201], the best values for vaporization at the normal boiling point (881°C at 1 atm) are reported as

$$L_v = 21.280 \text{ kcal/mole } (0.9256 \text{ kcal/g})$$

The value reported by Krakoviak [202] (L_v = 20.551 kcal/mole) is significantly lower; however, the values recommended by Weatherford *et al.* [5] (L_v = 21.226 kcal/mole), by Shpil'rain and Asinovskii [203] (L_v = 0.926 kcal/g), and by Golden and Tokar [19] (L_v = 21.29 kcal/mole) are in very good agreement. Recent measurements by Achener [196] yield a value of 21.40 kcal/mole ± 0.5%.

(2) *Potassium.* Stull and Sinke [201] recommended for vaporization under atmospheric pressure

$$L_v = 18.530 \text{ kcal/mole } (0.4739 \text{ kcal/g})$$

The value of 0.473 kcal/g as reported by Shpil'rain [203] is practically identical. Values reported by Krakoviak [202] (L_v = 18.487 kcal/mole), by Walling *et al.* [199] (18.29 kcal/mole), and by Weatherford *et al.* [5] (L_v = 18.468 kcal/mole) are insignificantly lower. Still somewhat lower are the recently measured data by Achener [204, 205] (L_v = 17.49 kcal/mole).

The entropy of vaporization at the boiling point can be found in Sec. 1-5.8(d).

1-5.3 *Critical Constants of Sodium and Potassium*

A number of investigators [13] have made strenuous efforts to estimate the critical constants of the alkali metals. In spite of this, the critical constants for sodium and potassium are still poorly known. This is evident from Table 1.13, which contains only the more recent U.S. contributions. The values of Miller [206] are recommended on the basis of the following evaluation.

The large errors assigned to these values arise from the fact that

---

*For vaporization under different pressures, the heat of vaporization can be obtained from the computer routines of Appendices 1-A and 1-B. Also, see Sec. 1-5.8(d).

TABLE 1.13 - Estimates of the Critical Constants of Sodium and Potassium

	Sodium	Potassium
Critical temp. (T_{cr}), °K		
Miller [206]	2733 ± 40	2287 ± 40
Dillon [210]	2573 ± 350	2223 ± 330
Morris [207]	2800	2300
Grosse [208]	2780 ± 300	2440 ± 300
Critical pressure (P_{cr}), atm		
Miller	408	167
Dillon	350 ± 70	160 ± 32
Morris	510	250
Grosse	490 ± 49	240 ± 24
Critical volume (V_{cr}), cm^3/gram mole		
Miller	0.126	0.216
Dillon	0.116 ± 0.023	0.209 ± 0.040
Morris	0.150	0.240
Grosse	0.128	0.217

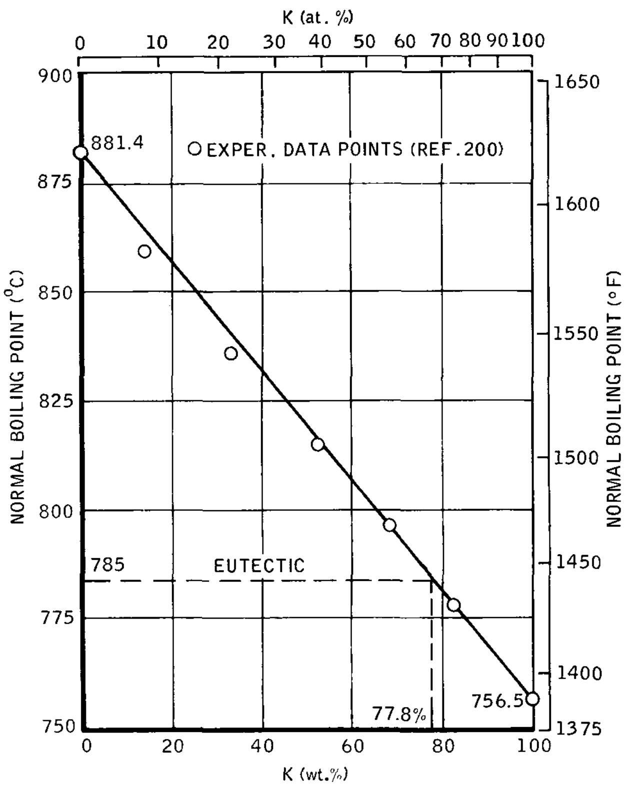

Fig. 1.15 Normal boiling point of sodium-potassium alloys.

investigators have been unable to measure the physical properties of sodium and potassium near their critical temperatures. To circumvent this difficulty, Grosse [208] and Morris [207] used the theory of corresponding states [209] to estimate critical constants. As presently developed, this theory holds that fluids behave similarly at "corresponding reduced conditions," i.e., where the reduced temperature, pressure, density, etc., are defined as

$$T_r = \frac{T}{T_{cr}}, \; P_r = \frac{P}{P_{cr}}, \text{ and } \rho_r = \frac{\rho}{\rho_{cr}}$$

respectively. Dillon *et al.* [69] and Dillon [210, 211] pointed out that the alkali metals deviate somewhat from this theory. Instead, they utilized (1) a rectilinear-diameter plot, (2) a Rowlinson plot, (3) a Kordes plot, and (4) a reduced rectilinear-diameter plot for all the alkali metals. From these they arrived at their best-value estimates in Table 1.13. Recently published works [212-214] discuss the fundamental difficulties that so far have prohibited a full understanding of the thermodynamics at the critical point.

Evidently because cesium has the lowest critical temperature among the alkali metals, the physical-property data for cesium are known closer to its critical point than those for the other alkali metals. Miller *et al.* [206], using these and certain theoretical and empirical relations, estimated the critical temperature, density, and pressure of cesium. Then these results and the law of corresponding states were used to estimate the physical properties of the other alkali metals at their critical points. Very recently, Oster [215] measured critical data for cesium right up to its critical point with a method that shows substantially less experimental scatter than the method of Dillon *et al.* [69]. The experimental cesium data of Oster agree with those predicted by Miller within less than 2%. Thus, by this partial experimental verification, the confidence in Miller's newly estimated critical data is substantially increased. Directly measured critical constants for sodium and potassium of equivalent accuracy are expected in the near future [36, 216].

1-5.4 *Thermal Expansion*

The linear expansion and volumetric expansion with temperature are inversely related to the change in density with temperature. The densities of solid and liquid sodium, potassium, and NaK were taken from Sec. 1-4.1 to provide this information.

(a) *Linear Expansion of Solid Sodium*

$$\ell = \ell_0(1 + 6.893 \times 10^{-5}t + 0.63 \times 10^{-7}t^2) \qquad (1.37)$$

where ℓ is the length at temperature t (°C) and ℓ_0 is the length at 0°C. This equation is valid from 0 to 96.6°C (within ±0.3%). Accordingly, the linear-expansion coefficient [defined as $\alpha = (1/\ell)\ (d\ell/dt)$] is $\alpha = 6.893 \times 10^{-5}$/°C if higher order terms are neglected. A measured value by Siegel and Quimby [217] is $\alpha = 6.84 \times 10^{-5}$/°C at 0° C.

(b) *Volumetric Expansion of Liquid Sodium*

$$V = V_0(1 + 2.4183 \times 10^{-4}t + 7.385 \times 10^{-8}t^2 + 15.64 \times 10^{-12}t^3) \qquad (1.38)$$

where V is the volume at temperature t (°C) and V_0 is the volume at 0°C. Accordingly, the volumetric-expansion coefficient [defined as $\beta = (1/V)\ (dV/dt)$] is $\beta = 2.418 \times 10^{-4}$/°C if higher order terms are neglected. Equation 1.38 is valid within ±0.4% from the melting point of sodium (97.82°C) to about 1350°C.

(c) *Linear Expansion of Potassium*

For the range from 0 to 95°C, the linear-expansion coefficient for potassium is approximately $\alpha = 8.3 \times 10^{-5}$/°C [15, 123], which appears to be essentially the same for the solid and the liquid phase.

(d) *Volumetric Expansion of Liquid Potassium*

$$V = V_0(1 + 2.581 \times 10^{-4}t + 13.080 \times 10^{-8}t^2 + 1.98 \times 10^{-12}t^3) \qquad (1.39)$$

This equation is valid from the melting point up to about 1250°C within ±0.4%. In the first approximation, the volumetric-expansion coefficient ($\beta \sim 2.58 \times 10^{-4}$) is about three times the linear-expansion coefficient.

Because of compressibility effects, the expansion coefficients are also dependent on pressure [123]. However, only at pressures in the range of 10^3 atm and above will these effects become substantial. For pressures up to about 50 atm, they remain practically negligible (well below 1%).

(e) *Volumetric Expansion of NaK*

$$V = V_0(1 + 2.77 \times 10^{-4}t) \qquad (1.40)$$

Accordingly, the volumetric-expansion coefficient, β, for NaK is $\beta = 2.77 \times 10^{-4}/°\mathrm{C}$. Equation 1.39 is valid within ±0.8% from its melting point to 700°C.

1-5.5 *Thermal Conductivity*

(a) *Definitions*

Thermal conductivity, k, is the proportionality factor between heat-flux density through a material and the temperature difference across the material. Specifically, it is defined as the conductive heat transfer through a material per unit time, cross-sectional area, and temperature difference. Thus the time rate of conduction, q, through a plane area, A, is given by

$$q = -kA \frac{dT}{dx} \tag{1.41}$$

where T is the temperature and x is the distance measured along the direction of heat flow, which is perpendicular to A.

The units of k used here are W/cm-°C. Values of k in other units can be obtained by multiplying values given by the factors listed in Sec. 1-3.

(b) *Solid Sodium*

No recent measurements of the thermal conductivity of solid sodium have been reported except for two low-accuracy values near the melting point measured by Evangelisti and Isacchini [218] during the course of their liquid-sodium conductivity measurements. The following equations, fitted by Thomson and Garelis [4], to the data of Hornbeck [219], are therefore recommended:

$$k\ (\mathrm{cal/sec\text{-}cm\text{-}°C}) = 0.324 - 0.00040t \quad (t \text{ in } °\mathrm{C}) \tag{1.42}$$

or

$$k\ (\mathrm{W/cm\text{-}°C}) = 1.356 - 0.00167t \quad (t \text{ in } °\mathrm{C}) \tag{1.43}$$

Thomson and Garelis estimate the accuracy of Eqs. 1.42 and 1.43 as about ±2% for the temperature range from 0 to 95°C.

(c) *Liquid Sodium*

Since publication of the previous edition of the Sodium-NaK Supplement [3], results of a set of measurements of sodium thermal conductivity covering nearly the entire range from melting point to boiling point by Evangelisti and Isacchini [218] has been published. The temperature gradient across a well-defined length of sodium in a cylindrical steel capsule was determined with thermocouples; the heat flux was derived from the measured temperature drop across a plug of stainless-steel AISI-304 with known thermal conductivity. The results for liquid sodium, spanning the range from 104 to 832°C, are consistent with a linear temperature dependence. A weighted least-squares fit was made to these results, with the weights based on the temperature-dependent errors given by the authors. These errors included random uncertainties of the order of 2% in the measurements of Evangelisti and Isacchini and 3% in the conductivity of the standard material. The results of this fit are given by

$$k\ (\mathrm{W/cm\text{-}°C}) = 0.918 \pm 0.013 - 4.9 \times 10^{-4}t \quad (t \text{ in } °\mathrm{C}) \tag{1.44}$$

The root-mean-square (rms) deviation of the measured values from this equation is 2.0%, which is in agreement with the reproducibility reported by Evangelisti and Isacchini; the overall rms standard deviation from all sources of error is calculated to be 3.8%.

Thomson and Garelis [4] recommended the following equation, based on measurements of earlier investigators:

$$k\ (\mathrm{cal/cm\text{-}sec\text{-}°C}) = 0.2166 - 1.16 \times 10^{-4}t \quad (t \text{ in } °\mathrm{C}) \tag{1.45}$$

or

$$k\ (\text{W/cm-°C}) = 0.907 - 4.85 \times 10^{-4}t \quad (t \text{ in °C}) \qquad (1.46)$$

This equation, although based on measurements below 515°C, is statistically almost indistinguishable from the fit to the results of Evangelisti and Isacchini, Eq. 1.44. Measurements made by Novikov *et al.* [220] and Nikol'skii [16] also agree, within error, with the latter fit.

Equation 1.44, based on the results of Evangelisti and Isacchini, is therefore recommended for temperatures below 900°C (see Table 1.14 and Fig. 1.16).

Golden and Tokar [19] also have carefully reviewed almost all existing direct and indirect data for the thermal conductivity of liquid sodium [Refs. 3, 4, 16, 75, and 219-223]. They found that up to about 700°C these data agree within about 5%. However, above the boiling point the data tend to diverge rapidly (about ±30% difference at 1400°C).

It is therefore recommended that either a simple extrapolation of the experimental results of Evangelisti and Isacchini or a semiempirical relation by Grosse [224] be used for values of the liquid thermal conductivity above 881°C (the boiling point at atmospheric pressure). The semiempirical relation by Grosse is given by

$$k = \left(\frac{b}{r_{\text{m.p.}}} \, \frac{T_{\text{cr}} - T}{b\left(T_{\text{cr}} - T_{\text{m.p.}}\right) + T_{\text{m.p.}}} \right) LT \qquad (1.47)$$

The expression in parentheses represents the electrical conductivity as a function of absolute temperature, T, and L is the Lorenz number (see Sec. 1-6.2). T_{cr} and $T_{\text{m.p.}}$ are the critical- and melting-point temperatures, $r_{\text{m.p.}}$ is the (liquid) electrical resistivity at melting, and b characterizes the semiempirical equilateral hyperbola used by Grosse to represent electrical conductivity in terms of reduced variables:

$$\left(\frac{1}{r^*} + b \right) (T^* + b) = b(1 + b) \qquad (1.48)$$

The reduced variables r^* and T^* are expressed in terms of critical-point and melting-point values as $r^* = r/r_{\text{m.p.}}$ and $T^* = (T - T_{\text{m.p.}})/(T_{\text{cr}} - T_{\text{m.p.}})$.

Since the free-electron density of the liquid vanishes at the critical point, the remaining electrical or thermal conductivity is that caused by the vapor state, which was assumed to be negligible over nearly all the liquid range. The Grosse equation provides a convenient method of requiring the liquid electrical or thermal conductivity to vanish at the critical temperature since, for $T^* = 1$, $1/r^*$ must be zero to satisfy the equation. With the following values of the parameters,

$r_{\text{m.p.}}$	$=9.64\times10^{-6}$ ohm-cm	[Sec.1-6.1(b)]
$t_{\text{m.p.}}$	$=97.8$°C	[Sec. 1-5.1]
T_{cr}	∿2800°K	[Grosse [224]]
b	$=0.118$	[Grosse [224]]
L	$=2.32\times10^{-8}$ W-ohm/°K^2	[Grosse [224]]

Equation 1.47 is in only fair agreement with the results of Evangelisti and Isacchini [218]. However, it is in good agreement with an independently proposed equation by Golden and Tokar [19] for a temperature range up to 1370°C.

$$k\ (\text{W/cm-°C}) = 0.930 - 0.581 \times 10^{-3}t + 1.173 \times 10^{-7}t^2 \quad (t \text{ in °C}) \qquad (1.49)$$

The value of k at higher temperatures as calculated by Grosse's method, depends strongly on the value chosen for the critical temperature, an uncertain anchor for the upper temperature end of the curve (see Fig. 1.17). There is no basis for making a choice

TABLE 1.14 - Thermal Conductivity (k)

Temperature		Liquid sodium		Liquid potassium		Eutectic NaK	
°C	°F	W/cm-°C	Btu/ft-hr-°F	W/cm-°C	Btu/ft-hr-°F	W/cm-°C	Btu/ft-hr-°F
50	122					0.224	12.9
100	212	0.869	50.2	0.522	30.1	0.232	13.4
150	302	0.844	49.8	0.498	28.8	0.240	13.9
200	392	0.820	47.4	0.477	27.6	0.247	14.2
250	482	0.796	46.0	0.458	26.5	0.252	14.6
300	572	0.771	44.5	0.440	25.4	0.256	14.8
350	662	0.747	43.1	0.424	24.5	0.260	15.0
400	752	0.722	41.7	0.408	23.6	0.262	15.1
450	842	0.698	40.3	0.393	22.7	0.263	15.2
500	932	0.673	38.9	0.378	21.8	0.263	15.1
550	1022	0.649	37.5	0.364	21.0	0.261	15.1
600	1112	0.624	36.1	0.350	20.2	0.259	15.0
650	1202	0.560	34.6	0.336	19.4	0.256	14.8
700	1291	0.576	33.2	0.323	18.7	0.251	14.5
750	1381	0.550	31.8	0.310	17.9	0.246	14.2
800	1471	0.526	30.4	0.297	17.2	0.239	13.8
850	1562	0.502	29.0	0.284	16.4	0.231	13.3
900	1652	0.477	27.6	0.272	15.7	0.222	12.8

between Eqs. 1.44 and 1.47 for temperatures not far above the boiling point. At higher temperatures, however, the Grosse correlation appears to be preferable because the temperature at which linear extrapolation of the equation by Evangelisti and Isacchini predicts zero conductivity (1870°C) is considerably lower than usual estimates of T_{cr} (see Sec. 1-5.3). A linear extrapolation appears to be highly questionable in this temperature regime.

(d) *Potassium*

The temperature dependence of the thermal conductivity of solid potassium is not very accurately known. No recent measurements are known [15], and Achener *et al.* [10] propose the following equation, which supposedly holds over the entire solid range down to 2.3°K:

$$k \text{ (cal/cm-sec-°K)} = 0.301 - 1.44\times10^{-4}T \quad (T \text{ in °K}) \qquad (1.50)$$

No accuracy statements concerning this equation have been made.

According to the critical survey by Coe [24] of various reported data [Refs. 16, 19, 92, 225 and 226] on the thermal conductivity of liquid potassium, the values obtained by Deem and Matolich [226] appear to be the most reliable. For the temperature region from 100 to 1150°C, he proposes the following equation:

$$k \text{ (W/cm-°C)} = 0.438 - 2.22 \times 10^{-4}t + \frac{39.5}{t + 273.2} \quad (t \text{ in °C}) \qquad (1.51)$$

The standard deviation is about 3% for 100°C < t < 800°C. Data for this equation are presented in Fig. 1.16 and Table 1.14.

Based on the same data, Caldwell and Walley [227] derived an equation of slightly different form:

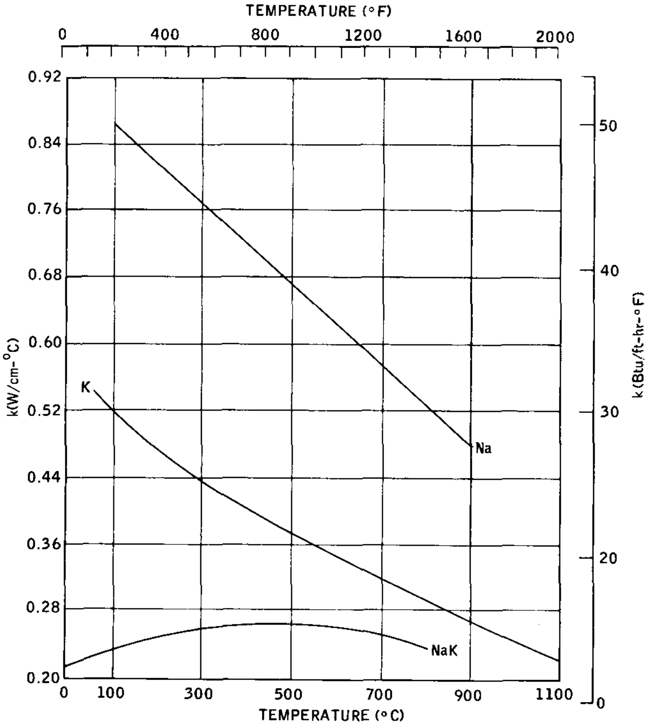

Fig. 1.16 Thermal conductivity (k) for liquid sodium, potassium, and NaK-78.

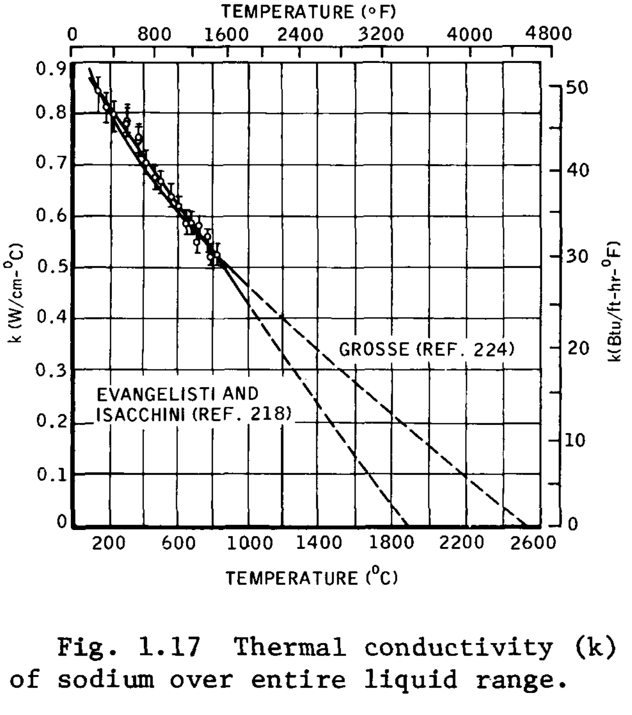

Fig. 1.17 Thermal conductivity (k) of sodium over entire liquid range.

$$k\ (\text{Btu/hr-ft-°F}) = 32.5 - 1.33\times10^{-2}t + 1.9\times10^{-6}t^{3} \quad (t \text{ in °F}) \qquad (1.52)$$

For temperatures above this range, Grosse [228] proposed an extrapolation scheme (similar to that for liquid sodium mentioned previously) which estimates the thermal conductivity of liquid potassium all the way up to the critical point. Since his scheme (as well as those proposed in Refs. 102, 103, 224) depends on the accuracy of the measured property data for the liquid (at or above ∿ 800°C) and for the saturated vapor at high temperatures, the estimates according to those schemes should improve as more reliable measurements in this temperature range become available.

(e) *NaK*

Apparently no new measurements of the thermal conductivity of eutectic NaK have been reported since the publication of the results by Ewing *et al.* [229, 230] and Drugas *et al.* [231] over the range 150 to 680°C. A least-squares parabola was fitted to the data of Ewing with the following result:

$$k\ (\text{W/cm-°C}) = 0.214 \pm 0.002 + 2.07\times10^{-4}t - 2.2\times10^{-7}t^{2} \quad (t \text{ in °C}) \qquad (1.53)$$

The root-mean-square deviation of this curve from the observations is about 0.8%.

The thermal conductivity of NaK is very sensitive to the precise composition near the eutectic value. Calculations by Powers [232] of the thermal conductivities of 78 and 80 wt.% NaK, based on measured electrical conductivities, indicate a difference of about 12% at 300°C. The NaK reported by Ewing *et al.* was 77.7 wt.% potassium. Nikol'skii [16] lists measured data for NaK-75 up to 700°C.

The thermal conductivity of NaK-77.7, as calculated with Eq. 1.53, is presented graphically in Fig. 1.16 and numerically in Table 1.14.

(f) *Thermal Conductivity of Sodium and Potassium Vapors*

Measurements of the thermal conductivity of any alkali-metal vapors are difficult because of the fairly high temperatures required involving radiation between the surfaces (such radiation can be absorbed partly by the alkali vapor [233]) and because of their corrosive chemical activity. Therefore reliable thermal-conductivity data are scarce, particularly for sodium. Furthermore, because of the nonideal gas behavior of alkali-metal vapors, their thermal conductivity depends not only on temperature but also on pressure.

Stefanov *et al.* [109] recently obtained data on sodium and potassium with a dilatometer method [234] over the temperature range 613 to 991°C and pressure range 0.034 to 0.69 atm.* Even more recently, Vargaftik and Voshchinin [235] reported on measurements with a slightly different experimental setup over essentially the same pressure and temperature range. They also proposed a correlation that links the thermal conductivity with the specific heat of the real sodium and potassium vapors. However, since the specific heat of the alkali-metal vapors is not accurately known either, the usefulness of this relation is limited. Some recent experimental data by Briggs [236] for superheated potassium vapor in the range from about 1000 to 1200°F are also in fairly good agreement with those reported in Refs. 109, 235, and 237.

Lee and Bonilla [237] used one of the hot-wire† methods [238] to measure the heat conductivity of cesium and rubidium vapors by first calibrating the hot wire in argon. In a parallel theoretical effort, they developed an analytical method to predict the thermal conductivities by using the potential-energy functions. Since they could show that their analytically predicted data matched fairly well with the measured data for rubidium and cesium, they applied the same analytical method to determine the thermal conductivities of the other alkali-metal vapors.

Their results and the corresponding data obtained by Stefanov *et al.* [109] and those obtained by Vargaftik and Voshchinin [235] are shown in Figs. 1.18 and 1.19.* The qualitative agreement between the results by Lee and Bonilla and Russian experimental data is reasonably good. The quantitative agreement is only fair, however.

Golden and Tokar [19] have reviewed additional earlier attempts [Refs. 5, 21, 112, 117 and 243] to calculate vapor conductivities. However, these attempts show even larger discrepancies (up to a factor of 10) from the recently measured data.

Recent attempts to measure the thermal conductivity of potassium vapor at Battelle Memorial Institute, which failed [24], emphasize the experimental difficulties, and there have yet been no published results (to our knowledge) of similar attempts at Southern

---

*Further details of this experimental procedure as well as a critical evaluation have recently been published [239, 240]. Their final data are slightly different from those reported originally in Ref.109.

†Hot-wire methods at low pressures [238, 241, 242] are affected by the "Knudsen effect," which makes the correct interpretation of experimental results considerably more difficult, even for permanent gases. For this reason the coaxial-cylinder method as described in Refs. 234 and 235 appears the most suitable.

*The set of curves by Lee and Bonilla [237] was chosen because it covers the widest pressure and temperature range. It does not necessarily mean that the accuracy of the data by Lee and Bonilla is superior to those of Refs. 109, 235, or 236.

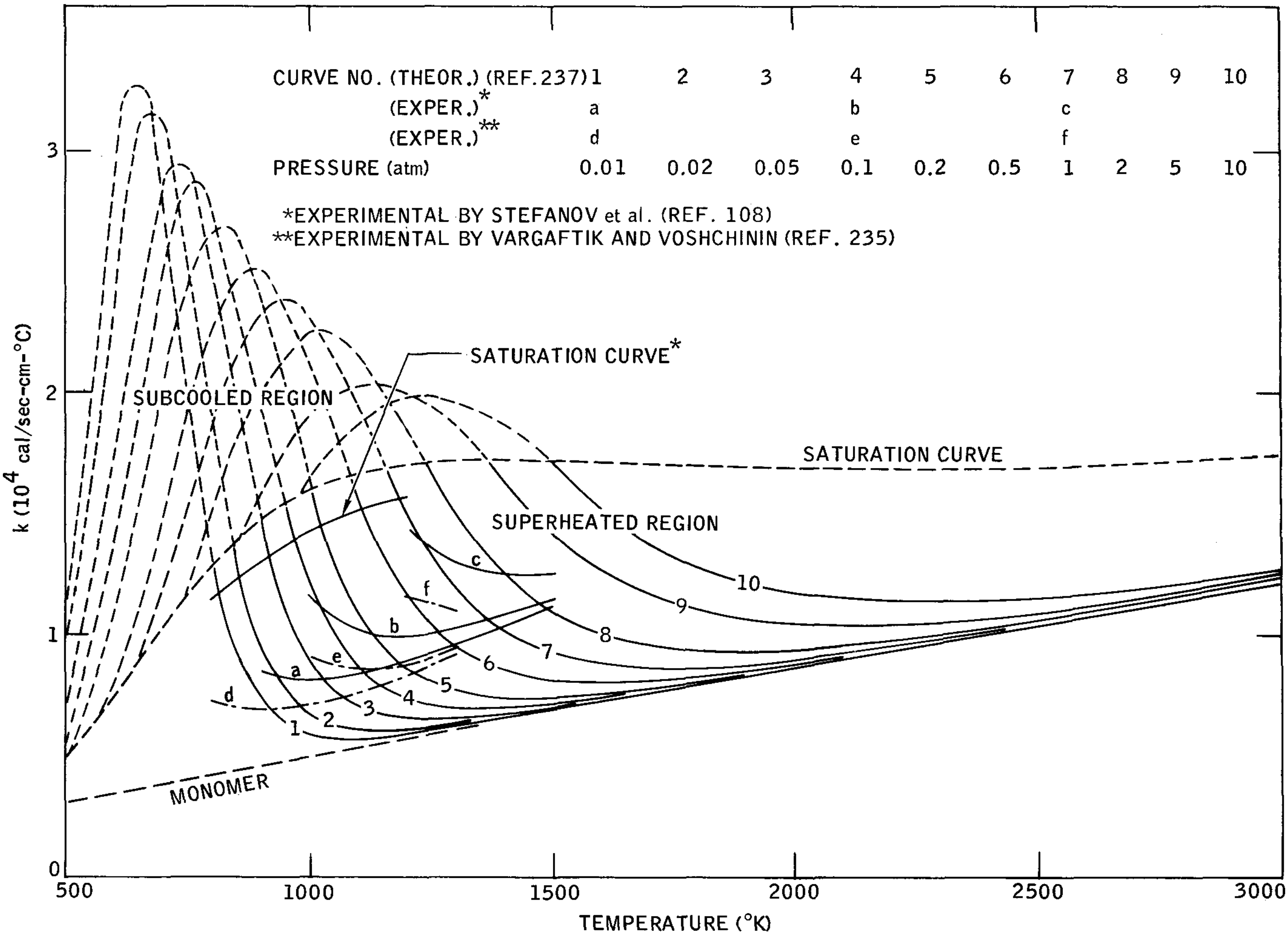

Fig. 1.18 Thermal conductivity (k) of sodium vapor.

Methodist University [244]. Achener and coworkers [120] will try to measure thermal conductivity of potassium vapor to 2000°F in the near future. Meanwhile, the data shown in Fig. 1.18 and 1.19 must be considered the best presently available.

No data have been found on thermal conductivities of mixed sodium-potassium vapors. Theoretically, they could be determined by methods outlined in Ref. 245.

1-5.6 *Thermal Diffusivity*

(a) *Definitions*

The thermal diffusivity of a material, α, is defined as the ratio of thermal conductivity to volume heat capacity, or

$$\alpha = \frac{k}{\rho c_p} \tag{1.54}$$

where k is thermal conductivity, ρ is density, and c_p is heat capacity. Thus it is a measure of the ability of a material to dissipate heat by conduction relative to its ability to retain heat. Thermal diffusivity is the property that governs thermal-transient behavior of the material involved, and its most commonly used dimension is square

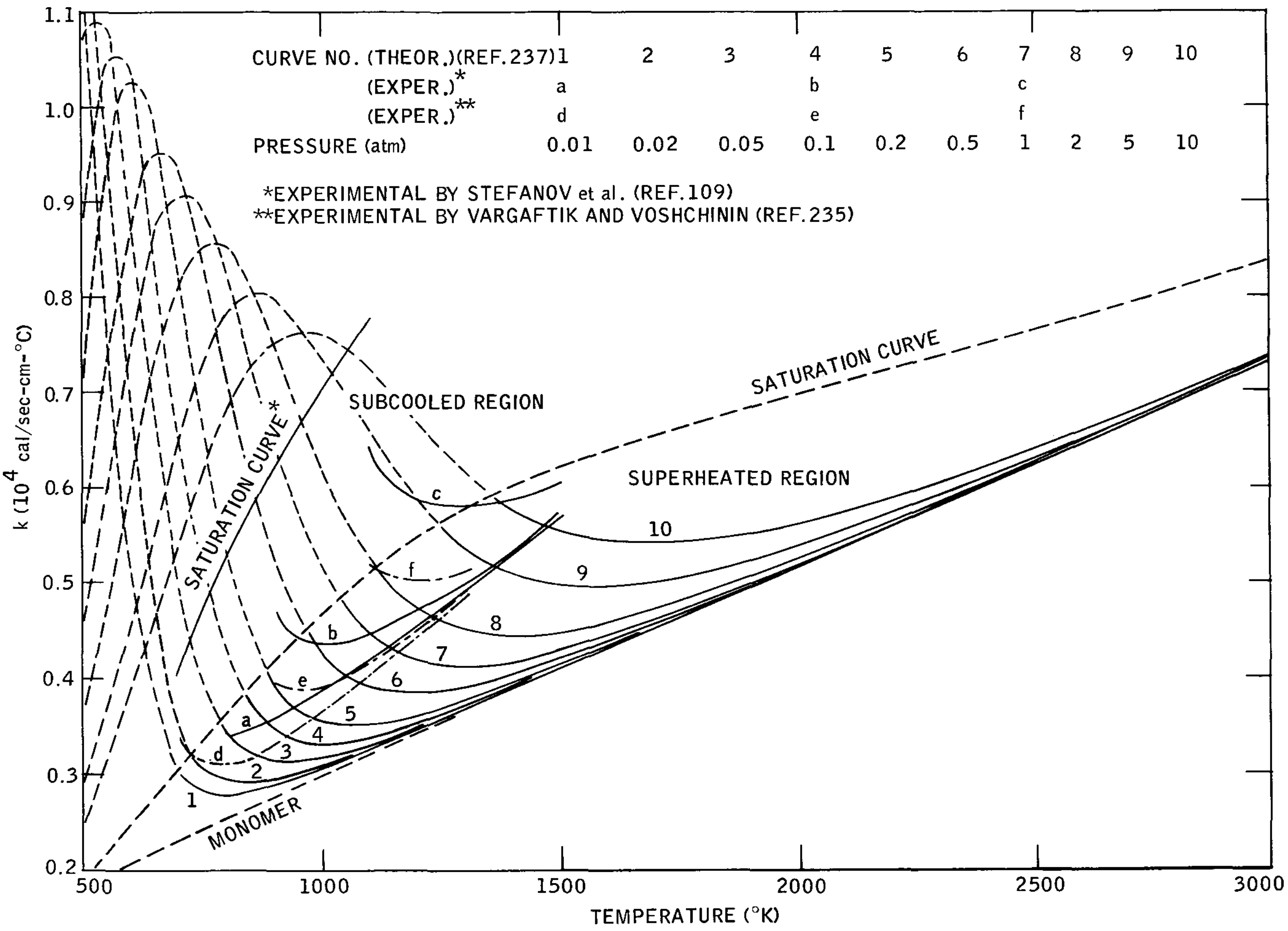

Fig. 1.19 Thermal conductivity (k) of potassium vapor.

centimeters per second. Even though Eq. 1.54 holds for solids, liquids, and gases, only the liquid diffusivity is being treated here.

(b) *Sodium*

The diffusivity of sodium as a function of temperature is plotted in Fig. 1.20. This curve was calculated from Eq. 1.54 by using the recommended equations for thermal conductivity (Eq. 1.44), density (Eq. 1.3), and specific heat (Eq. 1.56). Its estimated standard deviation is ±4%, depending almost entirely on the accuracy of the thermal conductivity measurements.

Direct measurements of α have been made by determining the transit time of a thermal pulse across a known distance [92,222]. These are in reasonable agreement with the calculated curve.

(c) *Potassium*

Equations 1.8, 1.51, 1.54 and 1.58 have been used for calculating the thermal diffusivity of liquid potassium. The results are shown in Fig. 1.20. They agree reasonably well with experimental data [92].

(d) *Eutectic NaK*

The thermal diffusivity of eutectic NaK-77.7 is plotted in Fig. 1.20. This curve was calculated from Eq. 1.54 by using the recommended equations for k

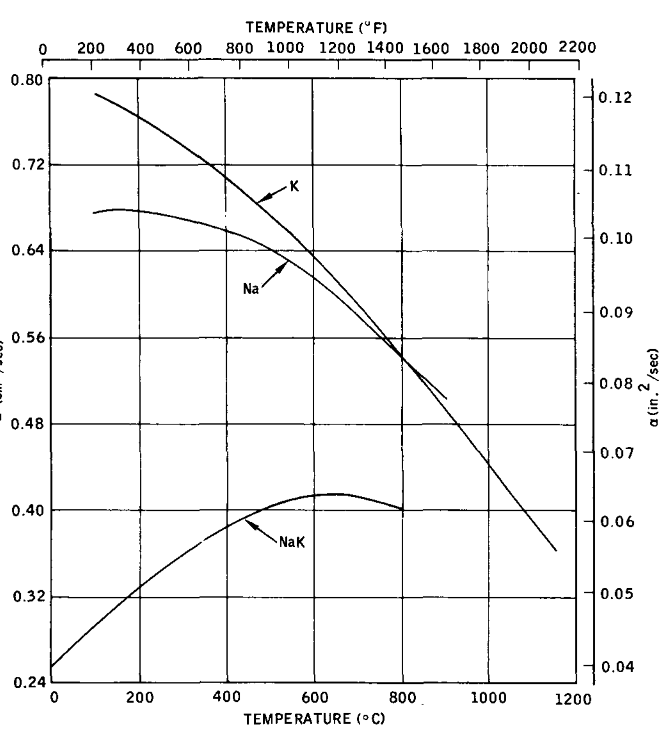

Fig. 1.20 Thermal diffusivity (α) for liquid sodium, potassium, and NaK-78.

(Eq. 1.53), ρ (Eq. 1.9 × 1.003), and c_p (Eq. 1.59). However, these data are in only fair agreement with experimental measurements [92].

1-5.7 *Prandtl Number*

The Prandtl number, Pr, a characteristic of a fluid, is the dimensionless ratio of kinematic viscosity to thermal diffusivity: $Pr = \nu/\alpha$. It may also be written as $Pr = \mu c_p/k$, where μ is absolute viscosity, c_p is specific heat, and k is thermal conductivity.

The Prandtl number is a measure of the importance of turbulent heat transfer relative to conductive heat transfer. The large values of thermal conductivity characteristic of metals lead to liquid-metal Prandtl numbers that are small compared with unity.

Prandtl numbers for liquid sodium, potassium, and eutectic NaK as a function of temperature are listed in Table 1.15. These were calculated from recommended values of thermal conductivity (Sec. 1-5.6), specific heat (Sec. 1-5.8 (b)), and viscosity (Sec. 1-4.2). The absolute accuracy is estimated as ±5%.

The Prandtl number of sodium and potassium vapor is of the order of 0.8 and does not change much with pressure and temperature. More precise values depend, of course, on more accurate knowledge of the vapor -transport properties, which is not yet available. For most practical applications, this approximate value of 0.8 should be adequate, however.

1-5.8 *Thermodynamic Relations*

(a) *Introduction*

The measurement and interpretation of the thermodynamic properties of a system, e.g., entropy, enthalpy and specific heat, in the liquid and solid phase is usually a relatively straightforward procedure. However, particularly with respect to alkali metals, the vapor phase can be complicated by the departure of the system from an ideal gas [246]. This departure is caused principally by the existence of diatomic and possibly other molecular species in the gas and by the variation of concentration of monomer, dimer, etc. with temperature and pressure. Since the literature on the thermodynamics of alkali vapors is quite extensive and still controversial to a certain extent, only the more important results are related here. For deeper study, the original literature must be consulted.

Departing from the usual practice of this chapter, we shall cover first the thermodynamic properties of the liquid and solid phases of sodium potassium and NaK together in Secs. 1-5.8 (b) and 1-5.8(c) and then the vapor properties in Secs. 1-5.8(d) and 1-5.8(e).

(b) *Heat Capacity and Specific Heat*

(1) *Definitions and Nomenclature.* The heat capacity of any system is the quantity of heat required to raise

TABLE 1.15 - Prandtl Number of Sodium, Potassium, and NaK-78 as a Function of Temperature

Temperature		Prandtl number		
°C	°F	Na	K	NaK-78
100	212	0.0108	0.0073	0.0211
200	392	0.0074	0.0054	0.0133
300	572	0.0058	0.0046	0.0098
400	752	0.0050	0.0041	0.0078
500	932	0.0046	0.0037	0.0064
600	1112	0.0042	0.0036	0.0057
700	1292	0.0040	0.0035	0.0052
800	1472	0.0039	0.0036	0.0051
900	1652	0.0040	0.0037	

the temperature of the system by one degree. If the weight of the material is that of the unit mass, the heat capacity is then called the specific heat of the substance. If the weight is that of 1 mole, the heat capacity is referred to as the molar heat capacity, or sometimes as the molecular heat. Since the heat capacity depends both on pressure and on specific volume, it is customary to distinguish between c_p (specific heat at constant pressure) and c_v (specific heat at constant volume).* The ratio of $c_p/c_v = \gamma$ (usually being in the range $1 \lesssim \gamma \lesssim 5/3$) is particularly important for compressibility effects in gases. However, it can also be defined for liquids and solids, for which it equals the ratio of the adiabatic to the isothermal compressibility (see Sec. 1-4.3 (a)) $\gamma = c_p/c_v = k_S/k_T$. According to an estimate by Trelin *et al.* [128], γ for liquid sodium rises almost linearly from 1.10 at 100°C to 1.43 at 800°C. For liquid potassium, γ ranges from about 1.12 to 1.34 for the same temperature interval. The γ values for NaK fall between those for sodium and potassium.

The specific heat is usually expressed in cal/g°C, which happens to be practically identical with Btu/lb°F.

(2) *Specific Heat of Solid Sodium.* Although several anomalies in the specific heat, c_p, of solid sodium have been reported in the literature [247], it seems now certain that these anomalies are restricted to the temperature region below $\sim$40°K [248-250], where the existence of two solid phases (due to martensitic transformation) has been demonstrated. (The temperature region below $\sim$40°K will, therefore, not be discussed here.) For the region $T \gtrsim 30$°K, the solid-sodium c_p curve is shown in Fig. 1.21. For the practically important temperature range $0°\text{C} \le t \le 97.8°\text{C}$, c_p can be expressed by the following equation [191] within about 0.4%:

$$c_p\ (\text{cal/g-°C}) = 0.2865 + 1.551\times10^{-4}t + 0.2516\times10^{-5}t^2 \quad (t \text{ in °C}) \qquad (1.55)$$

Martin [25] lists a sixth-order equation with only 0.16% deviation for about the same temperature range. His results are very close to those of Ginnings *et al.* [191]. Achener *et al.* [10] list a simple first-order equation that is said to be good within about 0.6%, but its extrapolation to temperatures well below 0°C appears doubtful.

Further discussions on the specific heat of solid sodium can be found in Refs. 13, 20, 42 and 252. The effect of high pressures (up to 20,000 atm) on the specific heat (both c_p and c_v) of sodium and potassium has been investigated recently by Rodionov [253].

(3) *Specific Heat of Liquid Sodium.* Stone *et al.* [25] made standard calorimetric measurements to obtain the specific heat of liquid sodium. As shown in Fig. 1.22, their data (circles) compare well with a curve constructed from Eq. 1.56. At about 640°C, c_p obviously has a minimum. Certain investi-

---

*For molar specific heat, a capital C is usually used in C_p and C_v.

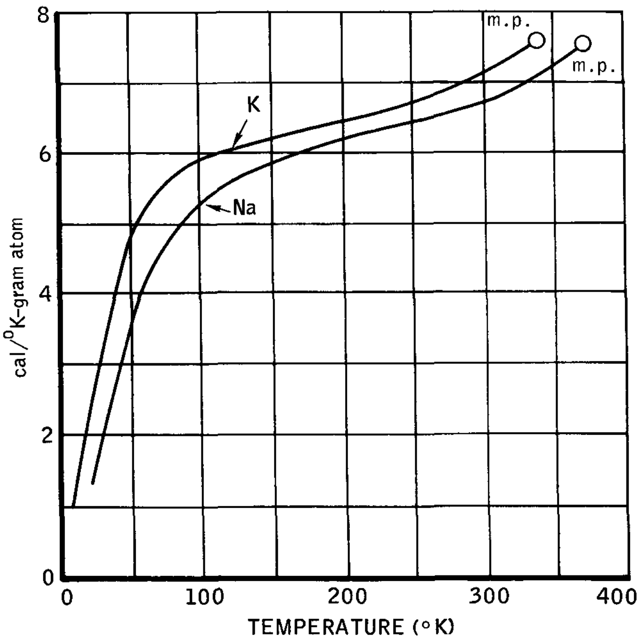

Fig. 1.21 Atomic heat (c_p) of solid sodium and potassium.

gators [254-256] have reported that c_p is essentially constant over a temperature range from about 100°C to as high as 1100°C, whereas others [42, 94] have reported a monotonic decline of c_p with temperature. Still others [251] report a steady decline to about 300°C and then essentially constant.

However, a recent investigation by Martin [25] closely confirms (over the limited range of 300 to 475°K) the older data by Ginnings *et al.* [191] which are therefore recommended here. The c_p data proposed by Evans *et al.* [20], which are based on a critical review of the older literature, are also quite close to those by Ginnings. So are data reported by Nikol'skii [16].

The results by Ginnings can be expressed by the following equation (said to be valid within 0.4% from the melting point to about 900°C):

$$c_p \text{ (cal/g-°C)} = 0.34324 - 1.3868\times10^{-4}t + 1.1044\times10^{-7}t^2 \quad (t \text{ in °C}) \qquad (1.56)$$

Data are presented in Fig. 1.22.

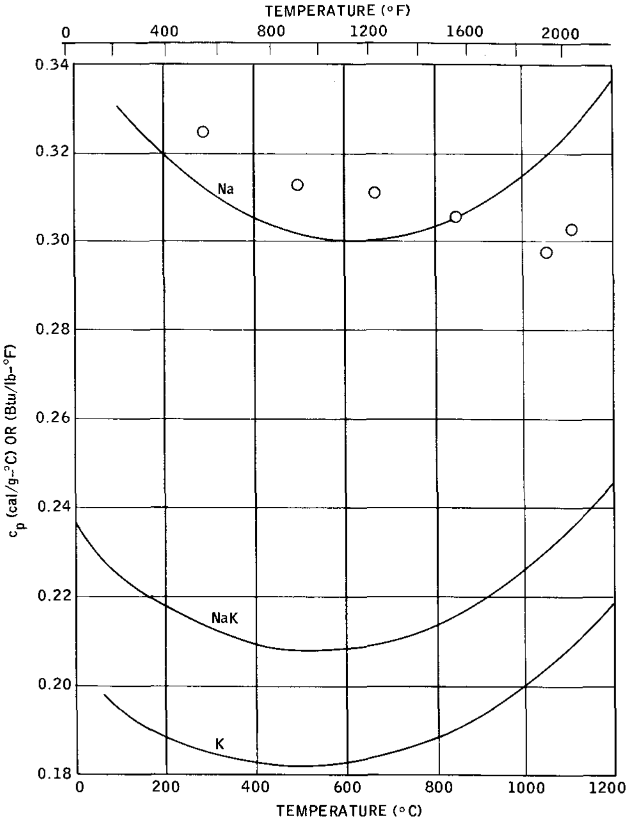

Fig. 1.22 Specific heat (c_p) of liquid sodium, potassium, and NaK-78.

The specific heat at constant volume, c_v, apparently has never been measured directly for liquid sodium. It has been determined by Trelin *et al.* [128] from measured values of c_p, the density, the thermal-expansion coefficient, and the isothermal compressibility according to the relation $c_p/c_v = k_S/k_T$.

(4) *Specific Heat of Solid Potassium.* In contrast to sodium, the specific heat of potassium seems to be well established all the way down to at least 0.2°K [258] because potassium does not show a martensitic transformation on cooling. The c_p curve for solid potassium, taken from Ref. 259, is shown in Fig. 1.21. According to Filby and Martin [258], these presently seem to be the most reliable data.

Only a linear equation for c_p was found in the literature [10]:

$$c_p \text{ (cal/g-°K)} - 0.1285 + 1.9116\times10^{-4}T \qquad (1.57)$$

where T is in °K in the range 100°K $\lesssim T \lesssim$ 337°K. It fits various sets of older data within about ±7%. Data of Ref. 259 are not considered, and therefore the equation should not be used below $\sim$ 100°K.

(5) *Specific Heat of Liquid Potassium.* The following second-order equation is recommended for the specific heat of liquid potassium for the temperature range from the melting point to about 1150°C.

$$c_p \text{ (cal/g-°C)} = 0.2004 - 0.8777\times10^{-4}t + 1.097\times10^{-7}t^2 \qquad (1.58)$$

Up to about 500°C, the error limit can be expected to be below 2%; between 500 and 1150°C, it rises to about 5%. The equation is based primarily on work by Douglas *et al.* [260], Lemmon *et al.* [31] and Deem *et al.* [193]. Up to about 450°C, these sources are in very close agreement. At higher temperatures (>750°C), there exist three single data points (taken at NRL) [26] that tend to support an extrapolation of the old Douglas data. Caldwell and Walley [227], who cite a very similar equation, also advise some caution when using their equation at higher temperatures. The minimum point in the specific heat of potassium lies around 500°C. The recommended relation is supported also by Russian measurements reported in Ref. 16. Data are presented in Fig. 1.22.

(6) *Specific Heat of NaK-78.* No data were found on the specific heat of the NaK solid phase.

Douglas, Ball and Ginnings [260], and Douglas [261] measured the heat capacity of a liquid NaK system from 0 to 800°C. Their results for NaK-78 are shown in Fig. 1.22 and correspond to the equation

$$c_p \text{ (cal/g-°C)} = 0.2320 - 8.82\times10^{-5}t + 8.2\times10^{-8}t^2 \quad (t \text{ in °C}) \qquad (1.59)$$

which is recommended here.

The data by Douglas *et al.* indicated that the specific heat of NaK can be calculated additively from the specific heat of sodium and potassium by using

$$(c_p)_{\text{NaK}} = X_{\text{Na}}(c_p)_{\text{Na}} + X_{\text{K}}(c_p)_{\text{K}} \qquad (1.60)$$

where X_{Na} and X_{K} are the weight fractions of sodium and potassium, respectively. However, they suggest that caution be exercised in the application of Eq. 1.60 to alloys of other materials.

On the other hand, Krier *et al.* [65] claim that Eq. 1.60 is not strictly true. Their data indicate substantial deviation from this rule for temperatures above -70°C for the alloy corresponding to Na_2K. The large deviation at 280.06°K coincides with the temperature at which Na_2K decomposes into its constituent elements. In addition, Krier *et al.* caution that the effective specific heat of the solid phase depends on the history of the alloy. To illustrate, the phase diagram (Sec. 1-4.1 (d)) shows that the liquid alloy corresponding to Na_2K begins to precipitate a solid phase when it is cooled to 20°C. The compound, Na_2K, forms by a peritectic reaction beginning at 7°C. If this reaction is not allowed to run to completion, the system below 7°C consists of Na_2K plus a mixture of sodium and potassium. Krier *et al.* found it necessary to cool through the two-phase region (20 to 7°C) as rapidly as possible to effect a complete peritectic transformation. Under these conditions the precipitated sodium is well dispersed, and the peritectic reaction occurs at a maximum rate. If the cooling through the two-phase region is slow (as it would be in a large system), the sodium particles apparently increase in size and retard the reaction. Thereafter the reaction is effectively incomplete.

(c) *Other Thermodynamic Properties of the Solid and Liquid Phase* *

The data on the enthalpy and entropy of liquid and solid sodium and potassium along the saturation line have been known for a considerable time [20, 191, 260] and appear to be rather accurate [262] since no superseding data have been published.

According to Refs. 14 and 191, the enthalpy H of solid and liquid sodium at saturation pressure can be expressed by the following equations with an estimated probable error of 0.1 to 0.2%.

$$H_c - H_{0c} = 1.19926t + 3.247\times10^{-4}t^2 + 3.510\times10^{-6}t^3 \qquad (1.61)$$

where H is in joules/g and t is in °C for a temperature range of 0 to 97.8°C.

$$H_\ell - H_{0c} = 98.973 + 1.436744t - 2.90244\times10^{-4}t^2 + 1.54097\times10^{-7}t^3 + 24000e^{-13600/(t + 273)} \qquad (1.62)$$

where H is in joules/g and t is in °C for a temperature range of 97.8 to 900°C.

The corresponding equations for the enthalpy of solid and liquid potassium according to Refs. 15 and 260 are

$$H_c - H_{0c} = 0.71040t + 1.0385\times10^{-3}t^2 \qquad (1.63)$$

where H is in joules/g and t is in °C for a temperature range of 0 to 63.2°C and the estimated accuracy is ±1 to 2% and

$$H_\ell - H_{0c} = 56.179 + 0.84074t - 1.5844\times10^{-4}t^2 + 1.0499\times10^{-7}t^3 \qquad (1.64)$$

where H is in joules/g, t is in °C for a temperature range of 63.2 to 800°C, and the estimated accuracy is ±0.3%.

Since only differences in H are of physical significance, the enthalpies are quoted as differences against the arbitrarily chosen H_{0c}, which is here the enthalpy of the solid phase at 0°C.

The following equations for the entropy of solid and liquid sodium (also at saturation pressure) [191] are recommended:

$$S_c - S_{0c} = 4.16241 \log (t+273) - 5.1036\times10^{-3}(t+273) + 5.2656\times10^{-6}(t+273)^2 - 9.14016 \qquad (1.65)$$

where S is in joules/g-°C and t is in °C for a temperature range of 0 to 97.8°C.

$$S_\ell - S_{0c} = 3.7526 \log (t+273) - 8.3303\times10^{-4}(t+273) + 2.3112\times10^{-7}(t+273)^2 - 8.67398 \qquad (1.66)$$

where S is in joules/g-°C and t is in °C for a temperature range of 97.8 to 900°C.

The equivalent equations for the entropy of solid and liquid potassium are [15, 260]

$$S_c - S_{0c} = 0.32938 \log (t+273) + 2.0770\times10^{-3}(t+273) - 1.36986 \qquad (1.67)$$

where S is in joules/g-°C and t is in °C for a temperature range of 0 to 63.2°C.

$$S_\ell - S_{0c} = 2.18919 \log (t+273) + 4.8862\times10^{-4}(t+273) + 1.5718\times10^{-7}(t+273)^2 - 5.04665 \qquad (1.68)$$

where S is in joules/g-°C and t is in °C for a temperature range of 63.2 to 800°C.

S_{0c} is the entropy at 0°C. Since 1 joule is equal to 0.2389 cal, the

---

*The specific heat has been treated in the previous section.

enthalpy and entropy values can easily be converted to cal/g and cal/g-°C units, respectively.

Ewing *et al.* [26] and Stone *et al.* [25] have combined the preceding equations for the solid and liquid phase and have converted them into engineering units. They also chose as the reference state the solid phase at 0°R. They took the absolute enthalpy and entropy at 32°F from Ref. 20. Under these conditions the equations for sodium for enthalpy and entropy have the following form:

$$H_{c\ell} = 0.389352T - 0.552955\times10^{-4}T^2 + 0.113726\times10^{-7}T^3 - 29.023 \qquad (1.69)$$

where $H_{c\ell}$ is the enthalpy in Btu/lb and T is the temperature in °R for $492°\text{R} \le T \le 2110°\text{R}$, which is between 32 and 1650°F.

$$S_{c\ell} = 0.896497 \log T - 0.10557\times10^{-4}T + 0.170408\times10^{-7}T^2 - 1.792026 \qquad (1.70)$$

where $S_{c\ell}$ is the entropy in Btu/lb °F and T is the temperature in °R for $492°\text{R} \le T \le 2110°\text{R}$, which is between 32 and 1650°F.

The equivalent equations for potassium are according to Ref. 26.

$$H_{c\ell} = 87.8783 + 0.2022t - 0.2177\times10^{-4}t^2 + 0.07741\times10^{-7}t^3 \qquad (1.71)$$

where $H_{c\ell}$ is the enthalpy in Btu/lb and and t is the temperature in °F for $32°\text{F} \le t \le 1472°\text{F}$.

$$S_{c\ell} = 0.52298 \log T - 0.64848\times10^{-4}T + 0.11589\times10^{-7}T^2 - 0.9646 \qquad (1.72)$$

where $S_{c\ell}$ is the entropy in Btu/lb°F and T is the temperature in °R for $492°\text{R} \le T \le 2110°\text{R}$, which is between 32 and 1650°F.

Equations 1.69 to 1.72 are being used in the computer subroutines of Appendices A and B.

There are only very few measured data for the enthalpy of NaK. For NaK 78, Douglas, Ball and Ginnings [260] give the following equation for the liquid NaK 78.26 enthalpy:

$$H_\ell - H_{0\ell} = 0.93860t - 1.09621\times10^{-4}t^2 + 7.0555\times10^{-8}t^3 + 0.05636t\times e^{-0.004055t} \qquad (1.73)$$

where H_ℓ is in joules/g and t is in °C for $0°\text{C} < t < 800°\text{C}$. The measured data fitted this curve within less than 0.1% and have been considered correct within 0.3% by Douglas, Ball and Ginnings [260].

No equation was found for the entropy of liquid Nak 78. It appears that our knowledge of the thermodynamic properties of liquid NaK alloys is by no means wholly satisfactory at present [89]. There is also very little information available on the enthalpy and entropy of mixing for the NaK alloys. Fig. 1.23 (taken from Refs. 89 and 263) shows the molar enthalpies of mixing ΔH^M as a function of the atomic fraction of sodium in the NaK alloy. This curve has been supported by recent theory [57].

For free energies and entropies of mixing, the only estimates that have been made [263] do not seem to be very accurate.

Cafasso *et al.* [89] have recently attempted by atomic absorption spectroscopy to determine the excess Gibbs energies of mixing, ΔG^{xs}, of NaK (Fig. 1.23). They combined their values with values for the enthalpy of mixing, ΔH^M, to obtain entropies of mixing, ΔS^{xs}. The difference between the two curves in Fig. 1.23 yields the value $T\Delta S^{xs}$, which is also shown in the figure. It shows that, in the range $X_{\text{Na}} \le 0.5$ it becomes clearly negative, which is surprising. Additional research work is apparently needed in this area.

So far, little reliable information has been found on the thermodynamics of NaK in the vapor phase. From a viewpoint of practical applications, this appears to be rather insignificant

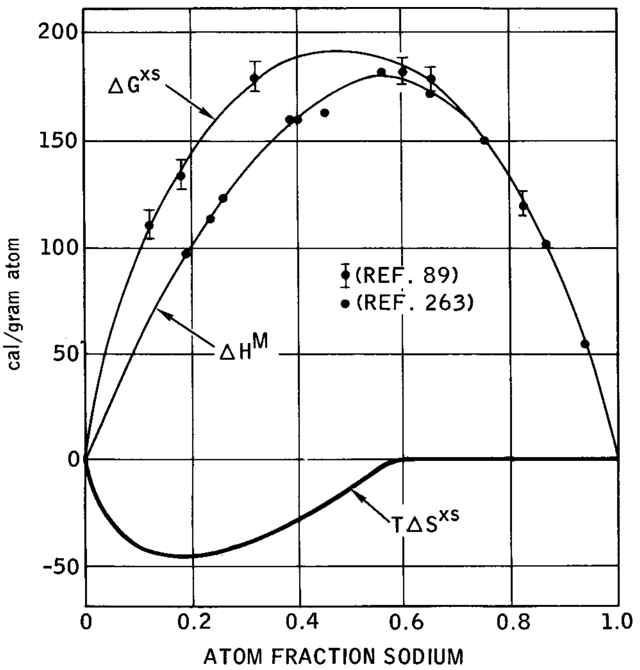

Fig. 1.23 Excess thermodynamic functions for the sodium-potassium system at 111°C.

since much of the advantage for the use of NaK is lost at high temperatures anyhow. In a first approximation, of course, NaK vapor can be treated as a mixture of two ideal gases (sodium vapor and potassium vapor) by applying Dalton's law and Raoult's law. Data on vapor pressure of NaK are therefore usually sufficiently accurate (see section on NaK vapor pressure (next section)). However, other thermodynamic data are less reliable [82].

(d) *Thermodynamic Properties of the Vapor Phase*

(1) *Saturation Vapor Pressure.* Sodium. Numerous pressure-temperature measurements of the saturated vapor of sodium have been made by several different methods [264]. Recently Golden and Tokar [19] made a critical analysis of the various measurements [Refs. 195, 196, 198, and 265-268] and equations [Refs. 4, 5, 18, 25, 265, 269 and 270] derived from "pooled" measurements and concluded that below ∿ 1250°K the most accurate is the equation of Ditchburn and Gilmour (Eq. 1.74) [269]. This equation (using common logarithms), derived from the work of eleven investigators, gives a normal boiling point of 1153.9°K (880.7°C, 1617°F):

$$\log p_s \text{ (atm)} = 6.354 - \frac{5567}{T} - 0.5 \log T \quad (T \text{ in °K valid up to } 1150\text{°K}) \qquad (1.74)$$

For higher temperatures, they prefer the equation of Stone *et al.* (Eq. 1.75) [25] which gives a normal boiling point of 1154.6°K (881.4°C, 1619°F):

$$\log p_s \text{ (atm)} = 6.6808 - \frac{5544.41}{T} - 0.16344 \log T \quad (T \text{ in °K valid above } 1150\text{°K}) \qquad (1.75)$$

Fig. 1.24 is a semilog plot of p_s vs. $1/T$, which shows that the relation can be delineated almost by a straight line. This means that the sodium vapor in this temperature range obeys the Clausius-Clapeyron equation [271] quite closely. However, Stone prefers the Kirchhoff type equation as exemplified by Eq. 1.75. The average deviation of his experimental data from Eq. 1.75 was determined as ±0.37%. A few singular data points obtained recently by Bohdansky and Schins [272] by a different method [273] tend to support Stone's data closely. Fig. 1.25 and Appendix D give values of pressure in atmospheres computed from Eqs. 1.74 and 1.75.

Potassium. Recently Coe [24] and Heimel [22] critically reviewed the numerous measurements of the saturation vapor pressures for potassium [Refs. 23, 26, 28, 31, 204, 270, 274 and 275]. They were found to be in fairly good agreement;* Heimel therefore proposed a

---

*Experimental data obtained recently by Rigney *et al.* [277] (but not considered by Coe or Heimel) also show the same type of good agreement in contrast to data reported in Ref. 278, which differ by about 20%.

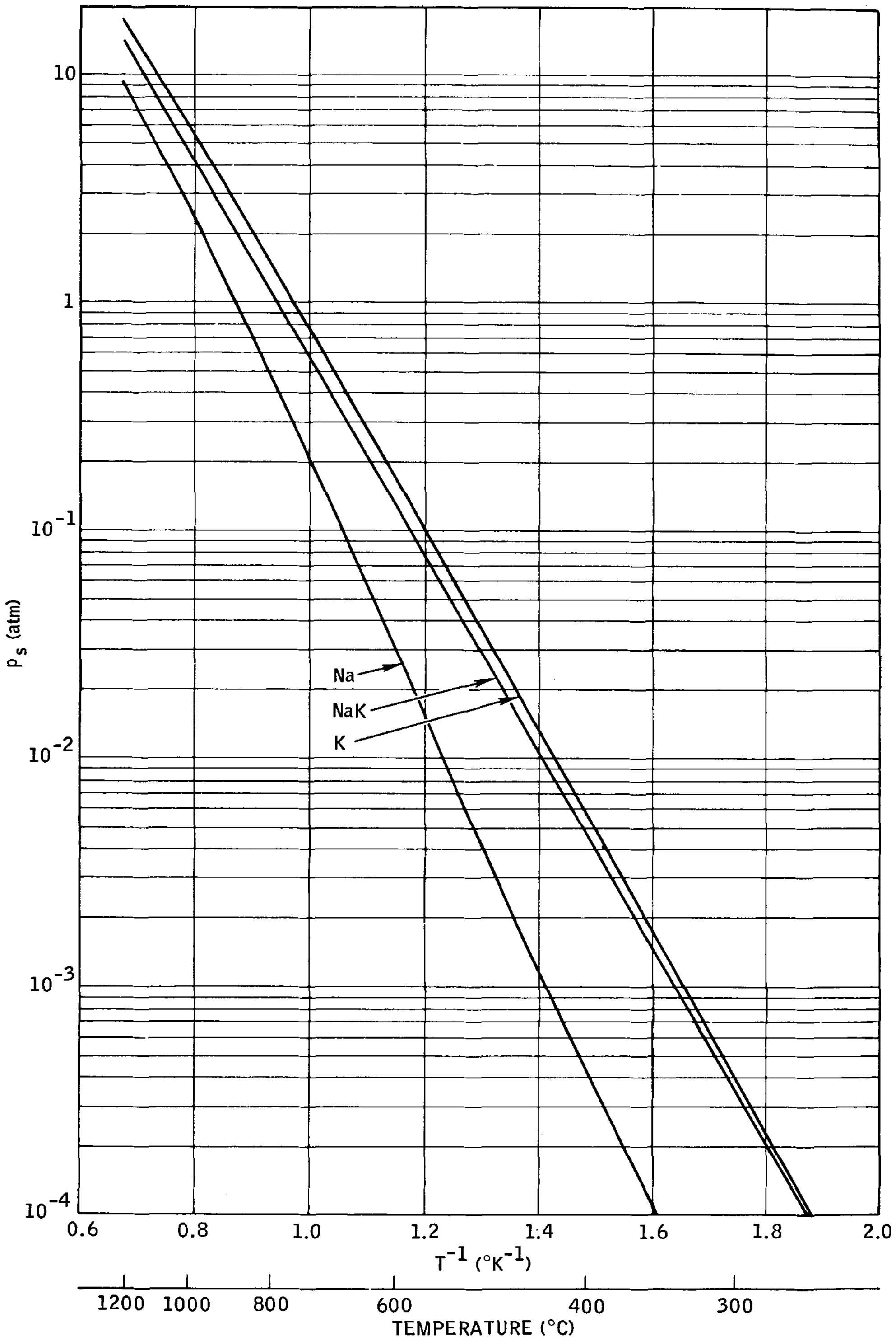

Fig. 1.24 Saturation pressure (p_s) of sodium, potassium, and NaK-78 as function of inverse absolute temperature.

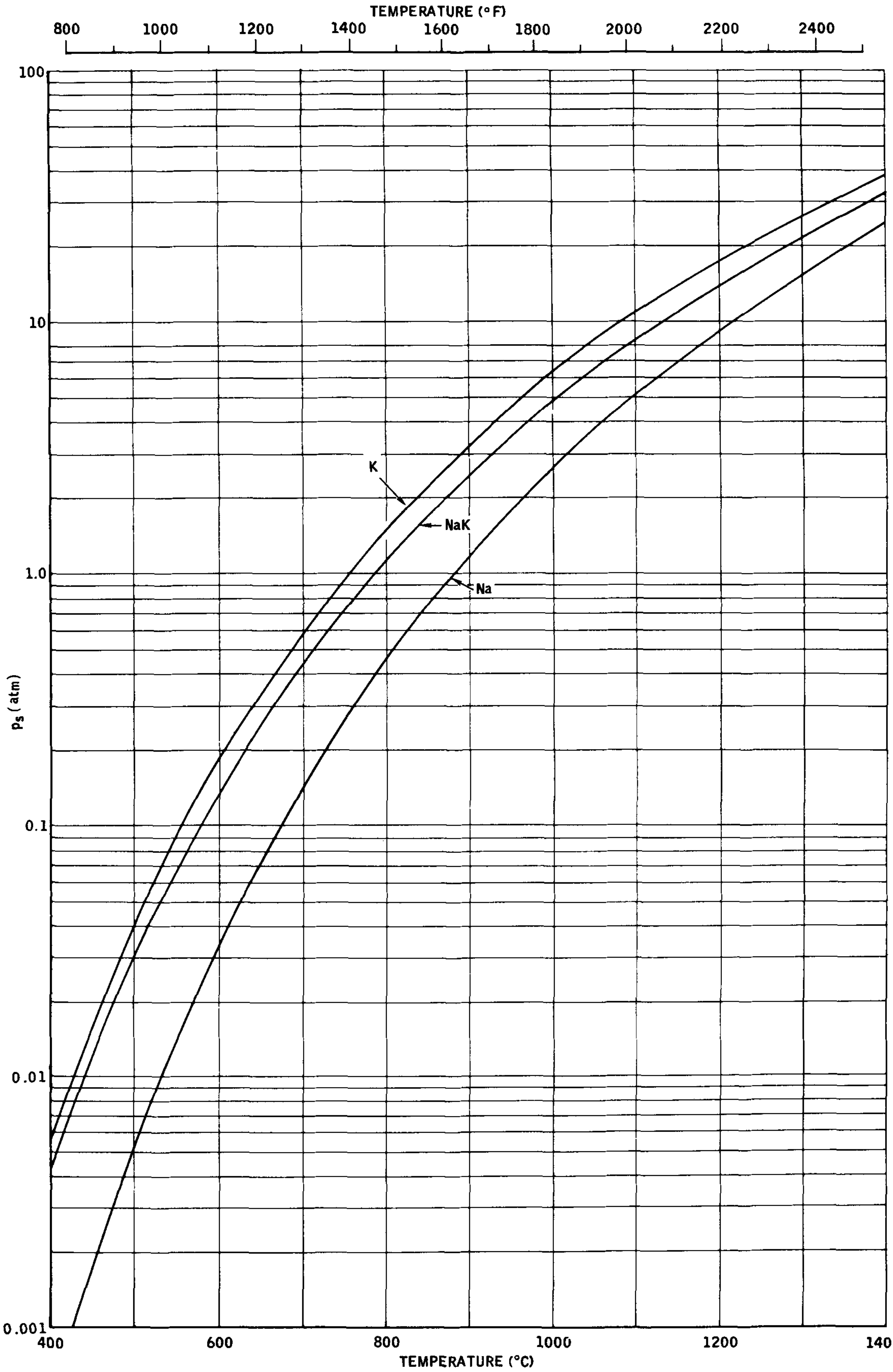

Fig. 1.25 Saturation vapor pressure (p_s) for sodium, potassium, and NaK-78.

single equation representing the pooled data within a standard deviation of 1.43%. With p_0 being the standard pressure of 1 atm and T being the absolute temperature (°K), his equation is

$$\log\left(\frac{p}{p_0}\right) = -\frac{4625.3}{T} + 6.59817 - 0.700643 \log T \qquad (1.76)$$

According to this equation the normal boiling point of potassium should be at 757.7°C, which is within the claimed accuracy limits. Very recently Bowles [276] measured the vapor pressure of potassium from 945 to 2170°K. His data show only a very small deviation (<1%) from Heimel's equation (Eq. 1.76); this adds additional weight for recommending it here. Only at low temperatures (<700°K) do significant discrepancies show up among the various sources. The numerical values of the potassium saturation vapor pressures are presented in Fig. 1.25 and Appendix 1-D.

Recent vapor-pressure measurements for low temperatures and very low pressures are very scarce. Only Buck and Pauly [274] report experimental data for sodium and potassium vapor in the region from 5×10^{-3} to 10^{-6} torr at temperatures between the normal melting point and about 190°C. Their results can be represented in this regime by the following equations:

$$\text{Na:}\quad \log p = 8.08 - \frac{5479}{T} \qquad (1.77)$$

$$\text{K}:\quad \log p = 7.56 - \frac{4587}{T} \qquad (1.78)$$

where p is in torr and T is in °K. The Ditchburn and Gilmore equation (Eq. 1.74) for sodium gives values that are about twice as high at 10^{-4} torr. Therefore some caution is advised in using Eq. 1.74 at these low pressures. For potassium, Eq. 1.76 is in good agreement with the data of Ref. 274 (at 10^{-4} torr within about 1%).

Eutectic NaK. Weatherford, Tyler and Ku [5] calculated the vapor pressure of NaK 77.7 in the temperature range of 722 to 1478°K, assuming the validity of Raoult's law, which is expressed by

$$p_{\text{NaK}} = N_{\text{Na}}p_{\text{Na}} + N_{\text{K}}p_{\text{K}} \qquad (1.79)$$

The results, shown in Fig. 1.25, are represented approximately by

$$\log p = 4.114 - \frac{4367}{T} \qquad (1.80)$$

where p is in atm and T is in °K.

The validity of Raoult's law for NaK between 942 and 1330°K has been verified experimentally to about 2% by Tepper *et al.* [75] and between 882 and 1212°K by Bonilla *et al.* [197]. (At lower temperatures, the validity of Eq. 1.80 should be regarded with some caution, considering the slightly strange appearance of the NaK curve in the lower right corner of Fig. 1.24.) Khanna [82] reports that the NaK system does, to a small degree, deviate positively from Raoult's law. The degree of deviation from ideality (case for which Raoult's law is applicable) generally depends on temperature and can be quantitatively expressed by the "activity coefficient" [271]. Khanna [82] has experimentally determined this coefficient for sodium and potassium in the NaK system at various temperatures.

(2) *Constitution of the Vapor and Dissociation Equilibrium.* At temperatures up to about 300°C, the saturated sodium (and potassium) vapors consist, for all practical purposes, of atoms only. At higher temperatures, dimerization is being observed, which increases with increasing temperature. For example, at the normal boiling point, about 16% of the vapor particles are Na_2 molecules. Specifically, the weight fraction X_2 of the Na_2 molecules present in sodium vapor depends on the equilibrium constant $k_2 = p_2/p_1^2$, where

p_2 is the partial pressure of the dimeric Na_2 species and p_1 is the partial pressure of the monomeric Na species in the reaction $Na_2 \rightleftarrows 2Na$. If p is the total pressure and if N_1 and N_2 are the mole fractions of Na and Na_2, respectively, the equilibrium constant k_2 also can be expressed in the following forms:

$$k_2 = \frac{p_2}{p_1^2} = \frac{N_2 p}{(N_1 p)^2} = \frac{N_2}{N_1^2 p} = \frac{N_2}{(1-N_2)^2 p} \tag{1.81}$$

For a tetramer equilibrium $Na_4 \rightleftarrows 4Na$, a corresponding equilibrium constant $k_4 = p_4/p_1^4$ can be defined. According to Stone [25], there has been no evidence so far for the existence of a trimer. The exact numerical value of k_2 (and similarly of k_4) can be determined from the total vapor pressure-temperature relation (see Sec.1-5.8(d)), the difference in the free-energy functions $(F^0 - H_0^0)$ for vaporization and dimerization, and the dimerization energy D_0^0 at 0°K. The corresponding equation is [19]

$$F_2^0 = -RT\,\ell n\, k_2 = (F^0-H_0^0)_2 - 2(F^0-H_0^0)_1 + D_0^0 \tag{1.82}$$

The thermodynamic properties of the ideal gaseous Na and Na_2 species are determined primarily by spectroscopic techniques [4, 279]. Although the values for the free-energy functions reported in the literature are in excellent agreement, the many reported values for D_0^0 agree only moderately well [280].

The effect of this disagreement is shown in Table 1.16 [280], which depicts the Na_2 fraction of sodium vapor at three different temperatures resulting from three different dimerization energies D_0^0. Although the increase in D_0^0 is only about 10%, the resulting Na_2 fractions for 800°K differ by almost 100%. Similarly, strong deviations result from inaccurate vapor-pressure measurements. Therefore the thermodynamic functions should be selected at least in such a way that the resulting properties are self-consistent. This is quite difficult, and perfect solution is not quite assured at this time. Golden and Tokar [19] have reviewed and discussed the various approaches in great detail. Since a similarly thorough discussion is beyond the scope of this handbook, only the more important results are reported here.

The recommended value of D_0^0 for sodium is 8420 cal per mole of Na. This value is in very close agreement with the values cited in Refs. 19, 25, 262 and 279.* The recommended value of D_0^0 for potassium is 5925 cal per mole of K, which has been favored by several investigators [20, 22, 279]; Ewing [26] recommends 6200 cal per mole of K.

(3) *Equations of State of the Real Vapor.*

The vapor-pressure equations of Sec. 1-5.8(d) are for saturation conditions only. In this case, which is of high practical importance for two-phase flows, the saturation pressure is a sole function of the temperature. For supersaturated conditions of alkali vapors (i.e., cases in which the vapor is no longer in thermodynamic equilibrium with the corresponding liquid phase), a more general equation must be used, namely, the "equation of state" for the vapor phase. Two versions of such an equation have been proposed for the alkali vapors: the "virial" type and the "quasi-chemical" type.

Virial equations. Pressure-volume-temperature measurements for sodium vapor were recently reported by Stone *et al.* [25] for the range 1750 to 2590°F. They could be fitted within ±0.26% by an equation of state of the following

---

*Frequently D_0^0 is also quoted in the literature in calories per mole of Na_2. These values are, of course, twice as high as those quoted here.

TABLE 1.16 - Dimer Fraction as Function of D_0^0

Temperature, °K	Mole fraction of Na_2		
	For D_0^0 = 8420 cal/mole of Na	For D_0^0 = 8765 cal/mole of Na	For D_0^0 = 9100 cal/mole of Na
800	3.9	5.8	7.6
1200	11.8	14.7	17.9
1600	18.5	21.4	24.4

virial form:

$$\frac{pV}{RT} = 1 + \frac{B}{V} + \frac{C}{V^2} + \frac{D}{V^3} \qquad (1.83)$$

where

B (ft^3/mole) = $-4.447 \times 10^{-5}\, T \exp(15554/T)$
C (ft^6/mole^2)= $0.2434 \exp(24958/T)$
D (ft^9/mole^3)= $-0.8119 \exp(31175/T)$

where T is measured in °R and V in ft^3/lb mole of the monomer. Or

B (cm^3/gram atom) = $-\ 0.1282 \times 10^{-5}\, T \exp(8641/T)$
C (cm^6/gram atom^2)= $0.3899 \times 10^{-2} \exp(13865/T)$
D (cm^9/gram atom^3)= $-\ 0.01301 \exp(17319/T)$

where T is measured in °K and V in cm^3/gram atom of the monomer.

The dimensions of p and R must be selected in such a way that the dimensions of pV are equal to those of RT.

Extensive PVT measurements for potassium vapor were reported by Ewing *et al.* [26] for the temperature range 1400 to 2525°F. Their data could be fitted (within ±0.26%) by an equation of state of the same form as the preceding. For potassium vapor the coefficients were:

B (ft^3/mole) = $-\ 1.322 \times 10^{-4}\, T \exp(12613/T)$
C (ft^6/mole^2)= $3.866 \exp(14703/T)$
D (ft^9/mole^3)= $-\ 28.81 \exp(18107/T)$

where T was measured in °R and V in ft^3/lb mole of the monomer. Or
Or

B (cm^3/gram atom) = $-0.3812 \times 10^{-5} T \exp(7007/T)$
C (cm^6/gram atom^2)= $6.193 \times 10^{-2} \exp(8168/T)$
D (cm^9/gram atom^3)= $-\ 0.4615 \times \exp(10059/T)$

where T is measured in °K and V in cm^3/gram atom of the monomer.

PVT measurements on potassium vapor from 1150 to 1479°K have recently been performed by Achener, Miller and Fisher [120]. Their data are in general agreement with those reported previously [Refs. 5, 26, 31 and 75], although for certain isolated conditions the deviation in the derived enthalpy and entropy values may become as large as 50%. Therefore the data of Achener, Miller and Fisher are not recommended.

Quasi-chemical equations. Stone *et al.* [25] and Ewing *et al.* [26] have also shown that their recent PVT measurements for sodium and potassium vapors can be satisfactorily interpreted by a "quasi-chemical" approach, assuming that sodium (or potassium) vapor is an ideal mixture of monomeric, dimeric, and tetrameric species. (However, since only the existence of the dimer among any potentially possible polymeric species has been verified by spectroscopic means, there still exists some possibility of different interpretations of their data.)

Their results can be fitted by the

following alternate equations of state (quasi-chemical type):

Sodium vapor:

$$\log k_2 = -4.3249 + \frac{7204.2}{T} \tag{1.84}$$

$$\log k_4 = -10.6798 + \frac{16325}{T} \tag{1.85}$$

$$pV = \frac{RT}{M_a} \tag{1.86}$$

Potassium vapor:

$$\log k_2 = -3.8611 + \frac{5312.5}{T} \tag{1.87}$$

$$\log k_4 = -10.1453 + \frac{13745}{T} \tag{1.88}$$

$$pV = \frac{RT}{M_a} \tag{1.89}$$

From the first two of the equations in each set, k_2 and k_4 can be determined as functions of temperature. The average molecular weight, M_a, can then be computed from the following three equations [26]:

$$k_2^1 = k_2 + 3k_4p^2 - 2k_2k_4p^3 \tag{1.90}$$

$$k_2^1 = \frac{N_2^1}{(N_1^1)^2 p} \quad (N_1^1 + N_2^1 = 1) \tag{1.91}$$

and

$$M_a = N_1^1 M_1 + N_2^1 (2M_1) \tag{1.92}$$

M_1 is the molecular weight of the monomer, and k_2^1 is an "apparent" equilibrium constant of dimerization, assuming that all association is taken to be dimerization. In any analog way, N_1^1 and N_2^1 represent the apparent mole fractions of the monomer and dimer in such a hypothetical case.

After M_a has been determined, the third equation in each set (Eq. 1.86 or 1.89) can be used to compute the specific volume V.

The true mole fractions N_2 and N_4 of the dimer and tetramer can then be computed by the following equations [26]:

$$N_2 = \alpha_1^2 p \left(\frac{M_a}{M_1}\right)^2 k_2 \tag{1.93}$$

and

$$N_4 = \alpha_1^4 p^3 \left(\frac{M_a}{M_1}\right)^4 k_4 \tag{1.94}$$

where

$$\alpha_1 = \frac{3M_1}{4M_a k_2 p} \left\{ \left[1 + \frac{8k_2 p}{9} \left(4 - \frac{M_a}{M_1} \right) \right]^{\frac{1}{2}} - 1 \right\} \tag{1.95}$$

(α_1 is the unassociated fraction of one initial mole of monomer.)

$$M_a = M_1(N_1 + 2N_2 + 4N_4) \tag{1.96}$$

$$N_1 + N_2 + N_4 = 1 \tag{1.97}$$

The following equations can be used to convert the mole fractions N to weight fractions X:

$$X_1 = \frac{N_1}{N_1 + 2N_2 + 4N_4} \tag{1.98}$$

$$X_2 = \frac{2N_2}{N_1 + 2N_2 + 4N_4} \tag{1.99}$$

and

$$X_4 = \frac{4N_4}{N_1 + 2N_2 + 4N_4} \tag{1.100}$$

Analog to Eq. 1.97, it can be observed that $X_1 + X_2 + X_4 = 1$.

The PVT data for saturated and superheated sodium and potassium vapor are shown graphically in Figs. 1.26 and 1.27; they are presented in numerical form in Appendix D.

(4) *Specific Heat of Sodium and Potassium Vapor.* No experimental data on the specific heat of alkali vapors have been found in the literature, and it is very likely that none exist.

There have been several attempts, however, to calculate the vapor specific heat. Coe [24] discusses various approaches [Refs. 5, 18, 26, 78 and 281] for potassium and shows that the results are quite different, up to several hundred percent at the higher temperatures around 1000°C. The lowest

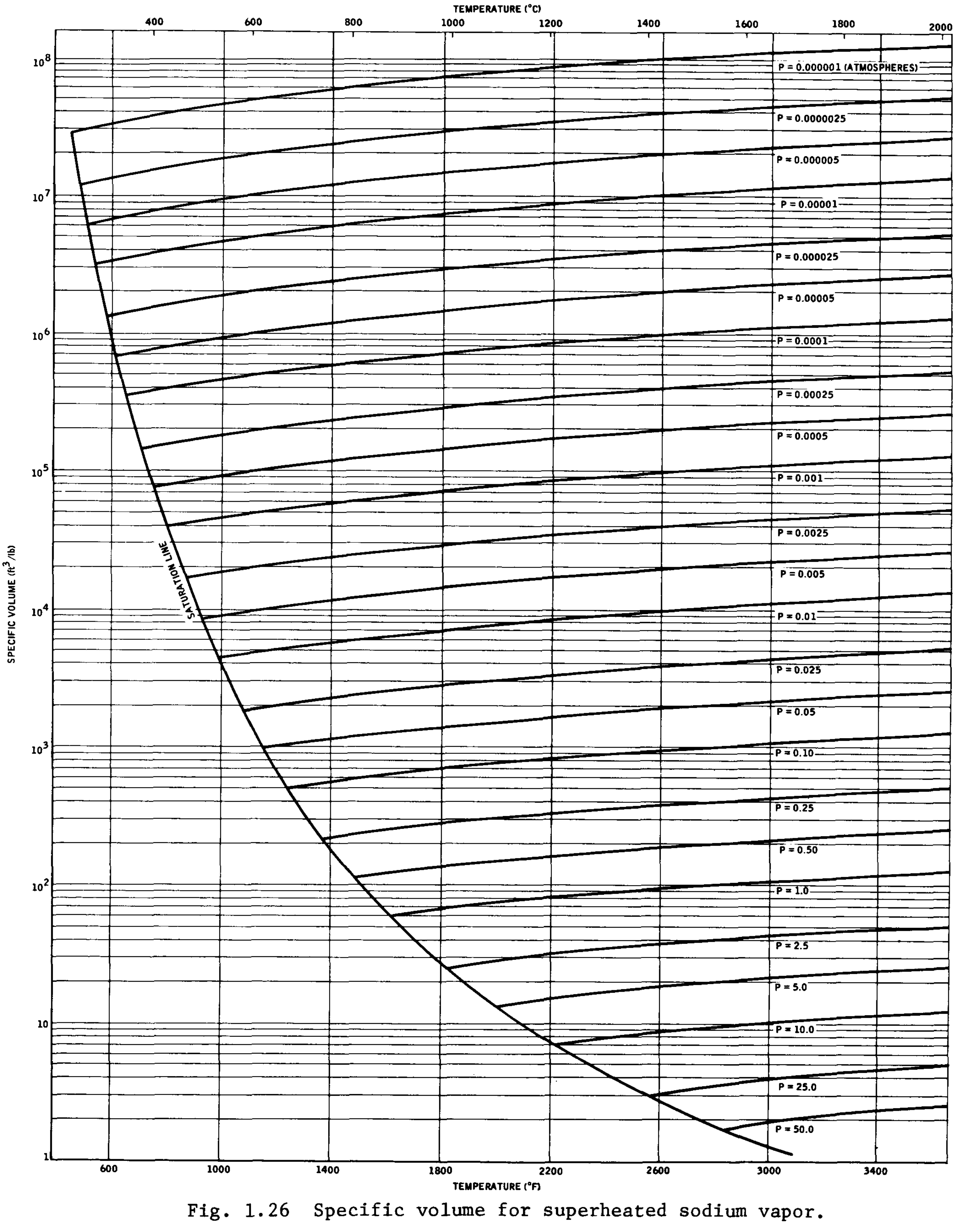

Fig. 1.26 Specific volume for superheated sodium vapor.

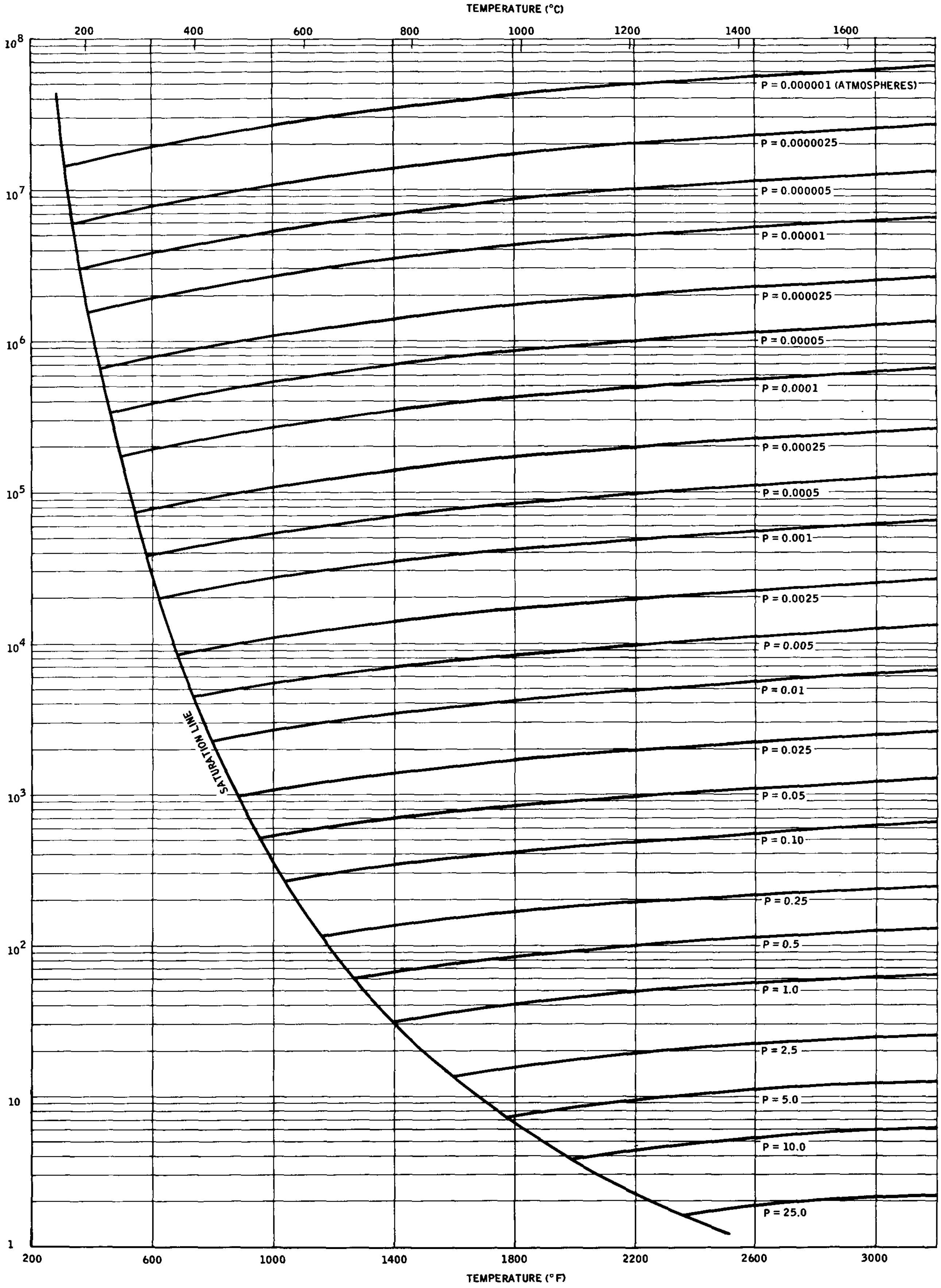

Fig. 1.27 Specific volume for superheated potassium vapor.

value is 4.9680 cal/mole-°C, which has been quoted by Evans *et al.* [20] and Weatherford, Tyler and Ku [5]. This is essentially a constant value (almost independent of temperature) and is practically the same for sodium and for potassium. It has been used by Golden and Tokar [19] in their computer programs for calculation of the vapor enthalpy of sodium. Therefore it is also the basis for the enthalpy values quoted in Appendix 1-D. Because an error in the specific heat value generates only a proportionally much smaller error in the total enthalpy values, it is very likely that the quoted enthalpies are nevertheless quite accurate.

Ewing *et al.* [26] and Stone *et al.* [25] determined the vapor specific heats of potassium and sodium by two different methods based partially on their PVT measurements. (Working equations for c_p of the monomeric sodium and potassium vapor were derived by Stone *et al.* [25] and Ewing *et al.* [26] from their own work and the earlier work of Evans *et al.* [20]. They are supposedly applicable from 0 to 3300°F and valid for monomeric gas at 1 atm:

Sodium vapor:

$$c_p \text{ (Btu/lb-°F)} = 0.21598 + 6.053\, e^{-37280/T} \quad (T \text{ in } °R) \tag{1.101}$$

Potassium vapor:

$$c_p \text{ (Btu/lb-°F)} = 0.12700 + 2.888\, e^{-28070/T} \quad (T \text{ in } °R) \tag{1.102}$$

Because their accuracy is doubtful, they should be used only with great caution.) Although the results from these two methods agree within about 6%, they are considerably higher than the value of Evans quoted previously (of the order of 12 cal/mole-°C). Their values are listed in numerical form in Appendix B of Refs. 25 and 26. Golden and Tokar [19] computed (with the aid of their NAPROP subroutine) the specific heat, c_p, of sodium vapor along the saturation curve by two different methods (virial and quasi-chemical approach) and developed two curves with a root-mean-square deviation of 6.2%. Heimel [22] recently computed c_p for potassium vapor using the theoretical "hard-sphere model." His values essentially rise from 5 cal/mole-°C at 150°C (∿ value of Evans) to 12 cal/mole-°C at 1000°C (∿ value of Ewing *et al.*). The values shown in Fig. 1.28 should therefore be considered as tentative values for the present. They were computed with the aid of the NAPROP subroutine of Ref. 19 and were taken from Appendix D of the same reference.

No data on c_v or $\gamma = c_p/c_v$ for sodium or potassium vapor have been found in the literature. In the first approximation, it can be assumed that $c_v = c_p - R$ (R being the gas constant).

(5) *Heat of Vaporization.* The vapor-pressure relations can theoretically be used to obtain the heat of vaporization by applying the well-known Clausius Clapeyron equation [117]. If Eq. 1.75 (based on the experimental data of Stone *et al.* [25]) is used, the heat of vaporization, ΔH_v, for sodium can be expressed as follows:

$$\Delta H_v = p_s\left(\frac{22982}{T} - 0.61344\right)(v_s^g - v_s^l) \tag{1.103}$$

v_s^g and v_s^l are the specific volumes of the gaseous and liquid phases, respectively. v_s^l (which is the inverse of the liquid density ρ) can be obtained from Eq. 1.3, and v_s^g can be obtained from the virial equation of state (Eq. 1.83). The corresponding equation for potassium, as taken from Ref.26, is:

$$\Delta H_v = jp_s\left(\frac{18717}{T} - 0.53299\right)(v_s^g - v_s^l) \tag{1.104}$$

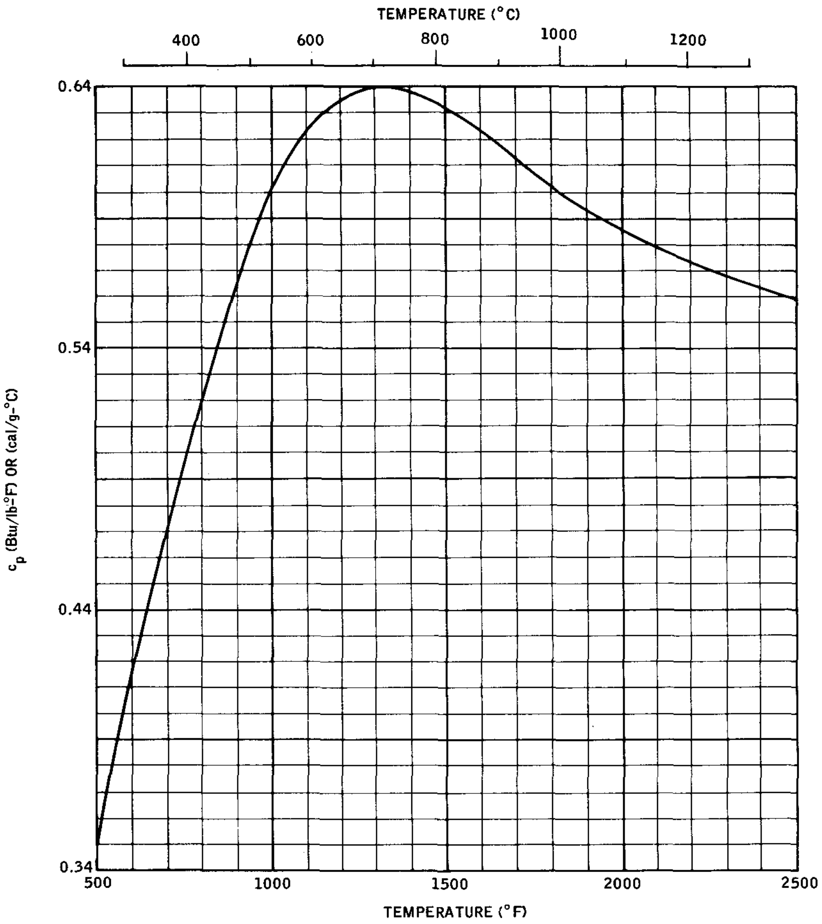

Fig. 1.28 Specific heat (c_p) of sodium vapor.

These equations are of limited practical usefulness, however.

Golden and Tokar [19] used the quasi-chemical approach to arrive at an equation for the heat vaporization of sodium. They used their equation in their NAPROP subroutine, which is reproduced in Appendix 1-A. The heat of vaporization, termed DHV in the computer language of Appendixes 1-A and 1-B, can easily be extracted by a suitable program. Corresponding comments apply for potassium.

The entropy change ΔS_v for vaporization at each saturation point can be obtained by dividing the appropriate enthalpy change ΔH_v by the absolute temperature ($\Delta S_v = \Delta H_v / T$), which has general validity.

(6) *Enthalpy and Entropy of the Real Vapor.* The final goal for these thermodynamic considerations is the determination of the enthalpy and the entropy of the real sodium and potassium vapor. Since there are no ways to measure them directly, they must be derived from equations that are based on other measured quantities.

Enthalpy. The enthalpy, H, per unit mass of saturated and superheated vapor can be determined with the equation

$$H^g = (H^g)^0 + \Delta H_2 X_2 + \Delta H_4 X_4 \qquad (1.105)$$

The term $(H^g)^0$ represents the absolute enthalpy of monomeric vapor at 1 atm (relative to a solid at 0°R), which, according to Ref. 25, is given for sodium by

$$(H^{g})^{0}\ (\text{Btu/lb}) = 2005.15 + 0.21598T + 12172e^{-43830/T} \quad (T \text{ in } ^{\circ}\text{R}) \qquad (1.106)$$

The last two terms in Eq. 1.105 represent the enthalpy changes contributed by each species of dimer and tetramer in moving from zero to some finite concentration, and it can be assumed [25] for the full temperature range that $\Delta H_2 = \Delta H_2^0/2M_1$ and $\Delta H_4 = \Delta H_4^0/4M_1$, where ΔH_2^0 and ΔH_4^0 are the enthalpy changes in sodium for the formation of one mole dimer and tetramer from the monomer, respectively.

$$\Delta H_2^0 = -\ 18.30 \text{ kcal/mole} = -\ 32948 \text{ Btu/lb mole}$$

$$\Delta H_4^0 = -\ 41.48 \text{ kcal/mole} = -\ 74661 \text{ Btu/lb mole}$$

The corresponding equation for potassium is

$$(H^{g})^{0}\ (\text{Btu/lb}) = 998.95 + 0.12700T + 24836e^{-39375/T} \quad (T \text{ in } ^{\circ}\text{R}) \qquad (1.107)$$

$$\Delta H_2^0 = -\ 13.50 \text{ kcal/mole} = -\ 24296 \text{ Btu/lb mole}$$

$$\Delta H_4^0 = -\ 34.92 \text{ kcal/mole} = -\ 62860 \text{ Btu/lb mole}$$

Entropy. The entropy of saturated and superheated alkali vapor along an isotherm can be computed by [25]

$$S^{g}_{i} = (S^{g})^{0} + \frac{\Delta H_2 X_2}{T} + \frac{\Delta H_4 X_4}{T} - \frac{R \ln p}{M_a} + \frac{X_2 R \ln k_2}{2M_1} + \frac{X_4 R \ln k_4}{4M_1} - \frac{R(N_1 \ln N_1 + N_2 \ln N_2 + N_4 \ln N_4)}{M_a} \qquad (1.108)$$

where the first term, $(S^{g})^{0}$, constitutes the entropy of monomeric vapor at 1 atm (relative to the solid at 0°R), which for sodium is given by [25]

$$(S^{g})^{0}\ (\text{Btu/lb-}^{\circ}\text{F}) = 0.23859 + 0.21598 \ln T \quad (T \text{ in } ^{\circ}\text{R}) \qquad (1.109)$$

The corresponding equation for the entropy of monomeric potassium vapor is [26]

$$(S^{g})^{0}\ (\text{Btu/lb-}^{\circ}\text{F}) = 0.18075 + 0.12700 \ln T + 0.7617e^{-31126/T} \quad (T \text{ in } ^{\circ}\text{R}) \qquad (1.110)$$

The computer subroutines listed in Appendixes 1-A and 1-B solve the preceding enthalpy and entropy equations (Eqs. 1.105 and 1.108) for sodium and potassium for any given pressure and temperature combination.

Numerical values for entropy and enthalpy are presented in the familiar form of a Mollier diagram in Figs. 1.29 and 1.30 and in Appendix 1-D. Furthermore, the computer program (as originally written by Golden and Tokar [19]) allows computation of these and other thermodynamic properties (such as specific volume, mean molecular weight, and composition) of sodium and potassium vapor in the range 500 to 2500°F for given pressures and temperatures.

(e) *Thermodynamic Properties of Sodium and Potassium Vapors at Very High Temperatures*

The thermodynamic properties of sodium and potassium vapors up to approximately 1400°C (∿2500°F), as based primarily on the work of Refs. 19, 26, etc., have been discussed previously. For vapors of even higher temperatures, the preceding procedures are no longer applicable since the alkali metals become ionized quite rapidly about 3000°F. Because of the relativity low ionization potential, nearly full ionozation is obtained for low pressures already at about 6000°K (∿11000°F).

So far practically no measurements of alkali-vapor properties have been reported for temperatures above approxi-

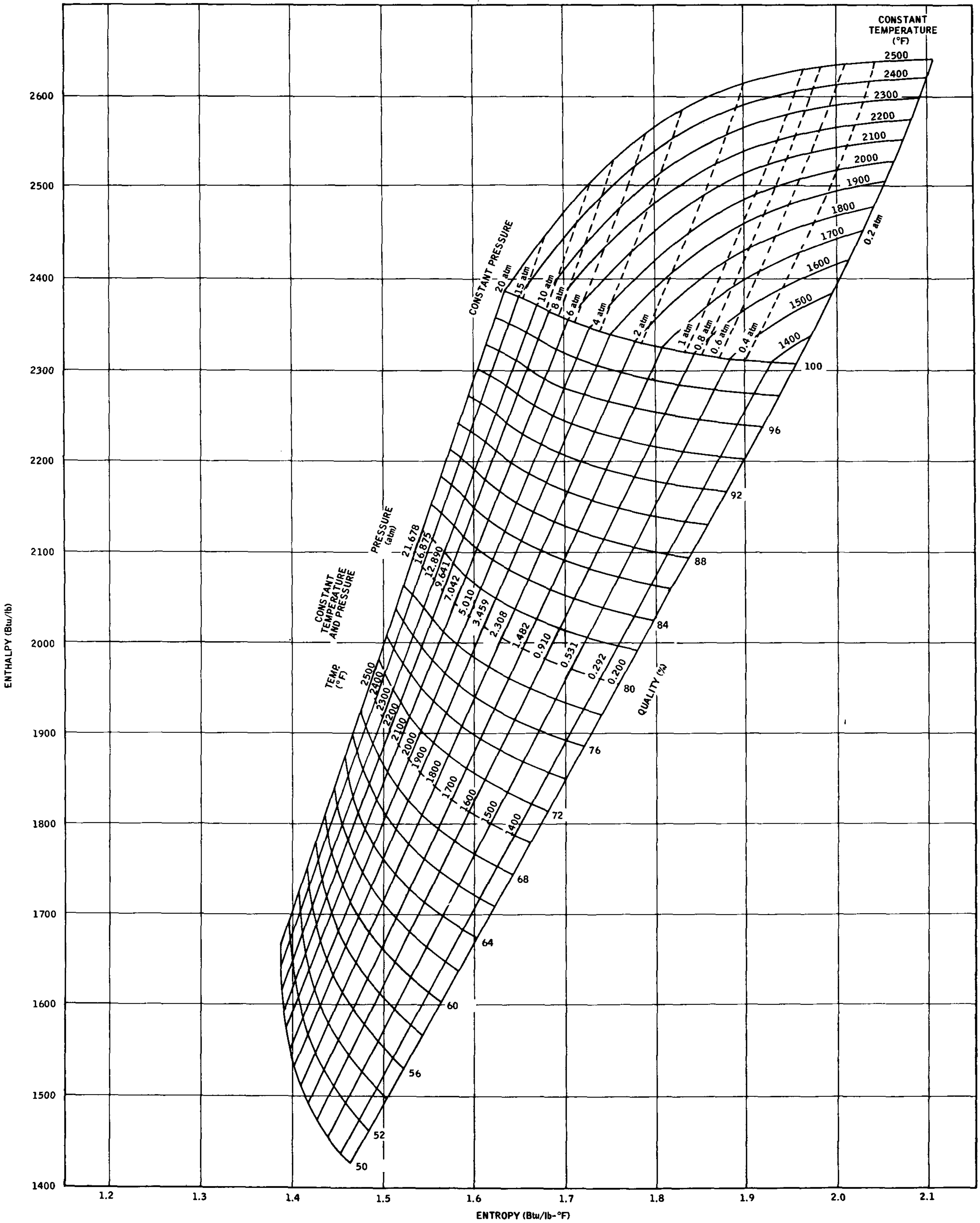

Fig. 1.29 Mollier diagram for sodium.

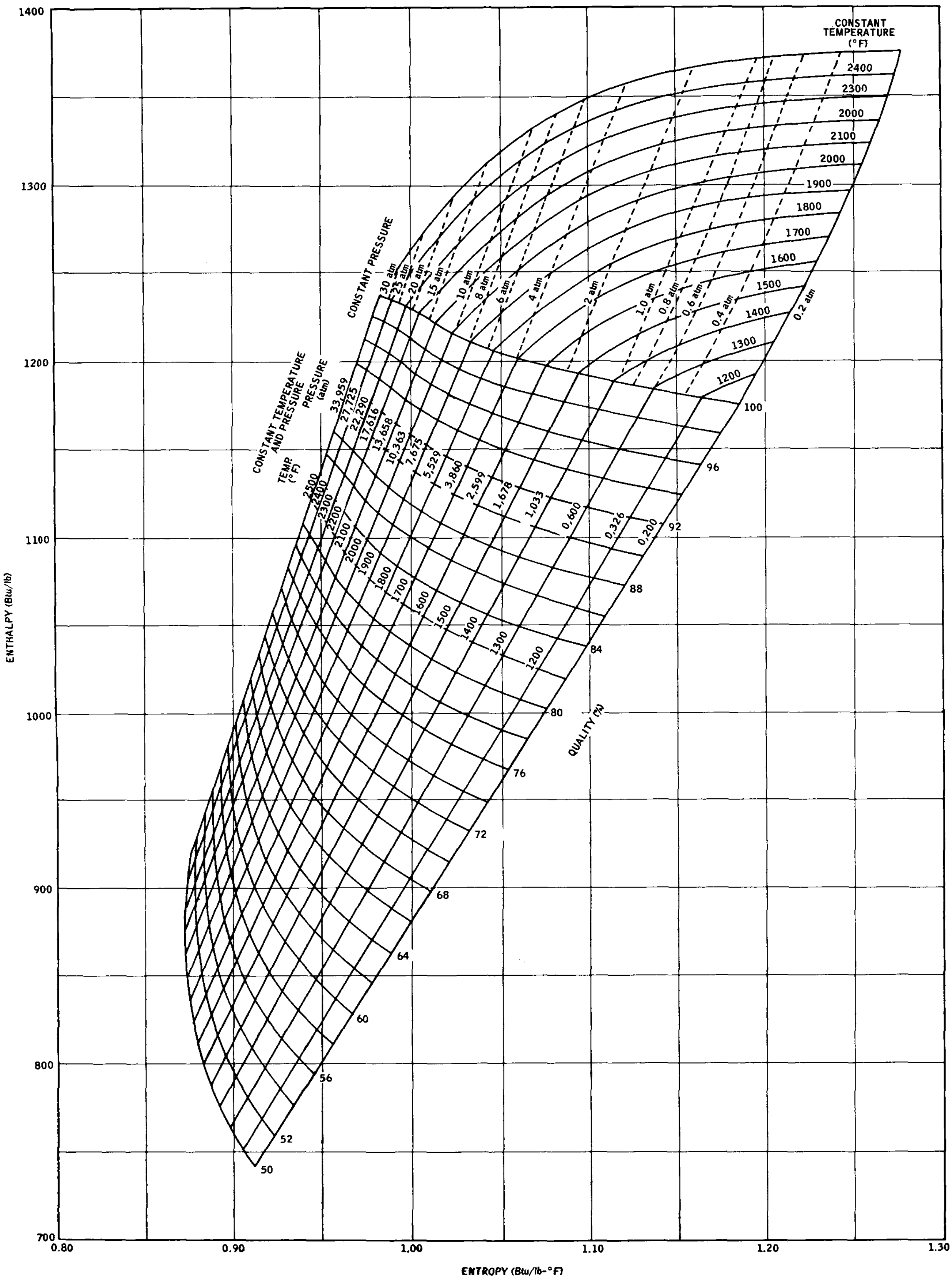

Fig. 1.30 Mollier diagram for potassium.

mately 1600°C (3000°F). This implies that no experimental data are available for either the critical or the supercritical state of sodium and potassium. The interesting subject of liquid-metals thermodynamics above the critical point has only very recently been touched upon experimentally with mercury [48]. However, several attempts have been made [112, 282-285] to compute the high-temperature properties of various alkali metals in thermodynamic equilibrium.

Milligan [282] has computed the enthalpy and entropy of ionized sodium and potassium vapor as functions of temperature and pressure. He has presented his results for 2000 to 25000°K in charts that resemble Mollier diagrams. His results differ slightly from those reported in Ref. 283, mainly because of the use of different reference energies.

Tables 1.17 and 1.18 (taken from Ref. 282) present enthalpy (H/RT_0), free energy ($-G/RT_0$), entropy (S/R), and heat capacity (C_p/R) as dimensionless quantities that can be converted to practical units by using suitable conversion factors from Sec. 1-3. The specific volume is given in units of cm^3/mole of un-ionized atoms.

The equilibrium composition for sodium vapor up to 10000°K has been reported in Ref. 283. Fig. 1.31, taken from this reference, shows the main results of the computation in graphical form.

Attempts have also been made to determine the transport properties of high-temperature alkali vapors [112], but only the interaction potential energies from which the transport coefficients can then be computed in a straightforward (though usually numerically tedious) manner have been determined. Since the referenced method ignores ionization and electronic excitation as well as dimerization, the results cannot be expected to be very accurate. The quoted uncertainty of ±25% is probably still optimistic.

Rynn [287] has theoretically determined the electron transport properties for fully ionized potassium plasma. His experimental data agree within 30% with his theoretical data in the temperature range from about 2400 to 3000°K. The electrical resistivity of dilute sodium and potassium plasmas is discussed briefly in Sec. 1-6.1(c).

(f) *Tables of Thermodynamic Properties*

A FORTRAN subroutine written by Golden and Tokar [19] for convenient computation of thermodynamic properties of sodium is reproduced as Appendix 1-A. This routine is based on the quasi-chemical approach. The latest experimental PVT data as reported by Stone *et al.* [25] and some previous work reported in Refs. 20, 191 and 269 were used. For given temperature and pressure, the routine calculates thermodynamic properties in any one of the following three regimes: subcooled liquid, saturated liquid and vapor, or superheated vapor.

Appendix 1-B is an exactly equivalent subroutine for computation of potassium thermodynamic properties. The coefficients in this routine are based mainly on the latest NRL experimental measurements as reported in Refs. 26 - 29. Critical reviews in the course of the preparation of this handbook, as well as by others [22, 24, 227], have considered the NRL data the most reliable. Thus far, however, no self-consistency checks (such as those performed in Ref. 19 for sodium) have been undertaken for the potassium data resulting from this new code.

Appendix 1-C lists an additional subroutine that computes the more important general properties for sodium, potassium, and NaK-78 as functions of temperature. See Appendixes 1-A, 1-B, and 1-C for further details on the practical use of these codes.

Most of the thermodynamic data in the tables of this chapter were prepared by these subroutines, which were slightly modified for this purpose. (Incidentally, it should be noted here that the tables were produced by a simple Teletype station printer connected to a time-shared computer (type SDS 940) via regular telephone lines. By storing these codes in the computer memory, the practicing engineer can call for any property value for any desired temperature, and within seconds he has the desired value printed out for him.)

Appendix 1-D contains tables of the thermodynamic properties of saturated and supersaturated sodium and potassium vapor as functions of pressure and temperature. In each pressure group of these tables, the first line pertains to the saturated condition and the remainder lists the supersaturated values for increasing temperatures (at 50°C steps) up to a maximum temperature of 1500°C. The data tabulated for the vapor are the enthalpy *H* (in cal/g and Btu/lb), the entropy *S* (in cal/g-°C and Btu/lb-°F), and the specific volume *V* (in cm^3/g and (ft^3/lb), as well as the dimensionless data of the compressibility factors *ZH*, the average molecular weight *ABARH*, and the dimer and tetramer mole fractions $N_2 = X2H$ and $N_4 = X4H$.

Golden and Tokar [19] point out that the general approach on which their computer code is based must still be considered tentative, even though it is based directly on the best experimental data available. It should be noted that vapor transport properties are not included in the code since the theoretical and experimental prerequisites for their correct calculations are not sufficiently advanced to be comparable in accuracy with the other properties. Generally, it can be stated, however, that the data which result from this computer code are self-consistent within about 1% and are probably absolutely accurate within a few percent. (These

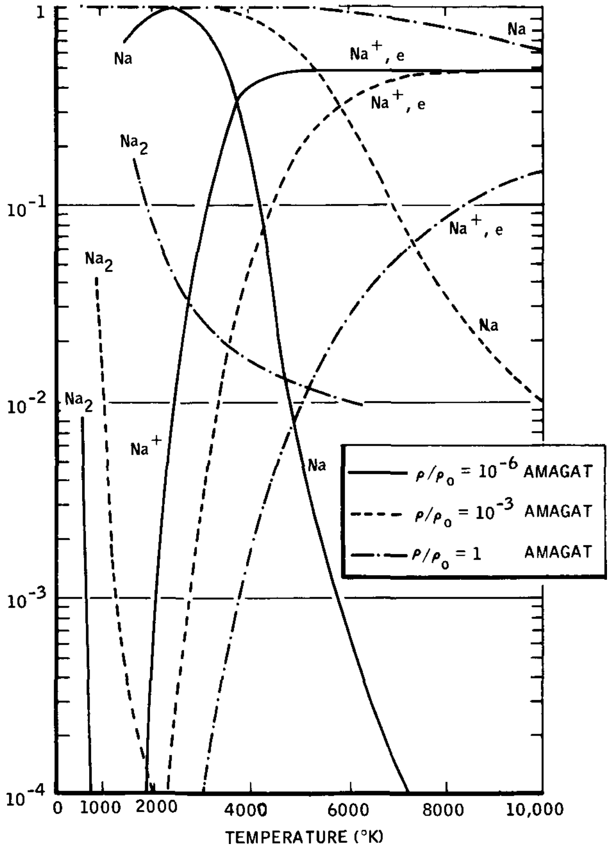

Fig. 1.31 Equilibrium compositions of sodium vapor at densities of 10^{-6}, 10^{-3}, and 1 amagat. (The amagat unit of density is the reciprocal of the amagat unit of volume, which is defined [286] for a real gas at the actual molar volume at 0°C and 1 atm pressure. It differs slightly from the molar volume of an ideal gas (22,414 cm^3/mole).)

(Text continues on page 76.)

TABLE 1.17 - Dimensionless Thermodynamic Properties

Pressure, atm*		Temperature, °K					
		2000	4000	6000	8000	10,000	12,000
100	$10^{-3}v$	1.271	3.137	4.925	6.939	9.669	13.14
	$-G/RT_0$	120.6	262.4	418.0	590.5	782.1	988.5
	H/RT_0	10.42	36.02	71.02	140.4	216.7	286.6
	S/R	17.90	20.38	22.26	24.95	27.28	29.03
	C_p/R	4.635	3.249	6.568	9.956	10.55	9.965
10	$10^{-3}v$	1.560	3.277	5.254	8.394	12.47	16.54
	$-G/RT_0$	135.3	295.6	470.5	670.8	900.2	1148
	H/RT_0	16.57	38.16	86.15	194.1	301.2	373.9
	S/R	20.75	22.79	25.34	29.53	32.82	34.64
	C_p/R	3.458	3.498	10.71	16.92	12.68	7.842
1	$10^{-3}v$	1.632	3.316	5.921	10.62	14.80	18.39
	$-G/RT_0$	151.8	329.4	527.8	770.3	1046	1554
	H/RT_0	18.11	40.40	126.2	285.4	369.0	416.9
	S/R	23.21	25.26	29.77	36.05	38.65	39.87
	C_p/R	2.630	4.771	20.75	17.43	8.107	6.097
0.1	$10^{-3}v$	1.640	3.393	7.481	12.27	15.74	19.09
	$-G/RT_0$	168.7	363.8	596.7	892.0	1208	1532
	H/RT_0	18.29	46.65	214.5	344.9	391.3	429.8
	S/R	25.53	28.03	36.93	42.23	43.68	44.65
	C_p/R	2.520	8.598	31.48	8.611	5.676	5.316
0.01	$10^{-3}v$	1.641	3.628	9.105	12.78	16.10	19.41
	$-G/RT_0$	185.5	399.7	684.2	1024	1374	1732
	H/RT_0	18.31	65.65	299.7	359.3	397.3	434.4
	S/R	27.84	31.78	44.79	47.22	48.39	49.32
	C_p/R	2.517	19.95	16.46	5.607	5.188	5.122
0.001	$10^{-3}v$	1.641	4.314	9.633	12.97	16.26	19.54
	$-G/RT_0$	202.4	440.1	782.3	1157	1542.2	1934
	H/RT_0	18.32	120.2	323.1	362.6	399.5	436.1
	S/R	30.14	38.26	50.33	51.90	53.03	53.94
	C_p/R	2.545	47.59	6.704	5.140	5.077	5.061
0.0001	$10^{-3}v$	1.642	5.626	9.756	13.07	16.36	11.66
	$-G/RT_0$	219.2	491.2	882.8	1292	1710	2135
	H/RT_0	18.37	222.9	326.8	363.9	400.8	437.5
	S/R	32.45	48.77	55.07	56.53	57.65	58.57
	C_p/R	2.637	55.16	5.236	5.043	5.023	5.015

*T_0 = 273.16°K;
R = 8.314 joules/mole-°K = 1.986 cal/mole-°K;
RT_0 = 2.271×10^6 joules/kg mole = 5.426×10^2cal/gram mole = 7.598 ft-lb/lb mole.

PHYSICAL PROPERTIES

of Sodium Vapor at High Temperatures [282]

Temperature, °K						
14,000	16,000	18,000	20,000	22,000	24,000	25,000
16.91	20.77	24.15	27.88	31.58	34.61	36.42
1206	1432	1669	1907	2150	2401	2526
349.0	405.3	453.1	500.3	545.6	583.0	604.4
30.34	31.37	32.20	32.88	33.47	33.96	34.20
8.987	8.086	7.171	6.755	6.444	6.161	6.081
20.16	23.84	27.16	30.71	33.93	37.42	38.86
1407	1672	1944	2220	2500	2783	2927
425.7	471.7	511.6	552.8	589.9	629.6	646.1
35.76	36.60	37.27	37.86	38.37	38.84	39.04
6.932	6.231	5.874	5.673	5.562	5.473	5.470
21.81	25.17	28.49	31.79	35.08	38.37	40.06
1630	1932	2238	2549	2863	3181	3340
457.4	495.8	533.4	470.6	507.6	644.6	663.9
40.73	41.44	42.06	42.60	43.09	43.54	43.75
5.595	5.413	5.325	5.273	5.244	5.267	5.334
22.40	25.73	29.01	32.29	35.60	38.88	40.58
1862	2198	2538	2883	3231	3582	3759
467.1	504.4	541.2	577.8	614.9	653.1	574.9
45.45	46.13	46.73	47.26	47.75	48.20	48.45
5.221	5.169	5.145	5.134	5.173	5.628	6.437
22.69	25.98	29.27	32.55	35.86	39.28	41.21
20.96	2466	2840	3218	3600	3986	4181
471.1	507.8	544.5	581.2	619.6	672.2	721.1
50.10	50.77	51.36	51.89	52.39	55.02	53.56
5.100	5.083	5.075	5.112	5.668	10.14	17.61
22.82	26.11	29.39	32.68	36.12	40.69	44.43
2332.2	2735	3143	3555	3971	4396	4618
472.8	509.4	546.1	583.8	637.1	817.0	1056
54.72	55.39	55.98	56.53	57.22	59.33	62.01
5.051	5.044	5.059	5.505	11.00	47.06	58.82
22.95	26.23	29.52	32.89	37.40	47.40	54.18
2567	3004	3446	3892	4347	4842	5120
474.2	510.9	547.9	595.5	781.0	1567	2113
59.34	60.01	60.61	61.29	63.67	72.94	79.04
5.010	5.012	5.214	9.653	54.41	151.4	137.4

TABLE 1.18 - Dimensionless Thermodynamic Properties

Pressure, atm*		Temperature, °K					
		2000	4000	6000	8000	10,000	12,000
100	$10^{-3}v$	1.371	3.133				
	$-G/RT_0$	125.5	274.6				
	$H\ RT_0$	14.38	38.87				
	S/R	19.11	21.41				
	C_p/R	3.493	4.074				
10	$10^{-3}v$	1.595	3.298	5.545	9.013	12.87	16.94
	$-G/RT_0$	141.0	307.8	494.8	712.9	956.6	1213
	H/RT_0	17.65	41.32	111.4	216.6	295.8	352.7
	S/R	21.67	23.89	27.60	31.74	34.21	35.63
	C_p/R	2.798	5.037	13.59	13.76	9.412	7.413
1	$10^{-3}v$	1.636	3.385	6.665	11.13	14.92	18.41
	$-G/RT_0$	157.7	342.2	557.9	820.9	1106	1401
	H/RT_0	18.25	47.58	167.4	287.0	344.3	386.9
	S/R	24.05	26.62	33.02	37.83	39.61	40.69
	C_p/R	2.564	8.034	22.10	10.80	6.685	5.810
0.1	$10^{-3}v$	1.641	3.602	8.398	12.38	15.74	19.08
	$-G/RT_0$	174.5	378.0	637.3	946.1	1268	1598
	H/RT_0	18.33	63.50	247.7	320.2	360.4	398.3
	S/R	26.34	30.15	40.29	43.24	44.49	45.45
	C_p/R	2.556	16.38	18.45	6.450	5.478	5.295
0.01	$10^{-3}v$	1.641	4.231	9.370	12.78	16.09	19.40
	$-G/RT_0$	191.4	417.9	731.6	1078	1435	799
	H/RT_0	18.37	108.2	285.9	328.5	365.8	402.8
	S/R	28.64	35.92	46.33	48.03	49.18	50.11
	C_p/R	2.613	36.03	7.957	5.343	5.179	5.129
0.001	$10^{-3}v$	1.642	5.484	9.656	12.96	16.25	19.53
	$-G/RT_0$	208.2	468.0	131.1	1212	1602	2000
	H/RT_0	18.47	194.7	293.8	331.1	367.9	404.6
	S/R	30.96	45.26	51.21	52.69	53.82	54.74
	C_p/R	2.801	43.77	5.471	5.124	5.085	5.073
0.0001	$10^{-3}v$	1.645	6.311	9.751	13.06	16.36	19.66
	$-G/RT_0$	225.1	230.1	931.7	1346	1770	2202
	H/RT_0	18.77	248.3	295.3	332.5	369.3	406.1
	S/R	33.31	53.16	55.87	57.33	58.45	59.37
	C_p/R	3.395	15.01	5.116	5.046	5.026	5.073

* T_0 = 273.16°K;
R = 8.314 joules/mole-°K = 1.986 cal/mole-°K;
RT_0 = 2.271 × 10^6 joules/kg mole = 5.426 × 10^2 cal/gram mole = 7.598 ft-lb/lb mole

of Potassium Vapor at High Temperatures [282]

Temperature, °K						
14,000	16,000	18,000	20,000	22,000	24,000	25,000
17.15	20.96	24.26	27.96	31.64	34.68	36.51
1275	1508	1752	1996	2245	2509	2630
331.8	382.9	426.7	472.3	517.2	556.4	581.1
31.36	32.29	33.06	33.71	34.30	34.81	35.09
8.087	9.512	6.852	6.596	6.517	5.841	7.392
2 .23	23.87	27.16	30.71	33.96	37.70	39.75
1479	1750	2028	2309	2596	2886	3033
398.1	441.9	480.8	522.3	563.5	623.3	668.0
36.63	37.43	38.08	38.67	39.23	39.94	40.44
6.462	6.044	5.829	5.869	5.798	10.53	14.56
21.80	25.15	28.48	31.84	35.57	40.84	44.52
1703	2010	2322	2639	2161	3293	3467
426.2	464.3	502.5	545.6	519.8	806.2	973.3
41.53	42.24	52.86	43.49	44.46	46.66	48.52
5.528	5.415	5.558	7.190	15.39	38.29	52.99
22.38	25.72	29.06	32.96	39.37	49.64	55.01
1934	2276	26.22	2975	3345	3755	3979
435.4	473.2	515.7	606.9	903.6	1471	1745
46.24	46.93	47.62	48.92	52.75	59.48	62.54
5.230	5.331	7.323	21.55	62.87	81.30	67.06
22.68	27.00	29.83	37.01	48.41	57.29	60.54
2169	2544	2926	3332	3795	4312	4508
439.6	479.7	571.1	962.7	1661	2065	2157
50.89	51.62	53.08	58.65	67.74	72.58	73.61
5.158	6.602	24.35	86.69	83.08	32.05	19.88
22.82	26.40	33.34	45.27	53.30	58.86	61.42
2404	2814	3248	3755	4324	4911	5208
442.1	511.3	917.2	1724	2075	2185	2220
55.53	56.78	63.21	74.84	79.45	80.77	80.77
5.563	19.22	102.5	84.09	23.45	10.47	8.873
23.01	28.54	40.74	48.71	54.06	59.05	61.52
2640	3094	3629	4243	4877	5517	5839
451.7	742.8	1670	2042	2138	2199	2227
60.32	65.50	86.40	88.84	87.10	87.82	83.14
10.00	95.35	100.5	20.76	9.261	7.810	7.645

accuracy limits must be kept in mind in using the tables of Appendix 1-D. Also, because of the accuracy limits, it is not necessary to print the Mollier charts at a larger scale.) Although Golden and Tokar [19] sometimes give five or even six significant figures in their tables, this should not be taken as an indication of absolute accuracy. For practical reasons (such as interpolations), however, it is usually desirable to have a larger number of significant figures available. That is also the reason why they are carried in the tables of this handbook.

For establishing more-precise thermodynamic data, more-accurate measurements on the specific heat of the liquid and vapor, the heat of vaporization, and the electrical conductivity of the vapor would be desirable [25, 26].

1-6 ELECTRICAL, NUCLEAR, AND MISCELLANEOUS PROPERTIES

1-6.1 *Electrical Resistivity*

(a) *Definitions*

Electrical resistivity* is the electrical resistance of a body of a given material with unit cross-sectional area and unit length. The most common unit for resistivity is the ohm-centimeter (Ωcm). The resistivity of good conductors (such as metals) is more conveniently expressed in a smaller unit, the microohm-centimeter (μΩcm), which is 10^{-6} of the standard unit. The inverse of the electrical resistivity is the electrical conductivity ($(\Omega\text{cm})^{-1}$ or mho/cm). The data reported in this section pertain to the resistivity at constant (atmospheric) pressure. The change in resistivity with temperature is caused by both the thermal-expansion effect and the change in resistivity with temperature at constant volume [288]. Since liquid alkali metals have unusually high compressibility and thermal expansion, the difference between the resistivity at constant pressure and at constant volume can be significant. The electrical resistivity of alkali metals at constant volume has been measured by several investigators [288-291], and their results are discussed briefly in the following section.

(b) *Electrical Resistivity of Sodium*

The resistivity of *solid sodium* has been measured by Dugdale and Gugan [289] from -223 to 22°C and also by others [Refs. 13, 14 and 292-294]. The results of Dugdale and Gugan, obtained by the use of self-supporting bare wires, appear to be superior because they were obtained with free wires and not with capillaries [295]. These results can be represented by

$$r_s(t) = 4.290 + 1.993 \times 10^{-2}t + 9.848 \times 10^{-6}t^2 \quad (t \text{ in } ^\circ\text{C}) \qquad (1.111)$$

which has an uncertainty of ±0.01 μΩcm for $-223^\circ\text{C} \lesssim t \lesssim 22^\circ\text{C}$. The resistivity at 0°C agrees within 0.5% with earlier data cited in Refs. 12-14.

For the temperature region between 22°C and the melting point, the same formula is recommended. The resistivity of the solid sodium is shown in Fig. 1.32 from 0°K to the melting point.

The resistivity of the solid at the melting point (6.5 μΩcm) was estimated as the average of the extrapolation of Eq. 1.111 and the measurement by MacDonald [299].

There is a marked increase (about 50%) in electrical resistance [194] as the melting point is passed which is

---

*Electrical resistivity is the property of liquid metals which, thus far, probably has attracted the widest interest from theoreticians. It can be computed from basic theory within about 20% [Refs. 48, 49, 51, 53, 236 and 296-298].

caused largely by the increase in specific volume [143]. Therefore different values are obtained for the resistivity at the melting point, depending on whether the equation for the solid or for the liquid sodium is being used.

The resistivity of solid sodium is affected significantly by high external pressures [Refs. 123, 293 and 299-301] and magnetic fields [13, 302]. At very low temperatures (<50°K), the resistivity is increasingly influenced by even very small amounts of impurities [303]. Sodium apparently does not become a superconductor [304].

Several recent measurements [Refs. 75, 223 and 305-307] of the resistivity of *liquid sodium* were analyzed. A least-squares fit of various power series to the combined data yielded the following recommended equation for the resistivity, r, as a function of the temperature, t (°C):

$$r\ (\mu\Omega\text{cm}) = 7.756 + 2.054 \times 10^{-2}t + 3.481 \times 10^{-5}t^2 \qquad (1.112)$$

which is valid within the temperature range of $98°\text{C} \leqslant t \leqslant 1100°\text{C}$ with an uncertainty of ±0.46 μΩcm. A third-order polynomial did not reduce the error significantly. While the least-squares analysis of the combined data ignores assumptions inherent in the method, it avoids the implication of the very small random errors exhibited by fits to single sets of data. However, the data of Tepper *et al.* [308] appear superior in terms of internal consistency and range, and therefore a third-order polynomial fit to these data can also be used:

$$r\ (\mu\Omega\text{cm}) = 6.144 + 3.504 \times 10^{-2}t + 5.695 \times 10^{-6}t^2 + 1.667 \times 10^{-8}t^3 \qquad (1.113)$$

which has an uncertainty of ±0.08 μΩcm within a range of $130°\text{C} \leqslant t \leqslant 1090°\text{C}$.

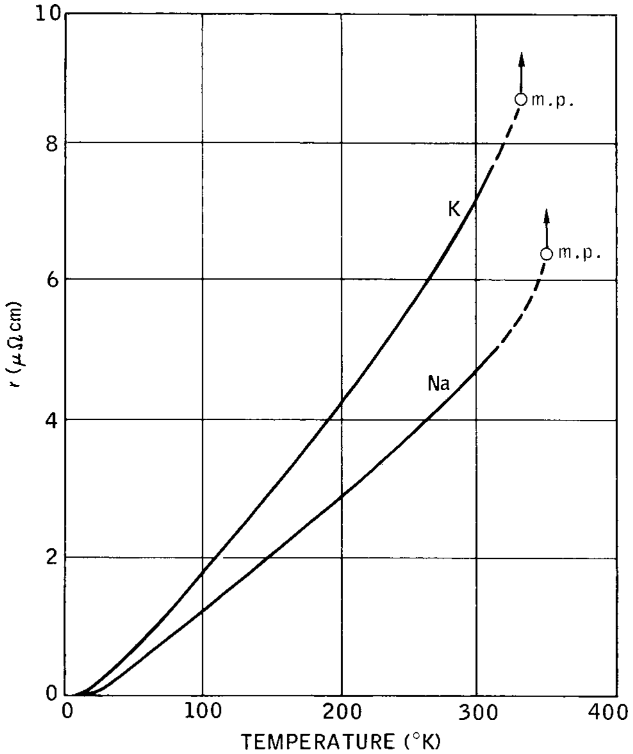

Fig. 1.32 Electrical resistivity (r) of solid sodium and potassium.

The use of these equations to estimate the resistivity at temperatures considerably above the measurement range leads to large uncertainties due to the increasing dominance of the higher power temperature terms. For this purpose, linear extrapolation of the specific resistivity with specific volume, v, is recommended [75, 306]. The specific resistivity, r', is related to resistivity, r, by

$$\frac{r'}{r} = \frac{\rho_t}{\rho_{\text{m.p.}}} = \frac{v_{\text{m.p.}}}{v_t} \qquad (1.114)$$

where ρ_t is the density at temperature t and $\rho_{\text{m.p.}}$ is the density of the liquid at the melting point.

Analysis of the combined data yields the equation

$$r'\ (\mu\Omega\text{cm}) = \frac{119.77}{\rho_t} - 119.67 \quad (\rho_t \text{ in g/cm}^3) \qquad (1.115)$$

with an uncertainty of ±0.6 μΩcm. The resistivity can then be obtained from Eq. 1.114. The error in the resistivity obtained in this manner is approximately ±0.6 r/r' μΩcm.

As a warning against overconfident extrapolation, the resistivities estimated by use of Eqs. 1.112, 1.113, and 1.115 at 1000, 1500, and 2000°C are presented in Table 1.19.

For the limited temperature range up to 1000°C, the computed values show hardly any discrepancies. The values from Eq. 1.113 are graphically presented in Fig. 1.33 and are listed in Table 1.20. Golden and Tokar [19] find also that the data by Tepper *et al.* [75, 308] represent a good average of the various sources that they reviewed in detail.

Very little is known conclusively on the effect of impurities on the electrical resistivity of liquid sodium. The influence of hydrogen and oxygen at 350°C has recently been determined experimentally. From a practical viewpoint, the use of such an effect [309] has been tried for a quantitative impurity monitoring device (rhometer) [310].

(c) *Electrical Resistivity of Potassium*

The electrical resistivity of *solid potassium*, as shown in Fig. 1.32, was reviewed by Wilson [15]. A significant increase of the electrical resistivity at the melting point was reported by Bidwell [292]. At lower temperatures (below 300°K), the electrical resistance of solid potassium was measured by Dugdale and Gugan [289]. As with all alkali metals, pressure has a significant influence on the electrical resistivity [292]; therefore resistivity is usually quoted in this region either for constant density or for constant (zero) pressure. The curves in Fig. 1.32 are for resistivities at ambient (∿ practically zero) pressure. The equivalent curves for resistivities at constant density would be about 20% lower.

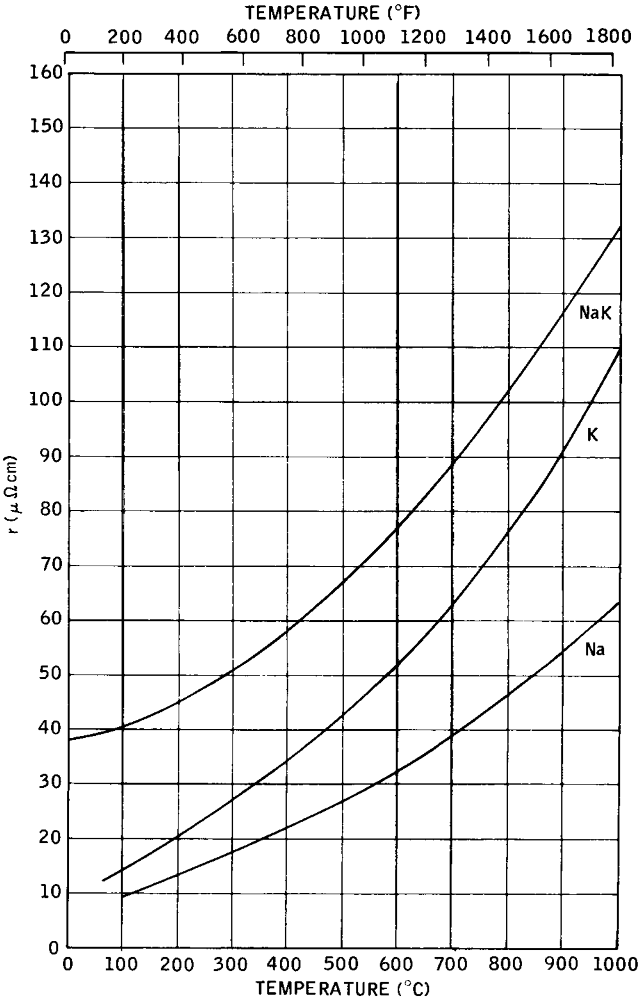

Fig. 1.33 Electrical resistivity (r) of liquid sodium, potassium, and NaK-78.

The electrical resistivity of *liquid potassium* was measured recently by several investigators [Refs. 223, 226, 308, 311 and 312]. The agreement among the various sources is rather good (about 3% variation).

From a recent evaluation by Coe [24], it can be assumed that the data by Tepper *et al.* [308] are in the best overall agreement with existing data; therefore the equation obtained by Tepper *et al.* by a least-squares fit is presented here.

Table 1.19 - Comparison of Estimated Resistivities of Liquid Sodium

Method	Resistivity, μΩcm		
	1000°C	1500°C	2000°C
Eq. 1.112 (second order)	63.1	116.9	188.1
Eq. 1.113 (third order)	63.6	127.7	232.4
Eq. 1.115 (specific resistivity)	63.6	71.8	255.6

$$r\ (\mu\Omega\text{in.}) = 2.6978 + 1.4055 \times 10^{-2}t - 2.0398 \times 10^{-6}t^2 + 3.5792 \times 10^{-9}t^3 \quad (t \text{ in } {}^\circ\text{F}) \qquad (1.116)$$

which has a standard deviation of 1% for 200°F $< t <$ 2000°F. This relation is presented in graphical form in Fig. 1.33; numerical data are given in Table 1.20. Recently Grosse [228] proposed a way to extrapolate the electrical and thermal conductivity data of liquid potassium all the way to the critical point.

The electrical conductivity of *potassium vapor* has been reported [313] to be 10^{-19} mho/cm at 1200°C and 1 atm and to be 10^{-5} mho/cm at 1200°C and 10 atm. There is no evidence of metallic conduction under these conditions. At still higher temperatures (above ∿ 2000°C), the electrical conductivity rises sharply owing to ionization. Because of the practical significance of alkali plasmas in magneto-gasdynamics, several investigators [282, 287, 314] have attempted to compute the high-temperature conductivities of both sodium and potassium plasmas. Figs. 1.34 and 1.35 show these attempts in graphical form for sodium and potassium.

The nonequilibrium electrical conductivity of a wet (i.e. two-phase) potassium vapor, investigated by Rowe and Kerrebrock [316] and Solbers and Kerrebrock [317], was found to be substantially below that of the dry vapor.

(d) *Electrical Resistivity of Sodium-Potassium Alloys*

The measurements of Tepper *et al.* [308] for NaK-77.47, Kapelner [35] for Nak-46.0, and Rahiser [318] for NaK-56 can be reproduced by the following equations:

NaK-78:

$$r\ (\mu\Omega\text{cm}) = 37.66 + 2.307 \times 10^{-2}t + 7.187 \times 10^{-5}t^2 \qquad (1.117)$$

which has an uncertainty of ±1.02μΩcm for 30°C $\leq t_c \leq$ 1100°C.

NaK-46:

$$r\ (\mu\Omega\text{cm}) = 31.14 + 3.327 \times 10^{-2}t + 4.196 \times 10^{-5}t^2 \qquad (1.118)$$

which has an uncertainty of ±0.87μΩcm for 20°C $\leq t \leq$ 860°C.

Table 1.20 - Electrical Resistivity

Temperature		Liquid sodium		Liquid potassium		NaK-78	
°C	°F	μΩcm	μΩin.	μΩcm	μΩin.	μΩcm	μΩin.
50	122					38.99	15.35
100	212	9.72	3.82	14.27	5.62	40.68	16.01
150	302	11.58	4.56	17.40	6.85	42.73	16.82
200	392	13.51	5.32	20.57	8.10	45.14	17.77
250	482	15.52	6.11	23.82	9.38	47.91	18.86
300	572	17.61	6.93	27.20	10.71	51.04	20.09
350	662	19.81	7.80	30.74	12.10	54.53	21.47
400	752	22.13	8.71	34.49	13.57	58.38	22.98
450	842	24.58	9.67	38.47	15.14	62.59	24.64
500	932	27.17	10.69	42.74	16.82	67.16	26.44
550	1022	29.91	11.77	47.33	18.63	72.08	28.38
600	1112	32.81	12.92	52.28	20.58	77.37	30.46
650	1202	35.90	14.13	57.63	22.69	83.02	32.68
700	1292	39.17	15.42	63.42	24.97	89.02	35.04
750	1382	42.65	16.79	69.70	27.44	95.38	37.55
800	1472	46.35	18.24	76.49	30.11	102.11	40.20
850	1562	50.27	19.79	83.85	33.01	109.19	42.99
900	1652	54.44	21.43	91.80	36.14	116.63	45.92
950	1742	58.86	23.17	100.40	39.52	124.43	48.99
1000	1832	63.54	25.01	109.67	43.17	132.59	52.20
1050	1922	68.50	26.97	119.66	47.11	141.12	55.55
1100	2012	73.76	29.04	130.42	51.34	149.99	59.05
1150	2102	79.32	31.22	141.97	55.89	159.23	62.69
1200	2192	85.19	33.54	154.36	60.77	168.33	66.47

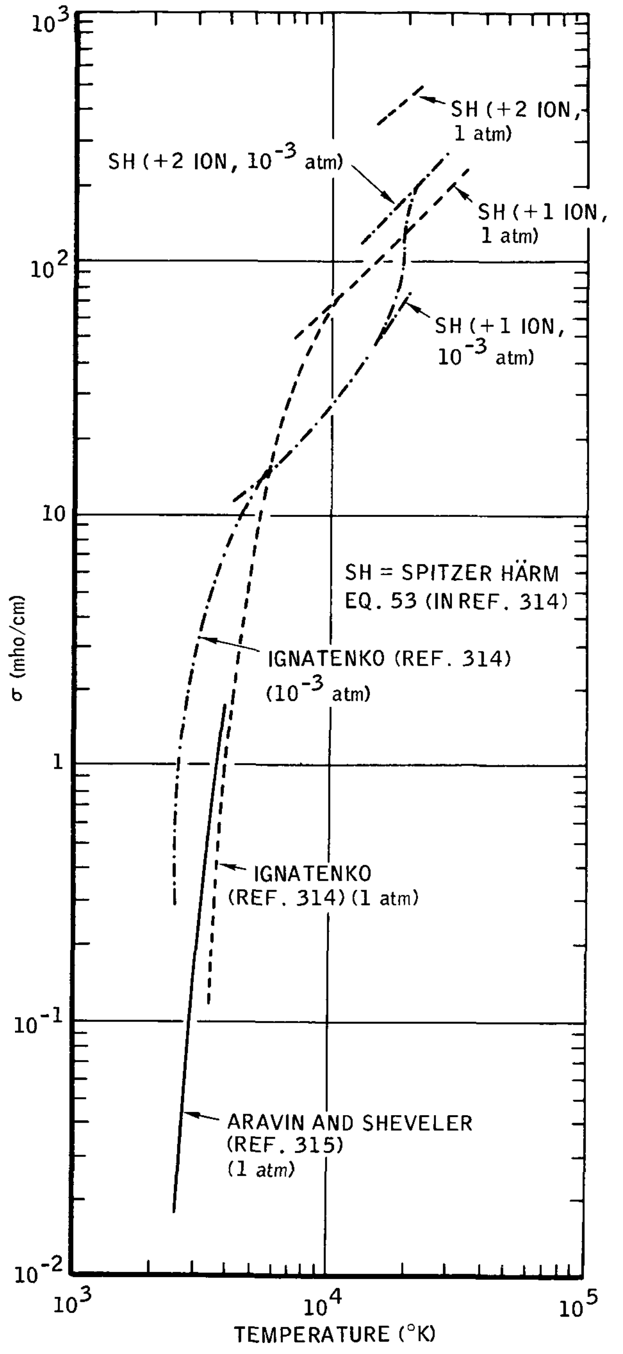

Fig. 1.34 Electrical conductivity of sodium plasma [282].

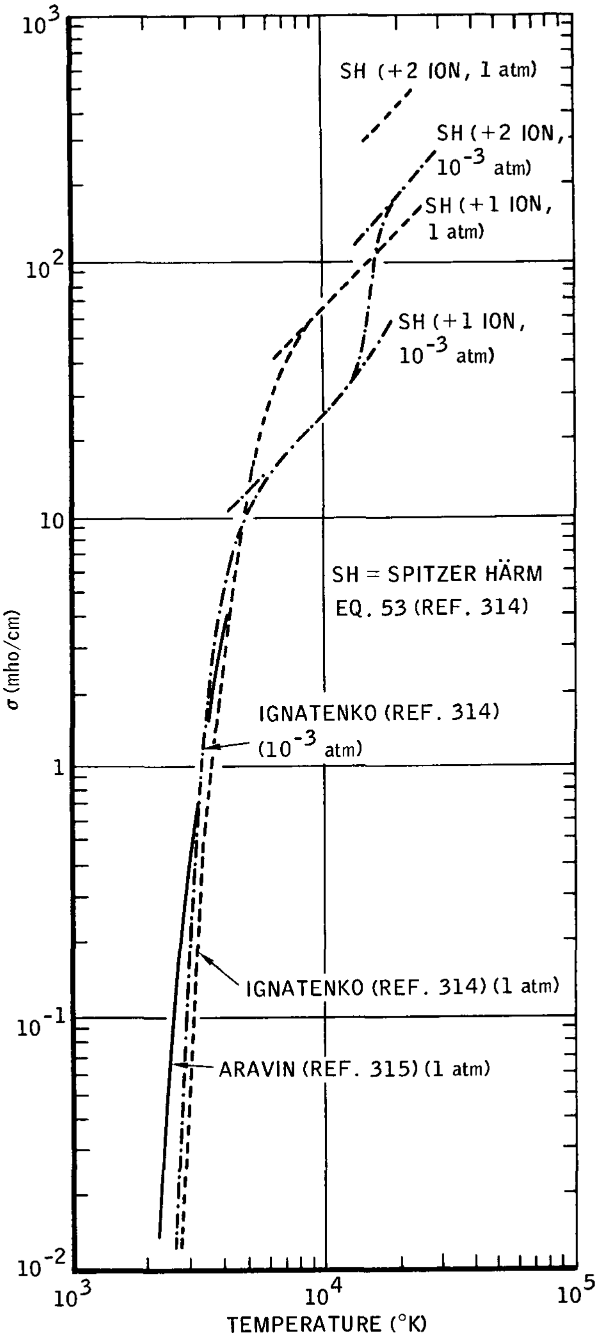

Fig. 1.35 Electrical conductivity of potassium plasma [282].

NaK-56:

$$r\ (\mu\Omega\text{cm}) = 36.76 + 4.539 \times 10^{-2}t + 4.091 \times 10^{-5}t^2 \qquad (1.119)$$

which has an uncertainty of ±0.51μΩcm for $100°\text{C} \le t \le 800°\text{C}$. Additional experimental data for NaK can be found in Refs. 229, 231 and 318.

For very dilute solutions of metals in sodium, Freedman and Robertson [305] determined the variation of resistivity, at 100°C, with solute concentration. For potassium in sodium, this is

$$r\ (100°\text{C}) = r_{\text{Na}}\ (100°\text{C}) + 0.838\ f = 9.72 + 0.838\ f \qquad (1.120)$$

where f is the atom fraction of potassium. This expression was derived from data for potassium concentrations below 1 at.%; it may be valid up to 5 to 10 at.% [297].

The variation of resistivity with composition at various temperatures is shown in Fig. 1.36. The experimental measurements at 46 and 56 wt.% suggest a possible ±4% uncertainty in the smoothed curves.

(e) *Contact Resistance*

Electric contact resistance between liquid sodium and stainless steel [319] depends on the degree of wetting. Unwetted surfaces can have a resistance equivalent to a 2-in. layer of stainless steel. Surfaces of 347 stainless steel, wetted completely by liquid sodium, were found to have a contact resistance of approximately $0.037 \mu\Omega/\text{in.}^2$, which is equivalent to a 0.001-in. layer of stainless steel. Essentially no change of this value was found in the temperature range 130 to 460°C for a current density from 0 to 7000 amp/in.^2. Sodium purity has very little influence on these values.

(f) *Electrical Resistivity at Constant Volume*

If $r_{\text{m.p.}}$ is the resistivity of the liquid metal at its melting temperature, $t_{\text{m.p.}}$, in °C, the electrical resistivity at constant volume can generally be expressed by [291]

$$r = r_{\text{m.p.}} + \left(\frac{\partial r}{\partial t}\right)_v (t - t_{\text{m.p.}}) \qquad (1.121)$$

The temperature coefficients $(\partial r/\partial t)_v$ are $0.021 \mu\Omega\text{cm}/°\text{C}$ for sodium and 0.030 $\mu\Omega\text{cm}/°\text{C}$ for potassium [291]. These results agree within 3% with those of Endo [288].

1-6.2 *Lorenz Number*

(a) *Definitions*

According to the Wiedemann-Franz-Lorenz law, the electrical and thermal conductivities of metals are proportional at a given temperature. The proportionality is given by

$$k = \frac{LT}{r} \qquad (1.122)$$

where r is the electrical resistivity, k is the thermal conductivity, and T is the absolute temperature. The proportionality constant, L, is called the Lorenz number. It is useful in estimating thermal conductivities when electrical conductivities are known [232, 320]. With the use of an improved version of the Wiedemann-Franz-Lorenz law, such a method is usually correct within ±5% up to about 900°C [230]. The quantum-theoretical value of L for a free electron gas is

$$L = \frac{\pi^2}{3} \left(\frac{k_0}{e}\right)^2 \qquad (1.123)$$

where k_0 is the Boltzmann constant and e is the electron charge. With the latest values of k_0 and e [321] the theoretical value of L is therefore

$$L = (2.4428 \pm 0.0002) \times 10^{-8}\ \text{W}\Omega/°\text{K}^2$$

The Lorenz number can also be determined experimentally from k, r, and T. For most metals, L differs from the theoretical free-electron-gas value by several percent because of nonelectronic conduction and other departures from the assumptions in the model.

(b) *Sodium*

Values of the Lorenz number for sodium below 850°C were derived from the recommended equations for electrical resistivity (Eq. 1.113) and thermal conductivity (Eq. 1.44). Some temperature dependence was apparent. The recommended value is

$$L = (2.32 \pm 0.05) \times 10^{-8}\ \text{W}\Omega/°\text{K}^2$$

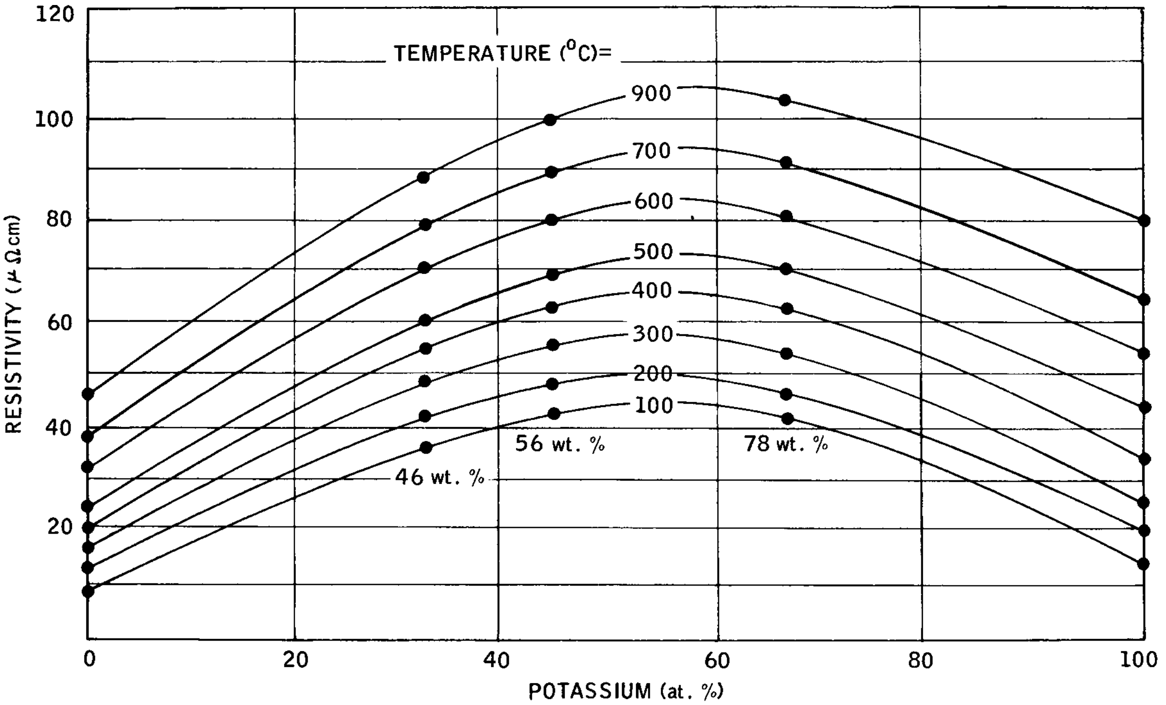

Fig. 1.36 Resistivity (ρ) of sodium-potassium alloys for various temperatures.

(c) *Potassium*

For temperatures below 800°C, the Lorenz number for potassium reportedly [223, 226] has a fairly constant (within 5%) average value of

$$L = 2.14 \times 10^{-8}\ \mathrm{W\Omega/^{\circ}K^2}$$

(d) *Eutectic NaK*

The Lorenz number for eutectic NaK was estimated from the thermal-conductivity measurements of Ewing *et al.* [229] (Eq. 153) for NaK-77.7 and the resistivity data of Tepper *et al.* [308] (Eq. 1.117) for NaK-77.5. The recommended value for temperatures up to 700°C is

$$L = (2.31 \pm 0.04) \times 10^{-8}\ \mathrm{W\Omega/^{\circ}K^2}$$

1-6.3 *Hall Effect*

When a magnetic field $\vec{B}$ is applied to a conductor carrying a current density $\vec{J}$, an electric field $\vec{E}_H$ (Hall field) is developed, given by

$$\vec{E}_H = R(\vec{J} \times \vec{B})$$

where R, the Hall coefficient, is -25×10^{-13} volt-cm/amp-gauss, or -25×10^{-11} m^3/amp-sec for sodium [13] (accuracy ±6%). Similar numbers have been reported by several independent workers [Refs. 290, 302, 313 and 322-325]; the theoretical value of R is supposed to be -25.6×10^{-13} volt-cm/amp-gauss [Refs. 298, 326, and 327].

The Hall constant is essentially the same for liquid and solid sodium. It decreases slightly with temperature (only by 3% from room temperature down to liquid-nitrogen temperature) and pressure (only by 5% from 0 to 15,000 atm) [328]. Within measuring accuracy it is independent of the magnetic-field strength, at least up to 25,000 gauss.

Reported values for the Hall constant for potassium vary from -35 to -49×10^{-13} volt-cm/amp-gauss [Refs. 290, 302, 323, 325 and 328]. The value of -49×10^{-13} volt-cm/amp-gauss (with a reported accuracy of ±5%) is recommended here. No recent data have been found on the Hall constant for NaK. It can be expected, however, that it changes monotonically with the at.%

ratio [236]. Older measurements [329, 330], as reported by Busch and Tieche [327] place the Hall constant for NaK (about 50 at.%) between -42 and $-44 \times 10^{-11} m^3$/amp-sec.

1-6.4 *Magnetic Permeability and Susceptibility*

(a) *Definitions*

The absolute magnetic permeability, μ, of a substance is defined in terms of the magnetic induction, B, and the magnetic-field intensity, H, by the equation $\mu = B/H$. The dimensionless ratio μ/μ_0 is the relative magnetic permeability μ_r (μ_0, the absolute permeability in vacuum equals $4\pi \times 10^{-7}$ volt-sec/amp-m in the international unit system, or 1.39×10^{-20} sec^2/cm^2 in the cgs system). The term $\mu_r - 1$ is called the magnetic susceptibility κ_m, and the ratio κ_m/ρ is the specific magnetic susceptibility χ. It is the χ that is usually quoted in the literature. The value of κ_m is dimensionless, whereas the dimension of χ obviously is the inverse of that of density. For most practical purposes, the magnetic permeability of the alkali metals can be considered to be equal to the vacuum permeability μ_0.

(b) *Magnetic Susceptibility of Sodium*

Sodium is a paramagnetic substance; hence the magnetic induction will be only slightly greater in sodium than in a vacuum for a given magnetic-field intensity. The presence of very small amounts of ferromagnetic materials will, however, lead to erroneous values for sodium. Oxygen, a common impurity, has a susceptibility of 3380×10^{-6} cm^3/g, or about 5000 times that of sodium, when in the liquid state.

Bowers [331] reports a room-temperature value of $+0.70 \pm 0.03 \times 10^{-6}$ cm^3/g for pure sodium from the Ethyl Corporation. The sample was vacuum melted and decanted to remove the insoluble oxide. No variation in susceptibility was observed with magnetic-field intensity suggesting the absence of any ferromagnetic impurities.

Venkateswarlu and Sriraman [332] obtained a value of $+0.60 \times 10^{-6}$ cm^3/g for a sample prepared in a similar manner. They extrapolated their results to an infinite magnetic field to remove ferromagnetic effects.

An unweighted average of the preceding two values together with two other measurements made since 1939, as noted by Venkateswarlu and Sriraman [332] gives a value of $0.64 \pm 0.04 \times 10^{-6}$ cm^3/g.

Venkateswarlu and Sriraman [332] measured the temperature dependence over the range of 30 to 250°C; Nachtrieb [333] extended this range up to 500°C. Their observed results are shown in Table 1.21. Collings [334] found that the magnetic susceptibility of sodium increases abruptly by 3% when passing through the melting point. The susceptibility of solid sodium decreases slowly with decreasing temperature [13, 335] (about -20% from the melting point down to 4°K).

(c) *Magnetic Susceptibility of Potassium*

The magnetic susceptibility of potassium is somewhat smaller than that of sodium. Its temperature dependence [332-334] is given in Table 1.21.

(d) *Magnetic Susceptibility of Sodium-Potassium Alloys*

Venkateswarlu and Sriraman [336] measured the susceptibility of a number of sodium and potassium alloys at temperatures from 30 to 250°C. The susceptibilities could be represented by a linear combination (known as "Wiedemann's law" [333]) of the sodium and potassium susceptibility. The data for NaK-78 in Table 1.21 can be calculated with the use of this relation.

(e) *Magnetic Prandtl Numbers*

For magnetohydrodynamic flows (see Chap. 4), a nondimensional fluid

Table 1.21 - Magnetic Susceptibility

Sodium		Potassium		Nak-78	
t, °C	χ, 10^{-6} cm^3/g	t, °C	χ, 10^{-6} cm^3/g	t, °C	χ, 10^{-6} cm^3/g
30	0.600	30	0.460	30	0.490
65	0.604	50	0.467	60	0.491
95	0.605	60	0.457	100	0.491
110	0.600	100	0.459	150	0.493
150	0.612	130	0.461	190	0.496
190	0.615	160	0.462	250	0.500
250	0.620	190	0.464		
		220	0.465		
		250	0.467		

property, the so-called magnetic Prandtl number β (sometimes called Batchelor number), becomes an important parameter. β is defined as $\beta = \mu\sigma\nu$, where μ is the magnetic permeability (as discussed previously for sodium and potassium: $\mu \approx \mu_0$), σ is the electric conductivity, which is the inverse of the electrical resistivity r (as discussed in Sec. 1-6.1), and ν is the kinematic viscosity (as discussed in Sec. 1-4.2). Numerical values for β are shown in Table 1.22 for liquid sodium, potassium, and NaK.

1-6.5 *Thermoelectric Potential*

The thermoelectric potential, or Seebeck potential, is the electrical potential difference observed between two points in a conductor which are at different temperatures [337]. Since a complete electrical circuit is usually needed to measure this potential, the potential is normally measured as the difference in potential between two conductors whose junctions are at different temperatures.

Bradley [338] measured the absolute thermoelectric power of liquid sodium and potassium by referencing it to copper, whose thermoelectric power had been determined separately. His data for the Seebeck coefficient (dE/dt) of sodium increase linearly from 9 to 15 μV/°C within the range from about 100 to 375°C. According to the same source, the Seebeck coefficient for liquid potassium ranges from 17 to 25 μV/°C from approximately 80 to 350°C.

More-recent measurements (with platinum serving as reference material) extending to 900°C have been reported by Bonilla *et al.* [339]. Their measured values for sodium and potassium are given in Table 1.23.

No reliable data on NaK-78 seem to exist. However, there are a few experimental data [338] on "dilute" solution of sodium in potassium and potassium in sodium. For solid sodium and potassium, the Seebeck coefficient decreases continuously down to 0 at 0° K. An extensive literature exists for this region [13].

1-6.6 *Nuclear Properties*

(a) *Sodium*

Sodium is an alkali metal having the atomic number 11 and a single naturally occurring isotope with an atomic weight of 22.9898 (based on the mass ^{12}C = 12.0000). Its ionization potential is 5.12 volts. The radioactive isotopes of sodium and their half-lives and emitted particles are listed in Table 1.24.

Of more importance than the radioactive isotopes of sodium in nuclear

TABLE 1.22 - Magnetic Prandtl Number (× 10^{-6})

Temperature		Sodium	Potassium	NaK-78
°C	°F			
50	122			2.603
100	212	9.485	5.061	1.925
150	302	6.418	3.449	1.506
200	392	4.651	2.526	1.224
250	482	3.541	1.944	1.021
300	572	2.797	1.552	0.868
350	662	2.272	1.272	0.749
400	752	1.886	1.048	0.654
450	842	1.594	0.867	0.556
500	932	1.367	0.728	0.482
550	1022	1.150	0.620	0.422
600	1112	0.983	0.533	0.372
650	1202	0.850	0.463	0.331
700	1292	0.742	0.405	0.297
750	1382	0.652	0.357	0.267
800	1472	0.578	0.316	0.242
850	1562	0.515	0.281	0.220
900	1652	0.462	0.251	0.202
950	1742	0.417	0.226	0.185
1000	1832	0.377	0.203	0.171
1050	1922	0.343	0.184	0.158
1100	2012	0.313	0.167	0.147
1150	2102	0.286	0.152	0.137
1200	2192	0.263	0.139	0.128

reactor operations are the radioactive isotopes that can be formed from neutron interactions with sodium in a nuclear reactor (see Table 1.25 [340]). The relative amounts are sensitive to the neutron spectrum in the particular reactor. In addition to the formation of ^{24}Na from simple neutron capture, ^{22}Na, ^{23}Ne, and ^{20}F result from the $(n, 2n)$, (n, p), and (n, α) reactions, respectively. Details of these reactions and decay schemes are given by Strominger *et al.* [341]. These reactions require energetic neutrons and would be found in appreciable amounts only in fast reactors. Neon-23 has a half-life of 38 sec and decays with β^- emission having end-point energies of 4.39, 3.95 and 2.4 MeV and gamma ray energies of 1.64 and 0.44 MeV. Fluorine-20 has a half-life of 11 sec and decays with the emission of a β^- particle with an end-point energy of 5.40 MeV, followed by a 1.63-MeV gamma ray.

For use in fast reactors, the ^{24}Na isotope with a half-life of 15 hr has most important implications. As long as no radioactive sodium escapes from the reactor, the beta radiation can be disregarded because of its relatively low energy [62]. However, the gamma radiation of this isotope requires special shielding of the primary sodium circuit.

Sodium has a neutron-capture cross section [342] σ_T at 0.025 eV of 0.53

TABLE 1.23 - Thermoelectric Potentials of Liquid Sodium and Potassium (in Millivolts) with Respect to Platinum*

Temp., °C	Pt/Na	Pt/K
25	0.029	0.183
50	0.053	0.368
75	0.070	0.563
100	0.084	0.736
125	0.094	0.926
150	0.109	1.124
175	0.122	1.327
200	0.136	1.536
225	0.153	1.753
250	0.175	1.988
275	0.202	2.221
300	0.226	2.466
325	0.263	2.727
350	0.301	3.028
375	0.341	3.337
400	0.390	3.666
425	0.446	4.008
450	0.497	4.360
475	0.551	4.717
500	0.615	5.075
525	0.699	5.439
550	0.789	5.824
575	0.888	6.204
600	0.996	6.624
625	1.110	7.031
650	1.225	7.455
675	1.350	7.884
700	1.470	8.316
725	1.591	8.758
750	1.731	9.218
775	1.856	9.672
800	2.016	10.168
825	2.173	10.643
850	2.316	11.143
875	2.461	11.637
900	2.629	12.150

*Cold junction is at 0°C. Platinum is positive at the cold junction in all cases.

barn and a total cross section at 0.025 eV of 3.9 barns. Its total cross section is fairly constant at approximately 3.1 barns until 2.85 keV where it has a large scattering resonance that rises to a value of approximately 370 barns. There are numerous resonances in σ_T between 0.12 and 1.0 MeV, as shown in Fig. 1.37.

References 343 and 344 contain a recent and comprehensive compilation of the neutron cross sections of sodium and potassium for the energy range from 0.01 eV to 20 MeV. Electron cross sections for alkali-metal atoms are reported in Ref. 345.

(b) *Potassium*

Potassium is an alkali metal with atomic number 19 and atomic weight 39.102 based on ^{12}C = 12.000. It has three naturally occurring isotopes [341] with mass numbers 39, 40, and 41 and abundances 93.10, 0.012, and 6.88%, respectively. The isotope ^{40}K is naturally radioactive with a half-life of 1.25×10^9 years; it decays in 89% of the cases with the emission of a 1.32-MeV β^- and in 11% of the cases by electron capture followed by a 1.46-MeV gamma ray. The ionization potential of potassium is 4.318 volts. Table 1.26 lists the radioactive isotopes of potassium with their principal decays.

As in the case of sodium, neutron reactions with potassium can produce numerous radioactive isotopes in a reactor (see Table 1.27 [340]). The important isotopes are ^{38}K and ^{39}Ar, which are produced from ^{39}K by (n, 2n) and (n,p) reactions, respectively [341]. Argon-39 has a 270-year half-life and decays by β^- emission with an end-point energy of 0.57 MeV. The (n,p) reaction with ^{41}K produces ^{41}Ar, which has a half-life of 1.83 hr and a predominant β^- group having an energy of 1.20 MeV followed by a gamma-ray energy of 1.29 MeV. The (n, α) reaction with ^{41}K produces ^{38}Cl, which decays with a half-life of 37.3 min by the emission of β^- and gamma rays having a total energy of about 4.9 MeV.

TABLE 1.24 - Sodium Radioactive Isotopes

Sodium isotope	Relative abundance, %	Half-life	Emitted particle	Decay product	Energy, MeV
20	<0.002	$\sim$0.39 sec	β^+, α	^{20}Ne, ^{16}F	E_{tot}15
21	$<10^{-6}$	23 sec	β^+	^{21}Ne	2.5
22	$<3.10^{-6}$	2.58 years	β^+, EC*	^{22}Ne	Mainly 0.54
			γ		1.30
24^m		$\sim$0.02 sec	β^-	^{24}Mg	$\sim$6
			γ		0.472
24	0.002	15 hr	β^-	^{24}Mg	1.39
			γ		1.37, 2.75
25	0.002	60 sec	β^-	^{25}Mg	3, 8, 2.8, 2.4
			γ		0.98, 0.58, 0.40, 1.61, 1.96
26		1.04 sec	β^-	^{26}Mg	$\sim$5

*Orbital electron capture.

TABLE 1.25 - Neutron Reactions of Sodium and Products Formed

Target nuclide	Natural abundance, %	Reaction	Product formed	Half-life	Type of radiation emitted	Energy of radiation	
						MeV	pJ
^{23}Na	100	(n,γ)	^{24}Na	15.0 hr	Gamma	1.37	0.219
		(n,γ)	^{24}Na	15.0 hr	Gamma	2.78	0.440
		(n,p)	^{23}Ne	38 sec	Gamma	0.44	0.0704
		(n,p)	^{23}Ne	38 sec	Gamma	1.65	0.264
		$(n,2n)$	^{22}Na	2.58 years	Gamma	1.28	0.205
		(n,α)	^{20}F	11 sec	Gamma	1.63	0.261
		(n,α)	^{20}F	11 sec	Beta	5.4	0.864

Potassium has a neutron-capture cross section [342] at 0.025 eV of 2.1 barns and a total cross section of about 4.36 barns. The total cross section is fairly constant below 10 eV, beyond which there are no measurements reported up to 0.01 MeV. Above 0.01 MeV, there appears to be detailed resonance structure in σ_T. For additional and more-detailed data on nuclear properties, see Refs. 13, 342 and 346.

1-6.7 *Miscellaneous Properties*

There exists a host of other properties of sodium and potassium (especially in the solid and vapor phases) which appear to be of rather limited importance for practical engineering applications at the present time and which will, therefore, not be discussed here. (Obviously the judging of the importance of certain characteristics is always somewhat arbitrary; other reviewers might well have arrived at another selection.) Most of the disregarded properties fall into the categories of electrical, optical, or structural and include, for example, data on electron emission and work function, photoelectric and thermomagnetic effects, contact potentials, secondary

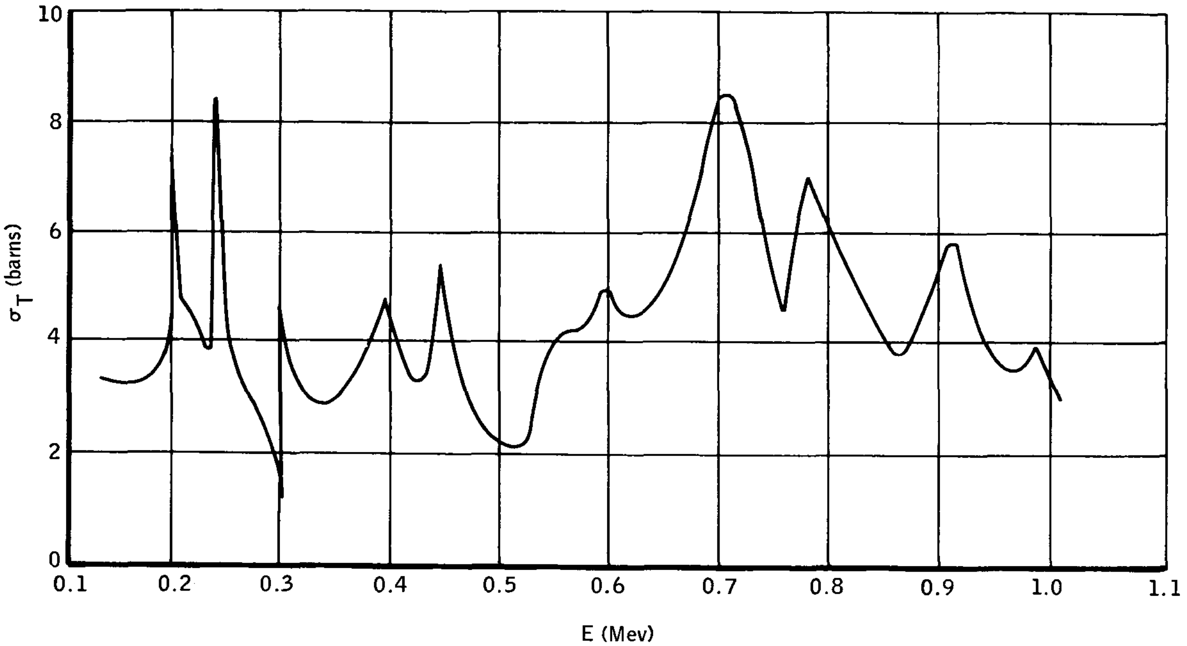

Fig. 1.37 Neutron cross section for sodium as a function of neutron energy.

TABLE 1.26 - Potassium Radioactive Isotopes

Isotope	Half-life	Emitted particle	Decay product	Energy, MeV
37	1.2 sec	β^+	^{37}Ar	5.1
38	7.7 min	β^+	^{38}Ar	2.7
		γ		2.2
	0.95 sec	β^+	^{38}Ar	5.1
40	1.25×10^9 years	β^-	^{40}Ca	1.32
		EC*	^{40}Ar	1.46
		γ		
42	12.4 hr	β^-	^{42}Ca	3.53, 2.01
		γ		1.53, 0.31
43	22 hr	β^-	^{43}Ca	0.24, 0.46, 0.83, 1.22, 1.84
		γ		0.220, 0.371, 0.388, 0.394, 0.591, 0.614, 1.01
44	22 min	β^-	^{44}Ca	1.5, 4.9
		γ		1.13, 2.01, 2.48, 3.6
45	20 min	β^-	^{45}Ca	Not identified
		γ		0.18, 1.7

*Orbital electron capture.

electron emission, ion emission, etc. A vast amount of data is also available for sodium and potassium on their atomic and ionic structure, atomic excitation, optical and X-ray spectra, photon cross section, X- and gamma-ray absorption and scattering, ionization and interaction with electrons, etc.

TABLE 1.27 - Neutron Reactions of Potassium and Products Formed

Target nuclide	Natural abundance, %	Reaction	Product formed	Half-life	Type of radiation emitted	Energy of radiation	
						MeV	pJ
^{39}K	93.1	(n,γ)	^{40}K	1.3×10^9 years	Beta	1.32	0.211
		(n,γ)	^{40}K	1.3×10^9 years	Gamma	1.46	0.2337
		(n,p)	^{39}Ar	260 years	Beta	0.57	0.0912
		$(n,2n)$	^{38}K	7.7 min	Gamma	2.2	0.352
		(n,α)	^{36}Cl	3×10^5 years	Beta	0.71	0.1207
		(n,d)	^{38}Ar	Stable			
		(n, np)	^{38}Ar	Stable			
^{40}K	0.0118	(n,γ)	^{41}K	Stable			
		(n,p)	^{40}Ar	Stable			
		$(n,2n)$	^{39}K	Stable			
		(n,α)	^{37}Cl	Stable			
		(n,d)	^{39}Ar	260 years	Beta	0.57	0.0912
		(n,np)	^{39}Ar	260 years	Beta	0.57	0.0912
^{41}K	6.88	(n,γ)	^{42}K	12.4 years	Gamma	1.52	0.2431
		(n,p)	^{41}Ar	1.83 hr	Gamma	1.3	0.208
		$(n,2n)$	^{40}K	1.3×10^9 years	Beta	1.32	0.211
		$(n,2n)$	^{40}K	1.3×10^9 years	Gamma	1.46	0.2337
		(n,α)	^{38}Cl	37.3 min	Gamma	1.6	0.256
		(n,α)	^{38}Cl	37.3 min	Gamma	2.2	0.352
		(n,d)	^{40}Ar	Stable			
		$(n,2p)$	^{40}Cl	1.4 min	Gamma	1.5	0.240
		$(n,2p)$	^{40}Cl	1.4 min	Gamma	2.75	0.440
		$(n,{}^3\mathrm{He})$	^{38}Cl	37.3 min	Gamma	1.6	0.256
		$(n,{}^3\mathrm{He})$	^{38}Cl	37.3 min	Gamma	2.2	0.352

Basic optical property data on sodium and potassium have become available in recent years. Also, certain mechanical and thermodynamical properties (such as elastic constants of the solid, Debye temperature, Grüneisen constant, etc.) are not included in this handbook because of their limited practical significance.

For a comprehensive and adequate introduction to this rapidly growing general field of the physics of liquid metals, Refs. 13, 48, 50, 51, 351, and 352 should be consulted. These are mostly general review articles that contain virtually hundreds of additional references to specific problems.

APPENDIXES

General Comments

Appendixes 1-A, 1-B and 1-C contain three computer subroutines (written in FORTRAN IV) that might be useful as part of a computer program requiring certain sodium, potassium, or NaK property values for its implementation, and Appendix 1-D gives data supplied through the subroutines of Appendixes 1-A and 1-B. It is suggested that the programmer familiarize himself with the details of each subroutine before he tries to incorporate it into a computer program. In many cases he might prefer to modify the subroutine to suit his particular needs.

The subroutine "NAPROP" in Appendix 1-A is taken verbatim from Ref. 19. It computes saturation properties in the units indicated in the last column as a function of pressure and temperature. (Only if the given values for the temperature and pressure match for the saturation condition within at least approximately 0.1% will the saturation properties be computed. Otherwise, the corresponding properties for the superheated vapor or the subcooled liquid will be computed.) The saturation properties which NAPROP computes are density, enthalpy, and entropy of the liquid and specific volume, enthalpy, and entropy of the vapor as well as the average molecular weight, mole fractions of the dimer and the tetramer, and the compressibility factors of the vapor. Included also is the heat of vaporization. If the p-T values fall into the superheated regime, the corresponding vapor properties are computed; if they fall into the subcooled regime, the corresponding liquid properties are computed.

Appendix 1-B carries a subroutine (POPROP) for the computation of the equivalent property values for potassium. (No equations for the subcooled liquid state of potassium are included, however.)
It has generally been patterned after the NAPROP subroutine of Appendix 1-A. However, it was intended primarily as a table-writing program for preparation of Appendix 1-D with the aid of a time-shared computer. These particular features will become evident to the cognizant programmer, who can easily modify the program to suit different purposes.

Appendix 1-C carries a subroutine (TRANP) for the computation of certain sodium, potassium and NaK properties that are functions of temperature only. It was supplied by Lawrence Radiation Laboratory of the University of California and can also be easily incorporated (in part or in its entirety) into any computer program that requires these properties. Most of the tables in Chap. 1 were prepared with the aid of this subroutine.

Appendix 1-D, which was prepared with the aid of subroutines NAPROP and POPROP, contains the vapor properties of sodium and potassium for saturated and supersaturated conditions.

APPENDIX 1-A: SODIUM PVT AND THERMODYNAMIC PROPERTIES SUBROUTINE (NAPROP)

```
          SUBROUTINE NAPROP (TEMPR.PATM)
          T = TFMPR
C         CALCULATION OF SATURATION PROPERTIES
      100 IF (T-2059.7) 110.110.112
      110 PSAT = (3.03266E6/T**.5)*(EXPF (-2.30733E4/T))                  ATM
      111 GO TO 120
      112 PSAT = (6.8817602E6/(T**.61344))*EXPF(-22981.96/T)               ATM
      113 GO TO 120
      120 HLS = .389352*T-.5529955E-4*(T)**2+.1137265-7*(T)**3-29.02       BTU/LB
      130 SLS = .289344*(LOGF(T))-1.105574-4*T+.170408E-7*(T**2)-1.792026  BTU/LBR
      140 DL = 59.566-7.9504E-3*(T-459.7)-.2872E-6*((T-459.7)**2)+.060354-9* LB/FT3
          1((T-459.7)**3)
      150 TWO = EXPF(-9.95845+(16588.3/T))                                 ATM-1
      160 FOUR + EXPF(-24.59115+(37568.7/T))                               ATM-3
      170 U = PSAT*TWO
      180 W = ((PSAT)**3)*FOUR
      190 X1 = 0.8
      200 X1P = X1
      203 X1 = X1-(W*(X1)**4+U*(X1)**2+X1-1.)/(4.*W*(X1)**3+2.*U*X1+1.)
      205 IF (ABSF(X1-X1P)/X1-1.$-6)210.210.200
      210 X2 = U*(X1)**2
      212 X4 = 1.-X1-X2
      214 ABAR = 22.991*(X1+2.*X2+4.*X4)
      216 VSAT = (.730229*T)/(ABAR*PSAT)                                   FT3/LB
      217 Z = 22.991/ABAR
      218 DHF 1 = 25980.7-2.21312*T+7.06278E-4*(T)**2-1.4526E-7*(T)**3     CAL/MNA1
      220 DHF 2= 2.*DHF1-18304.                                            CAL/MNA2
      222 DHF4 = 4.*DHF1-41478.                                            CAL/MNA4
      224 DHV = 1.8*(X1*DHF1+X2*DHF2+X4*DHF4)/ABAR                         BTU/LB
      226 HGS = HLS*DHV
      228 SGS = SLS+(DHV/T)
C         TEST FOR STATE, I.E., SUBCOOLED, SATURATED, SUPERHEATED
      250 IF(ABSF(PATM-PSAT)/PATM-1.E-4)463.463.260
      260 IF(PATM-PSAT)270.463.410
C         Calculation of superheated vapor properties
      270 UH = PATM*TWO
      272 WH = ((PATM)**3)*FOUR
      275 X1H = 0.8                                                        MOLEFRX1
      278 X1PH = X1H
      280 X1H = X1H-(WH*(X1H)**4+UH*(X1H)**2+X1H-1.)/(4.*WH*(X1H)**3+2.*UH*
          1X1H+1.)
      282 IF(ABSF(X1H-X1PH)/X1H-1.E-6)284.284.278
      284 X2H + UH*(X1H)**2                                                MOLEFRX2
      286 X4H = 1.-X1H-X2H                                                 MOLEFRX4
      288 ABARH = 22.991*(X1H+2.*X2H+4.*X4H)
      290 VH + (.730229*T)/(ABARH*PATM)                                    FT3/LB
      292 ZH = 22.991/ABARH
      294 BD = X1+2.*X2+4.*X4
      296 B2 = 2.*X2/BD                                                    WTFRX2S
      297 B4 = 4.*X4/BD                                                    WTFRX4S
```

```
     298  BDH = X1H+2.*X2H+4.*X4H
     300  B2H = 2.*X2H/BDH                                              WTFRX2H
     311  B4H = 4.*X4H/BDH                                              WTFRX4H
     303  HG1 = HGS+B2*716.54+B4*811.85
     305  HGH = HG1-B2H*716.54-B4H*811.85
     308  SG1 = SGS+B2*716.54/T+B4*811.85/T+(1.987180/ABAR)*LOGF(PSAT)-(B2/
          145.982)*(-19.78923+(32963.9/T))-(B4/91.964)*(-48.86704+(74697.5/
          2T))+(1.987180.ABAR)*(X1*LOGF(X1)+X2*LOGF(X2)+X4*LOGF(X4))
     310  SGH = SG1-B2H*716.54/T-B4H*811.85/T-(1.987180.ABARH)*LOGF(PATM)+
          (1B2H/45.982)*(-19.78923+(32963.9/T))+(B4H/91.964)*(-48.86704+(746
          297.5/T))-(1.987180/ABARH)*(X1H*LOGF(X1H)+X2H*LOGF(X2H)+X4H*LOGF
          (3X4H))
          PRINT 350
     350  FORMAT (3X.4HTEMP.7X.4HPRES.10X.2HVH.9X.2HZH.7X.3HHGI.8X.3HHGH.7X.3
          1HSGI.9X.3HSGH.5X.5HABARH.8X.3HX2H.9X.3HX4H)
          PRINT 351
     351  FORMAT (2X.5HDEG-F.7X.3HATM.8X.6HFT3/LB.16X.6HBTU/LB.4X.6HBTU/LB.4X
          1.7HBTU.LBF.5X.7HBTU.LBF.15X.6HMOL FR.6X.6HMOL FR)
     360  PRINT 370.T.PATM.VH.ZH.HGI.HGH.SGI.SGH.ABARH.X2H.X4H
     370  FORMAT (/.1X.F7.1.2(2X.E11.4).2X.F8.5.2(2X.F8.2).2X.F8.5.4XF8.5.2X
          1.F7.3.2(4X.F8.6))
          GO TO 80
C         CALCULATION OF SUBCOOLED LIQUID PROPERTIES
     410  DLP = -7.9504E-3-.5744E-6*(T-459.7(+.18105E-9*(T-459.7)**2
          HLC = HLS+(1./DL)*(1.+(T/DL)*DLP)*(PATM-PSAT)*2.721308
          SLC = SLS+2.721308*(1./(DL**2))*DLP*(PATM-PSAT)
          PRINT 415
     415  FORMAT (8X.4HTEMP.10X.4HPRES.11X.3HHLC.10X.3HSLC./.8X.5HDEG-F.9X.3H
          1ATM.10X.6HBTU/LB.7X.7HBTU/LBF)
     420  PRINT 450.T.PATM.HLC.SLC
     450  FORMAT(/.6X.F7.1.5X.E11.4.5X.F8.2.5X.F8.5)
          GO TO 80
C         OUTPUT SATURATION PROPERTIES
     463  T = T-459.7
          PRINT 10
     10   FORMAT (1H1.2X.5HTEMPF.6X.4HPSAT.7X.4hVSAT.8X.1HZ.7X.2HDL.6X.3HHLS.
          16X.3HDHV.6X.3HHGS.6X.3HSLS.6X.3HSGS.5X.4HABAR.5X.2HX2.7X.2HX4)
          PRINT 11
     11   FORMAT (2X.5HDEG-F.6X.3HATM.7X.6HFT3/LB.13X.6HLB/FT3.3X.6HBTU/LB.3X
          1.6HBTU/LB.3X.6HBTU/LB.2X.7HBTU/LBF.2X.7HBTU/LBF.10X.6HMOL FR.3X.6H
          2MOL FR)
          PRINT 470.T.PSAT.VSAT.Z.DL.HLS.DHV.HGS.SLS.SGS.ABAR.X2.X4
     470  FORMAT (/.F7.1.1X.E11.5.1X.E11.5.2X.F7.5.1X.F7.3.2X.F7.2.1X.F8.2.1X
          1.F8.2.1X.F8.5.1X.F8.5.1X.F7.3.1X.F8.6.2X.F7.6)
          80 RETURN
          51 END
```

APPENDIX 1-B: POTASSIUM PVT AND THERMODYNAMIC PROPERTIES SUBROUTINE (POPROP)

```
C:      PØTASSIUM P-V-T AND THERMODYNAMIC PRØPERTIES
   500  FØRMAT (//)
   510  FØRMAT (8X,4HTEMP,14X,2HZH,10X,5HABARH,10X,3HX2H,10X,3HX4H)
   520  FØRMAT (5X,1HC,8X,1HF)
   530  FØRMAT (F8.2,1X,F8.2,3(4X,E10.4),3X,E10.4)
        DISPLAY "TYPE PRESSURE IN ATM"
        ACCEPT PATM
        DISPLAY "LØWER AND UPPER LIMIT OF TEMPERATURE RANGE AND
        TEMPERATURE DIFFERENTIAL IN DEGREES C"
        ACCEPT TLØW,TUP,DELT
        WRITE (1,500)
        DISPLAY"                        P = ",PATM," ATM AB
S"
        WRITE (1,500)
        WRITE (1,510)
        WRITE (1,520)
        TEMP = TLØW
     5  IF (TEMP .GT. TUP) GØ TØ 80
C:      CALCULATIØN ØF SATURATIØN PRØPERTIES
        T = (TEMP + 273.16)*9.0/5.0
   112  PSAT = (1.3408E6/(T**.53299))*EXP[-18717.0/T]
   113  GØ TØ 120
   120  HLS = .2022*(T-459.0)-.2177E-4*(T-459.0)**2)+.07741E-
7       *((T-459.0)**3)+87.8783
   130  SLS = .227126*(ALØG[T])-.64848E-4*T+.11589E-7*(T**2)-.9646
   140  DL = 52.768-7.4975E-3*(T-459.7)-.5255E-6*((T-459.7)**2
)+.0498E-9*        ((T-459.7)**3)
   150  TWØ = EXP[-8.9033+(12250.1/T)]
   160  FØUR = EXP[-23.394+(31694.6/T)]
   170  U = PSAT*TWØ
   180  W = ((PSAT)**3)*FØUR
   190  X1 = 0.8
   200  X1P = X1
   203  X1 = X1-(W*(X1**4)+U*(X1**2)+X1-1.)/(4.*W*(X1**3)+2.*U
*X1+1.)
   205  IF (ABS[X1-X1P]/X1-1.E-6)210,210,200
   210  X2  = U*(X1**2)
   212  X4 = 1.-X1-X2
   214  ABAR = 39.102*(X1+2.*X2+4.*X4)
   216  USAT = (.730229*T)/(ABAR*PSAT)
   217  Z = 39.102/ABAR
   218  DHF1 = 21856.5-2.1734*T+7.0470E-4*(T**2)-1.6816E-7*(T*
*3)
   220  DHF2 = 2.*DHF1-13500.
   222  DHF4 = 4.*DHF1-34920.
   224  DHV = 1.8*(X1*DHF1+X2*DHF2+X4*DHF4)/ABAR
   226  HGS = HLS+DHV
   228  SGS = SLS+(DHV/T)
C:      TEST FØR STATE, I.E., SUBCØØLED, SATURATED, SUPERHEATED
```

```
   250  IF(ABS[PATM-PSAT]/PATM-1.E-4)463,463,260
   260  IF(PATM-PSAT)270,463,463
C:      CALCULATIØN ØF SUPERHEATED VAPØR PRØPERTIES
   270  UH = PATM*TWØ
   272  WH = ((PATM)**3)*FØUR
   275  X1H = 0.8
   278  X1PH = X1H
   280  X1H = X1H-(WH*(X1H**4)+UH*(X1H**2)+X1H-1.)/(4.*WH*(X1H
**3)+2.*UH*          X1H+1.)
   282  IF (ABS[X1H-X1PH]/X1H-1.E-6)284,284,278
   284  X2H = UH*(X1H**2)
   286  X4H = 1.-X1H-X2H
   288  ABARH = 39.102*(X1H+2.*X2H+4.*X4H)
   290  VH = (.730229*T)/(ABARH*PATM)
   292  ZH = 39.102/ABARH
   294  BD = X1+2.*X2+4.*X4
   296  B2 = 2.*X2/BD
   297  B4 = 4.*X4/BD
   298  BDH = X1H+2.*X2H+4.*X4H
   300  B2H = 2.*X2H/BDH
   301  B4H = 4.*X4H/BDH
   303  HGI = HGS+B2*310.67+B4*401.89
   305  HGH = HGI-B2H*310.67-B4H*401.89
        IF  (X2  .GT.  0.0)  GØ TØ 600
        XLØG2 = 0.0
        GØ TØ 610
   600  XLØG2 = X2*ALØG[X2]
   610  IF (X4   .GT.    0.0)  GØ TØ 620
        XLØG4 = 0.0
        GØ TØ 308
   620  XLØG4 = X4*ALØG[X4]
   308  SGI = SGS+B2*310.67/T+B4*401.89/T+(1.987180/ABAR)*ALØG
[PAAT]-(B2/        78.204)*(-17.66723+(24308.0/T))-(B4/156.4
14)*(-46.422+(62893.0/       T))+(1.987180/ABAR)*(X1*ALØG[X1]
+ XLØG2 + XLØG4)
        IF (X2H  .GT.  0.0)  GØ TØ 700
        XLØG2H = 0.0
        GØ TØ 710
   700  XLØG2H = X2H*ALØG[X2H]
   710  IF (X4H  .GT.  0.0)  GØ TØ 720
        XLØG4H = 0.0
        GØ TØ 310
   720  XLØG4H = X4H*ALØG[X4H]
   310  SGH = SGI-B2H*310.67/T-B4H*401.89/T-(1.987180/ABARH)*A
LØG[PATM]+(     B2H/78.204)*(-17.66700+(24308.0/T))+(B4H/
156.41)*(-46.42200+(62893.0/     T))-(1.987180/ABARH)*(X1
H*ALØG[X1H] + XLØG2H + XLØG4H)
        TFAR = T - 459.7
   HCGS = HGH/1.8
   VCGS = VH*62.428
   WRITE (1,530) TEMP, TFAR, ZH, ABARH, X2H, X4H
   IF (DELT  .EQ.  0.0)  GØ TØ 80
   TEMP = TEMP + DELT
```

```
      GØ TØ 5
  463 DISPLAY TEMP,"    SUBCØØLED ØR SATURATED STATE"
      IF (DELT  .EQ.  0.0)  GØ TØ 80
      TEMP = TEMP + DELT
      GØ TØ 5
  80  CØNTINUE
      END
```

APPENDIX 1-C: A DIGITAL COMPUTER SUBROUTINE FOR THE CALCULATION OF PROPERTIES (TRANP)*

The subroutine TRANP permits calculations of thermophysical properties of sodium, potassium, and NaK-78. All the properties included are functions of temperature only and are evaluated by using the recommended equations described in Chap. 1. The system of units is used for both input and output. Dummy branches are provided for the properties that remain to be analyzed, and, as these become available, they may be inserted in the appropriate section.

The calling sequence of the subroutine is as follows:

```
CALL TRANP (JFLUID, JPROP, TC, XX)
```

where

JFLUID is an integer code for the material in question
JPROP is an integer code for the property required
TC is the temperature in degrees C
XX is the output property value in units

The integer codes and the specific units are defined in the subroutine listing. As an example, consider the statement:

```
CALL TRANP (2, 8, 930., SPHEAT)
```

The TRANP subroutine would calculate the saturated liquid specific heat for sodium at 930°C and store the value under the name SPHEAT.

```
      SUBROUTINE TRANP (JFLUID,JPROP,TC,XX)
C
C     THIS PROGRAM IS WRITTEN IN FORTRAN IV
C
C     JFLUID MATERIAL                      JPROP   PROPERTY
C       1          SODIUM SOLID              1     ELECTRICAL RESISTIVITY (OHM-CM*E-6)
C       2          SODIUM SAT LIQUID         2     THERMAL CONDUCTIVITY (W/CM-DEG C)
C       3          SODIUM SAT VAPOR          3     SURFACE TENSION    (DYNE/CM)
C       4          NAK-77.2 SOLID            4     SONIC VELOCITY      (M/SEC)
C       5          NAK-77.2 SAT LIQUID       5     DENSITY            (G/CM**3)
C       6          NAK-77.2 SAT VAPOR        6     VISCOSITY        (0.1*G/CM-SEC)
C       7          POTASSIUM SOLID           7     VAPOR PRESSURE      (ATM)
```

---

* Prepared by J.H. Pitts, University of California, Lawrence Radiation Laboratory, Livermore, Calif., and T.C. Varljen, Westinghouse Electric Corp., Astronuclear Laboratory, Pittsburgh, Pa.

```
C       8        POTASSIUM SAT LIQUID       8    SPECIFIC HEAT       (CAL/G-DEG C)
C       9        POTASSIUM SAT VAPOR        9    KINEMATIC VISCOSITY (.01*CM**2/SEC
C                                                                    OR CENTISTOKES)
C
C
C
C     TC = TEMPERATURE IN DEGREES CENTIGRADE
C     XX = PROPERTY OUTPUT
C
C
      T  = TC
      JF = JFLUID
      JP = JPROP
      GO TO (1001, 1002, 1003, 1004, 1005, 1006, 1007, 1008, 1009),  JP
1001  GO TO (111, 112, 113, 113, 115, 113, 113, 118, 113),  JF
111   X  = 4.29+1.993E-2*T+9.848E-6*T**2
      GO TO 500
112   X  = 6.144+3.504E-2*T+5.692E-6*T**2  +1.667E-8*T**3
      GO TO 500
113   X  = 0.
      GO TO 500
115   X  = 37.66+2.307E-2*T  +7.187E-5*T**2
      GO TO 500
118   X  = 7.9896+6.3848E-2*T-15.175E-6*T**2+5.3020E-8*T**3
      GO TO 500
1002  GO TO (211, 212, 211, 211, 215, 211, 211, 218, 211), JF
211   X  = 0.
      GO TO 500
212   X  = .918-4.9E-4*T
      GO TO 500
215   X  = .214+2.07E-4*T -2.2E-7*T**2
      GO TO 500
218   X  = 0.438-2.22E-4*T+39.5/(T+273.16)
      GO TO 500
1003  GO TO (311, 312, 311, 311, 311, 311, 311, 318, 311), JF
311   X  = 0.
      GO TO 500
312   X  = 201.4-.1*7
      GO TO 500
318   X  = 115.7-0.064*T
      GO TO 500
1004  GO TO (411, 412, 411, 411, 415, 411, 411, 418, 411), JF
411   X  = 0.
      GO TO 500
412   X  = 2578.-0.52*T
      GO TO 500
415   X  = 2051.-0.53*T
      GO TO 500
418   X  = 1922.-0.54*T
      GO TO 500
1005 GO TO (511, 512, 513, 513, 515, 513, 513, 518, 513), JF
511   X  = .9725-20.11E-5*T-1.5E-7*T**2
```

```
      GO TO 500
512   X  = .9501-2.2976E-4*T-1.46E-8*T**2+5.638E-12*T**3
      GO TO 500
513   X  = 0.
      GO TO 500
515   DN2=.9501-2.2976E-4*T-1.46E-8*T**2+5.638E-12*T**3
      DN8=0.8415-2.172E-4*T-2.7DE-8*T**2+4.77E-12*T**3
      X  = 1./((.333/DN2)+(.666/DN8))
      GO TO 500
518   X  = 0.8415-2.172E-4*T-2.7DE-8*T**2+4.77E-12*T**3
      GO TO 500
1006  GO TO (611, 612, 613, 613, 615, 613, 613, 618, 613), JF
611   X  = 0.
      GO TO 500
612   DN = .9501-2.2976E-4*T -1.46E-8*T**2 +5.638E-12*T**3
      D3 = DN**(1./3.)
      IF (T.GT.500.) GO TO 6120
      X  = .1235*D3*EXP (697.*DN/(T+273.16))
      GO TO 500
6120  X  = .0851*D3*EXP (1040.*DN/(T+273.16))
      GO TO 500
613   X  = 0.
      GO TO 500
615   DN2= .9501-2.2976E-4*T-1.46E-8*T**2_5.638E-12*T**3
      DN8= 0.8415-2.172E-4*T-2.7DE-8*T**2+4.77E-12*T**3
      DN= 1./((.333/DN2)+(.666/DN8))
      D3= DN**(1./3.)
      IF (T.GT.400.) GO TO 6150
      X  = .116*D3*EXP (688.*DN/(T+273.16))
      GO TO 500
6150  X  = .082*D3*EXP (979.*DN/(T+273.16))
      GO TO 500
618   DN= 0.8415-2.172E-4*T-2.7DE-8*T**2+4.77E-12*T**3
      D3 = DN**(1./3.)
      IF (T.GT.380.) GO TO 6180
      X  = .1131*D3*EXP (680.*DN/(T+273.16))
      GO TO 500
6180  X  = .0799*D3*EXP (978.*DN/(T+273.16))
      GO TO 500
1007  T  = T+273.16
      GO TO (711, 711, 713, 711, 711, 716, 711, 711, 719), JF
711   X  = 0.
      GO TO 500
713   IF (T.GT.1250.) GO TO 7130
      X  = 10.**(6.354-5567./T -0.5*ALOG10(T))
      GO TO 500
7130  X  = 10.**(¢.6808-5544.41/T -0.61344*ALOG10(T))
      GO TO 500
716   X  = 10.**(4.114-4367./T)
      GO TO 500
719   X  = 10.**(5.992-4516./T -0.533*ALOG10(T))
      GO TO 500
1008  GO TO (811, 812, 813, 813, 813, 813, 813, 813, 813), JF
```

```
1008  GO TO (811, 812, 813, 813, 813, 813, 813, 813, 813), JF
811   X  = 0.47603+1.551E-4*T+0.2516E-5*T**2
      GO TO 500
812   X  = 0.34324-1.3868E-4*T+1.1044E-7*T**2
      GO TO 500
813   X  = 0.
      GO TO 500
1009  GO TO (911, 912, 911, 911, 915, 911, 911, 918, 911), JF
911   X  = 0.
      GO TO 500
912   DN =.9501-2.2976E-4*T -1.46E-8*T**2 +5.638E-12*T**3
      D3 = DN**(1./3.)
      IF (T.GT.500.) GO TO 9120
      V  = .1235*D3*EXP (697.*DN/(T+273.16))
      X  = .01*V/DN
      GO TO 500
9120  V  = .0851*D3*EXP (1040.*DN/(T+273.16))
      X  = .01*V/DN
      GO TO 500
915   DN2= .9501-2.2976E-4*T-1.46E-8*T**2+5.638E-12*T**3
      DN8= 0.8415-2.172E-4*T-2.7DE-8*T**2+4.77E-12*T**3
      DN = 1./((.333/DN2)+(.666/DN8))
      D3 = DN**(1./3.)
      IF (T.GT. 400.) GO TO 9150
      V  = .116*D3*EXP (688.*DN/(T+273.16))
      X  = .01*V/DN
      GO TO 500
9150  V  = .082*D3*EXP (979.*DN/(T+273.16))
      X  = .01*V/DN
      GO TO 500
918   DN = 0.8415-2.172E-4*T-2.7DE-8*T**2+4.77E-12*T**3
      D3 = DN**(1./3.)
      IF (T.GT.380.) GO TO 9180
      V  = .1131*D3*EXP (680.*DN/(T+273.16))
      X  = .01*V/DN
      GO TO 500
9180  V  = .0799*D3*EXP (978.*DN/(T+273.16))
      X  = .01*V/DN
500   XX = X
      RETURN
      END
```

APPENDIX 1-D: VAPOR PROPERTIES OF POTASSIUM AND

TABLE D.1 - Vapor Properties

Temperature °C	Temperature °F	Enthalpy H Cal/g	Enthalpy H Btu/lb	Entropy S Cal/g-°C or Btu/lb-°F	Specific volume V Cm^3/g
25 Atm					
1288.85	2351.91	681.0	1227.3	0.9914	0.1031×10^3
1300.00	2371.98	684.9	1232.8	0.9934	0.1045×10^3
1350.00	2461.98	698.2	1256.8	1.0018	0.1109×10^3
1400.00	2551.98	710.6	1279.1	1.0094	0.1170×10^3
1450.00	2641.98	722.3	1300.1	1.0164	0.1229×10^3
1500.00	2731.98	733.2	1319.9	1.0028	0.1286×10^3
10 Atm					
1086.59	1987.84	673.2	1211.8	1.0235	0.2402×10^3
1100.00	2011.98	677.0	1218.6	1.0263	0.2444×10^3
1150.00	2101.98	690.1	1242.2	1.0356	0.2596×10^3
1200.00	2191.98	702.1	1263.8	1.0439	0.2740×10^3
1250.00	2281.98	713.1	1283.6	1.0513	0.2879×10^3
1300.00	2371.98	723.4	1302.1	1.0579	0.3012×10^3
1350.00	2461.98	733.0	1319.5	1.0640	0.3142×10^3
1400.00	2551.98	742.2	1335.9	1.0697	0.3268×10^3
1450.00	2641.98	750.9	1351.6	1.0749	0.3391×10^3
1500.00	2731.98	759.3	1366.7	1.0799	0.3512×10^3
5 Atm					
966.25	1771.23	667.6	1201.7	1.0497	0.4538×10^3
1000.00	1831.98	676.7	1218.0	1.0567	0.4740×10^3
1050.00	1921.98	688.9	1240.1	1.0661	0.5025×10^3
1100.00	2011.98	700.1	1260.2	1.0744	0.5297×10^3
1150.00	2101.98	710.3	1278.6	1.0816	0.5558×10^3
1200.00	2191.98	719.8	1295.7	1.0882	0.5811×10^3
1250.00	2281.98	728.8	1311.8	1.0942	0.6058×10^3
1300.00	2371.98	737.3	1327.1	1.0997	0.6298×10^3
1350.00	2461.98	745.4	1341.8	1.1049	0.6535×10^3
1400.00	2551.98	753.3	1356.0	1.1097	0.6767×10^3
1450.00	2641.98	761.0	1369.8	1.1144	0.6997×10^3
1500.00	2731.98	768.4	1383.2	1.1188	0.7223×10^3
2.5 Atm					
866.03	1590.84	662.4	1192.3	1.0765	0.8564×10^3
900.00	1651.98	671.4	1208.5	1.0842	0.8957×10^3
950.00	1741.98	683.3	1230.0	1.0941	0.9509×10^3
1000.00	1831.98	694.0	1249.2	1.1026	0.1004×10^4
1050.00	1921.98	703.8	1266.8	1.1101	0.1053×10^4
1100.00	2011.98	712.8	1283.1	1.1167	0.1102×10^4
1150.00	2101.98	721.3	1298.5	1.1228	0.1150×10^4
1200.00	2191.98	729.5	1313.1	1.1284	0.1197×10^4
1250.00	2281.98	737.2	1327.1	1.1336	0.1243×10^4
1300.00	2371.98	744.8	1340.6	1.1385	0.1288×10^4

---

* The first line in each pressure group

SODIUM FOR SATURATED AND SUPERSATURATED CONDITIONS

of Potassium*

Specific volume V Ft^3/lb	Compressibility factor *ZH*	Average mol. weight ABARH	Dimer *X2H*	Tetramer *X4H*
		25 Atm		
0.1651×10	0.7864	0.4971×10^{2}	0.1684	0.3434×10^{-1}
0.1674×10	0.7918	0.4938×10^{2}	0.1654	0.3249×10^{-1}
0.1776×10	0.8140	0.4803×10^{2}	0.1521	0.2543×10^{-1}
0.1874×10	0.8332	0.4692×10^{2}	0.1400	0.2001×10^{-1}
0.1969×10	0.8499	0.4600×10^{2}	0.1290	0.1584×10^{-1}
0.2060×10	0.8643	0.4523×10^{2}	0.1190	0.1263×10^{-1}
		10 Atm		
0.3849×10	0.8421	0.4643×10^{2}	0.1436×10^{-1}	0.1461×10^{-1}
0.3916×10	0.8484	0.4608×10^{2}	0.1388×10^{-1}	0.1325×10^{-1}
0.4159×10	0.8693	0.4497×10^{2}	0.1223×10^{-1}	0.9295×10^{-2}
0.4390×10	0.8866	0.4410×10^{2}	0.1081×10^{-1}	0.6598×10^{-2}
0.4612×10	0.9008	0.4340×10^{2}	0.9587×10^{-1}	0.4747×10^{-2}
0.4826×10	0.9126	0.4284×10^{2}	0.8537×10^{-1}	0.3463×10^{-2}
0.5033×10	0.9224	0.4238×10^{2}	0.7635×10^{-1}	0.2561×10^{-2}
0.5235×10	0.9307	0.4200×10^{2}	0.6860×10^{-1}	0.1921×10^{-2}
0.5432×10	0.9378	0.4169×10^{2}	0.6190×10^{-1}	0.1459×10^{-2}
0.5625×10	0.9438	0.4142×10^{2}	0.5610×10^{-1}	0.1123×10^{-2}
		5 Atm		
0.7270×10	0.8724	0.4481×10^{2}	0.1243×10^{-1}	0.7276×10^{-2}
0.7593×10	0.8871	0.4407×10^{2}	0.1112×10^{-1}	0.5347×10^{-2}
0.8050×10	0.9049	0.4320×10^{2}	0.9470×10^{-1}	0.3443×10^{-2}
0.8485×10	0.9191	0.4253×10^{2}	0.8111×10^{-1}	0.2263×10^{-2}
0.8904×10	0.9306	0.4201×10^{2}	0.6994×10^{-1}	0.1518×10^{-2}
0.9309×10	0.9399	0.4159×10^{2}	0.6071×10^{-1}	0.1040×10^{-2}
0.9704×10	0.9476	0.4126×10^{2}	0.5305×10^{-1}	0.7270×10^{-2}
0.1008×10	0.9539	0.4098×10^{2}	0.4667×10^{-1}	0.5176×10^{-3}
0.1046×10	0.95923	0.4076×10^{2}	0.4132×10^{-1}	0.3752×10^{-3}
0.1084×10	0.9637	0.4057×10^{2}	0.3681×10^{-1}	0.2765×10^{-3}
0.1120×10	0.9674	0.4076×10^{2}	0.3297×10^{-1}	0.2071×10^{-3}
0.1157×10	0.9707	0.4028×10^{2}	0.2970×10^{-1}	0.1574×10^{-3}
		2.5 Atm		
0.1371×10^{2}	0.8956	0.4365×10^{2}	0.1059×10^{-1}	0.3509×10^{-2}
0.1434×10^{2}	0.9096	0.4298×10^{2}	0.9213×10^{-1}	0.2397×10^{-2}
0.1523×10^{2}	0.9261	0.4222×10^{2}	0.7553×10^{-1}	0.1402×10^{-2}
0.1607×10^{2}	0.9389	0.4164×10^{2}	0.6250×10^{-1}	0.8445×10^{-3}
0.1688×10^{2}	0.9489	0.4120×10^{2}	0.5223×10^{-1}	0.5238×10^{-3}
0.1766×10^{2}	0.9568	0.4086×10^{2}	0.4408×10^{-1}	0.3341×10^{-3}
0.1843×10^{2}	0.9631	0.4059×10^{2}	0.3755×10^{-1}	0.2189×10^{-3}
0.1918×10^{2}	0.9683	0.4038×10^{2}	0.3228×10^{-1}	0.1471×10^{-3}
0.1991×10^{2}	0.9724	0.4020×10^{2}	0.2798×10^{-1}	0.1011×10^{-3}
0.2064×10^{2}	0.9759	0.4006×10^{2}	0.2446×10^{-1}	0.7108×10^{-4}

---

pertains to the saturated condition.

TABLE D.1 - Vapor Properties

Temperature		Enthalpy H		Entropy S	Specific volume V
°C	°F	Cal/g	Btu/lb	Cal/g-°C or Btu/lb-°F	Cm^3/g
				2.5 Atm	
1350.00	2461.98	752.1	1353.8	1.1432	0.1333×10^4
1400.00	2551.98	759.3	1366.8	1.1476	0.1377×10^4
1450.00	2641.98	766.3	1379.4	1.1519	0.1422×10^4
1500.00	2731.98	773.3	1391.9	1.1560	0.1465×10^4
				1 Atm	
756.58	1393.84	656.2	1181.2	1.1134	0.1985×10^4
800.00	1471.98	667.3	1201.2	1.1238	0.2106×10^4
850.00	1561.98	678.5	1221.3	1.1339	0.2237×10^4
900.00	1651.98	688.4	1239.2	1.1424	0.2362×10^4
950.00	1741.98	697.4	1255.4	1.1499	0.2483×10^4
1000.00	1831.98	705.8	1270.5	1.1565	0.2601×10^4
1050.00	1921.98	713.8	1284.8	1.1626	0.2715×10^4
1100.00	2011.98	721.3	1298.5	1.1681	0.2828×10^4
1150.00	2101.98	728.7	1311.6	1.1734	0.2940×10^4
1200.00	2191.98	735.8	1324.5	1.1783	0.3050×10^4
1250.00	2281.98	742.8	1337.0	1.1829	0.3159×10^4
1300.00	2371.98	749.6	1349.4	1.1874	0.3268×10^4
1350.00	2461.98	756.4	1361.6	1.1917	0.3376×10^4
1400.00	2551.98	763.1	1373.6	1.1959	0.3484×10^4
1450.00	2641.98	769.8	1385.6	1.1999	0.3591×10^4
1500.00	2731.98	776.4	1397.5	1.2038	0.3697×10^4
				0.5 Atm	
687.13	1268.82	652.1	1173.0	1.1420	0.3759×10^4
700.00	1291.98	655.5	1179.9	1.1455	0.3831×10^4
750.00	1381.98	667.3	1201.2	1.1572	0.4096×10^4
800.00	1471.98	677.5	1219.6	1.1668	0.4346×10^4
850.00	1561.98	686.6	1235.9	1.1750	0.4587×10^4
900.00	1651.98	695.0	1251.0	1.1822	0.4819×10^4
950.00	1741.98	702.8	1265.0	1.1886	0.5046×10^4
1000.00	1831.98	710.2	1278.5	1.1945	0.5270×10^4
1050.00	1921.98	717.4	1291.4	1.2000	0.5490×10^4
1100.00	2011.98	724.4	1304.0	1.2051	0.5709×10^4
1150.00	2101.98	731.3	1316.4	1.2100	0.5925×10^4
1200.00	2191.98	738.0	1328.5	1.2147	0.6141×10^4
1250.00	2281.98	744.7	1340.5	1.2192	0.6355×10^4
1300.00	2371.98	751.3	1352.4	1.2235	0.6569×10^4
1350.00	2461.98	757.9	1364.3	1.2276	0.6782×10^4
1400.00	2551.98	764.4	1376.0	1.2317	0.6994×10^4
1450.00	2641.98	770.9	1387.7	1.2356	0.7206×10^4
1500.00	2731.98	777.4	1399.4	1.2395	0.7418×10^4

of Potassium (Continued)

Specific volume V Ft^3/lb	Compressibility factor *ZH*	Average mol. weight ABARH	Dimer *X2H*	Tetramer *X4H*
		2.5 Atm		
$0\ 2136 \times 10^{2}$	0.9787	0.3995×10^{2}	0.2153×10^{-1}	0.5096×10^{-4}
0.2207×10^{2}	0.9811	0.3985×10^{2}	0.1909×10^{-1}	0.3722×10^{-4}
0.2277×10^{2}	0.9831	0.3977×10^{2}	0.1704×10^{-1}	0.2766×10^{-4}
0.2348×10^{2}	0.9848	0.3970×10^{2}	0.1530×10^{-1}	0.2088×10^{-4}
		1 Atm		
0.3180×10^{2}	0.9189	0.4255×10^{2}	0.8430×10^{-1}	0.1290×10^{-2}
0.3374×10^{2}	0.9353	0.4180×10^{2}	0.6707×10^{-1}	0.6982×10^{-3}
0.3584×10^{2}	0.9493	0.4118×10^{2}	0.5223×10^{-1}	0.3587×10^{-3}
0.3735×10^{2}	0.9598	0.4073×10^{2}	0.4129×10^{-1}	0.1927×10^{-3}
0.3978×10^{2}	0.9676	0.4041×10^{2}	0.3314×10^{-1}	0.1079×10^{-3}
0.4166×10^{2}	0.9735	0.4016×10^{2}	0.2697×10^{-1}	0.6293×10^{-4}
0.4350×10^{2}	0.9781	0.3997×10^{2}	0.2226×10^{-1}	0.3805×10^{-4}
0.4531×10^{2}	0.9816	0.3983×10^{2}	0.1859×10^{-1}	0.2379×10^{-4}
0.4709×10^{2}	0.9844	0.3971×10^{2}	0.1571×10^{-1}	0.1534×10^{-4}
0.4886×10^{2}	0.9867	0.3962×10^{2}	0.1342×10^{-1}	0.1017×10^{-4}
0.5061×10^{2}	0.9885	0.3955×10^{2}	0.1157×10^{-1}	0.6925×10^{-5}
0.5235×10^{2}	0.9900	0.3949×10^{2}	0.1007×10^{-1}	0.4824×10^{-5}
0.5408×10^{2}	0.9912	0.3944×10^{2}	0.8841×10^{-2}	0.3434×10^{-5}
0.5580×10^{2}	0.9922	0.3940×10^{2}	0.7816×10^{-2}	0.2494×10^{-5}
0.5752×10^{2}	0.9930	0.3937×10^{2}	0.6958×10^{-2}	0.1844×10^{-5}
0.5923×10^{2}	0.9938	0.3934×10^{2}	0.6234×10^{-2}	0.1386×10^{-5}
		0.5 Atm		
0.6022×10^{2}	0.9328	0.4191×10^{2}	0.7020×10^{-1}	0.5926×10^{-3}
0.6136×10^{2}	0.9379	0.4168×10^{2}	0.6470×10^{-1}	0.4763×10^{-3}
0.6561×10^{2}	0.9539	0.4099×10^{2}	0.4768×10^{-1}	0.2117×10^{-3}
0.6963×10^{2}	0.9 50	0.4051×10^{2}	0.3586×10^{-1}	0.9981×10^{-4}
0.7347×10^{2}	0.9730	0.4018×10^{2}	0.2751×10^{-1}	0.4977×10^{-4}
0.7720×10^{2}	0.9788	0.3994×10^{2}	0.2151×10^{-1}	0.2615×10^{-4}
0.8084×10^{2}	0.9831	0.3977×10^{2}	0.1712×10^{-1}	0.1441×10^{-4}
0.8442×10^{2}	0.9863	0.3964×10^{2}	0.1385×10^{-1}	0.8301×10^{-5}
0.8795×10^{2}	0.9887	0.3954×10^{2}	0.1138×10^{-1}	0.4972×10^{-5}
0.9145×10^{2}	0.9906	0.3947×10^{2}	0.9472×10^{-2}	0.3086×10^{-5}
0.9492×10^{2}	0.9920	0.3941×10^{2}	0.7983×10^{-2}	0.1978×10^{-5}
0.9837×10^{2}	0.9932	0.3936×10^{2}	0.6803×10^{-2}	0.1306×10^{-5}
0.1018×10^{3}	0.9941	0.3933×10^{2}	0.5857×10^{-2}	Zero
0.1052×10^{3}	0.9949	0.3930×10^{2}	0.5089×10^{-2}	
0.1086×10^{3}	0.9955	0.3927×10^{2}	0.4460×10^{-2}	
0.1120×10^{3}	0.9960	0.3925×10^{2}	0.3939×10^{-2}	
0.1154×10^{3}	0.9965	0.3923×10^{2}	0.3503×10^{-2}	
0.1188×10^{3}	0.9968	0.3922×10^{2}	0.3136×10^{-2}	

TABLE D.1 - Vapor Properties

Temperature		Enthalpy H		Entropy S	Specific volume V
°C	°F	Cal/g	Btu/lb	Cal/g-°C or Btu/lb-°F	Cm³/g
			0.25 Atm		
626.65	1159.95	648.4	1167.1	1.1713	0.7133×10^4
650.00	1201.98	654.3	1177.7	1.1777	0.7384×10^4
700.00	1291.98	665.3	1197.5	1.1891	0.7894×10^4
750.00	1381.98	674.7	1214.6	1.1985	0.8378×10^4
800.00	1471.98	683.2	1229.9	1.2065	0.8843×10^4
850.00	1561.98	691.1	1244.0	1.2135	0.9296×10^4
900.00	1651.98	698.5	1257.3	1.2199	0.9740×10^4
950.00	1741.98	705.6	1270.2	1.2257	0.1017×10^5
1000.00	1831.98	712.5	1282.6	1.2312	0.1061×10^5
1050.00	1921.98	719.3	1294.8	1.2364	0.1104×10^5
1100.00	2011.98	726.0	1306.9	1.2413	0.1147×10^5
1150.00	2101.98	732.6	1318.8	1.2460	0.1189×10^5
1200.00	2191.98	739.2	1330.6	1.2505	0.1232×10^5
1250.00	2281.98	745.7	1342.3	1.2549	0.1274×10^5
1300.00	2371.98	752.2	1354.0	1.2591	0.1317×10^5
1350.00	2461.98	758.7	1365.6	1.2632	0.1359×10^5
1400.00	2551.98	765.1	1377.2	1.2672	0.1401×10^5
1450.00	2641.98	771.5	1388.8	1.2711	0.1443×10^5
1500.00	2731.98	778.0	1400.4	1.2749	0.1486×10^5
			0.1 Atm		
557.72	1035.88	643.9	1159.1	1.2107	0.1668×10^5
600.00	1111.98	653.7	1176.8	1.2220	0.1777×10^5
650.00	1201.98	663.5	1194.3	1.2327	0.1897×10^5
700.00	1291.98	671.9	1209.5	1.2415	0.2013×10^5
750.00	1381.98	679.7	1223.4	1.2491	0.2125×10^5
800.00	1471.98	686.9	1236.5	1.2559	0.2235×10^5
850.00	1561.98	693.9	1249.1	1.2622	0.2343×10^5
900.00	1651.98	700.7	1261.3	1.2680	0.2450×10^5
950.00	1741.98	707.4	1273.3	1.2735	0.2557×10^5
1000.00	1831.98	714.0	1285.2	1.2787	0.2664×10^5
1050.00	1921.98	720.5	1297.0	1.2837	0.2770×10^5
1100.00	2011.98	727.0	1308.6	1.2884	0.2876×10^5
1150.00	2101.98	733.5	1320.3	1.2930	0.2981×10^5
1200.00	2191.98	739.9	1331.9	1.2975	0.3087×10^5
1250.00	2281.98	746.3	1343.4	1.3018	0.3192×10^5
1300.00	2371.98	752.7	1355.0	1.3059	0.3297×10^5
1350.00	2461.98	759.1	1366.5	1.3100	0.3403×10^5
1400.00	2551.98	765.5	1378.0	1.3140	0.3508×10^5
1450.00	2641.98	771.9	1389.5	1.3178	0.3613×10^5
1500.00	2731.98	778.3	1401.0	1.3216	0.3718×10^5

of Potassium (Continued)

Specific volume V Ft^3/lb	Compressibility factor *ZH*	Average mol. weight ABARH	Dimer *X2H*	Tetramer *X4H*
		0.25 Atm		
0.1142×10^{3}	0.9444	0.4140×10^{2}	0.5805×10^{-1}	0.2679×10^{-3}
0.1182×10^{3}	0.9529	0.4103×10^{2}	0.4889×10^{-1}	0.1698×10^{-3}
0.1264×10^{3}	0.9664	0.4045×10^{2}	0.3450×10^{-1}	0.6773×10^{-4}
0.1342×10^{3}	0.9755	0.4008×10^{2}	0.2500×10^{-1}	0.2910×10^{-4}
0.1416×10^{3}	0.9817	0.3983×10^{2}	0.1858×10^{-1}	0.1340×10^{-4}
0.1489×10^{3}	0.9860	0.3965×10^{2}	0.1414×10^{-1}	0.6572×10^{-5}
0.1560×10^{3}	0.9891	0.3953×10^{2}	0.1099×10^{-1}	0.3412×10^{-5}
0.1630×10^{3}	0.9913	0.3944×10^{2}	0.8711×10^{-2}	0.1864×10^{-5}
0.1699×10^{3}	0.9930	0.3937×10^{2}	0.7025×10^{-2}	0.1066×10^{-5}
0.1768×10^{3}	0.9942	0.3932×10^{2}	0.5755×10^{-2}	Zero
0.1837×10^{3}	0.9952	0.3928×10^{2}	0.4781×10^{-2}	
0.1905×10^{3}	0.9959	0.3925×10^{2}	0.4023×10^{-2}	
0.1974×10^{3}	0.9965	0.3923×10^{2}	0.3424×10^{-2}	
0.2042×10^{3}	0.9970	0.3921×10^{2}	0.2945×10^{-2}	
0.2109×10^{3}	0.9974	0.3920×10^{2}	0.2557×10^{-2}	
0.2177×10^{3}	0.9977	0.3918×10^{2}	0.2240×10^{-2}	
0.2245×10^{3}	0.9980	0.3917×10^{2}	0.1977×10^{-2}	
0.2312×10^{3}	0.9982	0.3917×10^{2}	0.1757×10^{-2}	
0.2380×10^{3}	0.9984	0.3916×10^{2}	0.1573×10^{-2}	
		0.1 Atm		
0.2672×10^{3}	0.9569	0.4086×10^{2}	0.4474×10^{-1}	0.9205×10^{-4}
0.2846×10^{3}	0.9698	0.4031×10^{2}	0.3097×10^{-1}	0.3494×10^{-4}
0.3040×10^{3}	0.9796	0.3991×10^{2}	0.2073×10^{-1}	0.1222×10^{-4}
0.3224×10^{3}	0.9858	0.3966×10^{2}	0.1438×10^{-1}	0.4709×10^{-5}
0.3404×10^{3}	0.9897	0.3950×10^{2}	0.1030×10^{-1}	0.1977×10^{-5}
0.3580×10^{3}	0.9924	0.3939×10^{2}	0.7600×10^{-2}	Zero
0.3753×10^{3}	0.9942	0.3932×10^{2}	0.5752×10^{-2}	
0.3926×10^{3}	0.9955	0.3927×10^{2}	0.4455×10^{-2}	
0.4097×10^{3}	0.9964	0.3923×10^{2}	0.3521×10^{-2}	
0.4267×10^{3}	0.9971	0.3921×10^{2}	0.2833×10^{-2}	
0.4437×10^{3}	0.9976	0.3919×10^{2}	0.2317×10^{-2}	
0.4607×10^{3}	0.9980	0.3917×10^{2}	0.1923×10^{-2}	
0.4776×10^{3}	0.9983	0.3916×10^{2}	0.1617×10^{-2}	
0.4945×10^{3}	0.9986	0.3915×10^{2}	0.1375×10^{-2}	
0.5114×10^{3}	0.9988	0.3914×10^{2}	0.1182×10^{-2}	
0.5282×10^{3}	0.9989	0.3914×10^{2}	0.1026×10^{-2}	
0.5451×10^{3}	0.9991	0.3913×10^{2}	0.8984×10^{-3}	
0.5619×10^{3}	0.9992	0.3913×10^{2}	0.7927×10^{-3}	
0.5788×10^{3}	0.9992	0.3912×10^{2}	0.7046×10^{-3}	
0.5956×10^{3}	0.9993	0.3912×10^{2}	0.6304×10^{-3}	

TABLE D.1 - Vapor Properties

Temperature		Enthalpy H		Entropy S	Specific volume V
°C	°F	Cal/g	Btu/lb	Cal/g-°C or Btu/lb-°F	Cm^3/g
		0.05 Atm			
512.34	954.19	640.8	1153.5	1.2408	0.3180×10^5
550.00	1021.98	649.3	1168.8	1.2513	0.3369×10^5
600.00	1111.98	658.7	1185.7	1.2622	0.3607×10^5
650.00	1201.98	666.9	1200.4	1.2711	0.3833×10^5
700.00	1291.98	674.3	1213.9	1.2788	0.4054×10^5
750.00	1381.98	681.4	1226.6	1.2858	0.4271×10^5
800.00	1471.98	688.2	1238.9	1.2921	0.4486×10^5
850.00	1561.98	694.9	1250.9	1.2981	0.4700×10^5
900.00	1651.98	701.5	1262.7	1.3037	0.4912×10^5
950.00	1741.98	708.0	1274.4	1.3091	0.5124×10^5
1000.00	1831.98	714.5	1286.1	1.3142	0.5335×10^5
1050.00	1921.98	720.9	1297.7	1.3191	0.5546×10^5
1100.00	2011.98	727.3	1309.2	1.3238	0.5757×10^5
1150.00	2101.98	733.7	1320.8	1.3284	0.5968×10^5
1200.00	2191.98	740.1	1332.3	1.3328	0.6178×10^5
1250.00	2281.98	746.5	1343.8	1.3371	0.6388×10^5
1300.00	2371.98	752.9	1355.3	1.3412	0.6599×10^5
1350.00	2461.98	759.3	1366.7	1.3453	0.6809×10^5
1400.00	2551.98	765.7	1378.2	1.3492	0.7019×10^5
1450.00	2641.98	772.0	1389.7	1.3531	0.7229×10^5
1500.00	2731.98	778.3	1401.1	1.3569	0.7439×10^5
		0.025 Atm			
471.74	881.11	637.9	1148.2	1.2713	0.6072×10^5
500.00	931.98	644.1	1159.4	1.2794	0.6352×10^5
550.00	1021.98	653.4	1176.1	1.2908	0.6821×10^5
600.00	1111.98	661.4	1190.5	1.3000	0.7270×10^5
650.00	1201.98	668.7	1203.6	1.3080	0.7707×10^5
700.00	1291.98	675.6	1216.1	1.3151	0.8138×10^5
750.00	1381.98	682.3	1228.2	1.3217	0.8566×10^5
800.00	1471.98	688.9	1240.0	1.3279	0.8990×10^5
850.00	1561.98	695.4	1251.8	1.3337	0.9414×10^5
900.00	1651.98	701.9	1263.4	1.3392	0.9836×10^5
950.00	1741.98	708.3	1275.0	1.3445	0.1025×10^5
1000.00	1831.98	714.7	1286.5	1.3496	0.1067×10^5
1050.00	1921.98	721.1	1298.0	1.3545	0.1110×10^5
1100.00	2011.98	727.5	1309.5	1.3592	0.1152×10^5
1150.00	2101.98	733.9	1321.0	1.3637	0.1194×10^5
1200.00	2191.98	740.3	1332.5	1.3681	0.1236×10^5
1250.00	2281.98	746.6	1344.0	1.3724	0.1278×10^5
1300.00	2371.98	753.0	1355.4	1.3765	0.1320×10^5
1350.00	2461.98	759.4	1366.9	1.3806	0.1362×10^5
1400.00	2551.98	765.7	1378.3	1.3845	0.1404×10^5
1450.00	2641.98	772.1	1389.8	1.3884	0.1446×10^5
1500.00	2731.98	778.4	1401.2	1.3922	0.1488×10^5

of Potassium (Continued)

Specific volume V Ft^3/lb	Compressibility factor *ZH*	Average mol. weight ABARH	Dimer *X2H*	Tetramer *X4H*
		0.05 Atm		
0.5094×10^{3}	0.9646	0.4053×10^{2}	0.3653×10^{-1}	0.4051×10^{-4}
0.5398×10^{3}	0.9754	0.4008×10^{2}	0.2516×10^{-1}	0.1522×10^{-4}
0.5777×10^{3}	0.9842	0.3972×10^{2}	0.1597×10^{-1}	0.4645×10^{-5}
0.6141×10^{3}	0.9895	0.3951×10^{2}	0.1058×10^{-1}	0.1592×10^{-5}
0.6495×10^{3}	0.9927	0.3938×10^{2}	0.7296×10^{-2}	Zero
0.6843×10^{3}	0.9948	0.3930×10^{2}	0.5206×10^{-2}	
0.7187×10^{3}	0.9961	0.3925×10^{2}	0.3829×10^{-2}	
0.7529×10^{3}	0.9971	0.3921×10^{2}	0.2892×10^{-2}	
0.7869×10^{3}	0.9977	0.3918×10^{2}	0.2237×10^{-2}	
0.8208×10^{3}	0.9982	0.3917×10^{2}	0.1766×10^{-2}	
0.8547×10^{3}	0.9985	0.3915×10^{2}	0.1420×10^{-2}	
0.8885×10^{3}	0.9988	0.3914×10^{2}	0.1161×10^{-2}	
0.9222×10^{3}	0.9990	0.3913×10^{2}	0.9636×10^{-3}	
0.9560×10^{3}	0.9991	0.3913×10^{2}	0.8098×10^{-3}	
0.9897×10^{3}	0.9993	0.3912×10^{2}	0.6887×10^{-3}	
0.1023×10^{4}	0.9994	0.3912×10^{2}	0.5919×10^{-3}	
0.1057×10^{4}	0.9994	0.3912×10^{2}	0.5136×10^{-3}	
0.1090×10^{4}	0.9995	0.3911×10^{2}	0.4496×10^{-3}	
0.1124×10^{4}	0.9996	0.3911×10^{2}	0.3967×10^{-3}	
0.1158×10^{4}	0.9996	0.3911×10^{2}	0.3525×10^{-3}	
0.1191×10^{4}	0.9996	0.3911×10^{2}	0.3154×10^{-3}	
		0.025 Atm		
0.9726×10^{3}	0.9710	0.4026×10^{2}	0.2971×10^{-1}	0.1767×10^{-4}
0.1017×10^{4}	0.9788	0.3994×10^{2}	0.2163×10^{-1}	0.7702×10^{-5}
0.1092×10^{4}	0.9872	0.3960×10^{2}	0.1290×10^{-1}	0.2001×10^{-5}
0.1164×10^{4}	0.9919	0.3941×10^{2}	0.8113×10^{-2}	Zero
0.1234×10^{4}	0.9946	0.3931×10^{2}	0.5349×10^{-2}	
0.1303×10^{4}	0.9963	0.3924×10^{2}	0.3674×10^{-2}	
0.1372×10^{4}	0.9973	0.3920×10^{2}	0.2616×10^{-2}	
0.1440×10^{4}	0.9980	0.3917×10^{2}	0.1922×10^{-2}	
0.1508×10^{4}	0.9985	0.3915×10^{2}	0.1450×10^{-2}	
0.1575×10^{4}	0.9988	0.3914×10^{2}	0.1121×10^{-2}	
0.1643×10^{4}	0.9991	0.3913×10^{2}	0.8849×10^{-3}	
0.1710×10^{4}	0.9992	0.3912×10^{2}	0.7114×10^{-3}	
0.1778×10^{4}	0.9994	0.3912×10^{2}	0.5815×10^{-3}	
0.1845×10^{4}	0.9995	0.3912×10^{2}	0.4822×10^{-3}	
0.1912×10^{4}	0.9995	0.3911×10^{2}	0.4052×10^{-3}	
0.1980×10^{4}	0.9996	0.3911×10^{2}	0.3445×10^{-3}	
0.2047×10^{4}	0.9997	0.3911×10^{2}	0.2961×10^{-3}	
0.2114×10^{4}	0.9997	0.3911×10^{2}	0.2569×10^{-3}	
0.2182×10^{4}	0.9997	0.3911×10^{2}	0.2249×10^{-3}	
0.2249×10^{4}	0.9998	0.3910×10^{2}	0.1984×10^{-3}	
0.2316×10^{4}	0.9998	0.3910×10^{2}	0.1763×10^{-3}	
0.2383×10^{4}	0.9998	0.3910×10^{2}	0.1577×10^{-3}	

TABLE D.1 - Vapor Properties

Temperature °C	°F	Enthalpy H Cal/g	Btu/lb	Entropy S Cal/g-°C or Btu/lb-°F	Specific volume V Cm^3/g
0.01 Atm					
424.21	795.56	634.2	1141.6	1.3119	0.1431×10^6
450.00	841.98	639.6	1151.3	1.3194	0.1493×10^6
500.00	931.98	648.4	1167.1	1.3308	0.1608×10^6
550.00	1021.98	656.0	1180.8	1.3401	0.1718×10^6
600.00	1111.98	663.0	1193.5	1.3482	0.1826×10^6
650.00	1201.98	669.7	1205.6	1.3556	0.1933×10^6
700.00	1291.98	676.3	1217.4	1.3624	0.2039×10^6
750.00	1381.98	682.8	1229.1	1.3687	0.2144×10^6
800.00	1471.98	689.3	1240.7	1.3748	0.2250×10^6
850.00	1561.98	695.7	1252.3	1.3805	0.2355×10^6
900.00	1651.98	702.1	1263.8	1.3860	0.2460×10^6
950.00	1741.98	708.5	1275.3	1.3912	0.2565×10^6
1000.00	1831.98	714.9	1286.8	1.3963	0.2670×10^6
1050.00	1921.98	721.2	1298.3	1.4011	0.2776×10^6
1100.00	2011.98	727.6	1309.7	1.4058	0.2881×10^6
1150.00	2101.98	734.0	1321.2	1.4103	0.2986×10^6
1200.00	2191.98	740.3	1332.6	1.4147	0.3091×10^6
1250.00	2281.98	746.7	1344.1	1.4190	0.3195×10^6
1300.00	2371.98	753.0	1355.5	1.4231	0.3300×10^6
1350.00	2461.98	759.4	1367.0	1.4271	0.3405×10^6
1400.00	2551.98	765.8	1378.4	1.4311	0.3510×10^6
1450.00	2641.98	772.1	1389.9	1.4350	0.3615×10^6
1500.00	2731.98	778.5	1401.3	1.4387	0.3720×10^6
0.005 Atm					
392.16	737.87	631.6	1136.9	1.3428	0.2742×10^6
400.00	751.98	633.2	1139.9	1.3452	0.2780×10^6
450.00	841.98	642.3	1156.1	1.3579	0.3010×10^6
500.00	931.98	649.9	1169.8	1.3678	0.3230×10^6
550.00	1021.98	656.9	1182.4	1.3763	0.3445×10^6
600.00	1111.98	663.6	1194.5	1.3840	0.3658×10^6
650.00	1201.98	670.1	1206.2	1.3911	0.3870×10^6
700.00	1291.98	676.6	1217.9	1.3978	0.4081×10^6
750.00	1381.98	683.0	1229.5	1.4041	0.4291×10^6
800.00	1471.98	689.4	1241.0	1.4101	0.4502×10^6
850.00	1561.98	695.8	1252.5	1.4158	0.4712×10^6
900.00	1651.98	702.2	1264.0	1.4213	0.4922×10^6
950.00	1741.98	708.5	1275.4	1.4265	0.5132×10^6
1000.00	1831.98	714.9	1286.9	1.4315	0.5342×10^6
1050.00	1921.98	721.3	1298.3	1.4364	0.5552×10^6
1100.00	2011.98	727.6	1309.8	1.4410	0.5762×10^6
1150.00	2101.98	734.0	1321.2	1.4456	0.5972×10^6
1200.00	2191.98	740.4	1332.7	1.4499	0.6182×10^6
1250.00	2281.98	746.7	1344.1	1.4542	0.6392×10^6

of Potassium (Continued)

Specific volume V Ft^3/lb	Compressibility factor *ZH*	Average mol. weight ABARH	Dimer *X2H*	Tetramer *X4H*
		0.01 Atm		
0.2292×10^4	0.9779	0.3998×10^2	0.2248×10^{-1}	0.5837×10^{-5}
0.2392×10^4	0.9841	0.3973×10^2	0.1608×10^{-1}	0.2435×10^{-5}
0.2576×10^4	0.9911	0.3044×10^2	0.8879×10^{-2}	Zero
0.2752×10^4	0.9947	0.3930×10^2	0.5240×10^{-2}	
0.2925×10^4	0.9967	0.3923×10^2	0.3277×10^{-2}	
0.3096×10^4	0.9978	0.3918×10^2	0.2153×10^{-2}	
0.3266×10^4	0.9985	0.3915×10^2	0.1476×10^{-2}	
0.3435×10^4	0.9989	0.3914×10^2	0.1049×10^{-2}	
0.3604×10^4	0.9992	0.3913×10^2	0.7705×10^{-3}	
0.3773×10^4	0.9994	0.3912×10^2	0.5812×10^{-3}	
0.3941×10^4	0.9995	0.3911×10^2	0.4490×10^{-3}	
0.4110×10^4	0.9996	0.3911×10^2	0.3543×10^{-3}	
0.4278×10^4	0.9997	0.3911×10^2	0.2848×10^{-3}	
0.4446×10^4	0.9997	0.3911×10^2	0.2327×10^{-3}	
0.4614×10^4	0.9998	0.3910×10^2	0.1930×10^{-3}	
0.4783×10^4	0.9998	0.3910×10^2	0.1621×10^{-3}	
0.4951×10^4	0.9998	0.3910×10^2	0.1378×10^{-3}	
0.5119×10^4	0.9998	0.3910×10^2	0.1184×10^{-3}	
0.5287×10^4	0.9998	0.3910×10^2	0.1028×10^{-3}	
0.5455×10^4	0.9999	0.3910×10^2	0.8998×10^{-4}	
0.5623×10^4	0.9999	0.3910×10^2	0.7939×10^{-4}	
0.5791×10^4	0.9999	0.3910×10^2	0.7055×10^{-4}	
0.5960×10^4	0.9999	0.3910×10^2	0.6312×10^{-4}	
		0.005 Atm		
0.4393×10^4	0.9821	0.3981×10^2	0.1814×10^{-1}	0.2506×10^{-5}
0.4453×10^4	0.9840	0.3973×10^2	0.1617×10^{-1}	0.1856×10^{-5}
0.4822×10^4	0.9918	0.3942×10^2	0.8171×10^{-2}	Zero
0.5174×10^4	0.9955	0.3927×10^2	0.4479×10^{-2}	
0.5519×10^4	0.9973	0.3920×10^2	0.2634×10^{-2}	
0.5860×10^4	0.9983	0.3916×10^2	0.1643×10^{-2}	
0.6199×10^4	0.9989	0.3914×10^2	0.1079×10^{-2}	
0.6537×10^4	0.9992	0.3193×10^2	0.7393×10^{-3}	
0.6875×10^4	0.9994	0.3912×10^2	0.5255×10^{-3}	
0.7212×10^4	0.9996	0.3911×10^2	0.3855×10^{-3}	
0.7548×10^4	0.9997	0.3911×10^2	0.2908×10^{-3}	
0.7885×10^4	0.9997	0.3911×10^2	0.2246×10^{-3}	
0.8221×10^4	0.9998	0.3910×10^2	0.1772×10^{-3}	
0.8558×10^4	0.9998	0.3910×10^2	0.1424×10^{-3}	
0.8894×10^4	0.9998	0.3910×10^2	0.1164×10^{-3}	
0.9230×10^4	0.9999	0.3910×10^2	0.9653×10^{-4}	
0.9567×10^4	0.9999	0.3910×10^2	0.8110×10^{-4}	
0.9903×10^4	0.9999	0.3910×10^2	0.6895×10^{-4}	
0.1023×10^5	0.9999	0.3910×10^2	0.5925×10^{-4}	

TABLE D.1 - Vapor Properties

Temperature		Enthalpy H		Entropy S	Specific volume V
°C	°F	Cal/g	Btu/lb	Cal/g-°C or Btu/lb-°F	Cm^3/g
			0.005 Atm		
1300.00	2371.98	753.1	1355.6	1.4583	0.6602×10^6
1350.00	2461.98	759.4	1367.0	1.4624	0.6812×10^6
1400.00	2551.98	765.8	1378.4	1.4663	0.7022×10^6
1450.00	2641.98	772.1	1389.9	1.4702	0.7231×10^6
1500.00	2731.98	778.5	1401.3	1.4740	0.7441×10^6
			0.0025 Atm		
362.98	685.35	629.0	1132.3	1.3738	0.5262×10^6
400.00	751.98	635.9	1144.7	1.3840	0.5604×10^6
450.00	841.98	643.7	1158.6	1.3948	0.6045×10^6
500.00	931.98	650.7	1171.2	1.4039	0.6475×10^6
550.00	1021.98	657.3	1183.2	1.4120	0.6900×10^6
600.00	1111.98	663.9	1195.0	1.4195	0.7323×10^6
650.00	1201.98	670.3	1206.6	1.4265	0.7744×10^6
700.00	1291.98	676.7	1218.1	1.4332	0.8165×10^6
750.00	1381.98	683.1	1229.6	1.4394	0.8586×10^6
800.00	1471.98	689.5	1241.1	1.4454	0.9006×10^6
850.00	1561.98	695.8	1252.6	1.4511	0.9426×10^6
900.00	1651.98	702.2	1264.0	1.4565	0.9846×10^6
950.00	1741.98	708.6	1275.5	1.4617	0.1026×10^7
1000.00	1831.98	714.9	1286.9	1.4668	0.1068×10^7
1050.00	1921.98	721.3	1298.4	1.4716	0.1110×10^7
1100.00	2011.98	727.6	1309.8	1.4763	0.1152×10^7
1150.00	2101.98	734.0	1321.3	1.4808	0.1194×10^7
1200.00	2191.98	740.4	1332.7	1.4852	0.1236×10^7
1250.00	2281.98	746.7	1344.1	1.4894	0.1278×10^7
1300.00	2371.98	753.1	1355.6	1.4936	0.1320×10^7
1350.00	2461.98	759.4	1367.0	1.4976	0.1362×10^7
1400.00	2551.98	765.8	1378.5	1.5016	0.1404×10^7
1450.00	2641.98	772.1	1389.9	1.5054	0.1446×10^7
1500.00	2731.98	778.5	1401.3	1.5092	0.1488×10^7
			0.001 Atm		
32 .17	622.69	625.9	1126.6	1.4150	0.1248×10^7
350.00	661.98	629.8	1133.7	1.4212	0.1298×10^7
400.00	751.98	637.6	1147.7	1.4328	0.1407×10^7
450.00	841.98	644.5	1160.2	1.4424	0.1515×10^7
500.00	931.98	651.1	1172.1	1.4510	0.1621×10^7
550.00	1021.98	657.6	1183.7	1.4589	0.1726×10^7
600.00	1111.98	664.0	1195.3	1.4663	0.1831×10^7
650.00	1201.98	670.4	1206.8	1.4732	0.1936×10^7
700.00	1291.98	676.8	1218.3	1.4798	0.2041×10^7
750.00	1381.98	683.2	1229.7	1.4860	0.2146×10^7
800.00	1471.98	689.5	1241.2	1.4920	0.2251×10^7
850.00	1561.98	695.9	1252.6	1.4977	0.2356×10^7

of Potassium (Continued)

Specific volume V Ft^3/lb	Compressibility factor *ZH*	Average mol. weight ABARH	Dimer *X2H*	Tetramer *X4H*
		0.005 Atm		
0.1057×10^{5}	0.9999	0.3910×10^{2}	0.5141×10^{-4}	Zero
0.1091×10^{5}	0.9999	0.3910×10^{2}	0.4499×10^{-4}	
0.1124×10^{5}	0.9999	0.3910×10^{2}	0.3969×10^{-4}	
0.1158×10^{5}	0.9999	0.3910×10^{2}	0.3528×10^{-4}	
0.1192×10^{5}	0.9999	0.3910×10^{2}	0.3156×10^{-4}	
		0.0025 Atm		
0.8430×10^{4}	0.9855	0.3967×10^{2}	0.1461×10^{-1}	0.1070×10^{-5}
0.8977×10^{4}	0.9918	0.3942×10^{2}	0.8218×10^{-2}	Zero
0.9683×10^{4}	0.9958	0.3926×10^{2}	0.4119×10^{-2}	
0.1037×10^{5}	0.9977	0.3918×10^{2}	0.2249×10^{-2}	
0.1105×10^{5}	0.9986	0.3915×10^{2}	0.1320×10^{-2}	
0.1173×10^{5}	0.9991	0.3913×10^{2}	0.8233×10^{-3}	
0.1240×10^{5}	0.9994	0.3912×10^{2}	0.5400×10^{-3}	
0.1308×10^{5}	0.9996	0.3911×10^{2}	0.3699×10^{-3}	
0.1375×10^{5}	0.9997	0.3911×10^{2}	0.2629×10^{-3}	
0.1442×10^{5}	0.9998	0.3910×10^{2}	0.1928×10^{-3}	
0.1509×10^{5}	0.9998	0.3910×10^{2}	0.1454×10^{-3}	
0.1577×10^{5}	0.9998	0.3910×10^{2}	0.1123×10^{-3}	
0.1644×10^{5}	0.9999	0.3910×10^{2}	0.8863×10^{-4}	
0.1711×10^{5}	0.9999	0.3910×10^{2}	0.7123×10^{-4}	
0.1779×10^{5}	0.9999	0.3910×10^{2}	0.5821×10^{-4}	
0.1846×10^{5}	0.9999	0.3910×10^{2}	0.4827×10^{-4}	
0.1913×10^{5}	0.9999	0.3910×10^{2}	0.4055×10^{-4}	
0.1980×10^{5}	0.9999	0.3910×10^{2}	0.3448×10^{-4}	
0.2047×10^{5}	0.9999	0.3910×10^{2}	0.2962×10^{-4}	
0.2115×10^{5}	0.9999	0.3910×10^{2}	0.2570×10^{-4}	
0.2182×10^{5}	0.9999	0.3910×10^{2}	0.2250×10^{-4}	
0.2249×10^{5}	0.9999	0.3910×10^{2}	0.1985×10^{-4}	
0.2316×10^{5}	0.9999	0.3910×10^{2}	0.1764×10^{-4}	
0.2384×10^{5}	0.9999	0.3910×10^{2}	0.1578×10^{-4}	
		0.001 Atm		
0.1999×10^{5}	0.9891	0.3952×10^{2}	0.1093×10^{-1}	Zero
0.2079×10^{5}	0.9926	0.3939×10^{2}	0.7410×10^{-2}	
0.2255×10^{5}	0.9966	0.3923×10^{2}	0.3320×10^{-2}	
0.2426×10^{5}	0.9983	0.3916×10^{2}	0.1655×10^{-2}	
0.2596×10^{5}	0.9990	0.3913×10^{2}	0.9023×10^{-3}	
0.2765×10^{5}	0.9994	0.3912×10^{2}	0.5290×10^{-3}	
0.2934×10^{5}	0.9996	0.3911×10^{2}	0.3296×10^{-3}	
0.3102×10^{5}	0.9997	0.3911×10^{2}	0.2161×10^{-3}	
0.3270×10^{5}	0.9998	0.3910×10^{2}	0.1480×10^{-3}	
0.3438×10^{5}	0.9998	0.3910×10^{2}	0.1051×10^{-3}	
0.3607×10^{5}	0.9999	0.3910×10^{2}	0.7716×10^{-4}	
0.3775×10^{5}	0.9999	0.3910×10^{2}	0.5818×10^{-4}	

TABLE D.1 - Vapor Properties

Temperature		Enthalpy H		Entropy S	Specific volume V
°C	°F	Cal/g	Btu/lb	Cal/g-°C or Btu/lb-°F	Cm^3/g
			0.001 Atm		
900.00	1651.98	702.2	1264.1	1.5031	0.2461×10^7
950.00	1741.98	708.6	1275.5	1.5083	0.2566×10^7
1000.00	1831.98	714.9	1286.9	1.5133	0.2671×10^7
1050.00	1921.98	721.3	1298.4	1.5182	0.2776×10^7
1100.00	2011.98	727.7	1309.8	1.5228	0.2881×10^7
1150.00	2101.98	734.0	1321.3	1.5273	0.2986×10^7
1200.00	2191.98	740.4	1332.7	1.5317	0.3091×10^7
1250.00	2281.98	746.7	1344.1	1.5360	0.3196×10^7
1300.00	2371.98	753.1	1355.6	1.5401	0.3301×10^7
1350.00	2461.98	759.4	1367.0	1.5442	0.3406×10^7
1400.00	2551.98	765.8	1378.5	1.5481	0.3511×10^7
1450.00	2641.98	772.1	1389.9	1.5520	0.3616×10^7
1500.00	2731.98	778.5	1401.3	1.5558	0.3720×10^7
			0.0005 Atm		
304.30	579.72	623.6	1122.5	1.4463	0.2402×10^7
350.00	661.98	631.1	1136.0	1.4583	0.2605×10^7
400.00	751.98	638.2	1148.7	1.4688	0.2820×10^7
450.00	841.98	644.8	1160.7	1.4780	0.3032×10^7
500.00	931.98	651.3	1172.3	1.4864	0.3243×10^7
550.00	1021.98	657.7	1183.9	1.4942	0.3453×10^7
600.00	1111.98	664.1	1195.4	1.5015	0.3664×10^7
650.00	1201.98	670.5	1206.9	1.5085	0.3874×10^7
700.00	1291.98	676.8	1218.3	1.5150	0.4084×10^7
750.00	1381.98	683.2	1229.8	1.5213	0.4294×10^7
800.00	1471.98	689.5	1241.2	1.5272	0.4503×10^7
850.00	1561.98	695.9	1252.6	1.5329	0.4713×10^7
900.00	1651.98	702.2	1264.1	1.5383	0.4923×10^7
950.00	1741.98	708.6	1275.5	1.5435	0.5133×10^7
1000.00	1831.98	715.0	1287.0	1.5486	0.5343×10^7
1050.00	1921.98	721.3	1298.4	1.5534	0.5553×10^7
1100.00	2011.98	727.7	1309.8	1.5581	0.5763×10^7
1150.00	2101.98	734.0	1321.3	1.5626	0.5972×10^7
1200.00	2191.98	740.4	1332.7	1.5670	0.6182×10^7
1250.00	2281.98	746.7	1344.1	1.5712	0.6392×10^7
1300.00	2371.98	753.1	1355.6	1.5754	0.6602×10^7
1350.00	2461.98	759.4	1367.0	1.5794	0.6812×10^7
1400.00	2551.98	765.8	1378.5	1.5833	0.7022×10^7
1450.00	2641.98	772.1	1389.9	1.5872	0.7232×10^7
1500.00	2731.98	778.5	1401.3	1.5910	0.7441×10^7
			0.00025 Atm		
282.28	540.09	621.4	1118.5	1.4776	0.4629×10^7
300.00	571.98	624.4	1123.9	1.4827	0.4788×10^7
350.00	661.98	631.7	1137.1	1.4945	0.5221×10^7

of Potassium (Continued)

Specific volume V Ft^3/lb	Compressibility factor *ZH*	Average mol. weight ABARH	Dimer *X2H*	Tetramer *X4H*
		0.001 Atm		
0.3943×10^5	0.9999	0.3910×10^2	0.4494×10^{-4}	Zero
0.4111×10^5	0.9999	0.3910×10^2	0.3545×10^{-4}	
0.4279×10^5	0.9999	0.3910×10^2	0.2849×10^{-4}	
0.4447×10^5	0.9999	0.3910×10^2	0.2328×10^{-4}	
0.4615×10^5	0.9999	0.3910×10^2	0.1930×10^{-4}	
0.4783×10^5	0.9999	0.3910×10^2	0.1622×10^{-4}	
0.4951×10^5	0.9999	0.3910×10^2	0.1379×10^{-4}	
0.5120×10^5	0.9999	0.3910×10^2	0.1185×10^{-4}	
0.5288×10^5	0.9999	0.3910×10^2	0.1028×10^{-4}	
0.5456×10^5	0.9999	0.3910×10^2	0.9000×10^{-5}	
0.5624×10^5	0.9999	0.3910×10^2	0.7940×10^{-5}	
0.5792×10^5	0.9999	0.3910×10^2	0.7056×10^{-5}	
0.5960×10^5	0.9999	0.3910×10^2	0.6312×10^{-5}	
		0.0005 Atm		
0.3848×10^5	0.9913	0.3944×10^2	0.8770×10^{-2}	Zero
0.4173×10^5	0.9962	0.3924×10^2	0.2732×10^{-2}	
0.4518×10^5	0.9983	0.3916×10^2	0.1665×10^{-2}	
0.4857×10^5	0.9991	0.3913×10^2	0.8293×10^{-3}	
0.5195×10^5	0.9995	0.3911×10^2	0.4515×10^{-3}	
0.5532×10^5	0.9997	0.3911×10^2	0.2646×10^{-3}	
0.5869×10^5	0.9998	0.3910×10^2	0.1648×10^{-3}	
0.6205×10^5	0.9998	0.3910×10^2	0.1081×10^{-3}	
0.6542×10^5	0.9999	0.3910×10^2	0.7403×10^{-4}	
0.6878×10^5	0.9999	0.3910×10^2	0.5260×10^{-4}	
0.7214×10^5	0.9999	0.3910×10^2	0.3858×10^{-4}	
0.7550×10^5	0.9999	0.3910×10^2	0.2909×10^{-4}	
0.7886×10^5	0.9999	0.3910×10^2	0.2247×10^{-4}	
0.8223×10^5	0.9999	0.3910×10^2	0.1772×10^{-4}	
0.8559×10^5	0.9999	0.3910×10^2	0.1424×10^{-4}	
0.8895×10^5	0.9999	0.3910×10^2	0.1164×10^{-4}	
0.9231×10^5	0.9999	0.3910×10^2	0.9654×10^{-5}	
0.9567×10^5	0.9999	0.3910×10^2	0.8111×10^{-5}	
0.9903×10^5	0.9999	0.3910×10^2	0.6896×10^{-5}	
0.1024×10^6	0.9999	0.3910×10^2	0.5926×10^{-5}	
0.1057×10^6	0.9999	0.3910×10^2	0.5141×10^{-5}	
0.1091×10^6	0.9999	0.3910×10^2	0.4500×10^{-5}	
0.1124×10^6	0.9999	0.3910×10^2	0.3970×10^{-5}	
0.1158×10^6	0.9999	0.3910×10^2	0.3528×10^{-5}	
0.1192×10^6	0.9999	0.3910×10^2	0.3156×10^{-5}	
		0.00025 Atm		
0.7416×10^5	0.9930	0.3937×10^2	0.7021×10^{-2}	Zero
0.7669×10^5	0.9951	0.3929×10^2	0.4828×10^{-2}	
0.8363×10^5	0.9981	0.3917×10^2	0.1873×10^{-2}	

TABLE D.1 - Vapor Properties

Temperature		Enthalpy H		Entropy S	Specific volume V
°C	°F	Cal/g	Btu/lb	Cal/g-°C or Btu/lb-°F	Cm^{3}/g
		0.00025 Atm			
400.00	751.98	638.4	1149.2	1.5044	0.5645 × 10^{7}
450.00	841.98	644.9	1160.9	1.5134	0.6067 × 10^{7}
500.00	931.98	651.4	1172.5	1.5217	0.6488 × 10^{7}
550.00	1021.98	657.7	1184.0	1.5295	0.6908 × 10^{7}
600.00	1111.98	664.1	1195.4	1.5368	0.7328 × 10^{7}
650.00	1201.98	670.5	1206.9	1.5437	0.7748 × 10^{7}
700.00	1291.98	676.8	1218.3	1.5503	0.8168 × 10^{7}
750.00	1381.98	683.2	1229.8	1.5565	0.8588 × 10^{7}
800.00	1471.98	689.5	1241.2	1.5624	0.9007 × 10^{7}
850.00	1561.98	695.9	1252.6	1.5681	0.9427 × 10^{7}
900.00	1651.98	702.2	1264.1	1.5736	0.9847 × 10^{7}
9950.00	1741.98	708.6	1275.5	1.5788	0.1026 × 10^{8}
1000.00	1831.98	715.0	1287.0	1.5838	0.1068 × 10^{8}
1050.00	1921.98	721.3	1298.4	1.5886	0.1110 × 10^{8}
1100.00	2011.98	727.7	1309.8	1.5933	0.1152 × 10^{8}
1150.00	2101.98	734.0	1321.3	1.5978	0.1194 × 10^{8}
1200.00	2191.98	740.4	1332.7	1.6022	0.1236 × 10^{8}
1250.00	2281.98	746.7	1344.1	1.6065	0.1278 × 10^{8}
1300.00	2371.98	753.1	1355.6	1.6106	0.1320 × 10^{8}
1350.00	2461.98	759.4	1367.0	1.6146	0.1362 × 10^{8}
1400.00	2551.98	765.8	1378.5	1.6186	0.1404 × 10^{8}
1450.00	2641.98	772.1	1389.9	1.6224	0.1446 × 10^{8}
1500.00	2731.98	778.5	1401.3	1.6262	0.1488 × 10^{8}
		0.0001 Atm			
255.66	492.17	618.6	1113.5	1.5193	0.1103 × 10^{8}
300.00	571.98	625.4	1125.7	1.5309	0.1200 × 10^{8}
350.00	661.98	632.1	1137.8	1.5416	0.1306 × 10^{8}
400.00	751.98	638.6	1149.5	1.5512	0.1412 × 10^{8}
450.00	841.98	645.0	1161.1	1.5601	0.1517 × 10^{8}
500.00	931.98	651.4	1172.6	1.5683	0.1622 × 10^{8}
550.00	1021.98	657.8	1184.0	1.5761	0.1727 × 10^{8}
600.00	1111.98	664.1	1195.5	1.5834	0.1832 × 10^{8}
650.00	1201.98	670.5	1206.9	1.5903	0.1937 × 10^{8}
700.00	1291.98	676.8	1218.3	1.5968	0.2042 × 10^{8}
750.00	1381.98	683.2	1229.8	1.6031	0.2147 × 10^{8}
800.00	1471.98	689.5	1241.2	1.6090	0.2252 × 10^{8}
850.00	1561.98	695.9	1252.7	1.6147	0.2356 × 10^{8}
900.00	1651.98	702.3	1264.1	1.6201	0.2461 × 10^{8}
950.00	1741.98	708.6	1275.5	1.6253	0.2566 × 10^{8}
1000.00	1831.98	715.0	1287.0	1.6304	0.2671 × 10^{8}
1050.00	1921.98	721.3	1298.4	1.6352	0.2776 × 10^{8}
1100.00	2011.98	727.7	1309.8	1.6399	0.2881 × 10^{8}
1150.00	2101.98	734.0	1321.3	1.6444	0.2986 × 10^{8}

of Potassium (Continued)

Specific volume V Ft^{3}/lb	Compressibility factor *ZH*	Average mol. weight ABARH	Dimer *X2H*	Tetramer *X4H*
		0.00025 Atm		
0.9043×10^{5}	0.9991	0.3913×10^{2}	0.8341×10^{-3}	Zero
0.9719×10^{5}	0.9995	0.3911×10^{2}	0.4149×10^{-3}	
0.1039×10^{5}	0.9997	0.3911×10^{2}	0.2258×10^{-3}	
0.1106×10^{5}	0.9998	0.3910×10^{2}	0.1323×10^{-3}	
0.1173×10^{5}	0.9999	0.3910×10^{2}	0.8245×10^{-4}	
0.1171×10^{5}	0.9999	0.3910×10^{2}	0.5406×10^{-4}	
0.1308×10^{5}	0.9999	0.3910×10^{2}	0.3701×10^{-4}	
0.1375×10^{5}	0.9999	0.3910×10^{2}	0.2630×10^{-4}	
0.1442×10^{5}	0.9999	0.3910×10^{2}	0.1929×10^{-4}	
0.1510×10^{5}	0.9999	0.3910×10^{2}	0.1454×10^{-4}	
0.1577×10^{5}	0.9999	0.3910×10^{2}	0.1123×10^{-4}	
0.1644×10^{5}	0.9999	0.3910×10^{2}	0.8864×10^{-5}	
0.1711×10^{5}	0.9999	0.3910×10^{2}	0.7124×10^{-5}	
0.1779×10^{5}	0.9999	0.3910×10^{2}	0.5821×10^{-5}	
0.1846×10^{5}	0.9999	0.3910×10^{2}	0.4827×10^{-5}	
0.1913×10^{5}	0.9999	0.3910×10^{2}	0.4055×10^{-5}	
0.1980×10^{5}	0.9999	0.3910×10^{2}	0.3448×10^{-5}	
0.2048×10^{5}	0.9999	0.3910×10^{2}	0.2963×10^{-5}	
0.2115×10^{5}	0.9999	0.3910×10^{2}	0.2570×10^{-5}	
0.2182×10^{5}	0.9999	0.3910×10^{2}	0.2250×10^{-5}	
0.2249×10^{5}	0.9999	0.3910×10^{2}	0.1985×10^{-5}	
0.2316×10^{5}	0.9999	0.3910×10^{2}	0.1764×10^{-5}	
0.2384×10^{5}	0.9999	0.3910×10^{2}	0.1578×10^{-5}	
		0.0001 Atm		
0.1768×10^{6}	0.9948	0.3930×10^{2}	0.5222×10^{-2}	Zero
0.1922×10^{6}	0.9980	0.3917×10^{2}	0.1942×10^{-2}	
0.2093×10^{6}	0.9992	0.3913×10^{2}	0.7510×10^{-3}	
0.2262×10^{6}	0.9996	0.3911×10^{2}	0.3340×10^{-3}	
0.2430×10^{6}	0.9998	0.3910×10^{2}	0.1660×10^{-3}	
0.2598×10^{6}	0.9999	0.3910×10^{2}	0.9037×10^{-4}	
0.2766×10^{6}	0.9999	0.3910×10^{2}	0.5295×10^{-4}	
0.2935×10^{6}	0.9999	0.3910×10^{2}	0.2398×10^{-4}	
0.3103×10^{6}	0.9999	0.3910×10^{2}	0.2162×10^{-4}	
0.3271×10^{6}	0.9999	0.2910×10^{2}	0.1480×10^{-4}	
0.3439×10^{6}	0.9999	0.3910×10^{2}	0.1052×10^{-4}	
0.3607×10^{6}	0.9999	0.3910×10^{2}	0.7717×10^{-5}	
0.3775×10^{6}	0.9999	0.3910×10^{2}	0.5819×10^{-5}	
0.3943×10^{6}	0.9999	0.3910×10^{2}	0.4494×10^{-5}	
0.4111×10^{6}	0.9999	0.3910×10^{2}	0.3546×10^{-5}	
0.4279×10^{6}	0.9999	0.3910×10^{2}	0.2849×10^{-5}	
0.4447×10^{6}	0.9999	0.3910×10^{2}	0.2328×10^{-5}	
0.4615×10^{6}	0.9999	0.3910×10^{2}	0.1930×10^{-5}	
0.4783×10^{6}	0.9999	0.3910×10^{2}	0.1622×10^{-5}	

TABLE D.1 - Vapor Properties

Temperature		Enthalpy H		Entropy S	Specific volume V
°C	°F	Cal/g	Btu/lb	Cal/g-°C or Btu/lb-°F	Cm^3/g
			0.0001 Atm		
1200.00	2191.98	740.4	1332.7	1.6488	0.3091×10^8
1250.00	2281.98	746.7	1344.2	1.6530	0.3196×10^8
1300.00	2371.98	753.1	1355.6	1.6572	0.3301×10^8
1350.00	2461.98	759.4	1367.0	1.6612	0.3406×10^8
1400.00	2551.98	765.8	1378.5	1.6651	0.3511×10^8
1450.00	2641.98	772.1	1389.9	1.6690	0.3616×10^8
1500.00	2731.98	778.5	1401.3	1.6728	0.3721×10^8
			0.00005 Atm		
237.18	459.91	616.6	1109.9	1.5509	0.2133×10^8
250.00	481.98	618.6	1113.6	1.5546	0.2189×10^8
300.00	571.98	625.7	1126.3	1.5666	0.2403×10^8
350.00	661.98	632.2	1138.1	1.5770	0.2614×10^8
400.00	751.98	638.7	1149.6	1.5865	0.2824×10^8
450.00	841.98	645.0	1161.1	1.5953	0.3034×10^8
500.00	931.98	651.4	1172.6	1.6036	0.3244×10^8
550.00	1021.98	657.8	1184.0	1.6113	0.3454×10^8
600.00	1111.98	664.1	1195.5	1.6186	0.3664×10^8
650.00	1201.98	670.5	1206.9	1.6255	0.3874×10^8
700.00	1291.98	676.8	1218.3	1.6321	0.4084×10^8
750.00	1381.98	683.2	1229.8	1.6383	0.4294×10^8
800.00	1471.98	689.5	1241.2	1.6442	0.4504×10^8
850.00	1561.98	695.9	1252.7	1.6499	0.4713×10^8
900.00	1651.98	702.3	1264.1	1.6553	0.4923×10^8
950.00	1741.98	708.6	1275.5	1.6606	0.5133×10^8
1000.00	1831.98	715.0	1287.0	1.6656	0.5343×10^8
1050.00	1921.98	721.3	1298.4	1.6704	0.5553×10^8
1100.00	2011.98	727.7	1309.8	1.6751	0.5763×10^8
1150.00	2101.98	734.0	1321.3	1.6796	0.5973×10^8
1200.00	2191.98	740.4	1332.7	1.6840	0.6182×10^8
1250.00	2281.98	746.7	1344.2	1.6882	0.6392×10^8
1300.00	2371.98	753.1	1355.6	1.6924	0.6602×10^8
1350.00	2461.98	759.4	1367.0	1.6964	0.6812×10^8
1400.00	2551.98	765.8	1378.5	1.7004	0.7022×10^8
1450.00	2641.98	772.1	1389.9	1.7042	0.7232×10^8
1500.00	2731.98	778.5	1401.3	1.7080	0.7442×10^8
			0.000025 Atm		
219.96	427.91	614.7	1106.5	1.5826	0.4125×10^8
250.00	481.98	619.1	1114.5	1.5907	0.4384×10^8
300.00	571.98	625.9	1126.6	1.6021	0.4808×10^8
350.00	661.98	632.3	1138.2	1.6123	0.5229×10^8
400.00	751.98	638.7	1149.7	1.6218	0.5650×10^8
450.00	841.98	645.1	1161.2	1.6306	0.6069×10^8
500.00	931.98	651.4	1172.6	1.6388	0.6489×10^8

of Potassium (Continued)

Specific volume V Ft^3/lb	Compressibility factor *ZH*	Average mol. weight ABARH	Dimer *X2H*	Tetramer *X4H*.
		0.0001 Atm		
0.4952×10^{6}	0.9999	0.3910×10^{2}	0.1379×10^{-5}	Zero
0.5120×10^{6}	0.9999	0.3910×10^{2}	0.1185×10^{-5}	
0.5288×10^{6}	0.9999	0.3910×10^{2}	0.1028×10^{-5}	
0.5456×10^{6}	0.9999	0.3910×10^{2}	Zero	
0.5624×10^{6}	0.9999	0.3910×10^{2}		
0.5792×10^{6}	0.9999	0.3910×10^{2}		
0.5960×10^{6}	0.9999	0.3910×10^{2}		
		0.00005 Atm		
0.3416×10^{6}	0.9958	0.3926×10^{2}	0.4170×10^{-2}	Zero
0.3506×10^{6}	0.9969	0.3921×10^{2}	0.3014×10^{-2}	
0.3849×10^{6}	0.9990	0.3914×10^{2}	0.9732×10^{-3}	
0.4187×10^{6}	0.9996	0.3911×10^{2}	0.3758×10^{-3}	
0.4524×10^{6}	0.9998	0.3910×10^{2}	0.1670×10^{-3}	
0.4861×10^{6}	0.9999	0.3910×10^{2}	0.8305×10^{-4}	
0.5197×10^{6}	0.9999	0.3910×10^{2}	0.4519×10^{-4}	
0.5533×10^{6}	0.9999	0.3910×10^{2}	0.2647×10^{-4}	
0.5870×10^{6}	0.9999	0.3910×10^{2}	0.1649×10^{-4}	
0.6206×10^{6}	0.9999	0.3910×10^{2}	0.1081×10^{-4}	
0.6542×10^{6}	0.9999	0.3910×10^{2}	0.7403×10^{-5}	
0.6878×10^{6}	0.9999	0.3910×10^{2}	0.5260×10^{-5}	
0.7214×10^{6}	0.9999	0.3910×10^{2}	0.3858×10^{-5}	
0.7550×10^{6}	0.9999	0.3910×10^{2}	0.2909×10^{-5}	
0.7887×10^{6}	0.9999	0.3910×10^{2}	0.2247×10^{-5}	
0.8223×10^{6}	0.9999	0.3910×10^{2}	0.1773×10^{-5}	
0.8559×10^{6}	0.9999	0.3910×10^{2}	0.1424×10^{-5}	
0.8895×10^{6}	0.9999	0.3910×10^{2}	0.1164×10^{-5}	
0.9231×10^{6}	0.9999	0.3910×10^{2}	Zero	
0.9567×10^{6}	0.9999	0.3910×10^{2}		
0.9904×10^{6}	0.9999	0.3910×10^{2}		
0.1024×10^{7}	0.9999	0.3910×10^{2}		
0.1057×10^{7}	0.9999	0.3910×10^{2}		
0.1091×10^{7}	0.9999	0.3910×10^{2}		
0.1124×10^{7}	0.9999	0.3910×10^{2}		
0.1158×10^{7}	0.9999	0.3910×10^{2}		
0.1192×10^{7}	0.9999	0.3910×10^{2}		
		0.000025 Atm		
0.6608×10^{6}	0.9966	0.3923×10^{2}	0.3327×10^{-2}	Zero
0.7023×10^{6}	0.9984	0.3916×10^{2}	0.1512×10^{-2}	
0.7702×10^{6}	0.9995	0.3912×10^{2}	0.4870×10^{-3}	
0.8377×10^{6}	0.9998	0.3910×10^{2}	0.1879×10^{-3}	
0.9050×10^{6}	0.9999	0.3910×10^{2}	0.8354×10^{-4}	
0.9723×10^{6}	0.9999	0.3910×10^{2}	0.4153×10^{-4}	
0.1039×10^{7}	0.9999	0.3910×10^{2}	0.2259×10^{-4}	

TABLE D.1 - Vapor Properties

Temperature		Enthalpy H		Entropy S	Specific volume V
°C	°F	Cal/g	Btu/lb	Cal/g-°C or Btu/lb-°F	Cm^3/g
		0.000025 Atm			
550.00	1021.98	657.8	1184.0	1.6465	0.6909×10^{8}
600.00	1111.98	664.1	1195.5	1.6538	0.7329×10^{8}
650.00	1201.98	670.5	1206.9	1.6608	0.7749×10^{8}
700.00	1291.98	676.8	12 8.3	1.6673	0.8168×10^{8}
750.00	1381.98	683.2	1229.8	1.6735	0.8588×10^{8}
800.00	1471.98	689.5	1241.2	1.6795	0.9008×10^{8}
850.00	1561.98	695.9	1252.7	1.6851	0.9427×10^{8}
900.00	1651.98	702.3	1264.1	1.6906	0.9847×10^{8}
950.00	1741.98	708.6	1275.5	1.6958	0.1026×10^{9}
1000.00	1831.98	715.0	1287.0	1.7008	0.1068×10^{9}
1050.00	1921.98	721.3	1298.4	1.7056	0.1110×10^{9}
1100.00	2011.98	727.7	1309.8	1.7103	0.1152×10^{9}
1150.00	2101.98	734.0	1321.3	1.7148	0.1194×10^{9}
1200.00	2191.98	740.4	1332.7	1.7192	0.1236×10^{9}
1250.00	2281.98	746.7	1344.2	1.7235	0.1278×10^{9}
1300.00	2371.98	753.1	1355.6	1.7276	0.1320×10^{9}
1350.00	2461.98	759.4	1367.0	1.7316	0.1362×10^{9}
1400.00	2551.98	765.8	1378.5	1.7356	0.1404×10^{9}
1450.00	2641.98	772.1	1389.9	1.7395	0.1446×10^{9}
1500.00	2731.98	778.5	1401.3	1.7432	0.1488×10^{9}
		0.00001 Atm			
198.93	390.06	617.3	1102.2	1.6247	0.9882×10^{8}
200.00	391.98	612.5	1102.5	1.6250	0.9905×10^{8}
250.00	481.98	619.5	1115.1	1.6378	0.1097×10^{9}
300.00	571.98	626.0	1126.8	1.6488	0.1202×10^{9}
350.00	661.98	632.3	1138.3	1.6589	0.1307×10^{9}
400.00	751.98	638.7	1149.7	1.6683	0.1412×10^{9}
450.00	841.98	645.1	1161.2	1.6771	0.1517×10^{9}
500.00	931.98	651.4	1172.6	1.6854	0.1622×10^{9}
550.00	1021.98	657.8	1184.0	1.6931	0.1727×10^{9}
600.00	1111.98	664.1	1195.5	1.7004	0.1832×10^{9}
650.00	1201.98	670.5	1206.9	1.7073	0.1937×10^{9}
700.00	1291.98	676.8	1218.4	1.7139	0.2042×10^{9}
750.00	1381.98	683.2	1229.8	1.7201	0.2147×10^{9}
800.00	1471.98	689.5	1241.2	1.7260	0.2252×10^{9}
850.00	1561.98	695.9	1252.7	1.7317	0.2356×10^{9}
900.00	1651.98	702.3	1264.1	1.7371	0.2461×10^{9}
950.00	1741.98	708.6	1275.5	1.7424	0.2566×10^{9}
1000.00	1831.98	715.0	1287.0	1.7474	0.2671×10^{9}
1050.00	1921.98	721.3	1298.4	1.7522	0.2776×10^{9}
1100.00	2011.98	727.7	1309.8	1.7569	0.2881×10^{9}
1150.00	2101.98	734.0	1321.3	1.7614	0.2986×10^{9}
1200.00	2191.98	740.4	1332.7	1.7658	0.3091×10^{9}

of Potassium (Continued)

Specific volume V Ft^3/lb	Compressibility factor *ZH*	Average mol. weight ABARH	Dimer *X2H*	Tetramer *X4H*
		0.000025 Atm		
0.1106×10^{7}	0.9999	0.3910×10^{2}	0.1323×10^{-4}	Zero
0.1174×10^{7}	0.9999	0.3910×10^{2}	0.8246×10^{-5}	
0.1241×10^{7}	0.9999	0.3910×10^{2}	0.5406×10^{-5}	
0.1308×10^{7}	0.9999	0.3910×10^{2}	0.3702×10^{-5}	
0.1375×10^{7}	0.9999	0.3910×10^{2}	0.2630×10^{-5}	
0.1442×10^{7}	0.9999	0.3910×10^{2}	0.1929×10^{-5}	
0.1510×10^{7}	0.9999	0.3910×10^{2}	0.1454×10^{-5}	
0.1577×10^{7}	0.9999	0.3910×10^{2}	0.1123×10^{-5}	
0.1644×10^{7}	0.9999	0.3910×10^{2}	Zero	
0.1711×10^{7}	0.9999	0.3910×10^{2}		
0.1779×10^{7}	0.9999	0.3910×10^{2}		
0.1846×10^{7}	0.9999	0.3910×10^{2}		
0.1913×10^{7}	0.9999	0.3910×10^{2}		
0.1980×10^{7}	0.9999	0.3910×10^{2}		
0.2048×10^{7}	0.9999	0.3910×10^{2}		
0.2115×10^{7}	0.9999	0.3910×10^{2}		
0.2182×10^{7}	0.9999	0.3910×10^{2}		
0.2240×10^{7}	0.9999	0.3910×10^{2}		
0.2316×10^{7}	0.9999	0.3910×10^{2}		
0.2384×10^{7}	0.9999	0.3910×10^{2}		
		0.00001 Atm		
0.1583×10^{7}	0.9975	0.3919×10^{2}	0.2465×10^{-2}	Zero
0.1586×10^{7}	0.9976	0.3919×10^{2}	0.2387×10^{-2}	
0.1757×10^{7}	0.9993	0.3912×10^{2}	0.6059×10^{-3}	
0.1926×10^{7}	0.9998	0.3910×10^{2}	0.1949×10^{-3}	
0.2094×10^{7}	0.9999	0.3910×10^{2}	0.7520×10^{-4}	
0.2262×10^{7}	0.9999	0.3910×10^{2}	0.3342×10^{-4}	
0.2430×10^{7}	0.9999	0.3910×10^{2}	0.1661×10^{-4}	
0.2598×10^{7}	0.9999	0.3910×10^{2}	0.9039×10^{-5}	
0.2767×10^{7}	0.9999	0.3910×10^{2}	0.5295×10^{-5}	
0.2935×10^{7}	0.9999	0.3910×10^{2}	0.2398×10^{-5}	
0.3103×10^{7}	0.9999	0.3910×10^{2}	0.2162×10^{-5}	
0.3271×10^{7}	0.9999	0.3910×10^{2}	0.1480×10^{-5}	
0.3439×10^{7}	0.9999	0.3910×10^{2}	0.1052×10^{-5}	
0.3607×10^{7}	0.9999	0.3910×10^{2}	Zero	
0.3775×10^{7}	0.9999	0.3910×10^{2}		
0.3943×10^{7}	0.9999	0.3910×10^{2}		
0.4111×10^{7}	0.9999	0.3910×10^{2}		
0.4279×10^{7}	0.9999	0.3910×10^{2}		
0.4447×10^{7}	0.9999	0.3910×10^{2}		
0.4615×10^{7}	0.9999	0.3910×10^{2}		
0.4783×10^{7}	0.9999	0.3910×10^{2}		
0.4952×10^{7}	0.9999	0.3910×10^{2}		

TABLE D.1 - Vapor Properties

Temperature °C	Temperature °F	Enthalpy H Cal/g	Enthalpy H Btu/lb	Entropy S Cal/g-°C or Btu/lb-°F	Specific volume V Cm^3/g
			0.00001 Atm		
1250.00	2281.98	746.7	1344.2	1.7700	0.3196×10^9
1300.00	2371.98	753.1	1355.6	1.7742	0.3301×10^9
1350.00	2461.98	759.4	1367.0	1.7782	0.3406×10^9
1400.00	2551.98	765.8	1378.5	1.7822	0.3511×10^9
1450.00	2641.98	772.1	1389.9	1.7860	0.3616×10^9
1500.00	2731.98	778.5	1401.3	1.7898	0.3721×10^9
			0.000005 Atm		
184.18	363.51	610.6	1099.2	1.6567	0.1915×10^9
200.00	391.98	612.9	1103.3	1.6611	0.1983×10^9
250.00	481.98	619.6	1115.3	1.6732	0.2195×10^9
300.00	571.98	626.0	1126.8	1.6841	0.2405×10^9
350.00	661.98	632.4	1138.3	1.6942	0.2615×10^9
400.00	751.98	638.7	1149.7	1.7036	0.2825×10^9
450.00	841.98	645.1	1161.2	1.7124	0.3035×10^9
500.00	931.98	651.4	1172.6	1.7206	0.3244×10^9
550.00	1021.98	657.8	1184.0	1.7283	0.3454×10^9
600.00	1111.98	664.1	1195.5	1.7356	0.3664×10^9
650.00	1201.98	670.5	1206.9	1.7425	0.3874×10^9
700.00	1291.98	676.8	1218.4	1.7491	0.4084×10^9
750.00	1381.98	683.2	1229.8	1.7553	0.4294×10^9
800.00	1471.98	689.5	1241.2	1.7613	0.4504×10^9
850.00	1561.98	695.9	1252.7	1.7669	0.4713×10^9
900.00	1651.98	702.3	1264.1	1.7724	0.4923×10^9
950.00	1741.98	708.6	1275.5	1.7776	0.5133×10^9
1000.00	1831.98	715.0	1287.0	1.7826	0.5343×10^9
1050.00	1921.98	721.3	1298.4	1.7874	0.5553×10^9
1100.00	2011.98	727.7	1309.8	1.7921	0.5763×10^9
1150.00	2101.98	734.0	1321.3	1.7966	0.5973×10^9
1200.00	2191.98	740.4	1332.7	1.8010	0.6182×10^9
1250.00	2281.98	746.7	1344.2	1.8053	0.6392×10^9
1300.00	2371.98	753.1	1355.6	1.8094	0.6602×10^9
1350.00	2461.98	759.4	1367.0	1.8134	0.6812×10^9
1400.00	2551.98	765.8	1378.5	1.8174	0.7022×10^9
1450.00	2641.98	772.1	1389.9	1.8212	0.7232×10^9
1500.00	2731.98	778.5	1401.3	1.8250	0.7442×10^9
			0.0000025 Atm		
170.35	338.61	609.0	1096.3	1.6888	0.3717×10^9
200.00	391.98	613.1	1103.6	1.6967	0.3969×10^9
250.00	481.98	619.6	1115.3	1.7085	0.4390×10^9
300.00	571.98	626.0	1126.8	1.7194	0.4810×10^9
350.00	661.98	632.4	1138.3	1.7294	0.5230×10^9
400.00	751.98	638.7	1149.7	1.7388	0.5650×10^9
450.00	841.98	645.1	1161.2	1.7476	0.6070×10^9

of Potassium (Continued)

Specific volume V Ft^3/lb	Compressibility factor *ZH*	Average mol. weight ABARH	Dimer *X2H*	Tetramer *X4H*
		0.00001 Atm		
0.5120×10^{7}	0.9999	0.3910×10^{2}	Zero	Zero
0.5288×10^{7}	0.9999	0.3910×10^{2}		
0.5456×10^{7}	0.9999	0.3910×10^{2}		
0.5624×10^{7}	0.9999	0.3910×10^{2}		
0.5792×10^{7}	0.9999	0.3910×10^{2}		
0.5960×10^{7}	0.9999	0.3910×10^{2}		
		0.000005 Atm		
0.3068×10^{7}	0.9980	0.3917×10^{2}	0.1964×10^{-2}	Zero
0.3177×10^{7}	0.9988	0.3914×10^{2}	0.1196×10^{-2}	
0.3516×10^{7}	0.9996	0.3911×10^{2}	0.3031×10^{-3}	
0.3852×10^{7}	0.9999	0.3910×10^{2}	$0.9749 \times\times 10^{-4}$	
0.4189×10^{7}	0.9999	0.3910×10^{2}	0.3760×10^{-4}	
0.4525×10^{7}	0.9999	0.3910×10^{2}	0.1671×10^{-4}	
0.4861×10^{7}	0.9999	0.3910×10^{2}	0.8306×10^{-5}	
0.5197×10^{7}	0.9999	0.3910×10^{2}	0.4519×10^{-5}	
0.5534×10^{7}	0.9999	0.3910×10^{2}	0.2647×10^{-5}	
0.5870×10^{7}	0.9999	0.3910×10^{2}	0.1649×10^{-5}	
0.6206×10^{7}	0.9999	0.3910×10^{2}	0.1081×10^{-5}	
0.6542×10^{7}	0.9999	0.3910×10^{2}	Zero	
0.6878×10^{7}	0.9999	0.3910×10^{2}		
0.7214×10^{7}	0.9999	0.3910×10^{2}		
0.7550×10^{7}	0.9999	0.3910×10^{2}		
0.7887×10^{7}	0.9999	0.3910×10^{2}		
0.8223×10^{7}	0.9999	0.3910×10^{2}		
0.8559×10^{7}	0.9999	0.3910×10^{2}		
0.8895×10^{7}	0.9999	0.3910×10^{2}		
0.9231×10^{7}	0.9999	0.3910×10^{2}		
0.9567×10^{7}	0.9999	0.3910×10^{2}		
0.9904×10^{7}	0.9999	0.3910×10^{2}		
0.1024×10^{7}	0.9999	0.3910×10^{2}		
0.1057×10^{7}	0.9999	0.3910×10^{2}		
0.1091×10^{7}	0.9999	0.3910×10^{2}		
0.1124×10^{7}	0.9999	0.3910×10^{2}		
0.1158×10^{7}	0.9999	0.3910×10^{2}		
0.1192×10^{7}	0.9999	0.3910×10^{2}		
		0.0000025 Atm		
0.5954×10^{7}	0.9984	0.3916×10^{2}	0.1563×10^{-2}	Zero
0.6358×10^{7}	0.9994	0.3912×10^{2}	0.5989×10^{-3}	
0.7033×10^{7}	0.9998	0.3910×10^{2}	0.1516×10^{-3}	
0.7706×10^{7}	0.9999	0.3910×10^{2}	0.4875×10^{-4}	
0.8378×10^{7}	0.9999	0.3910×10^{2}	0.1880×10^{-4}	
0.9051×10^{7}	0.9999	0.3910×10^{2}	0.8355×10^{-5}	
0.9723×10^{7}	0.9999	0.3910×10^{2}	0.4153×10^{-5}	

TABLE D.1 - Vapor Properties

Temperature		Enthalpy H		Entropy S	Specific volume V
°C	°F	Cal/g	Btu/lb	Cal/g-°C or Btu/lb-°F	Cm^3/g
0.0000025 Atm					
500.00	931.98	651.4	1172.6	1.7558	0.6489×10^{9}
550.00	1021.98	657.8	1184.0	1.7636	0.6909×10^{9}
600.00	1111.98	664.1	1195.5	1.7709	0.7329×10^{9}
650.00	1201.98	670.5	1206.9	1.7778	0.7749×10^{9}
700.00	1291.98	676.8	1218.4	1.7843	0.8168×10^{9}
750.00	1381.98	683.2	1229.8	1.7905	0.8588×10^{9}
800.00	1471.98	689.5	1241.2	1.7965	0.9008×10^{9}
850.00	1561.98	695.9	1252.7	1.8033	0.9427×10^{9}
900.00	1651.98	702.3	1264.1	1.8076	0.9847×10^{9}
950.00	1741.98	708.6	1275.5	1.8128	0.1026×10^{10}
1000.00	1831.98	715.0	1287.0	1.8178	0.1068×10^{10}
1050.00	1921.98	721.3	1298.4	1.8227	0.1110×10^{10}
1100.00	2011.98	727.7	1309.8	1.8273	0.1152×10^{10}
1150.00	2101.98	734.0	1321.3	1.8319	0.1194×10^{10}
1200.00	2191.98	740.4	1332.7	1.8362	0.1236×10^{10}
1250.00	2281.98	746.7	1344.2	1.8405	0.1278×10^{10}
1300.00	2371.98	753.1	1355.6	1.8446	0.1320×10^{10}
1350.00	2461.98	759.4	1367.0	1.8487	0.1362×10^{10}
1400.00	2551.98	765.8	1378.5	1.8526	0.1404×10^{10}
1450.00	2641.98	772.1	1389.9	1.8565	0.1446×10^{10}
1500.00	2731.98	778.5	1401.3	1.8603	0.1488×10^{10}
0.000001 Atm					
153.30	307.92	607.0	1092.6	1.7314	0.8938×10^{-9}
200.00	391.98	613.2	1103.9	1.7435	0.9926×10^{9}
250.00	481.98	619.6	1115.4	1.7552	0.1097×10^{10}
300.00	571.98	626.0	1126.9	1.7659	0.1202×10^{10}
350.00	661.98	632.4	1138.3	1.7760	0.1307×10^{10}
400.00	751.98	638.7	1149.7	1.7854	0.1412×10^{10}
450.00	841.98	645.1	1161.2	1.7942	0.1517×10^{10}
500.00	931.98	651.4	1172.6	1.8024	0.1622×10^{10}
550.00	1021.98	657.8	1184.0	1.8101	0.1727×10^{10}
600.00	1111.98	664.1	1195.5	1.8174	0.1832×10^{10}
650.00	1201.98	670.5	1206.9	1.8243	0.1937×10^{10}
700.00	1291.98	676.8	1218.4	1.8309	0.2042×10^{10}
750.00	1381.98	683.2	1229.8	1.8371	0.2147×10^{10}
800.00	1471.98	689.5	1241.2	1.8430	0.2252×10^{10}
850.00	1561.98	695.9	1252.7	1.8487	0.2356×10^{10}
900.00	1651.98	702.3	1264.1	1.8542	0.2461×10^{10}
1950.00	1741.98	708.6	1275.5	1.8594	0.2566×10^{10}
1000.00	1831.98	715.0	1287.0	1.8644	0.2671×10^{10}
1050.00	1921.98	721.3	1298.4	1.8692	0.2776×10^{10}
1100.00	2011.98	727.7	1309.8	1.8739	0.2881×10^{10}
1150.00	2101.98	734.0	1321.3	1.8784	0.2986×10^{10}

of Potassium (Continued)

Specific volume V Ft^3/lb	Compressibility factor *ZH*	Average mol. weight ABARH	Dimer *X2H*	Tetramer *X4H*
		0.0000025 Atm		
0.1039×10^{8}	0.9999	0.3910×10^{2}	0.2259×10^{-5}	Zero
0.1106×10^{8}	0.9999	0.3910×10^{2}	0.1323×10^{-5}	
0.1174×10^{8}	0.9999	0.3910×10^{2}	Zero	
0.1241×10^{8}	0.9999	0.3910×10^{2}		
0.1308×10^{8}	0.9999	0.3910×10^{2}		
0.1375×10^{8}	0.9999	0.3910×10^{2}		
0.1442×10^{8}	0.9999	0.3910×10^{2}		
0.1510×10^{8}	0.9999	0.3910×10^{2}		
0.1577×10^{8}	0.9999	0.3910×10^{2}		
0.1644×10^{8}	0.9999	0.3910×10^{2}		
0.1711×10^{8}	0.9999	0.3910×10^{2}		
0.1779×10^{8}	0.9999	0.3910×10^{2}		
0.1846×10^{8}	0.9999	0.3910×10^{2}		
0.1913×10^{8}	0.9999	0.3910×10^{2}		
0.1980×10^{8}	0.9999	0.3910×10^{2}		
0.2048×10^{8}	0.9999	0.3910×10^{2}		
0.2115×10^{8}	0.9999	0.3910×10^{2}		
0.2182×10^{8}	0.9999	0.3910×10^{2}		
0.2249×10^{8}	0.9999	0.3910×10^{2}		
0.2316×10^{8}	0.9999	0.3910×10^{2}		
0.2384×10^{8}	0.9999	0.3910×10^{2}		
		0.000001 Atm		
0.1431×10^{8}	0.9988	0.3914×10^{2}	0.1156×10^{-2}	Zero
0.1590×10^{8}	0.9997	0.3911×10^{2}	0.2397×10^{-3}	
0.1758×10^{8}	0.9999	0.3910×10^{2}	0.6065×10^{-4}	
0.1926×10^{8}	0.9999	0.3910×10^{2}	0.1950×10^{-4}	
0.2094×10^{8}	0.9999	0.3910×10^{2}	0.7521×10^{-5}	
0.2262×10^{8}	0.9999	0.3910×10^{2}	0.3342×10^{-5}	
0.2430×10^{8}	0.9999	0.3910×10^{2}	0.1661×10^{-5}	
0.2598×10^{8}	0.9999	0.3910×10^{2}	Zero	
0.2767×10^{8}	0.9999	0.3910×10^{2}		
0.2935×10^{8}	0.9999	0.3910×10^{2}		
0.3103×10^{8}	0.9999	0.3910×10^{2}		
0.3271×10^{8}	0.9999	0.3910×10^{2}		
0.3439×10^{8}	0.9999	0.3910×10^{2}		
0.3607×10^{8}	0.9999	0.3910×10^{2}		
0.3775×10^{8}	0.9999	0.3910×10^{2}		
0.3943×10^{8}	0.9999	0.3910×10^{2}		
0.4111×10^{8}	0.9999	0.3910×10^{2}		
0.4279×10^{8}	0.9999	0.3910×10^{2}		
0.4447×10^{8}	0.9999	0.3910×10^{2}		
0.4615×10^{8}	0.9999	0.3910×10^{2}		
0.4783×10^{8}	0.9999	0.3910×10^{2}		

TABLE D.1 - Vapor Properties

Temperature		Enthalpy H		Entropy S	Specific volume V
°C	°F	Cal/g	Btu/lb	Cal/g-°C or Btu/lb-°F	Cm^3/g
0.000001 Atm					
1200.00	2191.98	740.4	1332.7	1.8828	0.3091×10^{10}
1250.00	2281.98	746.7	1344.2	1.8871	0.3196×10^{10}
1300.00	2371.98	753.1	1355.6	1.8913	0.3301×10^{10}
1350.00	2461.98	759.4	1367.0	1.8952	0.3406×10^{10}
1400.00	2551.98	765.8	1378.5	1.8992	0.3511×10^{10}
1450.00	2641.98	772.1	1389.9	1.9030	0.3616×10^{10}
1500.00	2731.98	778.5	1401.3	1.9068	0.3721×10^{10}

TABLE D.2 - Vapor

Temperature		Enthalpy H		Entropy S	Specific olume V
°C	°F	Cal/g	Btu/lb	Cal/g-°C or Btu/lb-°F	Cm^3/g
25 Atm					
1404.63	2560.32	1319.2	2374.6	1.6191	0.1877×100^3
1450.00	2641.98	1343.7	2418.8	1.6337	0.1982×10^3
1500.00	2731.98	1369.2	2464.6	1.6483	0.2093×10^3
10 Atm					
1211.24	2212.22	1308.9	2356.1	1.6762	0.4420×10^3
1250.00	2281.98	1330.5	2394.9	0.6907	0.4635×10^3
1300.00	2371.98	1356.1	2441.0	1.7074	0.4900×10^3
1350.00	2461.98	1379.6	2483.3	1.7223	0.5155×10^3
1400.00	2551.98	1401.2	2522.1	1.7355	0.5400×10^3
1450.00	2641.98	1421.1	2558.0	1.7474	0.5636×10^3
1500.00	2731.98	1439.7	2591.5	1.7581	0.5864×10^3
5 Atm					
1093.06	1999.49	1300.6	2341.1	1.7206	0.8387×10^3
1100.00	2011.98	1304.7	2348.4	1.7236	0.8463×10^3
1150.00	2101.98	1332.1	2397.8	0.7435	0.8994×10^3
1200.00	2191.98	1356.7	2442.0	1.7607	0.9501×10^3
1250.00	2281.98	1378.9	2482.0	1.7757	0.9985×10^3
1300.00	2371.98	1399.1	2518.4	1.7890	0.1044×10^4
1350.00	2461.98	1417.7	2551.8	1.8007	0.1089×10^4
1400.00	2551.98	1434.9	2582.9	1.8113	0.1133×10^4
1450.00	2641.98	1451.0	2611.9	1.8210	0.1175×10^4
1500.00	2731.98	1466.3	2639.4	1.8298	0.1216×10^4

---

*The first line in each pressure group

of Potassium (Continued)

Specific volume V Ft^3/lb	Compressibility factor *ZH*	Average mol. weight ABARH	Dimer *X2H*	Tetramer *X4H*
0.000001 Atm				
0.4952×10^8	0.9999	0.3910×10^2	Zero	Zero
0.5120×10^8	0.9999	0.3910×10^2		
0.5288×10^8	0.9999	0.3910×10^2		
0.5456×10^8	0.9999	0.3910×10^2		
0.5624×10^8	0.9999	0.3910×10^2		
0.5792×10^8	0.9999	0.3910×10^2		
0.5960×10^8	0.9999	0.3910×10^2		

Properties of Sodium*

Specific volume V Ft^3/lb	Compressibility factor *ZH*	Average mol. weight ABARH	Dimer *X2H*	Tetramer *X4H*
25 Atm				
0.3008×10^1	0.7840	0.2932×10^2	0.1788	0.3219×10^{-1}
0.3175×10^1	0.8057	0.2853×10^2	0.1634	0.2586×10^{-1}
0.3353×10^1	0.8271	0.2779×10^2	0.1479	0.2035×10^{-1}
10 Atm				
0.7081×10^1	0.8344	0.2755×10^2	0.1607×10^{-1}	0.1257×10^{-1}
0.7424×10^1	0.8526	0.2696×10^2	0.1438×10^{-1}	0.9660×10^{-2}
0.7850×10^1	0.8728	0.2633×10^2	0.1248×10^{-1}	0.6915×10^{-2}
0.8258×10^1	0.8899	0.2583×10^2	0.1086×10^{-1}	0.4990×10^{-2}
0.8650×10^1	0.9043	0.2542×10^2	0.9486×10^{-1}	0.3635×10^{-2}
0.9028×10^1	0.9164	0.2508×10^2	0.8314×10^{-1}	0.2676×10^{-2}
0.9393×10^1	0.9266	0.2481×10^2	0.7318×10^{-1}	0.1991×10^{-2}
5 Atm				
0.1343×10^2	0.8600	0.2673×10^2	0.1450×10^{-1}	0.5905×10^{-2}
0.1355×10^2	0.8634	0.2662×10^2	0.1414×10^{-1}	0.5567×10^{-2}
0.1440×10^2	0.8854	0.2596×10^2	0.1183×10^{-1}	0.3662×10^{-2}
0.1521×10^2	0.9035	0.2544×10^2	0.9944×10^{-1}	$0.2437 \times\times 10^{-2}$
0.1590×10^2	0.9183	0.2503×10^2	0.8394×10^{-1}	0.1644×10^{-2}
0.1673×10^2	0.9305	0.2470×10^2	0.7127×10^{-1}	0.1126×10^{-2}
0.1745×10^2	0.9405	0.2444×10^2	0.6089×10^{-1}	0.7835×10^{-3}
0.1815×10^2	0.9487	0.2423×10^2	0.5235×10^{-1}	0.5536×10^{-3}
0.1882×10^2	0.9555	0.2405×10^2	0.4530×10^{-1}	0.3972×10^{-3}
0.1948×10^2	0.9612	0.2391×10^2	$0.3944 \quad 10^{-1}$	$0.2894 \quad 10^{-3}$

---

pertains to the saturated condition.

TABLE D.2 - Vapor Properties

Temperature		Enthalpy H		Entropy S	Specific volume V
°C	°F	Cal/g	Btu/lb	Cal/g-°C or Btu/lb-°F	Cm^3/g
			2.5 Atm		
992.82	1819.08	1292.6	2326.8	1.7661	0.1589×10^4
1000.00	1831.98	1296.9	2334.5	1.7695	0.1604×10^4
1050.00	1921.98	1324.6	2384.3	1.7912	0.1708×10^4
1100.00	2011.98	1349.0	2428.2	1.8095	0.1807×10^4
1150.00	2101.98	1370.6	2467.2	1.8253	0.1901×10^4
1200.00	2191.98	1390.1	2502.2	1.8389	0.1991×10^4
1250.00	2281.98	2407.8	2534.1	1.8510	0.2078×10^4
1300.00	2371.98	1424.2	2563.5	1.8617	0.2162×10^4
1350.00	2461.88	1439.4	2591.0	1.8714	0.2243×10^4
1400.00	2551.98	1453.9	2617.0	1.8803	0.2323×10^4
1450.00	2641.98	1467.7	2641.8	1.8885	0.2402×10^4
1500.00	2731.98	1480.9	2665.7	1.8962	0.2480×10^4
			1 Atm		
881.46	1618.61	1283.4	2310.2	1.8281	0.3704×10^4
900.00	1651.98	1294.6	2330.3	1.8379	0.3802×10^4
950.00	1741.98	1321.6	2378.9	1.8608	0.4054×10^4
1000.00	1831.98	1344.7	2420.5	1.8796	0.4290×10^4
1050.00	1921.98	1364.8	2456.7	1.8955	0.4514×10^4
1100.00	2011.98	1382.7	2488.9	1.9090	0.4729×10^4
1150.00	2101.98	1398.9	2518.0	1.9208	0.4935×10^4
1200.00	2191.98	1413.8	2545.0	1.9314	0.5136×10^4
1250.00	2281.98	1427.9	2570.2	1.9409	0.5332×10^4
1300.00	2371.98	1441.2	2594.2	1.9497	0.5525×10^4
1350.00	2461.98	1454.0	2617.2	1.9579	0.5716×10^4
1400.00	2551.98	1466.4	2639.6	1.9656	0.5904×10^4
1450.00	2641.98	1478.5	2661.3	1.9728	0.6090×10^4
1500.00	2731.98	1490.3	2682.7	1.9797	0.6275×10^4
			0.5 Atm		
810.41	1490.72	1278.0	2300.4	1.8763	0.7052×10^4
850.00	1561.98	1301.2	2342.2	1.8982	0.7458×10^4
900.00	1651.98	1326.0	2386.8	1.9203	0.7938×10^4
950.00	1741.98	1346.9	2424.5	1.9381	0.8387×10^4
1000.00	1831.98	1365.0	2457.1	1.9530	0.8814×10^4
1050.00	1921.98	1381.2	2486.2	1.9658	0.9224×10^4
1100.00	2011.98	1395.9	2512.7	1.9770	0.9621×10^4
1150.00	2101.98	1409.7	2537.5	1.9871	0.1000×10^5
1200.00	2191.98	1422.7	2560.9	1.9963	0.1039×10^5
1250.00	2281.98	1435.2	2583.4	2.0049	0.1076×10^5
1300.00	2371.98	1447.3	2605.3	2.0129	0.1113×10^5
1350.00	2461.98	1459.2	2626.6	2.0204	0.1150×10^5
1400.00	2551.98	1470.8	2647.5	2.0276	0.1187×10^5
1450.00	2641.98	1482.3	2668.2	2.0345	0.1223×10^5
1500.00	2731.98	1493.6	2688.6	2.0411	0.1260×10^5

of Sodium (Continued)

Specific volume V Ft^{3}/lb	Compressibility factor *ZH*	Average mol. weight ABARH	Dimer *X2H*	Tetramer *X4H*
		2.5 Atm		
0.2545×10^{2}	0.8792	0.2614×10^{2}	0.1292	0.2704×10^{-2}
0.2570×10^{2}	0.8827	0.260×10^{2}	0.1252	0.2512×10^{-2}
0.2737×10^{2}	0.9045	0.2541×10^{2}	0.1009	0.1515×10^{-2}
0.2895×10^{2}	0.9220	0.2493×10^{2}	0.8179×10^{-1}	0.9307×10^{-3}
0.3045×10^{2}	0.9358	0.2456×10^{2}	0.6679×10^{-1}	0.5828×10^{-3}
0.3189×10^{2}	0.9468	0.2428×10^{2}	0.5500×10^{-1}	0.3728×10^{-3}
0.3328×10^{2}	0.9556	0.2405×10^{2}	0.4569×10^{-1}	0.2436×10^{-3}
0.3463×10^{2}	0.9626	0.2388×10^{2}	0.3829×10^{-1}	0.1625×10^{-3}
0.3594×10^{2}	0.9683	0.2374×10^{2}	0.3236×10^{-1}	0.1107×10^{-3}
0.3722×10^{2}	0.9729	0.2363×10^{2}	0.2759×10^{-1}	0.7688×10^{-4}
0.3848×10^{2}	0.9766	0.2353×10^{2}	0.2370×10^{-1}	0.5438×10^{-4}
0.3972×10^{2}	0.9797	0.2346×10^{2}	0.2051×10^{-1}	0.3915×10^{-4}
		1 Atm		
0.5934×10^{4}	0.8787	0.2557×10^{2}	0.1095	0.9368×10^{-3}
0.6080×10^{4}	0.9081	0.2531×10^{2}	0.9896×10^{-1}	0.7388×10^{-3}
0.6494×10^{4}	0.9286	0.2475×10^{2}	0.7560×10^{-1}	0.3959×10^{-3}
0.6872×10^{4}	0.9442	0.2434×10^{2}	0.5838×10^{-1}	0.2182×10^{-3}
0.7231×10^{4}	0.9560	012404×10^{2}	0.4563×10^{-1}	0.1239×10^{-3}
0.7575×10^{4}	0.9649	0.2382×10^{2}	0.3612×10^{-1}	0.7260×10^{-4}
0.7906×10^{4}	0.9717	0.2365×10^{2}	0.2896×10^{-1}	0.4383×10^{-4}
0.8228×10^{4}	0.9769	0.2353×10^{2}	0.2350×10^{-1}	0.2724×10^{-4}
0.8542×10^{4}	0.9810	0.2343×10^{2}	0.1939×10^{-1}	0.1740×10^{-4}
0.8851×10^{4}	0.9841	0.2336×10^{2}	0.1603×10^{-1}	0.1140×10^{-4}
0.9156×10^{4}	0.9866	0.2330×10^{2}	0.1346×10^{-1}	0.7658×10^{-5}
0.9457×10^{4}	0.9887	0.2325×10^{2}	0.1140×10^{-1}	0.5257×10^{-5}
0.9756×10^{4}	0.9903	0.2321×10^{2}	0.9755×10^{-2}	0.3684×10^{-5}
0.1005×10^{4}	0.9916	0.2318×10^{2}	0.8412×10^{-2}	0.2632×10^{-5}
		0.5 Atm		
0.1129×10^{4}	0.9117	0.2521×10^{2}	0.9552×10^{-1}	0.4091×10^{-3}
0.1194×10^{4}	0.9303	0.2471×10^{2}	0.7419×10^{-1}	0.2278×10^{-3}
0.1271×10^{4}	0.9479	0.2425×10^{2}	0.5455×10^{-1}	0.1122×10^{-3}
0.1343×10^{4}	0.9606	0.2393×10^{2}	0.4073×10^{-1}	0.5747×10^{-4}
0.1411×10^{4}	0.9699	0.2370×10^{2}	0.3092×10^{-1}	0.3062×10^{-4}
0.1477×10^{4}	0.9766	0.2354×10^{2}	0.2387×10^{-1}	0.1696×10^{-4}
0.1541×10^{4}	0.9815	0.2342×10^{2}	0.1872×10^{-1}	0.9751×10^{-5}
0.1603×10^{5}	0.9852	0.2333×10^{2}	0.1490×10^{-1}	0.5804×10^{-5}
0.1664×10^{5}	0.9880	0.2326×10^{2}	0.1203×10^{-1}	0.3568×10^{-5}
0.1724×10^{5}	0.9902	0.2321×10^{2}	0.9843×10^{-2}	0.2260×10^{-5}
0.1784×10^{5}	0.9919	0.2317×10^{2}	0.8148×10^{-2}	0.1472×10^{-5}
0.1843×10^{5}	0.9932	0.2314×10^{2}	0.6821×10^{-2}	Zero
0.1902×10^{5}	0.9942	0.2312×10^{2}	0.5769×10^{-2}	
0.1960×10^{5}	0.9950	0.2310×10^{2}	0.4925×10^{-2}	
0.2018×10^{5}	0.9957	0.2308×10^{2}	0.4241×10^{-2}	

TABLE D.2 - Vapor Properties

Temperature		Enthalpy H		Entropy S	Specific volume V
°C	°F	Cal/g	Btu/lb	Cal/g-°C or Btu/lb-°F	Cm^3/g
			0.25 Atm		
748.00	1378.38	1273.5	2292.3	1.9256	0.1345×10^5
750.00	1381.98	1274.7	2294.6	1.9269	0.1350×10^5
800.00	1471.98	1303.1	2345.6	1.9551	0.1449×10^5
850.00	1561.98	1325.9	2386.7	1.9770	0.1541×10^5
900.00	1651.98	1345.1	2421.1	1.9941	0.1627×10^5
950.00	1741.98	1361.6	2450.9	2.0083	0.1709×10^5
1000.00	1831.98	1376.5	2477.7	2.0206	0.1789×10^5
1050.00	1921.98	1390.2	2502.3	2.0314	0.1866×10^5
1100.00	2011.98	1403.0	2525.5	2.0413	0.1941×10^5
1150.00	2101.98	1415.4	2547.8	2.0504	0.2016×10^5
1200.00	2191.98	1427.4	2569.3	2.0589	0.2090×10^5
1250.00	2281.98	1439.0	2590.3	2.0669	0.2163×10^5
1300.00	2371.98	1450.5	2611.0	2.0744	0.2236×10^5
1350.00	2461.98	1461.9	2631.4	2.0817	0.2309×10^5
1400.00	2551.98	1473.1	2651.6	2.0886	0.2381×10^5
1450.00	2641.98	1484.2	2671.6	2.0953	0.2453×10^5
1500.00	2731.98	1495.3	2691.6	2.1018	0.2526×10^5
			0.1 Atm		
675.96	1248.71	1268.3	2283.0	1.9921	0.3171×10^5
700.00	1291.98	1282.7	2308.9	2.0078	0.3292×10^5
750.00	1381.98	1307.3	2353.2	2.0337	0.3525×10^5
800.00	1471.98	1327.0	2388.6	2.0536	0.3739×10^5
850.00	1561.98	1343.4	2418.2	2.0697	0.3942×10^5
900.00	1651.98	1358.0	2444.4	2.0829	0.4137×10^5
950.00	1741.98	1371.3	2468.4	2.0944	0.4327×10^5
1000.00	1831.98	1383.8	2490.9	2.1047	0.4514×10^5
1050.00	1921.98	1395.8	2512.5	2.1143	0.4699×10^5
1100.00	2011.98	1407.5	2533.6	2.1232	0.4882×10^5
1150.00	2101.98	1419.0	2554.2	2.1317	0.5063×10^5
1200.00	2191.98	1430.2	2574.5	2.1397	0.5244×10^5
1250.00	2281.98	1441.4	2594.5	2.1473	0.5425×10^5
1300.00	2371.98	1452.5	2614.5	2.1547	0.5605×10^5
1350.00	2461.98	1463.5	2634.3	2.1617	0.5785×10^5
1400.00	2551.98	1474.5	2654.1	2.1685	0.5964×10^5
1450.00	2641.98	1485.4	2673.8	2.1751	0.6143×10^5
1500.00	2731.98	1496.3	2693.4	2.1814	0.6323×10^5
			0.05 Atm		
627.98	1162.35	1264.9	2276.8	2.0433	0.6079×10^5
650.00	1201.98	1277.9	2300.2	2.0582	0.6296×10^5
700.00	1291.98	1301.8	2343.2	2.0849	0.6751×10^5
750.00	1381.98	1320.4	2376.8	2.1049	0.7170×10^5
800.00	1471.98	1336.0	2404.9	2.1209	0.7566×10^5
850.00	1561.98	1349.8	2429.7	2.1346	0.7949×10^5

of Sodium (Continued)

Specific volume V Ft^{3}/lb	Compressibility factor *ZH*	Average mol. weight ABARH	Dimer *X2H*	Tetramer *X4H*
		0.25 Atm		
0.2155×10^{3}	0.9231	0.2490×10^{2}	0.8266×10^{-1}	0.1759×10^{-3}
0.2162×10^{3}	0.9242	0.2487×10^{2}	0.8143×10^{-1}	0.1699×10^{-3}
0.2322×10^{3}	0.9463	0.2429×10^{2}	0.5648×10^{-1}	0.7311×10^{-4}
0.2469×10^{3}	0.9615	0.2391×10^{2}	0.3991×10^{-1}	0.3297×10^{-4}
0.2607×10^{3}	0.9719	0.2365×10^{2}	0.2878×10^{-1}	0.1563×10^{-4}
0.2738×10^{3}	0.9792	0.2347×10^{2}	0.2121×10^{-1}	0.7789×10^{-5}
0.2865×10^{3}	0.9842	0.2335×10^{2}	0.1594×10^{-1}	0.4070×10^{-5}
0.2989×10^{3}	0.9879	0.2327×10^{2}	0.1222×10^{-1}	0.2223×10^{-5}
0.3220×10^{3}	0.9905	0.2321×10^{2}	0.9536×10^{-2}	0.1265×10^{-5}
0.3230×10^{3}	0.9924	0.2316×10^{2}	0.7563×10^{-2}	Zero
0.3348×10^{3}	0.9939	0.2313×10^{2}	0.6089×10^{-2}	
0.3465×10^{3}	0.9950	0.2310×10^{2}	0.4970×10^{-2}	
0.3582×10^{3}	0.9959	0.2308×10^{2}	0.4107×10^{-2}	
0.3699×10^{3}	0.9965	0.2306×10^{2}	0.3434×10^{-2}	
0.3815×10^{3}	0.9971	0.2305×10^{2}	0.2901×10^{-2}	
0.3930×10^{3}	0.9975	0.2304×10^{2}	0.2474×10^{-2}	
0.4046×10^{3}	0.9978	0.2303×10^{2}	0.2129×10^{-2}	
		0.1 Atm		
0.5081×10^{3}	0.9363	0.2455×10^{2}	0.6776×10^{-1}	0.5673×10^{-4}
0.5274×10^{3}	0.9479	0.2425×10^{2}	0.5480×10^{-1}	0.3481×10^{-4}
0.5646×10^{3}	0.9653	0.2381×10^{2}	0.3589×10^{-1}	0.1320×10^{-4}
0.5990×10^{3}	0.9763	0.2354×10^{2}	0.2417×10^{-1}	0.5355×10^{-5}
0.6315×10^{3}	0.9835	0.2337×10^{2}	0.1674×10^{-1}	0.2321×10^{-5}
0.6628×10^{3}	0.9882	0.2326×10^{2}	0.1191×10^{-1}	0.1071×10^{-5}
0.6932×10^{3}	0.9913	0.2319×10^{2}	0.8702×10^{-2}	Zero
0.7231×10^{3}	0.9935	0.2314×10^{2}	0.6502×10^{-2}	
0.7587×10^{3}	0.9950	0.2310×10^{2}	0.4961×10^{-2}	
0.7820×10^{3}	0.9961	0.2307×10^{2}	0.3858×10^{-2}	
0.8111×10^{3}	0.9969	0.2306×10^{2}	0.3053×10^{-2}	
0.8401×10^{3}	0.9975	0.2304×10^{2}	0.2453×10^{-2}	
0.8690×10^{3}	0.9980	0.2303×10^{2}	0.1999×10^{-2}	
0.8979×10^{3}	0.9983	0.2302×10^{2}	0.1651×10^{-2}	
0.9266×10^{3}	0.9986	0.2302×10^{2}	0.1379×10^{-2}	
0.9554×10^{3}	0.9988	0.2301×10^{2}	0.1164×10^{-2}	
0.9841×10^{3}	0.9990	0.2301×10^{2}	0.9929×10^{-3}	
0.1012×10^{4}	0.9991	0.2301×10^{2}	0.8541×10^{-3}	
		0.05 Atm		
0.9738×10^{3}	0.9451	0.2432×10^{2}	0.5801×10^{-1}	0.2385×10^{-4}
0.1008×10^{3}	0.9554	0.2406×10^{2}	0.4657×10^{-1}	0.1440×10^{-4}
0.1081×10^{4}	0.9718	0.2365×10^{2}	0.2892×10^{-1}	0.4849×10^{-5}
0.1148×10^{4}	0.9817	0.2341×10^{2}	0.1859×10^{-1}	0.1772×10^{-5}
0.1212×10^{4}	0.9877	0.2327×10^{2}	0.2348×10^{-1}	Zero
0.1273×10^{4}	0.9915	0.2318×10^{2}	0.8513×10^{-2}	

TABLE D.2 - Vapor Properties

Temperature		Enthalpy H		Entropy S	Specific volume V
°C	°F	Cal/g	Btu/lb	Cal/g-°C or Btu/lb-°F	Cm^3/g
			0.05 Atm		
900.00	1651.98	1362.6	2452.7	2.1462	0.8323×10^5
950.00	1741.98	1374.7	2474.5	2.1567	0.8692×10^5
1000.00	1831.98	1386.4	2495.5	2.1664	0.9058×10^5
1050.00	1921.98	1397.8	2516.1	2.1755	0.9421×10^5
1100.00	2011.98	1409.0	2536.3	2.1841	0.9782×10^5
1150.00	2101.98	1420.2	2556.3	2.1923	0.1014×10^6
1200.00	2191.98	1431.2	2576.2	2.2001	0.1050×10^6
1250.00	2281.98	1442.2	2596.0	2.2077	0.1086×10^6
1300.00	2371.98	1453.1	2615.7	2.2149	0.1122×10^6
1350.00	2461.98	1464.0	2635.3	2.2219	0.1157×10^6
1400.00	2551.98	1474.9	2654.9	2.2286	0.1193×10^6
1450.00	2641.98	1485.8	2674.5	2.2352	0.1229×10^6
1500.00	2731.98	1496.7	2694.0	2.2415	0.1265×10^6
			0.025 Atm		
584.69	1084.44	1261.7	2271.0	2.0950	0.1166×10^6
600.00	1111.98	1270.7	2287.3	2.1060	0.1196×10^6
650.00	1201.98	1294.4	2329.9	2.1340	0.1286×10^6
700.00	1291.98	1312.5	2362.5	2.1546	0.1368×10^6
750.00	1381.98	1327.5	2389.5	2.1709	0.1446×10^6
800.00	1471.98	1340.8	2413.5	2.1848	0.1522×10^6
850.00	1561.98	1353.2	2435.7	2.1971	0.1596×10^6
900.00	1651.98	1364.9	2456.9	2.2079	0.1669×10^6
950.00	1741.98	1376.4	2477.6	2.2178	0.1742×10^6
1000.00	1831.98	1387.7	2497.8	2.2271	0.1814×10^6
1050.00	1921.98	1398.8	2517.8	2.2360	0.1886×10^6
1100.00	2011.98	1409.8	2537.7	2.2445	0.1958×10^6
1150.00	2101.98	1420.8	2557.4	2.2526	0.2030×10^6
1200.00	2191.98	1431.7	2577.1	2.2603	0.2101×10^6
1250.00	2281.98	1442.6	2596.7	2.2678	0.2173×10^6
1300.00	2371.98	1453.5	2616.3	2.2750	0.2244×10^6
1350.00	2461.98	1464.3	2635.8	2.2820	0.2316×10^6
1400.00	2551.98	1475.2	2655.3	2.2887	0.2387×10^6
1450.00	2641.98	1486.0	2674.8	2.2952	0.2459×10^6
1500.00	2731.98	1496.8	2694.3	2.3015	0.2530×10^6
			0.01 Atm		
533.57	992.41	1257.6	2263.8	2.1640	0.2768×10^6
550.00	1021.98	1266.8	2280.4	2.1760	0.2846×10^6
600.00	1111.98	1288.8	2319.9	2.2038	0.3062×10^6
650.00	1201.98	1305.4	2349.8	2.2239	0.3262×10^6
700.00	1291.98	1319.3	2374.9	2.2401	0.3452×10^6
750.00	1381.98	1331.9	2397.5	2.2539	0.3637×10^6
800.00	1471.98	1343.7	2418.8	2.2664	0.3820×10^6
850.00	1561.98	1355.2	2439.4	2.2778	0.4001×10^6
900.00	1651.98	1366.4	2459.5	2.2881	0.4181×10^6

of Sodium (Continued)

Specific volume V Ft^3/lb	Compressibility factor *ZH*	Average mol. weight ABARH	Dimer *X2H*	Tetramer *X4H*
0.05 Atm				
0.1333×10^{4}	0.9940	0.2312×10^{2}	0.6031×10^{-2}	Zero
0.1392×10^{4}	0.9956	0.2309×10^{2}	0.4389×10^{-2}	
0.1451×10^{4}	0.9967	0.2306×10^{2}	0.3272×10^{-2}	
0.1509×10^{4}	0.9975	0.2304×10^{2}	0.2493×10^{-2}	
0.1567×10^{4}	0.9980	0.2303×10^{2}	0.1936×10^{-2}	
0.1624×10^{4}	0.9984	0.2302×10^{2}	0.1531×10^{-2}	
0.1682×10^{4}	0.9987	0.2301×10^{2}	0.1229×10^{-2}	
0.1739×10^{4}	0.9989	0.2301×10^{2}	0.1001×10^{-2}	
0.1797×10^{4}	0.9991	0.2301×10^{2}	0.8269×10^{-3}	
0.1854×10^{4}	0.9993	0.2300×10^{2}	0.6906×10^{-3}	
0.1912×10^{4}	0.9994	0.2300×10^{2}	0.5879×10^{-3}	
0.1969×10^{4}	0.9995	0.2300×10^{2}	0.4969×10^{-3}	
0.2026×10^{4}	0.9995	0.2300×10^{2}	0.4274×10^{-3}	
0.025 Atm				
0.1869×10^{4}	0.9528	0.2412×10^{2}	0.4948×10^{-1}	0.9954×10^{-5}
0.1916×10^{4}	0.9599	0.2394×10^{2}	0.4166×10^{-1}	0.6714×10^{-5}
0.2060×10^{4}	0.9761	0.2355×10^{2}	0.2438×10^{-1}	0.1974×10^{-5}
0.2192×10^{4}	0.9853	0.2333×10^{2}	0.1488×10^{-1}	Zero
0.2317×10^{4}	0.9906	0.2320×10^{2}	0.9473×10^{-2}	
0.2438×10^{4}	0.9937	0.2313×10^{2}	0.6267×10^{-2}	
0.2557×10^{4}	0.9957	0.2308×10^{2}	0.4293×10^{-2}	
0.2674×10^{4}	0.9969	0.2306×10^{2}	0.3033×10^{-2}	
0.2791×10^{4}	0.9978	0.2304×10^{2}	0.2204×10^{-2}	
0.2906×10^{4}	0.9983	0.2302×10^{2}	0.1641×10^{-2}	
0.3022×10^{4}	0.9987	0.2301×10^{2}	0.1249×10^{-2}	
0.3137×10^{4}	0.9990	0.2301×10^{2}	0.9702×10^{-3}	
0.3252×10^{4}	0.9992	0.2300×10^{2}	0.7667×10^{-3}	
0.3366×10^{4}	0.9993	0.2300×10^{2}	0.6156×10^{-3}	
0.3481×10^{4}	0.9994	0.2300×10^{2}	0.5014×10^{-3}	
0.3596×10^{4}	0.9995	0.2300×10^{2}	0.4138×10^{-3}	
0.3710×10^{4}	0.9996	0.2299×10^{2}	0.3455×10^{-3}	
0.3825×10^{4}	0.9997	0.2299×10^{2}	0.2916×10^{-3}	
0.3939×10^{4}	0.9997	0.2299×10^{2}	0.2485×10^{-3}	
0.4054×10^{4}	0.9997	0.2299×10^{2}	0.2138×10^{-3}	
0.01 Atm				
0.4435×10^{4}	0.9616	0.2390×10^{2}	0.3989×10^{-1}	0.3102×10^{-5}
0.4558×10^{4}	0.9687	0.2373×10^{2}	0.3226×10^{-1}	0.1910×10^{-5}
0.4905×10^{4}	0.9827	0.2339×10^{2}	0.1751×10^{-1}	Zero
0.5225×10^{4}	0.9900	0.2322×10^{2}	0.1004×10^{-1}	
0.5530×10^{4}	0.9939	0.2313×10^{2}	0.6060×10^{-2}	
0.5827×10^{4}	0.9961	0.2307×10^{2}	0.3832×10^{-2}	
0.6119×10^{4}	0.9974	0.2304×10^{2}	0.2525×10^{-2}	
0.6410×10^{4}	0.9982	0.2303×10^{2}	0.1726×10^{-2}	
0.6698×10^{4}	0.9987	0.2301×10^{2}	0.1217×10^{-2}	

TABLE D.2 - Vapor Properties

Temperature		Enthalpy H		Entropy S	Specific volume V
°C	°F	Cal/g	Btu/lb	Cal/g-°C or Btu/lb-°F	Cm^3/g
0.01 Atm					
950.00	1741.98	1377.5	2479.5	2.2977	0.4361×10^6
1000.00	1831.98	1388.4	2499.2	2.3069	0.4540×10^6
1050.00	1921.98	1399.4	2518.9	2.3156	0.4720×10^6
1100.00	2011.98	1410.3	2538.5	2.3240	0.4898×10^6
1150.00	2101.98	1421.1	2558.1	2.3320	0.5077×10^6
1200.00	2191.98	1432.0	2577.6	2.3397	0.5256×10^6
1250.00	2281.98	1442.8	2597.1	2.3471	0.5435×10^6
1300.00	2371.98	1453.7	2616.6	2.3543	0.5613×10^6
1350.00	2461.98	1464.5	2636.1	2.3612	0.5792×10^6
1400.00	2551.98	1475.3	2655.6	2.3679	0.5970×10^6
1450.00	2641.98	1486.1	2675.0	2.3744	0.6149×10^6
1500.00	2731.98	1496.9	2694.5	2.3807	0.6327×10^6
0.005 Atm					
498.82	929.86	1254.7	2258.4	2.2165	0.5330×10^6
500.00	931.98	1255.3	2259.6	2.2175	0.5341×10^6
550.00	1021.98	1278.7	2301.7	2.2489	0.5779×10^6
600.00	1111.98	1295.5	2331.9	2.2706	0.6177×10^6
650.00	1201.98	1309.3	2356.8	2.2876	0.6556×10^6
700.00	1291.98	1321.7	2379.1	2.3022	0.6925×10^6
750.00	1381.98	1333.4	2400.2	2.3152	0.7289×10^6
800.00	1471.98	1344.7	2420.6	2.3271	0.7650×10^6
850.00	1561.98	1355.9	2440.6	2.3383	0.8010×10^6
900.00	1651.98	1366.9	2460.4	2.3483	0.8369×10^6
950.00	1741.98	1377.8	2480.1	2.3579	0.8727×10^6
1000.00	1831.98	1388.7	2499.7	2.3670	0.9084×10^6
1050.00	1921.98	1399.6	2519.3	2.3756	0.9442×10^6
1100.00	2011.98	1410.4	2538.8	2.3840	0.9799×10^6
1150.00	2101.98	1421.3	2558.3	2.3920	0.1015×10^7
1200.00	2191.98	1432.1	2577.8	2.3997	0.1051×10^7
1250.00	2281.98	1442.9	2597.3	2.4071	0.1087×10^7
1300.00	2371.98	1453.7	2616.7	2.4143	0.1122×10^7
1350.00	2461.98	1464.5	2636.2	2.4212	0.1158×10^7
1400.00	2551.98	1475.3	2655.7	2.4279	0.1194×10^7
1450.00	2641.98	1486.2	2675.1	2.4343	0.1229×10^7
1500.00	2731.98	1497.0	2694.6	2.4406	0.2165×10^7
0.0025 Atm					
466.99	872.56	1251.7	2253.1	2.2692	0.1027×10^7
500.00	931.98	1267.5	2281.5	2.2917	0.1085×10^7
550.00	1021.98	1285.0	2313.1	2.3158	0.1165×10^7
600.00	1111.98	1299.0	2338.2	2.3341	0.1240×10^7
650.00	1201.98	1311.3	2360.4	2.3495	0.1314×10^7
700.00	1291.98	1322.9	2381.3	2.3632	0.1387×10^7

of Sodium (Continued)

Specific volume V Ft^3/lb	Compressibility factor *ZH*	Average mol. weight ABARH	Dimer *X2H*	Tetramer *X4H*
		0.01 Atm		
0.6986×10^{4}	0.9991	0.2301×10^{2}	0.8840×10^{-3}	Zero
0.7273×10^{4}	0.9993	0.2300×10^{2}	0.6578×10^{-3}	
0.7560×10^{4}	0.9994	0.2300×10^{2}	0.5006×10^{-3}	
0.7847×10^{4}	0.9996	0.2299×10^{2}	0.3885×10^{-3}	
0.8133×10^{4}	0.9996	0.2299×10^{2}	0.3069×10^{-3}	
0.8420×10^{4}	0.9997	1.2299×10^{2}	0.2464×10^{-3}	
0.8706×10^{4}	0.9997	0.2299×10^{2}	0.2007×10^{-3}	
0.8992×10^{4}	0.9998	0.2299×10^{2}	0.1656×10^{-3}	
0.9278×10^{4}	0.9998	0.2299×10^{2}	0.1382×10^{-3}	
0.9564×10^{4}	0.9998	0.2299×10^{2}	0.1167×10^{-3}	
0.9850×10^{4}	0.9999	0.2299×10^{2}	0.9946×10^{-4}	
0.1013×10^{5}	0.9999	0.2299×10^{2}	0.8554×10^{-4}	
		0.005 Atm		
0.8538×10^{4}	0.9673	0.2376×10^{2}	0.3378×10^{-1}	0.1275×10^{-5}
0.8556×10^{4}	0.9678	0.2375×10^{2}	0.3321×10^{-1}	0.1226×10^{-5}
0.9257×10^{4}	0.9836	0.2337×10^{2}	0.1665×10^{-1}	Zero
0.9895×10^{4}	0.9911	0.2319×10^{2}	0.8913×10^{-2}	
0.1050×10^{5}	0.9949	0.2310×10^{2}	0.5071×10^{-2}	
0.1109×10^{5}	0.9969	0.2306×10^{2}	0.3048×10^{-2}	
0.1167×10^{5}	0.9980	0.2303×10^{2}	0.1923×10^{-2}	
0.1225×10^{5}	0.9987	0.2302×10^{2}	0.1266×10^{-2}	
0.1283×10^{5}	0.9991	0.2301×10^{2}	0.8645×10^{-3}	
0.1340×10^{5}	0.9993	0.2300×10^{2}	0.6097×10^{-3}	
0.1397×10^{5}	0.9995	0.2300×10^{2}	0.4423×10^{-3}	
0.1455×10^{5}	0.9996	0.2299×10^{2}	0.3291×10^{-3}	
0.1512×10^{5}	0.9997	0.2299×10^{2}	0.2504×10^{-3}	
0.1569×10^{5}	0.9998	0.2299×10^{2}	0.1943×10^{-3}	
0.1627×10^{5}	0.9998	0.2299×10^{2}	0.1535×10^{-3}	
0.1684×10^{5}	0.9998	0.2299×10^{2}	0.1232×10^{-3}	
0.1741×10^{5}	0.9998	0.2299×10^{2}	0.1003×10^{-3}	
0.1798×10^{5}	0.9999	0.2299×10^{2}	0.8282×10^{-4}	
0.1855×10^{5}	0.9999	0.2299×10^{2}	0.6914×10^{-4}	
0.1913×10^{5}	0.9999	0.2299×10^{2}	0.5835×10^{-4}	
0.1970×10^{5}	0.9999	0.2299×10^{2}	0.4973×10^{-4}	
0.2027×10^{5}	0.9999	0.2299×10^{2}	0.4277×10^{-4}	
		0.0025 Atm		
0.1645×10^{5}	0.9722	0.2364×10^{2}	0.2853×10^{-1}	Zero
0.1838×10^{5}	0.9831	0.2338×10^{2}	0.1716×10^{-1}	
0.1866×10^{5}	0.9916	0.2318×10^{2}	0.8468×10^{-2}	
0.1987×10^{5}	0.9955	0.2309×10^{2}	0.4496×10^{-2}	
0.2105×10^{5}	0.9974	0.2304×10^{2}	0.2548×10^{-2}	
0.2222×10^{5}	0.9984	0.2302×10^{2}	0.1529×10^{-2}	

TABLE D.2 - Vapor Properties

Temperature		Enthalpy H		Entropy S	Specific volume V
°C	°F	Cal/g	Btu/lb	Cal/g-°C or Btu/lb-°F	Cm^3/g
		0.0025 Atm			
750.00	1381.98	1334.2	2401.6	2.3757	0.1459×10^7
800.00	1471.98	1345.2	2421.5	2.3874	0.1531×10^7
850.00	1561.98	1356.2	2441.2	2.3985	0.1602×10^7
900.00	1651.98	1367.1	2460.8	2.4085	0.1674×10^7
950.00	1741.98	1378.0	2480.4	2.4179	0.1745×10^7
1000.00	1831.98	1388.8	2499.9	2.4270	0.1817×10^7
1050.00	1921.98	1399.7	2519.4	2.4356	0.1888×10^7
1100.00	2011.98	1410.5	2538.9	2.4439	0.1960×10^7
1150.00	2101.98	1421.3	2558.4	2.4519	0.2031×10^7
1200.00	2191.98	1432.1	2577.9	2.4596	0.2102×10^7
1250.00	2281.98	1442.9	259713	2.4670	0.2174×10^7
1300.00	2371.98	2453.8	2616.8	2.4742	0.2245×10^7
1350.00	2461.98	1464.6	2636.2	2.4811	0.2317×10^7
1400.00	2551.98	1475.4	2655.7	2.4878	0.2388×10^7
1450.00	2641.98	1486.2	2675.2	2.4943	0.2459×10^7
1500.00	2731.98	2497.0	2694.6	2.5006	0.2531×10^7
		0.001 Atm			
428.77	803.77	1247.8	2246.1	2.3391	0.2449×10^7
450.00	841.98	1257.8	2264.1	2.3543	0.2541×10^7
500.00	931.98	1275.4	2295.7	2.3802	0.2740×10^7
550.00	1021.98	1289.0	2320.3	2.3994	0.2927×10^7
600.00	1111.98	1801.1	2342.0	2.4155	0.3110×10^7
650.00	1201.98	1312.5	2362.6	2.4299	0.3291×10^7
700.00	1291.98	1323.7	2382.6	2.4430	0.3471×10^7
750.00	1381.98	1334.6	2402.4	2.4553	0.3650×10^7
800.00	1471.98	1345.5	2422.0	2.4669	0.3829×10^7
850.00	1561.98	1356.4	2441.6	2.4778	0.4007×10^7
900.00	1651.98	1367.3	2461.1	2.4878	0.4186×10^7
950.00	1741.98	1378.1	2480.6	2.4972	0.4365×10^7
1000.00	1831.98	1388.9	2500.1	2.5062	0.4543×10^7
1050.00	1921.98	1399.7	2519.6	2.5149	0.4722×10^7
1100.00	2011.98	1410.5	2539.0	2.5232	0.4900×10^7
1150.00	2101.98	1421.4	2558.5	2.5311	0.5079×10^7
1200.00	2191.98	1432.2	257719	2.5388	0.5257×10^7
1250.00	2281.98	1443.0	2597.4	2.5462	0.5436×10^7
1300.00	2371.98	1453.8	2616.8	2.5534	0.5614×10^7
1350.00	2461.98	1464.6	2636.3	2.5603	0.5793×10^7
1400.00	2551.98	1475.4	2655.7	2.5670	0.5971×10^7
1450.00	2641.98	1486.2	2675.2	2.5735	0.6149×10^7
1500.00	2731.98	1497.0	2694.6	2.5798	0.6328×10^7
		0.0005 Atm			
402.42	756.34	1244.9	2240.9	2.3921	0.4731×10^7

of Sodium (Continued)

Specific volume V Ft^3/lb	Compressibility factor *ZH*	Average mol. weight ABARH	Dimer *X2H*	Tetramer *X4H*
0.0025 Atm				
0.2337×10^{5}	0.9990	0.2301×10^{2}	0.9637×10^{-3}	Zero
0.2452×10^{5}	0.9993	0.2300×10^{2}	0.6338×10^{-3}	
0.2567×10^{5}	0.9995	0.2300×10^{2}	0.4326×10^{-3}	
0.2681×10^{5}	0.9996	0.2299×10^{2}	0.3050×10^{-3}	
0.2796×10^{5}	0.9997	0.2299×10^{2}	0.2212×10^{-3}	
0.2911×10^{5}	0.9998	0.2299×10^{2}	0.1646×10^{-3}	
0.3025×10^{5}	0.9998	0.2299×10^{2}	0.1252×10^{-3}	
0.3139×10^{5}	0.9999	0.2299×10^{2}	0.9719×10^{-4}	
0.3254×10^{5}	0.9999	0.2299×10^{2}	0.7678×10^{-4}	
0.3368×10^{5}	0.9999	0.2299×10^{2}	0.6163×10^{-4}	
0.3483×10^{5}	0.9999	0.2299×10^{2}	0.5019×10^{-4}	
0.3597×10^{5}	0.9999	0.2299×10^{2}	0.4141×10^{-4}	
0.3711×10^{5}	0.9999	0.2299×10^{2}	0.3457×10^{-4}	
0.3826×10^{5}	0.9999	0.2299×10^{2}	0.2918×10^{-4}	
0.3940×10^{5}	0.9999	0.2299×10^{2}	0.2487×10^{-4}	
0.4054×10^{5}	0.9999	0.2299×10^{2}	0.2138×10^{-4}	
0.001 Atm				
0.3923×10^{5}	0.9777	0.2351×10^{2}	0.2275×10^{-1}	Zero
0.4070×10^{5}	0.9845	0.2335×10^{2}	0.1569×10^{-1}	
0.4389×10^{5}	0.9930	0.2315×10^{2}	0.7007×10^{-2}	
0.4690×10^{5}	0.9965	0.2306×10^{2}	0.3422×10^{-2}	
0.4982×10^{5}	0.9981	0.2303×10^{2}	0.1808×10^{-2}	
0.5272×10^{5}	0.9989	0.2301×10^{2}	0.1022×10^{-2}	
0.5560×10^{5}	0.9993	0.2300×10^{2}	0.6127×10^{-3}	
0.5847×10^{5}	0.9996	1.2299×10^{2}	0.3859×10^{-3}	
0.6133×10^{5}	0.9997	0.2299×10^{2}	0.2537×10^{-3}	
0.6420×10^{5}	0.9998	0.2299×10^{2}	0.1731×10^{-3}	
0.6706×10^{5}	0.9999	0.2299×10^{2}	0.8854×10^{-3}	
0.6992×10^{5}	0.9999	0.2299×10^{2}	0.8854×10^{-4}	
0.7278×10^{5}	0.9999	0.2299×10^{2}	0.6586×10^{-4}	
0.7564×10^{5}	0.9999	0.2299×10^{2}	0.5010×10^{-4}	
0.7850×10^{5}	0.9999	0.2299×10^{2}	0.3888×10^{-4}	
0.8136×10^{5}	0.9999	0.2299×10^{2}	0.3071×10^{-4}	
0.8421×10^{5}	0.9999	0.2299×10^{2}	0.2465×10^{-4}	
0.8707×10^{5}	0.9999	0.2299×10^{2}	0.2007×10^{-4}	
0.8993×10^{5}	0.9999	0.2299×10^{2}	0.1656×10^{-4}	
0.9279×10^{5}	0.9999	0.2299×10^{2}	0.1383×10^{-4}	
0.9565×10^{5}	0.9999	0.2299×10^{2}	0.1167×10^{-4}	
0.9851×10^{5}	0.9999	0.2299×10^{2}	0.9948×10^{-5}	
0.1013×10^{5}	0.9999	0.2299×10^{2}	0.8555×10^{-5}	
0.0005 Atm				
0.7579×10^{5}	0.9812	0.2343×10^{2}	0.1912×10^{-1}	Zero

TABLE D.2 - Vapor Properties

Temperature		Enthalpy H		Entropy S	Specific volume V
°C	°F	Cal/g	Btu/lb	Cal/g-°C or Btu/lb-°F	Cm^3/g
0.0005 Atm					
450.00	841.98	1263.8	2274.9	2.4218	0.5121×10^7
500.00	931.98	1278.1	2300.7	2.4433	0.5499×10^7
550.00	1021.98	1290.4	2322.7	2.4608	0.5865×10^7
600.00	1111.98	1301.8	2343.3	2.4761	0.6227×10^7
650.00	1201.98	1312.9	2363.3	2.4902	0.6586×10^7
700.00	1291.98	1323.9	2383.1	2.5031	0.6944×10^7
750.00	1381.98	1334.8	2402.7	2.5154	0.7302×10^7
800.00	1471.98	1345.6	2422.2	2.5269	0.7659×10^7
850.00	1561.98	1356.5	2441.7	2.5378	0.8016×10^7
900.00	1651.98	1367.3	2461.2	2.5477	0.8373×10^7
950.00	1741.98	1378.1	2480.7	2.5571	0.8730×10^7
1000.00	1831.98	1388.9	2500.1	2.5661	0.9087×10^7
1050.00	1921.98	1399.7	2519.6	2.5748	0.9444×10^7
1100.00	2011.98	1410.6	2539.0	2.5831	0.9801×10^7
1150.00	2101.98	1421.4	2558.5	2.5911	0.1015×10^8
1200.00	2191.98	1432.2	2577.9	2.5987	0.1051×10^8
1250.00	2281.98	1443.0	2597.4	2.6061	0.1087×10^8
1300.00	2371.98	1453.8	2616.8	2.6133	0.1122×10^8
1350.00	2461.98	1464.6	2636.3	2.6202	0.1158×10^8
1400.00	2551.98	1475.4	2655.7	2.6269	0.1194×10^8
1450.00	2641.98	1486.2	2675.2	2.6334	0.1230×10^8
1500.00	2731.98	1497.0	2694.6	2.6397	0.1265×10^8
0.00025 Atm					
378.01	712.40	1242.0	2235.6	2.4451	0.9149×10^7
400.00	751.98	1251.3	2252.3	2.4604	0.9512×10^7
450.00	841.98	1266.9	2280.5	2.4857	0.1028×10^8
500.00	931.98	1279.5	2303.2	2.5049	0.1101×10^8
550.00	1021.98	1291.0	2323.9	2.5215	0.1174×10^8
600.00	1111.98	1302.2	2344.0	2.5364	0.1245×10^8
650.00	1201.98	1313.1	2363.7	2.5503	0.1317×10^8
700.00	1291.98	1324.0	2383.3	2.5632	0.1387×10^8
750.00	1381.98	1334.9	2402.8	2.5753	0.1460×10^8
800.00	1471.98	1345.7	2422.3	2.5868	0.1531×10^8
850.00	1561.98	1356.5	2441.8	2.5977	0.1603×10^8
900.00	1651.98	1367.3	2461.2	2.6077	0.1674×10^8
950.00	1741.98	1378.1	2480.7	2.6171	0.1746×10^8
1000.00	1831.98	1389.0	2500.2	2.6261	0.1817×10^8
1050.00	1921.98	1399.8	2519.6	2.6347	0.1888×10^8
1100.00	2011.98	1410.6	2539.1	2.6430	0.1960×10^8
1150.00	2101.98	1421.4	2558.5	2.6510	012031×10^8
1200.00	2191.98	1432.2	2578.0	2.6587	0.2103×10^8
1250.00	2281.98	1443.0	2598.4	2.6661	0.2174×10^8
1300.00	2371.98	2453.8	2616.8	2.6732	0.2245×10^8

of Sodium (Continued)

Specific volume V Ft^3/lb	Compressibility factor *ZH*	Average mol. weight ABARH	Dimer *X2H*	Tetramer *X4H*
		0.0005 Atm		
0.8203×10^{5}	0.9920	0.2317×10^{2}	0.7973×10^{-2}	Zero
0.8809×10^{5}	0.9964	0.2307×10^{2}	0.3528×10^{-2}	
0.9395×10^{5}	0.9982	0.2303×10^{2}	0.1716×10^{-2}	
0.9974×10^{5}	0.9990	0.2301×10^{2}	0.9057×10^{-3}	
0.1055×10^{6}	0.9994	0.2300×10^{2}	0.5118×10^{-3}	
0.1112×10^{6}	0.9996	0.2299×10^{2}	0.3065×10^{-3}	
0.1169×10^{6}	0.9998	0.2299×10^{2}	0.1930×10^{-3}	
0.1226×10^{6}	0.9998	0.2299×10^{2}	0.1268×10^{-3}	
0.1284×10^{6}	0.9999	0.2299×10^{2}	0.8658×10^{-4}	
0.1341×10^{6}	0.9999	0.2299×10^{2}	0.6103×10^{-4}	
0.1398×10^{6}	0.9999	0.2299×10^{2}	0.4427×10^{-4}	
0.1455×10^{6}	0.9999	0.2299×10^{2}	0.3293×10^{-4}	
0.1512×10^{6}	0.9999	0.2299×10^{2}	0.2505×10^{-4}	
0.1570×10^{6}	0.9999	0.2299×10^{2}	0.1944×10^{-4}	
0.1627×10^{6}	0.9999	0.2299×10^{2}	0.1535×10^{-4}	
0.1684×10^{6}	0.9999	0.2299×10^{2}	0.1232×10^{-4}	
0.1741×10^{6}	0.9999	0.2299×10^{2}	0.1003×10^{-4}	
0.1798×10^{6}	0.9999	0.2299×10^{2}	0.8283×10^{-5}	
0.1855×10^{6}	0.9999	0.2299×10^{2}	0.6915×10^{-5}	
0.1913×10^{6}	0.9999	0.2299×10^{2}	0.5836×10^{-5}	
0.1970×10^{6}	0.9999	0.2299×10^{2}	0.4974×10^{-5}	
0.2027×10^{6}	0.9999	0.2299×10^{2}	0.4278×10^{-5}	
		0.00025 Atm		
0.1465×10^{6}	0.9842	0.2335×10^{2}	0.1604×10^{-1}	Zero
0.1523×10^{6}	0.9898	0.2322×10^{2}	0.1022×10^{-1}	
0.1647×10^{6}	0.9959	0.2308×10^{2}	0.4018×10^{-2}	
0.1764×10^{6}	0.9982	0.2303×10^{2}	0.1770×10^{-2}	
0.1880×10^{6}	0.9991	0.2301×10^{2}	0.8599×10^{-3}	
0.1995×10^{6}	0.9995	0.2300×10^{2}	0.4532×10^{-3}	
0.2110×10^{6}	0.9997	0.2299×10^{2}	0.2560×10^{-3}	
0.2225×10^{6}	0.9998	0.2299×10^{2}	0.1533×10^{-3}	
0.2339×10^{6}	0.9999	0.2299×10^{2}	0.9653×10^{-4}	
0.2453×10^{6}	0.9999	0.2299×10^{2}	0.6345×10^{-4}	
0.2568×10^{6}	0.9999	0.2299×10^{2}	0.4329×10^{-4}	
0.2682×10^{6}	0.9999	0.2299×10^{2}	0.3052×10^{-4}	
0.2792×10^{6}	0.9999	0.2299×10^{2}	0.2213×10^{-4}	
0.2911×10^{6}	0.9999	0.2299×10^{2}	0.1646×10^{-4}	
0.3025×10^{6}	0.9999	0.2299×10^{2}	0.1252×10^{-4}	
0.3140×10^{6}	0.9999	0.2299×10^{2}	0.9721×10^{-5}	
0.3254×10^{6}	0.9999	0.2299×10^{2}	0.7679×10^{-5}	
0.3368×10^{6}	0.9999	0.2299×10^{2}	0.6164×10^{-5}	
0.3483×10^{6}	0.9999	0.2299×10^{2}	0.5019×10^{-5}	
0.3597×10^{6}	0.9999	0.2299×10^{2}	0.4141×10^{-5}	

TABLE D.2 - Vapor Properties

Temperature		Enthalpy H		Entropy S	Specific volume V
°C	°F	Cal/g	Btu/lb	Cal/g-°C or Btu/lb-°F	Cm^3/g
			0.00025 Atm		
1350.00	2461.98	1464.6	2636.3	2.6801	0.2317×10^8
1400.00	2551.98	1475.4	2655.7	2.6868	0.2388×10^8
1450.00	2641.98	1486.2	2675.2	2.6933	0.2460×10^8
1500.00	2731.98	1497.0	2694.6	2.6996	0.2531×10^8
			0.0001 Atm		
348.34	659.00	1238.2	2228.8	2.5153	0.2190×10^8
350.00	661.98	1238.9	2230.1	2.5166	0.2197×10^8
400.00	751.98	1256.0	2260.9	2.5462	0.2392×10^8
450.00	841.98	1268.8	2284.0	2.5673	0.2576×10^8
500.00	931.98	1280.4	2304.7	2.5851	0.2757×10^8
550.00	1021.98	1291.5	2324.7	2.6011	0.2936×10^8
600.00	1111.98	1302.4	2344.3	2.6159	0.3115×10^8
650.00	1201.98	1313.3	2363.9	2.6296	0.3294×10^8
700.00	1291.98	1324.1	2383.4	2,6425	0.3473×10^8
750.00	1383.98	1334.9	2402.9	2.6546	0.3651×10^8
800.00	1471.98	1345.7	2422.4	2.6661	0.3830×10^8
850.00	1561.98	1356.5	2441.8	2.6769	0.4008×10^8
900.00	1651.98	1367.3	2461.3	2.6869	0.4187×10^8
950.00	1741.98	1378.2	2480.7	2.6963	0.4365×10^8
1000.00	1831.98	1389.0	2500.2	2.7053	0.4543×10^8
1050.00	1921.98	1399.8	2519.6	2.7139	0.4722×10^8
1100.00	2011.98	1410.6	2539.1	2.7222	0.4900×10^8
1150.00	2101.98	1421.4	2558.5	2.7302	0.4079×10^8
1200.00	2191.98	1432.2	2578.0	2.7379	0.5257×10^8
1250.00	2281.98	1443.0	2597.4	2.7453	0.5436×10^8
1300.00	2371.98	1453.8	2616.8	2.7524	0.5614×10^8
1350.00	2461.98	1464.6	2636.3	2.7593	0.5793×10^8
1400.00	2551.98	1475.4	2655.7	2.7660	0.5971×10^8
1450.00	2641.98	1486.2	2675.2	2.7725	0.6150×10^8
1500.00	2731.98	1497.0	2694.6	2.7788	0.6328×10^8
			0.00005 Atm		
327.66	621.77	1235.3	2223.6	2.5684	0.4243×10^8
350.00	661.98	1243.6	2238.6	2.5835	0.4420×10^8
400.00	751.98	1257.7	2263.8	2.6083	0.4794×10^8
450.00	841.98	1269.5	2285.1	2.6280	0.5157×10^8
500.00	931.98	1280.6	2305.2	2.6453	0.5516×10^8
550.00	1021.98	1291.6	2324.9	2.6612	0.5874×10^8
600.00	1111.98	1302.5	2344.5	2.6758	0.6232×10^8
650.00	1201.98	1313.3	2364.0	2.6895	0.6589×10^8
700.00	1291.98	1324.1	2383.5	2.7024	0.6946×10^8
750.00	1381.98	1334.9	2402.9	2.7145	0.7303×10^8
800.00	1471.98	1345.7	2422.4	2.7260	0.7660×10^8

of Sodium (Continued)

Specific volume V Ft^3/lb	Compressibility factor *ZH*	Average mol. weight ABARH	Dimer *X2H*	Tetramer *X4H*
		0.00025 Atm		
0.3711×10^6	0.9999	0.2299×10^2	0.3457×10^{-5}	Zero
0.3826×10^6	0.9999	0.2299×10^2	0.2918×10^{-5}	
0.3940×10^6	0.9999	0.2299×10^2	0.2487×10^{-5}	
0.4054×10^6	0.9999	0.2299×10^2	0.2139×10^{-5}	
		0.0001 Atm		
0.3508×10^6	0.9874	0.2328×10^2	0.1269×10^{-1}	Zero
0.3519×10^6	0.9879	0.2327×10^2	0.1221×10^{-1}	
0.3832×10^6	0.9958	0.2308×10^2	0.4140×10^{-2}	
0.4127×10^6	0.9983	0.2302×10^2	0.1615×10^{-2}	
0.4417×10^6	0.9992	0.2300×10^2	0.7097×10^{-3}	
0.4704×10^6	0.9996	0.2299×10^2	0.3443×10^{-3}	
0.4991×10^6	0.9998	0.2299×10^2	0.1814×10^{-3}	
0.5277×10^6	0.9998	0.2299×10^2	0.1024×10^{-3}	
0.5563×10^6	0.9999	0.2299×10^2	0.6134×10^{-4}	
0.5849×10^6	0.9999	0.2299×10^2	0.3861×10^{-4}	
0.6135×10^6	0.9999	0.2299×10^2	0.2538×10^{-4}	
0.6421×10^6	0.9999	0.2299×10^2	0.1731×10^{-4}	
0.6706×10^6	0.9999	0.2299×10^2	0.1220×10^{-4}	
0.6992×10^6	0.9999	0.2299×10^2	0.8855×10^{-5}	
0.7278×10^6	0.9999	0.2299×10^2	0.6587×10^{-5}	
0.7564×10^6	0.9999	0.2299×10^2	0.5011×10^{-5}	
0.7850×10^6	0.9999	0.2299×10^2	0.3888×10^{-5}	
0.8136×10^6	0.9999	0.2299×10^2	0.3071×10^{-5}	
0.8422×10^6	0.9999	0.2299×10^2	0.2465×10^{-5}	
0.8707×10^6	0.9999	0.2299×10^2	0.2007×10^{-5}	
0.8993×10^6	0.9999	0.2299×10^2	0.1656×10^{-5}	
0.9279×10^6	0.9999	0.2299×10^2	0.1383×10^{-5}	
0.9565×10^6	0.9999	0.2299×10^2	0.1167×10^{-5}	
0.9851×10^6	0.9999	0.2299×10^2	Zero	
0.1013×10^7	0.9999	0.2299×10^2		
		0.00005 Atm		
0.6797×10^6	0.9894	0.2323×10^2	0.1062×10^{-1}	Zero
0.7081×10^6	0.9938	0.2313×10^2	0.6184×10^{-1}	
0.7681×10^6	0.9979	0.2303×10^2	0.2079×10^{-2}	
0.8262×10^6	0.9991	0.2300×10^2	0.8088×10^{-2}	
0.8837×10^6	0.9996	0.2299×10^2	0.3551×10^{-3}	
0.9410×10^6	0.9998	0.2299×10^2	0.1722×10^{-3}	
0.9982×10^6	0.9999	0.2299×10^2	0.9072×10^{-3}	
0.1055×10^7	0.9999	0.2299×10^2	0.5122×10^{-4}	
0.1112×10^7	0.9999	0.2299×10^2	0.3067×10^{-4}	
0.1169×10^7	0.9999	0.2299×10^2	0.1939×10^{-4}	
0.1227×10^7	0.9999	0.2299×10^2	0.1269×10^{-4}	

TABLE D.2 - Vapor Properties

Temperature		Enthalpy H		Entropy S	Specific volume V
°C	°F	Cal/g	Btu/lb	Cal/g-°C or Btu/lb-°F	Cm^3/g
		0.00005 Atm			
850.00	1561.98	1356.5	2441.8	2.7369	0.8017 × 10^8
900.00	1651.98	1367.4	2461.3	2.7468	0.8374 × 10^8
950.00	1741.98	1378.2	2480.7	2.7562	0.8731 × 10^8
1000.00	1831.98	1389.0	2500.2	2.7652	0.9087 × 10^8
1050.00	1921.98	1399.8	2519.6	2.7738	0.9444 × 10^8
1100.00	2011.98	1410.6	2539.1	2.7821	0.9801 × 10^8
1150.00	2101.98	1421.4	2558.5	2.7901	0.1015 × 10^9
1200.00	2191.98	1432.2	2578.0	2.7978	0.1051 × 10^9
1250.00	2281.98	1443.0	2597.4	2.8052	0.1087 × 10^9
1300.00	2371.98	1453.8	2616.9	2.8123	0.1122 × 10^9
1350.00	2461.98	1464.6	2636.3	2.8192	0.1158 × 10^9
1400.00	2551.98	1475.4	2655.7	2.8259	0.1194 × 10^9
1450.00	2641.98	1486.2	2675.2	2.8324	0.2230 × 10^9
1500.00	2731.98	1497.0	2694.6	2.8387	0.1265 × 10^9
		0.000025 Atm			
308.31	586.96	1232.5	2218.5	2.6216	0.8228 × 10^8
350.00	661.98	1246.0	2242.9	2.6471	0.8868 × 10^8
400.00	751.98	1258.5	2265.3	2.6694	0.9600 × 10^8
450.00	841.98	1269.8	2285.7	2.6883	0.1031 × 10^9
500.00	931.98	1280.8	2305.5	2.7054	0.1103 × 10^9
550.00	1021.98	1291.7	2325.0	2.7212	0.1175 × 10^9
600.00	1111.98	1302.5	2344.5	2.7358	0.1246 × 10^9
650.00	1201.98	1313.3	2364.0	2.7495	0.1317 × 10^9
700.00	1291.98	1324.1	2383.5	2.7623	0.1389 × 10^9
750.00	1381.98	1334.9	2402.9	2.7744	0.1460 × 10^9
800.00	1471.98	1345.7	2422.4	2.7859	0.1532 × 10^9
850.00	1561.98	1356.6	2441.8	2.7968	0.1603 × 10^9
900.00	1651.98	1367.4	2461.3	2.8067	0.1674 × 10^9
950.00	1741.98	1378.2	2480.7	2.8161	0.1746 × 10^9
1000.00	1831.98	1389.0	2500.2	2.8251	0.1817 × 10^9
1050.00	1921.98	139918	2519.6	2.8337	0.1888 × 10^9
1100.00	2011.98	1410.6	2539.1	2.8420	0.1960 × 10^9
1150.00	2101.98	1421.4	2558.5	2.8500	0.2031 × 10^9
1200.00	2191.98	1432.2	2578.0	2.8577	0.2103 × 10^9
1250.00	2281.98	1443.0	2597.4	2.8651	0.2174 × 10^9
1300.00	2371.98	1453.8	2616.9	2.8722	0.2245 × 10^9
1350.00	2461.98	1464.6	2636.3	2.8791	0.2317 × 10^9
1400.00	2551.98	1475.4	2655.7	2.8858	0.2388 × 10^9
1450.00	2641.98	1486.2	2675.2	2.8923	0.2460 × 10^9
1500.00	2731.98	1497.0	2694.6	2.8986	0.2531 × 10^9
		0.00001 Atm			
284.61	544.28	1228.9	2212.0	2.6920	0.1976 × 10^9

of Sodium (Continued)

Specific volume V Ft^3/lb	Compressibility factor *ZH*	Average mol. weight ABARH	Dimer *X2H*	Tetramer *X4H*
		0.00005 Atm		
0.1284×10^{7}	0.9999	0.2299×10^{2}	0.8660×10^{-5}	Zero
0.1341×10^{7}	0.9999	0.2299×10^{2}	0.6104×10^{-5}	
0.1398×10^{7}	0.9999	0.2299×10^{2}	0.4427×10^{-5}	
0.1455×10^{7}	0.9999	0.2299×10^{2}	0.3293×10^{-5}	
0.1512×10^{7}	0.9999	0.2299×10^{2}	0.2505×10^{-5}	
0.1570×10^{7}	0.9999	0.2299×10^{2}	0.1944×10^{-5}	
0.1627×10^{7}	0.9999	0.2299×10^{2}	0.1535×10^{-5}	
0.1684×10^{7}	0.9999	0.2299×10^{2}	0.1232×10^{-5}	
0.1741×10^{7}	0.9999	0.2299×10^{2}	0.1003×10^{-5}	
0.1798×10^{7}	0.9999	0.2299×10^{2}	Zero	
0.1855×10^{7}	0.9999	0.2299×10^{2}		
0.1913×10^{7}	0.9999	0.2299×10^{2}		
0.1970×10^{7}	0.9999	0.2299×10^{2}		
0.2027×10^{7}	0.9999	0.2299×10^{2}		
		0.000025 Atm		
0.1318×10^{7}	0.9912	0.2319×10^{2}	0.8877×10^{-2}	Zero
0.1420×10^{7}	0.9968	0.2306×10^{2}	0.3111×10^{-2}	
0.1537×10^{7}	0.9989	0.2301×10^{2}	0.1041×10^{-2}	
0.1653×10^{7}	0.9995	0.2300×10^{2}	0.4047×10^{-3}	
0.1767×10^{7}	0.9998	0.2299×10^{2}	0.1776×10^{-3}	
0.1882×10^{7}	0.9999	0.2299×10^{2}	0.8612×10^{-4}	
0.1996×10^{7}	0.9999	0.2299×10^{2}	0.4536×10^{-4}	
0.2111×10^{7}	0.9999	0.2299×10^{2}	0.2561×10^{-4}	
0.2225×10^{7}	0.9999	0.2299×10^{2}	0.1533×10^{-4}	
0.2339×10^{7}	0.9999	0.2299×10^{2}	0.9655×10^{-5}	
0.2454×10^{7}	0.9999	0.2299×10^{2}	0.6346×10^{-5}	
0.2568×10^{7}	0.9999	0.2299×10^{2}	0.4330×10^{-5}	
0.2682×10^{7}	0.9999	0.2299×10^{2}	0.3052×10^{-5}	
0.2797×10^{7}	0.9999	0.2299×10^{2}	0.2213×10^{-5}	
0.2911×10^{7}	0.9999	0.2299×10^{2}	0.1646×10^{-5}	
0.3025×10^{7}	0.9999	0.2299×10^{2}	0.1252×10^{-5}	
0.3140×10^{7}	0.9999	0.2299×10^{2}	Zero	
0.3254×10^{7}	0.9999	0.2299×10^{2}		
0.3368×10^{7}	0.9999	0.2299×10^{2}		
0.3483×10^{7}	0.9999	0.2299×10^{2}		
0.3597×10^{7}	0.9999	0.2299×10^{2}		
0.3711×10^{7}	0.9999	0.2299×10^{2}		
0.3826×10^{7}	0.9999	0.2299×10^{2}		
0.3940×10^{7}	0.9999	0.2299×10^{2}		
0.4054×10^{7}	0.9999	0.2299×10^{2}		
		0.00001 Atm		
0.3166×10^{7}	0.9930	0.2315×10^{2}	0.6992×10^{-2}	Zero

TABLE D.2 - Vapor Properties

Temperature		Enthalpy H		Entropy S	Specific volume V
°C	°F	Cal/g	Btu/lb	Cal/g-°C or Btu/lb-°F	Cm^3/g
0.00001 Atm					
300.00	571.98	1234.1	2221.5	2.7024	0.2036×10^9
350.00	661.98	1247.5	2245.6	2.7285	0.2221×10^9
400.00	751.98	1259.0	2266.2	2.7493	0.2401×10^9
450.00	841.98	1270.0	2286.0	2.7678	0.2580×10^9
500.00	931.98	1280.9	2305.6	2.7847	0.2759×10^9
550.00	1021.98	1291.7	2325.1	2.8004	0.2937×10^9
600.00	111.98	1302.5	2344.6	2.8150	0.3116×10^9
650.00	1201.98	1313.3	2364.0	2.8287	0.3294×10^9
700.00	1291.98	1324.1	2383.5	2.8415	0.3473×10^9
750.00	1381.98	1334.9	2402.9	2.8536	0.3651×10^9
800.00	1471.98	1345.7	2422.4	2.8651	0.3830×10^9
850.00	1561.98	1356.6	2441.8	2.8760	0.4008×10^9
900.00	1651.98	1367.4	2461.3	2.8859	0.4187×10^9
950.00	1741.98	1378.2	2480.7	2.8953	0.4365×10^9
1000.00	1831.98	1389.0	2500.2	2.9043	0.4543×10^9
1050.00	1921.98	1399.8	2519.6	2.9129	0.4722×10^9
1100.00	2011.98	1410.6	2539.1	2.9212	0.4900×10^9
1150.00	2101.98	1421.4	2558.5	2.9292	0.5079×10^9
1200.00	2191.98	1432.2	2578.0	2.9369	0.5257×10^9
1250.00	2281.98	1443.0	2597.4	2.9443	0.5436×10^9
1300.00	2371.98	1453.8	2616.9	2.9514	0.5614×10^9
1350.00	2461.98	1464.6	2636.3	2.9583	0.5793×10^9
1400.00	2551.98	1475.4	2655.7	2.9650	0.5971×10^9
1450.00	2641.98	1486.2	2675.2	2.9715	0.6150×10^9
1500.00	2731.98	1497.0	2694.6	2.9778	0.6328×10^9
0.000005 Atm					
267.93	514.26	1226.2	2207.1	2.7454	0.3839×10^9
300.00	571.98	1235.9	2224.7	2.7654	0.4082×10^9
350.00	661.98	1248.0	2246.5	2.7891	0.4445×10^9
400.00	751.98	1259.2	2266.5	2.8094	0.4804×10^9
450.00	841.98	1270.1	2286.1	2.8278	0.5161×10^9
500.00	931.98	1280.9	2305.7	2.8446	0.5518×10^9
550.00	1021.98	1291.7	2325.1	2.8603	0.5875×10^9
600.00	1111.98	1302.5	2344.6	2.8749	0.6232×10^9
650.00	1201.98	1313.3	2364.0	2.8886	0.6589×10^9
700.00	1291.98	1324.1	2383.5	2.9014	0.6946×10^9
750.00	1381.98	1334.9	2402.9	2.9135	0.7303×10^9
800.00	1471.98	1345.7	2422.4	2.9250	0.7660×10^9
850.00	1561.98	1356.6	2441.8	2.9359	0.8017×10^9
900.00	1651.98	1367.4	2461.3	2.9458	0.8374×10^9
950.00	1741.98	1378.2	2480.7	2.9552	0.8731×10^9
1000.00	1831.98	1389.0	2500.2	2.9642	0.9087×10^9
1050.00	1921.98	1399.8	2519.6	2.9728	0.9444×10^9

PHYSICAL PROPERTIES

of Sodium (Continued)

Specific volume V Ft³/lb	Compressibility factor ZH	Average mol. weight ABARH	Dimer X2H	Tetramer X4H
		0.00001 Atm		
0.3262×10^{7}	0.9955	0.2309×10^{2}	0.4509×10^{-2}	Zero
0.3558×10^{7}	0.9987	0.2301×10^{2}	0.1249×10^{-2}	
0.3846×10^{7}	0.9995	0.2300×10^{2}	0.4171×10^{-3}	
0.4133×10^{7}	0.9998	0.2299×10^{2}	0.1619×10^{-3}	
0.4419×10^{7}	0.9999	0.2299×10^{2}	0.7106×10^{-4}	
0.4705×10^{7}	0.9999	0.2299×10^{2}	0.3445×10^{-4}	
0.4991×10^{7}	0.9999	0.2299×10^{2}	0.1814×10^{-4}	
0.5277×10^{7}	0.9999	0.2299×10^{2}	0.1024×10^{-4}	
0.5563×10^{7}	0.9999	0.2299×10^{2}	0.6135×10^{-5}	
0.5839×10^{7}	0.9999	0.2299×10^{2}	0.3862×10^{-5}	
0.6135×10^{7}	0.9999	0.2299×10^{2}	0.2538×10^{-5}	
0.6421×10^{7}	0.9999	0.2299×10^{2}	0.1732×10^{-5}	
0.6707×10^{7}	0.9999	0.2299×10^{2}	0.1220×10^{-5}	
0.6992×10^{7}	0.9999	0.2299×10^{2}	Zero	
0.7278×10^{7}	0.9999	0.2299×10^{2}		
0.7564×10^{7}	0.9999	0.2299×10^{2}		
0.7850×10^{7}	0.9999	0.2299×10^{2}		
0.8136×10^{7}	0.9999	0.2299×10^{2}		
0.8422×10^{7}	0.9999	0.2299×10^{2}		
0.8708×10^{7}	0.9999	0.2299×10^{2}		
0.8993×10^{7}	0.9999	0.2299×10^{2}		
0.9279×10^{7}	0.9999	$0.2299 \times \times 10^{2}$		
0.9565×10^{7}	0.9999	0.2299×10^{2}		
0.9851×10^{7}	0.9999	0.2299×10^{2}		
0.1013×10^{7}	0.9999	0.2299×10^{2}		
		0.000005 Atm		
0.6151×10^{7}	0.9942	0.2312×10^{2}	0.5831×10^{-2}	Zero
0.6538×10^{7}	0.9977	0.2304×10^{2}	0.2264×10^{-2}	
0.7120×10^{7}	0.9993	0.2300×10^{2}	0.6254×10^{-3}	
0.7695×10^{7}	0.9997	0.2299×10^{2}	0.2086×10^{-3}	
0.8268×10^{7}	0.9999	0.2299×10^{2}	0.8100×10^{-4}	
0.8840×10^{7}	0.9999	0.2299×10^{2}	0.3553×10^{-4}	
0.9411×10^{7}	0.9999	0.2299×10^{2}	0.1722×10^{-4}	
0.1183×10^{7}	0.9999	0.2299×10^{2}	0.9074×10^{-5}	
0.1066×10^{8}	0.9999	0.2299×10^{2}	0.5123×10^{-5}	
0.1112×10^{8}	0.9999	0.2299×10^{2}	0.3067×10^{-5}	
0.1169×10^{8}	0.9999	0.2299×10^{2}	0.1931×10^{-5}	
0.1227×10^{8}	0.9999	0.2299×10^{2}	0.1269×10^{-5}	
0.1284×10^{8}	0.9999	0.2299×10^{2}	Zero	
0.1341×10^{8}	0.9999	0.2299×10^{2}		
0.1398×10^{8}	0.9999	0.2299×10^{2}		
0.1455×10^{8}	0.9999	0.2299×10^{2}		
0.1512×10^{8}	0.9999	0.2299×10^{2}		

TABLE D.2 - Vapor Properties

Temperature		Enthalpy H		Entropy S	Specific volume V
°C	°F	Cal/g	Btu/lb	Cal/g-°C or Btu/lb-°F	Cm^3/g
		0.000005 Atm			
1100.00	2011.98	1410.6	2539.1	2.9811	0.9801×10^{9}
1150.00	2101.98	1421.4	2558.5	2.9891	0.1015×10^{10}
1200.00	2191.98	1432.2	2578.0	2.9968	0.1051×10^{10}
1250.00	2281.98	1443.0	2597.4	3.0042	0.1087×10^{10}
1300.00	2371.98	1453.8	2616.9	3.0113	0.1122×10^{10}
1350.00	2461.98	1464.6	2636.3	3.0183	0.1158×10^{10}
1400.00	2551.98	1475.4	2655.7	3.0249	0.1194×10^{10}
1450.00	2641.98	1486.2	2675.2	3.0314	0.1230×10^{10}
1500.00	2731.98	1497.0	2694.6	3.0377	0.1265×10^{10}
		0.0000025 Atm			
252.23	486.00	1223.5	2202.4	2.7988	0.7464×10^{9}
300.00	571.98	1236.8	2226.3	2.8267	0.8173×10^{9}
350.00	661.98	1248.3	2246.9	2.8494	0.8873×10^{9}
400.00	751.98	1259.2	2266.7	2.8694	0.9609×10^{9}
450.00	841.98	1270.1	2286.2	2.8877	0.1032×10^{10}
500.00	931.98	1280.9	2305.7	2.9046	0.1103×10^{10}
550.00	1021.98	1291.7	2325.1	2.9202	0.1175×10^{10}
600.00	1111.98	1302.5	2344.6	2.9348	0.1246×10^{10}
650.00	1201.98	1313.3	2364.0	2.9485	0.1317×10^{10}
700.00	1291.98	1324.1	2383.5	2.9613	0.1389×10^{10}
750.00	1381.98	1334.9	2402.9	2.9735	0.1460×10^{10}
800.00	1471.98	1345.8	2422.4	2.9849	0.1532×10^{10}
850.00	1561.98	1356.6	2441.8	2.9958	0.1603×10^{10}
900.00	1651.98	1367.4	2461.3	3.0057	0.1674×10^{10}
950.00	1741.98	1378.2	2480.7	3.0151	0.1746×10^{10}
1000.00	1831.98	1389.0	2500.2	3.0241	0.1817×10^{10}
1050.00	1921.98	1399.8	2519.6	3.0326	0.1888×10^{10}
1100.00	2011.98	1410.6	2539.1	3.0410	0.1960×10^{10}
1150.00	2101.98	1421.4	2558.5	3.0490	0.2031×10^{10}
1200.00	2191.98	1432.2	2578.0	3.0567	0.2103×10^{10}
1250.00	2281.98	1443.0	2597.4	3.0641	0.2174×10^{10}
1300.00	2371.98	1453.8	2616.9	3.0713	0.2245×10^{10}
1350.00	2461.98	1464.6	2636.3	3.0782	0.2317×10^{10}
1400.00	2551.98	1475.4	2655.7	3.0849	0.2388×10^{10}
1450.00	2641.98	1486.2	2675.2	3.0913	0.2460×10^{10}
1500.00	2731.98	1497.0	2694.6	3.0976	0.2531×10^{10}
		0.000001 Atm			
232.84	451.09	1220.2	2196.4	2.8695	0.1799×10^{10}
250.00	481.98	1225.2	2205.5	2.8807	0.1863×10^{10}
300.00	571.98	1237.4	2227.3	2.9068	0.2044×10^{10}
350.00	661.98	1248.4	2247.2	2.9288	0.2223×10^{10}
400.00	751.98	1259.3	2266.8	2.9487	0.2402×10^{10}

of Sodium (Continued)

Specific volume Ft^3/lb	Compressibility factor ZH	Average mol. weight ABARH	Dimer $X2H$	Tetramer $X4H$
		0.000005 Atm		
0.1570×10^{8}	0.9999	0.2299×10^{2}	Zero	Zero
0.1627×10^{8}	0.9999	0.2299×10^{2}		
0.1684×10^{8}	0.9999	0.2299×10^{2}		
0.1741×10^{8}	0.9999	0.2299×10^{2}		
0.1798×10^{8}	0.9999	0.2299×10^{2}		
0.1855×10^{8}	0.9999	0.2299×10^{2}		
0.1913×10^{8}	0.9999	0.2299×10^{2}		
0.1970×10^{8}	0.9999	0.2299×10^{2}		
0.2027×10^{8}	0.9999	0.2299×10^{2}		
		0.0000025 Atm		
0.1195×10^{8}	0.9951	0.2310×10^{2}	0.4860×10^{-2}	Zero
0.1309×10^{8}	0.9988	0.2301×10^{2}	0.1134×10^{-2}	
0.1424×10^{8}	0.9996	0.2299×10^{2}	0.3129×10^{-3}	
0.1539×10^{8}	0.9998	0.2299×10^{2}	0.1043×10^{-3}	
0.1653×10^{8}	0.9999	0.2299×10^{2}	0.4050×10^{-4}	
0.1768×10^{8}	0.9999	0.2299×10^{2}	0.1776×10^{-4}	
0.1882×10^{8}	0.9999	0.2299×10^{2}	0.8613×10^{-5}	
0.1996×10^{8}	0.9999	0.2299×10^{2}	0.4537×10^{-5}	
0.2111×10^{8}	0.9999	0.2299×10^{2}	0.2561×10^{-5}	
0.2225×10^{8}	0.9999	0.2299×10^{2}	0.1533×10^{-5}	
0.2339×10^{8}	0.9999	0.2299×10^{2}	Zero	
0.2454×10^{8}	0.9999	0.2299×10^{2}		
0.2568×10^{8}	0.9999	0.2299×10^{2}		
0.2682×10^{8}	0.9999	0.2299×10^{2}		
0.2797×10^{8}	0.9999	0.2299×10^{2}		
0.2911×10^{8}	0.9999	0.2299×10^{2}		
0.3025×10^{8}	0.9999	0.2299×10^{2}		
0.3140×10^{8}	0.9999	0.2299×10^{2}		
0.3254×10^{8}	0.9999	0.2299×10^{2}		
0.3368×10^{8}	0.9999	0.2299×10^{2}		
0.3483×10^{8}	0.9999	0.2299×10^{2}		
0.3597×10^{8}	0.9999	0.2299×10^{2}		
0.3711×10^{8}	0.9999	0.2299×10^{2}		
0.3826×10^{8}	0.9999	0.2299×10^{2}		
0.3940×10^{8}	0.9999	0.2299×10^{2}		
0.4053×10^{8}	0.9999	0.2299×10^{2}		
		0.000001 Atm		
0.2881×10^{8}	0.9961	0.2307×10^{2}	0.3815×10^{-2}	Zero
0.2984×10^{8}	0.9978	0.2303×10^{2}	0.2106×10^{-2}	
0.3275×10^{8}	0.9995	0.2300×10^{2}	0.4546×10^{-3}	
0.3562×10^{8}	0.9998	0.2299×10^{2}	0.1252×10^{-3}	
0.3848×10^{8}	0.9999	0.2299×10^{2}	0.4175×10^{-4}	

TABLE D.2 - Vapor Properties

Temperature		Enthalpy H		Entropy S	Specific volume V
°C	°F	Cal/g	Btu/lb	Cal/g-°C or Btu/lb-°F	Cm^3/g
			0.000001 Atm		
450.00	841.98	1270.1	2286.2	2.9669	0.2580×10^{10}
500.00	931.98	1280.9	2305.7	2.9838	0.2759×10^{10}
550.00	1021.98	1291.7	2325.2	2.9994	0.2937×10^{10}
600.00	1111.98	1302.5	234416	3.0140	0.3116×10^{10}
650.00	1201.98	1313.3	2364.1	3.0277	0.3294×10^{10}
700.00	1291.98	1324.1	2383.5	3.0405	0.3473×10^{10}
750.00	1381.98	1334.9	2402.9	3.0527	0.3651×10^{10}
800.00	1471.98	1345.8	2422.4	3.0641	0.3830×10^{10}
850.00	1561.98	1356.6	2441.8	3.0750	0.4008×10^{10}
900.00	1651.98	1367.4	2461.3	3.0849	0.4187×10^{10}
950.00	1741.98	1378.2	2480.7	3.0943	0.4365×10^{10}
1000.00	1831.98	1389.0	2500.2	3.1033	0.4543×10^{10}
1050.00	1921.98	1399.8	2519.6	3.1119	0.4722×10^{10}
1100.00	2011.98	1410.6	2539.1	3.1202	0.4900×10^{10}
1150.00	2101.98	1421.4	2558.5	3.1282	0.5079×10^{10}
1200.00	2191.98	1432.2	2578.0	3.1359	0.5257×10^{10}
1250.00	2281.98	1443.0	2597.4	3.1433	0.5436×10^{10}
1300.00	2371.98	2453.8	2616.9	3.1505	0.5614×10^{10}
1350.00	2461.98	1464.6	2636.3	3.1574	0.5793×10^{10}
1400.00	2551.98	1475.4	2655.7	3.1641	0.5971×10^{10}
1450.00	2641.98	1487.2	2675.2	3.1705	0.6150×10^{10}
1500.00	2731.98	1497.0	2694.6	3.1768	0.6328×10^{10}

PHYSICAL PROPERTIES

of Sodium (Continued)

Specific volume Ft^3/lb	Compressibility factor *ZH*	Average mol. weight ABARH	Dimer *X2H*	Tetramer *X4H*
		0.000001 Atm		
0.4134×10^8	0.9999	0.2299×10^2	0.1620×10^{-4}	Zero
0.4420×10^8	0.9999	0.2299×10^2	0.7107×10^{-5}	
0.4706×10^8	0.9999	0.2299×10^2	0.3445×10^{-5}	
0.4991×10^8	0.9999	0.2299×10^2	0.1814×10^{-5}	
0.5277×10^8	0.9999	0.2299×10^2	0.1024×10^{-5}	
0.5563×10^8	0.9999	0.2299×10^2	Zero	
0.5849×10^8	0.9999	0.2299×10^2		
0.6135×10^8	0.9999	0.2299×10^2		
0.6421×10^8	0.9999	0.2299×10^2		
0.6707×10^8	0.9999	0.2299×10^2		
0.6992×10^8	0.9999	0.2299×10^2		
0.7278×10^8	0.9999	0.2299×10^2		
0.7564×10^8	0.9999	0.2299×10^2		
0.7850×10^8	0.9999	0.2299×10^2		
0.8136×10^8	0.9999	0.2299×10^2		
0.8422×10^8	0.9999	0.2299×10^2		
0.8708×10^8	0.9999	0.2299×10^2		
0.8993×10^8	0.9999	0.2299×10^2		
009279×10^8	0.9999	0.2299×10^2		
0.9565×10^8	0.9999	0.2299×10^2		
0.9851×10^8	0.9999	0.2299×10^2		
0.1013×10^9	0.9999	0.2299×10^2		

REFERENCES

1. R.R. Miller, Physical Properties of Liquid Metals, in *Liquid Metals Handbook*, Chap. 2, R.N. Lyon (Ed.), Report NAVEXOS-P-733, June 1950.

2. R.R. Miller, Physical Properties of Liquid Metals, in *Liquid Metals Handbook*, R.N. Lyon (Ed.), Report NAVEXOS-P-733 (Rev.), June 1952.

3. R.R. Miller and L.F. Epstein, Physical Properties - Sodium, in *Liquid Metals Handbook. Sodium - NaK Supplement*, USAEC Report TID-5277, July 1, 1955.

4. G.W. Thomson and E. Garelis, Physical and Thermodynamic Properties of Sodium, in *Sodium, Its Manufacture and Uses*, M. Sittig (Ed.), Chap. 9, Reinhold Publishing Corporation, New York, 1956.

5. W.D. Weatherford, Jr., J.C. Tyler, and P.M. Ku, *Properties of Inorganic Energy-Conversion and Heat-Transfer Fluids for Space Applications*, USAEC Report WADD-TR-61-96, Southwest Research Institute, November 1961.

6. W.D. Weatherford, Recent Data on the Thermophysical Properties of Alkali Metals, USAF Aerospace Fluids and Lubricants Conference, San Antonio, Texas, April 16-19, 1963, N63-17862.

7. K.H. Spiller, Zur Kenntnis der physikalischen Stoffeigenschaften von Flüssigmetallen, *Atomkernenergie*, 10: 127-138; 215-227 (1965).

8. K.H. Spiller, *Physico-Thermal Properties of Na-, K- and NaK-Alloys in the Temperature Range Between Boiling Point and About 1300°C*, Italian Report EUR-357.d, 1963.

9. S.S. Kutateladze, V.M. Borishanskii, I.I. Novikov, and O.S. Fedynskii, *Liquid Metal Heat Transfer Media* (translated from the Russian), Supplement No.2 of the Soviet Journal of Atomic Energy, (Atomnaia Energiia, Atomic Press, Moscow, 1958), Consultants Bureau, Inc., New York, 1959.

10. P.Y. Achener et al., *Thermophysical and Heat Transfer Properties of Alkali Metals*, USAEC Report AGN-8195 (Vols. 1 and 2), Aerojet-General Corp., April 1968.

11. G.F. Burdi, *SNAP Technology Handbook*, Vol. 1, Liquid Metals, USAEC Report NAA-SR-8617 (Vol. 1), North American Aviation, Inc., Aug. 1, 1964.

12. W. Mialki, Flüssige Metalle, Section 4329, pp. 350-359, in Landolt-Börnstein, 6th ed., Vol. IV/2c, Julius Springer, Berlin and New York, 1965.

13. *Gmelins Handbuch der Anorganischen Chemie*, 8th ed., Natrium Ergänzungsband. Lfg. 2, Chemie Verlag, Weinheim Germany, 1965.

14. W.H. Wilson, The Physical Properties of Sodium, in *Comprehensive Treatise on Inorganic and Theoretical Chemistry*, The Alkali Metals, J.W. Mellor (Ed.), Vol. II, Suppl. III, Part 2, John Wiley & Sons, Inc., New York and London, 1963.

15. W.H. Wilson, The Physical Properties of Potassium, in *Comprehensive Treatise on Inorganic and Theoretical Chemistry*, The Alkali Metals, J.W. Mellor (Ed.), Vol. II, Suppl. III, Part 2, John Wiley & Sons, Inc., New York and London, 1963.

16. N.A. Nikol'skii, Thermo-

physical Properties of Molten Metals and Alloys, in *Problems in Heat Transfer*, M.A. Mikheev (Ed.), USAEC Report AEC-tr.-4511, pp. 1-36, 1962.

17. J.L. Watts, *High-Temperature Properties of Liquid Metals*, USAEC Report UCID-15176, Lawrence Radiation Laboratory, July 21, 1967.

18. C.J. Meisl and A. Shapiro, *Thermodynamic Properties of Alkali Metal Vapors and Mercury*, 2nd Rev., Report R60FPD358-A, General Electric Co., Nov. 9, 1960.

19. G.H. Golden and J.V. Tokar, *Thermophysical Properties of Sodium*, USAEC Report ANL-7323, Argonne National Laboratory, August 1967.

20. W.H. Evans et al., Thermodynamic Properties of the Alkali Metals, *J. Res. Nat. Bur. Stand.*, 55: 83-95 (1955).

21. E.L. Dunning, *The Thermodynamic and Transport Properties of Sodium and Sodium Vapor*, USAEC Report ANL-6246, Argonne National Laboratory, October 1960.

22. S. Heimel, *Thermodynamic Properties of Potassium to 2100°K*, Report NASA-TND-4165, National Aeronautics and Space Administration, 1967.

23. A.W. Lemmon et al., *The Thermodynamic and Transport Properties of Potassium*, USAEC Report ORNL-3605, Vol. I, pp. 88-115, Oak Ridge National Laboratory.

24. H.H. Coe, *Summary of Thermophysical Properties of Potassium*, Report NASA-TND-3120, National Aeronautics and Space Administration, December 1965.

25. J.P. Stone et al., *High-Temperature Properties of Sodium*, Report NRL-6241, Naval Research Laboratory, Dec. 24, 1964.

26. C.T. Ewing et al., *High-Temperature Properties of Potassium*, Report NRL-6233, Naval Research Laboratory, Dec. 11, 1964.

27. J.P. Stone et al., High Temperature PVT Properties of Sodium, Potassium, and Cesium, *J. Chem. Eng. Data*, 11: 309-314 (1966).

28. J.P. Stone et al., High Temperature Vapor Pressures of Sodium, Potassium, and Cesium, *J. Chem. Eng. Data*, 11: 315-319 (1966).

29. J.P. Stone et al., High Temperature Specific Volumes of Liquid Sodium, Potassium, and Cesium, *J. Chem. Eng. Data*, 11: 320-322 (1966).

30. F. Tepper and F. Roehlich, *Thermophysical and Transport Properties of Liquid Metals*, Report AFML-TR-66-206, MSA Research Corp., May 31, 1966.

31. A.W. Lemmon et al., *Engineering Properties of Potassium*, USAEC Report BATT-4673-FINAL, Battelle Memorial Institute, Dec. 31, 1963.

32. L.G. Epel and J.R. Simmons, *Thermodynamic Diagrams for Lithium, Sodium and Potassium*, USAEC Report CF-59-11-67, Oak Ridge National Laboratory, Nov. 12, 1959.

33. T.H. Inatomi and W.C. Parrish, *Thermodynamic Diagrams for Sodium*, USAEC Report NAA-SR-62, North American Aviation, Inc., July 13, 1950.

34. A. Benton and T.H. Inatomi, The Thermodynamic Properties of

Sodium Vapor, *J. Chem. Phys.*, 20: 1946-1948 (1952).

35. S.M. Kapelner, *The Electrical Resistivity of Lithium and Sodium-Potassium Alloy*, USAEC Report PWAC-349, Pratt and Whitney Aircraft Div., United Aircraft Corp., June 30, 1961.

36. C.F. Bonilla, *High Temperature Thermal Properties of Gases and Vapors,* Progress Report, April 1967-March 1968, USAEC Report CU-2660-39, Columbia University, December 1967.

37. S.H. Fenney, *Bibliography on Liquid Metals*, 1964-1965, British Report TRG-Inf. Ser.-312 (Suppl. 1), November 1966.

38. A. Muccino (Comp.), *Liquid Metals, Liquid Metal Alloys and Their Applications*, Report AD-417111, Defense Documentation Center, September 1963.

39. G. Ervin, Jr., *Literature Survey on Properties of Sodium Vapor*, USAEC Report NAA-SR-Memo-4417, North American Aviation, Inc., Sept. 25, 1959.

40. O.E. Dwyer (Ed.), *High Temperature Liquid Metal Technology Review*, Brookhaven National Laboratory, Bimonthly Technical Progress Reviews Since 1962.

41. V. Ionescu and K.G. Lenhart (Comps.), *Fast Reactors*, Bibliographical Series, No. 22, International Atomic Energy Agency, Vienna, 1966 (STI/PUB/21/22).

42. R. Hultgren et al., *Selected Values of Thermodynamic Properties of Metals and Alloys*, John Wiley & Sons, Inc., New York, 1963.

43. R.P. Elliott, *Constitution of Binary Alloys, First Supplement*, McGraw-Hill Book Company, Inc., New York, 1965.

44. L. Green, *Table of Reactor Coolant Properties*, USAEC Report BNL-661, Brookhaven National Laboratory, Mar. 10, 1961.

45. R.C. Weast (Ed.), *Handbook of Chemistry and Physics*, 48th ed., Chemical Rubber Publishing Co., Cleveland, 1967.

46. B.J. McBride, S. Heimel, J.G. Ehlers, and S. Gordon, *Thermodynamic Properties to 6000°K for 210 Substances Involving the First 18 Elements*, Report NASA-SP-3001, National Aeronautics and Space Administration, 1963.

47. A.V. Gurvich et al., *Thermodynamic Properties of Individual Substances*, Vol. 1: Calculation of the Thermodynamic Properties, Part 3, Chapters 28 to 31, Report AD-659679 (FTD-HT-66-25; TT-67-63056).

48. N.E. Cusack, The Physics of Liquid Metals, *Contemp. Phys.,* 8: 583-606 (1967).

49. N.E. Cusack, The Electronic Properties of Liquid Metals, *Rep. Prog. Phys.,* 26: 361-410 (1963).

50. J.R. Wilson, The Structure of Liquid Metals and Alloys, *Metallurg. Rev.,* 10 (40): 385-590 (1965).

51. P.D. Adams, H.A. Davies, and S.G. Epstein (Eds.). *The Properties of Liquid Metals*, Taylor & Francis Ltd., London, 1967.

52. T.J. Hughes, *Liquids: Structure, Properties and Interactions*, Elsevier, Amsterdam, 1965.

53. J.M. Ziman, A Theory of the Electrical Properties of Liquid Metals. I. Monovalent Metals, *Phil. Mag.,* 8: 1013-1034 (1961).

54. A. Paskin, The Properties of Liquid Metals, *Phys. Today*, 19: 109-110 (November 1966).

55. J.R. Christman and H.B. Huntington, Theory of Molten Alkali Alloys. (I) NaK System, *Phys. Rev.*, 139: 83-90 (1965).

56. N.H. March, *Liquid Metals*, Pergamon Press Ltd., Oxford, 1968.

57. J.R. Christman, Theory of Molten Alkali Alloys. (II) Na-K, Na-Rb, Na-Cs, *Phys. Rev.*, 153: 217-224 (1967).

58. H. Knof, *Thermodynamics of Irreversible Processes in Liquid Metals*, Heywood Books, London, 1966.

59. R.F. Sweek and A. Amorosi, The U.S. Program on the Liquid Metal Fast Breeder Reactor, *Nucl. News,* 11 (3): 45-49 (March 1968).

60. M.A. Zipkin and R.N. Edwards (Eds.), Power Systems for Space Flight, Vol. II of *Progress in Astronautics and Aeronautics*, Academic Press, Inc., New York, 1963.

61. E.A. Mechtly, *The International System of Units, Physical Constants and Conversion Factors*, Report NASA-SP-7012, National Aeronautics and Space Administration, 1963.

62. W. Miakli, Natrium in der Kerntechnick, *Metall,* 13: 174-178 (1959).

63. M.H. Feldman, *Molecular Form of Vaporizing Sodium*, USAEC Report NAA-SR-123, North American Aviation, Inc., May 21, 1951.

64. J.P. Quin, The Preparation and Uses of Potassium, in *Comprehensive Treatise on Inorganic and Theoretical Chemistry*, The Alkali Metals, J.W. Mellor (Ed.), Vol. II, Suppl. III, Part 2, John Wiley & Sons, Inc. New York and London, 1963.

65. C.A. Krier et al., Low Temperature Heat Capacities and Related Properties of Potassium and Na_2K, *J. Phys. Chem.*, 61: 522-529 (1957).

66. D.L. Martin, Analysis of Alkali Metal Specific Heat Data, *Phys. Rev.,* 139: A150-A160 (1965).

67. E.B. Hagen, *Ann. Phys. Chem.,* 19: 436 (1883).

68. C.S. Barrett, X-ray Study of the Alkali Metals at Low Temperatures, *Acta Crystallogr.*, 9: 671-677 (1956)

69. I.G. Dillon, P.A. Nelson, and B.S. Swanson, *Critical Temperatures and Densities of the Alkali Metals*, USAEC Report ANL-7025, Argonne National Laboratory, August 1965.

70. E.I. Goltsova, Density of Lithium, Sodium and Potassium to 1500-1600°C, *High Temp.,* 4: 348-351 (1966).

71. C.T. Ewing and R.R. Miller, *Quarterly Progress Report No.1 on the Measurements of the Physical and Chemical Properties of the Sodium-Potassium Alloy*, Report NRL-P-3010, Naval Research Laboratory, Sept. 30, 1946.

72. I.I. Novikov et al., *At. Energ.,* 1: 92-106 (1956).

73. M. Nishibayashi, *Density and Viscosity of Molten Materials.* Part I. Density of Sodium and Sodium and Sodium Hydroxide, USAEC Report WADC-TR-53-308, Cincinnati University, November 1953.

74. M.E. Rinck, Density of Liquid

Sodium and Potassium, *Compt. Rend.*, 189: 39-41 (1929).

75. F. Tepper, J. Zelenak, F. Roehlich, and V. May, *Thermophysical and Transport Properties of Liquid Metals*, Report AFML-TR-65-99, MSA Research Corp., May 15, 1965.

76. J.P. Stone et al., *High-Temperature Properties of Sodium, Potassium and Cesium*, Report NRL-6128 Naval Research Laboratory, June 4, 1964.

77. C.A. Swenson, Compression of the Alkali Metals to 10,000 Atm at Low Temperatures, *Phys. Rev.*, 99: 423-430 (1955).

78. J.F. Walling and A.W. Lemmon, *The Experimental P - V - T Properties of Potassium to 1150°C*, USAEC Report BATT-T4, Battelle Memorial Institute, 1963; see also Report NASA-CR52950, 1963.

79. C.H. Liu, The Densities of Sodium and Potassium and Their Alloys, Report JPRS-42035, pp. 12-21 (1067), translated from *Acta Phys. Sinica*, 22: 757-764 (1966); (Chinese).

80. C.T. Ewing, Harold B. Atkinson, Jr., and Thomas K. Rice, *Quarterly Progress Report No. 7 on the Measurements of the Physical and Chemical Properties of the Sodium - Potassium Alloy*, USAEC file No. NP-340, Naval Research Laboratory, May 24, 1948.

81. O. Kubaschewski and J.A. Catterall, *Thermochemistry of Alloys*, Pergamon Press, Inc., London, 1956.

82. V.M. Khanna, Some Thermodynamic Properties of Sodium - Potassium Alloys, Ph. D. Thesis, New York University, 1963.

83. F.A. Kanda and G. Maxwell, *Phase Equilibria and Specific Volumes of Liquid Metals and Alloys*, USAEC Report NYO-2731-7, Syracuse University, May 1966.

84. R.C. Faxon, Density Studies of Liquid Metal Systems, Ph. D. Thesis, Syracuse University, 1966.

85. D.K.C. MacDonald et al., An Investigation of the Sodium Potassium Equilibrium Diagram, *Can. J. Phys.*, 34: 389-394 (1956).

86. E. Rinck, *Compt. Rend.*, 197: 49 (1933).

87. J.L. Van Bleiswijk, *Z. Anorg. Chem.*, Band S 152 (1912).

88. R.R. Miller, C.T. Ewing, R.S. Hartman, and H.B. Atkinson, Jr., *Quarterly Progress Report No. 3 on the Physical and Chemical Properties of the Sodium-Potassium Alloy*, Report NRL-C-3105, Naval Research Laboratory, April 1947.

89. F.A. Cafasso et al., Thermodynamic Properties and Ordering in Liquid NaK Alloys, *Advan. Phys.*, 16: 535-543 (1967).

90. Y.S. Chiong, Viscosity of Liquid Sodium and Potassium, *Proc. Roy. Soc.*, A157: 264-277 (1936).

91. J. Godfrey, *Viscosity of Sodium*, Technical Report of University of Cincinnati to General Electric Co. ANP Project Air Research and Development Command, Contract No. AI 33(038)-21102, Subcontract No. 6, 1952.

92. I.I. Novikov et al., Heat Transfer and Thermophysical Properties of Molten Alkali Metals, *Soviet J. At. Energy*, 1: 545-555 (1956).

93. N.A. Nikolskiy et al.,

Thermophysical Properties of Certain Metals and Alloys in the Molten State, Russian Report MCL-714/1, 1961. Report MCL-714/1, 1961.

94. E.E. Shpil'rain et al., Experimental Investigation of Thermal and Electrical Properties of Liquid Alkali Metals at High Temperatures, *High Temp.*, *3*: 870-874 (1965).

95. P.Y. Achener and D.L. Fisher, *Viscosity of Liquid Sodium and Lithium*, USAEC Report AGN-8191 (Vol. 5), Aerojet-General Corp., 1967.

96. C.T. Ewing et al., Viscosity of the Sodium-Potassium System, *J. Amer. Chem. Soc.*, *73*: 1168-1171 (1951).

97. C.T. Ewing et al., Viscosity of the Sodium-Potassium System, *J. Phys. Chem.*, *58*: 1086-1088 (1954).

98. E.N. da C. Andrade et al., *Proc. Phys. Soc. (London)*, *48*: 247-260 (1936).

99. A.G. Ward, *Structure and Molecular Forces in (a) Pure Liquids and (b) Solutions*, a general discussion held by the Faraday Society, p. 88, Gurney and Jackson, London, 1936.

100. E.H. Hall and J.M. Blocher, Jr., *The Viscosity of Saturated Liquid Potassium from 70 to 1150°C by the Oscillating Cylinder Method*, Report BATT-4673-T1, Battelle Memorial Institute, 1962.

101. D.V. Rigney, S.M. Kapelner, and R.E. Cleary, *Viscosity of Liquid Potassium to 900°C*, USAEC Report TIM-793, Pratt and Whitney Aircraft, June 22, 1964.

102. A.V. Grosse, Viscosities of Liquid Sodium and Potassium from Their Melting Points to Their Critical Points, *Science*, *147*: 1438-1441 (1965).

103. A.V. Grosse, Kinematic Viscosity of Metallic Mercury, Sodium, and Potassium over This Entire Liquid Range, *J. Inorg. Nucl. Chem.*, *28*: 31-39 (1966).

104. G. Cavalier, Measurements of the Viscosity of Undercooled Molten Metals, *The Physical Chemistry of Metallic Solutions and Intermetallic Compounds*, Symposium Proceedings, London, England, 1958, Vol. 2, pp. 4D1-4D12, Her Majesty's Stationery Office, London, 1959.

105. F. Sauerwald, The Measurement of the Viscosity of the Alkali Metals in Vacuum, *Z. Metallk.*, *26*: 259 (1934).

106. K. Gering and F. Sauerwald, The Viscosity of Pb, Cd, Zn, Ag, Sn, K and Na, *Z. Anorg. Allg. Chem.*, *223: 204* (1935).

107. G. Macur et al., Viscosity of NaK-78 at Low Temperatures, *J. Phys. Chem.*, *69*: 3782-3785 (1965).

108. M. Pingi and Y.T. Tien, On the Viscosity of Liquid NaK, Report JPRS-42035, pp. 1-11, 1967, translated from *Acta Phys. Sinica*, *22*: 749-756 (1966) (Chinese).

109. B.I. Stefanov et al., Viscosity and Thermal Conductivity of the Vapors of Sodium and Potassium, *High Temp.*, *4*: 131-132 (1966).

110. D.I. Lee, The Viscosity of the Alkali Metals Vapors, Doctoral Dissertation, Department of Chemical Engineering, Columbia University, November 1967.

111. D.I. Lee and C.F. Bonilla, The Viscosity of the Alkali Metal Vapors, in *The Alkali Metals*, Special Publication No. 22, Pt. 1, pp. 53-74, The Chemical Society, London, 1967.

112. R.H. Davies et al., High-Temperature Transport Properties of Alkali Metal Vapors, *Phys. Fluids, 8*: 444-452 (1965).

113. I. Johnson, Chen-Jung Huong, and J.D. Kemp, Chart for Getting Vapor Viscosities, *Chem. Eng., 61*: 195-196 (1954).

114. C.R. Wilke, A Viscosity Equation for Gas Mixtures, *J. Chem. Phys., 18*: 517-519 (1950).

115. J.O. Hirschfelder, C.F. Curtiss, and R.B. Bird, *Molecular Theory of Gases and Liquids* (1st ed., 2nd printing with corrections), p. 14, John Wiley & Sons, Inc., New York and London, 1954.

116. L. Pauling, *The Nature of the Chemical Bond*, 3rd ed., p. 403, Cornell University Press, Ithaca, N.Y., 1960.

117. W.D. Weatherford, Momentum Dynamics of Gas-Phase Physical Processes, *Bull. Amer. Phys. Soc., 6* (2): 41 (1961).

118. W.D. Weatherford, Viscosity Prediction for Alkali Metals, in *Bearing and Seal Design in Nuclear Power Machinery*, Symposium on Lubrication in Nuclear Applications, Miami Beach, Fla., June 5-7, 1967, R.A. Burton (Ed.), The American Society of Mechanical Engineers, New York, 1967.

119. A. Svehla, *Estimated Viscosities and Thermal Conductivities of Gases at High Temperatures*, Report NASA-TR-R-132, National Aeronautics and Space Administration, 1962.

120. P.Y. Achener, A.R. Miller, and D.L. Fisher, *Thermodynamic and Transport Properties of Potassium: PVT Properties*, USAEC Report AGN-8194 (Vol. 2), Aerojet-General Corporation, April 1967.

121. R.I. Beecroft and C.A. Swenson, An Experimental Equation of State for Sodium, *J. Phys. Chem. Solids. 18*: 329-344 (1961).

122. M.H. Rice, Pressure Volume Relationship for the Alkali Metals from Shock-Wave Measurements, *J. Phys. Chem. Solids, 26*: 483-492 (1965).

123. P.W. Bridgman, *The Physics of High Pressure*, G. Bell & Sons Ltd., London, 1931.

124. C.E. Monford and C.A. Swenson, An Experimental Equation of State for Potassium Metal, *J. Phys. Chem. Solids, 26*: 291-301 (1965).

125. G. Abowitz and R.B. Gordon, Compressibility of Liquid Sodium-Potassium Alloys, *J. Chem. Phys., 37*: 125-128 (1962).

126. T.E. Pochapsky, The Temperature Variation of the Compressibility of Molten Sodium, *Phys. Rev., 84*: 553-558 (1951).

127. A.W. Adamson, *Physical Chemistry of Surfaces*, 2nd ed., Interscience Publishers, New York, 1967.

128. V.S. Trelin et al., Experimental Data on the Velocity of Sound in Alkali Metals at Temperatures up to 800°C, *High Temp., 4*: 352-355 (1966).

129. J. Jarzynski and T.A. Litovitz, Ultrasonic Absorption in Liquid Sodium-Potassium Alloys, *J. Chem. Phys., 41*: 1290-1296 (1964).

130. S.V. Letcher and R.T. Beyer, Measurement of Ultrasonic Attenuation in Liquid Sodium and Potassium, *J. Acoust. Soc. Amer., 35*: 1571-1574 (1963).

131. S.P. Ying and C.C. Scott, *Attenuation Measurements of Sound and Performance of Ultrasonic Transducers*

in 600°F Liquid Sodium, USAEC Report APDA-180 (1965), and *Development of the Undersodium Ultrasonic Scanner*, USAEC Report APDA-290 (1967), Atomic Power Development Associates, Inc.

132. Yu. S. Trelin et al., Measurement of the Ultrasound Velocity in Molten Alkali Metals, *Soviet J. At. Energy, 9*: 955-957 (1960).

133. O.J. Kleppa, Ultrasonic Velocities of Sound in Some Metallic Liquids - Adiabatic and Isothermal Compressibilities of Liquid Metals at Their Melting Points, *J. Chem. Phys., 18*: 1331-1336 (1950).

134. A. Paskin, *Liquid State of Metals*, Annual Progress Report, USAEC Report BNL-50082, p. 131, Brookhaven National Laboratory, Dec. 31, 1967.

135. G.M.B. Webber and R.W.B. Stephens, Transmission of Sound in Molten Metals, in *Physical Acoustics*: Principles and Methods, Vol. IV, Pt. B, W.P. Mason (Ed.), pp. 53-97, Academic Press, Inc., New York, 1968 (contains an extensive reference list).

136. R.T. Beyer and A.B. Coppens, Sound Velocities, Nonlinearity and Equation of State for Liquids, in 5th International Congress on Acoustics, Liege, 1965, paper K46.

137. R.T. Smith et al., Sound Propagation in Liquid Metals, *Advan. Phys., 16*: 515-522 (1967).

138. S.V. Lechter and R.T. Beyer, Measurement of Magnetically Induced Sound Absorption in Liquid Sodium and Potassium, *Phys. Fluids, 7*: 375-378 (1964).

139. W. Westphal, Magnetohydrodynamische Dispersion and Absorption von Ultraschall, *Z. Phys., 168*: 33-342 (1962).

140. M.B. Gitis and I.G. Mikhailov, Propagation of Sound in Liquid Metals (Review), *Sov. Phys.-Acoust. (Engl. Transl.). 12*: 131-143 (1966).

141. D.H. Trevena, Liquids Under Tension, *Contemp. Phys., 8*: 185-195 (1967).

142. C.C. Addison et al., Liquid Metals, Part III. The Influence of Oxide Films on the Surface Tension of Liquid Sodium, *J. Chem. Soc. (London), 1955*: 3047-3050.

143. C.C. Addison, Liquid Sodium, *Endeavour, 26*: 91-95 (May 1967).

144. D.O. Jordan and D.E. Lane, The Surface Tension of Liquid Sodium and Liquid Potassium, *Aust. J. Chem., 18*: 1711 (1965).

145. F.E. Poindexter and M. Kernaghan, Surface Tension of Sodium, *Phys. Rev., 33*: 837 (1929).

146. C.C. Addison et al., Liquid Metals. Part I. The Surface Tension of Liquid Sodium: The Vertical-Plate Technique, *J. Chem. Soc., Pt. C, 1954*: 2861-2866.

147. C.C. Addison et al., Liquid Metals, Part II. The Surface Tension of Liquid Sodium: The Drop-Volume Technique, *J. Chem. Soc., 1955*: 2262-2264.

148. J.W. Taylor, The Surface Tension of Sodium, *J. Inst. Metals, 83*: 143-152 (1954-1955).

149. J. Bohdansky and H.E.J. Schins, The Surface Tension of the Alkali Metals, *J. Inorg. Nucl. Chem., 29*: 2173-2179 (1967).

150. A.N. Solov'ev and O.P. Makarova, Study of the Surface Tension of Liquid Sodium and Potassium, *High Temp., 4:* 187 (1966).

151. A.N. Solov'ev and A.B. Caplun, Approximate Calculation of the Surface Tension of Molten Alkali Metals, *High Temp.*, *4*: 476-479 (1966).

152. B. Longson and A.W. Thorley, The Wetting Behavior of Some Alloys Based on Iron, Nickel and Chromium in Liquid Sodium, in *The Alkali Metals* The Chemical Society, London, 1967.

153. C.F. Bonilla, *High-Temperature Thermal Properties of Gases and Vapors*, Progress Report, 1964-65, USAEC Report CU-2660-16, Columbia University, March 1965.

154. C.F. Bonilla, *High-Temperature Thermal Properties of Gases and Vapors During the Year 1965/66*, Progress Report, USAEC Report CU-2660-26, Columbia University, February 1966.

155. J.W. Chung, *Capillary Properties of Alkali Metal Systems.* 1. Surface Tension of Potassium Under Argon, USAEC Report CU-2660-24, Columbia University, 1965.

156. J.W. Cooke, Thermophysical Property Measurements of Alkali Liquid Metals, in *Proceedings of 1963 High-Temperature Liquid-Metal Heat Transfer Technology Meeting, Oak Ridge, September 1963*, USAEC Report ORNL-3605 (Vol. 1), pp. 66-87, Oak Ridge National Laboratory, November 1964.

157. J.W. Taylor, *The Surface Tension of Liquid Metals and Alloys*, British Report AERE-M/TN-24, May 4, 1954.

158. J.W. Taylor, The Surface Tension of Alkali Metals, *Phil. Mag.*, *46*: 867-876 (1955).

159. D. Germer and H. Mayer, Messung der Oberflächenspannung der flüssigen Alkalimetalle im Ultra-Hoch vakuum, *Z. Phys.*, *210*: 391-402 (1968).

160. A. Quaterman and W.L. Primak, The Capillary Rise, Contact Angle and Surface Tension of Potassium, *J. Amer. Chem. Soc.*, *72*: 3035-3038 (1950).

161. V.G. Zhivov, *Tr. Vses. Alumin.-Magnieryi Inst.*, *14*: 99 (1937).

162. G. Quincke, Uber die Kapillaritätskonstanten geschmolzener Körper, *Ann. Phys.*, *135*: 621 (1868).

163. D.H. Bradhurst and A.S. Buchanan, Surface Properties of Liquid Sodium and Sodium Potassium Alloys in Contact with Metal-Oxide Surfaces, *Aust. J. Chem.*, *14*: 397-408 (1961).

164. S.C. Carniglia, *Interactions of Graphite with Liquid Sodium*, USAEC Report BNL-489, pp. 159-167, Brookhaven National Laboratory, 1957.

165. T.A. Coultas and R. Cygan, *Compatibility of Sodium, Graphite and Stainless Steel*, USAEC Report NAA-SR-258, North American Aviation, Inc., July 8, 1953.

166. V.N. Yeremenko and Y.V. Naydich, *The Wetting of Refractory Compounds with Liquid Metals*, Report JPRS-5006, translated from *Acad. Nauk Ukr. RSR, Kiev*, 1958 (contains an extensive reference list).

167. J.W. Taylor, Wetting by Liquid Metals, in *Metallurgy and Fuels*, Vol. 2, H.M. Finniston and J.P. Howe (Eds.), Pergamon Press Inc., New York, London, 1959.

168. M.H. Wahl, *Wetting with Sodium*, Technical Report No. 43, USAEC file No. NP-5811, Mine Safety Appliances Co., Nov. 7, 1955.

169. B.R.T. Frost, *The Wetting of Solids by Liquid Metals*, British Report AERE-R-387, 1957.

170. C.C. Addison et al., Liquid Metals. Pt. V. The Role of Oxide Films in the Wetting of Iron, Cobalt and Nickel by Liquid Sodium and by Solutions of Barium and Calcium in Liquid Sodium, *J. Chem. Soc., 1962*: 2699-2705.

171. C.C. Addison and E. Iberson, Liquid Metals, Pt. XI. The Wetting of Chromium, Molybdenum and Tungsten by Liquid Sodium, *J. Chem. Soc., 1965*: 1437-1440.

172. D.T. Livey and P. Murray, The Wetting Properties of Solid Oxides and Carbides by Liquid Metals, in *Sintered High-Temperature and Corrosion-Resistant Materials, Plansee Proceedings, 1955*, pp. 375-404, Pergamon Press Ltd., London, 1955.

173. D.O. Jordan and J.E. Lane, The Wetting of Some Transition Metals by Liquid Sodium and Potassium, *Aust. J. Chem., 19*: 1093-1102 (1966).

174. G.G. Bentle et al., *Wetting Temperatures of Fuel Element Components with Sodium and NaK*, USAEC Report TID-7526 (Pt. 1), pp. 16-27, Ames Laboratory, 1957.

175. D.O. Jordan and J.E. Lane, The Wetting of Solid Metals by Liquid Alkali Metals, in *The Alkali Metals*, Special Publication No. 22, pp. 147-152, The Chemical Society, London, 1967.

176. N.H. Nachtrieb, Self-Diffusion in Liquid Metals, *Advan. Phys., 16*: 309-323 (1967).

177. J. Rohlin and A. Lodding, Selbstdiffusion in geschmolzenem Kaliummetall, *Z. Naturforsch., 17a*: 1081-1085 (1962).

178. A. Lunden et al., Der Isotopieefekt bei Stromdurchgang in geschmolzenem Kaliummetall, Z. Naturforsch., 10a: 924-926 (1955).

179. A. Lodding and A. Klemm, Die effektive Diffusion in flüssigen Metallen bei der Isotopenüberfuhrung, *Z. Naturforsch., 17a*: 1085-1088 (1962).

180. A.R.E. Lodding, Isotope Transport Phenomena in Liquid Metals, *Gothenburg Studies Phys., 1* (1961).

181. A. Lodding and A. Ott, Isotope Thermotransport in Liquid Potassium, Rubidium, and Gallium, *Z. Naturforsch., 21a*: 1344-1347 (1966).

182. R.B. Bird et al., The Equation of State and Transport Properties of Gases and Liquids, in *Handbook of Physics*, 2nd ed., E.V. Condon and H. Odishaw (Eds.), McGraw-Hill Book Company, Inc., New York, 1967.

183. R.E. Meyer and N.H. Nachtrieb, Self-Diffusion in Liquid Sodium, *J. Chem. Phys., 23*: 1851-1854 (1955).

184. N.H. Nachtrieb et al., Self-Diffusion in Solid Sodium, *J. Chem. Phys., 20*: 1185-1194 (1952).

185. R.J. Cvetanovic and D.J. LeRoy, Diffusion Coefficients of Sodium Vapor in Nitrogen, *J. Chem. Phys., 20*: 343-344 (1952).

186. J.B. Ott and J.R. Goates, *Thermodynamic Investigation of Alkali Metal Mixtures*, USAEC Report COO-1707-1, Brigham Young University, Jan. 15, 1968.

187. Ye. G. Ponyatovskiy, The Melting Points of Lithium and Sodium Under Pressures up to 30,000 kg/cm^2, *Fiz. Met. Metalloved., 11*: 476-477 (1961); translated as Report NP-tr-727.

188. R.C. Newton et al., The Fusion Curves of the Alkali Metals

up to 50 Kilobars, *J. Geophys. Res.*, *67*: 2559-2566 (1962).

189. E.A. Kraut and G.C. Kennedy, New Melting Law at High Pressures, *Phys. Rev.*, *151*: 668 (1966).

190. H.D. Luedemann and G.C. Kennedy, The Melting Curves of Lithium, Sodium, Potassium and Rubidium to 80 kB, *J. Geophys. Res.*, *73*: 2795-2805 (1968).

191. D.C. Ginnings et al., Heat Capacity of Sodium Between 0° and 900°C, The Triple Point and Heat of Fusion, *J. Res. Nat. Bur. Stand.*, *45*: 23 (1950).

192. S.A. Hluchan, Pressure and Temperature Transducers for High Temperature and Nuclear Radiation Environments, a paper presented at the National Telemetering Conference, June 2, 1964, Los Angeles, Calif.

193. H.W. Deem, E.A. Eldridge, and C.F. Lucks, *The Specific Heat from 0° to 1150°C and Heat of Fusion of Potassium*, Report BATT-4673-T2, Battelle Memorial Institute, Aug. 31, 1962.

194. L.S. Kothari et al., Scattering of Cold Neutrons in Liquid Metals and the Entropy of Disorder, *Phil. Mag.*, *8* (1): 560-567 (1956).

195. M.M. Makansi et al., Determination of the Vapor Pressure of Sodium, *J. Phys. Chem.*, *59*: 40-42 (1955).

196. P.Y. Achener and J.T. Jouthas, *The Latent Heat of Vaporization and Vapor Pressure of Sodium*, USAEC Report AGN-8191 (Vol. 1), Aerojet-General Nucleonics, July 1966.

197. C.F. Bonilla et al., Vapor Pressure of Alkali Metals. Rubidium, Cesium and Sodium-Potassium Alloy (NaK) up to 100 psi, *Trans. Quart. Amer. Soc. Metals (ASM)*, *55* (3): 877-890 (1962).

198. A.K. Fischer, Quasistatic Vapor Pressure Measurements on Reactive Systems in Inert Atmosphere Box, *Rev. Sci. Instr.*, *37*: 717-719 (1966).

199. J.F. Walling, H.K. Nuzum, and A.W. Lemmon, Jr., *The Vapor Pressure and Heat of Vaporization of Potassium from 480° to 1150°C*, Report BATT-4673-T3, Battelle Memorial Institute, Apr. 30, 1963.

200. D.R. Stull and G.C. Sinke, *Thermodynamic Properties of the Elements*, Advances in Chemistry Series, Vol. 19, American Chemical Society, Washington, D.C., 1956.

202. A.I. Krakoviak, Superheat Requirements with Boiling Liquid Metals, in *Proceedings of 1963 High-Temperature Liquid-Metal Heat Transfer Technology Meeting, Oak Ridge, September 1963*, USAEC Report ORNL-3605 (Vol. 1), p. 313, Oak Ridge National Laboratory, November 1964.

203. E.E. Shpil'rain and E.I. Asinovskii, The Calculation of Latent Heats of Vaporization of Alkali Metals, *Inzh.-Fiz. Zh., Akad. Nauk. Belorusskoi SSR*, *5*: 35-40 (1962).

204. P.Y. Achener, *Alkali Metals Evaluation Program - The Determination of the Latent Heat of Vaporization and Vapor Pressure of Potassium for 1000 to 1900°F*, USAEC Report AGN-8141, Aerojet-General Nucleonics, April 1965.

205. P.Y. Achener, Latent Heat of Vaporization of Potassium: Its Experimental Determination, in *The Alkali Metals*, The Chemical Society, London, 1967.

206. D. Miller et al., Estimation of Vapor and Liquid Density and Heat of

Vaporization of the Alkali Metals to the Critical Point, *International Conference on the Safety of Fast Reactors; Aix en Provence, September 19-22, 1967*, paper No. II-B/8, Commissariat á l'Energie Atomique, 1967.

207. E. Morris, *An Application of the Theory of Corresponding States to the Prediction of the Critical Constants of Metals*, British Report AWRE-O-67/64, 1964.

208. A.V. Grosse, *The Liquid Range of Metals and Some of the Physical Properties at High Temperatures*, in USAEC file No. NP-10895, 1960.

209. J.F. Walling and A.W. Lemmon, On the Corresponding States Behavior of Sodium, Potassium, Rubidium and Cesium, *J. Phys. Chem.*, *68*: 534-537 (1964).

210. I.G. Dillon, Measurement of Densities and Estimation of Critical Properties of the Alkali Metals, *J. Chem. Phys.*, *44*: 4229-4328 (1966).

211 I.G. Dillon, Measurement of Densities of Alkali Metals in the Region of the Critical Point by a Gamma Radiation Counting Technique, Ph.D. Thesis, Illinois Institute of Technology, 1965.

212. V.V. Sycher, Some Problems in Thermodynamics at the Critical Point, *High Temp.*, *5*: 169-172 (1967).

213. P. Heller, Experimental Investigation of Critical Phenomena, *Rep. Progr. Phys.*, *30* (2): 731-828 (1967).

214. L. Kadanoff, Static Phenomena Near Critical Points: Theory and Experiment, *Rev. Mod. Phys.*, *39*: 395-431 (1967).

215. G.F. Oster, High Temperature Saturated Liquid and Vapor Densities and the Critical Point of Cesium, Ph.D. Dissertation, Nuclear Engineering Division, Columbia University. N.Y., 1967.

216. I.L. Silver, High Temperature Vapor Pressures and Critical Points of Alkali Metals, forthcoming dissertation, Nuclear Engineering Division, Columbia University, N. Y.

217. S. Siegel and S.L. Quimby, The Thermal Expansion of Crystalline Sodium Between 80°K and 290°K, *Phys. Rev.*, *54*: 76-78 (1938).

218. R. Evangelisti and F. Isacchini, The Thermal Conductivity of Sodium in the Temperature Range 90-850°C, *Int. J. Heat Mass Transfer*, *8*: 1303-1317 (1965).

219. J.W. Hornbeck, Thermal and Electric Conductivities of the Alkali Metals, *Phys. Rev.*, *2*: 217-240 (1913).

220. I.I. Novikov et al., The Heat Transfer and High-Temperature Properties of Liquid Alkali Metals, *J. Nucl. Energy*, *2* (4): 387 (1957).

221. C.T. Ewing, J.A. Grand, and R.R. Miller, Thermal Conductivity of Liquid Sodium and Potassium, *J. Amer. Chem. Soc.*, *74*: 11 (1952).

222. I.I. Rudnev et al., Diffusivity of Sodium and Lithium, *Sov. J. At. Energy*, *11*: 877-880 (1961).

223. S.M. Kapelner and W.D. Bratton, *The Electrical Resistivity of Sodium, Potassium, Rubidium and Cesium in the Liquid State*, USAEC Report PWAC-376 Pratt and Whitney Aircraft Div., United Aircraft Corp., June 30, 1962.

224. A.V. Grosse, *Thermal Conductivity of Liquid Metals over Their Entire Liquid Range, i.e., from the Melting Point to the Critical*

Point, in Relation to Their Electrical Conductivities and the Fallacy of Dividing Metals into Normal and Abnormal Thermally Conducting Ones, USAEC Report TID-21737, Temple University, Dec. 7, 1964.

225. C.T. Ewing et al., Thermal Conductivity of Liquid Sodium and Potassium, *J. Amer. Chem. Soc., 74*: 11-14 (1952).

226. H.W. Deem and J. Matolich, *The Thermal Conductivity and Electrical Resistivity of Liquid Potassium and the Alloy Nb-1 Zr,* Report BATT-4673-T6, Battelle Memorial Institute, Apr. 30, 1963.

227. R.T. Caldwell and D.M. Walley, *Physical and Thermodynamic Properties of Potassium,* Report AFAOK-TR-66-104, Garrett Corp., July 1, 1966.

228. A.V. Grosse, Electrical and Thermal Conductivity of Metallic Potassium over Its Entire Liquid Range, i.e., from the Melting Point (336.4K) to the Critical Point (2450K), *J. Inorg. Nucl. Chem., 28* 795-802 (1966).

229. C.T. Ewing et al., Thermal Conductivity of Mercury and Two Sodium-Potassium Alloys, *J. Phys. Chem., 59*: 524-528 (1955).

230. C.T. Ewing et al., Thermal Conductivity of Metals, in Liquid Metals Technology, Part I, *Chem. Eng. Progr., Symp. Ser. 53,* No. 20 (1957).

231. P.G. Drugas, I.R. Rehn, and W.D. Wilkinson, *Resistivity of NaK,* USAEC Report ANL-5115, Argonne National Laboratory, Oct. 2, 1953.

232. A.E. Powers, *Application of the Ewing Equation for Calculating Thermal Conductivity from Electrical Conductivity,* USAEC Report KAPL-2146, Knolls Atomic Power Laboratory, Apr. 7, 1961.

233. A.E. Wechsler, *Characteristics of Metal Vapor,* Report AD-631469, Arthur D. Little, Inc., January 1966.

234. D.L. Timrot and E.E. Totskii, Dilatometer Method for the Experimental Determination of the Thermal Conductivity of Corrosive Gases and Vapors at High Temperatures, *High Temp., 3*: 685-690 (1965).

235. N.B. Vargaftik and A.A. Voshchinin, Experimental Study of the Thermal Conductivity of Sodium and Potassium Vapors, *High Temp., 5:* 715-722 (1967).

236. D.E. Briggs, Thermal Conductivity of Potassium Vapor, Ph.D. Thesis, University of Michigan, 1968.

237. C.S. Lee and C.F. Bonilla, Thermal Conductivity of the Alkali Metal Vapors and Argon, in *7th Conference on Thermal Conductivity, Gaithersburg, Md., Nov. 13-16, 1967,* USAEC Report CONF-671110-3, National Bureau of Standards.

238. J.R. Peterson and C.F. Bonilla, The Development of a Frequency Response Analysis Technique for Thermal Conductivity Measurement and Its Application to Gases at High Temperatures, in *Advances in Thermophysical Properties at Extreme Temperatures and Pressures, Third Symposium, Purdue University, Lafayette, Indiana, March 22-25, 1965,* S. Gratch (Ed.), pp. 264-276, The American Society of Mechanical Engineers, New York, 1965.

239. D.L. Timrot and E.E. Totskij, Measurement of the Thermal Conductivity of Sodium and Potassium Vapors as a Function of Temperature and Pressure, *High Temp., 5*: 708-714 (1967).

240. D.L. Timrot et al., Experi-

mental Apparatus for the Investigation of the Thermal Conductivity of Alkali Metal Vapors by the Dilatometric Method, *High Temp.*, *6*: 133-137 (1968).

241. L. Lees and C.Y. Liu, Kinetic Theory Description of Conductive Heat Transfer from Fine Wires, *Phys. Fluids*, *5*: 1137-1148 (1962).

242. H.J. Bomelburg, *A Method for Determining the Heat Conductivity of a Gas with a Single AC Heated Hot Wire*, Report BRL-1107, Ballistic Research Laboratories, 1960.

243. W.D. Weatherford, J.C. Tyler, and P.M. Ku, *Properties of Inorganic Working Fluids and Coolants for Space Applications*, Report WADC-TR-59-598, Southwest Research Institute, June 13, 1960.

244. H.A. Blum, *Determination of Thermal Conductivity of Low Vapor Pressure Materials: Sodium Vapor*, Status Report N66-15614, Southern Methodist University, 1965.

245. J.N. Butler and R.S. Brokaw, Thermal Conductivity of Gas Mixtures in Chemical Equilibrium, *J. Chem. Phys.*, *26*: 1636-1643 (1957).

246. C.T. Ewing et al., High Temperature Properties of Alkali-Metal Vapors, in *The Alkali Metals*, The Chemical Society, London, 1967.

247. T.M. Dauphinee et al., A New Semi-Automatic Apparatus for Measurement of Specific Heats and the Specific Heat of Sodium Between 55 and 315°K, *Proc. Roy. Soc. (London), Ser. A*, *221*: 267-276 (1954).

248. J.D. Filby and D.L. Martin, Specific Heats Below 30K of Lithium Metal of Various Isotopic Compositions and of Sodium Metal, *Proc. Roy. Soc. (London), Ser. A*, *276*: 187-203 (1963).

249. G.L. Pickard and F.E. Simon, The Atomic Heats of Palladium, Sodium and Mercury at Low Temperatures, *Proc. Phys. Soc.*, *343*: 1-9 (1948).

250. D.L. Martin, The Specific Heat of Sodium from 20 to 300°K, *Proc. Roy. Soc. (London), Ser. A*, *254*: 433-443 (1960).

251. D.L. Martin, Specific Heat of Sodium from 300 to 475°K, *Phys. Rev.*, *154*: 571-575 (1967).

252. L.G. Carpenter, Some Properties of Sodium and Potassium Near Their Melting Points, *J. Chem. Phys.*, *21*: 2244-2245 (1953).

253. K.P. Rodionov, Influence of Pressure on the Heat Capacity of Metals, *Sov. Phys.-Tech. Phys. (Engl. Transl.)*, *11*: 955-959 (1967).

254. E.A. Mit'kina, Experimental Determination of the True Specific Heats of Uranium, Thorium and Other Metals, *Sov. J. At. Energy (Engl. Transl.)*, *7*: 669-670 (1959).

255. P.Y. Achener and D.L. Fisher, *Alkali Metals Evaluation Program. The Specific Heat of Liquid Sodium and Lithium*, USAEC Report AGN-8191 (Vol. 6), Aerojet-General Corp., June 1967.

256. I.M. Pchelkin, The Specific Heat of Molten Metals, in *Problems of Heat Transfer*, M.A. Mikheev (Ed.), USAEC Report AEC-tr-4511, 1959.

257. N.A. Nikolskii et al., Thermophysical Properties of Some Metals and Alloys in a Molten State, *Vop. Teploobmena, Akad. Nauk. SSSR, Energ. Inst.*, *28*: 11-45 (1959).

258. J.D. Filby and D.L. Martin, The Specific Heats Below 320°K of Potassium, Rubidium and Cesium, *Proc. Roy. Soc. (London), Ser. A*, *284*: 83-107 (1965).

259. C.A. Krier et al., Low Temperature Heat Capacities and Related Properties of Potassium and Na_2K, *J. Phys. Chem., 61*: 522-529 (1957).

260. T.B. Douglas, Anne F. Ball and D.F. Ginnings, Heat Capacity of Potassium and Three Potassium Alloys Between 0° and 800°C, USAEC Report AECU-1017, National Bureau of Standards, 1951; also *J. Amer. Chem. Soc., 74*: 2472-2478 (1952).

261. T.B. Douglas, Specific Heat of Liquid Metals and Liquid Salts, *Trans. ASME, 79*: 23-28 (1957).

262. M. Makansi et al., Thermodynamic Properties of Sodium, *J. Chem. Eng. Data, 5*: 441-452 (1960).

263. T. Yokokawa and O.J. Kleppa, Heats of Mixing in Binary-Liquid-Alkali-Metal Mixtures, *J. Chem. Phys., 40*: 46-54 (1964).

264. An. N. Nesmeyanov, *Vapor Pressure of the Elements,* Academic Press, Inc., New York, 1963.

265. K.J. Bowles and L. Rosenblum, *Vapor Pressure of Sodium from 0.5 to 120 Atmospheres,* Report NASA-TN-D-2849, National Aeronautics and Space Administration, May 1965.

266. E.S. Sowa, Sodium Vapor Pressure to 25 Atmospheres, *Nucleonics, 21 (10)*: 76 (1963).

267. P.L. Kirillov and N.S. Grachev, Determination of Sodium Vapor Pressure at Temperatures from 880 to 1300°C, *J. Eng. Phys., 11 (5)*: 3 (1959).

268. Y.K. Vinogradov and L.D. Yolyak, Experimental Determination of the Saturated Vapor Pressure of Sodium and Potassium, *High Temp., 4*: 50 (1966).

269. R.W. Ditchburn and J.C. Gilmour, The Vapor Pressure of Monatomic Vapors, *Rev. Mod. Phys., 13*: 310-327 (1941).

270. W.T. Hicks, Evaluation of Vapor Pressure Data for Mercury, Lithium, Sodium and Potassium, *J. Chem. Phys., 38*: 1873-1880 (1963).

271. S. Glasstone, *Elements of Physical Chemistry,* D. Van Nostrand Company, Inc., Princeton, N.J., 1958.

272. J. Bohdansky and H.E.J. Schins, Vapor Pressure of Different Metals in the Pressure Range of 50 to 4000 Torr, *J. Phys. Chem., 71*: 215-217 (1967).

273. J. Bohdansky and H.E.J. Schins, New Method for Vapor Pressure Measurements at High Temperatures and Pressures, *J. Appl. Phys., 36*: 3683-3684 (1964).

274. U. Buck and H. Pauly, Vapor Pressure Measurements of the Alkali Metals, *Z. Phys. Chem., 44*: 345-352 (1965).

275. R.J. Thorn and G.H. Winslow, Correction of the Potassium Vapor Pressure Equation by Use of the Second Virial Coefficient, *J. Phys. Chem., 65*: 1297-1302 (1961).

276. K.J. Bowles, *Vapor Pressure of Potassium to 2170°K,* Report NASA-TND-4535, National Aeronautics and Space Administration, 1968.

277. D.V. Rigney, S.M. Kapelner and R.E. Cleary, *The Vapor Pressure of Potassium Between 1065 and 1500°K,* USAEC Report TIM-810, Pratt and Whitney Aircraft, June 1965.

278. N.S. Grachev and P.L. Kirillov, *Experimental Determination of Potassium Vapor Pressure in the 550°*

to 1280°C Temperature Range, Report NASA-TT-F-66, translated from *Inzh.-Fiz. Zh., Akad. Nauk Belorus. SSR.*, *3*(6): 62-65 (June 1960).

279. G. Herzberg, *Molecular Spectra and Molecular Structure, I, Spectra of Diatomic Molecules*, 2nd ed., D. Van Nostrand Company, Inc., Princeton, N.J., 1950.

280. W. Mialki and H.J. Freund, Zur Thermodynamik der Alkalimetalle, *Metall*, *18*: 1-7 (1964).

281. J.P. Stone et al, *High-Temperature Properties of Sodium, Potassium and Cesium*, Project Report No. 14, Report NRL-6128, Naval Research Laboratory, June 4, 1964.

282. J.H. Milligan, Jr., Thermodynamic Properties of the Alkali Metals Considered as Dilute Plasmas, Ph.D. Thesis, Purdue University, 1965.

283. J. Pomerantz and R. Piacesi, *The Equilibrium Composition and Thermodynamic Properties of Sodium Vapor from 400° to 10,000°K*, Report NOLTR-62-170, Naval Ordnance Laboratory, Apr. 11, 1963.

284. M. Griffel, Thermodynamic Functions of Potassium Vapor, *J. Chem. Phys.*, *21*: 1908 (1962).

285. L. Gurvich et al., Thermodynamic Functions of Monatomic and Diatomic Gases over a Wide Temperature Range. V. Alkali Metals in the Ideal Gas State up to 10,000°K, *Russ. J. Phys. Chem.*, *36*: 108-110 (1962).

286. D.E. Gray (Ed.), *American Institute of Physics Handbook*, 2nd ed., pp. 4-158, McGraw-Hill Book Company, Inc., New York, 1963.

287. N. Rynn, Macroscopic Transport Properties of a Fully Ionized Metal Plasma, *Phys. Fluids*, *7*: 284-291 (1964).

288. H. Endo, The Temperature Dependence of the Resistivity of Liquid Alkali Metals at Constant Volume, *Phil. Mag.*, *8*(8): 1403-1415 (1963).

289. J.S. Dugdale and D. Gugan, The Effect of Pressure on the Electrical Resistance of Lithium, Sodium and Potassium at Low Temperatures, *Proc. Roy. Soc. (London), Ser. A*, *270*: 186-211 (1962).

290. D.K.C. MacDonald, Electrical Resistance in Liquid Metals and the Change on Melting, *Phil. Mag.*, *4*: 1283-1285 (1959).

291. R.A. Swalin et al., Electrical Resistivity of Liquid Sodium from the Melting Point to 350°C, *Bull. Amer. Phys. Soc., Ser. II*, *13*: 43 (1968).

292. C.C. Bidwell, Electrical Resistance and Thermoelectric Power of the Alkali Metals, *Phys. Rev.*, *23*: 357-376 (1924).

293. F.J. Bradshaw and S. Pearson, The Electrical Resistivity of Sodium Between 78°K and 372°K, *Proc. Phys. Soc.*, *B69*: 441-448 (1956).

294. D.K.C. MacDonald, Self-Diffusion in the Alkali Metals, *J. Chem. Phys.*, *21*: 177-178 (1953).

295. J.S. Dugdale and D. Gugan, The Effect of Capillary Constraints on the Electrical Resistivity of Sodium and Potassium, *J. Sci. Instr.*, *40*: 28-29 (1963).

296. N.E. Cusack and J.E. Enderby, A Note on the Resistivity of Liquid Alkali and Noble Metals, *Proc. Phys. Soc. (London)*, *75*: 395-407 (1960).

297. B.A. Green, Size Effect in Electrical Resistivity of Alloy,

Phys. Rev., *126*: 1402-1405 (1962).

298. B. Springer, *Resistivity and Hall Effect in Liquid Metals*, Thesis, USAEC Report TID-19959 (Rev.), University of Chicago, 1963.

299. A.W. Lawson, The Effect of Hydrostatic Pressure on the Electrical Resistivity of Metals, *Progr. Met. Phys.*, *6*: 1-44 (1956).

300. R.A. Stager and H.G. Drickamer, Effect of Temperature and Pressure on the Resistance of Alkali Metals, *Phys. Rev.*, *132*: 124-127 (1963).

301. J.M. Dickey et al., Resistivities and Thermopowers of the Alkalis Under Pressure, *Proc. Phys. Soc.*, *92*: 460-475 (1967).

302. E. Justi, Elektrischer Widerstand, magnetische Widerstandsänderung und Hall-Effekt der Alkali Metalle, *Ann. Phys.*, *3*: 183-198 (1948).

303. F. Pawlek and D. Rogalla, Der elektrische Widerstand von Silber, Kupfer, Aluminum, Zink und Natrium zwischen 4 and 298°K in Abhängigkeit von den Verunreinigungen, *Metall*, *20*: 949-956 (1966).

304. H. Weyerer, Supraleitung und Elektronenpaar-Modell, *Z. Naturforsch.*, *A*, *13*: 286-295 (1958).

305. J.F. Freedman and W.D. Robertson, Electrical Resistivity of Liquid Sodium, Liquid Lithium and Dilute Liquid Sodium Solutions, *J. Chem. Phys.*, *34*: 769-780 (1961).

306. A.N. Solov'ev, Variation of the Electrical Resistance of Liquid Metals with Specific Volume, *High Temp.*, *1*: 37-40 (1963).

307. R. Evangelisti et al., Experimental Determination of the Lorenz Number of Liquid Sodium, *Energ. Nucl.*, *12*: 601-604 (1965).

308. F. Tepper et al., *Thermophysical and Transport Properties of Liquid Metals*, Report MSAR-64-36, MSA Research Corporation, 1964.

309. M. N. Arnol'dov et al., Effect of Dissociating and Thermally Stable Gaseous Impurities on the Electrical Resistivity of Alkali Metals, *High Temp.*, *5*: 723-726 (1967).

310. J.P. Petrek and E.C. Kovacic, Evaluation of Impurity Monitoring Devices Tested in a Dynamic System, in *Alkali Metal Coolants*, Symposium Proceedings, Vienna, 1966, International Atomic Energy Agency, Vienna, 1967 (STI/PUB/143).

311. B.E. Semyachkin and A.N. Solov'yev, Experimental Determination of the Electrical Resistance of Liquid Alkali Metals up to 1000°C, Report FTD-MT64-285, pp. 350-352, translated from *J. Appl. Mech. and Tech. Phys.*, *2*: 176-177 (1964).

312. A.N. Solov'yev, Experimental Definition of Electrical Conductivity of Liquid Sodium, Potassium, and Lithium, *J. Appl. Mech. and Tech. Phys.*, *1* (1963).

313. W. Braunbeck, Über die elektrische Leifähigkeit komprimierter Metalldämpfe, *Z. Phys.*, *97*: 482-492 (1935).

314. V. Ignatenko, Calculation of the Electrical Conductivity of Vapors of Alkali Metals and Copper, *Sov. Phys. - Tech. Phys. (Engl. transl.)*, *7*: 86-88 (1962).

315. G. Aravin and V. Sheveler, *Thermal Ionization and Electrical Conductivity in Some Mixtures and Combustion Products*, Report AD-637118

(FTD-MT-64-87), translated from *Zh. Prik. Mekh. Fiz.*, *2*: 20-31 (1962).

316. A.W. Rowe and J.L. Kerrebrock, *Nonequilibrium Electric Conductivity of Wet and Dry Potassium Vapor*, Report APL-TDR-64-106, Aero Propulsion Laboratory, 1964.

317. A. Solbers and J.L. Kerrebrock, *Condensation and Electrical Conduction in Metallic Vapors*, Report AFAPL-TR-67-21, 1967.

318. R.H. Rahiser, *Electrical Resistivity of Sodium and Sodium-Potassium Alloys*, Technical Report 24, USAEC file No. NP-4656, Mine Safety Appliances Co., July 17, 1953.

319. L.B. Vandenberg, *Electrical Contact Resistance Between Sodium and Stainless Steel*, USAEC Report KAPL-1502, Knolls Atomic Power Laboratory, Feb. 14, 1956.

320. F. Roehlich, *The Electrical Resistivity and Thermal Conductivity of Liquid Alkali Metals to 2000°F*, Report MSAR-64-111, Mine Safety Appliances Research Corp., 1964.

321. E.R. Cohen and J.W.M. Dumond, Our Knowledge of the Fundamental Constants of Physics and Chemistry in 1965, *Rev. Mod. Phys.*, *37*: 537-594 (1965).

322. J.M. Luttinger, in *The Fermi Surface*, Proceedings of an International Conference held at Cooperstown, New York, Aug. 22-24, 1960, W.A. Harrison and M.B. Webb (Eds.), John Wiley & Sons, Inc., New York, 1960.

323. F.J. Studer and W.D. Williams, The Hall Effect in Sodium, Potassium and Cesium, *Phys. Rev.*, *47*: 291-295 (1935).

324. C. Zener, Hall Effect of the Alkali Metals, *Phys. Rev.*, *47*: 636 (1935).

325. J. Langeheime, Der Halleffekt der vier Alkalimetalle Natrium, Kalium, Rubidium and Casium beim Ubergang vom festen in flussigen Zustand, Ph.D. Dissertation, Bergakademie Clausthal, Technische Hochschule, Clausthal-Zellerfeld, Germany, 1968.

326. G. Busch and Y. Tieche, Hall Effect flüssiger Metalle, *Helv. Phys. Acta*, *35*: 273 (1962).

327. G. Busch and Y. Tieche, Electrical Resistivity and Hall Effect of Molten Metals and Semiconductors, *Phys. Kondens. Mater.*, *1: 78-104* (1963).

328. T. Deutsch et al., Pressure Dependence of the Hall Constant for Alkali Metals, *Phys. Rev.*, *124*: 753-763 (1961).

329. J. Kikoin and I Fakidow, Halleffekt in flüssigen Metallen, *Z. Phys.*, *71*: 393-402 (1931).

330. H. Zahn, Zur Auffassung des Halleffekts, *Naturwissenschaften*, *18*: 848-849 (1930).

331. R. Bowers, Magnetic Susceptibility of Sodium Metal, *Phys. Rev.*, *100*: 1141-1144 (1955).

332. K. Venkateswarlu and S. Sriraman, Magnetic Susceptibility of Alkali Elements, Part I: Sodium and Potassium, *Z. Naturforsch.*, *132*: 451-455 (1958).

333. N.H. Nachtrieb, Magnetic Susceptibility of Some Liquid Metals, Molten Salts and Their Solutions, *J. Phys. Chem.*, *66*: 1163-1166 (1962).

334. E.W. Collings, Magnetic Susceptibility of the Alkali Metals

Through Their Melting Point, *Phys. Kondens. Mater.*, *3*: 335-344 (1965).

335. E. W. Collings, Magnetic Susceptibility of Sodium at Low Temperatures, *Phil. Mag.*, *11*(8): 617-619 (1965).

336. K. Venkateswarlu and S. Sriraman, Magnetic Susceptibility of Alkali Elements, Part II: Liquid Alloys of Sodium and Potassium, *Z. Naturforsch.*, *13a:* 455-458 (1958).

337. D. K. C. MacDonald, *Thermoelectricity: An Introduction to the Principles*, John Wiley & Sons, Inc., New York, 1962.

338. C. C. Bradley, The Experimental Determination of the Thermoelectric Power in Liquid Metals and Alloys, *Phil. Mag.*, *7:* 1337-1347 (1962).

339. C. F. Bonilla et al., Thermoelectric Potentials of Molten and Refractory Metals, I. Seebeck Potentials of Sodium, Potassium, Rubidium, Cesium, and Mercury vs. Platinum and Other Metals, in *Proceedings of 1963 High-Temperature Liquid-Metal Heat Transfer Technology Meeting, Oak Ridge, September 1963*,, USAEC Report ORNL-3605 (Vol. 1), pp. 116-138, Oak Ridge National Laboratory, November, 1964.

340. L. Soffer, *Activation of Sodium, Lithium, and Potassium in Compact Fast Reactors and Its Effects on Shielding*, Report NASA-TM-X-1512, National Aeronautics and Space Administration, 1968.

341. D. Strominger et al., Table of Isotopes, *Rev. Mod. Phys.*, *30*: 585-904 (1958).

342. D. J. Hughes and R. B. Schwartz, *Neutron Cross Sections*, 2nd ed., USAEC Report BNL-325 (1958); D. J. Hughes et al., *Neutron Cross Sections*, Suppl. No. 1, 2nd ed., USAEC Report BNL-325 (1960); J. R. Stehn et al., *Neutron Cross Sections*, Vol. 1, Z = 1 to 20, 2nd. ed., Suppl. No. 2 (1964), Brookhaven National Laboratory.

343. J. D. Garrison and M. K. Drake, *Neutron and Gamma Ray Production Cross Sections for Sodium, Magnesium, Chlorine, Potassium, and Calcium*, Report GA-7829 (Pt. 2), General Dynamics Corp., 1967.

344. M. K. Drake, *Neutron and Gamma Ray Production Cross Sections for Sodium, Magnesium, Chlorine, Potassium, and Calcium*, Report GA-7829 (Pt. 5), General Dynamics Corp., 1967.

345. I. P. Zapesochnyi, Absolute Cross Sections for the Excitation of Levels of Alkali Metal Atoms by Low Energy Electrons, *High Temp.*, *5*: 6-11 (1967).

346. W. Kunz and J. Schintmeister, *Nuclear Tables*, Pts. I and II, Pergamon Press Ltd., Oxford, 1964.

347. A. V. Sokolov, *Optical Properties of Metals*, American Elsevier Publishing Company, New York, 1967.

348. M. H. El Naby, Die Optischen Konstatnen des Kaliums im Wellenlängenbereich von 3650 bis 20000 Å, *Z. Phys.*, *174:* 268-279 (1963).

349. B. Hietel, Die Optischen Eigenschaften des Alkalimetalls Natrium, Ph.D. Dissertation, Bergakademie Clausthal, Technische Hochschule, Clausthal-Zellerfeld, West Germany, 1965.

350. H. Mayer and B. Hietel, Experimental Results on the Optical Properties of the Alkali Metals, in *Optical Properties and Electronic Structure of Metals and Alloys*, F. Abelès (Ed.), pp. 47-59, North-Holland Publishing Company, 1966.

351. E. M. Samarin (Ed.), *Structure and Properties of Liquid Metals*, USAEC Report AEC-tr-4879, translated by Lydia

Venters from *Akad. Nauk SSR*, 1952.

352. P. A. Egelstaff, *An Introduction to the Liquid State*, Academic Press Inc., London and New York, 1967.

SUPPLEMENTAL READING LIST

Achener, P. Y., and J. T. Jouthas, *Thermodynamic and Transport Properties of Potassium Thermal Conductivity of the Vapor,* USAEC Report AGN-8194 (Vol. 1), Aerojet-General Corporation, November 1968.

Aldridge, R. V., The Hall Effect in Liquid Alkali Amalgams, *Phil Mag.*, *8*: 1-10 (1968).

Alfonia, A. V., B. A. Nevzorov, and O. V. Starkov, Influence of Dissolved Oxygen on the Electric Resistance of Liquid *Sodium*, *At. Energ.* (*USSR*), *24*: 477-478 (1968).

Bakanova, A. A., I. P. Dudoladov, and R. F. Trunin, Compression of Alkali Metals by Strong Shock Waves, *Sov. Phys. - Solid State* (*Engl. Transl.*), *7*: 1307-1313 (1965).

Ewing, C. T., J. P. Stone, J. R. Spann, and R. R. Miller, Molecular Association in Sodium, Potassium and Cesium Vapors at High Temperatures, *J. Phys. Chem., 71:* 473-477 (1967).

Grosse, A. V., Analysis of Experimental Data on Viscosity and Self-Diffusion of Liquid Metals and Their Correlation by a Simple Kinetic Theory of Liquids, *Rev. Int. Hautes Temp. Réfract.*, *4*: 171-182 (1967).

Grosse, A. V. , Surface Tension of the Alkali Metals from their Melting Points to their Critical Temperatures along the Saturation Line, *Rev. Int. Hautes Temp. Réfract.*, *5*: 97-104 (1968).

Hoffman, H. W., and B. Cox, *A Preliminary Collation of the Thermodynamic and Transport Properties of Potassium,* USAEC Report ORNL-TM-2126, Oak Ridge National Laboratory, July 1968.

Kalakutskaya, N. A.,Viscosity of the Liquid Alkali Metals Potassium, Sodium,and Lithium at High Temperatures up to 1500°C, *High Temp., 6:* 436-440 (1968).

Pasternak, A. D., and D. R. Olander, Diffusion in Liquid Metals, *J. AIChE, 13:* 1052-1057 (1967).

Swalin, R. A., On the Fluctuation Model of Diffusion in Liquid Metals, *Z. Naturforsch.*, *23*A: 805-813 (1968).

Swalin, R. A., *Diffusion Studies in Liquid Metals*, Progress Report, May 16, 1967 - June 15, 1968, USAEC Report COO-841-15, Minneapolis Institute of Technology, 1968.

Tamaki, S. and I. Shiota, Heat of Mixing in Liquid Alloys, *Phys. Kondens. Mater., 7:* 383-389 (1968).

Chapter 2

Chemistry

Principal Author: H.E. JOHNSON

Contributing Authors: R.L. McKISSON, R.L. EICHELBERGER and D.C. GEHRI

2-1 INTRODUCTION

This chapter evaluates the state-of-the-art of analysis methods for determination of impurities in sodium and NaK and for interactions of sodium and NaK with gases, liquids, and solids. Emphasis is placed on information needed in the design of Liquid Metal Fast Breeder Reactor (LMFBR) systems. Most of the chemical-analysis methods developed for impurities in sodium are adaptable for application to sodium-potassium alloys. However, changes and improvements in analytical-chemistry technology necessitate a comprehensive survey and bibliography of potential future techniques.

This chapter includes topics discussed supplementally in other parts of this series. For example, Chap. 1 lists and discusses properties of all the alkali metals, and this chapter and Vol. V, Chap. 2, contain supplemental information on such properties (i.e., the chemistry of the interactions of solids with sodium and NaK). Likewise, in-line monitoring methods as techniques of impurity analysis are discussed from a different point of view in Vol. III, Chap. 4. Sampling devices of interest to chemical-analysis methods are also described in Vol. III, Chap. 3. Cover gases, discussed in this chapter in the light of their importance for monitoring sodium and NaK systems, are also discussed in Vol. III, Chaps. 2, 3 and 4. Chemical reactions of liquid metals with water, air (fire), and fission products are also discussed in Vol. III, Chap. 2. Also pertinent are the sodium-purity specifications and purification methods discussed in Vol. V, Chap. 1.

2-2 GENERAL DISCUSSION

2-2.1 *Chemistry of the Alkali Metals*

Lithium, sodium, potassium, cesium, rubidium and francium are active metals of low density and similar chemical properties found in Group IA of the Periodic Table. These metals react with other elements to form compounds that are usually very stable. Their high chemical reactivity is due to the

---

*See Sec. 2-4, Chemical Interactions.

presence of a single electron in the outer shell. The valence electron is more readily lost from the alkali metals of higher atomic weight than from those of lower atomic weight because of the increasing number of electrons shielding the positive charge of the nucleus from the valence electron. Consequently the chemical reactivity of the alkali metals increases with atomic weight. The compounds formed by the interaction of the alkali metals with other elements and compounds are generally ionic because one valence electron is lost. The ion is left with a stable rare-gas electron configuration of 2, 10, 18, 36, 54 and 86 electrons about the nucleus (Table 2.1). Consequently alkali-metal ions are stable in contrast to the highly reactive alkali-metal atoms [1].

TABLE 2.1 - Electronic Configuration of the Alkali Metals*

Element	Atomic number	*K*†	*L*		*M*			*N*				*O*			*P*			*Q*
		1*s*††	2*s*	2*p*	3*s*	3*p*	3*d*	4*s*	4*p*	4*d*	4*f*	5*s*	5*p*	5*d*	6*s*	6*p*	6*d*	7*s*
Lithium	3	2	1															
Sodium	11	2	2	6	1													
Potassium	19	2	2	6	2	6		1										
Rubidium	37	2	2	6	2	6	10	2	6			1						
Cesium	55	2	2	6	2	6	10	2	6	10		2	6		1			
Francium	87	2	2	6	2	6	10	2	6	10	14	2	6	10	2	6		1

† Shells are *K*, *L*, *M*, *N*, *O*, *P* and *Q*.
†† Subshells are *s*, *p*, *d*, *f*, etc.

Since the chemistry of sodium and NaK is similar to that of all the alkali metals, a brief comparison with the chemical behavior of Li, K, Rb and Cs will add perspective and clarity to more detailed discussions of sodium and NaK. We are concerned here with some major chemical interactions of the alkali metals with other elements and compounds, rather than with properties, which are discussed in Chap. 1.

The alkali metals are among the most chemically reactive elements known. Their chemical reactivity can be illustrated by their reactions with such common elements, mixtures, and compounds as air, oxygen, water, hydrogen, nitrogen and carbon or its compounds. Their relative chemical properties depend on their ionization potentials (ionization potential measures the relative ease with which an element parts with its outer electrons). Since ionization potential decreases with increasing atomic weight, lithium is expected to be the least reactive and cesium the most reactive of the five common alkali metals, but actually the largest difference in reactivity is between lithium and sodium. Lithium is not only the least reactive but also the least typical of the alkali metals. It does not react with dry oxygen at room temperature but will react in the presence of moisture to form the monoxide, Li_2O. Sodium is stable toward dry oxygen but forms both the monoxide, Na_2O, and the peroxide, Na_2O_2, at room temperature

---

*From I.M. Kolthoff, P.J. Elving and E.B. Sandell (Eds.), Treatise on Analytical Chemistry. II: *Analytical Chemistry of the Elements I*: 324. Interscience Publishers, New York, 1961.

in the presence of moist air. Potassium reacts slowly with dry oxygen and with moist air to form the monoxide, K_2O, the peroxide, K_2O_2, and the superoxide, KO_2. Rubidium and cesium react similarly to potassium, but more rapidly [2].

A similar increase in rate can be expected for the reaction of alkali metals with water to liberate hydrogen. Lithium reacts slowly with water at room temperature. Sodium can be added in small pieces to water below 40°C without igniting, but potassium, rubidium and cesium react with increasing vigor until it becomes almost impossible to prevent ignition. Hydrogen reacts with alkali metals to form hydrides of the form MH. Nitrogen reacts readily only with lithium; above lithium's melting point (186°C), forms Li_3N with sufficient rapidity to necessitate handling lithium under cover gases such as argon or helium rather than nitrogen. Sodium reacts with CO_2 above 200°C to form sodium oxide and carbon plus a trace of sodium oxalate. Potassium forms the oxide but yields 17% potassium oxalate. The heavy alkali metals potassium, rubidium and cesium readily form lamellar compounds with graphite, in which the alkali metals are believed to be loosely bonded between parallel graphite planes. Sodium and lithium form lamellar graphite compounds only in the presence of impurities such as hydroxides or oxides [2].

2-2.2 *Importance of Impurity Determination in Sodium and Sodium-Potassium Alloys*

The contaminants known to increase corrosion rates of materials normally used in sodium, NaK, and other alkali metals are carbon, oxygen, hydrogen, and nitrogen (C,O,H,N). The effects of these elements in sodium and NaK, systems are very briefly summarized. The presence of carbon in sodium is of importance because austenitic stainless steels are subject to carburization. Above 1000°F the increase in carburization rate can be significant. Carbon transfer from ferritic to austenitic stainless steel can also occur in secondary systems but at a lower rate because the temperatures are lower. Oxygen in sodium enhances the corrosion rate of austenitic stainless steel and the rate of embrittlement of refractory metals. Hydrogen may be of moderate importance in causing hydrogen embrittlement of refractory metals at low temperature and plugging in cold zones in the event of gross contamination from a hydrogen source, such as water. Sodium reacts with water to release hydrogen, which reacts with more sodium to form the hydride. The decrease in solubility of the oxide and the hydride in sodium with decrease in temperature can cause plugging if water in-leakage occurs. In the presence of a few parts per million of calcium or barium in sodium, nitrogen can be transported rapidly from cover gas to metal surfaces, causing nitriding of sodium-containing stainless-steel surfaces or nitride embrittlement of refractory metals. Nitrogen is sometimes used as a cover gas or may be present because of air in-leakage.

Chemical analysis and in-line monitoring methods are important in the determination of (C,O,H,N) and their species in alkali metals. The utilization and development of these methods and techniques depend on their value in assessing the interaction of such impurities with containment materials. These contaminants establish the corrosion potential of the coolant and the resultant life expectancy of the containment system and components. Trace metallic elements provide an indication of corrosion products in the sodium. Impurities and fission products present either in the sodium or in the cover gas may be indicators of contamination, in-leakage, and corrosion.

Chemical analysis methods are sufficiently reliable for sodium- and NaK-contaminant monitoring and generally provide more accurate and sensitive data than are obtainable from current in-line monitoring devices. Consequently analytical methods establish the primary standards against which in-line measurement techniques must be calibrated. In-line monitoring devices for oxygen, hydrogen and carbon are under development. Analysis methods developed for sodium are usually adaptable to sodium-potassium alloys.

The purification effectiveness of cold traps, hot traps, or other contaminant-removal devices in the coolant is established by monitoring changes by chemical-analysis methods and by in-line monitoring techniques. Thus monitoring of the sodium by sampling-chemical-analysis methods and in-line devices is part of the purification process since monitoring tells what needs to be removed and how effective the removal has been. Surveillance of coolant impurity level is of practical importance for monitoring reactor conditions. Upgrading the usability, performance, sensitivity, and reliability of surveillance methods assists reactor operations in monitoring plant conditions. Research on the alkali metal-C,O,H,N system is a general prerequisite to establishment of valid analytical methods.

The presence and significance of impurities in sodium and cover gases in various reactor and test systems are reviewed by Alexanderson and co-workers [3, 4], Ashley *et al.* [5], Berger *et al.* [6], Broom *et al.* [7], Darley *et al.* [8, 9], Dickinson and Leppard [10], Duffy and Jens [11], Foust *et al.* [12], Hansen [13], Johnson [14], Lagowski and Havlena [15], Miller and Hallinan [16], Peterson and Cubitt [17], Phillips [18], and Woodruff, Durand and Owens [19]. Impurity-level specifications for reactor-grade sodium and for systems-quality sodium are discussed by Murbach, Bodine and Heath [20].

2-3 ANALYTICAL CHEMISTRY

2-3.1 *Oxygen - General Review*

Methods used to analyze for the oxygen content of sodium include mercury amalgamation (originally developed by Pepkowitz and Judd (21), vacuum distillation, butyl bromide separation, getter-plus-vacuum fusion, spectroscopy, liquid-ammonia separation, thermal and fast-neutron activation, and fluorination [22, 23]. The mercury-amalgamation and vacuum-distillation methods have undergone the most development. The mercury-amalgamation method is reported to be valid down to about 5 ppm, but it does not discriminate between such compounds as Na_2O, Na_2O_2, NaOH, NaH and Na_2CO_3. (Oxygen content is generally determined by measuring total alkalinity assuming that all the oxygen is present as Na_2O.) The method is therefore subject to error. Precision methods under ultraclean conditions are required. Both the mercury-amalgamation and the vacuum-distillation methods are presently recommended for fast-flux test facility and reactor applications. The vacuum-distillation method, like mercury amalgamation, is capable of measuring oxygen down to low levels but does not discriminate between the various compounds in which oxygen may appear. In addition to mercury amalgamation and vacuum distillation, getter-plus-vacuum-spark-source mass spectrometry are promising methods that appear to be capable of determining oxygen at levels of 10 ppm or lower with reasonable precision. Only limited work has been done in this area. An American Society for Testing Materials standard for the analysis of oxygen in sodium, entitled *The Amalgamation Method for the Determination of Oxygen in Sodium*, is presently in preparation.

Hobart [23] reviewed liquid-ammonia separation, thermal- and fast-neutron activation, and fluorination methods. The liquid-ammonia method, originally proposed for the determination of oxygen in lithium [24], has also been applied to the analysis of oxygen in sodium [25]. The alkali metal is dissolved in liquid ammonia; then the insoluble oxides are filtered from the solution. The filtered residues are then dissolved in water and titrated

[26]. Dutina and Simpson found that this method provides relatively good separations. Low temperatures are desirable, and a glass system is necessary. The potential chemical reduction of the oxide species and the inability to examine offgases during dissolution are disadvantages. Also, in-line applications are limited because of the required glass construction. The fluorination method involves reaction of alkali-metal samples with $KBrF_4$ to form fluorides and to displace molecular oxygen and nitrogen, but it has only been applied to the analysis of oxygen in lithium. Oxygen and nitrogen are measured by conventional gasometric techniques. The advantages of this approach are specificity for oxygen and the ability to completely release oxygen. Disadvantages are the need for complex equipment, hazardous reagents, and tedious procedure. Activation methods are briefly described in a later section. These methods are reported to be somewhat complex in procedure and equipment and in need of development.

The Karl Fischer titration method, developed by Steinmetz and co-workers [27,28] for the determination of oxygen in lithium, was succesfully used to measure low amounts of oxygen in sodium. The sodium oxide is dissolved in alcohol and reacted with an organic acid for conversion to an equivalent amount of water. The water is then titrated with the Karl Fischer reagent. Analysis of a series of samples gave a mean value of 3 ppm of oxygen and a standard deviation of ±1.5 ppm. The method has an advantage over the usual amalgamation titration or photometric method in that all the sodium does not have to be separated from the sodium oxide.

A 1961 report [29] from Battelle Memorial Institute (BMI) reviewed various new approaches to the problem of determining oxygen content to below 10 ppm in sodium. Table 2.2 [30], which was partially derived from the BMI report, lists 18 methods, categorized as unevaluated and evaluated, together with principles and remarks. The six methods thought to have the greatest potential were further reduced to the three most feasible methods. The main effort of BMI was to determine the suitability of nonchemical methods such as ellipsometry, polarography, coulometry, mass spectrometry, and arc-emission spectrography for low-level oxygen detection. It was concluded that all methods except ellipsometry should be specific for oxygen. Practical difficulties prevented experimental demonstration of these otherwise technically feasible methods. At that time additional development of coulometry and fused-salt polarography as potential oxygen-monitoring techniques and of arc-emission spectrography as a laboratory calibration technique applicable to many impurities was recommended. Coulometry is based on the dependence of electrical current on the number of ions transferred through an electrolyte. Decrease in electrical current through an oxide film on a reactive metal reflects the buildup of oxide by reduction of sodium oxide. Aluminum was found to be more promising than zirconium or tantalum for use as the reactive-metal electrode. Polarography, which is based on the interpretation of the curve plotted from current-voltage ratio resulting during the electrolysis of reducible or oxidizable substances, offers versatility in impurity detection but presents problems in the choice of electrolyte.

Emission spectroscopy can be used to determine oxygen in sodium ranging from 1 to 1000 ppm if techniques can be devised to volatilize and remove the metal. Emission spectroscopy is not adaptable for use as a continuous monitor but can be used as a standard laboratory technique for determination and analysis of many impurities. The BMI tests with sodium, calcium, and

TABLE 2.2 - Potential Oxygen-in-Sodium Analytical Techniques*

Technique	Principle	Remarks
		Unevaluated
Electron-spin resonance	Measure magnetic susceptibility oxygen with respect to sodium	Not good in the presence of traces of nickel, iron, or cobalt; other interferences may exist. Relatively new field; few general data amassed
Nuclear magnetic resonance	Measure interaction of oxygen with sodium nuclei resulting in a broadening of the steep sodium resonance peak	Not necessarily specific for oxygen and not a particularly sensitive phenomenon. May require cryogenic operation
Hall effect	Alteration of Hall coefficient of sodium resulting from dissolved impurities	Not specific for oxygen but extremely sensitive effects noted in semiconductors; sodium, however, is a metallic conductor. Lattice defects in pure material can produce effects similar to impurities. May require cryogenic operation and careful freezing to avoid strains
Oxygen radioactivation	Measure the radioactive decay of ^{19}O	Extremely difficult in the presence of high ^{24}Na activity
Thermoelectric potential	Monitor changes in thermoelectric potential with impurity change	No direct evidence of sensitivity; probably not selective for oxygen. Little prior experimentation exists
Infrared and ultraviolet absorption	Measure attenuation of transmitted or reflected infrared and ultraviolet radiation by sodium impurities	Probably not extremely sensitive although band absorption may provide selectivity. Selection of window material may present difficulty
Melting-point depression	Measure depression of sodium melting point as influenced by dissolved impurities	Sensitivity of 1 ppm oxygen per 3×10^{-4}°F predicted. Extreme accuracy required for temperature control and measurement. Technique probably lacks selectivity. The same general potentiality should hold for other colligative properties, such as vapor-pressure lowering, osmotic pressure, and boiling-point elevation

TABLE 2.2 - Potential Oxygen-in-Sodium Analytical Techniques* (Continued)

Technique	Principle	Remarks
		Unevaluated
Drop-time method	(Plugging-indicator refinement) determine sodium drop-time from free end of a capillary tube as a function of temperature	Not specific for oxygen accuracy dependent upon temperature-solubility data; increased precision results from potential precision of drop-time determination. Surface-tension effects may increase sensitivity
Getter reaction potential	Measure the electrical potential developed between the system sodium and a reactive metal	Probably not specific for oxygen. Thermoelectric interference expected; no good experimental evidence found. Sodium-resistant electrical-insulating seal may present difficulties
Getter resistance, optical properties, or weight change	Measure changes in oxygen content of a reactive metal exposed to system sodium by changes in electrical resistance, or weight gain	Large variations expected in blank reactive metal will influence reaction rates with sodium impurity. Specificity of these approaches is not explicit. Clean insertion and removal of getter from sodium system may be extremely difficult; in situ measurements probably very difficult
Concentration cell+	Measure the electropotential between a Na-Na_2O half-cell of known concentration and the sodium system	Calculations indicate adequate sensitivity at low impurity levels and manageable temperature sensitivity. Specificity for oxygen in doubt. The problem of a stable, nonreactive oxygen-ion conductor for the barrier between the cell and the system appears formidable
Fused-salt polarography	(See Organic polarography)	Basically as favorable as organic polarography; potentially specific, sensitive, and may be adaptable as semicontinuous monitor. The problem of obtaining and maintaining purity of a nonreactive fused-salt electrolyte formidable

(Table continues on following page.)

TABLE 2.2 - Potential Oxygen-in-Sodium Analytical Techniques* (Continued)

Technique	Principle	Remarks
		Evaluated
Electrical resistivity	Measure change in electrical resistance of sodium with change in impurity level	Not specific for oxygen. Expected to be sensitive to dissolved impurities only if atomic ordering of liquid sodium is sufficiently high. BMI results in disagreement with feasibility demonstrated by L.R. Blake (UKAEA)††
Ellipsometry	Measure change in degree of rotation and elliplicity of reflected polarized light as a function of impurity level	Not specific for oxygen. Potentially a continuous monitor; however, experiments at BMI were hindered by lack of compatibility between sodium sample and viewing window
Organic polarography	The determination of sodium impurity by electroreduction using an organic electrolyte	Specific for oxygen; other impurities exhibiting electroreduction or electro-oxidation might also be determined. Lack of satisfactory organic electrolyte prevented experimental confirmation of feasibility
Coulometry	The determination of sodium impurity by applying Faraday's law to the conduction of metal ions through an electrolytic oxide film on a getter metal	Specific for oxygen. Promises capability as a continuous monitor. BMI results clouded by ambiguous electrical behavior of films; however, qualified confirmation of feasibility was obtained
Mass spectrometry	Mass determination of oxygen evolved from residue after in situ distillation of sodium sample	Specific for oxygen. BMI experiments hampered by sample size limitations imposed by available mass spectrometer. Qualified success obtained
Arc-emission spectrography	Excitation and spectral determination of oxygen released during high-energy arc heating of residue after in situ distillation of sodium sample	Specific for oxygen. Promises versatility in the potential capacity to determine a large range of impurities. Preliminary BMI studies hampered by interference from electrode materials and difficulties in volatilization of sodium from sample
(Isotope Dilution[δ])		

(Table footnotes on following page.)

TABLE 2.2 - Potential Oxygen-in-Sodium Analytical Techniques* (Continued)

Footnotes to Table 2.2

---

*From K.T. Claxton, Review of Solubility Data for the Liquid Sodium-Oxygen System, *J. Nucl. Energy*, *19*: 849 (1965).

†Cu-Cu_2O has been shown to be a superior reference electrode to Na-Na_2O. The concentration cell is now considered to be specific for oxygen.

††UKAEA is the United Kingdom Atomic Energy Authority

§A promising isotope dilution method under development at Brookhaven National Laboratory (BNL) is discussed in Sec. 2-3.4.

---

magnesium established that it is possible to produce the spectrum of oxygen-containing compounds of these metals and that the intensity of the spectrum is proportional to the amount of oxygen present. A suitable means of introducing and volatilizing the sodium metal needs to be devised. A possible method would be extrusion of a solid sodium sample directly into the arc-excitation chamber carrying out sodium distillation; oxygen-containing impurities would be left on the bottom and sides of a graphite cup for arcing and analysis. An additional dividend in this procedure might be the detection of trace-element impurities and gases not volatilized with the sodium, but carbon cannot be determined if graphite electrodes are used. The method has potential value in regard to speed and sensitivity of analysis.

Another technique for the determination of oxygen levels at low compositions in alkali metals was reported by Herald [31], whose theoretical investigation of the effect of oxygen impurities on the freezing points of potassium, rubidium, and cesium indicated that levels of oxygen impurities in alkali metals as low as 10 ppm are detectable and measurable. Additional studies were recommended to evaluate the role of carbon impurities in lowering the freezing points of alkali metals. McKisson [32] reported that measurement of oxygen in potassium by this method is only marginally feasible because the temperature depression per part per million of oxygen is too small to measure accurately and because dissolved substances other than oxygen depress the melting point.

Results obtained by oxygen analyses depend on sampling techniques since slight amounts of air contamination erroneously increase oxygen measurements. Sampling methods are discussed in Sec. 2-3.8 and in Vol. III, Chap. 3.

(a) *Mercury-Amalgamation Method*

The mercury-amalgamation method depends on the selective reaction of mercury with sodium to form an amalgam that can be separated from the sodium oxide. The oxygen content is determined by titrating the water-soluble oxide residue with standard acid or by flame photometric analysis of the sodium. The original sodium content is determined by titration of the sodium amalgam. The determination of amounts as low as 5 to 10 ±2 ppm of oxygen in sodium has been reported. The method was reported promising for the determination of oxygen in sodium in the <10 ppm range and for utility in Fast Flux Test Facility (FFTF) service [22].

Improved versions of the Pepkowitz-Judd [21] method are the most suitable methods presently available for the laboratory analysis of oxygen in sodium. Inherent difficulties should be recognized, however, to ensure proper care in the required manipulations and awareness of limitations.

Although oxygen in sodium exists predominantly as Na_2O, the compounds Na_2O_2, NaOH, and Na_2CO_3 may also be included, and the residue separated from the sodium amalgam may contain any of these oxide compounds, as well as NaH. Repeated mercury extractions are necessary to obtain complete separation.

Great care must be taken to prevent contamination of the sodium during sampling, handling, and separation steps. The amalgamation and separation steps are done in a dry box under an inert-gas atmosphere. According to a study by Goldberg [33], the maximum impurity concentration allowable for inert atmospheres used in the analysis of alkali metals is 5 ppm moisture, 10 ppm oxygen, 5 ppm hydrogen, 10 ppm nitrogen (in handling lithium), and 10 ppm carbon dioxide. These concentration maximums should be adjusted, depending on the type of analysis to be made. Oxygen and moisture impurities in inert-gas atmospheres used in oxygen determinations can be controlled to 1 to 2 ppm [34, 35].

Procedures and refinements for analyzing oxygen in sodium by the amalgamation technique are given by Boltz, Kermoshchuk, and Meacham [36], Hobart [23], and Scarborough and De Vries [37]. Their methods vary mainly in ways of determining oxygen content, whether by various titration techniques or by flame photometry. Scarborough and De Vries [38] investigating methods of reducing blank values to determine oxygen in sodium at 0 to 10 ppm, reported that the principal source of the blank, adsorbed water on amalgamation-extraction glassware, can be most effectively reduced by high-temperature vacuum drying. By vacuum drying at 300°C and transferring under vacuum to the inert-atmosphere box, they were able to reduce the blank equivalent to oxygen to 1.3 ± 0.3 μg. Various modifications of amalgamation handling techniques developed by Goldberg [39] were claimed to reduce the required amount of mercury and the time of analysis from several hours to less than 1 hr. Sodium-potassium eutectic alloys can be analyzed in the same manner as sodium [1].

Claxton [30], reviewing oxygen analysis methods used to obtain solubility data, listed the three basic steps involved in analysis: (1) separation of the sodium from the oxide portion, (2) chemical or physical analysis of the oxide residue, and (3) chemical or physical analysis of the separated sodium. Two methods of separation, amalgamation and vacuum distillation, were used. The oxide residue was analyzed (1) by dissolving the residue to form a sodium hydroxide solution and then titrating with a dilute acid to a phenolphthalein end point to determine the hydroxyl ion equivalent to the sodium oxide or (2) by determining the sodium equivalent to oxygen with a flame photometer and measuring the intensity of the 5960-Å line of sodium with an internal standard such as lithium. The separated sodium was analyzed (1) by adding a known excess of HCl to the sodium amalgam to form sodium chloride and back titrating the excess acid with sodium hydroxide to a phenolphthalein end point and (2) by using the known volume and density of the sample, as in the vacuum-distillation method.

To assist in oxygen calculations, Claxton listed the forms that oxygen may take in the sodium: sodium monoxide (Na_2O), sodium peroxide (Na_2O_2), sodium superoxide (NaO_2), and sodium ozonide (NaO_3) [see Secs. 2-4.1(q) and 2-4.5 (a)]. If such other impurities as hydrogen, carbon, or moisture are present in the sodium or the atmosphere, sodium hydroxide (NaOH), sodium hydride (NaH), sodium carbonate (Na_2CO_3), sodium carbide (Na_xC_y), or sodium nitride (Na_xN_y) may also be present.

Mercury amalgamation is a well-established method of separating sodium from sodium oxide. This technique separates NaOH, NaH, Na_2CO_3, and Na_2O_2, as well as Na_2O from the sodium, although Na_2O normally predominates. Subsequent titration to establish total alkalinity or flame photometry to determine the sodium content of the separated residue does not distinguish between all the possible compounds, even though the oxygen content is usually calculated on the assumption that only Na_2O is present. High precision and accuracy have been claimed for the mercury-amalgamation method but considerable care must be taken in the chemical manipulations to prevent error. Metallic sodium remaining unseparated in the residue, will give a positive error. A negative error can be introduced during titration if the distilled water used to dissolve the residue has absorbed CO_2 and is not neutral. Mercury, which is used in large quantities, must be highly purified to prevent the addition of contaminants. Glassware must be clean and thoroughly dried. If proper precautions are taken, the amalgamation method is potentially useful to about 5 ppm but is not readily adaptable to in-line monitoring requirements.

(b) *Vacuum Distillation*

Vacuum distillation, first developed by Humphreys [40], is a method for separating sodium from its nonvolatile impurities. The sodium is drawn into a cup and distilled under vacuum; then the residue is analyzed by radiological or chemical means. A principal advantage of the method is its utility for highly radioactive liquid-metal systems. As described by White [41], the sodium is removed from the sodium oxide by distillation at 800°F at a pressure of less than 5μ Hg. The samples are taken from a high-temperature static or dynamic system and transferred under pressure to a hemispherical cup for distillation. The oxides in the residue are dissolved in water to form the hydroxide, which is then titrated with HCl using methyl orange indicator. This method is not specific for oxides since other sodium compounds may also be present in the residue.

Various refinements in the technique of vacuum distillation were described by McPheeters and Williams [42] and by Bergstresser, Waterbury, and Metz [43] of Los Alamos Scientific Laboratory (LASL). The sodium is drawn into a sample cup and heated at 400°C under a vacuum of pressure less than 5μ Hg. The nonvolatile residue is then dissolved in acid and analyzed for sodium content by flame spectrophotometry. Oxygen can be determined from 0 to 10 ppm with an estimated error of ±2.5 ppm. Later modifications are reported capable of reducing the error to ±0.5 ppm. The oxygen is assumed to be present as Na_2O, but this can be misleading because the residue may contain various combinations of sodium, oxygen, carbon, and fission-product elements from the reactor system. The nature of the distillation residues is being investigated at LASL [44, 45].

The experiments of Dutina and Simpson [26] indicated that a distillation system is feasible for application to in-line monitoring. The residue formed during distillation can be isolated and enclosed with only minor difficulty. Certain compounds, such as sodium hydride, may decompose at the high separation temperatures, however. Walker et al. [46] reported on British experience with the vacuum-distillation method. Sensitivity is high because large sample weights can be used. Low blank values of the order of 1 to 3 ppm can be maintained since no contaminating reagents are added during the distillation-separation step when the system is under high vacuum. Thermal decomposition of sodium oxide was negligible; recovery experiments resulted in a standard deviation of 1 ppm and bias less than 1 ppm of oxygen at the 5-ppm level in a 7-g sample. The loss of Na_2O by reduction with carbon was also found to be insignificant. The specificity of the method depends on the impurities present and, to some extent, on whether titration or flame photometry is used to determine the oxygen content. Oxides such as CaO or MgO are titratable but will not interfere with the determination of Na_2O by flame photometry. Common metals capable of reducing sodium oxide include Al, Ba, Be, Ca, Mg, Sr, Th, Ti, U, and Zr [30]. Oxides of the alkaline-earth group which remain stable under distillation can then be determined by titration but not by flame photometry. Sodium hydride decomposes to sodium and hydrogen, but sodium hydroxide decomposes to its oxide. Sodium carbonate requires a separate analysis technique [46].

The vacuum-distillation method is particularly adaptable to reactor systems because it is capable of providing accurate determinations down to 1 to 10 ppm in radioactive loops and where in-line monitoring techniques are convenient. Errors due to the presence of various compounds in the residue can be reduced by proper selection of analytical technique and by supplemental analyses to determine the types and content of the contaminating impurities.

Claxton [30] concluded that amalgamation may give high results and distillation may give low results. The errors in the amalgamation method result mainly from the separation and measurement of impurities other than oxides, and those in the vacuum-distillation method result from single-stage distillation of oxides into the distillate. Subsequent titration steps common to both methods may give low results also.

Vacuum distillation is a well-established method of separating sodium from its oxide and impurity residue. The method is not specific for Na_2O since compounds such as Na_2CO_3, Na_2O_2, and NaOH (decomposed to Na_2O at >400°C) remain in the residue although NaH is dissociated and lost at distillation temperature. Loss of sodium oxide due to reduction by carbon is a possibility; however, radiotracer tests do not indicate that losses occur from this cause. Reduction by metals such as Al, Ba, Be, Ca, Mg, Sr, Th, Ti, U, and Zr is, however, a possibility. Separation of the Na_2O during the normal single-stage distillation step does not appear to be a problem in spite of the fact that highly purified sodium is obtained by triple distillation. Large sample weights can be used to improve the sensitivity of determination. Location of the high-vacuum-distillation sampler in the sodium system itself reduces the possibility of contamination during distillation and the subsequent step in which only the residue is removed. Blank values are difficult to establish but are apparently reducible to values as low as 1 to 3 ppm. The accuracy and precision of the method are good if the apparatus is suitably designed and exacting care is taken during manipulations. The method is feasible for in-line monitoring applications and for radioactive systems.

(c) *Getter-Plus-Vacuum Fusion*

An undeveloped method for use with sodium systems is getter-plus-vacuum-fusion analysis of the oxygen content of tabs, such as zirconium, exposed to an alkali metal. The oxygen content of the metal tabs is determined by vacuum-fusion analysis. This method is specific but is of questionable value for low oxygen concentrations (<10 pp) in sodium. Distribution coefficients have been determined for the solid Zr(*O*) and liquid K(*O*) systems, but not for the Zr(*O*)-Na(*O*) system. Litman and Prados [47] investigating the distribution of oxygen between zirconium and liquid potassium at 815°C, found that the distribution ratio is sufficiently reproducible to make the method a useful analytical procedure for the determination of oxygen in potassium. Recoveries of oxygen in potassium were reported to be good from less than 100 to several thousand ppm. Gettering techniques provide oxygen-concentration averages over given exposure periods. Further development will be required for this method to supplement analytical techniques and operational checks by plugging meter.

Little experimentation has been done to determine oxygen content in sodium by getter-plus-vacuum-fusion methods. Goble, Albrecht, and Mallett [48], however, using titanium as a getter, attempted to determine low levels of oxygen in sodium after exposure of 2 to 4 hr. Results were inexact.

The getter-plus-vacuum-fusion method is specific for oxygen and is potentially capable of determining low concentrations of oxygen but provides only average-value data over an exposure period. Oxygen determinations are limited by the accuracy of vacuum-fusion analyses. An empirical factor derived from test conditions must be used. Much less effort has been expended on this method than on the amalgamation and distillation techniques.

(d) *Butyl Bromide Method*

Sodium can be separated from sodium oxide by reaction with excess *n*-butyl bromide in hexane with sodium by the following reaction:

$$2C_4H_9Br + 2Na \rightarrow C_8H_{18} + 2NaBr \quad (2.1a)$$

Sodium oxide will not react with the butyl bromide. The residue left behind (Na_2CO_3, NaOH, or Na_2O_2, as well as Na_2O) is then dissolved in water for titration of residue content. Moisture in reagents, necessitating careful dehydration, limits the general acceptability of the technique. The method has low precision and lacks discrimination [22, 49].

DeBruin [50, 51] reported on a method for the determination of oxygen in sodium by infrared spectrophotometry. In the original method, which uses butyl bromide, the reaction mixture containing the unreacted oxide is dissolved in water and reacted with excess carbon dioxide to convert the oxide to bicarbonate. The solution is freeze dried to a powder and pressed into a clear disk for infrared spectrophotometric analysis of specific absorption bands. In a later modification of the method, the sodium metal is first reacted with *n*-amyl chloride by

$$2C_5H_{11}Cl + 2Na \rightarrow C_{10}H_{22} + 2NaCl \quad (2.1b)$$

Infrared analysis was then made on the product, NaCl, which contained the impurity sodium monoxide. The sodium monoxide was converted by atmospheric carbon dioxide to sodium carbonate which absorbs strongly at 11.38 μ. The latter procedure is claimed to have a detection limit of 20 ppm with an accuracy of ±20%.

Although the butyl bromide method has been known for a number of years, it has not been used extensively. The method is not discriminatory since it analyzes for Na_2CO_3, Na_2O_2, and NaOH as well as Na_2O. Sensitivity and precision do not compare well with the more commonly used methods because of the difficulty of preparing and maintaining reagents and glassware free of moisture. The use of larger samples does not help since with larger samples more reagent is needed. The method is not recommended at the present level of development.

(e) *Activation Methods*

Claxton [30] outlined reactions on which the radioactivation methods are based:

Reaction	*Half-life*
$^{16}O(t,n)^{18}F$	112 min
$^{16}O(n,p)^{16}N$	7.35 sec

Reaction	*Half-life*
$^{16}O(\gamma,n)^{15}O$	124 sec
$^{16}O(\alpha,pn)^{18}F$	112 min
$^{16}O(^{3}He,p)^{18}F$	112 min

Fast-neutron activation has potential as a laboratory-standards method but is not applicable to reactors where sodium activity is high. Activation by the $^{16}O(n,p)^{16}N$ reaction requires neutrons of energies above 10 Mev at fluxes from 10^8 to 10^{11} neutrons/cm^2/sec [22]. The possibility of the presence of oxide impurites other than sodium oxide is a limitation of this technique. All the oxygen present, including oxides such as CaO, ZrO_2, MgO, and Al_2O_3, which are not reducible by sodium, are measured by this technique. Problems are caused by the possibility that containers may be oxygen contaminated and by the short half-life of the ^{16}N. Argonne National Laboratory (ANL) [52], analyzing for total oxygen by fast-neutron activation using the $^{16}O(n,p)^{16}N$ reaction, reported satisfactory oxygen determinations at levels down to 50 ppm.

General Atomics [53, 54], in an investigation of the neutron-proton reaction on ^{16}O to determine oxygen in potassium, concluded that this method is best from considerations of time per analysis, equipment availability and cost, concentration, sensitivity, and convenience. The lower limit of detection for a single determination was 25 μgm of oxygen which corresponds to 3.5 ppm oxygen in 7 g of potassium. At 1 ppm the uncertainty would be ±0.7 ppm for a single determination. The best available capsule material for low oxygen content potassium samples is oxygen-free high-conductivity (OFHC) copper. Two large NaI (Tl) crystals were recommended as the most sensitive detection system for ^{16}N. An automated activation-analysis system was recommended to eliminate the need for a highly trained analyst.

Interference from fluorine can affect results since fluorine is the only element other than oxygen that yields ^{16}N when bombarded with fast neutrons. To find its contribution to the total ^{16}N, we must determine fluorine separately by measuring ^{19}O from the $^{19}F(n,p)^{19}O$ reaction or the ^{18}F from the $^{19}F(n,2n)^{18}F$ reaction to correct the oxygen to its proper value. This method, though it has advantages of potential speed, sensitivity, and automation of analysis, does not distinguish between such compounds as Na_2O, NaOH, and Na_2CO_3, nor is it more accurate than existing techniques [30].

Photon activation can be used to determine oxygen concentration in sodium if interference from other radioactive species produced can be kept low. Holm and Sanders [55], investigating various detector geometries, found one that minimized interference so that 30 ppm oxygen was measured and 3 ppm should be detectable. They were able to reduce interference and improve sensitivity by a method that distinguishes between pure positron emitters and emitters of positrons with coincident high-energy gamma rays. Future improvements using a pair of large crystal detectors and a multiparameter pulse-height analyzer are believed to be possible. At LASL [44] the (γ,n) activation technique is used to evaluate the distillation method for oxygen analysis. This method, which is capable of measuring oxygen specifically rather than by alkalinity or sodium content, is used to study the nature of the residue left by vacuum distillation of the sodium. According to LASL the theoretical sensitivity of the technique should be <1 ppm.

The neutron-activation method is specific for total oxygen but cannot distinguish between the various oxygen species coexisting in the sodium or the oxides present in the containment material. The method can be useful in establishing an upper limit to check for positive errors in other techniques. Sensitivity is good (<10 ppm) but requires relatively large samples (~10 g). Accuracy and precision are generally good. Equipment costs and technical requirements are high. The nondestructive nature of the technique may be an advantage under certain circumstances. The method is basically a laboratory tool, being of limited value for primary reactor systems because of the high-sodium-activity background. Matrix and container background activity is a limitation of the technique. Photon-activation methods have good potential for determinations of oxygen in sodium to <1 ppm.

2-3.2 *Carbon - General Review*

Carbon-analysis methods used by various laboratories were compared in two series of "round robins" sponsored by the U.S. Atomic Energy Commission [36]. Participants were provided with carbon samples from a common source of sodium, and final comparisons were made of results, analytical methods, and procedural details. General conclusions reached from the program were that improvements in analytical methods had been made but that further work was needed in sodium source preparation, sampling, and handling techniques. Several methods were reported to have moderately good precision in determining either "total" or "elemental" carbon in sodium at levels above 10 ppm. The low-temperature oxidation methods were reported to yield somewhat higher results with better interlaboratory agreement than the high-temperature oxidation techniques. However, there was no apparent difference in the level of total or elemental carbon among the six batches of round-robin samples. Tests were classified as (1) total-carbon determination, (2) elemental-carbon determination, (3) carbonate-carbon determination, (4) water-acid carbon determination, and (5) water-dissolution carbon determination. These categories, with brief descriptions by Dutina [57], are given in Table 2.3. (Elemental carbon is that remaining after the sodium is distilled or the sample is dissolved and acidified.) The gases evolved in categories 3 to 5 are collected and measured. The nontotal carbon methods indicate that carbon exists in sodium in a variety of chemical species.

Analysis methods, though they include many variations, are generally based on "dry" or "wet" combustion, tab carburization, or isotope dilution [22]. The dry-combustion method depends on the combustion of carbon in sodium, by means of oxygen diluted in inert gas, to form carbon dioxide as a final product. The CO_2 can be measured by manometer, conductometer, or gas chromatograph. In the wet-combustion method, the carbon in the sodium is oxidized to CO_2 by the Van Slyke oxidizing agent. In general, the dry-combustion method provides small blanks and is used to determine total-carbon content; the wet-combustion method gives higher blanks and is generally used to determine elemental carbon. However, wet oxidation using the Van Slyke oxidizing agent can yield total carbon if all off-gases are collected. Variations of the dry-combustion method include addition of potassium dichromate as an oxidizing flux or addition of sulfuric acid to the product to release CO_2. Oxidation at high temperature (1100°C) in quartz is required to completely decompose the Na_2CO_3 formed by the interaction of CO_2 with Na_2O without the introduction of possible CO_2-containing compounds. Wet-oxidation methods produced erroneous results in some early experiments because carbon-containing gases released when the water reacted with the metal and when the resultant alkaline solution acidified were not collected. Dry oxidation or combustion

TABLE 2.3 - Methods for Converting Carbon in Sodium to a Gaseous Form [57]

1. Total-carbon determination
High-temperature direct oxidation (1100°C)
Low-temperature direct oxidation (650°C) followed by acidification
Water-acid dissolution and direct low-temperature oxidation of sulfate slurry (600°C)
Wet oxidation of slurry by Van Slyke's solution following water-acid dissolution (180°C)

2. Elemental-carbon determination
High-temperature oxidation (direct after distillation) (600°C)
Low-temperature oxidation (of sulfate slurry) (600°C)
Wet oxidation (Van Slyke)

3. Carbonate carbon determination
Acidification of water dissolution

4. "Water-acid" carbon determination
Water dissolution (Acidification)

5. "Water dissolution" carbon determination
Water dissolution

of the carbon to carbon dioxide appears to be the most suitable method for determining total carbon at low concentrations.

Carburization of the surface of austenitic stainless-steel tabs, determined by microhardness or metallographic analyses, is a method used by Atomics International [58, 59] to monitor for "effective" carbon level. The effective carbon content in the sodium is that form of carbon in true solution resulting in surface carburization. The correlation of carbon-analysis determinations with carburization-decarburization reactions remains a basic problem. This work is a significant step in correlating effective carbon content with resultant carburization potential. (See Table 2.4.)

In the isotope-dilution technique, a known quantity of ^{13}C is added to unknown ^{12}C impurity, the carbon is oxidized to carbon dioxide by wet or dry oxidation, and the ratio of $^{13}CO_2$ to $^{12}CO_2$ is measured. At 10 to 30 ppm (50 to 150µg in a 5-g sample), the method has a reported accuracy uncertainty (95% confidence limit) of ±2 to 5 ppm of elemental carbon in sodium [60]. (See Isotopic dilution, Table 2.4.)

Photonuclear-activation determinations of carbon in sodium from 10 to 100 ppm were reported by the National Bureau of Standards [61]. Precision of the analysis is 5% relative standard deviation for a single determination. This technique requires approximately 30 min per sample for analysis.

The sodium-carbon system is complex. Kelly, Hobart and Bjork [62] stated that significant amounts of methanides, acetylides, and various gases were formed by aqueous dissolution of the reaction products of sodium with various carbon compounds. In an experiment at Atomics International, methane was found in the helium bubbled through carbon-saturated sodium [63]. Gas chromatography was used for both tests. Varied species of carbon in sodium were found in cold traps in operational loops at Mine Safety Appliances Research Corporation (MSA) [64]. One of the cold traps was operated for 1400 hr at 250°F with a high-carbon environment due to sodium flow through a bed of graphite rods at 1200°F.. Found in the trap were 0.05 lb

TABLE 2.4 - Summary of Analytical Chemistry Methods for Oxygen and Carbon in Sodium [22]

Analytical technique	Potential for utility in FFTF service	Pro	Con
		Oxygen	
Mercury amalgamation	Good (only because of Pro item 2)	1. Broad experience available 2. Potential for determinations at <10 ppm	1. Difficult manipulation involved 2. Not discriminatory 3. Many potential sources for error
Vacuum distillation[*]	Good	1. Broad experience available 2. Sample handling only after sodium distillation	1. Not discriminatory 2. Problems with precision have been encountered
Butyl bromide extraction	Poor	None apparent	1. Not discriminatory 2. Low precision 3. Water-free reagents are a necessity
Getter plus vacuum fusion	Fair (possible opportunity for use in conjunction with carbon-determination tabs)	1. Specific for oxygen 2. Possibly capable of low-oxygen-level determination	1. Sparse background; needs further investigation 2. Will provide only an average indication over exposure period
Spectroscopy	Good (some form of spectroscopy will be a necessary analytical tool for trace-element impurities in sodium)	1. Potential for determination at <10 ppm 2. Potential for analysis without sample transfer	Sparse background; needs developmental effort
		Carbon	
Carburization tabs	Good	1. Specific for effective carbon and carburization potential 2. Experience available	1. Difficult manipulations involved 2. Only good for indications of past carbon history
Wet combustion	Poor	Experience available	Difficult manipulations involved

---

[*] The potential sensitivity for this method as reported by Walker *et al.* [46] is 1 ppm (see Table 2.6).

(Table continues on following page.)

TABLE 2.4 - Summary of Analytical Chemistry Methods for Oxygen and Carbon in Sodium [22] (Continued)

Analytical technique	Potential for utility in FFTF service	Pro	Con
		Carbon	
Dry combustion	Good (low-temperature method)	1. Experience available 2. Some encouraging utilization during round-robin analyses	Difficult manipulations involved
Isotopic dilution	Fair	No need for complete carbon conversion to CO_2	1. Difficult manipulation involved 2. ^{13}C additions must be stringently controlled with regard to quantity

of carbon; significant quantities of carbon dioxide, acetylene, and hydrocyanic acid; and traces of methane, ethane, ethylene, carbonyl sulfide, hydrogen sulfide, cyanogen, and oxymonocyanogen. The relative quantities of CO_2, C_2H_2, and HCN led the investigators to assume that sodium carbide or some acetylene-producing compound such as a carbonyl is responsible for the carburization of austenitic steels. For additional information on carbon in sodium, see Secs. 2-4.1 (k), 2-4.2 (c) and (d), and 2-4.5 (c) and, for information on the analysis of cyanides, Sec. 2-3.5.

(a) *Dry-Combustion Method*

The Stoffer-Phillips [65] method for the dry oxidation of carbon in sodium was later found by Kallman and Liu [66] to give no better than 50% recoveries of CO_2 from samples containing about 100 ppm of carbon. In the Stoffer-Phillips method, the sample is ignited in a stream of O_2 to convert the carbon to CO_2, which is then absorbed and weighed. Oxidation temperatures of 950°C or higher were required to obtain satisfactory recoveries. The quartz of the combustion boat reacts with the Na_2CO_3 to assist in the liberation of CO_2. The partial interaction of the oxidation products CO_2 and Na_2O to form Na_2CO_3 caused low recoveries. Subsequent experiments showed that temperatures of 1100°C were needed for complete recovery of carbon from Na_2CO_3 in the time allotted for the analysis. Sodium carbonate begins to dissociate at about 700°C and increases to a vapor pressure of about 1 mm at 950°C.

Kallman and Liu [66] oxidized the sodium samples at 600°C in an argon-oxygen mixture so that all the CO_2 reacted with the Na_2O to form the thermally stable Na_2CO_3. The product was later acidified with H_2SO_4 to release and measure the CO_2. This method appears to be reliable; the experimenters claimed that low blanks could be attained by careful operation. However, the apparatus was reported to be cumbersome and the manipulations intricate for routine analysis of a large number of samples.

A high-temperature dry-oxidation method using a gas chromatograph was developed by Atomic Power Development Associates (APDA) [67]. This method is applicable to the determination of total carbon in sodium in the range 10 to 150 ppm using 0.2- to 0.4-g samples of sodium and reportedly gives results with a relative error of ±5 to 10%. In this procedure the sample is oxidized at a temperature of 1100°C for 1 hr in an atmosphere of oxygen in helium. Intermediate compounds are believed to form in the combustion chamber by the interaction of CO_2 and Na_2O to form Na_2CO_3 and the reaction of Na_2O and $Na_2CO_3$with silica (SiO_2) to form Na_2SiO_3. The carbon is converted in steps to CO_2, which is collected in trap-cooled liquid nitrogen and is subsequently measured by gas chromatography. The sample is loaded into the combustion tube before the run in the dry oxygen-free argon atmosphere of a glove box.

Argonne National Laboratory [52] reported on experiments using dry oxidation in low-pressure (150-torr) ultrapure oxygen to form a residue of mixed sodium oxide and sodium carbonate. Tests of two methods for releasing the carbon dioxide from the residue by heating to 1100°C, cold trapping to collect the CO_2, and using manometric measurements of pressure resulted in reagent blanks of 4 µg. Treatment of the residue with sulfuric acid to release and measure the carbon dioxide by gas chromatography resulted in reagent blanks of 1.5 to 2 µg. Actual determinations of carbon content gave good agreement for average results, but variations in individual results indicated sampling problems.

Classical combustion-gravimetric methods have been adapted for the determination of trace amounts of carbon in sodium by Gardner and Ashley [68]. In this method the sample is contained in an aluminum capsule, reacted with a flux consisting of boric anhydride and vanadium pentoxide, and oxidized in oxygen at 1100°C. An average recovery of 96% with a standard deviation of 10 ppm was reported for 40 samples containing 0 to 200 ppm carbon.

Walker *et al.* [46] in a review of carbon analysis methods, claimed that dry oxidation at high temperature is simple and rapid. Low blanks can be achieved, but the sensitivity is poor since the sample size is limited to 0.1 to 0.3 g The low-sample-weight difficulty encountered with the high-temperature-oxidation method was reportedly overcome by the Kallman-Liu method of direct oxidation at low temperature (600°C) and the subsequent release of the CO_2 by acidification. Sensitivities of about 5 ppm were attained by use of 3- to 5-g samples. The formation of carbon monoxide is a possible source of error since the supply of oxygen is limited to control the rate of oxidation. Neither of the two direct-oxidation methods selects between the various forms of carbon.

Epstein [69], reviewing both the dry- and wet-combustion methods of determining carbon in sodium, stated that the dry-combustion method is promising in the presence of silica since the intermediate product Na_2CO_3 is converted to CO_2 by reaction

$$Na_2CO_3 + SiO_2 \rightarrow Na_2SiO_3 + CO_2 \qquad (2.2)$$

The CO_2 was not completely released until the reaction was carried out at 1100°C in quartz boats. A promising alternative is oxidization of the sample at 600 to 800°C and acidification with H_2SO_4 to break down the carbonate. Correlation of the form of carbon with carburizarion-decarburization reactions is currently unsatisfactory. The state of carbon in alkali metals needs further investigation as part of both analytical and materials programs.

Walker *et al.* [46] reported on a method that combines separation by distillation with combustion of the residue in an oxygen excess at 1200°C. The method for carbon is similar to that for oxygen except that silica crucibles are used instead of nickel. Satisfactory recoveries of 3, 6, and 12 ppm carbon in sodium at a standard deviation of 0.5 ppm were reported. Checks on the loss of carbon from interaction with sodium oxide indicated that carbon is not lost during distillation. Distillation methods for determining free and total carbon using 6 to 10 g of sodium have been in routine use at Culcheth and Dounreay for several years; blanks equivalent to 1.5 ppm have been obtained.

The high-temperature dry-combustion method yields total carbon in sodium with a sensitivity of about 5 ppm with moderately good precision, but carbon species cannot be individually determined by this method. Low analytical blanks (1 to 5 μg) can be achieved if extreme care is taken to prevent contamination. Sample weights are limited to about 1/2 g for the high-temperature oxidation method; however, weights can be increased to 3 to 5g with the lower-temperature oxidation-plus-acidification procedure. The use of reagent in the acidification step generally increases blank values. An advantage of the high-temperature method is that no reagents are necessary, but precautions must be taken to prevent downstream deposition of Na_2O in a colder zone of the furnace where it may react with CO_2 to form Na_2CO_3.

(b) *Wet-Oxidation Method*

In the wet oxidation method proposed by Pepkowitz and Porter [70], sodium is converted to sulfate, carbon is oxidized to carbon dioxide by means of the Van Slyke sulfuric acid-chromic acid oxidizing agent, and the carbon dioxide is collected and measured in a gasometer. The method reportedly has a standard deviation of ±0.001% for precision and is valid for determining elemental carbon but not for total carbon. According to Walker *et al.* [46] the wet-oxidation method can, under certain assumptions, be used to obtain a total-carbon figure by obtaining the sum of three fractions; the fractions are the gases evolved (1) during the hydrolysis of the carbide content, (2) from the acidification of the carbonate content, and (3) from the oxidation of the elemental carbon to carbon dioxide by the Van Slyke reagent. Elemental carbon is measured on the final step. The high-carbon blank added with the Van Slyke reagent and the limitation of the sensitivity of the method to about 10 ppm are serious disadvantages.

Epstein [69] reported that the wet-oxidation technique using the Van Slyke reagent as the oxidant produced erroneous results because only about half of the total carbon was actually determined since carbon-containing gases (as well as large amounts of hydrogen) were released upon reaction of the sodium sample with water and later upon acidification. Dutina *et al.* [71] determined total carbon by modifying the Pepkowitz-Porter method [70] to permit collection and analysis by gas chromatography of carbon-containing gases released during dissolution of the sodium and subsequent acidification. Improvements in preparing Van Slyke oxidant are claimed to reduce the blank by a factor of 2.5; this reduction would permit measurement of carbon concentrations at 10 ppm with a precision of ±5 ppm.

Although improvements have been reported, the wet-oxidation method of analyzing for elemental carbon in sodium is handicapped because of the somewhat erratic and relatively high blanks resulting from the addition of the Van Slyke reagent. The method is reported, however, to have a sensitivity of about 10 ppm with moderately good precision. Collection of carbon-containing gases released during hydrolysis and acidification prevents negative errors and permits determination of total carbon.

(c) *"Carbonate" Carbon Determination*

A method for the determination of carbonate carbon in sodium [72], in which the sodium sample is carefully dissolved in water and the evolved carbon dioxide is collected and measured by gas chromatography, gave standard deviations of 0.2 to 0.26 ppm and relative standard deviations of 4 to 7%. Other possible methods (not all have been specifically applied to determine carbonate) are based on such techniques as infrared and mass spectrometry, colorimetry, electroconductivity, and gas chromatography. Infrared-spectrometric measurement of CO_2 is not sufficiently sensitive. Isotope dilution using mass spectrometry has been applied to the determination of elemental carbon and could apply equally to carbonate determination. Colorimetric measurements have been used for CO_2 but were not specific for the complex equilibria of carbonates found in aqueous solutions. In addition to their method for total carbon, Kallman and Liu [66] developed a method to determine carbonate carbon. The sample is first reacted with moist argon to completely convert the sodium to NaOH; the carbonate remains as Na_2CO_3. Reaction with water and dilute H_2SO_4 then releases the CO_2 for absorption into $Ba(OH)_2$ solution and for conductometric measurement. Gas chromatography has been used for the determination of CO_2 content. For information on a recent method using distillation separation of the sodium and conductometric determination of the carbon dioxide evolved after acidification of distillation residue, see Walker and France [73].

The classical gravimetric method of analyzing for carbonates is not generally used for the determination of carbonates in reactor systems. The suitability of such techniques as mass and infrared spectrometry and colorimetry has not been established. The best available methods of determining carbonate are measurement of the evolved CO by chromatography or electroconductivity [66, 72].

2-3.3 *Hydrogen - General Review*

Hydrogen in sodium is determined by vacuum extraction, amalgamation, and isotope dilution. The vacuum-extraction method depends on the ability of hydrogen to permeate thin-walled iron or nickel membranes at high temperature. The method has been subject to the criticism that hydrogen does not completely permeate the capsule wall; however, reported recoveries are good. Various mercury-amalgamation separation methods using gas chromatography to determine hydrogen present in the free state, as a hydroxide or as a hydride, have been reported. This method is said to be suitable for the simultaneous analysis of hydrogen and oxygen at low concentrations. Further effort should be made to use gas chromatography or other suitable methods to identify and determine the separation products resulting from amalgamation of the sodium with mercury.

Vacuum extraction is a commonly used method of determining total hydrogen in sodium. Isotope-dilution methods, which utilize more complex analytical techniques to determine total hydrogen, have no particular advantages over the diffusion method. The accuracy and sensitivity of the two methods are good. The amalgamation technique, which can be used to release hydrogen from sodium, is of particular interest because it reportedly may be adaptable to the simultaneous analysis of both oxygen and hydrogen. Hydroxide hydrogen, nonhydroxide hydrogen, and total hydrogen can be determined by careful control of amalgamation temperatures. The classical combustion-gravimetric method has also been successfully adapted to measure hydrogen in sodium.

(a) *Vacuum-Extraction Method*

In the vacuum-extraction method, the sample is sealed in an iron or steel capsule and heated to 700°C in a vacuum. Quantitative removal of hydrogen either as the hydride or hydroxide occurs at this temperature. After it permeates the wall, the collected hydrogen gas is measured by a manometer or gas chromatograph. In the original method of Pepkowitz and Proud [74], the hydrogen was converted to water over hot copper oxide and measured by pressure decrease. Sensitivity was improved down to 1 ppm by better capsule cleaning and degassing to reduce blanks, by continuous removal of gases from the capsule to speed up diffusion, and by the passage of gases through a palladium thimble to make the measurements more specific for hydrogen [75]. A glove box was used during capsule loading and sealing to prevent contamination. Using some of these improvements, Dutina and Simpson [76] replaced the manometer with a gas chromatograph, which is more specific for hydrogen. This combination of vacuum extraction and gas chromatography gave a sensitivity of 1 ppm in a 5-g sample with a precision of approximately ±0.7 at 1 σ. Reported recovery averages (~98 to 99%) indicate that the hydrogen is completely released and diffuses through the capsule to be quantitatively trapped and measured. Good recoveries for the diffusion method were reported by Pepkowitz and Proud [74] and Walker and Seed [75].

Other membrane-permeation methods have been developed. Permeation of hydrogen through a Pd-Ag alloy is the basis for the Fisher Serfass Hydrogen Analyzer [77]. The use of nickel as the permeable membrane is discussed under in-line monitoring devices.

(b) *Isotope-Dilution Method*

Various isotope-dilution methods, including the use of deuterium or tritium, have been developed. The deuterium is heated with the alkali metal to set up equilibrium conditions. The isotope ratio in the gas phase, determined by mass spectrometer, is used to calculate the hydrogen content [78]. Reported recoveries on 2-g samples were at the standard deviation level of ±2 ppm for spikes ranging from 5 to 250 ppm hydrogen.

In a later tritium isotope-dilution method, Evans and Herrington [79], used a Geiger counter to obtain final measurements. Equilibrium was established between the tritiated hydrogen and the hydrogen in the sample by heating in a sealed borosilicate tube at 420°C for 10 min. Satisfactory recoveries from 140 to 4000 ppm were reported.

(c) *Amalgamation Method*

A promising alternate to the vacuum-extraction method, the gas-chromatographic determination of the hydrogen released during mercury amalgamation and hydrolysis of the residue, developed by Naud and Sannier [80], is reported sensitive to 0.1 ppm and adaptable for the simultaneous determination of oxygen content. Only hydrogen as hydride or in the free state is determined by this method. Sodium hydride and sodium hydroxide were differentiated by controlling the amalgamation temperature. Since analysis temperatures were held below 300°C, only nonhydroxide hydrogen was evolved. Goldberg [81] developed an amalgamation method to determine hydrogen in sodium, potassium, and NaK in which water is added under vacuum to the residue containing the hydride. The liberated hydrogen is then pumped by Toepler pump through a desiccant into an evacuated, calibrated sample bulb for determination by gas chromatography.

A later development [77], a modification of the Naud and Sannier method [80], uses a two-stage vacuum-reflux technique with mercury as the refluxing medium and measures evolved hydrogen quantitatively by gas chromatography. The mercury removes the sodium, which prevents recombination of the liberated hydrogen with sodium to again form sodium hydride. Hydroxide hydrogen, nonhydroxide hydrogen, and total hydrogen can be determined by careful control of the amalgamation temperature. Further investigation is needed to determine the presence of dissolved hydrogen, sodium hydride, and/or hydrocarbons in the reactor sodium. Experiments [77] indicated that hydrogen was liberated quantitatively from sodium hydride at 200°C and from sodium hydroxide at 370°C if temperatures are carefully controlled at those levels. The method is reportedly applicable to the determination of 0.2 to 100 µg of hydrogen in sodium with a relative standard deviation of ±5%.

A mass spectrometer was used by Grundy and Hamer [82] to analyze for gases evolved during amalgamation of sodium and subsequent hydrolysis of the residue with distilled water and dilute sulfuric acid. Gases evolved were found to consist of hydrogen, argon, carbon dioxide and various hydrocarbons including methane, ethane, ethylene and acetylene. The authors report that the method is sufficiently sensitive to detect individual impurities of the order of 0.1 ppm. Agreement was reported with hydrogen results and with sodium carbonate levels measured by an alternate procedure.

(d) *Gravimetric-Combustion Method*

Gardner and Ashley [83] adapted the classical combustion-gravimetric-hydrogen method to the determination of hydrogen in sodium. The sample, contained in an aluminum capsule, is first reacted with a silica-sand flux at 1000°C under an argon blanket and is then oxidized under oxygen to form water, which is absorbed in $Mg(ClO_4)_2$ and weighed. Fifty control samples ranging from 0 to 600 ppm hydrogen were recovered at 100% with a standard deviation of 8 ppm.

2-3.4 *Research and Development Programs and Method Summaries*

Investigation of other methods for the analytical determination of carbon, oxygen and hydrogen in alkali metals [84] include (1) paramagnetic experiments to measure the variation in magnetic moments due to the presence of impurities in sodium, (2) experiments to determine surface-tension changes of sodium as affected by contaminants, (3) extraction in organic solvents to determine sodium oxide in sodium, and (4) mass-spectrometric analysis of off-gases from the refluxing of sodium at high temperatures. The program was briefly evaluated [85] as follows:

Technique	*Evaluation*
Magnetic effects	Lacks specificity and sensitivity
Surface tension	Offers promise as an analytical tool for impurity measurement; sensitivity yet to be established
Organic solvent extraction	Terminated because of lack of accuracy, difficulty in maintaining reagent purity, and interfering side reactions
Mass spectrometry	Duplication of work at other facilities; funding terminated before performance of critical experiment

Table 2.4 lists and evaluates analytical methods for the analysis of oxygen and carbon in sodium for FFTF applications, giving important information on specificity, sensitivity, precision, utility and related factors. Tables 2.5 and 2.6 outline techniques, specificity and statistical data for leading methods of hydrogen, oxygen and carbon analysis.

(a) *Internal-Friction Techniques*

A promising method reported by Smith and Kassner* of analysis for interstitial impurity concentrations to <1 ppm involves the equilibration, with respect to the interstitial element, of refractory metal wires in liquid sodium. The high sensitivity of internal friction to low-interstitial-impurity concentrations in body-centered-cubic metals permits accurate determination of these impurities in several refractory metals. Since each interstitial element (O, N, C, and probably H) has a characteristic internal-friction peak, all these elements may possibly be analyzed for in one test. Because oxygen is probably the most significant impurity in sodium corrosion, emphasis has been initially placed on this element. The oxygen-analysis method involves the equilibration, with respect to oxygen activity, of tantalum wires in liquid sodium and the subsequent measurement of the oxygen concentration in the tantalum by internal-friction techniques. The oxygen concentration in the sodium is then related to the oxygen in tantalum by the distribution coefficient (ppm O in Ta/ppm O in Na), calculated from the best available free-energy and solubility data.

(b) *Isotope-Dilution Method*

An isotope-dilution method to determine the oxygen content of sodium is being developed at BNL [86]. In this method a known amount of ^{18}O is added to sodium before separation of the residue by amalgamation or vacuum distillation. The total oxygen content of the residue is then converted to carbon monoxide by reaction with graphite at sufficiently high temperatures. Then the ratio of ^{18}O to ^{16}O is determined by mass spectrometry to determine the initial oxygen content.

(c) *X-Ray Spectrometry*

X-ray spectrometry is a promising tool that has not been effectively utilized for analyzing impurities in sodium. As with other techniques, problems in handling the alkali metals must be overcome. This method determines a large variety of impurities quite rapidly and with good precision and accuracy. Elements with atomic numbers of 12 and above can be detected; limits of detection vary between 5 and 200 ppm depending on the particular element.

(d) *Spark-Source Mass Spectrometry*

Spark-source mass spectrometry is a potential method of analyzing for impurities in sodium, though problems in sample removal and integration of spectra must be solved. The attractive features of the mass-spectrographic technique [22] are as follows:

1. A basic sensitivity of subparts per million detection, usually from 3 to 30 ppb (atomic). Even allowing for interferences, photographic fog and other deleterious factors, very few elements have poorer than 1 ppm detection limits in a given matrix.

2. Approximately equal sensitivity for all elements. There are no blind spots.

3. Small-size-sample requirements. Only one set of sample electrodes is required for a complete analysis.

4. Generally unambiguous identification of elements and almost entire lack of dependence on the form in which the impurity is present. For example, oxygen would be detected whether

---

*D.L. Smith and T.F. Kassner, Argonne National Laboratory, personal communication, 1968; also Argonne National Laboratory, *Metallurgy Division Annual Progress Report for 1966*, United States Atomic Energy Commission Report ANL-7299.

TABLE 2.5 - Separation Methods*

Impurity	Technique	Method
Hydrogen	Diffusion	Separate H_2 by diffusion through the wall of an iron capsule containing the sodium
	Isotope dilution	Isotopic exchange of H_2 in sample with D_2 or T_2; separate by thermal dissociation; measure isotopic ratios
Oxygen	Butyl bromide extraction	React sodium with alkyl halide; titrate residual alkali
	Amalgamation	React sodium with mercury; remove amalgam, leaving Na_2O, which is determined by titration
	Vacuum distillation	Distill off sodium, leaving residue of Na_2O, for determination by titration or flame photometry
Carbon	High-temperature combustion	React sodium with oxygen at above 1000°C; measure evolved CO_2
	Low-temperature combustion	React sodium with oxygen at 500°C to Na_2CO_3; measure CO_2 evolved with acid
	Van Slyke oxidation	React sodium with water under argon; acidify; wet oxidize C; measure CO_2 manometrically
	Vacuum distillation	Distill sodium, leaving residue of carbon; determine by combustion in excess oxygen; measure CO_2 manometrically

present as M_2O, M_2O_2, M_2CO_3, or dissolved O_2.

The sample is prepared in an inert atmosphere or vacuum and then transferred to an evacuated spark chamber or a spark chamber filled with an inert gas. Analysis to less than 10 ppm of oxygen and carbon in solid lithium has been reported. Claxton [30] stated that the mass-spectrographic method for the analysis of oxygen in sodium is as promising, but as difficult, as the emission spectrographic method. Attempts to determine metallic constituents in trace amounts and to determine nonmetals by letting the spark burn through a vacuum-encapsulated gold foil to volatilize the sample were unsuccessful [87, 88]. An alternate procedure, "wiping" sodium on the electrodes under vacuum, appears promising. This method is presently reported to be suitable for the qualitative analysis of any elements (metal or nonmetal) in sodium and to be potentially suitable for quantitative determination. Because of contamination problems, oxygen, carbon and nitrogen are among the most difficult of the elements to determine in sodium. Data-processing techniques are being developed for more rapid and efficient operation.

Spark-source spectrometry is a promising method of determining the metallic and nonmetallic impurities in

---

*From J.A.J. Walker, E.D. France, J.L. Drummond and A.W. Smith, *Methods for the Analysis of Oxygen, Hydrogen and Carbon in Sodium*, British Report TRG-Report-1271, p. 2, June 14, 1966.

TABLE 2.6 - Comparative Methods for Hydrogen, Oxygen and Carbon*

Constituent	Technique	Specificity	Potential sensitivity, ppm	Potential coefficient of variation at 10 ppm	Time/ analysis, hr	Rate/day in routine use at UKAEA
Hydrogen	Diffusion	H_2 in solution NaH	0.2	±5	10	4
	Isotopic dilution	NaOH	2	±20	4	
Oxygen	Butyl bromide extraction	Na_2O Na_2CO_3 NaH NaOH	10	±100	2	
	Mercury amalgamation (Goldberg)†	Na_2O Na_2CO_3 NaH NaOH	10	±100	1	
	Vacuum distillation	Na_2O Na_2CO_3 NaOH	1	±10	6	10 samples in quadruplicate
Carbon	High-temperature combustion	Total C	25††	±100	1/2	
	Low-temperature combustion	Total C	5	±75	1	
	Vacuum distillation	Total C	1	±10	10	
	Wet oxidation	Free C	5	±50	1	
	Vacuum distillation	Free C	1	±10	12	5 samples in triplicate

*From J.A.J. Walker, E.D. France, J.L. Drummond and A.W. Smith, *Methods for the Analysis of Oxygen, Hydrogen, and Carbon in Sodium*, British Report TRG-Report-1271, p. 6, June 14, 1966.

†To be superseded by an ASTM standard method in preparation entitled *The Amalgamation Method for the Determination of Oxygen in Sodium Metal.*

††Reported by Bradley and Meacham [67] to be 10 ppm; see Sec. 2-3.2(a).

sodium with excellent sensitivity. The difficulty of introducing a representative sample into the mass spectrometer is one of the important problems under examination. Utilization of the technique for quantitative as well as for qualitative determinations is currently under development.

2-3.5 *Nitrogen*

The standard Kjeldahl method for determining nitrogen has been adapted to the analysis of nitrogen in sodium. In the method adopted at Los Alamos [89], the sample is dissolved in ethanol and flushed in an argon-gas stream. Water is added, and the evolved nitrogen, in the form of ammonia, is distilled into dilite boric acid solution and tritated with 0.01*N* hydrochloric acid to a mixed methyl red-bromocresol green indicator end point. Reported recovery for standard ammonium chloride solutions ranging in concentration from 1 to 100 ppm was 100% with an average standard deviation of 2.5% relative. Slow dissolution of the samples with water alone was somewhat hazardous and gave high, erratic results. Substitution with 95% ethanol allowed the process to proceed less violently and gave consistent results. Colorimetric methods can be used to measure the ammonia content in the distillate by dissolving an aliquot of the distillate with Nessler's reagent, which reacts to give a yellow color (Nessler's reagent connot be used in the presence of ethanol). The absorbance is measured with a spectrophotometer at 420 mμ. The method is reported to be valid for determining nitride nitrogen but not total nitrogen in sodium. Comparitively little effort has been expended for developing nitrogen-analysis methods.

Experiments by Hobart and Bjork [90] showed that cyanide can be formed in sodium by the reaction of nitrogen (added as ammonium, azide or gaseous nitrogen) with carbon (added as free carbon, carbonate or oxalate) [see Sec. 2-4.2(d)]. The Kjeldahl method may therefore be valid to determine nitride nitrogen but not to determine total nitrogen in sodium. If cyanide is present, hydrolysis of the samples will not cause formation and release of ammonia. Wet-oxidation methods for carbon analysis will cause loss of the cyanide as HCN. Dry combustion would add the cyanide carbon to any other carbon and thus lose its identity. Various methods could be developed for analyzing cyanide in sodium depending on the chromatographic determination of HCN, which is evolved after dissolution and acidification of the sample, or on fluorometric or colorimetric techniques [91, 92]. Kirtchik [93] reported application of the Kjeldahl method to the analysis of potassium.

Nitrogen in alkali metals is generally determined by some variation of the Kjeldahl technique. Good recoveries and precision have been reported for this technique with sodium, but only nitride nitrogen (not total nitrogen) is recovered. Since cyanides present in sodium are not converted to ammonia, other methods, such as chromatography, fluorometry or colorimetry, are required to determine cyanide content.

2-3.6 *Trace-Metal Analysis*

Certain trace metals of importance can be quantitatively measured by spectrophotometry, in which the metal reacts with certain compounds to form colored complexes. Emission spectroscopy is another method of qualitatively or quantitatively scanning the metallic trace elements present in sodium. The sample is generally converted to a chloride or a sulfate before excitation by electric arc. This method is less sensitive and less accurate than spectrophotometry but provides a broad and relatively quick technique to scan trace-metal-impurity content. Carrier-precipitation techniques to concentrate trace metals in high-purity sodium have been used in both emission and atomic-absorption spectrometry. Atomic-absorption spectrometry and spark-source mass spectrometry are promising new techniques to determine trace-metal constituents in sodium [see Sec. 2-3.4(d) for a discussion of spark-source mass spectrometry]. Radioactive fission and corrosion products in primary sodium and Na-K systems can be best detected by gamma-ray spectrometry. Requirements for chemical separation depend on the sophistication of radiation-measurement equipment available and the sensitivity of detection desired. Since a small number of radionuclides of possible interest do not emit X rays or gamma rays, specific chemical separations may be required. The separated sample can then be analyzed by beta-counting techniques. Crouthamel [94], Heath [95] and O'Kelley [96] reported further information on detecting and measuring nuclear radiation.

Korkisch and Orlandini [97] described a method of separating metal ions from sodium matrices.

Generally, trace metals in sodium can be determined most accurately by colorimetric methods. Emission spectroscopy is a very sensitive and a relatively rapid method of detecting a wide variety of trace metals but is less accurate and precise than colorimetric methods. For some requirements the analyst may have to adapt his technique from methods applied to the determination of the required metallic impurity in matrices other than sodium. Atomic-absorption spectrometry, a relatively new and sensitive technique, has been successfully used to determine trace metals in sodium. Spark-source mass spectrometry, which is at the experimental stage of development, shows considerable promise for determining all trace metals in sodium with excellent sensitivity.

(a) *Iron, Chromium and Nickel*

Iron, chromium and nickel react with certain compounds to form colored complexes whose optical densities are related to the original concentration of metal ions [98]. Spectrophotometric determinations, made by comparing optical densities of the unknowns to previously prepared standard curves, provide a quantitative measurement of concentration. Iron forms an orange-red complex with orthophenanthroline at a pH of approximately 4.0. The optical density of chromium in the hexavalent state is determined at 540 mμ in the form of a red-violet complex with diphenylcarbazide. Nickel is measured at 530 mμ as a complex red-colored salt formed with dimethylglyoxime. Supplemental information and procedures are given by Sandell [99]. Florence [100] reported on a method of estimating traces of nickel in sodium metal by complexing with cyanide, removing iron and chromium interference, and measuring absorbance of the complex at 268 mμ. Scarborough, Bingham and DeVries [101] developed a method to determine 0- to 10-ppm traces of iron, chromium, nickel and other metals in high-purity sodium using atomic absorption. At 1 ppm, 95% confidence limits, a precision of ±10% (relative) was attained. [See Sec. 2-3.6(e) on emission spectrography.]

(b) *Calcium*

Various methods used to determine calcium in sodium are:

1. Photometric measurements of optical density resulting from the presence of highly colored naphthalhydroxamate formed by the precipitation of calcium as calcium naphthalhydroxamate dissolved in (disodium ethylene-diaminetetraacetate dihydrate) (EDTA salt) [98].
2. Titration with di-Na-EDTA [98].
3. Separation of the calcium from large amounts of sodium salts with 8-hydroxyquinoline, followed by oxalate precipitation and titration, with 0.01*N* potassium permanganate [102].

Sensitivities are 0.1 μg for the first method, 30 μg for the second, and 0.1 mg for the third. Measurement in the first method is made by spectrophotometer at 410 mμ, and the optical density is related to a standard curve. [See Sec. 2-3.6(e) on emission spectrography.]

(c) *Potassium*

Potassium is best determined by flame photometry, a method of analysis in which light emitted by substances brought to excitation in a flame is measured. Since sodium emission interferes with potassium emission, the concentration of sodium must be kept below certain levels.

The flame-photometric method described by Sabol and Lockhart [98] is capable of determining 10 μg of potassium if the sodium content does not exceed 1.5 mg/ml. The potassium is determined in a flame photometer using an oxygen-hydrogen flame. Excessive sodium content will cause the sodium line to overlap the potassium line. Sandell [99] described the separation of the potassium from sodium by the cobaltinitrite technique, which involves precipitation of potassium in large amounts of sodium with sodium cobaltinitrite in cold solution or with silver cobaltinitrite, which gives $K_2AgCo(NO_2)_6$ when chloride is absent.

(d) *Barium*

A method reported by Dutina [103] to determine barium in sodium at concentrations as low as 250 ppm involves the precipitation of barium as the chromate followed by spectrophotometric measurement of the chromium concentration. The percentage of barium in sodium [104] can also be determined gravimetrically by precipitating as $BaSO_4$. [See Sec. 2-3.6 (e) on emission spectrography.]

(e) *Analysis by Emission Spectrography* [1, 105]

Emission spectrography depends on the measurement of light emitted by atoms excited by electrical discharge, in contrast to flame photometry in which high temperature is produced by the combustion of gases. This method is rapid, requiring only very small quantities in either solid or solution form with the use of suitable electrodes. Metallic elements in sodium can be determined after they are converted to chlorides or sulfates. Analysis sensitivities are usually in low parts per million. Iron, chromium, nickel, and calcium, as well as many other metals, can be determined either qualitatively or quantitatively. Emission spectrography is not the most suitable method of determining alkali metals, because the lower limit of detection is too high. Since the alkali metals are relatively volatile and have low excitation potentials, their presence in large amounts can reduce the sensitivity for the other elements. Various factors contribute to minimizing the suppressive effect of the alkali metal, including the buffering effect of the graphite, the deep anode cup, the high amperage, and the complete burning. Precautions must be taken to prevent contamination in handling, which can lead to serious error.

Specific procedures for analyzing impurities by emission spectroscopy have been reported by Westinghouse Electric Corp. [106], General Electric Company [107], Pratt and Whitney Aircraft [108], and Atomics International [109]. A 3.4-m Ebert Electronics Corp. spectrograph was used at Westinghouse to determine 30 elements in sodium at concentrations of 1 to 1000 ppm. The sample was hydrolyzed, converted to chloride, mixed with graphite, and excited by a d-c arc. Standard spectra prepared from NaCl are recorded concurrently with samples. Accuracies of 10 to 50%, depending on the impurity and its concentration, were reported. Table 2.7 lists impurities, estimated limits of detection, and wavelengths. Similar procedures were used at General Electric [107]. Sulfuric and hydrochloric acid were used for neutralization, and specific procedures were worked out for groupings of the elements. Table 2.8 lists procedures, elements, range, and sensitivity. In

TABLE 2.7 - Spectrographic Determination of Impurities in Sodium* [106]

Element	Estimated limit of detection,† ppm	Wavelength, Å	Element	Estimated limit of detection,† ppm	Wavelength, Å
Ag	1	3280.7	Mo	10	3132.6
Al	10	3082.1	Na		
As			Nb	800	3094.2
Au			Ni	10	3012.0
B	30	2947.7	P		
Ba	3	4554.0	Pb	30	2833.1
Be	30	3131.1	Rb	10	7947.6
Bi	10	3067.7	Sb	250	2598.1
Ca	3	3968.5	Si	10	2516.1
Cd	50	3261.1	Sn	30	3175.0
Co	3	3453.5	Sr	3	4607.3
Cr	3	2849.8	Th	800	2837.3
Cs	20	8521.1	Ti	30	3372.8
Cu	3	3247.5	Tl		
Fe	10	2598.4	U		
In	50	3256	V	10	3184.0
K	30	7968.0	W	800	2946
Li	1	6707.8	Zn	100	3302.6
Mg	3	2795.5	Zr	20	3438.2
Mn	2	2794.8			

*Impurities in sodium as NaCl.

†Limits of detection may vary slightly with photographic emulsion.

the Pratt and Whitney [108] procedure for sodium and NaK, the sample was dissolved in absolute alcohol, dried, hydrolyzed, and converted to carbonate. The carbonate was mixed with Li_2CO_3; then a measured amount was mixed in the electrode of a Jaco 3.4-m Ebert mounting-plane grating spectrograph. Semiquantitative results were reported by visual comparison against film. Concentrations of Fe, Ni, Cr, Al, Be, Ca, Si, and Mg can be detected to 0.01 to 10 ppm. The refractory metals, such as Nb, Mo, Ti, and Zr, can be detected at concentrations of 10 to 100 ppm. Atomics International [109] used a 3-m Baird-Atomic, Inc., emission spectrograph to determine the following trace elements at 1 to 100 ppm: Ag, Al, B, Ba, Be, Bi, Ca, Cd, Co, Cr, Cs, Cu, Fe, In, K, Li, Mg, Mn, Mo, Nb, Ni, Pb, Rb, Si, Sn, Ti, V, Zn, and Zr. The sodium containing the impurities was first dissolved in methanol, then acidified with HCl, and evaporated to dryness as NaCl. Spectrographic lines for the individual impurities were compared to corresponding element lines on standard plates using a comparator made by National Spectrographic Laboratories, Inc. Specialized spectrographic analyses can be done on certain impurity elements by use of CdS carrier precipitation, which acts to concentrate and enhance their response [110]. Limits of detection by this method for determining five metallic elements are: Co, 0.1 μg; Cr, 0.5 μg; Fe, 1.0 μg; Mn, 0.5 μg;

TABLE 2.8 - Spectrographic Determination of Impurities in Sodium [107]

Procedure*	Element	Range, ppm	Spectrographic limit, ppm	Procedure	Element	Range, ppm	Spectrographic limit, ppm
I-A	Beryllium	1 to 10		I-A	Molybdenum	2 to 200	
	Bismuth	5 to 50	2		Nickel	1 to 100	2
	Cobalt	2 to 100			Palladium	2 to 100	
	Indium	1 to 100			Silver	2 to 10	
	Iron	2 to 100	5		Thallium	10 to 100	
	Lead	5 to 200	2		Tin	10 to 200	
	Magnesium	10 to 100	10		Titanium	10 to 200	
	Manganese	2 to 50	2		Vanadium	2 to 200	
I-B	Mercury	2 to 200	5				
II	Boron		6	II	Copper		
	Cadmium	1 to 10			Silicon		
III	Aluminum			III	Calcium		400
	Barium				Strontium		
IV	Rare Earths	Range varies with different elements, usually 1 to 10 ppm.					

*Samples are dissolved by the dropwise addition of deionized water under an inert atmosphere, neutralized with hydrochloric or sulfuric acid, evaporated, and loaded into craters drilled in graphite electrodes. The electrodes are arced to burn the samples and excite the impurity spectra. Different procedures are used, depending on the elements sought.

Procedure 1-A (General impurities, except Hg, B, Cd, Si, Cu, and alkaline rare earths)
Sample: Pyrex cups, 1 g Na
Acid: 18N H_2SO_4, then 2N H_2SO_4 to the phenolphthalein end point
Spectrographic: 50 mg, 15 amp, 2 min, Gaertner, 2200 to 3500 Å

Procedure 1-B (Mercury)
Sample: Pyrex cups, 2 samples, 5 g Na each
Acid: 2N HCl, titrate to the methyl orange end point +10 ml conc. HCl
Spectrographic: Stir with 1 g Cu, arc Cu 30 sec at 12 amp d-c Gaertner, 2200 to 3500 Å or Baird 2.7°

Procedure II (Cd, B, Si, Cu)
Sample: Steel cups, 1 g Na
Acid: 18N H_2SO_4, then 2N H_2SO_4 to the phenolphthalein end point
Spectrographic: 75 mg, 15 amp, 2 min, Baird 2.7° plus filters

(Footnote continues on following page.)

Footnote to Table 2.8 (Continued)

Procedure III	(Al, Ca, Sr, Ba)
(Sample and acid	same as Procedure II)
Spectrographic:	10 mg a-c arc, Baird 5.2° + filters
Procedure IV	(Rare earths)
Sample:	Steel cups 5 g Na
Acid:	2*N* HCl, titrate to the methyl orange end point, use Fe^3 carrier, precipitate with NH_4^+, etc.
Spectrographic:	Solution on flat electrode, Baird d-c arc

and Ni, 0.5 μg.

(f) *Supplemental Methods for Trace-Metal Analysis*

Methods of trace-metal analysis not previously discussed are briefly outlined, with references, in Appendix 2-A at the end of this chapter [See also Sec. 2-3.4(d) on spark-source mass spectrometry].

2-3.7 *Nonmetals*

Nonmetals in sodium are generally determined with good sensitivity, accuracy, and precision by spectrophotometric and turbidimetric methods. In some cases methods must be adopted from analysis techniques used for matrices other than sodium.

(a) *Chlorine*

The chloride ion forms an insoluble precipitate with silver nitrate which can be detected by turbidity. In this method the sodium sample is dissolved in water and then converted to the nitrate by the addition of nitric acid. When silver nitrate is added to this solution, silver chloride forms, producing a turbidity measurable by spectrophotometer. Sensitivity of this method is 1 to 10 ppm detected to ±10% [111].

(b) *Boron*

Boron was determined in sodium colorimetrically. In a method reported by UKAEA [112] the sodium is dissolved in water under argon and heated to dryness before formation of rosocyanin complex by addition of curcumin in acid. Spectrophotometric measurement is reported capable of obtaining 0.1 to 1 ppm with a precision of ±20% at the 0.5-ppm level.

Logie [113] applied ion-exchange membranes to the separation and determination of boron in sodium metal. In this technique the sodium is converted to hydroxide and the boron to borate, and the solution is electrolyzed in a cell having electrode compartments separated by a cation-exchange membrane. The borate remains in the anionic compartment, and the sodium ions migrate into the cationic compartment.

(c) *Supplemental Methods for Nonmetal Analysis*

Methods for analyzing nonmetals not previously discussed are briefly outlined, with references, in Appendix 2-A at the end of this chapter. [See also Sec. 2-3.4(d) on spark-source mass spectrometry and Sec. 2-3.6 for a brief discussion of fission and activation product detection.]

2-3.8 *Sampling*

Varied approaches, including dip buckets, overflow cups, bypass flow-through tubes, evacuated bulbs, thief tubes, solid extrusions, and cup-distillation techniques, have been used to sample for sodium. Most of these methods have also been used to obtain samples for oxygen analysis and other impurities. It is difficult to obtain samples uncontaminated by atmospheric gases, particularly when low-level impurity concentrations are present in the sodium. Austenitic stainless steel is generally used for sampling, but pyrex can be used for some purposes at temperatures under 250°C. Flow-through samplers have the advantage of cleaning themselves before sampling. A flow-through sampler may be simply a bypass line parallel to the main line containing tubing connected by Swagelok fittings. The sampler can be chilled to freeze the sodium before crimping and removing to the laboratory for analysis. Sampling difficulties are caused by reactivity of alkali metals with atmospheric gases, moisture, and some containment materials As part of the LMFBR cladding program, Murbach [114] demonstrated that sodium can be dispensed, sampled, and analyzed at <10 ppm with a satisfactory degree of confidence. Oxygen-equivalent blanks obtained for flow-through samplers and retorts used to sample sodium were found to be 3.2 ± 0.8 ppm for samplers made of stainless-steel tubing, 2.0 ± 1.0 ppm for samplers made of nickel tubing, and 7.4 ± 1.5 ppm for retort samplers. Since the solubility of most impurities is temperature dependent, problems of impurity loss due to precipitation and segregation should also be considered [1]. Luner, Cosgarea, and Feder [115], for example, observed that reactor-grade liquid sodium, which freezes in clean quartz or stainless-steel tubes, contains more than three times the concentration of carbon on the walls than in central core. Scott [116] reviewed and evaluated sodium-sampling techniques and described a conceptual design for sampling sodium from both reactor and FFTF systems. The final choice for the FFTF sampling system will require further experimental investigation in the areas of impurity segregation, sampler preconditioning, general sampler preconditioning, general sampler requirements, blind-leg problems, the temperature of high-temperature seals, and the effects of atmospheric exposure on sample ends. See Madsen [117] for a review and evaluation of various sampler types used in the primary sodium system of the Enrico Fermi Atomic Power Plant (EFAPP). Development and standardization of samplers for specific impurities, particularly oxygen and carbon, are needed to improve the reliability of corresponding analysis methods. Sampling specifications are under preparation by an ASTM task group. Sampling devices are discussed in more detail in Vol. III, Chap. 3.

Inert gases can be sampled in metal or glass bulbs. The ready possibility of air contamination necessitates careful design of the sampling system to avoid air inleakage. Bakeout of the sample bulb under vacuum and repeated purging and evacuation of the bulb are essential for analysis of trace constituents [1]. Various gas-sampling devices are described and illustrated in Vol. III, Chap. 3.

The best sampler design for alkali metals or cover gases depends on test requirements. Flow-through-type alkali-metal samplers are recommended for dynamic systems because of their ability, with proper handling, to obtain representative contamination-free samples. Gas-sampling devices, to be used for trace-element analysis, must be thoroughly outgassed and purged.

2-3.9 *In-Line Monitoring Devices*

In-stream impurity-monitoring devices are, for the most part, in the experimental stages. Plugging meters are widely used, but most laboratories still design their own devices. Devices that are specific for a given impurity and have at least partially demonstrated their utility are the most promising, e.g., the electrochemical oxygen cell, which is commercially available, and the hydrogen detector. Other potential in-line methods include some inert-gas monitors discussed elsewhere. The possibility that cover-gas monitoring by gas chromatography may provide clues to carburizing potential and NaH activity has been explored only with small experimental systems. Gas chromatography has also been applied to the detection of hydrogen in cover-gas systems as a result of water inleakage. A description of in-line monitoring systems is also presented in Vol. III, Chap. 4. Davis [118] reported on in-line impurity-measuring instruments for liquid sodium, and Miller and Hallinan [16] reported on fission-product detection devices.

The most promising in-line monitoring devices, judged on the bases of durability, specificity, speed, sensitivity, and accuracy, appear at present to be the electrochemical cell for oxygen and diffusion monitors for hydrogen and carbon.

(a) *Oxygen and General Impurity Monitors*

In-line monitoring devices complement chemical methods because they are designed to provide continuous and/or fast-acting measurements, whereas chemical analysis methods are intended to provide sensitive and accurate measurements. The plugging meter is the in-line impurity-measurement device that has reached the highest state of utility even though it has limited specificity for oxygen or other impurities [see the discussion of the plugging meter in Vol. III, Chap. 4] The electrochemical cell and the resistivity meter (rhometer or Blake meter) are promising in-line impurity meters. The electrochemical cell is reported to be specific for oxygen, but the resistance meter has limited specificity.

A plugging meter is a relatively simple device for obtaining impurity concentrations in sodium by determining the temperature at which sodium flow can be restricted through an orifice plate. Concentrations of specific impurities can be obtained from known solubility curves from the saturation-precipitation temperature. The meter can be used as an oxide and/or a hydride meter when no other soluble impurities are present.

Minushkin [119] and Minushkin and Kolodney [120] reported that the electrochemical cell has a range from 1 to 100 ppm and is capable of rapid and continuous detection of small changes at low oxygen concentrations. In this device a solid electrolyte separates an inner reference electrode from the sodium and thus forms a galvanic cell which develops a voltage that is a direct measure of the thermodynamic activity (or effective concentration) of oxygen in the sodium. The meter has a ThO_2-Y_2O_3 solid electrolyte and a reversible oxygen-Cu, Cu_2O, reference electrode. A particular advantage is the specificity of the instrument for oxygen. Oxygen-level changes of 20% are detectable with no appreciable error if temperatures are controlled within 10°F. Sodium flow rates from 1/4 to 1 gpm have no effect on meter calibration or response in oxygen content. Cell life is reported to be better than 6 months at 600°F. Improvements are needed in the electrolyte and in the ceramic-to-metal seal. Recommended operating temperatures [121] are below 650°F; however, the device has been operated successfully at temperatures as high as 1000°F (see Davis [118]).

The resistivity meter developed at Dounreay and APDA depends on an increase in resistance with increase in oxygen. This type of meter is capable of continuous operation up to 1000°F but is limited by its lack of discrimination and by its sensitivity to temperature level. Test evaluation [122, 123] of the Blake resistivity meter in a liquid-sodium loop indicated that it is reliable and suitable for service in a radioactive environment as well as in a typical sodium-filled loop. Though the instrument was successfully calibrated for the oxide-concentration range of 10 to 80 ppm, improvements were needed to stabilize the signal, as well as to extend the range of the meter to make it suitable for commercial applications above 600°F. The determination of oxygen contamination was reported to be excellent. Carbon contamination interferes with the oxygen readings, but the amount of interference was not determined. The formation of submicron-size carbon particles with the resultant two-phase system causes difficulty. In addition, the device is very sensitive to hydrogen contamination.

A d-c electrical-resistivity meter being developed at LASL [45] appears promising for the in-line measurement of oxygen in sodium. A testing program to evaluate its capabilities and limitations and those of the United Nuclear Corp. electrolytic cell over a range of impurity concentrations, flow, and temperature conditions is under way.

The niobium corrosion meter depends on the differential flow rates through parallel niobium and stainless-steel orifice plates caused by corrosive reaction of the niobium with oxygen in the sodium. Davis and Draycott [124] reported that the meter can be used for a long time but not under high oxygen concentrations. Little detailed information on performance is available.

(b) *Hydrogen Monitors*

A hydrogen detector developed at Atomics International [125, 126] depends on the diffusion of hydrogen through the wall of a thin nickel tube into an evacuated chamber. The increase in thermal conductivity of the gas mixture in the evacuated region is detectable by the pressure indication of a Pirani vacuum gage. The device was reported to be capable of detecting as little as 1 ppm of hydrogen in a flowing stream of sodium at temperatures from 500 to 1200°F with a response time of 5 sec. Tests [123] of a similar nickel-diffusion-tube hydrogen monitor indicated that the hydrogen evolution rate was low and that the meter did not respond to massive water injections but an acceptable signal could be generated by sealing off the vacuum pump and reading the rise in pressure. A variation of this design [121] is a palladium tube plated on the inside with nickel. A hydrogen pressure difference is maintained across the membrane surface by catalytic conversion of the hydrogen to water as it emerges from the membrane surface. An electrochemical cell for the continuous measurement of hydrogen in sodium up to 650°C (1200°F) is being developed by United Nuclear Corp. The sensor is a hydrogen-concentration cell with an electrolyte containing hydride ions. Current status and future plans for the program are discussed by Fuhrman *et al.* [127].

(c) *Carbon Monitors*

Efforts are also under way to develop an in-line carbon meter suitable for sodium service. This device, developed by United Nuclear Corp. [128] is a diffusion meter in which the carbon diffuses through an iron or other metallic membrane to react with a low-pressure gas stream, such as dry or wet hydrogen. The decarburizing gas reacts with the carbon to be measured as CO or CH_4 in the flowing gas stream. Hydrogen reacts with carbon to form methane, and water vapor reacts to form carbon monoxide and hydrogen. Preliminary study indicated that a moist Ar-H mixture was a better decarburizing gas than dry hydrogen and that iron and nickel were the most promising diaphragm materials. Exploratory tests showed that both dry hydrogen and moist argon-hydrogen can remove carbon from iron more rapidly than carbon-saturated sodium can supply it to iron at 1300°F. In a series of thermal convection loop tests run at United Nuclear Corp. [129], a definite correlation was found between the carbon readings in sodium and the carburization rate of iron and stainless-steel tabs. The tests showed that oxygen greatly enhances the carburizing effectiveness of elemental carbon in sodium at 1400°F. Unstable carbides such as iron or sodium carbide cause a significant carburizing potential in sodium without the addition of oxygen. Probe materials through which carbon diffuses are under further investigation. Iron containing 1% nickel transmits as high a carbon flux as Armco iron but exhibits considerable grain growth. Iron alloys with 18 and 30% nickel are less attractive as probe materials than is pure nickel.

(d) *In-Line-Monitoring Development Program for Oxygen, Carbon, and Hydrogen*

In-line approaches under recent development by MSA include (1) physical-property changes of metals due to carburization, (2) electrical sensing of particles in liquid metals, (3) sodium oxide determination by electrical potential concentration in which sodium is concentrated at the anode of an electrolytic cell, and (4) continuous hydrogen monitoring [84]. A final evaluation of the program as summarized later by MSA follows:

Technique	Evaluation
Physical-property change	Immeasurable response at low contaminant levels
Electrical sensing of particles	Lacked validity
Electrical potential concentration	"No-go" with respect to both impurity concentration and detection
Continuous hydrogen monitoring	Erratic results; lacked promise of direct contact system at APDA

2-3.10 *Cover-Gas Monitoring*

Cover gases of large sodium reactor systems have been monitored to detect fission products indicative of cladding failure and to detect air inleakage or other contaminants. For smaller systems and for experimental work, methods have been developed to detect the impurities present in inert gases. Gas chromatography, however, provides a relatively inexpensive tool to detect a variety of impurities. Correct selection of column materials and detectors, coupled with anticipated developments in the future, indicate further improvements in sensitivity and accuracy. Supplemental methods may be necessary for some systems for impurities such as oxygen and water vapor. Table 2.9, which gives Fermi argon gas specifications, is from Yevick [130], who describes auxiliary inert-gas systems including cover-gas specifications.

TABLE 2.9 - Fermi Argon-Gas Specifications*

Composition	As-purchased	Purified
Ar	99.996%	99.998%
O_2	10 ppm	Trace
N_2	10 ppm	10 ppm
H_2	5 ppm	5 ppm
CO_2	5 ppm	Trace
H_2O	5 ppm	Trace

The most promising and inexpensive method of determining the varied impurity elements of interest in cover gases, (i.e., H_2O_2, N_2, CO, CO_2, water vapor, and various low-molecular-weight hydrocarbons) is gas chromatography. Recent developments in column materials and detectors indicate that these impurities are detectable at low levels. Mass spectrometry, however, is a basic tool for determining trace amounts of impurities in cover gases as well as for providing standards for gas chromatography. A variety of additional monitoring techniques to detect impurities in cover gases are listed in Tables 2.10 to 2.12. Some of these methods are not suitable for rapid

---

*From J.B. Yevick, *Fast Reactor Technology: Plant Design*, The M.I.T. Press, Cambridge, Mass., 1966.

TABLE 2.10 - Recommended Laboratory Methods for Determination of Impurities in Inert Gases[*]

Determination	Approximate possible sensitivity	Method
General methods	5 to 10 ppm[†]	Mass spectrometry
	1 to 50 ppm[†]	Gas chromatography
	1 to 10 ppm	Emission spectrography
Total impurities	0.5%	Measure gas pressure at constant volume and temperature before and after removing impurities, or measure gas volume at constant pressure and temperature before and after removing impurities
		Determine each impurity separately and add the values for the separate impurities
Purity of lamp-grade argon	3 ppm water and water-forming impurities	Fill a clear-glass tungsten-filament-type electric light bulb with sample, heat the filament under controlled conditions, and examine the glass for streaks
Acetylene	1 ppm	Colorimetric Ilosvay: Red copper acetylide is formed with ammoniacalcuprous chloride solution* (sensitivity can be increased by prior concentration of acetylene on refrigerated silica gel)
Carbon dioxide	1 ppm	Absorption sample in barium hydroxide solution and back-titrate with standard hydrochloric acid with phenolphthalein as indicator
Carbon monoxide	1 ppm	Oxidize sample over hot copper oxide at 300°C and determine carbon dioxide formed
Hydrocarbons	1 ppm	Oxidize sample over hot copper oxide at 900°C and determine carbon dioxide formed
Hydrogen	1 ppm	Oxidize sample over copper oxide at 300°C and determine moisture formed, or mix with oxygen and burn over hot platinum
Nitrogen	10 ppm	Measure volume of sample (at constant pressure) before and after treating with molten lithium
Nitrous oxide		Mass spectrometry
Oxygen	1 ppm	Mix with hydrogen, burn over platinum, and determine moisture formed
	7 ppm	React with a hot tungsten filament of an electric light bulb, and examine the filament for oxide formation
	10 ppm	Gas chromatography

(Table continues on following page.)

TABLE 2.10 (Continued)

Determination	Approximate possible sensitivity	Method
Water vapor	0.03 ppm	Freeze out moisture from a measured volume of gas in a trap at -183°C, and then warm the trap and measure pressure of water vapor
	5 ppm	Determine dew point
	<0.01%	Absorb on phosphorus pentoxide or other drying agent and weigh

[*] From I.M. Kolthoff, P.J. Elving, and E.B. Sandell (Eds.), Treatise on Analytical Chemistry. II: *Analytical Chemistry of the Elements I*: 268-269. Interscience Publishers, New York, 1961.

[†] Depending on the nature of the impurity and the sensitivity of the detector.

[‡] The Ilosvay reagent is an ammoniacal solution of cuprous chloride made by reducing cupric chloride in aqueous solution with hydroxylamine hydrochloride.

---

routine-monitoring applications. Frequently the high-rate techniques require equipment that is unreliable and often needs costly recalibration. The highly reliable techniques may require types of equipment unsuitable for a commercial system and involve time-consuming analytical procedures. For most purposes a gas chromatograph or mass spectrometer is recommended; however, the specific methods listed in Tables 2.10 to 2.12 may be more practical for individual impurities.

(a) *Gas Chromatography*

Impurities can be detected in inert gases by gas chromatography, supplemented by other methods using commercial units such as oxygen analyzers and moisture monitors. Gas chromatography can be used to determine the impurities oxygen, nitrogen, methane, hydrocarbons, carbon monoxide and dioxide, hydrogen, and water vapor. The sensitivity of detection varies considerably, however, for these impurities in various inert gases. Oxygen, nitrogen, methane, and carbon monoxide are reportedly [131] detected in helium at 1 to 2 ppm; in argon, however, the sensitivity is an order of magnitude poorer. In-line gas chromatography [132] is used to detect oxygen and nitrogen in helium to 1.5 ppm and methane and carbon monoxide in helium to 3 ppm, using Linde Co. Molecular Sieve Type-5A columns and thermal-conductivity detectors. If argon is present in the helium, oxygen cannot be detected because argon and oxygen have similar elution times. Dutina and Simpson [76] reported on the use of gas chromatography to determine hydrogen and other impurities in argon cover gas over sodium. Both hydrogen and nitrogen, apparently from atmospheric contamination, were observed. Using helium carrier gas in a two-column silica gel and molecular sieve with hot-wire-filament detectors, they found the following sensitivities: hydrogen, 30 ppm; carbon dioxide, 200 ppm; carbon monoxide, 100 ppm; oxygen, 150 ppm; nitrogen, 300 ppm. and methane, 100 ppm. The bulb used for inert-gas sampling is described. Johnson [63] bubbled helium through carbon-saturated sodium and measured the released gaseous impurities hydrogen, methane, and nitrogen by gas chromatography. Measurements of H_2 and CH_4 concentrations were used to correlate gas analysis with NaH activity and carbon activity based on the reactions

$$C + 2H_2 \rightarrow CH_4 \qquad (2.3)$$

$$Na + 1/2H_2 \rightarrow NaH \qquad (2.4)$$

TABLE 2.11 - Other Methods for Determination of Impurities in Inert Gases*

Determination	Approximate possible sensitivity	Type†	Method
Combustible impurities	1 ppm	C	Oxidize sample over platinized silica gel or other suitable catalyst to give carbon dioxide and/or water vapor
Impurities, general		C	Electrical: Flow gases through an electrolytic rectifier; the leakage current determines the extent of impurities
	0.05%	C	Electrical: Voltage across a discharge tube is a function of the concentration of total impurities; total pressure of 3.5 mm Hg is used
		C	Electrical: Voltage across a uniform-current arc in a stream of argon is a function of impurities
Noncondensable impurities (e.g., O_2 or N_2) in xenon		L	Condense xenon by liquid nitrogen and measure the pressure of the residual gas
Carbon dioxide	1 ppm	L-C	Bubble gas through a calcium carbonate slurry, and measure the pH
Hydrogen in argon		C	Spectroscopic: High-frequency, electrodeless discharge at 0.1 to 10 mm Hg pressure gives $H\alpha$ and $H\beta$ lines
Hydrogen (in absence of oxygen)	0.1 ppm	C	Colorimetric: Reduction of methylene blue-palladous chloride solution at pH 3.9
Hydrogen	6 ppm	C	Sonic: The concentration of hydrogen is automatically determined by measuring the phase shift of sound waves at 150 kc
	1 ppm	L	Spectroscopic: High frequency, electrodeless discharge excites gas at 2 to 20 mm Hg pressure; the $H\beta$ line is isolated by an interference filter
Hydrogen fluoride	10 μg	L	Conductometric: Aqueous boric acid solution is used to scrub gas sample
Nitrogen in argon		C	Spectroscopic: High frequency, electrodeless discharge at 0.1 to 10 mm Hg pressure gives nitrogen-band spectra
		C	Electrical: Voltage across a uniform-current arc in a stream of argon is measured
Nitrogen in helium	1 ppm	L	Spectroscopic: High-frequency, electrodeless discharge with gas at about atmospheric pressure

(Table Continues on following page)

TABLE 2.11 (Continued)

Determination	Approximate possible sensitivity	Type[†]	Method
Nitrogen	0.2%	L	Absorb in molten lithium; each determination takes 10 min
	0.1%	L	Absorb by molten lithium at 180 to 200°C; reaction is complete in 15 min
	0.01%	L	Absorb in molten lithium at 500°C for 1 hr
	10 ppm	L	Absorb by titanium at 1050°C in a silica tube; determine nitrogen in the titanium by a modified Kjeldahl method. (Not reproducible at 0 to 10 ppm nitrogen)
	1 ppm	L	Spectroscopic: High-frequency, electrodeless discharge excites gas at 2 to 20 mm Hg pressure; nitrogen-bands are isolated by an interference filter
Oxygen	0.1%	L	Absorb by molten lithium at 180 to 200°C; reaction is complete in 15 min
	0.002%	L	Colorimetric: Absorption in cuprous ammonium salt solution
	0.02%		
	0.01%	L	Absorb in molten lithium at 500°C for 1 hr
	0.003%	L	Quench fluorescence of trypaflavine
	0.001%	L	Colorimetric: Oxygen reacts with the reduced form of sodium anthraquinone-β-sulfonate in alkaline solution
	20 μg	L	Colorimetric: Absorption in alkaline aqueous pyrogallol
	<1 ppm	L	Optical: Oxygen is absorbed on sodium metal, and the thickness of the oxide film is determined optically
	1 ± 0.1 ppm	L	Colorimetric: Improved Winkler method; oxygen reacts with manganous potassium iodide solution to give iodine; color is measured in O-oxylene
Water vapor	0.1%	L	Absorb by molten lithium at 180 to 200°C; reaction is complete in 15 min
	0.5 ppm	C	Optical: Absorption of 1216 Å radiation (vacuum ultraviolet) by water vapor

---

[*] From I.M. Kolthoff, P.J. Elving, and E.B. Sandell, (Eds.) Treatise on Analytical Chemistry. II: *Analytical Chemistry of the Elements I*: 280-281. Interscience Publishers, New York, 1961.

[†] C, continuous plant-stream method; L, laboratory method. In many cases, laboratory methods may be adapted for use as continuous plant-stream methods.

TABLE 2.12 - Recommended Continuous-Flow Methods for Determination of Impurities In Streams of Inert Gases*

Determination	Approximate maximum sensitivity	Method
Overall purity of an inert gas	10 to 50 ppm	Thermal conductivity
Individual impurities	25 ppm†	Plant-type mass spectrometry
	2 ppm‡	Gas chromatography
Acetylene	1 ppm	Nondispersive infrared absorption
Carbon dioxide	1 ppm	Nondispersive infrared absorption
	5 ppm	Measurement of pH of sodium bicarbonate solution
Total hydrocarbons	1 ppm	Combustion, followed by carbon dioxide determination
Hydrogen	1 to 2 ppm	Combustion with added oxygen over a catalyst, followed by determination of moisture
	10 ppm	Combustion with added oxygen over a catalyst and measurement of temperature of the catalyst
Nitrogen in argon	3 ppm	Continuous liquefaction and distillation of the sample and measurement of thermal conductivity of the nitrogen concentrate
Oxygen	0.01%	Magnetic analyzer, 0 to 1% full scale
	0.1 ppm	Hersch electrolytic cell
	5 ppm	Combustion with added hydrogen over a catalyst and measurement of temperature of the catalyst
Water vapor	1 ppm	Electrolysis of phosphorus pentoxide and absorbed water in a special cell, with measurement of electrolysis current

*From I.M. Kolthoff, P.J. Elving, and E.B. Sandell (Eds.), Treatise on Analytical Chemistry. II: *Analytical Chemistry of the Elements I*: 276. Interscience Publishers, New York, 1961.

†The sensitivity can sometimes be increased by modification of available instruments.

‡This sensitivity is reached only in special cases by use of a very sensitive detector.

Recent developments in detectors promise considerable improvement in sensitivity of detection for impurities in cover gases. The helium-ionization detector operates on the principle that metastable helium atoms (*He) will ionize all compounds having lower ionization potentials than the excitation energy of *He. Such gases as H_2, Ar, O_2, N_2, CH_4, CO, and CO_2 can be ionized since their ionization potentials are below that of helium. Concentrations of these gases as low as 10 ppb can be detected by the helium-ionization detector according to Dimick and Rigali [133].

(b) *Mass Spectrometry*

T.F. Lyon discussed the use of the mass spectrometer to measure the concentration of oxygen, nitrogen, and hydrogen in a vacuum-purged helium inert-gas welding chamber. Detection limits are stated to be between 1 and 2 ppm for these impurities. Qualitative measurements can be made for other impurities. Mass spectrometry has been used [135] to analyze for trace impurities, such as H_2, N_2, O_2, Ar, CH_4, CO, and CO_2, in ultrapure gases to sensitivities of 0.1 ppm or better. Since gas chromatography is not an absolute method and its analytical standards are difficult to synthesize, mass spectrometry can be used to determine its standards as well as to analyze routine gas samples.

(c) *Other Methods*

Other methods of analyzing helium and argon for impurity content are reviewed by Limoncelli [131]. Water in helium or argon can be detected by a cold-mirror dew-point meter or by an electrolytic hygrometer. Oxygen in helium or argon can be detected by bubbling the gas through a cuprous sulfate solution, which becomes oxidized to the cupric ion; the impurity is thus measurable by color change. Lyon [134] discussed an oxygen analyzer (Beckman model 80) and an electrolytic hygrometer (Beckman model 27901) capable of detecting approximately 0.1 ppm oxygen and 0.05 ppm water vapor to monitor inlet-gas purity.

The Connecticut Aeronautical Nuclear Experimental Laboratory (CANEL) Materials Laboratory Manual [136] specified that a measured inert-gas sample be passed through an ammoniacal cuprous chloride solution. The oxygen in the inert gas oxidizes the colorless cuprous ion to the intensely blue cupric complex for visual comparison with standard solutions.

The coulometric Ag-Cd or Ag-Pb electrode system based on the electrolytic reduction of oxygen in the sample stream is also used for the determination of oxygen in flowing cover-gas systems. The coulometric Lockwood & McLorie Inc., model 0-1000 oxygen analyzer for continuous monitoring of helium streams for oxygen was found [137] to be capable of determining less than 1 ppm of oxygen with response time of about 30 sec at gas flow rate of 200 cm^3/min. This method, unlike a comparable gas-chromatographic method, is not sensitive to interference by argon. Hydrocarbons in helium or argon can be measured continuously and nonspecifically by the increase in ionization of a hydrogen-gas flame caused by the injection of the hydrocarbons. Nitrogen in argon is determined by passing a gas sample through a glow-discharge light cell in which nitrogen produces a measurable line of ultraviolet light [131].

APDA [122] developed a continuous hydrogen monitor for argon cover gas with a detection range from 100 to 2000 ppm and a maximum response time of 20 sec. The detection device was based on the comparative thermal conductivity of clean and dirty gas streams. The monitor met specifications below 2000 ppm but required constant manual surveillance.

See Ref. 1 and Tables 2.10, 2.11, and 2.13 for various other methods for laboratory and in-stream monitoring of impurities in inert gases. In general, preference should be given to the recommended methods.

2-4 CHEMICAL INTERACTIONS

In this survey of the chemical behavior of sodium and NaK, the emphasis is placed on the interactions of these metals with the elements. The discussion of interactions with compounds is limited to those materials whose reactions with sodium or NaK are of concern in nuclear reactor technology or are potentially hazardous. Source references relating to other aspects of sodium technology are noted in the pertinent sections.

2-4.1 *Interactions with the Elements*

This section, which deals primarily with the interactions of binary elemental systems, presents phase diagrams, equilibrium data for solubilities, and pertinent thermodynamic data relating to binary systems. Selected ternary-alloy systems of particular concern to nuclear reactor technology are also discussed.

(a) *Group 0 Elements - He, Ne, Ar, Kr, and Xe*

The rare gases are slightly soluble in the alkali metals, as shown by the measurements of Dhar [138, 139], of Slotnick, Kapelner, and Cleary [140] and of Mitra [141].

(1) *Helium.* No measurements of the solubility of helium in sodium or in NaK have been reported. However, Epstein [142] estimated values of the solubility of helium in sodium at 232°C (459°F) and 482°C (900°F) to be 1.6×10^{-11} and 1.3×10^{-7} (cm^3 He at STP/cm^3 Na), respectively. These values become 1.83×10^{-14} mole He/mole Na at 232°C and 1.59×10^{-10} mole He/mole Na at 482°C. The measured values of argon and krypton in sodium, shown in Fig. 2.1, are higher than these estimated values.

(2) *Neon.* No measurements of the solubility of neon in sodium or in NaK have been reported.

(3) *Argon.* Dhar [138] measured the solubility of argon in sodium in the temperature range 340°C (644°F) to 480°C (896°F) and in the pressure range 3.4 to 9.1 atm. The solubility of argon follows Henry's law. Dhar's data are described by the expression,

$$\log S \text{ (mole Ar/mole Na/ atm)} = -4.01 - \frac{3450}{T(^\circ\text{K})} \qquad (2.5)$$

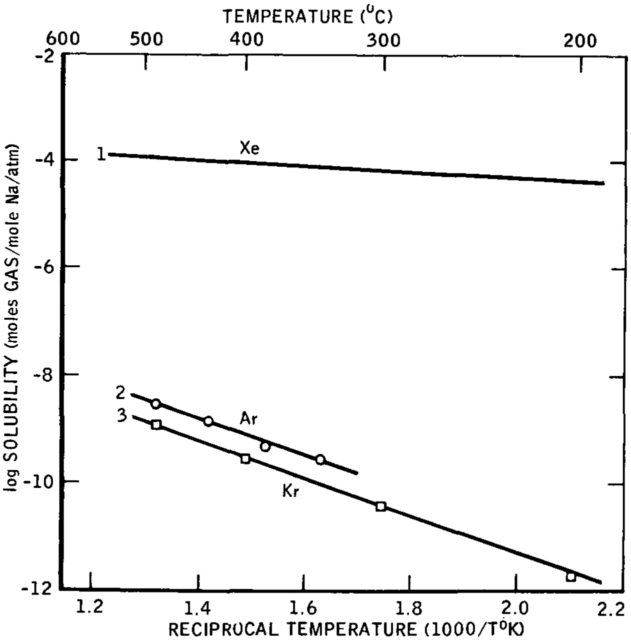

Fig 2.1 Solubilities of rare gases in sodium. (Curve 1 is from Ref. 141; curve 2, from Ref. 138; and curve 3, from Ref. 139.

for which the ΔH (solution) is 15.8 kcal/mole of argon. The data are shown in Fig. 2.1.

Savage *et al.* [143] reported two experiments in which flowing NaK-78 contacted argon gas at about 730°C (1350°F) in a surge tank and then cooled as it flowed through the system. Argon gas was accumulated in a cold leg. An estimate of the solubility of argon in NaK-78 was made from the flow rates of the NaK, the rate of removal of argon from the surge tank, and the assumption that no entrainment of argon occurred. The average value from the two experiments is 10^{-5} mole Ar/liter NaK/atm for a temperature of 730°C (1350°F) and an argon pressure of 25 psia (1.7 atm). This is about one order of magnitude larger than the extrapolation of the argon-in-sodium data in Fig. 2.1. This is not an unreasonable difference, based on the difference between the solubilities of helium in lithium and potassium shown in Fig. 2.2. If the molecular weight of the alkali metal has the same effect on argon solubility as it does on helium solubility, the one-order-of-magnitude difference between the solubility in NaK-78 and in sodium is reasonable. However, the measurement technique gave less accurate results than those reported in Figs. 2.1 and 2.2, so that the derived value should be viewed primarily as an unconfirmed estimate of the solubility of argon in NaK-78.

(4) *Krypton.* Dhar's data [139] for the solubility of krypton in sodium in the temperature range 202 to 480°C (396 to 896°F) for only one pressure level, 18 to 19 psia, are described by the expression

$$\log S \text{ (mole Kr/mole Na/atm)} = -4.34 - \frac{3500}{T(^\circ\mathrm{K})} \qquad (2.6)$$

for which the ΔH (solution) is 16 kcal/mole of krypton. These data are also shown in Fig. 2.1.

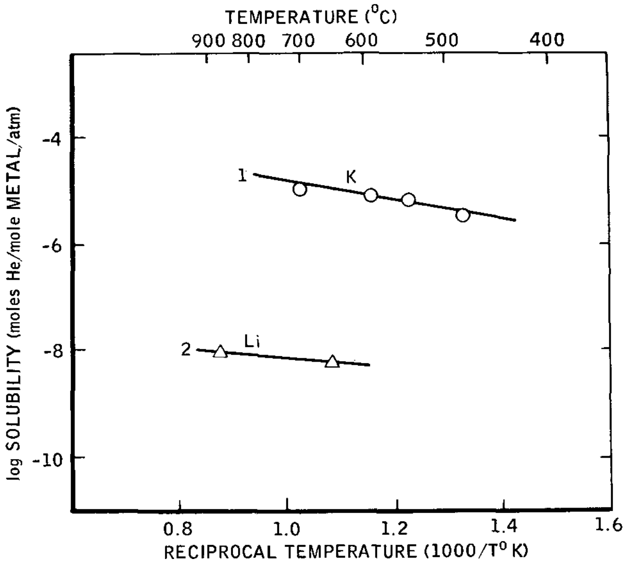

Fig. 2.2 Solubilities of helium in alkali metals. (Both curves 1 and 2 are from Ref. 140.)

(5) *Xenon.* Mitra [141], using a radioactive-tracer technique to measure the solubility of xenon in sodium at 1 atm, derived the following expression for the solubility:

$$\log S \text{ (mole Xe/mole Na)} = -3.248 - \frac{522}{T(^\circ\mathrm{K})} \qquad (2.7)$$

for which the ΔH (solution) is 2.4 kcal/mole. The curve, plotted in Fig. 2.1, is about four decades above the curves for argon and krypton in sodium. The temperature limitations in Eq. 2.7 are not noted in Mitra's abstract [141], but Yevick [144], who referred to Mitra's work, indicated that the data were taken at 100 to 200°C (212 to 392°F).

(6) *Helium Solubility in Lithium and in Potassium.* Slotnick *et al.* [140] measured the solubility of helium in potassium at temperatures from 482 to 704°C (900 to 1300°F) and at pressures from 1 to 3 atm, and the solubility of helium in lithium at temperatures from 649 to 871°C (1200 to 1600°F) at a pressure of 2.38 atm. In the former study the helium solubility was found to follow Henry's law. The data are described by the expressions

$$\log S \text{ (mole He/mole K/atm)} = -3.30 - \frac{1550}{T(^\circ\mathrm{K})} \qquad (2.8)$$

and

$$\log S \text{ (mole He/mole Li/atm)} = -7.33 - \frac{840}{T(^\circ\mathrm{K})} \qquad (2.9)$$

for which the ΔH (solution) values are 7.1 kcal/mole of helium and 3.85 kcal/mole of helium, respectively. The data are shown in Fig. 2.2.

(b) *Hydrogen*

The H-Na system has been investigated by many experimenters; Ref. 145

gives a good summary of the system. Hydrogen is soluble in sodium and in NaK and forms the compounds NaH and KH. In low concentrations hydrogen remains in solution in sodium (or NaK) and is in equilibrium with a partial pressure of hydrogen in the gas phase. At higher hydrogen concentrations and at moderate temperatures, two condensed phases exist, a hydrogen-saturated liquid-metal phase and a solid metal-saturated hydride phase. Finally, at hydrogen concentrations approaching 50 at.%, only a sodium-saturated solid solution of NaH exists at equilibrium with its decomposition pressure of hydrogen. The K-H system and, in essence, the (NaK-78)-H system behave similarly to the Na-H system.

Information on techniques of preparing alkali hydrides and on their chemical properties can be found in the works of Littlewood [146], Mellor [147, 148], Kirk and Othmer [149], and Sittig [150].

(1) *Sodium Hydride.* NaH has a ΔH_f^0 (298) of -13.490 kcal/mole and a ΔF_f^0 (298) of -8.023 kcal/mole [151]. These values were taken from the calorimetric measurements of Gunn and Green [152] and of Messer, Fasolino and Thalmayer [153]. Gunn and Green found the $\Delta H^\circ f$ (298) of NaD(sol) to be - 13.34 kcal/mole. These values of $\Delta H^\circ f$ (298) are considered more accurate than those determined by extrapolating (to 298°K) the high-temperature data obtained from equilibrium-hydrogen-dissociation pressures over NaH(sol) mixtures. Hérold, [154], measuring equilibrium hydrogen pressure over NaH in the temperature range 289 to 415°C (552 to 779°F), obtained the expression

$$\log P \text{ (torrs)} = 11.66 - \frac{6100}{T(°\text{K})} \qquad (2.10)$$

from which a ΔH_f value of -13.95 kcal/mole is calculated. The log P curve is plotted in Fig. 2.3.

Banus, McSharry, and Sullivan [155], measuring the dissociation pressure of hydrogen over NaH(sol) in the temperature range 500 to 600°C (932 to 1112°F), obtained the equilibrium-hydrogen-pressure expression

$$\log P \text{ (torrs)} = 10.49 - \frac{5070}{T(°\text{K})} \qquad (2.11)$$

from which a ΔH_f value of -11.61 kcal/mole is calculated. This log P curve is also plotted in Fig. 2.3.

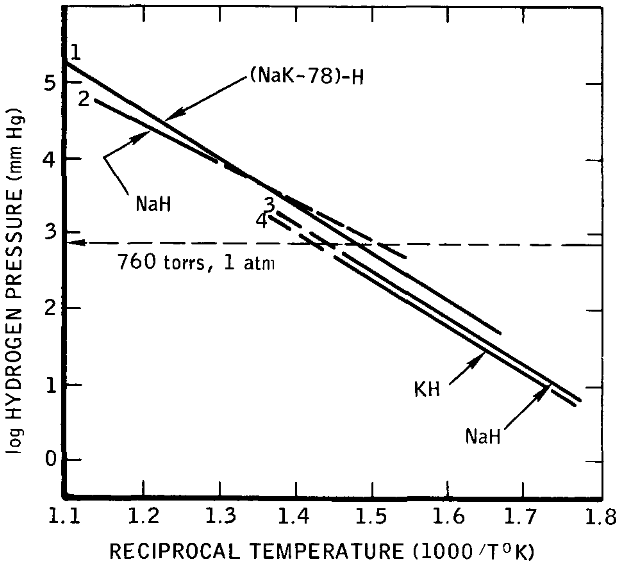

Fig. 2.3 Dissociation pressures of NaH, KH, and (NaK-78)-H. (Curve 1 is from Ref. 143; curve 2, from Ref. 155; and 154).

Extrapolations of the curves of Eqs. 2.10 and 2.11 to P = 760 torrs are shown in Fig. 2.3. The equation of Banus *et al.* [155] gives a temperature of 675°K (402°C, 756°F), and that of Hérold [154] gives 694°K (421°C, 790°F). The Joint Army-Navy-Air Force (JANAF) tables [151] quoted a decomposition temperature value of ~700°K (~427°C, ~801°F). Littlewood [146] gave a report and survey of early work on NaH.

(2) *Potassium Hydride.* The ΔH_f^0 (298) of KH(sol) is reported in the JANAF tables [151] as -13.819 kcal/mole, a value taken from the data of

Gunn and Green [152]. The value -15.16 kcal/mole reported by Messer *et al.* [153] was discounted. JANAF reported a ΔF_f^0 (298) value of -8.316 kcal/mole for KH(sol). Gunn and Green measured the ΔH_f^0 (298) of KD(sol) to be -13.238 kcal/mole.

Hérold [154] reported the dissociation pressure of KH(sol) in the temperature range 289 to 415°C (552 to 779°F),

$$\log P\ (\text{torrs}) = 11.69 - \frac{6175}{T(^\circ\text{K})} \qquad (2.12)$$

from which a ΔH_f value of -14.1 kcal/mole is calculated. The log P curve is plotted in Fig. 2.3. The temperature corresponding to P = 760 torrs is 701°K (428°C, 802°F), and that used in JANAF tables [151] is ~690°K (~417°C, ~783°F).

(3) *(NaK-78)-H System.* The reaction of hydrogen with NaK-78 has been investigated as a part of various SNAP programs. Savage *et al.* [143, 156, 157] reported the saturation pressure of hydrogen over NaK-78 in the temperature range 330 to 704°C (626 to 1299°F) as

$$\log P\ (\text{torrs}) = 12.14 - \frac{6280}{T(^\circ\text{K})} \qquad (2.13)$$

Equation 2.13, plotted in Fig. 2.3, falls near the NaH and KH curves. The ΔH_f value is -14.33 kcal/mole, which is similar to the values of Hérold [154] for NaH and KH.

(4) *Hydrogen Pressure-Composition Data for the Na-H System.* The pressure-composition isotherms of Addison, Pulham and Roy [158] for solutions of hydrogen in sodium at 250 to 330°C (482 to 626°F) are shown in Fig. 2.4.

McClure and Halsey [159] measured the pressure-composition relations at 260 to 350°C (500 to 662°F). The curvatures of their isotherms are different from those of all the other investigators of this system, and their data are therefore neglected in this review.

Results of the measurements of Banus *et al.* [155] of the hydrogen-dissociation pressures of Na-NaH mixtures at 500 to 600°C (932 to 1112°F) are shown in Figs. 2.5 and 2.6. A two-phase region occurs in the nominal 80 to 30% NaH range. Using these data, Banus *et al.* computed the constants for the equilibrium-dissociation-hydrogen pressures over NaH-Na mixtures given in Table 2.13.

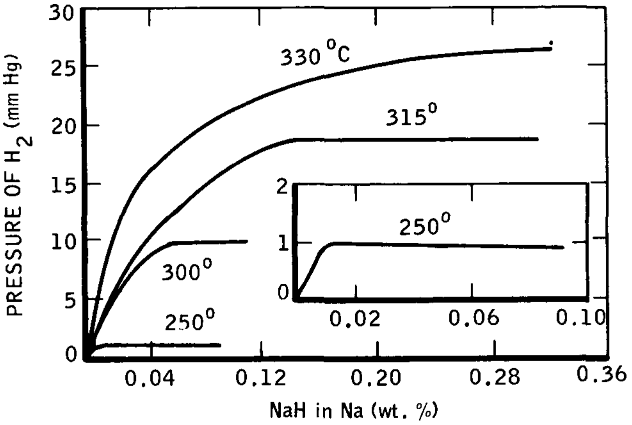

Fig. 2.4 Pressure-composition isotherms for solutions of hydrogen in liquid sodium.

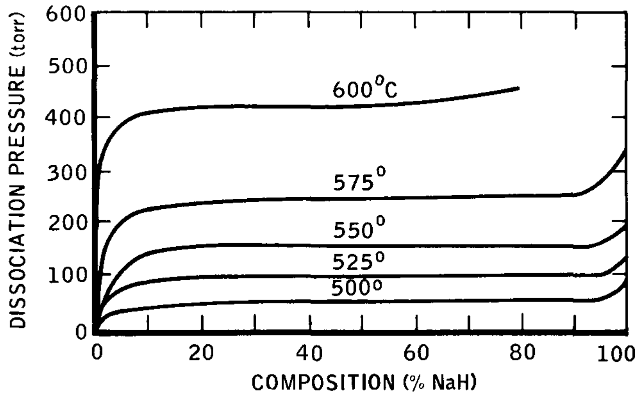

Fig. 2.5 Experimental isotherms.

(5) *Hydrogen-Pressure-Composition Data for (NaK-78)-H System.* Savage *et al.* [143] and Compere and Savolainen [160] reported results of the same study of the pressure and temperature dependence of the concentration of hydrogen in unsaturated NaK-78 as

$$\log \frac{S\ (\text{ppm H}_2)}{P_{\text{H}_2}^{\frac{1}{2}}\ (\text{atm})} = 2.06 + \frac{240}{T(^\circ\text{K})} \qquad (2.14)$$

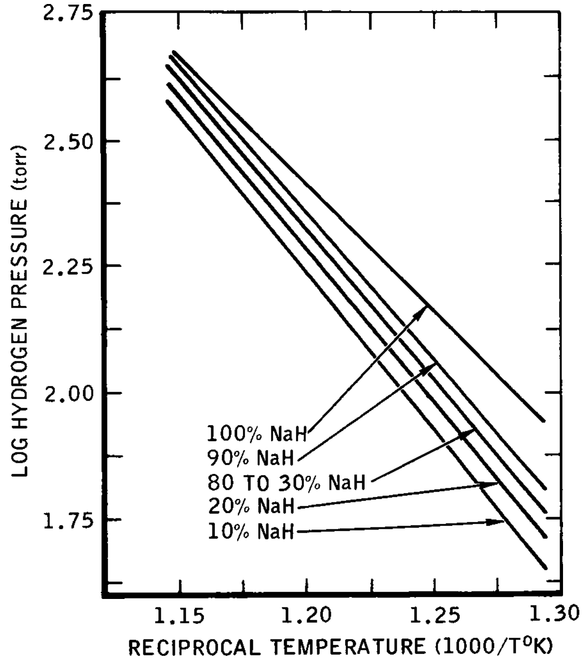

Fig. 2.6 Isocomposition curves.

TABLE 2.13 - Empirical Constants for the Integrated Clausius-Clapeyron Equation for NaH*

$$\left[\log P\ (\text{torrs}) = A - \frac{B}{T(^\circ\text{K})}\right]$$

NaH, %	*A*	*B*
100	10.49	5070
90	11.32	5806
80 to 30	11.47	5958
20	11.55	6058
10	11.70	6222

*From M.O. Banus, J.J. McSharry and E.A. Sullivan, The Sodium-Sodium Hydride-Hydrogen System at 500-600°C, *J. Amer. Chem. Soc.*, 77: 2007 (1955).

Equation 2.14 represents the results of measurements made at 330 to 704°C (626 to 1299°F) with hydrogen pressures from 4 to 727 torrs.

The experiments of Savage *et al.* [143] involved the transfer of hydrogen through a weld-sealed iron capsule containing the NaK-78. The amounts of hydrogen involved in the transfers into and out of the capsule were measured to obtain the data shown in Fig. 2.7. The slopes of the curves support the $P^{\frac{1}{2}}$ dependence shown in Eq. 2.14. The vertical breaks in the 300, 330, and 400°C curves correspond to the solubilities of hydrogen in NaK-78 at those temperatures.

(6) *Solubility of Hydrogen in Sodium.* Addison *et al.* [158] reported the saturation solubility of hydrogen in sodium at 250 to 330°C (482 to 626°F) to be represented by

$$\log S\ (\text{wt.\% H}) = 6.211 - \frac{5021}{T(^\circ\text{K})} \qquad (2.15)$$

This equation is plotted in Fig. 2.8, together with the data of Williams, Grand and Miller [161, 162] on the solubility of hydrogen (as NaH) in sodium in the temperature range 240 to 445°C (464 to 833°F). The curve suggested by Williams *et al.* has a slightly higher slope than that of Eq. 2.15. Addison *et al.* [158] compared the two sets of data and concluded that, because the low-temperature data of Williams *et al.* are subject to greater error than are the high-temperature data and because their low-temperature data fall on a continuous curve with the Williams high-temperature data, the best representation of all the findings is Eq. 2.15.

Table 2.14 shows the solubility data of these two sources converted to wt.% hydrogen.

In recent work at APDA [163], the solubility of hydrogen in sodium was reported to be 15 wppm (0.0015 wt.%) at 320°C (608°F), which is lower than the values reported in Table 2.14.

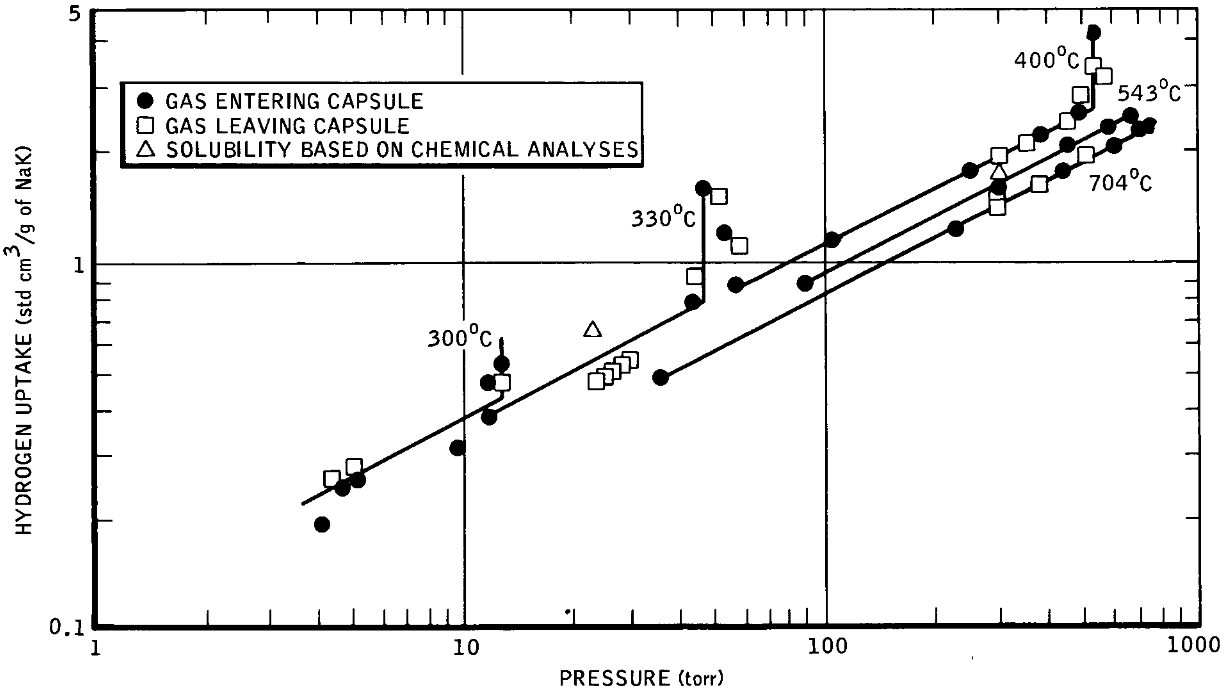

Fig. 2.7 Pressure-composition curves for hydrogen in NaK-78.

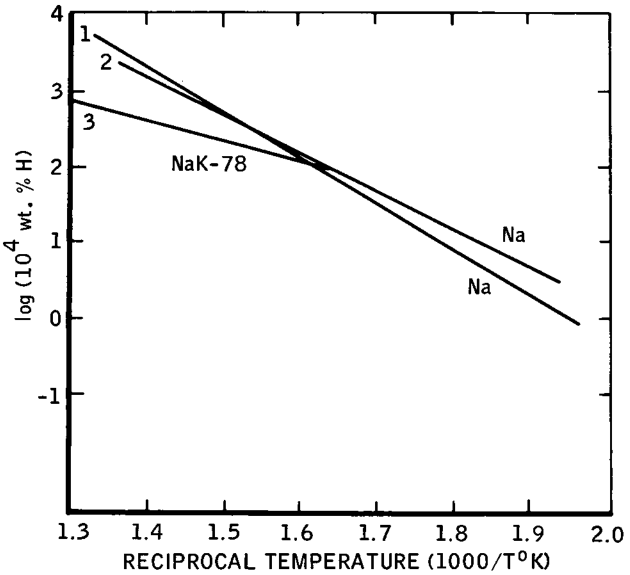

Fig. 2.8 Solubility of hydrogen in sodium and in NaK-78. (Curve 1 is from Ref. 161; curve 2, from Ref. 158; and curve 3, from Ref. 143.)

TABLE 2.14 - Solubility of Hydrogen in Sodium

Temperature		Solubility, wt.% H	
°C	°F	Ref. 158	Refs. 161, 162
250	482	0.00042	0.00021
300	572	0.0022	0.00167
315	599	0.0052	
330	626	0.0104	
350	662		0.0125
400	752		0.0605
445	833		0.1785

(7) *Solubility of Hydrogen in NaK-78.* Savage *et al.* [143] and Compère and Savolainen [160] reported results of the same study of the solubility of hydrogen in NaK-78 at 330 to 704°C (626 to 1299°F):

$$\log S\ (\text{wt.\% H}) = 2.69 - \frac{2900}{T(°\text{K})} \qquad (2.16)$$

The fact that the curve for NaK-78 in Fig. 2.8 has a substantially lower slope than curves for sodium is noted by the authors, but no explanation is offered.

Savage *et al.* [143] also discussed the behavior of hydrogen in NaK-78 to which 1 to 4 wt.% lithium was added to act as a soluble getter.

(c) *Group IA Metals - Li, K, Rb, Cs*

(1) *Lithium.* The Na-Li system was recently studied by Kanda and coworkers [164, 165] using a novel liquid-density method of measuring miscibility limits. Their data are in general agreement with those of Howland and Epstein [166], whose phase diagram was reproduced in the compilation of Elliott [167], and with those of Salmon and Ahmann [168] as reported by Hansen and Anderko [169]. The phase diagram shown in Fig. 2.9 is a composite of the diagrams given by Kanda *et al.* and by Elliott. The principal change from that given by Elliott is that the consolute temperature of 306 ± 1°C determined by Kanda *et al.* [164] is used (that shown by Elliott was 442 ± 10°C).

(2) *Potassium.* The Na-K system was studied by MacDonald, Pearson, and Towle [170], Orton, Shaw, and Williams [171], Rinck [172], and others (see Hansen and Anderko [169] for additional references). Early workers did not find the solid solutions noted by MacDonald *et al.* (see Fig. 2.10), who used a resistivity measurement for alloys isothermally at equilibrium. The diagram shown by Hansen and Anderko is similar except for minor changes in the peritectic and eutectic temperatures and the presence of the solid solutions. This earlier diagram was taken primarily from the thermal analysis work of Rinck.

Gingrich and Henderson [173], examining the liquid alloys for molecules in the liquid, concluded that no permanent compounds exist. This conclusion is supported by the work of Orton *et al.* [171] who used a monochromatic X-ray beam in a focusing Geiger diffractometer as a search tool.

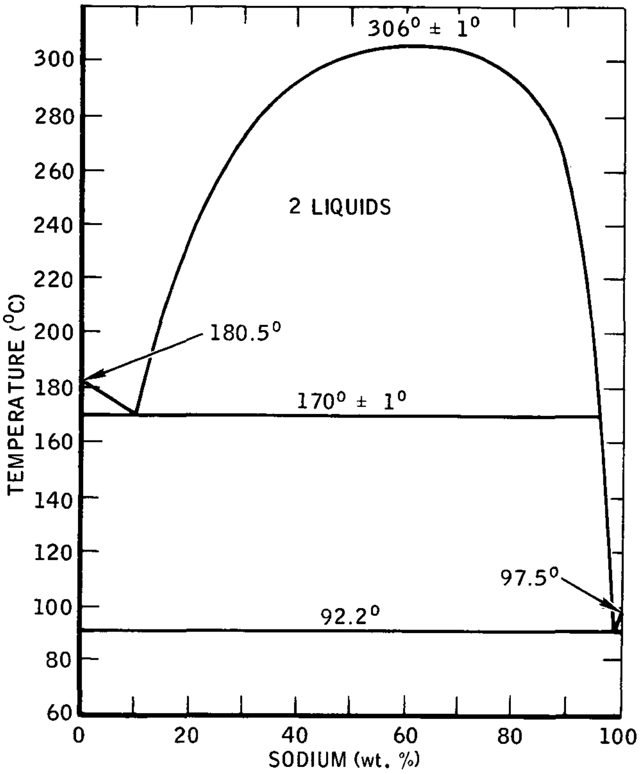

Fig 2.9 Sodium-lithium system.

The existence of the compound Na_2K

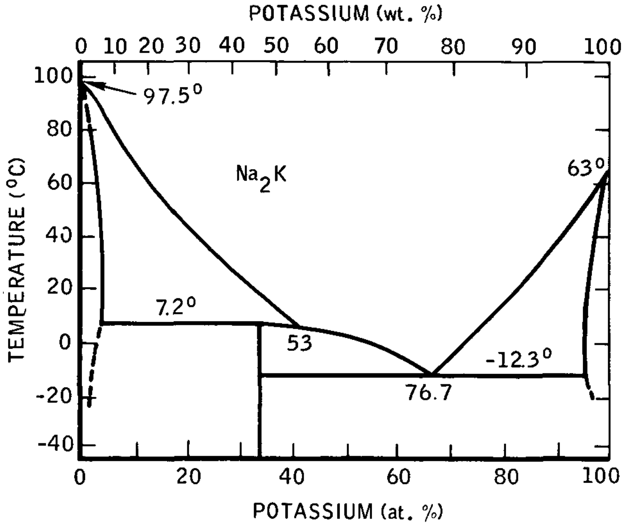

Fig. 2.10 Sodium-potassium system.

TABLE 2.15 - Heats of Formation of Na-K Alloys*

Ref.	Temp., (°C)	66.6 at.% Na (Na_2K)	50 at.% Na	33.3 at.% Na
175	18	+2.93	+0.14	-1.94
176	110	+0.10	+0.09	+0.11
177	25	+2.14 ± 0.1	+1.43 ± 0.1	+2.13 ± 0.1
	110	+0.53 ± 0.1	+0.36 ± 0.1	+0.53 ± 0.1

*ΔH_f^0 in kcal/gram mole of composition shown.

was first established by Van Bleiswijk [174]. Its heat of formation was studied by Joannis [175], Kawakami [176], and McKisson and Bromley [177]. The results of investigations of other compositions in the Na-K system are given in Table 2.15. The values given by McKisson and Bromley are recommended.

(3) *Rubidium.* The Na-Rb system was investigated by Rinck [178], Goria [179], and Böhm and Klemm [180]. The diagram shown in Fig. 2.11 was prepared by Hansen and Anderko [169] from the data of Rinck and of Goria, which are quite consistent. Also, the data of Böhm and Klemm are in good agreement with the diagram.

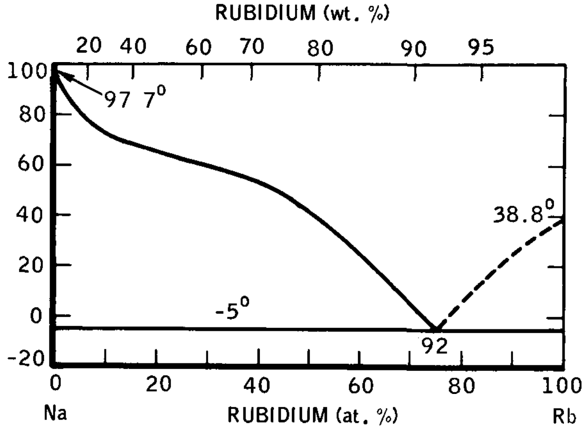

Fig. 2.11 Sodium-rubidium system. (From M. Hansen and K. Anderko, *Constitution of Binary Alloys*, p. 1001. McGraw-Hill Book Company, Inc., New York, 1958.)

Tepper, King, and Greer [181] studied low-melting ternary alloys of the alkali metals and determined that the lowest melting alloy in the Na-K-Rb system melts at -25°C (-13°F). The composition of this alloy is not given, however.

(4) *Cesium.* The Na-Cs system was studied by Rinck [182] and by Goria [183] using a thermal-arrest technique. One compound, Na_2Cs, which decomposes peritectically at -8°C, was identified by both investigators and by Böhm and Klemm [180], who used a magnetic measurement. The diagram shown in Fig. 2.12 was developed.

Tepper *et al.* [181] studied the low-melting ternary alloys of the alkali metals and determined the liquidus curves for the Na-K-Cs system shown in Fig. 2.13. The ternary eutectic is at 13.5 wt.% Na, 46.5 wt.% K, and 40 wt.% Cs, with a melting point of -79°C (-110°F).

(d) *Group IB Metals - Cu, Ag, and Au*

(1) *Copper.* Hansen and Anderko [169] reported the conclusion of Zintl, Goubeau, and Dullenkopf [184] that there are no Na-Cu compounds. The examination of Zintl *et al.* consisted of titrating a solution of sodium in ammonia with a solution of cuprous iodide in ammonia, with a potentiometric detection method.

The solubility of copper in sodium was measured by Eichelberger and

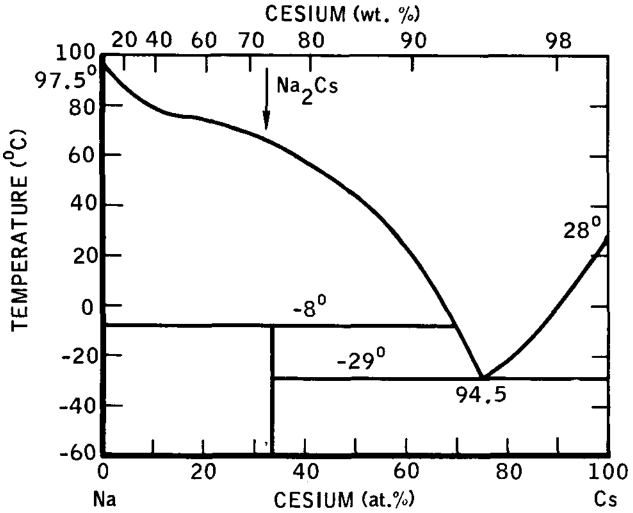

Fig. 2.12 - Sodium cesium system. (From M. Hansen and K. Anderko, *Constitution of Binary Alloys*, 578. McGraw-Hill Book Company, Inc., New York, 1958.)

McKisson [185] in the temperature range 250 to 726°C (482 to 1339°F) using a capsule technique. However, because their data taken at 250 to 350°C showed a large amount of scatter, they concluded that the low-temperature data were not reliable and used only the data taken above 350°C for their analysis. Singer and Becker [186] measured the solubility at 255 to 547°C (491 to 1017°F) using a dip-cup technique, and Humphreys [187] measured the solubility at 500 to 700°C (932 to 1292°F) using a radioactive-tracer technique. The results of all three investigations are in very good agreement as is shown in Fig. 2.14. The expression describing the composite solubility curve [185] is

$$\log S\ (\text{wppm Cu}) = 5.957 - \frac{3431}{T(°\text{K})} \quad (2.17)$$

Walker, Pratt and Mott [188] also measured the solubility of copper in sodium in the temperature range 222 to 640°C (432 to 1184°F) using a dip-cup sampling technique. Their results lie above those described by Eq. 2.17 and have a ΔH (solution) of 9.24 kcal/gram atom of copper.

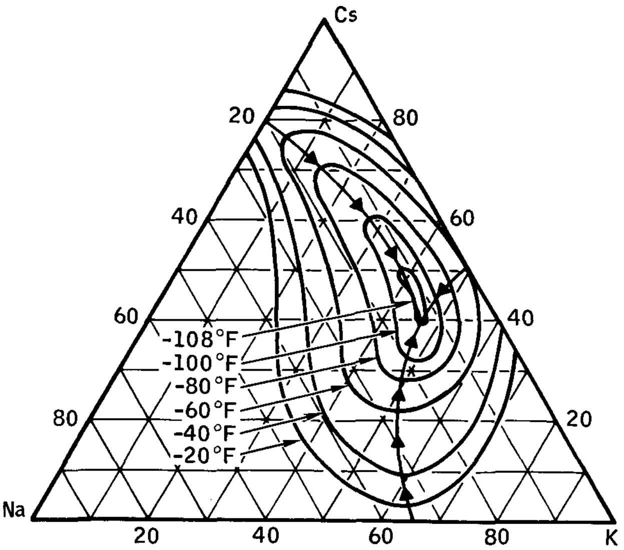

Fig. 2.13 Sodium-potassium-cesium system.

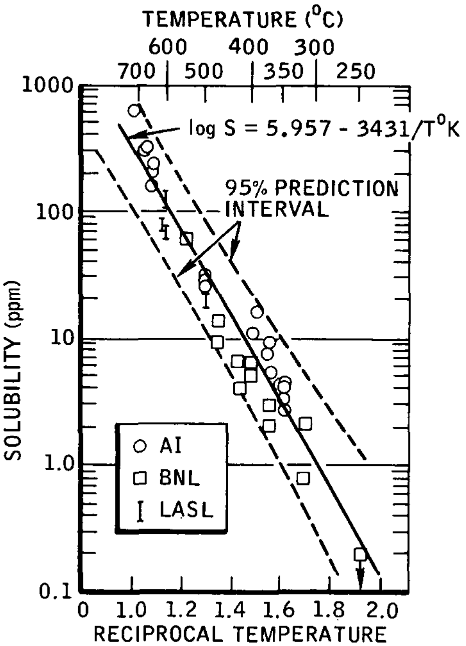

Fig. 2.14 Solubility if copper in sodium.

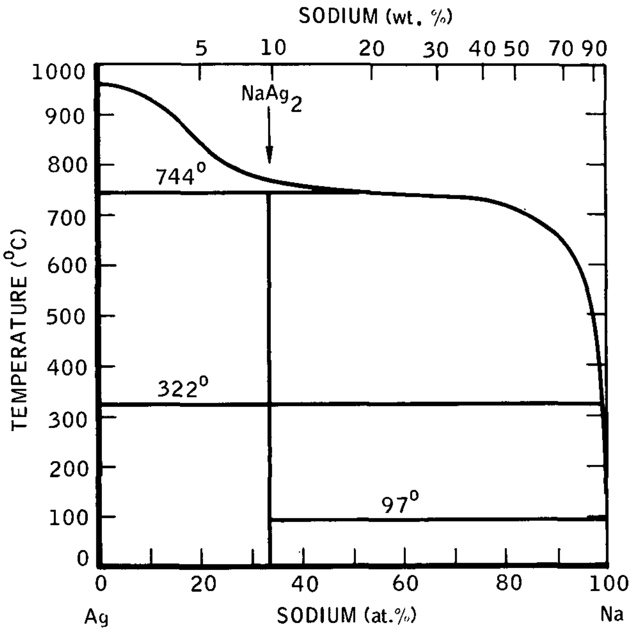

Fig. 2.15 Sodium-silver system.

$$\log X\ (\text{at.\% Cu}) = -0.5173 - \frac{2018.7}{T(°\text{K})} \tag{2.17a}$$

(2) *Silver.* In a study of the Na-Ag system, Kienast and Verma [189] first showed the existence of the compound $NaAg_2$, which is thought to decompose peritectically at 744°C and to have a phase transformation at 322°C. The phase diagram incorporating these findings is shown in Fig. 2.15. The liquidus given by Hansen and Anderko [191], and derived from the data of Quercigh and Bruni [190] and Mathewson [191], is substantially the same as that given in the figure.

The solubility of silver in sodium was determined by researchers at BNL [192]. Their data are fitted by the expression

$$\log S\ (\text{wppm Ag}) = 7.248 - \frac{1493}{T(°\text{K})} \tag{2.18}$$

at 100 to 500°C (212 to 932°F).

Lamprecht [193] measured the solubility of silver in sodium and reported his results in the form of an equation,

$$\log X\ (\text{atom fraction Ag}) = 0.899 - \frac{1642}{T(°\text{K})} \tag{2.19}$$

(3) *Gold.* The data of Kienast and Verma [189] for the Na-Au system showed the presence of three intermetallic compounds, Na_2Au, NaAu, and $NaAu_2$. The third, $NaAu_2$, is congruent melting at 1005°C, but the others decompose peritectically as shown in Fig. 2.16, taken from Elliott [167]. This work resolved the uncertainties shown in the diagram presented by Hansen and Anderko [169].

The liquidus in the temperature range 100 to 600°C (212 to 1112°F) is described by

$$S\ (\text{wt.\% Au}) = -11 + 0.52t - 6 \times 10^{-4}\ t^2\ (°\text{C}) \tag{2.20}$$

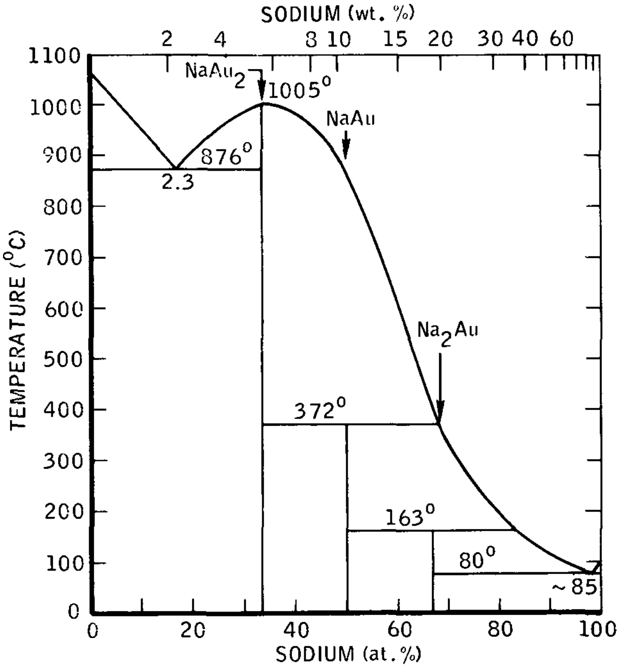

Fig. 2.16 Sodium-gold system. (From R.P. Elliot, *Constitution of Binary Alloys, First Supplement*, 96. McGraw Hill Book Company, Inc., New York, 1965.)

(e) *Group IIA Metals - Be, Mg, Ca, Sr, and Ba*

(1) *Beryllium.* No equilibrium data on the Na-Be system were found. Bett and Draycott [194] reporting on a compatibility study of beryllium in NaK containing oxygen, quoted corrosion rates and noted that the beryllium oxide product does not adhere to the beryllium metal, so that in heavily contaminated sodium very significant losses of beryllium were observed. Stang *et al.* [195] summarized the corrosion and mechanical-property effects on beryllium exposed to static and flowing sodium and NaK.

(2) *Magnesium.* The Na-Mg system was studied by Mathewson [196]. The diagram shown in Fig. 2.17 is taken from his data and from the compilation of Hansen and Anderko [169]. The following expression for the solubility of magnesium in sodium was determined by curve-fitting the estimated liquidus curve in the temperature range 97.5 to 638°C (208 to 1180°F)

$$S\ (\text{wt.\% Mg}) = -0.1414 + 1.248 \times 10^{-3}t + 2.08 \times 10^{-6}t^2\ (^\circ\text{C}) \qquad (2.21)$$

Any values calculated from Eq. 2.21 should be used as estimates only.

(3) *Calcium.* The Na-Ca system was studied by Rinck [197] using thermal analysis and metal-salt equilibration. Hansen and Anderko [169] used his results in their diagram (Fig. 2.18). Lorenz and Winzer [198] also measured the locations of the boundaries of the miscibility gap using metal-salt equilibria in the system Na-Ca-Cl.

An expression for the Na-Ca liquidus (the solubility of calcium in sodium) is given by Jackson [199]:

$$\log S\ (\text{wt.\% Ca}) = 2.5629 - \frac{1545.6}{T(^\circ\text{K})} \qquad (2.22)$$

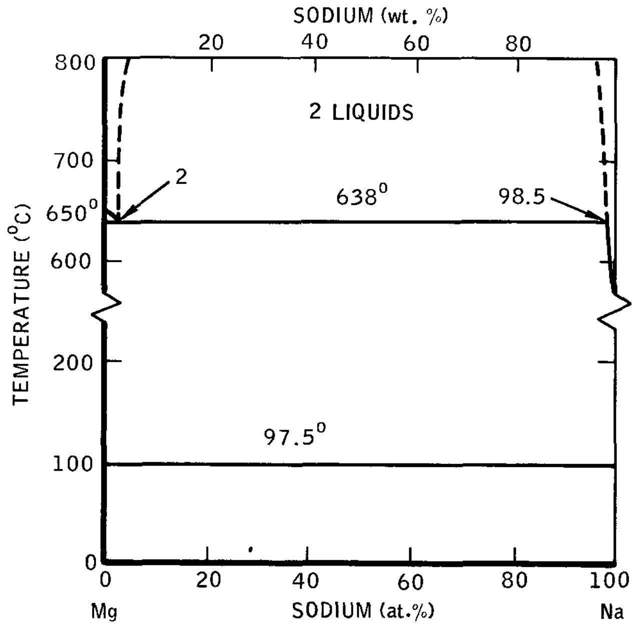

Fig. 2.17 Sodium-magnesium system. (From M. Hansen and K. Anderko, *Constitution of Binary Alloys*, 909. McGraw-Hill Book Company, Inc., New York 1958.)

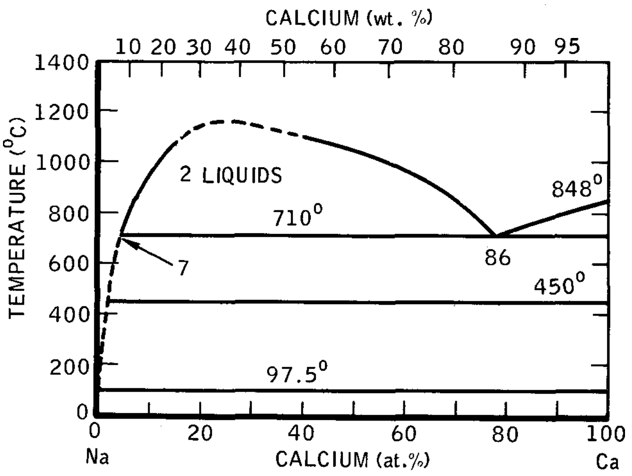

Fig. 2.18 Sodium-calcium system. (From M. Hansen and K. Anderko, *Constitution of Binary Alloys*, 404. McGraw-Hill Book Company, Inc., New York, 1958.)

(4) *Strontium.* Remy, Wolfrum, and Haase [200], reported the simple eutectic diagram shown in Fig. 2.19 for the Na-Sr system. It was also shown by Elliott [169]. No compounds and no solid solubility were found. Kanda and Keller [201], using thermal analysis, differential thermal analysis, high-temperature densitometry, and X-ray analysis to study the system, reported the tentative diagram shown in Fig. 2.20. No compounds are evident. The liquidus shows a more convex curvature than that of Fig. 2.19, and more detail is shown in the strontium-rich end of the diagram.

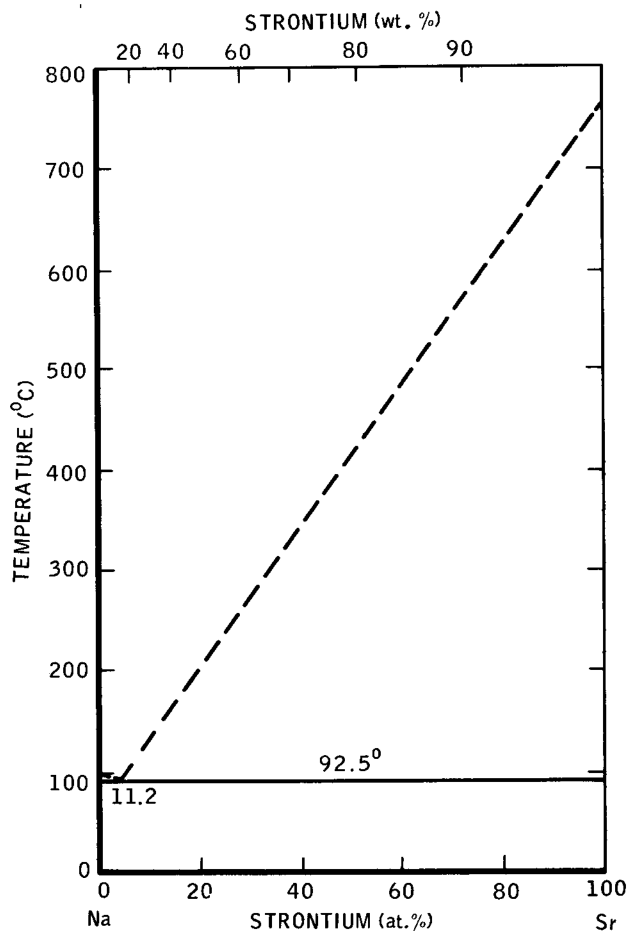

Fig. 2.19 Sodium-strontium system. (From R.P. Elliott, *Constitution of Binary Alloys, First Supplement*, 651. McGraw-Hill Book Company, Inc., New York, 1965.)

Kanda [202] indicated that the eutectoid region shown in dashed lines is quite tentative and is based on an interpretation of some weak X-ray lines. Additional work will be required to confirm its existence.

(5) *Barium.* The Na-Ba system was studied by Remy *et al.* [200], Kanda and Keller [201], Kanda and King [203], Kanda, Stevens and Keller [204], and Gould [205]. The results of these experiments are not consistent. Elliott [169], using the data of Remy *et al.* as most probably correct, derived the diagram shown in Fig. 2.21. According to Remy *et al.*, three congruent melting compounds $Na_{12}Ba$, Na_6Ba, and NaBa are formed in the system. The third, NaBa, is shown to be rather high melting, 510°C (950°F).

Kanda *et al.* [201, 204], on the other hand, did not find NaBa to be congruent melting, but instead found the compound to decompose peritectically at 197°C (387°F). They reported the existence of the compound Na_4Ba, but neither Na_6Ba nor $Na_{12}Ba$ was found (see their phase diagram in Fig. 2.22). Since the work of Kanda *et al.* was done

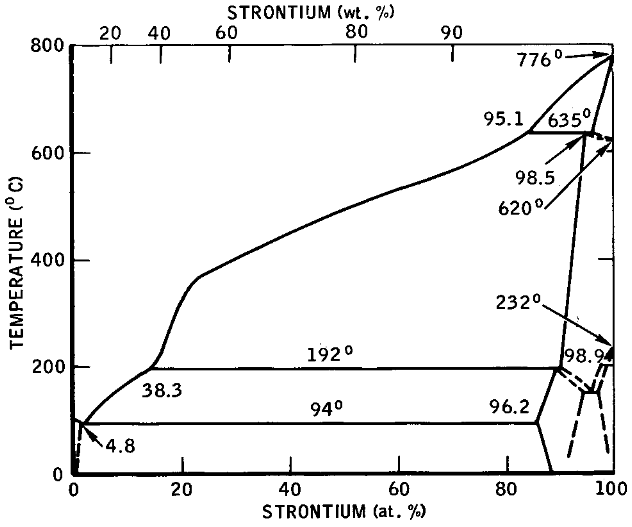

Fig. 2.20 Sodium-strontium system [201].

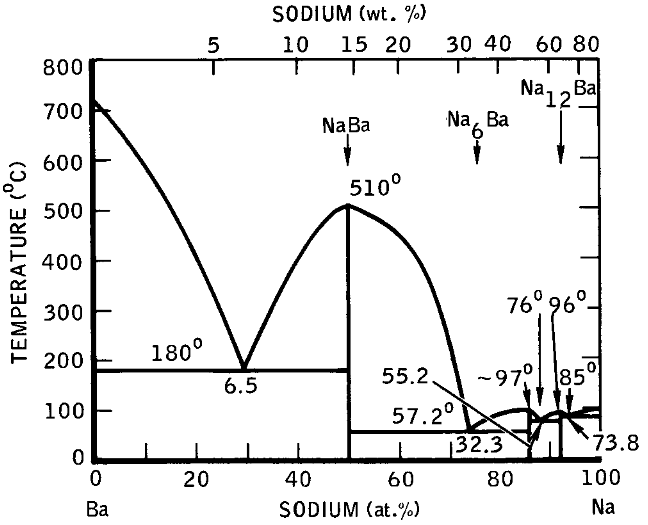

Fig. 2.21 - Sodium-barium system. (From R.P. Elliott, *Constitution of Binary Alloys, First Supplement*, 152. McGraw-Hill Book Company, Inc., New York, 1958.)

with great care on pure materials, it is difficult to understand how the compound NaBa could melt congruently at 510°C and not be observed. Therefore their phase diagram is recommended.

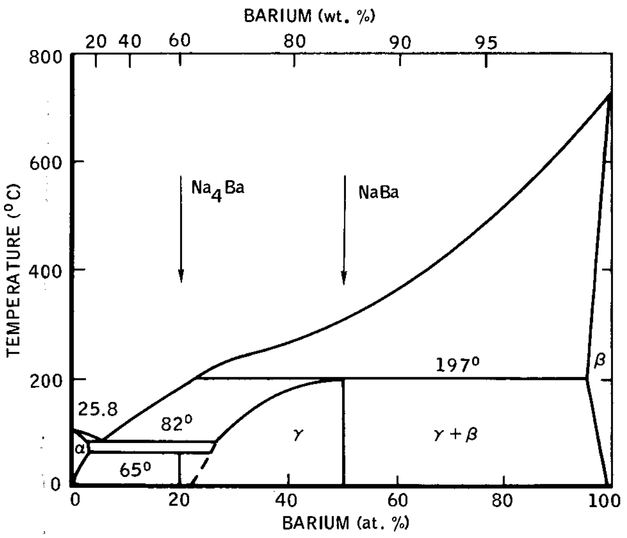

Fig. 2.22 - Sodium-barium system [201, 204].

(f) *Group IIB Metals - Zn, Cd, and Hg*

(1) *Zinc.* The Na-Zn system was studied by Häusler [206], and earlier by Mathewson [207], Zintl, Goubeau, and Dullenkopf [208] and Zintl and Haucke [209]. One compound, established as $NaZn_{13}$ by Zintl and Haucke [209], exists, but the principal feature of the system is the presence of two liquid phases in the temperature range above 557°C. There is generally good agreement among the reports, although a compound, $NaZn_4$, reported by Kraus and Kurtz [210] and Burgess and Rose [211] to form in ammonia solutions was not confirmed by the other experimenters. Figure 2.23 shows the diagram presented by Hansen and Anderko [169].

Lamprecht, [193] measuring the solubility of zinc in sodium in the temperature interval 100 to 300°C (212 to 572°F), reported his results as

$$\log X \text{ (mole fraction Zn)} = 0.998 - \frac{2562}{T(°\text{K})} \qquad (2.23)$$

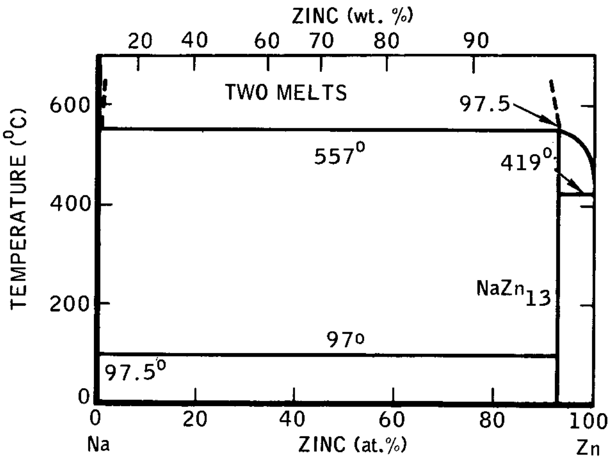

Fig. 2.23 - Sodium-zinc system. (From M. Hansen and K. Anderko, *Constitution of Binary Alloys*, 1010. McGraw-Hill Book Company, Inc., New York, 1958.)

(2) *Cadmium.* The Na-Cd system was studied by several authors [212-216] using thermal analysis. The existence of the compound $NaCd_2$ is confirmed by all, but there was some doubt regarding the composition of the $NaCd_6$ compound [169]. Allaria [215] established that this compound has a range of composition, as was suggested by Kurnakow and Kusnetzow [212, 213].

In Mathewson's [214] diagram a two-liquid-phase region was proposed, but the evidence is weak, and the phase diagram shown in Fig. 2.24 is the best available.

The heat of formation of $NaCd_2$ was measured by Seith and Kubaschewski [217], Biltz and Haase [218], and Roos [219]. The first two experiments are in good agreement, ΔH_f^0 (298) $\doteq$ -8.1 kcal/mole for $NaCd_2$. Seith and Kubaschewski [217] also reported the $\Delta H^o f$ (298) value for $NaCd_6$ as -12.6 kcal/mole.

Weeks and Davies [216] measured the solubility of cadmium in sodium at 0 to 15 at.% cadmium using a crucible containing the solution and a dip-cup sampling technique. Hot-trapped sodium was used to minimize any interference in the results from the oxygen content of the sodium. The solubility curve in the temperature range 100 to 210°C is described by the expression

$$\log S \text{ (wt.\% Cd)} = 3.101 - \frac{970}{T(°\text{K})} \qquad (2.24)$$

These values are lower than those of earlier experiments, and the authors suggested that their technique is less susceptible to subcooling effects than is the thermal-arrest method.

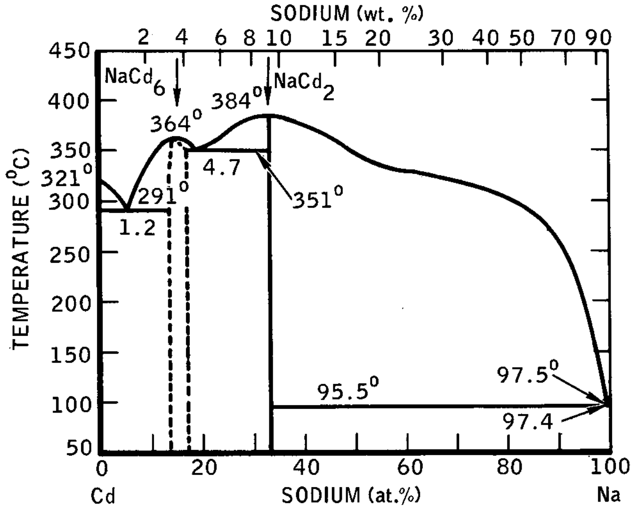

Fig. 2.24 Sodium-cadmium system. (From M. Hansen and K. Anderko, *Constitution of Binary Alloys*, 430. McGraw-Hill Book Co., Inc., New York, 1958.)

(3) *Mercury.* The Na-Hg system has been studied rather extensively. Figure 2.25, from Hansen and Anderko [169], was based primarily on the work of Kurnakow [220], Schüller [221], and Vanstone [222]. Seven intermetallic compounds have been identified: $NaHg_4$, $NaHg_2$, Na_7Hg_8, NaHg, Na_3Hg_2, Na_5Hg_2, and Na_3Hg.

Although the thermal-analysis data did not confirm the presence of the compound Na_3Hg, its existence was established by Klemm and Hauschulz [223] using magnetic-susceptibility measurements.

The data of several researchers on the heats of formation of the Na-Hg compounds are summarized in Table 2.16, and the recommended values are indicated.

(g) *Group IIIA Elements - B, Al, Ga, In, and Tl*

(1) *Boron.* Moissan [226] reported that boron does not dissolve in boiling sodium [167]. Hagenmuller *et al.* [227] reported that the compound NaB_6 is formed from the elements at 900°C (1652°F). No solubility data were found.

(2) *Aluminum.* The Al-Na system consists primarily of a two-liquid-phase field above the melting point of aluminum [228, 229]. This is confirmed by Fink, Willey, and Stumpf [230], who established the monotectic composition at 0.18 wt.% sodium at 659°C (1218°F). The diagram shown in Fig. 2.26 is from Hansen and Anderko [169].

The data of Brush [231] for the solubility of aluminum in sodium at

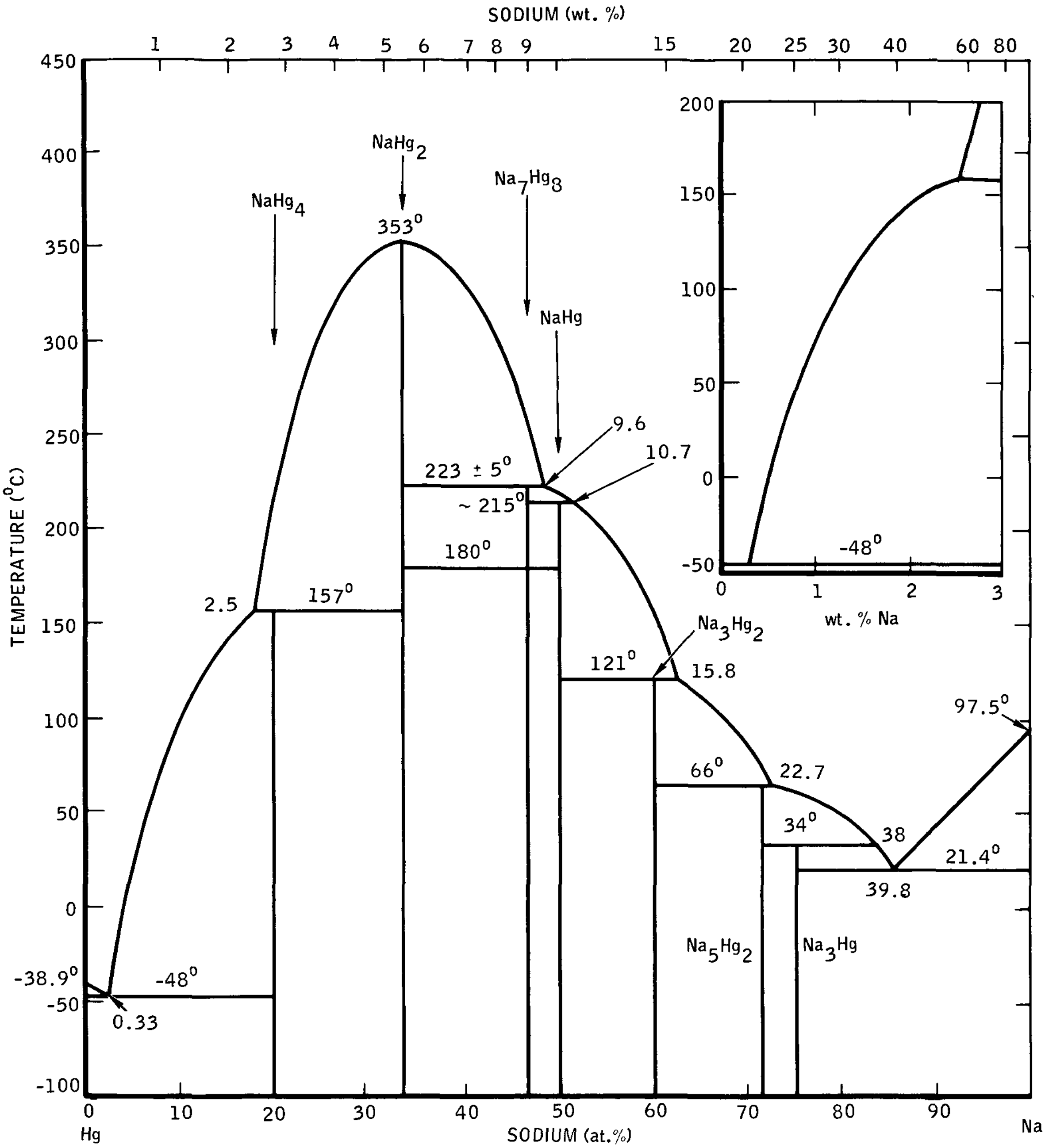

Fig. 2.25 - Sodium-mercury system. (From M. Hansen and K. Anderko, *Constitution of Binary Alloys*, McGraw-Hill Book Company, Inc., New York, 1958.)

150 to 500°C (302 to 932°F) show some scatter and are best represented by

$$S \text{ (wppm Al)} = 1.4 + 0.057t \text{ (°C)} \quad (2.25)$$

Scheuer [232] found the solubility of sodium in liquid aluminum to increase from 0.1 wt.% at 700°C (1292°F) to 0.13 wt.% at 800°C (1472°F). Ransley and Neufeld [233] found it to be 0.14 wt.% at the monotectic and to rise to 0.25 wt.% at 775°C (1427°F).

The solubility of sodium in solid

TABLE 2.16 - Heats of Formation of Na-Hg Compounds

Compound	ΔH_f^0 (298), kcal/mole	Ref.	Recommended value, kcal/mole
Na_3Hg	-11.6	224	-11.6
	-9.3	225	
	-12.9	218	
Na_3Hg_2	-20.7	225	-21.5
	-22.5	224	
NaHg	-5.7	225	-5.7
Na_7Hg_8	-84.4	225	-84.4
$NaHg_2$	-18.7	225	-18.7
	-18.0	224	
$NaHg_4$	-22.4	225	-21
	-19.5	224	

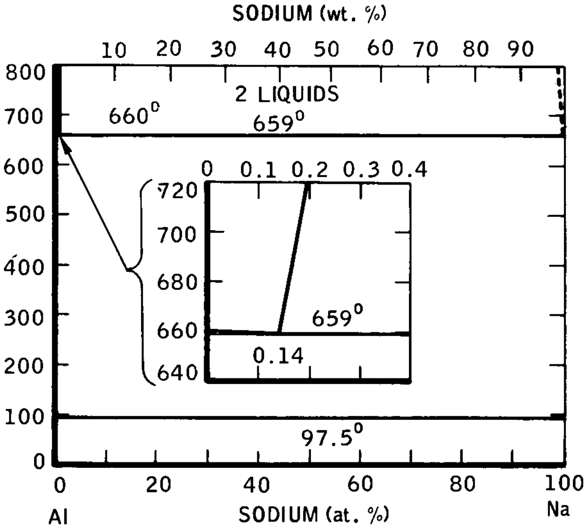

Fig. 2.26 Sodium-aluminum system. (From M. Hansen and K. Anderko, *Constitution of Binary Alloys*, 117. McGraw-Hill Book Company, Inc., New York, 1958.)

aluminum is reported as <0.003 wt.% at 659°C (1218°F) and decreases to 0.002 wt.% at 550 to 650°C (1022 to 1202°F) [169].

(3) *Gallium.* Feschotte and Rinck [234] developed the phase diagram for the Na-Ga system. In a later study they showed the peritectic compound previously shown as $NaGa_3$ to be $NaGa_4$. The composition of the compound Na_5Ga_8 was confirmed within 0.2 at.% by resistivity methods, and a minor change in the gallium-rich eutectic from 30 to 29.75°C (85.5°F) was found [236]. The phase diagram shown in Fig. 2.27 is a composite of their data.

Results of measurements of the solubility of gallium in sodium by chemical analysis of equilibrated mixtures [237, 238] are: 500°C (932°F), 3.0 at.%; 450°C (842°F), 1.2 at.%; 300°C (572°F), 0.13 at.%; 200°C (392°F), 0.05 at.%; and 98°C (208°F), 0.015 at.%. An expression that fits these data in the temperature range 100 to 300°C (212 to 572°F) is

$$\log X \text{ (at.\% Ga)} = 0.867 - \frac{1010}{T(°K)} \qquad (2.26)$$

(4) *Indium.* The Na-In system has been examined, but the phase relations are not yet clearly defined. Heycock

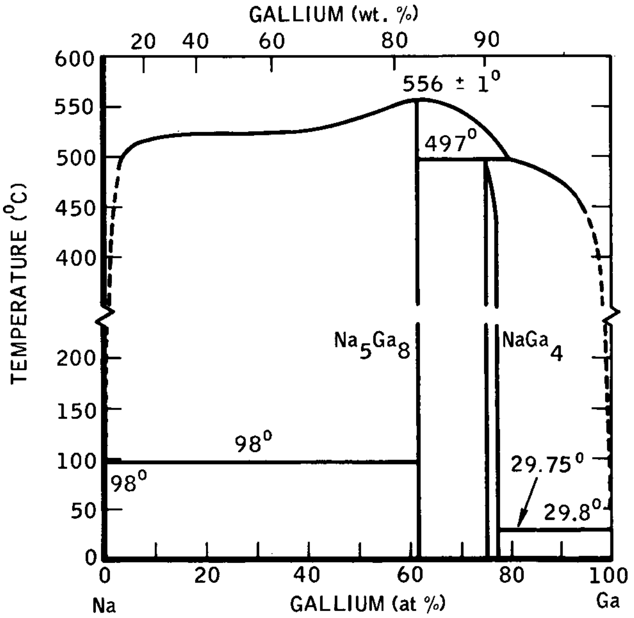

Fig. 2.27 Sodium-gallium system.

and Neville [239], investigating sodium-rich compositions, found a eutectic at 96.0 to 96.2°C for 1.2 to 2.0 wt.% (0.28 to 0.45 at.%) indium.

The compound NaIn was identified by Zintl and Neumayr [240]. Heberlein [241] studied the system at 50 at.% sodium, but his results are not accurate [169]. A liquidus temperature of 420°C (788°F) was found at 30 to 50 at.% sodium.

Davies [242], determining the solubility of indium in sodium in the temperature range 100 to 300°C (212 to 572°F), found the sodium-rich eutectic temperature to be 94.9°C. An extrapolation of his solubility data indicates that the eutectic composition is about 0.25 at.% (1.236 wt.%) indium. The solubility curve is represented by

$$\log X \text{ (atom fraction In)} = 1.89 - \frac{1620}{T(°\text{K})} \qquad (2.27)$$

Lamprecht's results [195] for the solubility of indium in sodium are described by

$$\log X \text{ (atom fraction In)} = 1.939 - \frac{1597}{T(°\text{K})} \qquad (2.28)$$

(5) *Thallium.* The Na-Tl system was extensively studied by Grube and Schmidt [243] using thermal and electrical-resistance techniques. The liquidus curve agreed well with that of earlier workers [169]. The intermetallic phases found were Na_6Tl, Na_2Tl, NaTl, and $NaTl_2$, as shown in Fig. 2.28.

The heat of formation of NaTl was determined by Kubaschewski [244] to be -9.0 ± 0.6 kcal/mole.

(h) *Group IIIB Metals - Sc, Y, and La*

(1) *Scandium.* No report of studies of the Na-Sc system was found.

(2) *Yttrium.* No report of studies of the Na-Y system was found.

(3) *Lanthanum.* Mässenhausen's [245] attempted study of the Na-La system by a thermal-analysis technique was unsuccessful because of experimental difficulties [169].

(i) *Sixth-Period Rare-Earth Metals - Ce, Pr, and Others*

(1) *Cerium.* No report of studies of the Na-Ce system was found other than the solubility measurements of Lamprecht [193], who found the solubility to be quite low and to decrease as the temperature increased. The temperature dependence is therefore very much in doubt, but the level of solubility may be correct at $\sim 10^{-8}$ mole fraction of cerium or $\sim$0.06 wppm at 100 to 300°C.

(2) *Praseodymium and Others.* No report of studies of systems of sodium and these sixth-period rare earths was found.

(j) *Seventh-Period Rare-Earth Metals - Th, Pa, U, and Pu*

(1) *Thorium.* Grube and Botzenhardt [246], using the thermal-analysis technique to study the Na-Th system, reported a phase diagram showing the compound Na_4Th. The diagram was disputed by L.R. Kelman, who was quoted by Hansen and Anderko [169] as having observed that thorium is not attacked by sodium at temperatures up to 800°C (1472°F), but the supporting details for his statement are not known. The diagram of Grube and Botzenhardt is not shown since observations by other experimenters indicate that it may be erroneous.

Bett and Draycott [194] studied the use of thorium as an oxygen getter in sodium and reported weight-change data for thorium tabs in contaminated sodium. The oxide product was found to be adherent.

Pearlman [247] reported static-corrosion data for thorium exposed to sodium and NaK containing 200 to 250 ppm oxygen at 750°C (1382°F) for 720 hr. Weight gains of 2 mg/cm^2/month were found. At 611°C (1132°F) a weight gain of 4.5 mg/cm^2/month was found in 144 hr. These data are also reported

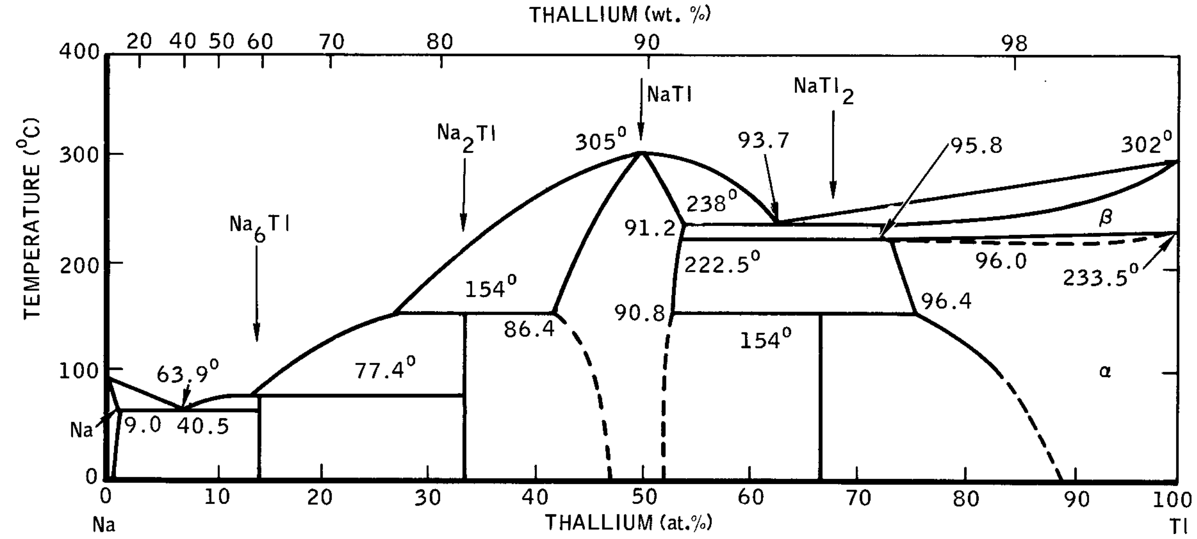

Fig. 2.28 - Sodium-thallium system. (From M. Hansen and K. Anderko, *Constitution of Binary Alloys*, McGraw-Hill Book Company, Inc., New York, 1958.

in the summary by Stang *et al.* [195].

(2) *Protactinium.* No report of studies of the Na-Pa system was found.

(3) *Uranium.* The Na-U system was examined by Foote, [248] who reported that massive uranium is not appreciably attacked by liquid sodium at 500°C (932°F). Katz and Rabinowitch [249] also reported Foote's experience.

Douglas, [250] measuring the solubility of uranium in sodium at 97.8°C using a cryoscopic technique, concluded, "... not more than a very few hundredths of one percent by weight of uranium dissolves in liquid sodium at 97.8°C. The actual solubility may be many times smaller than this." The melting-point depression of sodium, which is due to its saturation with uranium, is 0.001 to 0.003°C, but it was shown by Douglas that the depression due to the presence of other impurities was 0.035°C.

Douglas [250] reported that the solubility of uranium in liquid sodium is <0.05 wt.% at 550°C (1022°F). Rough and Bauer [251] reported a private communication from the Atomic Energy Research Establishment that no evidence of reaction between uranium and sodium was observed after "long periods of time" at 550°C (1022°F).

Pearlman [247] reported the results of static tests of the corrosion of uranium and uranium alloys in sodium and in NaK containing several different levels of oxygen impurity at 200 to 649°C (392 to 1200°F). Hoffman [252] and Davis and Draycott [124] reported corrosion rates for uranium exposed to flowing sodium and NaK at 400 to 677°C (752 to 1250°F). These data are also reported in the summary by Stang *et al.* [195].

(4) *Plutonium.* Schonfeld [253] reported that the results of attempts to produce alloys of plutonium and sodium suggest that the metals are completely immiscible in both liquid and solid states.

(k) *Carbon*

The interactions of sodium with carbon are among the most important in reactor technology. Unfortunately, they are also among the least understood because of complications arising from carbon transport [see Sec. 2-4.2

(f) and Chap. 3] and the interactions of carbon with other nonmetallic impurities in the Na (liq) environment [see Secs. 2-4.2(c) and (d)]. We are primarily concerned here with the Na-C binary system and hence with the solubility and interactions of elemental carbon in sodium.

The studies of the Na-C system have involved the preparation of the acetylide Na_2C_2 and the lamellar compounds, and a number of measurements of the solubility of carbon in sodium. The compound Na_2C_2, which has a ΔF_f^0 (298) of -6.57 kcal/mole [254], has not been prepared by a direct combination of the elements at temperatures below 800°C, and the high-temperature preparation involves the use of sodium vapor [255]. The evolution of C_2H_2 upon hydrolysis of Na (liq) has been suggested as evidence for the existence of Na_2C_2 in solution, but Addison, Hobdell, and Pulham [256] concluded that its solubility in Na (liq) is less than 1 wppm below 200°C. They prepared a film of Na_2C_2 on Na (liq) by reacting Na (liq) with C_2H_2, and the film did not dissolve even at 300°C. Since Na_2C_2 decomposes to the elements above 200°C, it was concluded that the solubility of carbon itself was less than 1 wppm at 300°C.

Asher and Wilson [257] prepared a compound of the approximate formula $C_{64}Na$ by the reaction of powdered graphite and $\sim$3% Na (liq) at 400°C. This same compound was prepared [258] by the action of Na(g) on a hollow graphite cylinder at 450°C. In both instances the composition was verified by X-ray analysis. The structure was of the lamellar type often observed in the reactions of the heavier alkali metals with graphite. This kind of reaction can cause disintegration of the bulk graphitic structure, as was observed by Greening and Davis [259] for a NaK alloy containing only 1% potassium. In the absence of contaminants such as H_2O, O_2, or N_2, Dzurus, Hennig, and Montet [260] were unable to prepare the $C_{64}Na$ species or any other lamellar Na-C compound under conditions similar to those used by Asher and Wilson. However, the role of the nonmetallic contaminants in promoting the attack of graphite by Na (liq) is not understood and may be catalytic or even indicative of ternary compound formation.

Preliminary results of a study at Atomics International [261] of the solubility of elemental carbon in Na (liq) do not agree with the very low solubilities reported from studies at ANL [115, 262]. Nothing has yet been published on a study at Harwell, England [263]. Some previous work by Gratton [264], although probably pertinent to the Na-C-O system, has been rejected as a valid study of the Na-C system [115]. This work seems to indicate, however, that the solubility of carbon in oxygen-contaminated sodium is much greater than it is in relatively pure sodium at the same temperature. Earlier work at ANL [52, 265, 266] has been dismissed by the researchers themselves because of sampling and analytical problems. Data from all these sources are shown in Fig. 2.29. We will not attempt to choose a carbon solubility from among these widely discordant results. Note, however, that the differences between the ^{14}C data obtained at ANL and the data obtained by combustion techniques at ANL and at Atomics International are similar in direction and magnitude to those found when tracer techniques are compared to more conventional "wet-chemical" techniques for determining the solubilities of iron and nickel in Na (liq).

The problems associated with the accurate determination of the solubility of carbon in sodium are well illustrated by the results of the USAEC-sponsored round robin analysis for carbon impurities in sodium [56]. These results not only differed widely among the many participating laboratories for ostensibly identical samples but also showed very large data scatter for many of the individual determi-

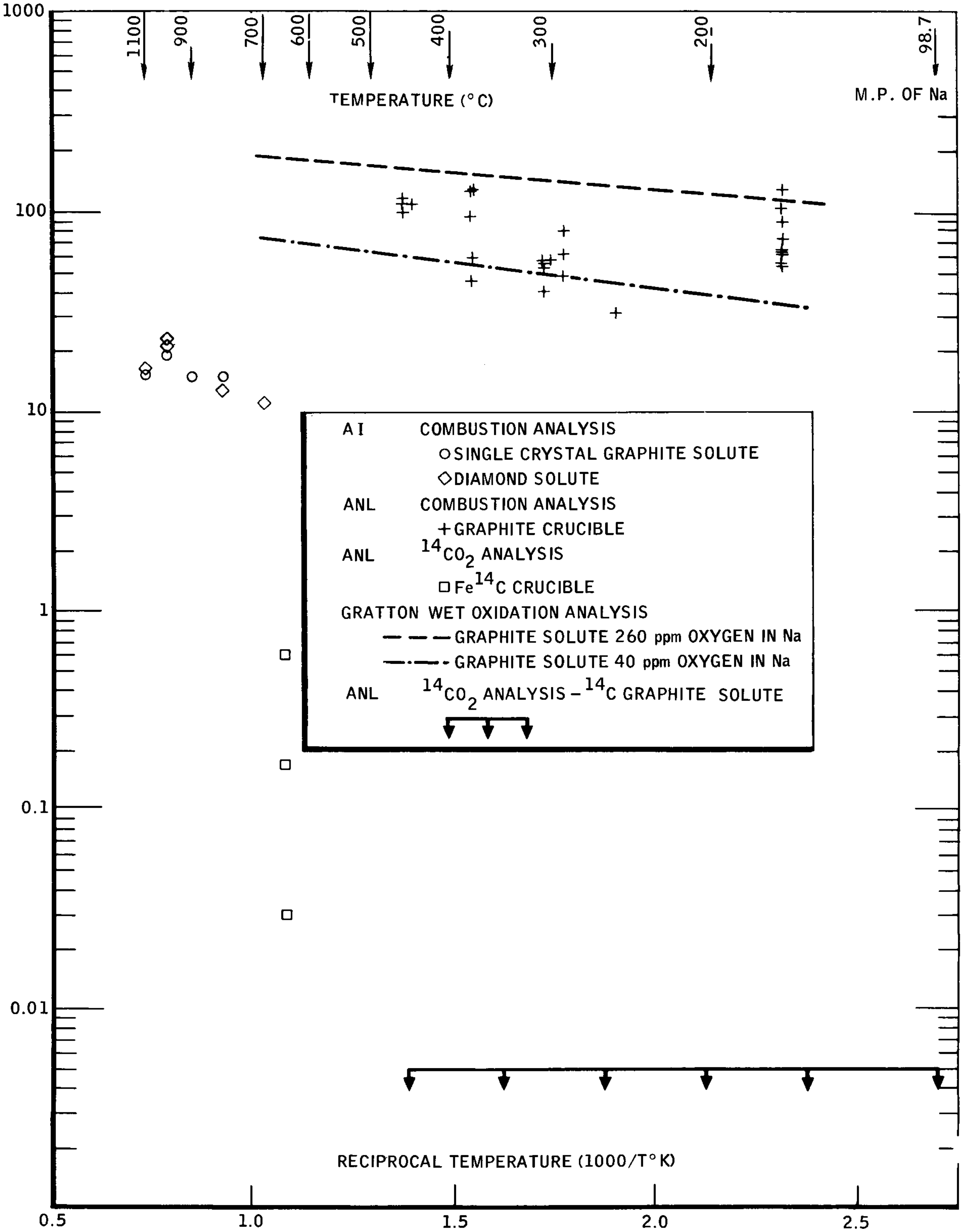

Fig. 2.29 - Solubility of carbon in sodium. (Atomics International combustion-analysis data are from Ref. 261; ANL combustion-analysis data, from Refs. 52, 265, and 266; ANL $^{14}CO_2$-analysis data, from Refs. 262 and 268; Gratton's wet-oxidation-analysis data, from Ref. 264; and ANL $^{14}CO_2$-analysis-^{14}C graphite-solute data, from Ref. 115.)

nations of a single laboratory. Among the reasons advanced for the failure of this comprehensive study to yield more definitive results were inadequate analytical techniques, inappropriate sampling procedures, and possible interactions of the sodium samples with containment materials. All the analytical techniques currently used for carbon-solubility studies require conversion of the carbon to CO_2 and subsequent measurement of the total CO_2 or of the tagged $^{14}CO_2$ evolved. If demonstrated carbon recovery is assumed to be an adequate measure of the validity of these techniques, the reasons for the apparent disagreement must be sought elsewhere.

Considerable evidence has been amassed [267-270] for the existence of particulate carbon dispersed in a Na (liq) system. These observations have direct implications in determining sampling procedures for measuring true solubility. One solution to this problem is to sample through fine-porosity filters, a routine procedure at ANL. An alternate method is to use solute materials (e.g., the diamonds used at Atomics International [261]) which are not likely to produce particulates. As an aid to understanding this phenomenon, Cefasso [271] attempted to prepare stable and well-characterized dispersions of colloidal carbon in sodium by ultrasonics and/or arc-discharge techniques. Another problem, which may be quite apart from particulation, is the observed migration of carbon to the walls of the sample container [269] and the resultant nonhomogeneity of the sample. The reasons for this migration are not understood but could very well be related to the physical and chemical interactions of carbon with containment materials.

Such interactions have been observed to occur in a variety of Na-C multicomponent systems. [For a more detailed discussion, see Sec. 2-4.2 (f).] Of more immediate concern is the comment of Davies [272] on the ANL work suggesting that, on the basis of similar work at Dounreay, the rate of deposition of ^{14}C on the walls of a stainless-steel container may be greater than the rate of dissolution in Na (liq) and hence may result in very low observed "solubilities." The ANL group [262] subsequently analyzed both the container and the Na (liq) for ^{14}C and found that deposition does occur, but the highest observed solubility in the Na (liq) itself was ~0.6 ppm. The reverse phenomenon, transfer of carbon from a nickel container to the sodium, has been suggested as a possible explanation for some anomalous blank experiments at Atomics International [261]. Anderson and Sneesby's observation [59] that Na (liq) containing 15 to 18 ppm carbon and less than 40 ppm oxygen was in virtual equilibrium with uncarburized 304 stainless steel at 670°F, although not suggested as a measure of solubility, is often used in engineering calculations and illustrates the importance of recognizing the effects of containment materials.

In connection with solubility measurements and in terms of the interactions of sodium with graphite moderators, it is pertinent to inquire what carbon species might exist in a Na (liq) solution. Much of the available information on this subject is indirect, resulting from observations of the products of amalgamation, dissolution, and hydrolysis of sodium samples [26, 62, 82, 267]. [See the discussion of these results in Secs. 2-4.2 and 2-4.5.]

No specific studies have been made of the solubility of carbon in NaK, although one analytical technique was specifically developed for use with the alloy [65]. The work of Tepper and Greer [273] on the solubility of carbon in cesium in the temperature range 330 to 670°C provides the only other data available for the solubility of carbon in alkali metals. Their results indicated a solubility of 12 to 53 wppm, but particulates were observed, and independent verification is therefore desirable.

Such verification is being sought in efforts to determine the solubility of carbon in sodium, but obviously from the foregoing discussion, much work remains before it can be obtained. From the standpoint of reactor technology, it is also obvious that the Na-C binary system must be understood before the ternary systems such as Na-C-O and Na-C-N and the mechanisms responsible for carbon transport in reactor systems can be adequately studied and properly understood.

(*l*) *Group IVA Elements - Si, Ge, Sn, and Pb*

(1) *Silicon*. The Na-Si system has been studied by several authors [274-277]. The compound NaSi was first synthesized by Hohmann [276], who reported that it dissociates in vacuum at 420°C (788°F). A decomposition temperature of 410°C (770°F) for NaSi was given by Hagenmuller *et al.* [227], who studied the thermal-decomposition behavior of the sodium silicides and reported the existence of a complex phase, Na_8Si_{46}.

A compound, probably $NaSi_2$, was prepared by Nowotny and Scheil [275] by reduction of SiO_2 with sodium. Moissan [274] also reported the preparation of the sodium silicides.

(2) *Germanium*. The principal finding from several studies [169, 276-279] of the Na-Ge system is the presence of a compound NaGe [276], which is stable only in an inert atmosphere and dissociates in vacuum at 480°C (896°F).

Hagenmuller *et al.* [227] reported that NaGe decomposes in the temperature range 320 to 380°C (608 to 716°F) to form two new phases, one having the formula $NaGe_4$. The second phase is described as Na_xGe_{136}.

(3) *Tin*. The Na-Sn system has been studied in considerable detail, as indicated by Hansen and Anderko [169], whose phase diagram is shown in Fig. 2.30. This diagram is based on the work of Hume-Rothery [280]. Nine compounds have been identified, but none appear to have any appreciable solid-solution ranges. There is still some doubt about the formula of one of the compounds, Na_4Sn or $Na_{15}Sn_4$. Hume-Rothery gave Na_4Sn, but Zintl and Harder [281] prepared the compound in a sodium-rich solution, extracted the excess sodium with liquid ammonia, and identified it as $Na_{15}Sn_4$.

The heats of formation of Na-Sn compounds have been measured by several authors [224, 225, 282-287]. The recommended values of the $\Delta H^\circ f$ (298) of the various compounds are: Na_4Sn, -15 kcal/mole; Na_2Sn, -14.5 kcal/mole; Na_4Sn_3, -35 kcal/mole; NaSn, -11 kcal/mole; and $NaSn_2$, -12 kcal/mole.

The solubility of tin in liquid sodium at the melting point of sodium is reportedly very small [229, 288]. Lamprecht [193] measured the solubility of tin in sodium in the temperature interval 120 to 260°C (248 to 500°F) and gave the following expression for the solubility:

$$\log X \text{ (atom fraction Sn)} = 2.356 - \frac{2312}{T(^\circ\mathrm{K})} \qquad (2.29)$$

This equation also fits the data of Davies [289], who measured the solubility of tin in sodium in the temperature interval 300 to 400°C (572 to 752°F). Heycock and Neville [290] reported that the freezing point of tin is reduced from 232°C (450°F) to 220°C (428°F) by the addition of 0.96 wt.% sodium. No solubility of sodium in solid tin was detected by Hume-Rothery [280], but more recent work by Pokrovsky and Galanina [291] indicated that sodium is soluble up to 0.48 wt.% in solid tin.

(4) *Lead*. The Na-Pb system has been extensively studied, but there are still unresolved questions about the details of the phase diagram.

Figure 2.31 represents a composite of two diagrams of Hansen and Anderko

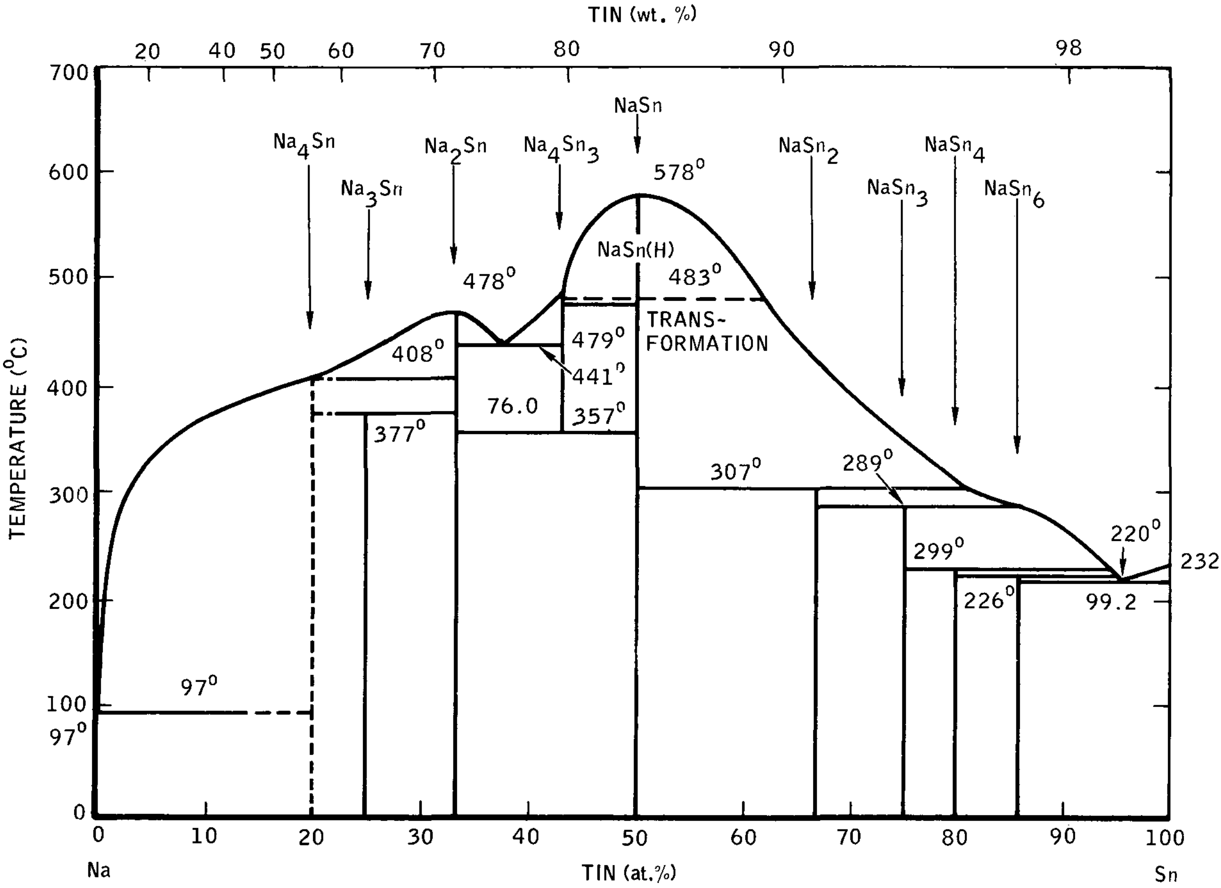

Fig. 2.30 - Sodium-tin system. (From M. Hansen and K. Anderko, *Constitution of Binary Alloys*, McGraw-Hill Book Company, Inc., New York, 1958)

[169], who gave a good review of this system. Though there are still some questions regarding the compositions of the two lead-rich eutectics, the compromise chosen by Hansen and Anderko is accepted here. The diagram is based largely on the studies of Mathewson [292] Calingaert and Boesch [293], and Krohn, Werner, and Shapiro [294]. The compound shown in Fig. 2.31 as $Na_{15}Pb_4$ was identified by the single-crystal work of Zintl and Harder [283] and confirmed by Shoemaker, Weston and Rathler [295]. In earlier work there was a controversy regarding the composition of the phase; the compounds Na_4Pb, $Na_{31}Pb_8$, and $Na_{15}Pb_4$ were suggested [169].

The compound Na_2Pb was reported by Calingaert and Boesch [293] but Shoemaker *et al.* [295] found the compounds Na_5Pb_2 and Na_9Pb_4 but not Na_2Pb (see Fig. 2.31).

The compound NaPb was shown by Mathewson [292] and Calingaert and Boesch [293] to have a composition range of 48 to 50 at.% lead.

The beta phase, whose homogeneity limits fall outside the composition $NaPb_3$, has the cubic Cu_3Au structure [296, 297]. However, the data of several workers who investigated the phase show differences in the extent of its phase field [169]. Figure 2.31 shows a range in general agreement with that given by Zintl and Harder [296].

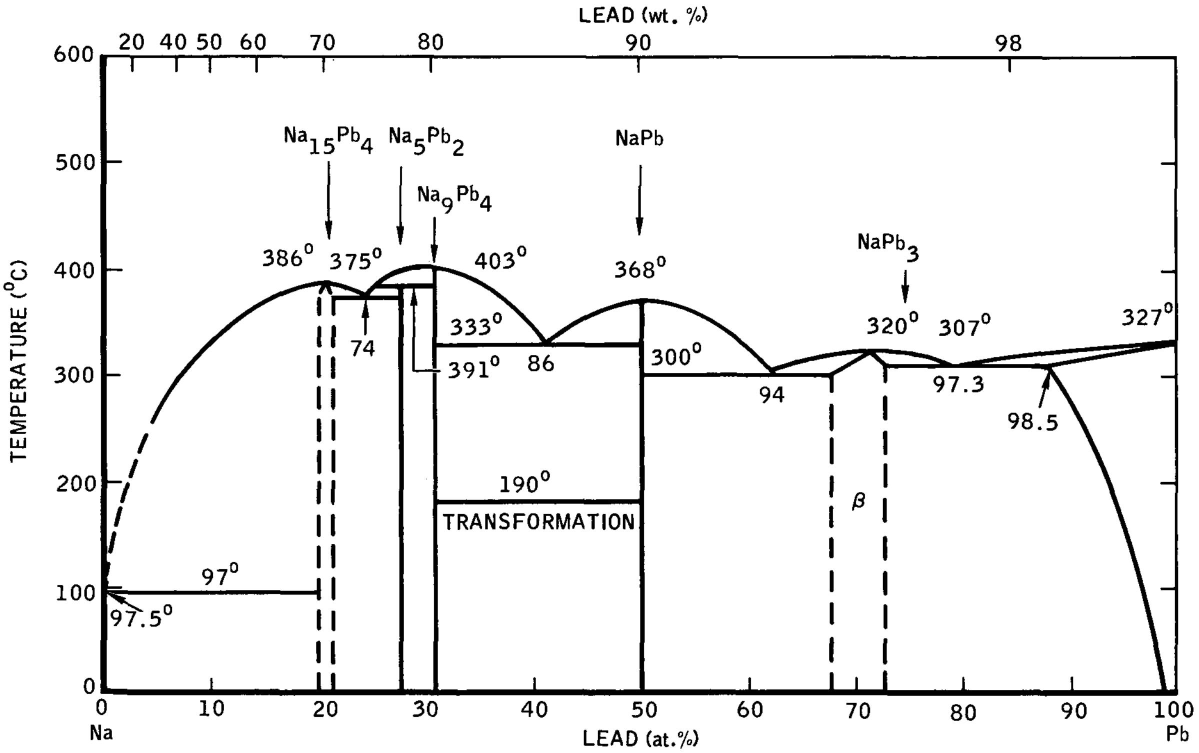

Fig. 2.31 Sodium-lead system. (From M. Hansen and K. Anderko, *Constitution of Binary Alloys*, 1002. McGraw-Hill Book Company, Inc., New York, 1958.)

The heats of formation, ΔH_f^0 (298), of Na-Pb alloys were measured by Seith and Kubaschewski [217] and Kraus and Ridderhof [298]. The preferred values [217] are: Na_4Pb, −20 kcal/mole; Na_5Pb_2, −35 kcal/mole; NaPb, −11.6 kcal/mole; and "$NaPb_3$," −15.2 kcal/mole.

Lamprecht [193] measured the solubility of lead in sodium in the temperature interval 120 to 250°C (248 to 482°F) and reported the solubility expression

$$\log X \text{ (atom fraction Pb)} = 3.515 - \frac{2639}{T(°K)} \tag{2.30}$$

Several investigations of the solubility of sodium in solid lead have given contradictory results, but Falkenhagen and Hofmann [299] showed that lead can be greatly supersaturated with sodium (up to 24 at.%). This may be the reason for the discrepancies in the high-lead region of the phase diagram. The solid solubility curve shown in Fig. 2.31 is described in the temperature interval 0 to 300°C (32 to 572°F) by

$$S \text{ [wt.\% Na in Pb (sol)]} = 0.173 + 1.15 \times 10^{-3}t + 1.027 \times 10^{-5}t^2 \text{ (°C)} \tag{2.31}$$

(m) *Group IVB Metals - Ti, Zr, and Hf*

(1) *Titanium*. No report on the Na-Ti system was found.

(2) *Zirconium*. Siegel *et al*. [300] offered a comment on the Na-Zr system: "No evidence has been found to indicate a significant solubility of zirconium in sodium or the converse." No

measurement of the solubility of zirconium in pure sodium has been reported. However, zirconium reacts with hydrogen, oxygen, nitrogen, and carbon impurities in sodium and acts as a getter for them. The products, especially the oxide, are adherent and protective, as described by Eichelberger [301], Mackay, [302] Carter, Eichelberger, and Seigel, [303] and Davis and Draycott [124].

The interaction of NaK and zirconium, described by Davis and Draycott [124], primarily involves an oxygen-gettering action.

(3) *Hafnium.* No report of the Na-Hf system was found. However, the solubility of hafnium in potassium was studied by Eichelberger, McKisson, and Johnson [304] in the temperature range 1200 to 1380°C (2192 to 2516°F). The solubility values found (118 wppm hafnium at 1200°C and 103 and 48 wppm hafnium at 1380°C) were quite uncertain.

Eichelberger *et al.* [304] also measured the solubility of hafnium in lithium at 1000 to 1400°C (1832 to 2552°F). The values found showed little temperature dependence and can best be represented by the single value 6 ± 2 wppm hafnium over the entire temperature range.

(n) *Nitrogen.* Three Na-N compounds have been reported. Zehnder [305] and Dennis and Browne [306] established the compounds sodium nitride (Na_3N), which dissociates at 300°C (572°F) and explodes when heated above 350°C (662°F) [145], and sodium azide (NaN_3), which decomposes at about 300°C (572°F) by the slow evolution of nitrogen and melts above 365°C (689°F). The heat of formation [145] of NaN_3, ΔH_f^0 (298), is 5.08 kcal/mole, and the free energy of formation is 23.76 kcal/mole.

The diazide compound $Na(N_3)_2$ is noted by Elliott [167] based on information given in a Japanese patent [307].

The solubility of nitrogen was studied by Cafasso [308] using a ^{15}N tracer technique. A known mixture of N_2 containing 20.4 mole % $^{15}N_2$, 77.9 mole % $^{14}N_2$, and 1.6 mole % $^{14}N^{15}N$ was used in an effort to understand the nature of the dissolution process and to determine if N_2 dissolves as a molecule. When exsolved, the dissolved N_2 was found to have essentially the same molecular isotopic composition. Thus Cafasso concluded that N_2 dissolved as a molecule. From the amounts of N_2 dissolved at 500°C (932°F), an average solubility of $(2.5 \pm 1.5) \times 10^{-7}$ std cm^3 N_2/cm^3 Na was found. This corresponds to $(4.37 \pm 1.75) \times 10^{-10}$ mole N_2/mole Na at 500°C (932°F). This value is consistent with the data of Dhar [138, 139] for the solubility of argon and krypton in sodium at 500°C (932°F), which, by Eq. 2.5 and 2.6, is 3.4×10^{-9} mole Ar/mole Na and 1.07×10^{-9} mole Kr/mole Na, respectively.

Although the solubility of nitrogen is small, the transfer of nitrogen in sodium from one material to another has been noted by several experimenters [195, 309-312] Nitrogen transfer behavior is also discussed in Secs. 2-4.5(b) and in Vol. V, Sec. 2-6.

(o) *Group VA Elements - P, As, Sb, and Bi*

(1) *Phosphorus.* No reports of the Na-P phase diagram were found. The Gmelin handbook [145] described the properties and behavior of the phosphides of sodium, Na_3P, Na_2P, NaP, and Na_2P_5.

The compound Na_3P was prepared by Brauer and Zintl [313], Morozova, Bol'shakova, and Lukniykh, [314] and Peterson and Logan [315]. Its heat of formation, ΔH_f^0 (298), was found by Morozova *et al.* [314] to be -32.0 ± 1.0 kcal/mole.

The compound Na_2P was prepared by Legoux [316] and by Royen, Zschaage, and Wutschel [317], who also reported that it decomposes in vacuum at 380°C (816°F) to yield sodium and NaP. The compound NaP was prepared by Royen *et al.* [317].

The compound Na_2P_5 was prepared by heating NaP in vacuum at 460 to 480°C

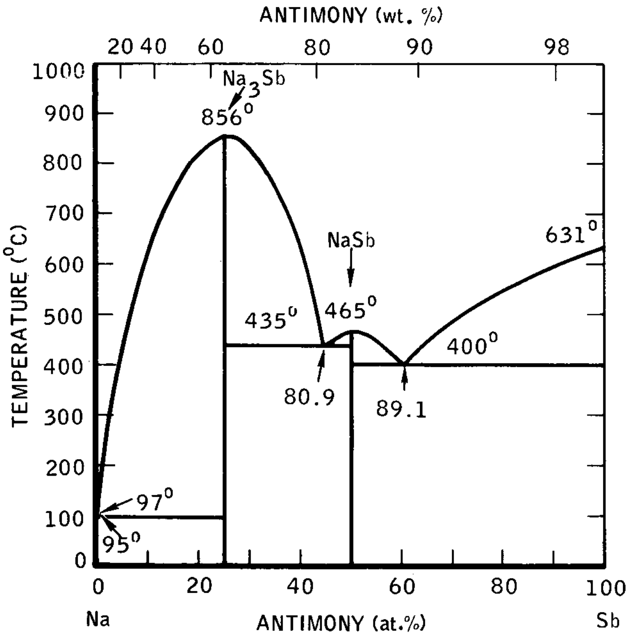

Fig. 2.32 Sodium-antimony system. (From M. Hansen and K. Anderko, *Constitution of Binary Alloys*, 1002. McGraw-Hill Book Company, Inc., New York, 1958.)

(860 to 896°F). Na_2P_5 sublimes and a residue of Na_3P remains [317].

(2) *Arsenic.* No reports of studies of the Na-As system were found, although the preparation of Na_3As, Na_3As_3, Na_3As_5, and Na_3As_7 in a liquid-ammonia medium was reported by Zintl *et al.* [208]. The ΔH_f^0 (298) of Na_3As was determined by Morozova *et al.* [314] to be -52.0 ± 1 kcal/mole.

(3) *Antimony.* The Na-Sb system was studied by thermal techniques by Mathewson, [318] whose data are used in the phase diagram shown in Fig. 2.32. Two compounds are shown, Na_3Sb and NaSb. Tammann [288] showed that the sodium-rich liquidus temperature rises sharply with small additions of antimony to sodium. The high-antimony region of the diagram was corroborated by X-ray techniques [319].

The heat of formation, ΔH_f^0 (298), of Na_3Sb, measured by Kubaschewski and Seith [224], was -47.2 kcal/mole. Morozova *et al.* [314] reported -50.8 ± 1 kcal/mole for ΔH_f^0 (298) for Na_3Sb. The heat of formation, ΔH_f^0 (298), of NaSb, measured by Weibke and Kubaschewski [320], was -15.8 kcal/mole. Kraus [321] reported a measurement of the free energy of formation of an $NaSb_x$ composition as -43.0 kcal/gram atom sodium. Additional information on Na-Sb compounds can be found in the Gmelin handbook [145]. Lamprecht [193] reported the following expression for the solubility of antimony in sodium:

$$\log X \text{ (atom fraction Sb)} = -1.453 - \frac{1831}{T(°K)} \qquad (2.32)$$

(4) *Bismuth.* The Na-Bi system was studied in detail by thermal analysis by Kurnakow and Kustnetzow [212] and by Mathewson [322]. The phase diagram shown in Fig. 2.33 is based on that shown by Hansen and Anderko [169]. However, the melting point of Na_3Bi is 840°C (1544°F) instead of the 775°C

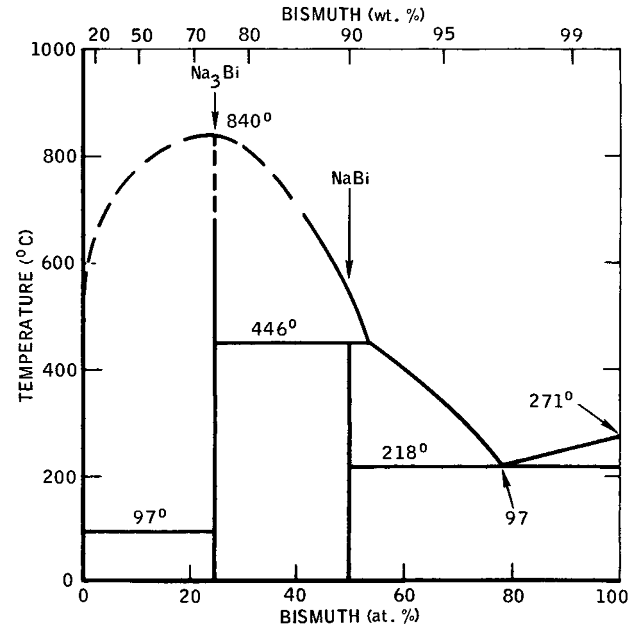

Fig. 2.33 Sodium-bismuth system.

(1427°F) given by Hansen and Anderko. The higher value was found by Fischer, Johnson, and Wovel [323], during a study of the liquid-vapor equilibria in the system. Vapor pressures, activities, and activity coefficients for both sodium and bismuth are given over the entire composition range, as is an analysis and discussion of the excess chemical potentials and the free energy of mixing in the system.

The two compounds NaBi and Na_3Bi are formed both by direct combination of sodium and bismuth and by precipitation from solutions in liquid ammonia. [208, 319]

Walker *et al.* [188] reported the following expression for the solubility of bismuth in distilled sodium in the temperature range 252 to 563°C (486 to 1045°F):

$$\log X \text{ (at.\% Bi)} = 5.0038 - \frac{4188.9}{T(°\mathrm{K})} \tag{2.32a}$$

from which a ΔH (solution) of 19.2 kcal/gram atom bismuth was computed. This expression, which defines the liquidus at the low-bismuth end of the phase diagram, was used in preparing the diagram shown in Fig. 2.33.

The heat of formation, ΔH_f^0 (298), of Na_3Bi was found by Kubaschewski and Seith [224] to be -45.6 kcal/mole (±6%). Morozova *et al.* [314] reported a ΔH_f^0 (298) of -48.2 ± 0.5 kcal/mole for Na_3Bi. The heat of formation, ΔH_f^0 (298), of NaBi was reported by Weibke and Kubaschewski [312] as -15.6 ± 1.0 kcal/mole. Kraus [321] reported the free energy of formation of an $NaBi_x$ composition to be -44.2 kcal/gram atom sodium. Additional information on the Na-Bi compounds can be found in the Gmelin handbook [145].

(p) *Group VB Metals - V, Nb, and Ta*

(1) *Vanadium.* No report of studies of the Na-V system was found. However, Stang *et al.* [195] summarized corrosion studies of vanadium and vanadium alloys in sodium. Greenberg, Ruther, and Levin [324] and Champeix, Darras, and Sannier [325] reported findings on the corrosion behavior of vanadium-base alloys. Evans and Thorley [326] reported work on the corrosion of commercially pure vanadium in sodium.

(2) *Niobium.* No report of the Na-Nb system was found. However, Kovacina and Miller [327] measured the "solubility" of niobium (columbium) from the alloy Cb-1% Zr in distilled and gettered sodium using a radioactive-tracer technique. The solubility values reported were, at 803°C (1477°F), 17.9 wppm; at 1008°C (1846°F), 7.5 wppm; at 1181°C (2158°F), 35.2 wppm; and at 1380°C (2516°F), 243 wppm. The author noted that the 17.9-wppm value is certain to be in error. These data are also reported in essence by Stang *et al.* [195].

Eichelberger [301] reported that niobium corrodes at the rate of 1 mg/cm^2/day in 600°C (1112°F) sodium cold trapped at 145°C (293°F). In hot-trapped sodium no measurable loss was observed in 1070 hr at 550°C (1022°F). Evans and Thorley [326] reported their findings on the corrosion rate of niobium in sodium.

(3) *Tantalum.* The solubility of tantalum in sodium was measured by Grand *et al.* [328] using a technique in which the tantalum-saturated liquid was irradiated and the tantalum was determined radiochemically. The reported solubilities are 2.9 wppm at 525°C (977°F), 0.19 wppm at 425°C (797°F), and 0.032 wppm at 325°C (617°F). These results (Fig. 2.34) were discussed and evaluated by Anthrop [329], who suggested that, because of the presence of a number of other impurity elements in the sodium, the results of Grand *et al.* may have been affected by a systematic error in the experimental procedure.

(q) *Oxygen.* From the viewpoint of using sodium in practical heat-transfer systems or as a reaction medium, a

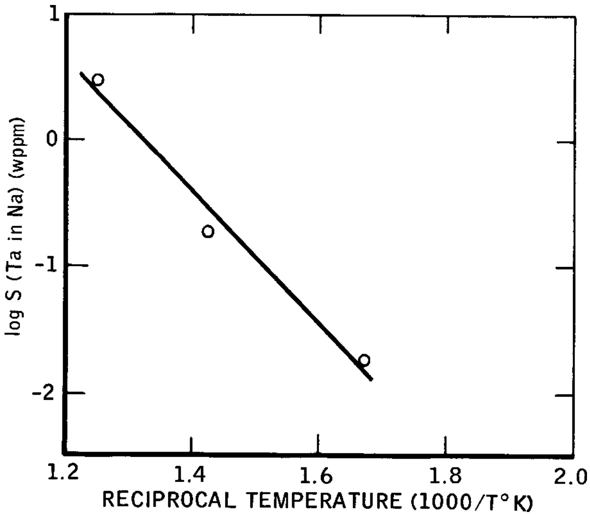

Fig. 2.34 Solubility of tantalum in sodium.

knowledge of the interaction of sodium and oxygen is of the greatest importance. Since the presence of oxygen impurity can be the controlling factor in many corrosion and mass-transfer processes, the control of oxygen concentration in sodium systems is a major concern (see Vol. V, Chap. 1).

The reaction of oxygen with sodium can produce the monoxide, peroxide, or superoxide. The heats and free energies of formation [$\Delta H^\circ f$ (298) and $\Delta F\overset{\circ}{f}$ (298)] of these compounds are, respectively, -99.400 and -90.125 kcal/mole for Na_2O (sol), -122.000 and -106.817 kcal/mole for Na_2O_2 (sol), and -62.300 and -52.282 kcal/mole for NaO_2 (sol) (all values are from Ref. 151).

These data show that the most stable Na-O compound per gram atom of oxygen is the monoxide; therefore this is the product expected in oxygen-saturated sodium. At temperatures above 298°K, the relative stability of the monoxide increases. The peroxide forms in an excess of oxygen, and the superoxide forms under a high pressure of oxygen [150]. Although opinions vary regarding the rate at which sodium peroxide decomposes in excess sodium, there is no disagreement on the fact that the oxide in equilibrium with oxygen-saturated liquid sodium is solid Na_2O (melting point, 1132°C [330]). "Sodium ozonide" has been reported as a product of the reaction between sodium and ozone in liquid ammonia [145, 331] and as a product of the reaction of ozonized oxygen and NaOH [332].

The solubility of oxygen (or of Na_2O, since at equilibrium in excess sodium the amount of dissolved oxygen is independent of the source from which it came) in sodium has been measured by Salmon and Cashman [333], Walters [334], Bogard and Williams [335], Noden and Bagley [336], Jahns and Weidmann [337], Thorley [338], Dorner [339], Bergstresser *et al.* [43] and Hall, Perkins, and Rutkauskas* [340], but the data are not in good agreement. Smith [341], reviewing the work reported in Refs. 333 to 336, concluded that there were systematic errors, particularly in the mercury-amalgamation methods used for oxygen determination. Claxton [30, 342] reviewing the same four papers, as well as Ref. 338, concluded after correlating all the data in several ways [30] that the best expression for oxygen solubility was of the form $\log S = A + (B/T)$, in which S is oxygen solubility, A and B are constants, and T is absolute temperature. In his second report Claxton [342] included data from Ref. 340, recorrelated all the data using an expression of the form $\log S = K\,[(1/T) - (1/T_m)]$, in which K is a constant and T_m is the melting point of Na_2O, and suggested that the solubility curve consists of a low-temperature portion and a high-temperature portion, intersecting somewhere between 215 and 315°C.

---

*For a more detailed discussion of the work described in Ref. 340, see V.J. Rutkauskas, *Determination of the Solubility of Oxygen in Sodium by Vacuum Distillation*, USAEC Report LA-3879, Los Alamos Scientific Laboratory, July 15, 1968.

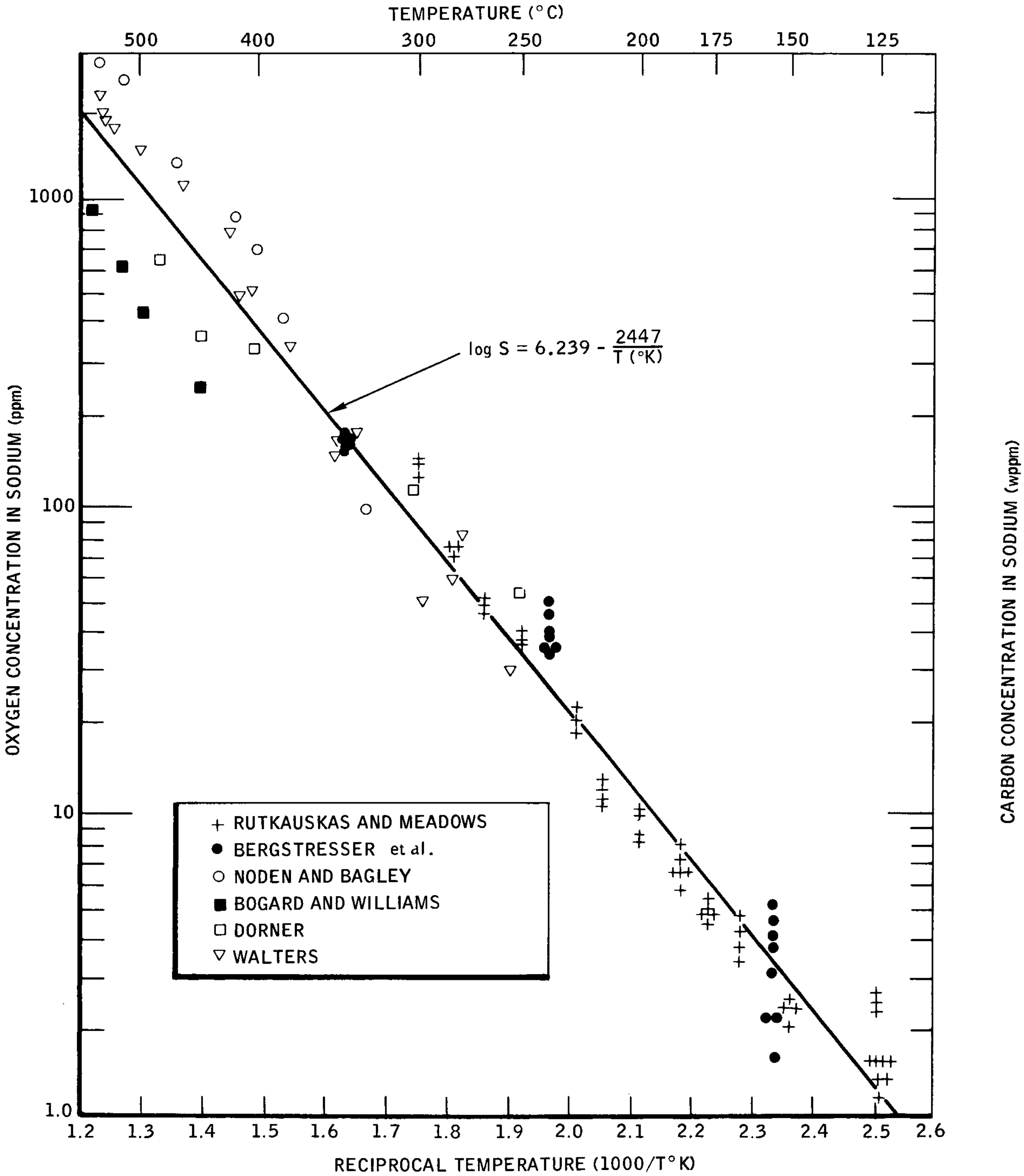

Fig. 2.35 Solubility of oxygen in sodium - recommended curve. [Data are from Hall, Perkins and Rutkauskas [340], Bergstresser *et al.* [43], Noden and Bagley [336], Bogard and Williams [335], Dorner [339], and Walters [334].]

Dorner [339], in a brief discussion of Refs. 30 and 333 to 337, argued against the two-line representation for the solubility. Eichelberger [343] reviewed all these references and evaluated the experimental procedures and

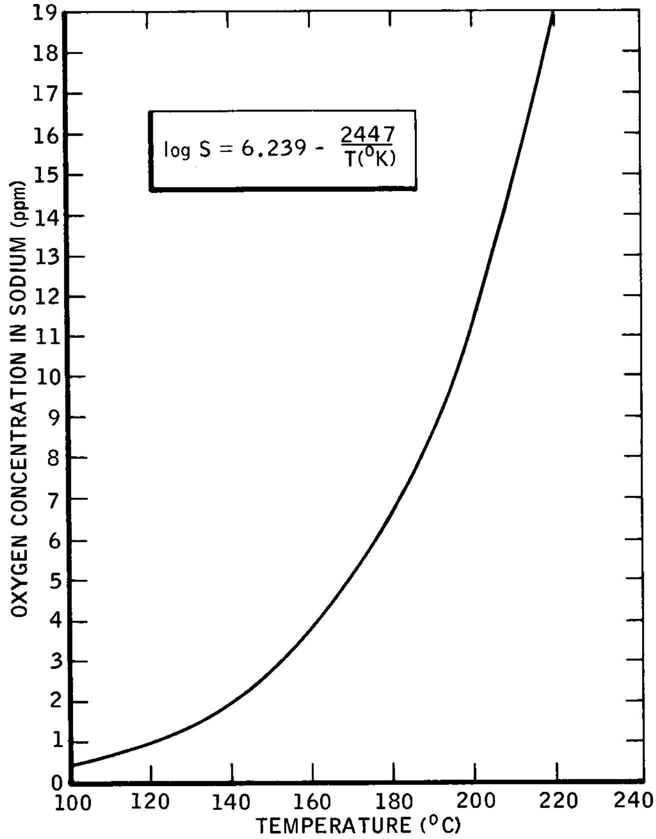

Fig. 2.36 Oxygen solubility in sodium - low-temperature portion, plotted linearly.

analytical chemistry used. His recommended solubility curve is shown in Fig. 2.35; the low-temperature portion is replotted in Fig. 2.36 for easy reference. The equation for the recommended solubility curve is

$$\log S \text{ (wppm O)} = 6.239 - \frac{2447}{T(°\text{K})} \qquad (2.33)$$

The recommended solubility curve represents a linear regression line for 107 data points from six experiments [43, 334-336, 339, 340]. No data are included from Salmon and Cashman [339] or Thorley [338] because only generalized curves, and not individual data points, were available from these investigators.

The 212 points from the seven references in which individual data points were presented are shown in Fig. 2.37. The 107 points used for the regression line were chosen on the basis of the following reasoning. Although various methods were used to prepare samples of sodium saturated with oxygen (Na_2O) at the test temperatures, only two analytical methods were used to determine the oxygen content of the sodium. Thorley [338], Bergstresser *et al.* [43] and Hall, Perkins, and Rutkauskas [340] used the distillation technique to separate the Na_2O from sodium; all the other investigators used mercury amalgamation for the separation, in different modifications of the amalgamation procedure. These methods are discussed in detail earlier in this chapter. The distillation method has been developed at LASL (and presumably at Culcheth also although, as noted, individual data points are not available for Thorley's work) to a point where it seems to be reasonably free of systematic errors or variable blank phenomena. In a study of analytical methods for oxygen in sodium, Prach [344] reported a zero blank for the distillation analysis. Therefore all the data points derived by this analytical method were used.

Until the middle 1960's sodium-system technology was not sufficiently well developed to require oxygen analyses in the concentration range below 20 or 30 wppm. Therefore there was no strong impetus to refine the amalgamation method for accurate analyses at low oxygen levels. Smith [341] concluded that the method used in the 1950's was of doubtful accuracy below 400 wppm. Subsequent study of the method by Prach [344] and by Scarborough and DeVries [38] has shown that there is a blank associated with the method and that the blank originates primarily in moisture adsorbed on the surface of the glassware used, with some contribution from the glass itself. In routine work the blank can range from 4 to 10 μg of oxygen equivalent even when the glassware is vacuum

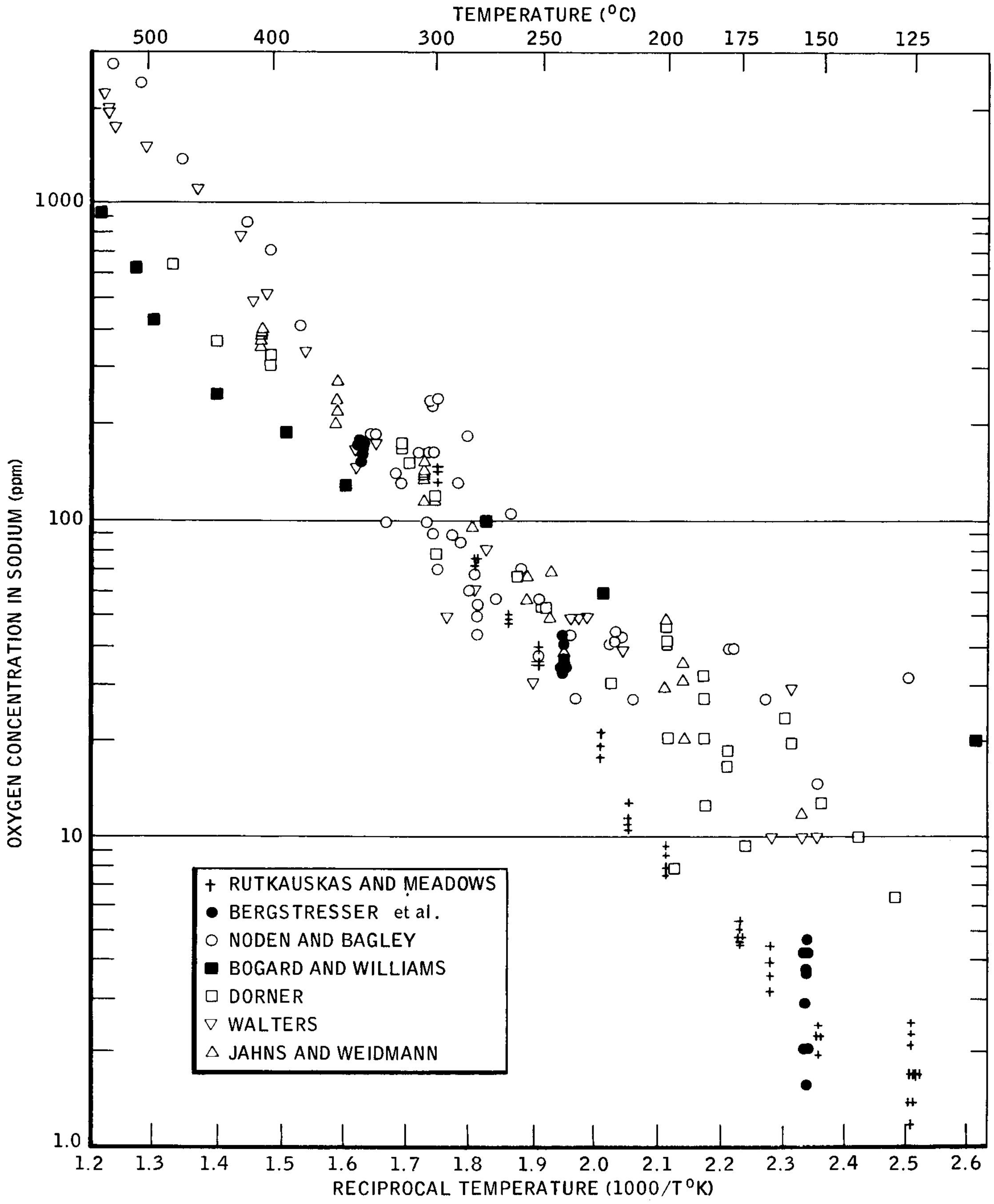

Fig. 2.37 Oxygen solubility in sodium - all data. [Data are from Hall, Perkins, and Rutkauskas [340], Bergstresser *et al.* [43], Noden and Bagley [336], Bogard and Williams [335], Dorner [339], Walters [334], and Jahns and Weidman [337].]

dried at 150°C before use. In earlier applications of the method, the blank was undoubtedly higher and more variable. By vacuum drying overnight at 300°C and transferring the glassware to the analytical station in an evacuated container, Scarborough and DeVries were able to reduce the blank to 1.3

± 0.3 μg. Evidently earlier determinations of dissolved oxygen in sodium include a sizable blank. A blank of 5 or 10 μg in a 1-g sample will go unnoticed at high oxygen levels, but it may not be neglected at lower concentrations of oxygen. The presence of such a blank provides a reasonable explanation for the apparent change in slope for the oxygen solubility curve proposed by Claxton and others. Because of the effect of the blank, no results of amalgamation analyses are included below 250°C, at which temperature the solubility is about 35 wppm.

In addition to the analytical blank, which includes a contribution from reaction with the analytical glassware during analysis, there is a varying and unmeasurable uncertainty in experiments in which the sodium was sampled in glass. Many researchers, taking note of this, used stainless-steel apparatus for the high-temperature experiments. Since a reaction with glass is always a possibility, though perhaps not severe at low temperature, no experiments run or sampled in glass apparatus are included in the data from which the recommended solubility curve was derived. Table 2.17 gives a summary of the sources of data points from which Figs. 2.35 to 2.37 were derived.

The data were used to derive the best straight line in the form log S (wppm) = $A + (B/T)$. This treatment of the data implies that the heat of solution (in the term "B") is constant over the temperature range. Although the heat of solution probably will not be strictly constant over such a wide range, it will change slowly and continuously; thus the straight line is a better representation than a line showing an abrupt change in slope at some temperature. The heat of solution derived from the line shown in Fig. 2.35 is 11.2 kcal per mole of Na_2O.

Complete data from all references, a total of 212 points, are plotted in Fig. 2.37. Comparison of Figs. 2.35 and 2.37 shows that many data points that were excluded fall close to the derived line. The previously mentioned criteria for the inclusion of data points were held rigorously, however. Note that the 21 points above 240°C from Jahns and Weidmann [339] would not appreciably alter the recommended line even though the work was done in glass apparatus. On the other hand, many of the experiments in glass of Noden and Bagley [336] are much above the line. The four points from Bogard and Williams [335], for which stainless-steel apparatus was used, are included although they fall much below the derived line.

TABLE 2.17 - Sources of Data for Oxygen Solubility Curve

Reference	Total data points	Temperature range of points, °C	Data points used	Reason for exclusion of some points
Bergstresser *et al.* [43]	22	155 to 340	22	
Hall *et al.* [340]	52	125 to 300	52	
Walters [334]	25	152 to 549	17	Analytical blank <250°C
Noden and Bagley [336]	46	127 to 540	7	Glass solubility apparatus
Bogard and Williams [335]	10	110 to 555	4	Glass solubility apparatus
Dorner [339]	30	130 to 480	5	Glass samplers
Jahns and Weidmann [337]	27	156 to 406	None	All-glass apparatus
Salmon and Cashman [333]	?	115 to 495	None	Only average data reported
Thorley [338]	?	114 to 292	None	Only average data reported

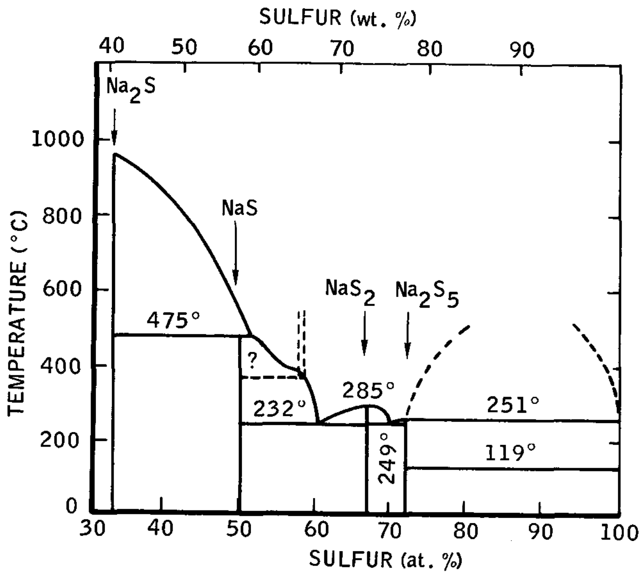

Fig. 2.38 Sodium-sulfur system. (From *Gmelins Handbuch der anorganischen Chemie*. Natrium, System-Nummer 21, p. 1059, Verlag Chemie, Weinheim, 1966.)

In addition to Claxton's generalized expressions for oxygen solubility [30, 342] Subbotin, Kirillov, and Kozlov [345] published a "generalization of the data of several papers and the results of our experiments," but did not discuss any of the data from which they derived their expression. Kassner and Smith [346] used the data of Hall, Perkins, and Rutkauskas [340] and the sampled-in-steel high-temperature points of Noden and Bagley [336] to derive a solubility curve similar to that in Fig. 2.35, but with a slightly steeper slope.

(r) *Group VIA Elements - S, Se, and Te*

(1) *Sulfur.* The Na-S system was studied by several authors, some of whom are cited by Kohlmeyer and Brinkman [347] and by Erametsa and Karlsson [348]. The Gmelin handbook [145] summarizes the published information and presents the phase diagram of Pearson and Robinson [349] shown in Fig. 2.38. Four compounds are found, Na_2S, NaS, NaS_2, and Na_2S_5. In addition, a two-liquid-phase region is shown in the high-sulfur region. Earlier diagrams by Hansen [350] showed many more compounds, but these are now thought to be in error. The polysulfides familiar in aqueous solutions are not reflected in the binary system.

The standard heat of formation at 298°K of Na_2S(sol) is -89.0 kcal/mole [151] and the standard free energy of formation at 298°K is -86.368 kcal/mole [151]. No solubility data for sulfur in sodium were found.

(2) *Selenium.* A thermal-analysis study of the Na-Se system was performed by Mathewson [351], whose phase diagram is shown in Fig. 2.39. The melting point of the most refractory compound, Na_2Se, is in doubt because of containment problems. Five compounds have been established, Na_2Se, Na_2Se_2, Na_2Se_3, Na_2Se_4, and Na_2Se_6 [145]. Of these,

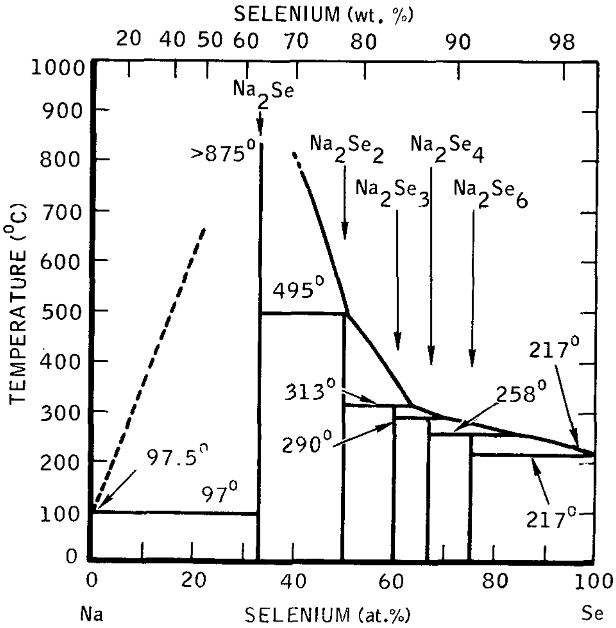

Fig. 2.39 Sodium-selenium system. (From M. Hansen and K. Anderko, *Constitution of Binary Alloys*, 1007, McGraw-Hill Book Company, Inc., New York, 1958.)

Na_2Se is the most stable; the others are polyselenide structures of lower stability.

The heat of formation, $\Delta H^{o}{}_{f}(298)$, of Na_2Se has been reported by Rossini *et al.* [352] to be -63.0 kcal/mole, by Maslov [353] to be -63.4 kcal/mole, and by Mulder and Schmidt [354] to be -82.0 kcal/mole.

(3) *Tellurium.* The Na-Te system was studied by Pellini and Quercigh [355], and by Kraus and Glass [356] using thermal analysis. The data of Walker *et al.* [188] for the solubility of tellurium in sodium in the temperature range 222 to 572°C (432 to 1062°F) show a significantly lower solubility value at 570°C than do those of Pellini and Quercigh (0.17% vs. ~10%). The phase diagram shown in Fig. 2.40 is based on the composite data of Pellini and Quercigh, Kraus and Glass, and Walker *et al.*

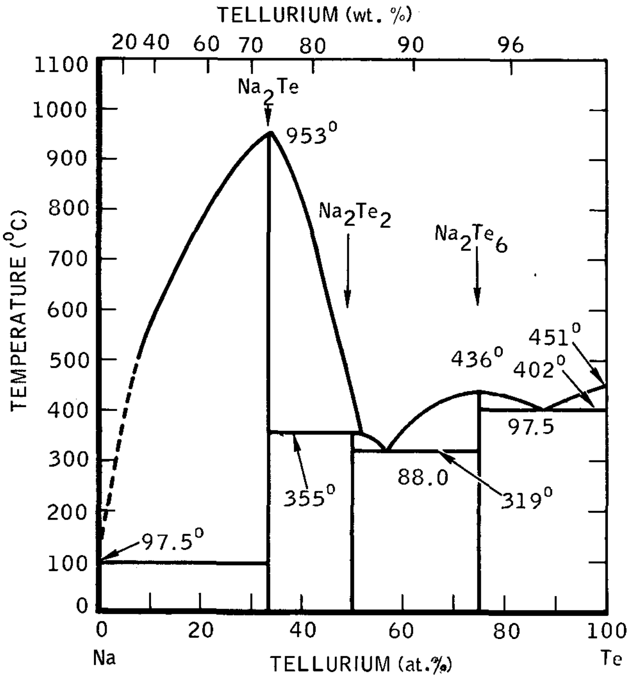

Fig. 2.40 Sodium-tellurium system. (From M. Hansen and K. Anderko, *Constitution of Binary Alloys,* 1007. McGraw-Hill Book Company, Inc., New York, 1958.)

Three compounds are formed by direct mixing of the elements, Na_2Te, Na_2Te_2, and Na_2Te_6, but a number of polytellurides can be prepared in liquid ammonia [298].

The heat of formation, ΔHOf (298), of Na_2Te has been reported by Rossini *et al.* [352] to be -84.0 kcal/mole, and by Kraus and Ridderhoff [218], by the direct combination of the elements, to be -60.0 kcal/mole. The former value is preferred. The heat of formation, ΔHO_f (298) of Na_2Te_2 was reported by Kubaschewski [244] to be -120 kcal/mole and by Rossini *et al.* to be -101.5 kcal/mole. The latter value is preferred. Additional information on the Na-Te compounds can be found in the Gmelin handbook [145].

(s) *Group VIB Metals - Cr, Mo, and W*

(1) *Chromium.* Eichelberger *et al.* [357] found that the solubility of chromium in sodium in the temperature range 700 to 1000°C (1292 to 1832°F) could be expressed by the single value 2.5 ± 1 wppm chromium. The temperature dependence is less than the uncertainty in the analytical procedures.

(2) *Molybdenum.* No study of the Na-Mo system was found. However, the solubility of molybdenum in potassium was measured by McKisson *et al.* [358] from 1000 to 1200°C (1832 to 2192°F). The results are described by

$$\log S \text{ (wppm Mo)} = 4.8 - \frac{5600}{T(°K)} \qquad (2.34)$$

Eichelberger *et al.* [304] found the solubility of molybdenum in lithium from 1400 to 1620°C (2552 to 2948°F) to be 4.5 wppm molybdenum at 1400°C and 11 wppm molybdenum at 1620°C.

(3) *Tungsten.* No study of the Na-W system was found. However, the solubility of tungsten in potassium was measured by Eichelberger *et al.* [304] from 1390 to 1580°C (2534 to 2876°F). The solubility values found were 40 wppm tungsten at 1390°C and 61 wppm tungsten at 1580°C.

The measured values of Eichelberger *et al.* [304] for the solubility of

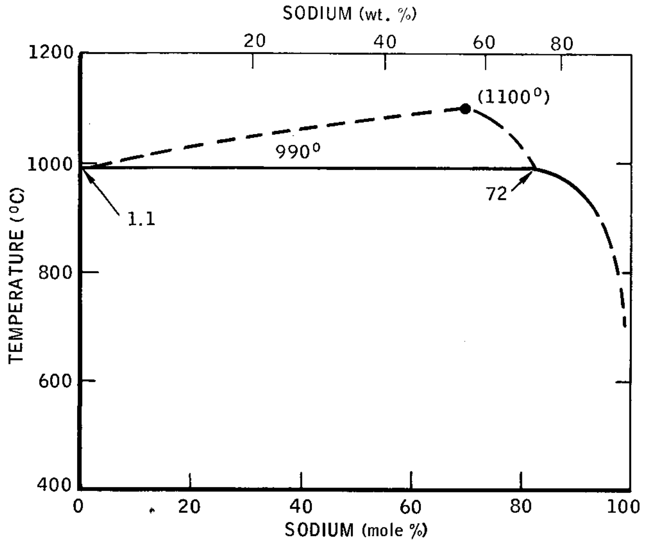

Fig. 2.41 Sodium-sodium flouride system. [From M.A. Bredig, J.W. Johnson, W.T. Smith, Jr., Miscibility of Liquid Metals with Salts. I. The Sodium-Sodium Halide Systems, *J. Amer. Chem. Soc.*, *77:* 307 (1955).]

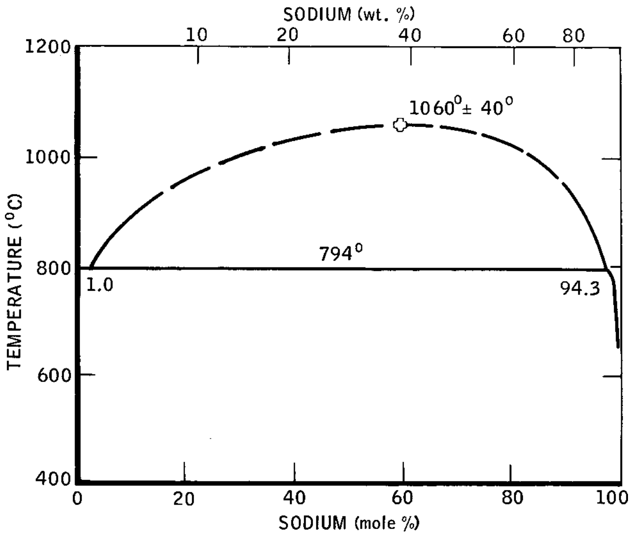

Fig. 2.42 Sodium-sodium chloride sys- - tem. [From M.A. Bredig, J.W Johnson, and W.T. Smith, Jr., Miscibility of Liquid Metals with Salts. I. The Sodium-Sodium Halide Systems, *J. Amer. Chem. Soc.*, *77:*307 (1955).]

tungsten in lithium from 1200 to 1600°C (2192 to 2912°F) ranged from $\sim$1 to 2.5 wppm and had an uncertainty of about ±1 wppm.

(t) *Group VIIA Elements - F, Cl, Br, and I*

(1) *Fluorine.* Bredig, Johnson, and Smith [359] studied the Na-NaF system and presented the phase diagram shown in Fig. 2.41 The $\Delta H^\circ f$ (298) of NaF (sol) is - 137.10 kcal. mole and its $\Delta F^\circ f$ (298) is -129.87 kcal/mole [151]. The Gmelin handbook [145] describes preparation and properties of NaF in detail.

(2) *Chlorine.* Bredig *et al.* [359] also studied the Na-NaCl system and presented the phase diagram shown in Fig. 2.42. The $\Delta H^\circ f$ (298) of NaCl (sol) is - 98.26 kcal/mole, and its $\Delta F^\circ f$ (298) is -91.79 kcal/mole [151]. The Gmelin handbook [145] describes the preparation and properties of NaCl in detail.

The solubility of sodium in molten sodium chloride was given by Sittig [150], who reported the results of Lorenz and Winzer [198] and of Stockem [360]: at 800°C (1472°F), 3.4 wt.% Na [360] and 4.2 wt.% Na [198]; and at 850°C (1562°F), 15 to 20 wt.% Na [198].

(3) *Bromine.* Bredig *et al.* [359] studied the Na-NaBr system and presented the phase diagram shown in Fig. 2.43. The $\Delta H^\circ f$ (298) of $\text{NaBr}_\circ$(sol) is -86.38 kcal/mole, and its ΔFf (298) is 83.48 kcal/mole [151]. The Gmelin handbook [145] describes the preparation and properties of NaBr in detail.

(4) *Iodine.* Bredig *et al.* [359] studied the Na-NaI system and presented the diagram shown in Fig. 2.44. The ΔH°_f (298) of NaI (sol) is -68.80 kcal/mole, and its ΔF°_f (298) is -68.01 kcal/mole [151]. The Gmelin handbook [145] described the preparation and properties of NaI in some detail.

(u) *Group VIIB Metals - Mn and Re*

(1) *Manganese.* No study of the Na-

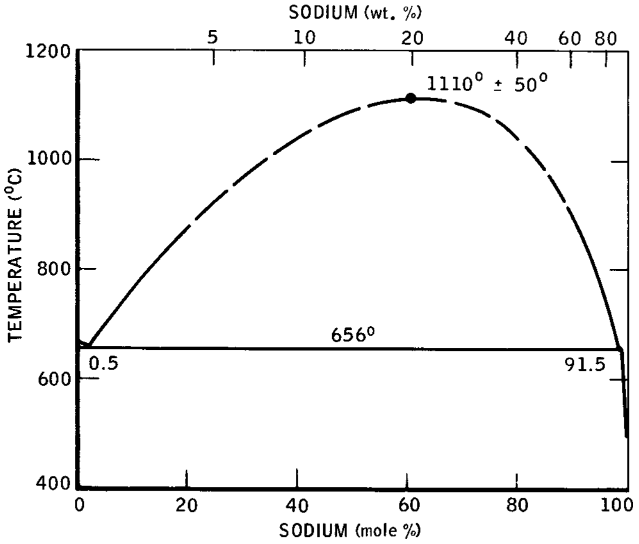

Fig. 2.43 Sodium-sodium bromide system. [From M.A. Bredig, J.W. Johnson, and W.T. Smith, Jr., Miscibility of Liquid Metals with Salts. I. The Sodium-Sodium Halide Systems, *J. Amer. Chem. Soc.* *77:* 307 (1955).]

Mn system was found.

(2) *Rhenium.* No study of the Na-Re system was found. However, the solubilities of rhenium in potassium and in lithium have been measured in the temperature range 1200 to 1600°C (2192 to 2912°F). For potassium the solubility was found to be <1 wppm over the temperature range investigated and for lithium, 1.1 ± 0.5 wppm. The temperature dependences were all within the limits of uncertainty of the analytical procedures [304].

(v) *Group VIIIB Metals - Fe, Co, Ni, Ru, Rh, Pd, Os, Ir, and Pt*

(1) *Iron.* The solubility of iron in liquid sodium has been studied by several investigators [361-366]. Figure 2.45 shows the data summary given in Anthrop's [329] review. The data points shown by Anthrop have been deleted to maintain maximum clarity. However, the scatter of the data about the lines shown ranges from ±10% for

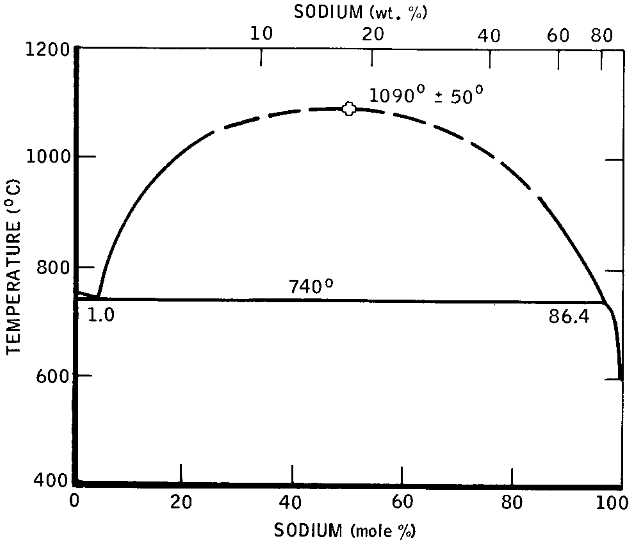

Fig. 2.44 Sodium-sodium iodide system. [From M.A. Bredig, J.W. Johnson, and W.T. Smith, Jr., Miscibility of Liquid Metals with Salts. I. The Sodium-Sodium Halide Systems, *J. Amer. Chem. Soc.*, *77:* 307 (1955).]

the solubility of iron in the $Na-Na_2O-NaOH$ solutions of Baus *et al.* [361] to ±30% for the solubility in $Na-Na_2O$ solutions.

Epstein [364] reported an expression for the solubility of iron in sodium of unknown purity in the temperature range 231 to 473°C (448 to 883°F):

$$S \text{ (wppm Fe)} = -1.47 + 0.030t \text{ (°C)} \quad (2.35)$$

Baus *et al.* [361] and Bogard [362] measured the solubility of iron in sodium of various levels of oxygen content using ^{59}Fe tracer material. Their data show an unmistakable increase in iron "solubility" with increased oxygen content in the sodium (their "pure" sodium has been estimated to have about 30 ppm oxygen impurity [329]). Their curve for the solubility of iron in "pure" sodium is described by [361, 362]

$$\log S \text{ (wppm Fe)} = -0.7764 - \frac{1028}{T(°K)} \quad (2.36)$$

Rodgers *et al.* [363] measured the solubility of iron in sodium, using both nickel and stainless-steel static systems and electromagnetically pumped loops, one of nickel and the other of stainless steel. The analyses were made by the thiocyanate method. They noted that an appreciable amount of nickel dissolved during the tests but determined to their satisfaction that there was no interference from this source. A composite of their solubility data is shown as a best-fit line in Fig. 2.45.

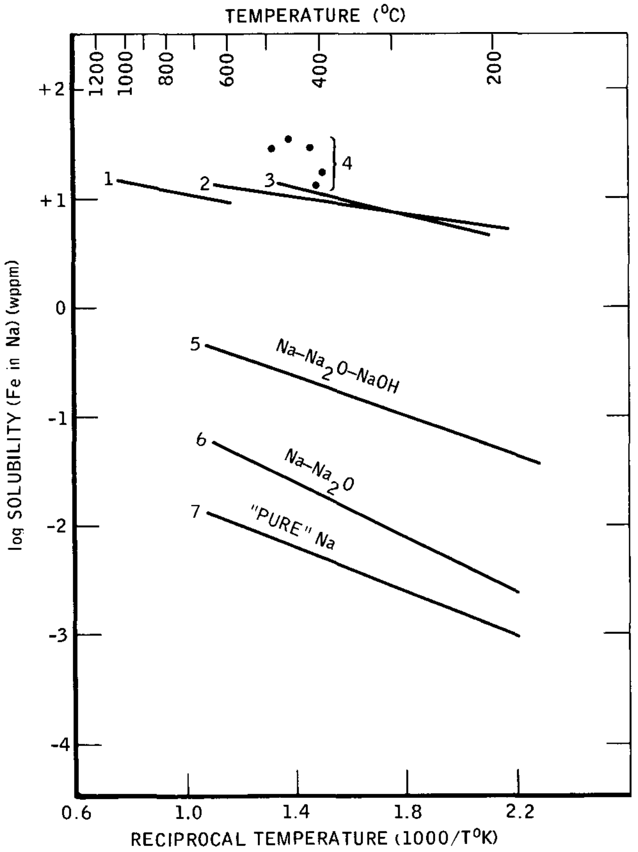

Fig. 2.45 Solubility of iron in sodium. (Data for curve 1 are from Ref. 366; curve 2, from Ref. 363; curve 3, from Ref. 364; curve 4, from Ref. 365; and curves 5, 6, and 7, from Refs. 361 and 362.)

Weeks and co-workers [365] studied the solubility of iron in sodium using both spectroscopic and radioactive-tracer analytical techniques in an effort to resolve the differences in the results of earlier workers. Their test system consisted of a stirred volume of high-purity sodium contained in the sample material. Dip-cup samples were taken after the system had come to temperature equilibrium. The spectroscopically determined solubility values are shown as points in Fig. 2.45. The data obtained in the tracer work are scattered but generally fall in the 0.1 to 1.0 wppm range in the temperature interval from 390°C (734°F) to 550°C 1022°F). This is two orders of magnitude below the spectroscopic (normal iron) data.

Eichelberger and McKisson [366] studied the solubility of iron in sodium using a capsule technique in which the iron-saturated sodium was poured from the sample crucible into an iron-free collector vessel at temperature. Fractionally distilled sodium containing less than 5 wppm oxygen was used. The tests, which were carried out at 600 to 1000°C (1112 to 1832°F), yielded the expression

$$\log S \text{ (wppm Fe)} = 1.549 - \frac{517}{T(°\text{K})} \qquad (2.37)$$

This curve is also shown in Fig. 2.45.

A single determination of the solubility of iron in NaK-78 was made by Drugas and Kelman [367], who reported the solubility to be 15 ± 3 ppm at 700°C. This value agrees well with the higher range data shown in Fig. 2.45.

An examination of the solubility data for iron in sodium obtained by wet-chemical techniques (Fig. 2.45) indicates that there is a general agreement of the "solubility" of iron in sodium. However, the existence of an oxygen-concentration effect on the iron solubility is clearly shown by the ^{59}Fe tracer work; similar increases would be expected in the observed iron solubilities measured by wet-chemical techniques in solutions containing Na_2O and NaOH. However, the sensitivity of the iron solubility to oxygen content of the sodium may be less than that of the refractory metals. The most puzzling aspect of the iron-solubility problem is the very low solubility values obtained with radioactive-tracer techniques. The presence of 5 to 25 wppm iron in iron-saturated sodium is a proved observation on which four laboratories agree. But it has also been shown that the amount of radioactive iron found in presumably saturated solutions is much less than 0.1 wppm iron. No explanation for this anomaly has been offered.

(2) *Cobalt.* The solubility of cobalt in sodium was measured by Grand *et al.* [328] by irradiating cobalt-saturated sodium and using radioactive-tracer techniques to determine the cobalt content. They reported 1.00 wppm at 525°C (977°F), 0.021 wppm at 425°C (797°F), and 0.028 wppm at 365°C (689°F). The oxygen content of the sodium used was thought to be 10 to 20 ppm. Anthrop [329] expressed the belief that there may have been a systematic error in the measurements. The data of Grand *et al.* are shown in Fig. 2.46, along with Anthrop's least-squares curve.

(3) *Nickel.* The solubility of nickel in sodium was investigated by Rodgers *et al.* [363] using (1) two static systems, one of stainless steel and the other of nickel, and (2) one pumped loop of nickel. The dimethylglyoxime wet-chemical method of analysis was used, and the results are shown as a line on Fig. 2.47. The oxygen concentration of the solvent sodium was estimated to be less than 100 wppm; however, variations in oxygen content from 50 to 650 wppm did not affect the nickel-solubility values. (This is in contrast to oxygen-dependence experience in iron systems.)

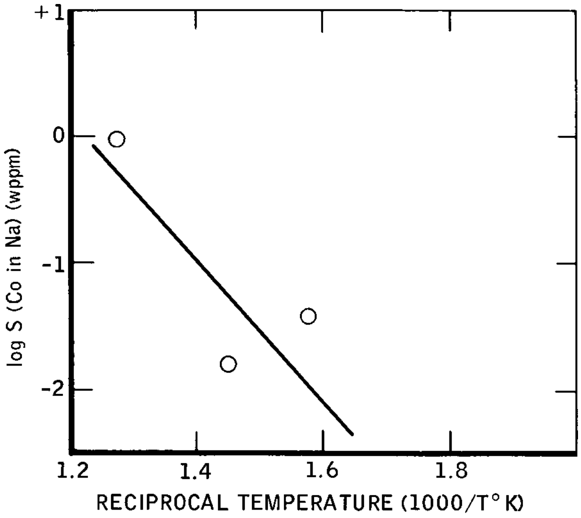

Fig. 2.46 Solubility of cobalt in sodium.

Kovacina and Miller [368] used the radioactive tracer ^{63}Ni to measure the solubility of nickel in vacuum-distilled sodium (20 to 50 wppm oxygen). Their data are shown as a line in Fig. 2.47. They found a marked effect of oxygen concentration in the sodium on the apparent solubility of nickel.

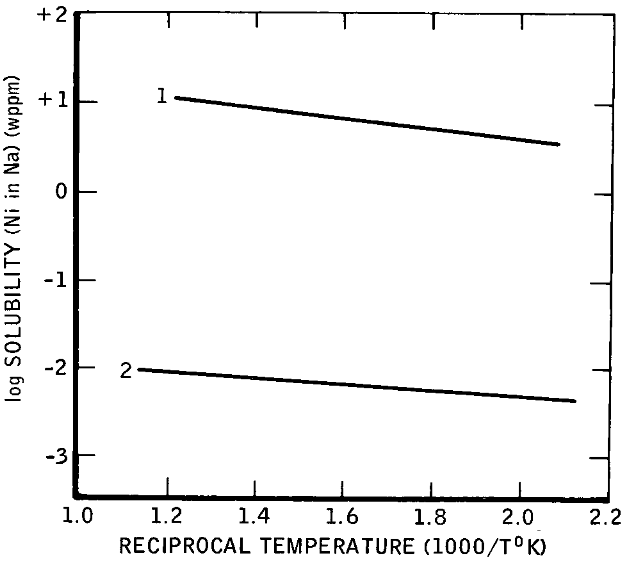

Fig. 2.47 Solubility of nickel in sodium. (Curve 1 is from Ref. 363 and curve 2, from Ref. 368.)

At 600°C (1112°F) in sodium containing 30, 430, 770 and 1130 wppm oxygen, the "solubilities" found were 0.012, 0.04, 0.12, and 0.20 wppm, respectively.

Weeks and co-workers [365] initiated a study of the solubility of nickel in sodium using a heated container made of the solute metal and a dip-cup sampling technique. The reported results were scattered, and no curve was proposed. The values ranged from about 1 to 5 wppm at 500°C (932°F) to 0.4 to 0.9 wppm at 450°C (842°F).

Thorley and Tyzack [369] reported on the corrosion behavior of nickel alloys in sodium, and De Van [370] reported on the corrosion behavior of nickel alloys in sodium and NaK-56.

(4) *Ruthenium.* No studies of the Na-Ru system were found.

(5) *Rhodium.* No studies of the Na-Rh system were found.

(6) *Palladium.* Hansen and Anderko [169] cited a report of Tammann [288] that the solidification point of sodium is depressed by 0.4°C by the addition of 2.8 wt.% palladium.

(7) *Osmium.* No study of the Na-Os system was found.

(8) *Iridium.* No study of the Na-Ir system was found.

(9) *Platinum.* Only limited studies of the Na-Pt system have been reported. Hansen and Anderko [169], reviewing the early work, cited Tammann [288], who found the freezing point of sodium to be essentially unaffected by the addition of up to 1.5 wt.% platinum. These early workers found that sodium liquid and vapor attack platinum above 450°C (842°F) and that, upon cooling, pure platinum precipitates from the solution. No estimates of the extent of the solubility of platinum in sodium were made, however.

Nash, Boyden, and Whittig [371], prepared and identified the compound $NaPt_2$ by reacting the elements.

2-4.2 *Interactions with Selected Inorganic Compounds*

This section describes briefly the interactions of sodium and/or NaK with those inorganic compounds considered most relevant to reactor technology in terms of safety, corrosion, impurity formation, or the chemistry of laboratory methods for basic chemical studies. These interactions are conveniently divided into subsections containing descriptions of the chemistry of ternary systems, as opposed to the binary systems of Sec. 2-4.1 When NaK is considered, however, the systems become quaternary. For example, the subsection on Na-H-O contains the interactions of H_2O and NaOH with sodium or, in the case of NaK, the interactions of H_2O, NaOH, and KOH. Addison [372, 373] described the basic factors involved in the use of liquid alkali metals as reaction media, and Feder [374] presented a similar discussion. *Fast Reactor Technology: Plant Design* [144], Chap. 2, provides an excellent review of the more current literature on this same subject from an engineering point of view. Finally, the comprehensive works of Mellor [147, 148], Sittig [150], and the Gmelin Institute [145] provide discussions and extensive lists of references for the specific interactions discussed here, as well as other interactions beyond the scope of this handbook.

(a) *Interactions in the Na(NaK)-H-O System*

Studies of the interactions of water with sodium or NaK have been largely based on safety considerations, and in many cases detailed chemical information was not the object of the work. When such information was obtained, the particular experimental conditions involved proved to be the controlling factor in the nature of the chemical reactions. In addition to the usual variables of temperature, pressure, and the physical states and relative amounts of reactants and products, the reactions were found to depend on a variety of experimental conditions less subject to simple description. Table 2.18 lists the possible reactions in the Na(NaK)-

TABLE 2.18 - Sodium (NaK)-Hydrogen-Oxygen Reaction Equations

Equation	Equation No.
$Na + H_2O = NaOH = \frac{1}{2}H_2$	2.38
$2Na + H_2O = NaOH + NaH$	2.39
$Na + NaOH = Na_2O + \frac{1}{2}H_2$	2.40
$2Na + NaOH = Na_2O + NaH$	2.41
$NaH = Na + \frac{1}{2}H_2$	2.42
$NaH + H_2O = NaOH + H_2$	2.43
$2Na + \frac{1}{2}O_2 = Na_2O$	2.44
$Na_2O + H_2O = 2NaOH$	2.45
$2Na + O_2 = Na_2O_2$	2.46
$2Na + Na_2O_2 + 2H_2O = 4NaOH$	2.47
$NaK_2 + 3H_2O = 2KOH + NaOH + {}^3/{}_2H_2$	2.48
$3NaK_2 + KOH + NaOH = 2Na_2O + 7K + H_2$	2.49
$H_2 + \frac{1}{2}O_2 = H_2O$	2.50

H-O system without specifying reaction conditions. The standard heats and free energies of formation of the reactants and products are provided for convenience in Table 2.19. These kinds of reactions and the significance of the experimental studies in determining which might be important under given conditions have been reviewed by Ford [375] and are briefly discussed here.

The reaction of Na (sol) with ice at temperatures down to -200°C has been followed [376] by means of the evolution of H_2(gas), but the rate of reaction [148] is not appreciable at temperatures lower than -98°C. Above -98°C the reaction can become violent if forceful contact is made between the ice and the sodium [377, 378]. The reaction probably proceeds according to Eq. 2.38 (in Table 2.18), but the reasons for the violence have not been investigated.

Below the melting point of NaOH

TABLE 2.19 - Heats and Free Energies of Formation of Selected Na-H-O Compounds

Compound (state)	ΔHO_f (298), kcal/mole	ΔFO_f (298), kcal/mole	Ref.
H_2O(gas)	-57.798	-54.636	151
H_2O(liq)	-68.320	-56.720	254
Na(liq)	+0.575	+0.119	151
NaH(sol)	-13.490	-8.023	151
NaH(gas)	+29.700	+24.602	151
Na_2O(sol)	-99.400	-90.125	151
Na_2O(liq)	-93.966	-84.691	151
Na_2O_2(sol)	-122.000	-106.817	151
NaOH(sol)	-102.240	-91.188	151
NaOH(liq)	-100.353	-89.981	151

(319.1°C), Eq. 2.38 is generally accepted as representing the primary reaction of Na(liq) and H_2O(gas or liq) [375]. The possibility of reaction with Eq. 2.39 as an intermediate step and the subsequent dissociation of NaH according to Eq. 2.42 cannot, however, be eliminated. Naud [379] found that the NaH decomposition reaction was important in Na-H-O systems under vacuum at 280°C. In all cases where O_2 is excluded from the system, the reaction of Na(liq) and H_2O(gas) has been found to proceed smoothly [380]. Much of the violence normally associated with the Na(liq)-H_2O(liq) reaction has been ascribed [380] to the secondary combination of evolved H_2(gas) with O_2 according to Eq. 2.50 Kilpatrick, Baker and McKinney [381] found that 30 to 50% of the H_2(gas) yield in a NaK-H_2O reaction is consumed by the subsequent reaction with O_2.

Equations 2.40 and 2.41 have been suggested as possible secondary reactions above the melting point of NaOH. Williams [382], in fact, concluded that NaH is stable in Na(liq) above 385°C and that its formation by Eq. 2.39 or 2.41 results in a solution of NaH in Na(liq). The "solubility" of NaH, Na_2O, and NaOH in Na(liq) at these temperatures therefore results in a complex equilibrium in which reaction mechanisms as well as species are extremely difficult to determine. In addition, Williams showed that the dissociation of NaH depends on the total pressure above the melt and not on the partial pressure of H_2. He concluded that NaH decomposition occurs by a vaporization or sublimation process at temperatures at which NaH dissolves in Na(liq). At temperatures below 385°C, the NaH-H_2 equilibrium involved the predicted dissociation pressure of NaH, which can be calculated [383] from the equilibrium suggested by Eq. 2.42.

The formation or dissociation of NaH as it occurs in the Na-H_2O reactions is not completely understood under conditions different from those in Williams' experiments. Woollen, Scott, and Dell [384] found, for example, that NaH was present in the reaction products of Na(liq) and steam in the temperature range 280 to 450°C, but no NaH could be detected at a reaction temperature of 500°C. Thus the reaction was assumed to proceed according to Eq. 2.38 at the high temperature. Naud's [379] assertion that NaH can be completely decomposed in a Na(liq)-NaOH melt under vacuum at 320°C also raises questions about the nature of the NaH-NaOH-Na(liq) equilibria. In excess H_2O NaH could probably be hydrolyzed according to Eq. 2.43, thus affording a different mechanism for its removal from the system.

The reactions of Na and O_2 to give oxides is included in Table 2.18 for two reasons: (1) the formation of Na_2O by Eq. 2.44 is known [385] to be catalyzed by the presence of H_2O(gas) or H_2(gas), and (2) Na_2O is an observed product of the reaction of Na(liq) with NaOH (Eq. 2.40 or 2.41) above the melting point of NaOH. The possibility that Na_2O will hydrolyze in excess H_2O (Eq. 2.4 5) must also be considered in the Na-H-O systems under discussion. Humphreys [386] demonstrated that Na_2O_2 could be hydrolyzed by traces of H_2O (gas) after Na(liq) had been oxidized with excess O_2 (Eq. 2.46 followed by Eq. 2.47). Safety studies at KAPL [387] indicated that O_2(gas) concentrations of 5 vol.% or less drastically reduced the rate of the Na-O_2 reactions. The catalytic effect of H_2O (gas) was demonstrated by Gracie and Droher [388], who found that O_2(gas) concentrations had to be reduced to less than 1.3 vol.% to get similar results in the presence of substantial amounts of water vapor.

The solubility of NaOH in Na(liq) determined by Bogard and Williams [335], is given in Table 2.20. A conceptual difficulty not unlike that of describing the "solubility" of Na_2O, NaH, or Na_2CO_3 in sodium is encountered in discussing these data. Since these molecular species can be recovered from Na(liq) by controlled distillation or precipitated out of Na(liq) by changing temperature, such a solubility seems reasonable. A molecular-solubility mechanism or solute species is, however, not necessarily implied by these observations. The solubility of these compounds has been and will continue to be discussed without apology, but the reader should draw his own conclusions about physical significance. The phase rule of classical thermodynamics, of course, allows a certain freedom in describing the species used in calculating the thermodynamic properties of a given system.

TABLE 2.20 - NaOH Solubility in Metallic Sodium [335]

Temp. °C	NaOH, wt.%
110	0.004
150	0.006
200	0.012
250	0.022
300	0.031
350	0.042

The reactions of NaK with H_2O are similar to those for the Na-H_2O system, and one possibility is illustrated by Eq. 2.48. Since Na_2O has been shown to be the stable oxide in a NaK-O system [389], the subsequent reaction of the mixed hydroxides can be represented by Eq. 2.49. Both NaOH and KOH can be recovered by precipitation from the NaK-H_2O reaction products [390], but the much lower observed melting point for the mixed hydroxides (as low as 166°C) suggests that Eq. 2.49 will be a more important part of the NaK-H-O scheme than the corresponding reactions (Eqs. 2.40 and 2.41) for the Na-H-O system [391]. The existence and stability of the hydrides of sodium and potassium have not been investigated in the NaK-H-O system. The most hazardous species that might exist is K_2O_4, which is known to explode under a variety of conditions [392]. If O_2 is excluded, however, the formation of K_2O_4 is unlikely, and the NaK-H_2O reaction presents no greater hazard than the corresponding Na-H_2O reactions under the same conditions.

The safety aspects of the Na(NaK)-H_2O reactions are discussed in Vol. III, Chap. 2, and the implications of these reactions as they apply to the design of steam-generator systems for fast breeder reactors are discussed in Vol. II, Chap. 4. The foregoing discussion was therefore limited to the probable reaction products in Na(NaK)-H-O systems and the conditions under which they can be formed. This kind of information can be, and has been, applied to calculations of the thermodynamics of the reactions by making certain simplifying assumptions about the processes involved. Salmon [393], for example, calculated the temperatures produced by the overall reaction

$$2\mathrm{Na(liq)} + \mathrm{H_2O(gas)} \rightarrow \mathrm{Na_2O(sol)} + \mathrm{H_2(gas)} \qquad (2.51)$$

assuming both a constant volume and a constant-pressure process for tube leaks in a sodium-heated steam generator. This reaction is equivalent to the sum of Eqs. 2.38 and 2.40 of Table 2.18 and represents the most probable overall reaction under the conditions of his calculation.

This kind of calculation could also be performed for a different choice of reactions and/or reaction products from Table 2.18. Perhaps the best guide for this choice, for an initial set of reaction conditions, is given by Ford [395], who provided an excellent discussion as well as a comprehensive reference list of the pertinent literature. Table 2.19 should also prove a valuable tool since many of the literature references are not explicit about the source or quality of their thermodynamic data.

(b) *Interactions in the* Na(NaK)-H-N *System*

Studies of the interactions of NH_3 with sodium or NaK which are of primary interest in reactor technology are concerned with the use of NH_3(liq) as a solvent. Although many articles have appeared in the literature on the subject of metal-ammonia systems, no general agreement has been reached as to the exact nature of the solutions. The two solution models currently favored are the "polaron" or modified electron-cavity model of Jortner [394] and the "cluster" or localized electron-solvated metal ion model of Becker, Lindquist, and Adler [395]. Neither of these models, however, is individually capable of explaining the observed physical and chemical properties of the solutions over the full ranges of temperature and composition. [396]

The solubilities of sodium, potassium and mixtûres of sodium and potassium in NH_3(liq) have been measured over wide temperature ranges. The solubilities of the mixtures show three branches [397] corresponding to the solubility of pure sodium, pure potassium, and the compound NaK_2. The individual solubilities of sodium and potassium reported by Jolly [398] are presented in Table 2.21. An unusual feature of Na-NH_3 or K-NH_3 solutions is the existence of a liquid-liquid miscibility gap characterized by two separate immiscible solutions of the metal existing in equilibrium. The density of these phases is also unusual, in that the heavier blue-colored phase is less concentrated in metal than the less-dense bronze-colored phase. It is not surprising, therefore, that a solution of lithium in NH_3(liq) has the lowest specific gravity of any known liquid. To illustrate the temperature dependence of these phenomena and to provide a more complete description of the Na-NH_3 system, Jolly [398] constructed the phase diagram shown in Fig. 2.48.

Two advantages of using ammonia for the dissolution of sodium are the selectivity of the process and its relative nonviolence. Sodium dissolves quite readily in NH_3(liq), but impurities such as NaH and Na_2CO_3 are essentially insoluble [399]. Sodium hydroxide is only sparingly soluble [400] (∿ 2 mg/1000 g of NH_3 at -45°C) and can be recovered in the residue of the NH_3 dissolution along with the Na_2CO_3 and NaH. The compound Na_2O which ammonolyzes according to the reaction [399]

$$Na_2O + NH_3(liq) \rightarrow NaOH + NaNH_2 \quad (2.52)$$

can also be recovered as NaOH. The compound $NaNH_2$, whose solubility in NH_3(liq) is somewhat greater than that of NaOH, [145] can also be produced by the reaction

TABLE 2.21 - Solubilities of Sodium and Potassium in Liquid Ammonia*

Temp., °C	Gram atoms metal/ 1000 g NH_3
Sodium	
22	9.56
0	10.00
-30	10.63
-33.8	10.72
-33.5	10.93
-50	10.89
-70	11.29
-105	11.79
Potassium	
0	12.4
-33.2	11.86
-33.5	12.05
-50	12.3
-100	12.2

---

*From W.L. Jolly, Metal-Ammonia Solutions, in F.A. Cotten (Ed.), *Progress in Inorganic Chemistry*, Vol. I, p. 235, Interscience Publishers, New York, 1959. See this volume for a list of the original papers from which the data are taken.

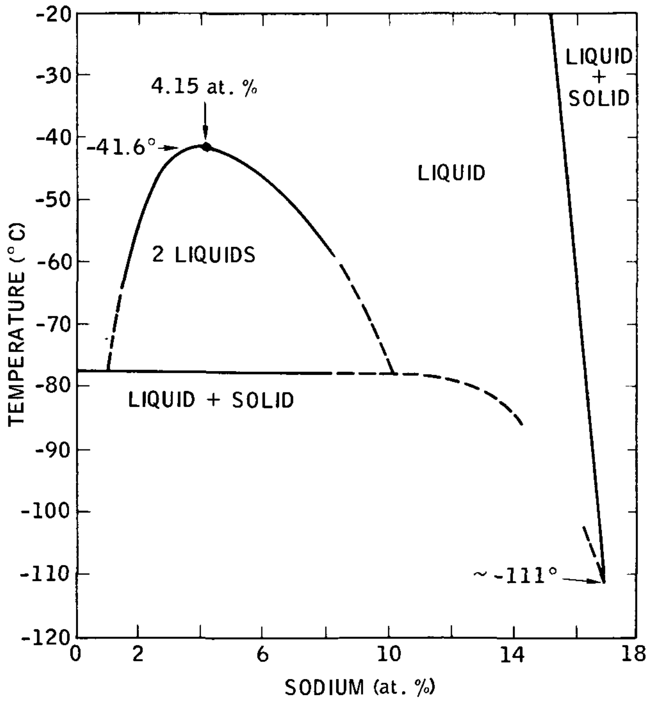

Fig. 2.48 Sodium-ammonia system.

$$Na + NH_3(liq) \rightarrow NaNH_2 + \tfrac{1}{2}H_2 \tag{2.53}$$

which proceeds very slowly at low temperatures but is catalyzed by the presence of many metals, including iron, aluminum and chromium [401]. When no catalysts are present, the heat effects of Na-NH_3 dissolution are small [ΔH (solution) at -33°C for a 0.4$\underline{M}$ solution is +1.4 kcal/mole [402]] and the process therefore proceeds smoothly.

On the basis of these observations, NH_3(liq) was suggested as a leaching agent for cleaning sodium-contaminated equipment [399], as a solvent for species studies [26], and even as a solvent in the quantitative analysis of impurities in sodium coolants [25]. More information about the behavior of alkali metals dissolved in ammonia can be found in reviews on solution models [391, 403]; reactions of inorganic and organic reagents with metal-ammonia solutions [148, 404, 405]; and studies of the thermodynamic and physicochemical properties [398, 401-411].

(c) *Interactions in the Na(NaK)-C-O System*

The interactions of the carbon oxides with sodium or NaK are important in reactor technology primarily as they relate to the C-O impurities that may exist in the liquid metals. The relatively higher solubility of carbon in oxygen-contaminated sodium, discussed in Sec. 2-4.1(k), is almost universally attributed to the formation of C-O species. The nature of these species for the CO(gas)-Na(liq) reaction, studied by Sinclair, Davies and Drummond [412] has been loosely described as "sodium carbonyl" [see Sec. 2-4.5(e)]. This careful study discusses the conflicting reports of previous investigators on the nature and extent of the reaction under a variety of conditions and suggests explanations for the apparent conflicts. In the absence of strict definition and control of reaction conditions, the characterization or prediction of the reaction products in CO-Na or CO_2-Na systems is as difficult as it is for the H_2O-Na reactions discussed in Sec. 2-4.2(a).

An explosive reaction occurs when sodium and solid CO_2 are brought together by impact [413], but there is apparently no reaction when CO_2(gas) contacts Na(sol) at room temperature [414]. At 350°C Na (liq) reacts with CO_2(gas) to form Na_2CO_3 and free carbon [415]. At lower temperatures the rate of production of Na_2CO_3 is increased by the presence of H_2O; Na_2O and NaOH are formed by the Na-H_2O reaction and immediately combine with CO_2(gas) to produce carbonate. Other products observed and reported for the CO-Na and CO_2-Na reactions include NaCO [416], Na_2C_2 [417], $Na_2C_2O_4$ [418], and HCOONa [419]. The formation and stability of these products depend largely on reaction temperature, the phase in which reaction occurs, and the possibility of decomposition or recombination reactions.

The compound Na_2CO_3 is probably the

most stable formed in these reactions, and its solubility in Na(liq) was measured by Williams *et al.* [161] in the temperature range 150 to 385°C. The validity of these data, however, was questioned by Hill [121], who observed a much lower solubility when attempting to dissolve Na_2CO_3 in flowing Na(liq) at temperatures up to 450°C. As a result of these discrepancies, a program was begun at APDA [420] to determine the solubility of Na_2CO_3 in Na(liq). Preliminary data from this program [421] indicated a solubility at least an order of magnitude lower than that obtained by Williams *et al.*

The discrepancy between the results of the two studies may be caused by the removal of Na_2CO_3 from the Na_2CO_3-Na (liq) phase prior to analysis. Two reactions that may occur are

$$Na_2CO_3 \rightarrow Na_2O + CO_2(gas) \qquad (2.54)$$

and

$$4Na + Na_2CO_3 \rightarrow 3Na_2O + C \qquad (2.55)$$

The free energy of reaction (Eq. 2.54) is +33 kcal at 1100°C [69], and it is even more positive at lower temperatures. This reaction is thermodynamically improbable at the temperatures of the solubility measurements. Pepkowitz and Porter [70] cited a ΔF of -19.6 kcal (temperature is not specified) for reaction 2.55, which could therefore be a potential problem in Na_2CO_3 solubility measurements. The standard analytical procedure for determining Na_2CO_3 is the acidification of an aqueous solution of the Na_2CO_3-Na phase and measurement of the evolved CO_2(gas). The sensitivity and accuracy of this technique was also studied as a part of the APDA program. The conclusion was reached that procedural problems in the technique are another potential source for the disagreement between APDA and Williams *et al.* [161].

Although the reactions of NaK with CO or CO_2 have not been studied explicitly, the alloy would probably react according to the respective properties of sodium and potassium individually. Potassium is much more reactive with CO than is sodium as illustrated by the ease of formation of an explosive carbonyl at lower temperatures [415] than the corresponding reaction with sodium. Generalizations about the NaK reactions can probably be made from the published results for sodium by considering the greater reactivity of potassium. The fact that mixtures of Na_2CO_3 and K_2CO_3 melt at lower temperatures than Na_2CO_3 alone [147], should also be considered in assessing the relative importance of carbonates in NaK systems.

(d) *Interactions in the Na(NaK)-C-N System*

Until recently the presence and possible significance of cyanide in alkali-metal coolants have been largely ignored by workers in reactor technology. Although Ornig [422] established the effectiveness of cyanide as a carburizing agent for steel in a fused-salt mixture of cyanide, cyanate and carbonate, no one has detected significant quantities of cyanide or cyanide-producing species under conditions approaching those of a reactor environment. For example, less than 1 ppm cyanide was detected in samples from the primary and secondary coolant systems of Experimental Breeder Reactor No. II (EBR-II), and similar results were obtained with an as-received sample of U.S. Industrial Chemicals Co. (USI) sodium [423]. However, Hobart and Bjork [90] showed that significant quantities of cyanide could be produced by adding various carbon and nitrogen species to Na(liq) at 500 and 700°C. Further, Cafasso [271] reported a solubility of NaCN in Na(liq) at 550°C of 750 ± 110 wppm. If this work is accepted as a true measure of solubility, the warning of Hobart and Bjork about "the possible presence of cyanide in (alkali-metal) systems" assumes renewed importance.

The cyanides are important in two

related areas: first, the carburizing potential of the cyanide species in Na(liq) and, second, the contribution of such species to the total carbon present in the system. This contribution is indeterminate in some of the currently used carbon-analysis techniques. Dutina and Simpson [26] demonstrated by X-ray analysis that NaCN can be recovered intact from an amalgam of a solid-sodium sample deliberately contaminated with NaCN, but the solute form of cyanide in high-temperature Na(liq) has not been studied except for the inferences that can be drawn from the work of Hobart and Bjork [90] and Cafasso [271] and others. Hobart and Bjork were able to produce and detect cyanide by adding $(NH_4)_2C_2O_4 \cdot H_2O$ to Na(liq) at 500°C, at which temperature NaCN is normally solid (~564°C). Their Na_2CO_3-NaN_3, C-N_2, and Na_2CO_3-N_2 additions at 700°C are probably less indicative of true solubility because the melting point of NaCN was exceeded. Similarly it should be noted that Cafasso's solubility was determined very close to this melting point. The work at ANL [424] included a preliminary solubility value of 0.4 wppm NaCN at 500°C which was rejected because of the observed segregation of cyanide on solidification of sodium in the sampling pipettes and the attendant sampling problem. Passing vapor mixtures of Na, CO, and N_2 through a 60-watt lamp [425] also produces NaCN. Since one of the proposed mechanisms [426] for carbon transport in a Na(liq) system involves CO(gas), such a reaction could be important and bears further study.

Thus in many respects the Na-C-N system is similar to the Na-C-O system; e.g., solubilities, solute species, and reaction mechanisms in a Na(liq) environment have not been completely established. Since no specific information about the interaction of NaK with cyanide has been found, detailed study will be required if the indications from current sodium-interaction studies are proved valid. Discussions of other cyanide-producing reactions and a more complete description of the chemistry of NaCN can be found in the work of the Gmelin Institute [145], Mellor [148], and Sittig [150].

(e) *Interactions in Na(NaK)-O Ternary Systems*

The interactions of sodium or NaK with oxides are of interest primarily as they relate to the corrosion of containment materials and oxide fuels or to oxygen gettering as a purification process. Since Na_2O is the stable oxide in oxygen-contaminated Na(liq) or NaK coolants [389] even with as much as 99.8% potassium, a comparison of the thermodynamic stability of a given oxide with respect to Na_2O is a useful procedure. Glassner [427] provided graphical compilations of the free energies of formation of various oxides as a function of temperature. These data or data from the JANAF tables [151] or from Wicks and Block [254] can serve as a basis for such comparisons. Weeks and Klamut [428] pointed out a basic error in using these data indiscriminately for the systems of interest in reactor environments. The free energies of formation of Na_2O and the other oxides depend on the oxygen level in the system as well as on the system temperature; this introduces an additional variable in the calculation. On this basis Ta_2O_5 is said to be thermodynamically stable toward Na(liq) containing ≥ 25 ppm oxygen at 900°C but will be attacked by Na(liq) containing 10 ppm oxygen at the same temperature. Other complications in applying free-energy criteria to Na(liq)-oxide interactions have been discussed by Epstein and Weber [429] and include srrors in measured or calculated thermodynamic data, effects of alloying metals on the formation of the oxide, formation of stable lower oxides, and the surface free energy of the oxide layer. The surface free energy of solid oxides was calculated by Livey and Murray [430], but this effect is usually overshadowed by the other assumptions and approximations in the more rigorous thermodynamic treatments of the Na-O ternary systems.

Several of these more rigorous treatments have been presented, including an updated version [431] of the previously mentioned work of Weeks and Klamut, a calculation of oxygen distribution coefficients in refractory-metal-alkali-metal systems by DiStefano and Hoffman [312], and a report by Kassner and Smith [346] on the use of thermodynamic equilibria as a basis for determining kinetic factors in the Na-O-Nb and Na-O-Ta systems. Each of these approaches involves the postulation of a model for the interactions under study as well as simplifying assumptions about the thermodynamics involved. Some of the problems in constructing such a model for assessing "the role of oxygen in promoting the attack of refractory metals by alkali metals" were listed by Chandler and Hoffman [432]. The list includes the effects of oxygen on the solubility of the refractory metal in the alkali metal, the formation of low-melting eutectics of the various oxides present, the low-melting or sublimation temperatures of certain oxides of refractory metals, and the formation of soluble polyoxides.

The work of Horsley [433] on the Na-O-Fe system provided an early indication of the formation of metastable polyoxides in a Na(liq) environment. His evidence for the existence of $(Na_2O)_2 \cdot FeO$ in sodium contaminated with large amounts of oxygen generated interest in studies of the interactions of other metallic oxides with sodium. Addison and co-workers at the University of Nottingham [434-436], studying the reactions of MoO_2, WO_2, UO_2, Nb_2O_5, and CrO_3 with Na(liq) and K(liq), observed some relatively stable ternary oxides such as $Na_3Mo_2O_6$, $Na_3W_2O_6$, Na_3NbO_4, K_3NbO_4, and Na_2CrO_3. No similar reaction, however, was observed between UO_2 and Na(liq) up to 600°C. Sienko's studies [437] of the solid-state interactions between alkali metals and the transition-metal oxides Sc_2O_3, TiO_2, Ta_2O_5, and WO_3 provided additional information about the basic chemical nature of the ternary oxides. The vapor-phase reaction between sodium or potassium and MoO_3 and WO_3 has also been investigated [438]. Other studies of ternary oxides of this kind have been done by Hoppe [439] and by Hagenmuller *et al.* [440].

Most of the work on the Na(NaK)-O ternary systems, however, has been concerned with corrosion rates and/or oxygen gettering. A complete discussion of these corrosion results is found in Vol. V, Chap. 2. Loftness, Ruebsamen, and Coultas [441] studied the corrosion of a large number of refractory materials in Na(liq), and the corrosion resistance of various ceramic oxides was reviewed by Cook [442]. Kelman [443] considered the effect of NaK on a number of structural materials, and Stang *et al.* [195] provided another general source of information in this area. Additional information can be found in the proceedings of numerous conferences on corrosion and related subjects; for a few of the more pertinent works, see Refs. 444 to 449.

Oxygen gettering by refractory metals is a technique often used for purification of sodium [450, 451]. The basic reaction involved can be represented by

$$aM + bNa_2O \rightarrow M_a O_b + 2bNa \qquad (2.56)$$

where M represents the refractory metal. This reaction is usually subject to the simplified thermodynamic treatment discussed previously. Thus the metal that forms the most stable oxide (i.e., whose ΔF_f per gram atom of oxygen is lowest) is usually the most efficient oxygen getter. On this and other bases, zirconium and titanium have been suggested as prime candidates. Williams [450] found that a 50 wt.% Zr-50 wt.% Ti alloy was more efficient than zirconium alone, but its fabrication qualities were not desirable.

Thermodynamically, uranium is a more efficient oxygen getter than zirconium, and it was previously stated that UO_2 was observed to be stable in a Na(liq) environment up to 600°C. Using the simple free-energy approach, Epstein and Nigriny [452] predicted that UO_2 will not be reduced by Na(liq) at temperatures up to 1000°C. Two factors, however, could complicate the Na(liq)-UO_2 system. The first, indicated by the report of Pepper, Stubbles, and Tottle [453], is that a ternary oxide, Na_3UO_4, can be formed by reacting Na, Na_2O, and UO_2. Epstein and Nigriny, considering this factor in the reduction of otherwise stable oxides by Na(liq), concluded that oxide reduction was indeed possible if such ternary compounds were formed in the reaction. The second complicating factor is the known nonstoichiometry of the UO_2 phase, which can also result in oxygen transfer to the sodium. This complication, although not previously mentioned, is an additional factor to be considered in several other Na(liq)-oxide reactions of interest in reactor technology. For the composition and properties of uranium oxides and a number of other nonstoichiometric compounds, see Ref. 454. A wide variety of procedures [455, 456] has been investigated to protect fuel elements and to ensure that UO_2 will not be attacked by Na(liq).

The interactions of sodium or NaK with SiO_2 merit separate discussion, primarily because of the laboratory use of glass in low-temperature sodium experiments and because quartz is often used as an acid flux in the dry-combustion technique for the determination of carbon in sodium. Consideration of tests run at KAPL and ANL prompted Epstein and Weber [429] to conclude that glass should not be used in Na(liq) systems above 250°C. In a more quantitative experiment by Naud [379] the off-gases from the reaction of Na(liq) with pyrex were collected and analyzed. From these data it was concluded that Na(liq) attacked pyrex at temperatures as low as 150°C, but the nature and vigor of the reaction were different from those at 340°C, as evidenced by the type and quantity of gases produced. Finely divided quartz is said to be attacked by Na(liq) at all temperatures above the melting point of sodium [430], but the more dense bulk material is said [457] to be stable in a Na(liq) environment up to 870°C. A detailed discussion of the Na_2O-SiO_2 system, including phase diagrams, is presented by Glasser [457], and additional information about the behavior of SiO_2 in Na(liq) is given by Mellor [448].

The simple free-energy approach for comparing the thermodynamic stability of a given oxide with Na_2O, which is known to be the stable oxide in sodium or NaK systems, is often useful in predicting the interactions of these alkali metals with structural materials and oxide fuels. Such phenomena as oxygen gettering and the attack of alkali metals on oxide fuels are specific examples of the applicability of this approach. Other considerations, such as the effect of oxygen concentration on the free-energy of formation of Na_2O or other oxides and the chemical formation of ternary oxides, can also be important and have been included in more rigorous models for the behavior of oxygen in the Na-O ternary systems. Other aspects of the interaction of sodium with oxides, the reactions of Na_2O with materials of interest, and reviews of the literature in these areas are provided in the work of the Gmelin Institute [145], Mellor [148], and Sittig.

(f) *Interactions in Na(NaK)-C Multicomponent Systems*

The interactions of sodium or NaK with carbides are of interest for reasons that in many respects parallel those given for oxides. Comparisons of the thermodynamic stability of Na_2C_2 with carbide phases in contact with the alkali metals, however, are of little use since Na_2C_2 is not usually found in the liquid metal [269, 458, 459]. In fact, the exact nature of the carbon-bearing species in a Na(liq) environment has not been unambiguously established (see Sec. 2-4.5). Therefore many corrosion studies were done in multicomponent systems in which carbon is transported through the alkali metal from a phase of high carbon activity to one of lower activity, but the alkali-metal phase itself was considered only as a transfer medium and was not characterized. Some rather different and conflicting transport mechanisms for carbon in liquid sodium have been postulated [426, 460], but each is limited by the lack of definitive species information.

The carburization or decarburization of structural materials can result in undesirable effects such as embrittlement and corrosion. Studies of these phenomena have been largely limited to engineering corrosion tests, which provide a minimum of specific chemical information. The results of these tests are discussed in Vol. V, Chap. 2, from the standpoint of mechanical properties. See Refs. 195 and 442 for specific information about the corrosion and compatibility of various ceramic and cermet compositions in contact with liquid alkali metals. These ceramics and cermets are largely composed of refractory carbides, whose properties make them suitable for use in high-temperature liquid-metal environments such as those envisioned for fast-breeder reactors. Additional general information about Na-C multicomponent systems can also be found in conference proceedings [444-449].

An interesting phenomenon relating to carbon transfer was observed at the liquid-metals laboratory at Culcheth, England, when zirconium was used in a hot-trapping purification scheme for sodium. Although the process was designed to reduce the oxygen content of the sodium, it was observed and reported to Epstein [461] that zirconium was also an effective getter for carbon present in the loop. In this case, the simple free-energy approach seems to be valid since ZrC is a very stable carbide. In some other cases, however, the complications of solubility effects, nonstoichiometry of carbide phases, surface free energy of carbide phases, errors in measured or calculated thermodynamic data, and the inability to calculate the carbon activity (free energy) in the liquid metal make such simple predictions questionable. Basic data are available for the surface free energy of carbides, [430] and Storms [462] provided a good review of the properties of refractory carbides, but the incorporation of this information into an effective model for carburization reactions is difficult, at best.

Perhaps the most widely studied carburization reactions are those involving austenitic stainless steels in multicomponent Na-C systems containing a carburizing phase. [59, 463, 464] It has been postulated that the thermodynamic stability of $Cr_{23}C_6$, which is the normal carbide formed in alloys of 5.7 wt.% chromium or more [465], is fundamental to the carburization reaction. [466] Another stable chromium carbide, Cr_7C_3, has been observed to form in alloys of 0.4 to 5.7 wt.% chromium. The very rapid decarburization of ferritic alloys such as $2\frac{1}{4}$ Cr-1 Mo, in hot sodium [467] cannot be explained by simple thermodynamic arguments. Campbell and Tyzak [466] attempted to provide a model for the carburization of stainless steel and to provide some inferences about decarburization reactions as well.

The problem of the attack of carbide fuels by alkali-metal coolants and the subsequent transfer of carbon to cladding material or other parts of the system has also been the subject for numerous studies. Frost [468], in a comprehensive review of the properties of the carbides of uranium, provided basic information relevant to the interactions of uranium carbides with alkali metals. McKisson *et al.* [469] approached this phenomenon for carbide fuels on the basis of free energy and phase equilibria. Many of the conclusions they reached had been previously verified experimentally by Webb [470] and by Elkins [471]. The major complications in this kind of system, the nonstoichiometry of the fuel carbides and the effects of oxygen, were emphasized by Storms and Huber [472] in their reevaluation of ΔH_f for two uranium carbide compositions. If these complications are considered and are corrected for or eliminated, such systems seem quite amenable to the simple thermodynamic approach. For example, 304 stainless steel was found to be compatible (no carbon transfer) with hypostoichiometric uranium monocarbide (<4.8 wt.% carbon) at temperatures up to 1000°C, but hyperstoichiometric UC (>4.8 wt.% carbon) significantly carburized the stainless steel [471] at 650°C. Therefore the Na(liq) was an efficient carbon-transfer medium when a UC_2 carburizing phase was present but did not transfer carbon from hypostoichiometric UC, which is thermodynamically more stable than $Cr_{23}C_6$.

Among the very few universally valid generalizations about the interactions of carbides with sodium or NaK are: (1) the probable carburization of austenitic stainless steels in the presence of a carbon source, (2) the decarburization of ferritic alloys in the presence of a carbon sink, and (3) the attack on, and subsequent transfer of carbon from, hyperstoichiometric carbide fuels. Until the nature of the carbon species responsible for the observed transport is elucidated, even these generalizations must be used with care. In contrast, the resistance of many ceramic and cermet carbide compositions is well established and seems to be predictable on the basis of thermodynamic-stability data and the physical properties of the materials.

2-4.3 *Interactions with Organic Compounds*

This section deals primarily with the interactions of sodium and NaK with the organic materials which have been considered as auxiliary coolants and with the organic compounds frequently used as solvents or cleaning agents. Sodium is used extensively as a reducing agent in the preparation of organic chemicals. Information relating to this behavior can be found in standard organic chemistry textbooks and reference works.

(a) *Hydrocarbons*

Sodium and NaK are inert toward hydrocarbons that do not have an active hydrogen or an acetylene hydrogen. Alkyne hydrogen atoms are replaced by sodium, and the hydrogen is liberated. At the melting point of sodium, the reaction between acetylene and sodium produces ethylene plus monosodium acetylide [256]; at higher temperatures Na_2C_2 is formed [473]. Substituted acetylenes undergo rearrangements like that in which butyne-1 is formed from dimethyl acetylene [473].

Aryl hydrocarbons are relatively inert to sodium at low temperatures unless an active hydrogen is present. However, benzene can be polymerized to diphenyl at 200 to 300°C in sodium. At higher temperatures the aryl hydrocarbons are decomposed by sodium. McKisson and Horton [474] studied the effect of sodium on tetralin as a function of temperature. A significant amount of decomposition occurred at 360°C (675°F). More-complex aryl compounds tend to react more readily. In general, NaK alloy shows an activity similar to that of pure sodium, although some materials, such as styrene and substituted styrenes, react more readily with NaK than with sodium. Apparently, the potassium is a more active agent than sodium in these systems [473].

(b) *Halogen Derivatives*

Sodium reacts with many halogenated organic materials. In most cases the organic radicals condense with the formation of the sodium halide [148]. The Wurtz, Wurtz-Freund, Fittig, and Wurtz-Fittig reactions are typical. These reactions are usually carried out in suitable solvents and proceed under good control. However, the sodium-organic halide reactions are not always smooth. Polysubstituted halogen derivatives of methane have been found to explode in contact with sodium [145]. The quantitive decomposition of CCl_4 by Na-Hg was reported in 1921 [148, 475]. Further, the use of sodium or NaK alloys with hydrocarbons as detonators was recognized as early as 1925 [476, 477]. "Explosions which previously were difficult to detonate, or which were not detonated at all, are easily detonated with alkali metal using a relatively small quantity of material. The sensitivity of NaK with CCl_4 to shock is 150 to 200 times greater than that of mercury fulminate" [473, 476]. The compounds CH_2Cl_2 and $CHCl_3$, also known to be detonators with NaK, are reported to yield a "very strong" explosion [473]. The CH_3Cl and NaK reaction yields only a "moderately strong" explosion.

Combinations of bromoform and potassium, barium, and carbon tetrachloride, potassium and 1, 1, 2, 2-tetrachloroethane, potassium and pentachloroethane, and potassium and 1, 1, 2, 2-tetrabromoethane have been known to explode spontaneously at room temperature shortly after mixing [413]. Although combinations of these five halogen-substituted hydrocarbons with sodium do not always explode spontaneously, a very dangerous explosion potential exists. Lenze and Metz [413] described other combinations of chemicals and their explosive and combustive tendencies.

(c) *Oxygen Derivatives*

(1) *Alcohols*. Sodium or NaK reacts with alcohols to form sodium alcoholates, RONa, and hydrogen. Primary alcohols react more readily than secondary or tertiary alcohols, and heavy alcohols react more slowly than the lighter ones. For this reason *n*-butyl alcohol is frequently used to dissolve and remove sodium or NaK from components and parts. Ethyl alcohol reacts more rapidly and sometimes catches fire.

(2) *Aldehydes*. Sodium reacts with aldehydes in ammonia solutions, but the reaction may involve the ammonia-aldehyde addition product $R{\cdot}CHOH{\cdot}NH_2$, which has a sodium-replaceable hydrogen and forms $R{\cdot}CHONa{\cdot}NH_2$. Sodium does not react with dry methyl-ethyl-acetaldehyde, but, in the presence of moisture, the aldehyde is reduced to amyl alcohol [478]. Sodium reacts with benzaldehyde to form a number of products, such as benzyl alcohol, benzoin, and benzyl benzoate [473].

(3) *Ketones*. Sodium reacts with ketones to form (1) a sodium derivative, with evolution of hydrogen,

$$R{\cdot}CH_2{\cdot}CO{\cdot}R + Na \rightarrow R{\cdot}CH{:}CONa{\cdot}R + \tfrac{1}{2}H_2 \tag{2.57}$$

or (2) a dimolecular product, such as sodium pinacone,

$$2CH_3{\cdot}CO{\cdot}CH_3 + 2Na \rightarrow [(CH_3)_2CONa]_2 \tag{2.58}$$

In general, if the carbon adjacent to the C-O group has a labile hydrogen, the replacement reaction occurs; in other cases the pinacone reaction occurs. Discussion of the more-complex reactions of sodium with specific aldehydes and ketones [473, 150], is beyond the scope of this book.

(4) *Ethers*. Sodium does not attack the simple ethers, but those which boil above 200°C are rapidly decomposed. The aryl ethers tend to rearrange to form alcohols in the presence of sodium [150].

(5) *Acids*. Sodium reacts with or-

ganic acids to form the sodium salts and hydrogen.

(6) *Esters.* Sodium reacts with most esters to form complex esters [473, 150].

(d) *Nitrogen Derivatives*

(1) *Amines.* Sodium reacts with amines in the presence of metallic catalysts to replace one hydrogen of the $\cdot NH_2$ group, although the rate of the reaction is quite variable [474, 150].

(2) *Imines.* Sodium reacts with imines to form the sodium salts, and, in time, more-complex condensation products.

(3) *Azo Compounds.* Sodium reacts with azo compounds either by adding two sodium atoms or by causing their decomposition with the liberation of nitrogen.

(4) *Nitro Compounds.* Sodium reduces nitro compounds in ammonia or in alcohol solutions. In the absence of such solvent agents, sodium reacts with the nitro group to give compounds having the structure $R \cdot N(Na) \cdot ONa$ [150].

(5) *Nitriles.* Sodium reacts with nitriles to produce amines or to form polymers or a variety of other products [150]. Side reactions from alkyl nitriles include the formation of NaCN plus a variety of alkene products.

2-4.4 *Interaction Kinetics*

Studies of the interaction rates of sodium with a number of materials range from attempts to derive kinetic rate laws to gross measurements of burning rates. The generalizations that reaction rates increase with increasing temperature, gas pressure, and area of contact with solids are aplicable in most cases. The following sections discuss the results of some specific work that falls under the broad definition of kinetics.

(a) *Na-H_2O Reactions*

Addison and Manning [383] studied the sodium-water-vapor reaction at temperatures above 125°C and for water-vapor pressures of 15 to 65 torr. The reaction was smooth and nonviolent. As soon as a continuous layer of NaOH formed on the surface of the sodium (this required a very short time and depended on the temperature and water-vapor pressure), the rate of reaction followed a parabolic law, $\Delta p = kt^{1/2}$, where Δp is the pressure change, t is time, and k is a constant. The diffusion of water vapor through the NaOH film became the rate-controlling step. However, after several seconds the rate dropped below that described by the $t^{1/2}$ relation. Above 300°C the rate study was further complicated by the reaction of the NaOH film with the liquid sodium; the rate of this latter reaction became controlling at the higher pressures studied. The variety of reactions possible in this system, discussed in Sec. 2-4.2 (a), makes definitive kinetic study very difficult.

Furman [479] studied the reaction of dilute water vapor (100 to 400 volume ppm) in helium with sodium at 200 to 350°C. The reaction rate was followed by measuring the amount of hydrogen in the effluent gas at a controlled rate of flow of the incoming gas. At the start of a typical experiment at 138 ppm H_2O and a helium flow rate of 100 ml/min, all the H_2O reaching the sodium surface reacted. As a surface film formed on the sodium, the rate decreased. Hydrogen was detected in the effluent after 4 min of flow, and the rate of hydrogen formation became essentially constant after 9 min. At higher flow rates (e.g., 1000 ml/min) the results were similar, the first hydrogen being detected at a shorter time and the steady state being reached sooner. The surface of the sodium was covered by a discontinuous layer of Na_2O, with bright metal visible in the cracks. The rate of reaction was linear with the H_2O concentration in the helium. The reaction apparently followed the equation

$$2Na(liq) + H_2O(gas) = Na_2O(sol) + H_2(gas) \qquad (2.59)$$

The author postulated that no NaOH was formed because of the low pressure of hydrogen.

A very specific study of the reaction of sodium in dilute amalgams with deaerated liquid H_2O was reported by Shaede and Walker [480]. By careful kinetic studies using scavengers for solvated electrons and hydroxide ions, they concluded that hydrogen atoms are not formed when sodium in dilute amalgams reacts with neutral or alkaline water. The species formed was judged to be solvated electrons, which are then precursors of gaseous hydrogen in unscavenged reactions.

The possibility of gross interaction of water and sodium in large-scale industrial installations has engendered numerous studies of rates of reaction and pressure buildup. The problem is discussed in Vol. III, Chap. 2. Ford's [375] comprehensive survey report on sodium-water reactions includes a discussion of reaction rates applicable to specific reactor situations.

(b) *Na-O_2 Reactions*

The rate of reaction of sodium with oxygen has been studied for solid, liquid, and gaseous sodium. Cathcart, Hall, and Smith [481] used a differential manometer to measure the rate of reaction of solid sodium with dry oxygen passed over hot CuO, Ascarite, and $Mg(ClO_4)_2$ at five temperatures between -79 and +48°C. The most striking feature of the oxidation curves was the slowness of the oxidation rate. The ratio of oxide volume to metal volume for equivalent amounts of metal is much less than 1, and a linear rate of oxidation might be expected according to the Pilling-Bedworth rule [482]. The reaction did not, however, fit an equation of the form $x^n = kt$ (where x is amount of reaction, k and n are constants, and t is time). Since neither a logarithmic equation nor the inverse logarithmic relation of Cabrera and Mott [483] yielded a satisfactory fit, it was concluded that the dry oxidation of sodium does not conform to a conventional mechanism.

A similar method was used by Besson and Touzain [484], to follow the oxidation of liquid sodium in the temperature range 98 to 145°C. With very dry oxygen and triple-distilled sodium, the rate of reaction was slow below 110°C and could be described by the equation $x^n = kt$ for a total time up to three weeks. The value of n fell between 1 and 3, was constant for a given temperature, and was independent of oxygen pressure. The factor k was found to be a function of temperature and pressure. Above 110°C the experiments were less reproducible, the sodium spontaneously igniting during some experiments. The reaction rate after a variable period of time, sometimes several hundred minutes, could be described by $(x - x_0)^n = k(t - t_0)$, where x_0 is the extent of reaction and t_0 is the time after which the oxidation followed a specific rate expression.

Mellor [148] discussed several studies of the reaction of sodium vapor with oxygen.

The effect of the presence of water vapor on the rate of oxidation of potassium and sodium was studied by Hatterer and Thevenin [485], who also list previous work on the oxidation of these metals. Water vapor in the oxygen markedly increased the oxidation rate for solid sodium. The results indicated that water is necessary for potassium to oxidize at a measurable rate at room temperature.

The rate of burning of sodium in air has been studied extensively (see Pool Fires, Vol. III, Chap. 2).

(c) *Na-CO Reactions*

Kinetic studies by Sinclair, Davies, and Drummond [412] in the temperature range 200 to 500°C and CO pressures to 1 atm indicated that the reaction between sodium and CO goes through at least three stages: (1) an initial rapid but small reaction of several minutes' duration, (2) an induction period with slow reaction (up to several hours), and (3) a rapid exothermic reaction. The rate of CO absorption at each stage appeared to be independent of temperature and pressure, but the duration of the first two stages decreased as the temperature increased. Species formed in the reaction are discussed in Sec. 2-4.5 (e).

2-4.5 *Reaction Mechanisms and Chemical Species in Sodium*

This interesting topic encompasses the general area of sodium as a reaction medium. The distinction between two-phase interactions (Sec. 2-4.2) and interactions and species in solution in sodium cannot be clearly drawn at the present state of knowledge, although some attempts to do this are discussed in the following subsections. Mostly, deductions were drawn from observations made in experiments planned for other purposes and were not the basis for definitive reports.

Addison *et al.* [436] discussed the nature of liquid alkali metals as reaction media. Their major conclusion was that species present in sodium can be very different from those found in molecular solvents because of the presence of conduction-band electrons in the liquid metal. They suggested that the usual concepts of stoichiometry in chemical compounds need not prevail, since electrons in atomic orbitals of solute elements can interact with sufficiently energetic conduction-band electrons in the sodium. However, the difficulty in determining what species are present in solution remains since experimental methods generally involve isolation of reaction products by vaporization of the solvent sodium or dissolution of the sodium in an "inert" solvent such as liquid ammonia.

(a) *Metal-Oxygen Systems*

Oxygen is without doubt the most important impurity in sodium from the point of view of corrosion and mass transfer; much work has been reported on O-Na studies and the effect of oxygen on other interactions in sodium. These studies are reported elsewhere in this chapter.

Oxygen in sodium is generally considered to be present as sodium monoxide, Na_2O, since this compound is left when sodium is distilled away from a solution of oxygen in sodium or when the sodium is dissolved in mercury. The monoxide is the most stable compound in the Na-O system [see Sec. 2-4.1 (q)], but no definitive experiments showing that the dissolved oxygen species is indeed Na_2O have been reported. On the basis of experiments on the oxidation of zirconium in liquid sodium, Bowman and Cubicciotti [486] suggested that oxygen might be present as oxide anions, O^{2-}. Nevzorov [487] reported some convincing experimental evidence that oxygen in sodium migrates to the anode when as little as 2 amp (unknown current density) is passed through sodium at 300°C for an hour; greater transfer occurs at higher currents and temperatures. He concluded that the polarization of negative oxygen ions in solution caused the migration of oxygen. An attempt by Andrews, Barker, and Werner [488] was less conclusive. After passing a current at a density of 950 amp/sq in. through sodium for 1400 hr, the analysis of the positive and negative ends of the cell showed 252 and 203 wppm of oxygen, respectively. This difference is not sufficient to permit conclusions to be drawn, considering the uncertainty in sampling and analysis. Attempts at BNL [365] proved inconclusive also. It was thought that mixing may have occurred during or after the tests in this case.

A number of oxygen-metal complexes have been isolated from sodium. The most important of these is the Fe-Na double oxide, $(Na_2O)_2 \cdot FeO$, first identified by Horsley [433]. This compound, like the other double oxides mentioned, was isolated from sodium containing gross amounts of oxygen impurity, but it is reasonable to conclude that similar species exist in solution and provide a mechanism for transport of the metals through a system [489]. Weeks and Klamut [428, 431] gave a plausible thermodynamic argument for the stability of the Fe-Na double oxide in sodium; however, their argument is based on iron-solubility data that are not generally accepted.

The differential stability and/or solubility with temperature of this kind of compound has been suggested by a number of authors [428, 431, 487] to explain material transfer from hot to cold regions in a sodium circuit.

Niobium [490-492], tantalum [493, 494], and molybdenum [495] were found to form double oxides with sodium or potassium in the presence of excess liquid metal. The formation of such compounds is probably responsible for mass transfer of these and other metals in sodium systems. Mausteller and Batutis [496], in radioactive-tracer experiments, found that the transfer of Fe, Co, Ta, Mn, and Sb was strongly enhanced by the addition of 100 ppm of oxygen to the sodium system.

(b) *Metal-Nitrogen Systems*

The interaction of sodium with nitrogen [discussed in Sec. 2-4.1 (n)] is not extensive in a true binary system of the two elements. The presence of other elements in the sodium, especially the alkaline earths and carbon, promotes reaction with nitrogen.

Early observations of sodium-stainless steel systems having nitrogen as a cover gas showed that some degree of nitriding occurred (see Gill and Bokros [309] and Brush and Rodd [310]), indicating that some chemical mechanism exists for introducing nitrogen into sodium. A series of experiments by MSA [497, 478] showed general nitriding when the oxygen level was very high but did not unequivocally relate the nitrogen transport to the presence of other impurities (e.g., Ca or Li) nor show that the nitrogen is transported as a soluble species.

Addison *et al.* [372] found that a significant amount of nitrogen was taken up by sodium with 1 or 2% calcium, strontium, or barium dissolved in it. The apparent compositions of the "compounds" formed were $Ca_{2.41}N$, $Sr_{2.23}N$, and Ba_3N. These compounds were not shown to exist in solution. After removal of the excess sodium by distillation, the residue had no sodium in it; the sodium was reported to be simply the medium in which the metal-nitrogen reactions took place and did not participate in the formation of products.

The addition of carbon to the Ba-Na solution with nitrogen cover gas caused formation of a product that contained barium, carbon and nitrogen. The presence of barium was necessary for the absorption of N_2 below 700°C. The authors postulated that at the lower temperatures barium can donate electrons to the carbon, perhaps as an intercalation complex of electrons in graphite, which then can form various CN_x^{-n} entities. The final product probably has the empirical formula Ba_2CN_4, plus some Ba_3N. Again the question of what is present in the dissolved state cannot be answered, but entities (perhaps ions) of these elements, singly and in combination, must be present.

(c) *Metal-Carbon Systems*

The form in which carbon is present in liquid sodium has been the subject of considerable experimental work and conjecture. The most definitive work, some of which is discussed briefly here, is from the University of Nottingham [256, 372], ANL [115, 267, 499], the Institute for Physical Energy of the Committee for the Utilization of Atomic Energy (Moscow) [426], and the General Electric Vallecitos Laboratory [26, 500]. The transfer of carbon through sodium from one material to another and its importance to reactor technology are discussed in Vol. V, Chap. 2.

Although all the reports cited show evidence of the presence of carbon in liquid sodium, no evidence indicating that carbon is in solution as an elemental entity containing only carbon is presented. In fact, as seen in Sec. 2-4.1 (k), there is some doubt that carbon is soluble to a measurable extent (i.e., a few tenths of a part per million). Carbon can, however, be present in sodium and may exist as particles, perhaps even of colloidal dimensions [271].

Compounds containing carbon have been isolated from sodium in a number of ways. The vapor phase over sodium heated to 300°C in a Knudsen cell was examined on a mass spectrograph by I. Johnson and co-workers [267, 501]. When reagent-grade sodium was used, peaks attributed to hydrocarbon fragments were found at many mass numbers. Masses from 207 to 312 were found, indicating that heavy hydrocarbons may exist in liquid sodium for considerable periods of time. D.L. Johnson [63], who isolated CH_4 from the gas phase over a circulating sodium system using gas chromatography, detected no CO nor CO_2 in any experiments up to his highest temperature, 650°C (1200°F).

Luner and Anderson [267, 502] extracted sodium at 125°C with high-purity nonane in an attempt to remove and identify the compounds whose mass peaks were seen. Spectrophotometric examination of the extracts failed to show any absorption between 2200 and 4000 Å; this indicates that aromatic compounds were not present in amounts as great as 5 ppm of carbon.

Dutina and Simpson [26, 500] found considerable H_2 and CH_4 (several tens of parts per million) in the gases evolved during heating of sodium at 250°C under vacuum and also in the gases evolved during amalgamation of sodium with mercury. Doubting the existence of sodium alkyls, they suggested that the methane arises from the reaction

$$4NaH + C \rightarrow CH_4 + 4Na \tag{2.60}$$

They found no carbonyls but stated that the sensitivity of their identification methods for carbonyls (X-ray diffraction, ultraviolet absorption) was not known. In the acidified aqueous solutions from four different samples of contaminated sodium, they found from less than five to nearly 600 ppm of carbon as cyanide, CN^-.

This work by Dutina and Simpson is part of a program to isolate relatively large amounts of impurities from sodium by distillation, amalgamation, and solution in ammonia. Unfortunately only a few experimental observations have been reported, but interested readers should see current reports from the General Electric Vallecitos Laboratory.

Grundy and Hamer [82] made a similar separation of impurities by dissolving away the sodium with mercury, as in an analysis for oxygen by the amalgamation method, and examining the gases evolved by mass spectrometry. After amalgamation they dissolved the residue in water, added acid, and observed the spectra of the gases at each step. Their sodium was taken from operating sodium systems and sampled in nickel; then a 2-g core was cut from the sodium in the sample cup. The components of the gas evolved during each operation were

Amalgamation:	H_2, CH_4, C_2H_4
H_2O solution of residue:	H_2, CH_4, C_2H_2
Acidification of H_2O:	CO_2

Grundy and Hamer suggested that the methane found could have been present in the sodium in solution either as methane or as methyl sodium, $NaCH_3$. They postulated that other sodium alkyls may be the precursors of the heavier hydrocarbons noted in various other studies.

Addison *et al.* [256], studying the reaction of acetylene with sodium, postulated a two-step mechanism:

$$2Na + 2C_2H_2 \rightarrow 2[Na^+(C_2H)^-] +$$

2H (atomic) on the Na surface (2.61)

$$2H + C_2H_2 \text{ (adsorbed ?)} \rightarrow C_2H_4 \quad (2.62)$$

Adding these two reactions gives

$$2Na + 3C_2H_2 \rightarrow 2[Na^+(C_2H)^-] + C_2H_4 \quad (2.63)$$

They substituted methylacetylene for acetylene and reported that this mechanism was verified in general. In practice, however, some H_2 is also formed. They reported that, when the vapor space over the sodium was evacuated to remove C_2H_4 and H_2, the Na_2C_2 formed remained on the surface of the sodium. These results suggest that stable hydrocarbon species may be present in sodium, but there is no way to show that they are actually dissolved.

Lyashenko and Nevzorov [426] studied the transport of carbon through sodium, as measured by the carburization and decarburization of various metals. The carbon transport was thought to depend completely on the presence of oxygen; i.e., no pure carbon species seemed to be responsible for carrying carbon throughout the system.

(d) *Metal-Hydrogen Systems*

Hydrogen interacts with liquid sodium to an appreciable extent, as noted in Sec. 2-4.1 (b). The hydrogen species existing in sodium is not known, however. Addison *et al.* [158] wrote, "There is no existing evidence on which we can base conclusions regarding species present in solutions of hydrogen in liquid sodium." They suggested that the dissolved species is not NaH, H^+, or H_2 but is more probably H^0 or H^- and pointed out that the concept of unit charge on a dissolved hydrogen atom is not valid in liquid-metal solutions. Williams *et al.* [382], studying various equilibria in the Na-H-O system, concluded that NaH is stable in liquid sodium and has a measurable solubility but said nothing explicit about the species actually present in the solution. A discussion of hydrogen and carbon species in sodium is included in Sec. 2-4.5(c).

(e) *Metal-Carbon-Oxygen Systems*

Undoubtedly the presence of oxygen in sodium systems greatly influences the amount of carbon that can be carried by the sodium. Without concerning ourselves with whether the carbon found was actually in solution [see Sec. 2-4.1 (k)] we should note that Gratton [264] found a significant enhancement of the apparent solubility of carbon when the oxygen level in the sodium was increased from 40 to 260 ppm. Lyashenko and Nevzorov [426] found that carbon transfer in sodium systems requires the presence of oxygen in the sodium. Their experiments showed that much more carbon was transferred under some conditions than corresponded to a C:O ratio of 1:1; this indicates that the carbon was transferred in the form of an oxygen complex that was then decomposed.

Miller [416] found that the product of reaction of CO with sodium was "hexasodium hexacarbonyl," $(NaCO)_6$, and that this compound was stable in contact with sodium at 280 to 340°C. It must therefore have a certain solubility in the sodium and can constitute a possible carbon-containing species in liquid sodium. The same reaction (CO + Na) was studied in detail by Sinclair *et al.* [412], who isolated the sodium salt of hexahydroxybenzene, the sodium salt of tetrahydroxy-*p*-benzoquinine, and sodium rhodizonate ($Na_2C_6O_6$) from the reaction at various stages. At early stages of the reaction, no such products could be isolated by distilling away the excess sodium at 300°C even though a significant amount of CO had been absorbed by the sodium. Therefore it might be conjectured that the form in which the carbon was present in the sodium was a precursor to the compounds isolated and was perhaps a C-O species which had not yet formed the stable six-membered carbon ring and which was decomposed to volatile species at 300°C.

Sodium carbonate is a product of many reactions in liquid sodium in which both carbon and oxygen are present, but it has not been shown that there is a dissolved carbonate species that is important as a carrier of carbon in sodium systems. Oxygen seems to be necessary for carbon to be present in sodium, and, in the very dilute systems encountered when sodium is used as a heat-transfer medium, the important species contain both carbon and oxygen in some as yet unresolved stoichiometry or configuration.

(f) *Metal-Hydrogen-Oxygen Systems*

Various experiments have shown that there is an important interaction between hydrogen and oxygen in liquid sodium, as discussed in Sec. 2-4.2(a) and 2-4.2(e). Although the actual species present in the sodium are not determined, a soluble O-H species in equilibrium with H_2(gas) over the sodium was shown to exist by Woollen *et al.* [384] and Addison *et al.* [372]. Woollen's group injected superheated steam into liquid sodium at 282 to 450°C and found only hydrogen in the off-gas; no oxygen or water vapor was detected. When argon was subsequently injected in place of the steam, in effect reducing the hydrogen overpressure, more hydrogen appeared in the off-gas as the equilibrium shifted. Addison's group noted that the addition of only a few parts per million of oxygen to a sodium system with a given equilibrium hydrogen overpressure markedly alters the hydrogen pressure; this implies a reaction in the sodium between hydrogen and oxygen in some form. It is convenient and useful to talk of hydroxide ion in liquid sodium, and the equilibria that can be written [see Sec. 2-4.2(a)] based on identifiable gaseous species support this assumption. There is, however, no experimental evidence that the O-H species in sodium does contain a 1:1 ratio of oxygen to hydrogen or has a particular charge associated with it.

(g) *Metal-Carbon-Nitrogen Systems.*

A familiar analytical-chemistry procedure to detect nitrogen in organic compounds involves fusion with sodium and subsequent test for the presence of cyanide ion in aqueous solution. It can be inferred, therefore, that carbon and nitrogen can react in sodium to form cyanide. Addison *et al.* [372] found no reaction of nitrogen cover gas with sodium containing carbon unless the temperature of the sodium was 700°C or higher. At this temperature they postulated that conduction-band electrons in the sodium are sufficiently energetic to activate the carbon and enable it to react with nitrogen. If this reasoning is correct, they pointed out, nitrogen-to-carbon ratio in the sodium should vary with the sodium-to-carbon ratio; this was the case in their experiments. However, the carbon cannot be in solution to a very great extent [see Sec. 2-4.1(k)], so the reaction must be a heterogeneous one. The observation that NaCN is the residue left after removal of the excess sodium by distillation can only imply that a C-N species is present in solution in sodium. The observations of Addison *et al.* on the addition of carbon to a Ba-N_2-Na system are discussed in Sec. 2-4.5(b).

Hobart and Bjork [20] found CN^- in the aqueous solution of sodium which had been heated to 500 to 700°C with large amounts of oxalate, carbonate, or carbon as carbon sources and NaN_3 or nitrogen gas as nitrogen sources. The CN^- found corresponded to 8 to 68% of the carbon added, with nitrogen in excess. The solubility of NaCN in sodium is discussed in Sec. 2-4.2(d).

The isolation of cyanide from sodium solutions is a strong indication, but not proof, that an entity containing a chemically bound C-N grouping exists in solution.

Appendix 2-A

SUPPLEMENTAL ANALYTICAL METHODS FOR IMPURITIES IN ALKALI METALS*

Item	Impurity	Method	Ref.*
1	Ag	See items 91 and 96.	
2	Al	See items 90 and 95.	
3	As	Arsenic can be determined in a number of metals, including sodium, by a procedure based on the Marsh test. The arsenic mirror formed is dissolved in iodine chloride and hydrochloric acid, and the sample is titrated with iodate using an extraction end point.	a
4	Au	See item 96.	
5	B	The sodium sample is completely dissolved in water; then the solution is neutralized and evaporated to dryness, and the residue is extracted with slightly acid ethyl alcohol. The alcoholic extracts are made alkaline and evaporated in the presence of a small amount of glycerol. First curcumin solution and then an oxalic-hydrochloric acid solution are added to the residue. The color is developed for 1 hr at 60°C. The color of the boron-curcumin complex is read at 550 mμ. The reported accuracy is ±20% relative, and the method can be applied to samples containing 1 or more ppm of Boron. The average recovery is 72%.	b
6	B	See items 92 and 96.	
7	Ba	See items 92 and 94.	
8	Be	See item 92.	
9	Bi	In acid solution containing gelatin, bismuth with bromopyrogallol-red forms a blue color, the extinction of which is measured at 635 mμ. The solution is maintained at pH 2 and at a constant ionic strength of 0.2 by adding of KNO_3. The precision (6 determinations, 95% confidence level) is ±6.7% for 0.1 to 0.5 μg, ±5.2% for 0.5 to 1 μg, and ±3.2% for 1 to 5 μg Bi/ml.	c
10	Br	See item 95.	

---

*See reference list at the end of this appendix for lettered references; numbered references are those cited in text (references previously discussed are not included). Some references are taken from E.E. Garcia and B.D. LaMont, *An Annotated Bibliography of Analytical Methods for Alkali Metals*, USAEC Report WCAP-2540, Westinghouse Electric Corp., March 1961.

Item	Impurity	Method	Ref.
11	Ca	Calcium is titrated to a visible end point with an EDTA salt (disodium ethylene-diaminetetraacetate dihydrate). Calcein indicator is used to make the method applicable in the presence of magnesium.	107
12	Ca	Calcium in an alcoholic solution of NaK is titrated with EDTA using Eriochrome Black T as an indicator. A small amount of cyanide is added to eliminate the interference of trace metals. Any magnesium present is also titrated. This procedure is designed for the determination of 50 to 1000 ppm of calcium in NaK.	136
13	Ca	The sample, containing 0.1 to 1 mg Ca and 1 g Na is acidified and diluted to volume. The flame intensity is measured at 622 mμ and referred to a calibration curve made with solutions containing 1 g Na in 100 ml and 0 to 100 ppm Ca. For 0.1 mg the error is 30% and for 1 mg 3%.	d
14	Ca	A 5- to 50-g sample of sodium is dissolved in ethyl or methyl alcohol, acidified with hydrochloric acid, evaporated to dryness, and baked at 110 to 130°C for 4 to 12 hr. . The weight of this residue gives the total sodium as NaCl. Water is added to the residue to form a saturated solution, which is cooled to 0°C and saturated with dry hydrogen chloride. The supernatant solution is filtered through a porous glass filter. Potassium (as perchlorate), calcium (as oxalate), and magnesium (as oxinate) are determined in the filtrate. Good results are reported in samples containing 3 to 8 mg K, 0.1 to 0.4 mg Ca and 0.4 mg Mg.	e
15	Ca	Microgram amounts of calcium in reactor-grade sodium are determined in 1- to 1.5-g samples. The samples are dissolved in ethyl alcohol and converted to the chloride. Calcium is precipitated with sodium naphthalhydroxamate, and the precipitate is dissolved in EDTA. The amount of the highly colored naphthalhydroxamate released is proportional to the calcium present. The absorbance is measured at 410 mμ for amounts of calcium over 10 μg. A tenfold increase in sensitivity is obtained by reading at 339 mμ.	f
16	Ca	See items 92, 94, 95 and 96.	
17	Cd	Cadmium is determined by solvent extraction of the complex formed between 2,2'-bipyridyl-Fe II and CdI_4^{2-}. The solution is added to 2,2'-bipyridyl-$(NH_4)_2SO_4 \cdot FeSO_4 \cdot 6H_2O$-KI reagent, the pH adjusted to 6.5 with dilute H_2SO_4 or dilute NaOH, and the complex extracted by shaking with 10 ml of dichloroethane. The mixture is set aside for 20 min, and then the organic layer is transferred to a flask containing anhydrous Na_2SO_4 (1 g) and shaken till the solution is trans-	g

Item	Impurity	Method	Ref.
		parent. The extinction is measured at 526 mμ with dichloroethane or a reagent blank solution as reference. Beer's law is obeyed from 0.4 to 2.8 ppm of Cd^{2+}. The color is stable at 15 to 20° for > 6 hr. There is no interference from up to 1500 ppm of NO_3^-, Cl^-, or SO_4^{2-}, or 40 ppm of Zn(II), but as little as 0.4 ppm, of Pb(II), Hg(II), or Bi(III) interferes; EDTA causes serious interference.	
18	Cd	The sample (1 to 2 g uranium metal, oxide or other insoluble compound) was converted into the nitrate, which, after dissolution in 20 ml of 5*N* HNO_3, was extracted (the apparatus is described) with 200 ml of tributyl phosphate-kerosine (1:10). If the separated aqueous phase contained 0.05 to 1.5 μg Cd per ml, it was evaporated to dryness, the residue was dissolved in 1 ml of 1*N* HNO_3, and the solution, diluted to 5 ml with methanol, was sprayed into a 15-cm acetylene-air-nitrogen flame. The absorption of cadmium at 2288 Å was compared with that produced by a standard cadmium solution. The sensitivity and coefficient of variation of the method were 0.015μg Cd/ml and 1.5% at 0.5 μg/ml, respectively. If the aqueous phase contained 0.003 to 0.1 μg Cd/ml, the residue after evaporation was dissolved in 1 ml of 1*N* HNO_3, and the solution was made up to 5 ml with H_2O. The absorption was measured by using an oxyhydrogen flame in a 70-cm absorption cell. The sensitivity and coefficient of variation were 0.001 μg Cd/ml and 8% (at 0.007 μg/ml), respectively.	h
19	Cd	See item 96.	
20	Cl	Spectrophotometry of silver with copper diethyldithiocarbamate (I) solution in benzene was used to determine Cl^- down to 1 μg by proportion of AgCl from HNO_3 solution of pH 1.0 to 2.0 in the presence of phenolphthalein (as carrier for the AgCl) and determination of unconsumed Ag^+. Other halides, CrO_4^{2-}, $Cr^{7}O_{7}^{2-}$, and cations that react with copper diethyldithiocarbamate interfere.	i
21	Cl	Clark's method using $Hg(NO_3)_2$-diphenylcarbazone was modified. The neutral test solution (10 ml) containing 0.1 to 1.0 ppm Cl^- is shaken with 1 ml each of 0.025*N* HNO_3 and a solution 550 micromoles in both $Hg(NO_3)_2$ and KBr, benzene (10 ml), and 0.02% ethanolic diphenylcarbazone (1 ml). The extinction is measured at 562 mμ. From 0.01 to 0.2 ppm Cl^- can be determined in a 50-ml sample by use of 1 ml 0.1*N* HNO_3.	j
22	Cl	See items 95 and 96.	
23	Co	The sodium metal is reacted with water and neutralized with hydrochloric acid, and the cobalt is determined by reaction with 2-nitroso-1-naphthol. The colored complex	k

Item	Impurity	Method	Ref.
		is extracted with carbon tetrachloride, and the absorbance is measured at 535 mμ. As little as 0.1 ppm Co can be detected in sodium metal by using a 10-g sample.	
24	^{60}Co	Cobalt-60 is determined by a carrier technique using an ion-exchange-separation procedure. The cobalt fraction obtained from ion-exchange separation is prepared for counting by precipitation as $2K_3Co(NO_2)_6.3H_2O$ by the addition of potassium nitrite in the presence of acetic acid.	98
25	Co	Cobalt is determined by activation analysis in which the sodium is irradiated in the MTR. The sample is completely dissolved, known amounts of inactive carriers are added, and the sample is treated with HF-HNO_3-H_2SO_4 and then with H_2O_2. Gross separations of the elements and decontamination steps follow. The samples are counted on standard β-counting equipment.	
26	Co	See items 90, 91, 92, 93 and 94.	
27	Cr	Microgram amounts of chromium are determined in concentrated solutions of alkali metals by extraction in the sexivalent state with a 0.2*M* solution of tri-*n*-octylphosphine oxide in benzene from either a chloride or sulfate solution. The chromium-diphenylcarbazide complex is then formed directly in the benzene solution by addition of an alcoholic solution of diphenylcarbazide. As chromium is extracted only in the sexivalent state, an oxidant is added. Argentic oxide was found to be a satisfactory oxidant in sulfuric acid solutions. The coefficient of variation of the method was 9% for 2 to 10 μg of chromium.	*l*
28	Cr	Chromium is determined colorimetrically with *s*-diphenylcarbazide reagent after oxidation with ammonium persulfate.	107
29	Cr	Small amounts of chromium and vanadium are separated from the alkali hydroxide solution by means of Dowex-1 in hydroxide form. Chromium and vanadium are absorbed from a 1*M* solution of the hydroxides and eluted together by 2*M* ammonium carbonate. The eluate is evaporated to small volume, and aliquots are taken for the determination of chromium with diphenylcarbazide and of vanadium by the indirect ferrous-*o*-phenanthroline method.	*m*
30	^{51}Cr	Chromium-51 is determined by a carrier technique using an ion-exchange-separation procedure. The chromium fraction obtained from ion-exchange separation is prepared for counting by precipitation as $BaCrO_4$ from an ammonium acetate buffer solution.	98
31	Cr	See items 90, 91, 92 and 93.	

Item	Impurity	Method	Ref.
32	Cs	Cesium, (as well as rubidium) is determined spectrographically in sodium metal by the following method: Cesium is concentrated by passing a solution of the sample through an ion-exchange column. The cesium is eluted from the resin with dilute hydrochloric acid, and the solution is subjected to analysis by the Lundegardh flame technique. Rubidium is determined directly on a solution of the sample. The precision of the method is estimated to be ±20% (99.5% confidence level). Cesium concentrations of > 0.2 ppm (and rubidium concentrations of > 5 ppm) can be determined. Cesium (as well as rubidium) is determined spectrographically in Na-K alloy by the following method: The sample is dissolved in methanol, dilute hydrochloric acid is added, and the resultant solution is evaporated to dryness. The residue is dissolved in 1% hydrochloric acid, and cesium and rubidium are determined by the Lundegardh flame technique on a Hilger Large Glass Prism Spectrograph. Cesium concentrations of > 50 ppm (and rubidium concentrations of > 10 ppm) can be determined. The precision of the method is estimated to be ±20% (99.5% confidence level).	*n*
33	Cs	See items 84, 85 and 88.	
34	Cu	Two metals are described. Copper is determined spectrophotometrically by using neo-cuproine or by atomic absorption spectrophotometry (AAS) after the copper is separated from the sodium by coprecipitation with the lanthanum hydroxide. The neo-cuproine procedure, which does not require separation of sodium, is more precise, but somewhat more limited in sensitivity than AAS, and is more subject to interferences from other impurities.	*o*
35	Cu	Copper is determined by a colorimetric method using biquinoline. The method was verified from 1 to 10 ppm.	358
36	Cu	See items 90 and 94.	
37	Fe	Iron is determined colorimetrically with *o*-phenanthroline reagent.	107
38	Fe	This method describes the determination of iron in potassium, molybdenum, and tantalum. Iron is reduced to the bivalent state with ascorbic acid and hydroxylamine hydrochloride. The Fe(II), which forms a red complex with bathophenanthroline, is determined spectrophotometrically. Ammonium tartrate is added to complex the molybdenum and tantalum, and boric acid is present to complex the fluoride ion. The standard deviation from 1 to 12 μg is 0.7 μg Fe. Standard deviation from 80 to	358, *p*

Item	Impurity	Method	Ref.
		100 μg is 3.1 μg and from 100 to 250 μg, 5.9 μg Fe. The method is adapted from that reported by Penner and Inman.	
39	^{59}Fe	Iron-59 is determined by a carrier technique using an ion-exchange-separation procedure. The iron fraction obtained from ion-exchange separation is prepared for counting by precipitation as $Fe(OH)_3$ by means of ammonium hydroxide.	98
40	Fe	See items 90, 92, 93, 94 and 95.	
41	Hf	A procedure based on the extraction of zirconium ions with a solution of tri-*n*-octylphosphine oxide in cyclohexane and the formation of a zirconium-catechol violet complex in the organic extract, is successfully applied to the determination of zirconium (20 to about 1000 ppm) in niobium. Alloying amounts of Cr, Co, Mo and W do not interfere. Hafnium ions are also extracted into a solution of tri-*n*-octylphosphine oxide in cyclohexane. Hafnium produces a colored complex with catechol violet in the organic extract; the procedure is therefore equally applicable to the determination of hafnium provided that zirconium is absent and can be used to determine hafnium and zirconium in alkali metals.	*q*
42	Hg	A spectrochemical method is used for the determination of mercury in sodium or Na-K alloy in concentrations as low as 0.5 ppm. The mercury is isolated from the sodium or NaK by amalgamation on copper powder in an acidified chloride solution. The dried copper powder is arced in a conventional d-c arc, a special electrode cap being used to ensure reproducible volatilization of the mercury. The analysis line used is Hg: 2536.5. No internal standard is used, and the accuracy of the method is ±20% of the amount of mercury present.	*r*
43	Hg	See item 91.	
44	In	See item 96.	
45	K	Potassium must be separated from the bulk of the sodium to determine 1 to 10 ppm by flame photometry. Sodium metal is dissolved in methanol, neutralized with hydrochloric acid, and the methanol removed by evaporation. To the NaCl residue, 500 μg of ammonium ion are added, and potassium and ammonium are precipitated with tetraphenylboron reagent. The precipitate is dissolved in a mixture of tetrahydrofuran-water, and potassium is determined by flame photometry. At 1 ppm the error is ±5%. A blank is carried through the procedure.	*s*
46	K	Potassium is determined by flame photometry. The sample is dissolved in deionized water in an inert atmosphere and	107

Item	Impurity	Method	Ref.
		acidified with hydrochloric acid. The potassium content is compared against standards made up in a matrix similar to the unknown sample. The luminosity (percent transmittance) is read at 766 mμ against a deionized water blank by using a Beckman DU flame spectrophotometer with a didymium filter.	
47	K	Potassium is precipitated by tetraphenyl boron from a cold, dilute hydrochloric acid solution. The reagent will precipitate K, Cs, Rb, Hg, Ag and ammonia but will not precipitate sodium. Only two of these interferences must be considered, ammonia and mercury. Care must be taken to avoid ammonia contamination during the procedure. NaK samples are dissolved in mercury and subsequently extracted from the amalgam with sulfuric acid, in which mercury has limited solubility. This procedure is designed for the determination of 10 to 25 mg K in as much as a tenfold excess of sodium.	136
48	K	Potassium is precipitated as potassium cobaltinitrite containing ^{60}Co. Before precipitation, 0.5 to 0.8 g of sodium is dissolved in methanol, neutralized with hydrochloric acid, and diluted to volume. An aliquot of the solution is acidified with acetic acid, and the potassium is precipitated with the cobalt salt.	*t*
49	K	See items 14, 92, 94, 95 and 96.	
50	Li	Lithium [and potassium - see Sec. 2-3.6(c)] are determined in a buffered solution using a flame photometer adapted with a large-bore oxygen-hydrogen burner. The measured emission is compared with the emission from the known standard solution. The sodium concentration must stay below 1.5 mg/ml, or sodium emission will interfere with the lithium and potassium lines.	98
51	Li	Lithium is determined by flame photometry. The sample is dissolved in deionized water in an inert atmosphere and acidified with hydrochloric acid. The potassium content is compared with standards made up in a matrix similar to the unknown sample. The luminosity (percent transmittance) is read at 670 mμ against a deionized water blank using a Beckman DU flame spectrophotometer with a didymium filter.	107
52	Li	See items 92, 94 and 96.	
53	Mg	See items 14, 90, 92, 94 and 95.	
54	Mn	Manganese is oxidized to the red-violet permanganate ion in an acid solution with ammonium persulfate. Photometric measurements are made with a spectrophotometer at approximately 535 mμ, and the optical density is related to a standard curve.	98

Item	Impurity	Method	Ref.
55	Mn	Manganese is determined spectrophotometrically as the permanganate ion. The manganese is oxidized with potassium periodate to the permanganate ion, and the optical density of the unknown is compared with standard solutions at 535 mμ.	358
56	^{54}Mn	Manganese-54 is determined by a carrier technique using an ion-exchange-separation procedure. The manganese fraction obtained from ion-exchange separation is prepared for counting by precipitation as $MnNH_4PO_4.H_2O$ from an ammoniacal phosphate solution.	98
57	Mn	See items 90, 92, 93 and 94.	
58	Mo	The determination of molybdenum and tungsten in niobium involves the formation of the intensely colored complex of molybdenum with toluene-3,4-dithiol in an aqueous medium, its extraction into carbon tetrachloride, the reduction of tungsten, and the formation and extraction of its complex. The recommended reagent is stable for at least 90 days. Both the molybdenum and the tungsten dithiol complexes are formed quantitatively within 5 min. Interlaboratory evaluation of the method reveals standard deviations of about 1.5% within laboratory and about 2.9% between laboratories. The method is valid in the presence of alkali metals and most other metals.	*u*
59	Mo	Molybdenum is determined by developing a red-colored complex with a mixture of sodium thiocyanate and stannous chloride. Butylacetate is used to extract this complex. The optical density, measured photometrically at 515 mμ, is related to a standard curve.	98
60	Mo	Dithiol reacts with molybdenum in solution to give the green complex of Mo(VI). Iron(II) added as ferrous sulfate accelerates the reaction between dithiol and molybdenum at room temperatures. Citric acid complexes tungsten and prevents its reaction with dithiol, and boric acid is present to complex the fluoride ion. The average standard deviation from 1 to 50 μg is 0.5 μg Mo. The method is based on that published by Sandell.	99, 358
61	Mo	See items 90 and 92.	
62	Nb	4-(2-Pyridylazo)-resorcinol (PAR) forms a 1:1 purple-colored complex (λ_{max} = 550 mμ) with Nb(V) in an acetate-tartrate medium at pH 5.8. This is suitable for the spectrophotometric determination of niobium to 0.1 ppm. The color is formed within 45 min and is stable for several days thereafter; the molecular extinction coefficient, $\varepsilon_{550\ m\mu}$ = 38,700, is as high as that reported for the well-known thiocyanate procedure, and the stability is very much superior. The interference of over 40 ions was	

Item	Impurity	Method	Ref.
		examined at 1000 µg in the presence of excess of cyanide and EDTA; only U(VI), V(V), and phosphate interfere. Vanadium may be masked by addition of zinc ions and uranium by ammonium oxalate. 1000 µg of tantalum exhibit weak color formation with the reagent, but this can be eliminated with only a slight decrease in the sensitivity of the niobium reaction by the addition of larger amounts of tartrate. This procedure does not necessitate an extraction and is easier to operate than the standard methods. The method is valid in the presence of alkali metals, molybdenum, and titanium.	
63	Nb	In strong hydrochloric acid solutions niobium forms a yellow thiocyanate complex that is extracted with di-ethyl ether and can be determined spectrophotometrically. Tartaric acid is added to prevent hydrolysis of tantalum, stannous chloride is added to reduce the iron, and boric acid is present to complex the fluoride ion. The method used is that of Bukhsh and Hume (*w*). The average deviation from 20 to 70 µg Nb is 2.2 µg.	358, *w*
64	Nb	Niobium is determined by colorimetry using 4-(2-pyridylazo)-resorcinol. The method was verified from 5 to 30 ppm ±5%.	358
65	Nb	The standard comparator method of activation analysis was used to determine the niobium and zirconium content of equilibrated sodium samples. The limits of measurement are estimated at 2 µg Nb and 1 µg Zr; this corresponds to ∿ 0.1 ppm for a 15-g sample.	327
66	Nb	See item 92.	
67	Ni	Nickel is determined colorimetrically with dimethylglyoxime reagent. The sodium metal is dissolved under an inert atmosphere with methanol. Water is added to methanol solution, and the combined solution is heated to evaporate the methanol. Ammonium citrate, iodine solution, and dimethylglyoxime are added to an aliquot of the sample containing less than 0.3 mg of nickel in a 50-ml volume. After 10 min the optical density is read against a reagent blank at 540 mµ.	107
68	^{63}Ni	Nickel-63 is determined by a carrier technique using an ion-exchange-separation procedure. Nickel is determined by a radioactive technique using ^{63}Ni as the tracer. The nickel is separated from the sodium by standard carrier technique. The isotopically exchanged nickel is electrolytically deposited on a platinum tab for counting in a windowless proportional counter using high-purity methane as the ionizable gas.	368

Item	Impurity	Method	Ref.
69	Ni	See items 90, 92, 93, 94, and 95.	
70	P	The phosphorus is converted to a phosphate and determined spectrophotometrically as molybdenum blue. The sensitivity of the method is 1 ppm. The method is applicable to alkali metals.	358
71	P	The heteropoly blue colorimetric method is used to determine phosphorus at an optimum concentration range of 0.1 to 1.2 ppm. Orthophosphate and molybdate ions react in dilute acid to form molybdophosphoric acid, which is reduced by hydrazine sulfate in 1*N* H_2SO_4 at 100°C to give the heteropoly blue color. The absorbance is read at 830 mμ in 1-cm absorption cells and conforms to Beer's law. The following ions do not interfere: Al, Cd, Cr(III), Cu(II), Co(II), Ca, Fe(II), Mg, Mn(II), Ni, Zn, ammonium, chloride, bromide, acetate, citrate, silicate, fluoride, vanadate, and borate. Tin(II), nitrate, and arsenate do interfere.	111
72	Rare earths	A carrier distillation method for quantity determination of trace amounts of rare earths in HCl solution evaporated on graphite matrix can be applied to the analysis of all rare-earth elements. The detection limit obtained for individual elements was from 0.02 to 0.16 γ/sample (except for ytterbium, when it was 0.0008 γ/sample). The deviations of the analytical curves for the individual rare-earth elements were investigated as they are affected by addition of all other rare-earth elements in concentrations at the upper limit of the procedure. It was established that the influence of additional elements varies for each element and for the different lines of the same elements. The interpolation error for maximum difference in composition between the sample and spectrographic standards was calculated in 30 references.	x
73	Rare earths	A spark is struck between a pellet, prepared from the mixed oxides and carbon powder (1:9), and an upper carbon electrode, and the spectra are photographed. The comparison element is scandium, added as Sc_2O_3 (1.25 parts per 100 of oxides). The analytical pairs of lines (Å) used are for europium [Eu(II) 3907.11 and Sc(I) 3907.48, or, with <50% of Dy_2O_3 in the mixed oxides, Eu(II) 3688.44 and Sc 3651.80]; for terbium in the presence of <20% of dysprosium [Tb 3324.40 and Sc(II) 3372.15, with higher concentration of dysprosium, the sample is diluted with Y_2O_3]; for holmium [Ho 3456.00 and Sc(II) 3372.14 - the results are practi-	y

Item	Impurity	Method	Ref.
		cally independent of the concentration of dysprosium]; for thulium [Tm 3131.26 and Sc(II) 3372.15 - erbium and holmium do not affect the results, but >60% of dysprosium does]; and for lutetium [Lu 3077.60 and Sc(II) 3372.15 - the accuracy is practically independent of the concentration of yttrium].	
74	Pb	See item 90.	
75	Rb	See items 32, 91, 92, and 94.	
76	Re	This method is a simple, sensitive, and accurate spectrophotometric determination of rhenium based on complexation with α-furildioxime. The rhenium-dioxime complex is formed on reduction of perrhenate by tin(II) chloride in the presence of a large excess of α-furildioxime. The absorbance of the complex is measured at 532 mμ. Beer's law is followed within 0.2% for 20 to 300 μg of rhenium in 50 ml of solution. The method is free from most interferences, except molybdenum, which is overcome by prior extraction of the molybdenum-ethyl xanthate complex by chloroform. The method was later modified so that molybdenum and tungsten could be determined in the same solution as the rhenium. Rhenium was extracted into chloroform as the tetraphenylarsonium complex, and a color developed with furildioxime was measured spectrophotometrically. The sensitivity could be increased by reducing the volume of the final solution from 50 to 25 ml. The method was successfully applied with improved sensitivity to alkali metals. The method is valid in the presence of alkali metals, copper, molybdenum, tungsten and many other metals.	*z, aa*
77	S	Sulfur is oxidized (wet) to sulfate and reduced to sulfide, which is determined spectrophotometrically with *p*-amino-dimethylaniline. The sensitivity of the method is 1 ppm. The method is applicable to alkali metals.	358
78	S	See item 96.	
79	Sb	See item 91.	
80	Si	The heteropoly blue colorimetric method is used to determine silicon in the concentration range of 10 to 60 μg/100 ml solution using a cell depth of 1 cm. Molybdosilicic acid is formed at pH 1.6 and reduced to the heteropoly blue. After 20 min the absorbance is read at 815 mμ. The color is stable for 12 hr. The absorbance conforms to Beer's law.	111
81	Si	See items 90 and 95.	

Item	Impurity	Method	Ref.
82	Sn	See item 90.	
83	Sr	See items 91, 92, and 94.	
84	Ta	Tantalum is extracted from hydrochloric acid-hydrofluoric acid solution into isobutyl methyl ketone and back-extracted into buffered EDTA solution. The excess of fluoride is complexed with Al(III). Phenylfluorone is then added to form the colored tantalum-phenylfluorone complex, and its absorbance is measured at 530 mμ on a spectrophotometer. The method can be used in the presence of alkali metals. Niobium and tin show serious interferences.	bb
85	Ta	Phenylfluorone forms a bright red complex with tantalum in slightly acid solution. Interference from some metals present as impurities is avoided by a preliminary extraction of tantalum with isobutyl ketone from an HCl-HF medium. EDTA is added to complex coextracted metals, and boric acid is added to complex the fluoride ion. The method is applicable to the determination of tantalum in alkali metals in the absence of molybdenum and iron.	358
86	Ta	Both molybdenum and iron form colored complexes with phenylfluorone and thus interfere with the determination of tantalum by the previously described method (item 85). When more than 1 mg of an interfering element is expected to be present in the portion taken for color development, a preliminary separation by solvent extraction is required. Under the proper conditions methylisobutyl ketone (hexone) will extract tantalum preferentially from aqueous solution.	358
87	Ta	See item 92.	
88	Ti	See items 90, 92, and 95.	
89	Th	A simple, direct colorimetric determination of thorium extracted from chloride solution with di-(2-ethylhexyl)-orthophosphoric acid is described; the color is developed in the organic phase by adding arsenazo (III) and then isopropanol. Two different procedures are outlined for different thorium levels; maximum absorbance occurs at 660 nanometers, and Beer's law is obeyed within limited ranges. Molar extinction coefficients for the two methods are $4.93 \cdot 10^4$ and $8.77 \cdot 10^4$, respectively. The more sensitive method yielded 0.696 μg Th/ml, with 0.0028 as standard deviation. The effects of the various parameters were studied. Of 69 foreign cations tested, U(VI), Se(IV), Ti(IV), Y, and the rare earths interfered seriously.	cc

Item	Impurity	Method	Ref.
		Of the common anions, only large amounts of sulfate interfered slightly. Several ways of overcoming interferences are suggested, with particular reference to uranium. Several extensions of the method are outlined; 2 ppb Th in aqueous media can be determined by modifying the extraction step. The procedure also appears to be extremely sensitive for the light rare-earth elements. The method can be used for determining thorium in alkali metals.	
90	Trace elements	Al, Cr, Co, Cu, Fe, Pb, Mg, Mn, Mo, Ni, Si, Sn, Ti, V, and Zr are determined in sodium or NaK by the porous-cup spectrographic technique. Palladium is used as an internal standard. The samples are dissolved in ethyl alcohol and converted to the chloride before the determination.	dd
91	Trace elements	Five-gram samples of NaK were irradiated for 14 days in the Harwell reactor. Samples were cooled one week and dissolved in methyl alcohol. Radiochemical and ion-exchange separations were applied. The following elements were determined by their radioactivity: Hg, Cr, Rb, Cs, Ag, Sb, Sr, and Co.	ee
92	Trace elements	A general review of methods of determining metallic impurities in alkali metals is presented. Included are colorimetric methods for Fe, Ni, Ba, Cr, V, and B; gravimetric methods for K, Ca, and Mg in sodium; flame photometric methods for Li, Na, K, Mg, Ca, and Sr as major constituents or as minor impurities; spectrographic methods for Be, Co, Cr, Fe, Ni, Nb, Mn, Mo, Ta, Ti, U, V, W, and Zr; and activation methods for Rb and Cs in Na-K alloys. (This review includes references used elsewhere in this report.)	1
93	Trace elements	A method for determining trace-level concentrations of Cr, Mn, Fe, Co, and Ni from 0 to 10 ppm in a 1-g sample of sodium using atomic absorption spectrometry is presented. Carrier precipitation on lanthanum hydroxide is used to remove the difficulty associated with aspirating a solution of high salt content. At 1 ppm 95% confidence limits for precision of ±10% (relative) are attained. Approximately 5 hr is required for sampling these 5 elements in a 1-g sample, including sample dissolution and standard preparation.	101
94	Trace elements	Cation analysis of marine waters (Gulf of Mexico coastal waters) was accomplished by atomic absorption spectrometry, which appears ideally suited to water analysis	ff

Item	Impurity	Method	Ref.
		for major and trace cations because of its inherent speed, sensitivity, and precision. Two types of interferences are noted: (1) chemical complexing of P, Al, and Si with alkaline earths, which results in a decrease in absorption; (2) light scattering caused by sample solutions containing > 1% total solids (seawater is such a sample). The trace components were determined in normal seawater and in concentrated seawater. The major cations in seawater were determined by diluting it with distilled water to place the ions in a linear concentration range. Elements determined were Li, Na, Mg, K, Ca, Mn, Fe, Co, Ni, Cu, Zn, Rb, Sr, and Ba.	
95	Trace elements	A spark-source mass spectrograph was used to determine Br, Zn, Ni, Fe, Ti, K, Ca, Cl, Si, Al, and Mg as impurities in sodium.	*gg*
96	Trace elements	Chloride (10- to 100-ppm range) is determined turbidimetrically with silver nitrate, after alcohol dissolution and neutralization with HNO_3. Cesium is determined by a neutron-activator technique (sensitivity in parts per billion). Uranium analyses employ a fluorescence method after evaporation of a dissolved sample and fusing with a NaF-LiF mixture (sensitivity in 0.5-ppm range). Sulfur is obtained by a turbidimetric procedure, after sulfate conversion and acidification. Ca, B, Li, Ag, Au, Cd, In, and K are determined spectrochemically. The procedure involves alcohol solution, acidification, evaporation, and mixing with spectrographic-grade powdered graphite. A total of 41 elements can be determined as impurities in sodium metal by this procedure.	22
97	U	See items 92 and 96.	
98	V	See items 29, 90 and 92.	
99	W	See items 58 and 92.	
100	Zn	See items 94 and 95.	
101	Zr	A sensitive colorimetric method for the determination of zirconium was developed for use in organic extracts containing tri-*n*-octylphosphine oxide (TOPO) in cyclohexane. The method is based on the absorbance of the zirconium-pyrocatechol violet complex in a TOPO cyclohexane-ethyl alcohol medium at a wavelength of 655 mμ. The molar absorbance index for this complex at 655 mμ is about 40,000. The complex conforms to Beer's law up to a concentration of 10 μg Zr/ml. This method is useful for determining zirconium extracted from a chloride medium in the presence of large amounts of Al, U, V, Fe, and Cr; moderate amounts of thorium do not interfere. Molybdenum, titanium, and	*hh*

Item	Impurity	Method	Ref.
		hafnium interfere with the method. The procedure is applicable in the presence of milligram amounts of phosphate and sulfate ions. The method is useful for determining zirconium extracted from a nitrate medium in the presence of Al, Ti, Mo, V, Fe, and Cr; however, uranium, thorium, and hafnium interfere. Microgram amounts of phosphate and sulfate ions can be tolerated. This method has the common advantage of most extraction methods in that zirconium present in an aqueous sample can be extracted into a smaller organic volume. The coefficient of variation for the determination of zirconium by this method is less than 3%. This method can be used for determining zirconium in alkali metals.	
102	Zr	Zirconium is determined colorimetrically with alizarin reagent.	107
103	Zr	See items 41, 65, 90 and 92.	

APPENDIX 2-A

REFERENCES

a. A.J. Hegedus and M. Dvorsky, The Microtitrimetric Determination of Traces of Arsenic in Tungsten, Molybdenum, and in Other Metals, *Microchim. Acta, 1961*: 169.

b. J. Rynasiewicz, M.P. Sleeper, and J.W. Ryan, Boron in Sodium Metal, Determination of Microgram Amounts by Alcohol Extraction, *Anal. Chem., 26*: 935 (1954).

c. V. Suk and M. Smetanova, Bromopyrogallol Red as Colorimetric Reagent. 1. Photometric Determination of Bismuth, *Collect. Czech. Chem. Commun., 30*(8): 2532-2537 (1965) (In German).

d. W. Schuhknecht, Flame Photometric Determination of Small Amounts of Calcium in the Presence of Large Amounts of Sodium, Z. *Anal. Chem., 157*: 338 (1957).

e. L. Silverman and K. Trego, Determination of Small Amounts of Potassium, Calcium and Magnesium in Sodium and Its Compounds, *Analyst, 78*: 717 (1953).

f. D.K. Banerjee, C.C. Budke and F.D. Miller, Spectrophotometric Determination of Traces of Calcium in Sodium, *Anal. Chem., 33*: 418 (1961).

g. K. Kotsuji, Spectrophotometric Determination of Anions by Solvent Extraction with Metal-Chelate Cations. VIII. Determination of Cadmium, *Bull. Chem. Soc. Jap., 38*(6): 988-992 (1965).

h. J. Stupar, B. Podobnik and J. Kôrosin, Determination of Cadmium in Uranium Compounds by Atomic Absorption Spectrophotometry, *Croat. Chem. Acta, 27*: 141-148 (1965).

i. T. Hattori and T. Kuroha, Indirect Spectrophotometric Determination of Small Amounts of Chloride, *Jap. Anal. 13*(8): 749-753 (1964).

j. S. Utsumi and T. Okutani, Spectrophotometric Determination of Less Than One Part per Million of Chloride, *J. Chem. Soc. Jap., Pure Chem. Sect.*, *85*(9): 543-547 (1964).

k. L. Silverman and R.L. Seitz, Determination of Microgram Amounts of Cobalt in Sodium Metal: 2-Nitroso-1-Naphthol Spectrophotometric Method, *Anal. Chim. Acta, 20*: 340 (1959); see also Spectrophotometric Determination of Cobalt in Sodium Metal, USAEC Report NAA-SR-4005, Atomics International, Oct. 15, 1959.

l. C.K. Mann and J.C. White, Extraction of Chromium with Trioctylphosphine Oxide from Acidic Solutions of Alkali Metal Salts and Its Determination in situ as the Chromium-Diphenylcarbazide Complex, *Anal. Chem. 30*: 989 (1958).

m. D.L. Manning, W.K. Miller and R. Rowan, Jr., Determination of Submicrogram Quantities of Chromium and Vanadium in Alkali Hydroxides, USAEC Report ORNL-1396, Oak Ridge National Laboratory, Sept. 8, 1952.

n. United Kingdom Atomic Energy Authority, Industrial Group, *The Analysis of Sodium Metal and Sodium-Potassium Alloy (Collected Capenhurst Methods*), British Report IGO-AM/CA-110, March 1958.

o. J.M. Scarborough, The Determination of Trace Level Copper in Sodium by Colorimetric and Atomic Absorption Spectrophotometry, paper presented at the 155th National Meeting of the American Chemical Society, San Francisco, Apr. 2, 1968.

p. E.M. Penner and W.R. Inman, Extraction and Determination of Iron as the Bathophenanthroline Complex in High-Purity Niobium, Tantalum, Molybdenum, and Tungsten Metals, *Talanta, 9*: 1027 (1962).

q. D.F. Wood and J.T. Jones, The Determination of Zirconium (and Hafnium) in Niobium and Other Metals'with Catechol Violet, *Analyst, 90*: 125 (March 1965).

r. F.P. Landis and J.R. Pelrine, *The Determination of Mercury in NaK*, USAEC Report KAPL-67, Knolls Atomic Power Laboratory, Jan. 31, 1952.

s. K.H. Neeb and W. Bebauhr, Flame Photometric Determination of Small Amounts of Potassium in Sodium and Its Compounds After Enrichment with Ammonium Tetraphenyl-Borate, *Z. Anal. Chem., 162*: 167 (1958).

t. I.M. Korenman *et al.*, Radiometric Determination of Potassium in Sodium Metal, A Ternary Alloy and Electrolytes, *Trudy Khim. i Khim. Tekhnol., 1959*: 94.

u. W. Hobart and E.P. Hurley, Spectrophotometric Determination of Molybdenum and Tungsten in Niobium with Dithiol, *Anal. Chim. Acta, 27*: 144 (1962).

v. R. Belcher, T.V. Ramakrishna and T.S. West, Absorptiometric Determination of Niobium with 4-(2-Pyridylazo)-Resorcinol as Reagent, *Talanta, 10*: 1013 (1963).

w. M.N. Bukhsh and D.N. Hume, Colorimetric Determination of Niobium in the Presence of Tantalum, *Anal. Chem., 27*: 116 (1955).

x. B. Strzyzewska, Z. Radwan and J. Minczewski, Spectrographic Determination of Trace Amounts of Rare Earths. III. Determination of All Rare Earth Elements by the Carrier Distillation Method, *Appl. Spectrosc., 20*(4): 236-240 (1966).

y. L.O. Fadeeva, M.F. Zakhariya and L.I. Karpenko, Spectrographic Determination of Individual Rare Earth Elements in Their Mixed Oxides, *Khim. Prom., Inform. Nauk-Tekhn. Zb., 1964*(2): 76. (Ukrainian)

z. J.H. Landrum and H.L. Henicksman, The Separation of Rhenium from Copper, Molybdenum and Tungsten and Its Spectrophotometric Determination, USAEC Report LA-3550, Los Alamos Scientific Laboratory, June 1966.

aa. V.W. Meloche, R.L. Martin and W.H. Webb, Spectrophotometric Determination of Rhenium with Alpha-Furildioxime, *Anal. Chem., 29*: 527 (1957).

bb. J.H. Hill, The Spectrophotometric Determination of Trace Amounts of Tantalum, *Analyst, 91*: 659 (1966).

cc. E. Cerrai and G. Ghersini, Spectrophotometric Determination of Thorium with Arsenazo III in the Organic Phase After Extraction with Di-(2-Ethylhexyl)orthophosphoric Acid, *Anal. Chim. Acta, 37*: 295 (1967).

dd. G.I. Goodfellow, A.L. Wilson, T.H. Boyd, L. Lloyd and P.A. Sarin, *The Determination of Trace Elements in Metallic Sodium and Sodium-Potassium Alloy by the Porous-Cup Technique,* British Report SCS-R-329, Aug. 31, 1954.

ee. A.A. Smales, The Determination of Trace Impurities in Liquid Metal Coolants by Radioactivation Methods, *Proceedings of the International Conference on the Peaceful Uses of Atomic Energy, Geneva, 1955,* Vol. 9, pp. 273 ff. United Nations, New York, 1956.

ff. G.K. Billings and R.C. Hariss, Cation Analysis of Marine Waters by Atomic Absorption Spectrometry, Gulf of Mexico Coastal Waters, *Tex. J. Sci., 17*(1): 129-138 (1965).

gg. G.G. Cookson, W. Fletcher and R. Tushingham, A Commentary on the Spark Source Mass Spectrograph, Report CONF-721-9, papers presented at the 8th Conference on Analytical Chemistry in Nuclear Technology, Gatlinburg, Tenn., Oct. 6-8, 1964, Oak Ridge National Laboratory.

hh. J.P. Young and J.C. White, The Extraction of Zirconium with Tri-*n*-octyl-phosphine Oxide and Its Direct Determination in the Organic Phase with Pyrocatechol Violet, *Talanta, 1*: 263 (1958).

REFERENCES

1. I.M. Kolthoff, P.J. Elving and E. B. Sandell (Eds.), Treatise on Analytical Chemistry, *Part II, Analytical Chemistry of the Elements,* I, Interscience Publishers, New York, 1961.

2. R.E. Robinson and I.L. Mador, Alkali Metal Derivatives, in *Encyclopedia of Polymer Science and Technology, 1*: 639-658 (1964).

3. E.L. Alexanderson, C.E. Branyan and W.R. Olson, Operating Experience at the Enrico Fermi Atomic Power Plant, in *Fast Reactor Technology, National Topical Meeting, Detroit, Apr. 26-28, 1965,* ANS-100, pp. 41-56, American Nuclear Society, Hinsdale, Ill., 1965.

4. E.L. Alexanderson, Enrico Fermi Atomic Power Plant Operating Experience Through 100 Mwt, in *Fast Reactors, National Topical Meeting, San Francisco, Apr. 10-12, 1967,* ANS-101, pp. 1.21-1.45, American Nuclear Society, Hinsdale, Ill., 1967.

5. R. Ashley, R.J. Beeley, F.L. Fillmore, W.J. Hallett, B.R. Hayward and A.A. Jarrett, *SRE Fuel Element Damage,* Final Report, USAEC Report NAA-SR-4488 (Suppl.), Atomics International, June 30, 1961.

6. S. Berger *et al., Hallam Nuclear Power Facility, Reactor Operations Analysis Program.* Semiannual Progress Report No. 4, Feb. 29, 1964 - Sept. 30, 1964, USAEC Report NAA-SR-10743, Atomics International, May 15, 1965.

7. K.M. Broom, Jr., *et al.,* Post Irradiation Chemical Analysis of SNAP-8 Experimental Reactor Coolant, *Nucl. Appl., 2*: 519 (1966).

8. D.K. Darley *et al., Hallam Nuclear Power Facility, Reactor Operations Analysis Program,* Semiannual Progress Report No. 2, Mar. 1, 1963 - Aug. 31, 1963, USAEC Report NAA-SR-9265, Atomics International, Mar. 1, 1964.

9. D.K. Darley *et al., Hallam Nuclear Power Facility, Reactor Operations Analysis Program,* Semiannual Progress Reprot No. 3, Sept. 1, 1963 - Feb. 29, 1964, USAEC Report NAA-SR-9799, Atomics International, Sept. 15, 1964.

10. R.W. Dickinson and J.A. Leppard, Summary of SCTI Experience, in *Fast Reactors, National Topical Meeting, San Francisco, Apr. 10-12, 1967,* ANS-101, pp. 8.35-8.42, American Nuclear Society, Hinsdale, Ill., 1967.

11. J.G. Duffy, W.H. Jens, J.G. Feldes, K.P. Johnson and W.J. McCarthy, Jr., Investigation of the Fuel Melting Incident at the Enrico Fermi Atomic Power Plant, in *Fast Reactors, National Topical Meeting, San Francisco, Apr. 10-12, 1967,* ANS-101, pp. 2.15-2.37, American Nuclear Society, Hinsdale, Ill., 1967.

12. O.J. Foust *et al., Hallam Nuclear Power Facility, Reactor Operations Analysis Program.* Semiannual Progress Report No. 1, Sept. 1, 1962 - Feb. 28, 1963, USAEC Report NAA-SR-8401, Atomics International, July 1, 1963.

13. A.I. Hansen, *The Effects of Long-Term Operation on SRE Sodium System Components,* USAEC Report NAA-SR 11396, Atomics International, Aug. 1, 1965.

14. H.E. Johnson, *Transfer Corrosion and Activity in the SRE Primary Sodium System,* USAEC Report NAA-SR-5363, Atomics International, Oct. 30, 1961.

15. J.P. Lagowski and E. Havlena, Impurities in the Primary Sodium and Cover Gas of the Enrico Fermi Atomic

Power Plant, in *Alkali Metal Coolants*, Symposium Proceedings, Vienna, 1966, International Atomic Energy Agency, Vienna, 1967 (STI/PUB/143).

16. W.C. Miller and C.J. Hallinan, *S8DS Fission Product Detection System*, Report NAA-SR-Memo-12087, Atomics International, Oct. 5, 1966.

17. R.E. Peterson and R.L. Cubitt, Operation of the Plutonium Fueled Fast Reactor LAMPRE, in *Fast Reactors, National Topical Meeting, San Francisco, Apr. 10-12, 1967*, ANS-101, American Nuclear Society, Hinsdale, Ill., 1967.

18. J.L. Phillips, Full Power Operation of the Dounreay Fast Reactor, in *Fast Reactor Technology, National Topical Meeting, Detroit, Apr. 26-28, 1965*, ANS-100, pp. 7-24, American Nuclear Society, Hinsdale, Ill., 1965.

19. R.W. Woodruff, R.E. Durand and J.E. Owens, SRE and HNPF Operating and Modification Experience, in *Fast Reactors, National Topical Meeting, San Francisco, Apr. 10-12, 1967*, ANS-101, pp. 2.45-2.61, American Nuclear Society, Hinsdale, Ill., 1967.

20. E.W. Murbach, J.E. Bodine and N.W. Heath, *The Systems-Quality Sodium Loop Design, Construction, and Startup*, USAEC Report NAA-SR-12327, Atomics International, May 31, 1967.

21. L.P. Pepkowitz and W.C. Judd, Determination of Sodium Monoxide in Sodium, *Anal. Chem.*, *22*: 1285 (1950).

22. E.M. Simons, J.H. Stang, S.J. Basham, W.A. Glaeser and J.C. Bell, *Sodium Technology Support Program for Pacific Northwest Laboratories, Battelle Memorial Institute FFTF Studies, FY1965*, USAEC Report BMI-X-10129, Battelle Memorial Institute, July 9, 1965.

23. E.W. Hobart, *Status of Methods for Determining Carbon, Oxygen, and Nitrogen in Alkali Metals*, USAEC Report TIM-900, Pratt and Whitney Aircraft, Apr. 1, 1965.

24. R.J. Jaworowski, J.R. Potts and E.W. Hobart, The Determination of Oxygen in Lithium, *Anal. Chem.*, *35*: 1275 (1963).

25. V. Attas and C. Boudier, *Determination of Oxygen in Sodium by Liquid Ammonia*, USAEC Report ORNL-tr-931, translated by Gregory L. Boisvert, Oak Ridge National Laboratory, from French Report DRP/ML/FAR-R.-160, March 1965.

26. D. Dutina and J.L. Simpson, *Sodium Mass Transfer. XXIV. Methods for Separation and Identification of Sodium Impurities*, USAEC Report GEAP-5020, General Electric Company, March 1967.

27. N.I. Sax and H. Steinmetz, *Determination of Oxygen in Lithium Metal*, USAEC Report ORNL-2570, Nuclear Development Corp. of America, Oct. 31, 1958.

28. H. Steinmetz and B. Minushkin, *Experimental Determination of Contaminants in Sodium*, USAEC Report NDA-2154-6, United Nuclear Corp., Aug. 30, 1961.

29. D.R. Grieser, G.G. Cocks, E.H. Hall, W.M. Henry and J. McCallum, *Determination of Oxygen in Sodium at Concentrations Below 10 ppm*, USAEC Report BMI-1538, Battelle Memorial Institute, Aug. 23, 1961.

30. K.T. Claxton, Review of Solubility Data for the Liquid Sodium-Oxygen System, *J. Nucl. Energy*, *19*: 849 (1965).

31. R.H. Herald, *Study of the Feasibility of a Technique for Determining the Impurity Content of Liquid Alkali Metals*, Report APL-TDR-64-101,

Wright-Patterson Air Force Base, Ohio, September 1964.

32. R.L. McKisson, *Analysis of Freezing Point Depression Technique of Determining Impurity Content of Alkali Metal,* Report AI-TDR-9404, Atomics International, Mar. 25, 1964.

33. G. Goldberg, *The Effects of Trace Impurities of Moisture, Oxygen, Hydrogen, Nitrogen and Carbon Dioxide in Glove Box Atmospheres on the Analysis of Alkali Metals,* USAEC Report ORNL-TM-1357, Oak Ridge National Laboratory, Dec. 10, 1965.

34. D.D. Adams, Vacuum/Atmosphere Corporation Recirculation Inert Atmospheres Purification Systems, paper presented at the 10th Conference on Analytical Chemistry in Nuclear Technology, Gatlinburg, Tenn., Sept. 27-29, 1966.

35. M.E. Smith, J.M. Hansel and G.R. Waterbury, *An Inert Atmosphere Enclosure for the Preparation of Samples Prior to the Determination of Oxygen,* USAEC Report LA-3344, Los Alamos Scientific Laboratory, May 20, 1965.

36. D.F. Boltz, J.O. Kermoshchuk and S.A. Meacham, *The Determination of Oxygen in Sodium Metal,* USAEC Report APDA-168, Atomic Power Development Associates, Inc., July 2, 1965.

37. J.M. Scarborough and P.F. DeVries, *Determination of Oxygen in Sodium by the Amalgamation Method,* USAEC Report NAA-SR-12250, Atomics International, Sept. 25, 1967.

38. J.M. Scarborough and P.F. DeVries, Characterization of Blank Correction in Determination of Oxygen in Sodium by the Amalgamation Method, *Anal. Chem. 39*: 826 (1967).

39. G. Goldberg, *The Rapid Determination of Low Concentrations of Oxygen and Hydrogen in Alkali Metals by a Modified Amalgamation Technique,* USAEC Report ORNL-P-539, Oak Ridge National Laboratory.

40. J.R. Humphreys, Jr., Sampling and Analysis for Impurities in Liquid Sodium Systems, Chemical Engineering Progress Symposium Series 53, No. 20, pp. 7-10, American Institute of Chemical Engineers, New York, 1957.

41. J.C. White, *Procedure for the Determination of Oxygen in Sodium and NaK by the Distillation Method,* USAEC Report CF-56-4-31, Oak Ridge National Laboratory, Apr. 5, 1956.

42. C.C. McPheeters and J.M. Williams, A Comparison of Three Methods of Oxygen Concentration Measurement in Sodium, in *Alkali Metal Coolants,* Symposium Proceedings, Vienna, 1966, p. 429, International Atomic Energy Agency, Vienna, 1967, (STI/PUB/143).

43. K.S. Bergstresser, G.R. Waterbury and C.F. Metz, *Determination of Trace Amounts of Oxygen Added to Metallic Sodium,* USAEC Report LA-3343, Los Alamos Scientific Laboratory, May 1965.

44. Los Alamos Scientific Laboratory, *Quarterly Status Report on the Advanced Plutonium Fuels Programs,* July 1 - Sept. 30, 1967, USAEC Report LA-3820, Nov. 14, 1967.

45. Los Alamos Scientific Laboratory, *Quarterly Status Report on the Advanced Plutonium Fuels Program,* Oct. 1 - Dec. 31, 1967, USAEC Report LA-3880, Feb. 20, 1968.

46. J.A.J. Walker, E.D. France, J.L. Drummond and A.W. Smith, *Methods for the Analysis of Oxygen, Hydrogen, and Carbon in Sodium,* British Report TRG-Report-1271, June 14, 1966.

47. A.P. Litman and J.W. Prados,

The Partitioning of Oxygen Between Zirconium and Liquid Potassium, USAEC Report ORNL-P-984, Oak Ridge National Laboratory, 1964.

48. P.H. Goble, W.M. Albrecht, and M.M. Mallett, Determination of Oxygen in Sodium, in R.W. Dayton and C.R. Tipton, Jr., *Progress Relating to Civilian Applications During February 1957,* USAEC Report BMI-1173, pp. 67-68, Battrle Memorial Institute, Mar. 1, 1957; *Progress Relating to Civilian Applications During April 1957,* USAEC Report BMI-1181, Battelle Memorial Institute, May 1, 1957; *Progress Relating to Civilian Application During May 1957,* USAEC Report BMI-1189, Battelle Memorial Institute, June 1, 1957; and *Progress Relating to Civilian Applications During June 1957,* USAEC Report BMI-1201, Battelle Memorial Institute, July 1, 1957.

49. J.C. White, W.J. Ross, and R. Rowan, Jr., Determination of Oxygen in Sodium, *Anal. Chem., 26*: 210 (1954).

50. H.J. de Bruin and L.E. Smythe, Determination of Traces of Oxygen in Sodium by Infrared Spectrophotometry, *Nature (London), 182*: (1958).

51. H.J. de Bruin, Determination of Traces of Oxygen in Sodium by Infrared Spectrophotometry, *Anal. Chem., 32*: 360 (1960).

52. Argonne National Laboratory, *Chemical Engineering Division Research Highlights,* May 1964-April 1965, USAEC Report ANL-7020.

53. E.L. Steele and H.R. Lukens, Jr., *Development of Neutron Activation Analysis Procedures for the Determination of Oxygen in Potassium.* First and Second Quarterly Report, Period Ending Dec. 26, 1963, Report GA-4855, General Dynamics Corp., Jan. 10, 1964.

54. E.L. Steele, H.R. Lukens, Jr., and V.P. Guinn, *Development of Neutron Activation Analysis Procedures for the Determination of Oxygen in Potassium.* Final Peport, Period Ending Dec. 15, 1964, Report GA-5982, General Dynamics Corp.

55. D.M. Holm and W.M. Sanders, *Interference Reduction and Sensitivity Improvement in Activation Analysis,* USAEC Report LA-DC-7931, Los Alamos Scientific Laboratory, 1964.

56. R.W. Lockhart, R.C. Blair, D. Dutina, J.L. Jaech, and W.W. Sabol, *Results of the USAEC Round-Robin Analysis for Carbon Impurity in Sodium,* USAEC Report GEAP-4602, General Electric Company, March 1964.

57. D. Dutina, The Current State-of-the Art of Alkali Metal Analysis, in *AEC-NASA Liquid Metals Information Meeting, Gatlinburg, Tenn., Apr. 21-25, 1965,* p. 1, USAEC Report CONR-750411, Oak Ridge National Laboratory.

58. J.A. Leppard, Carburization Potential in Sodium Systems, in *Fourth Sodium Components Development Program Information Meeting, Los Angeles, Apr. 14, 1964,* USAEC Report COO-1213-30.

59. W.J. Anderson and G.V Sneesby, *Carburization of Austenitic Stainless Steel in Liquid Sodium,* USAEC Report NAA-SR-5282, Atomics International, Sept. 1, 1960.

60. K.Y. Eng, R.A. Meyer, and C.D Bingham, Determination of Carbon in Sodium by Isotope Dilution Mass Spectrommetry, *Anal. Chem., 36:* 1832 (1964).

61. National Bureau of Standards, *1967 Technical Highlights of the National Bureau of Standards Annual Report, Fiscal Year 1967,* Miscellaneous Publication 293, Superintendent of Documents, U.S. Government Printing Office, Washington, 1967.

62. K.J. Kelly, E.W. Hobart, and R.G. Bjork, Studies Concerning the Chemical State of Carbon, Nitrogen, and Oxygen in Alkali Metals, in *AEC-NASA Liquid Metals Information Meeting, Gatlinburg, Tenn., Apr. 21-23, 1965,* USAEC Report CONF-659411, pp. 74-68, Oak Ridge National Laboratory.

63. D.L. Johnson, *Chromatographic Analysis of Gases over Liquid Sodium,* USAEC Report NAA-SR-8448, Atomics International, Sept. 15, 1964.

64. S.J. Rodgers, C.A. Palladino, and T.J. Wildeman, *Effect of High-Temperature Sodium on the Mechanical Properties of Candidate Alloys for the LMFBR Program,* USAEC Report MSAR-67-203, Mine Safety Appliances Research Corp., December 1967.

65. K.G. Stoffer and J.H. Phillips, Determination of Carbon in Sodium Potassium Alloy, *Anal. Chem., 27*: 773 (1955).

66. S. Kallman and R. Liu, The Determination of Total Carbon and Sodium Carbonate in Sodium Metal, *Anal. Chem., 36*: 590 (1964).

67. H. Bradley and S.A. Meacham, *Determination of Carbon in Sodium by a High-Temperature Combustion Method Utilizing Gas Chromatography,* USAEC Report APDA-164, Atomic Power Development Associates, Inc., Nov. 25, 1964.

68. R.D. Gardner and W.H. Ashley, *The Gravimetric Determination of Trace Amounts of Carbon in Sodium Metal,* USAEC Report LA-3035, Los Alamos Scientific Laboratory, January 1964.

69. L.F. Epstein, Effects of Impurities. C. Carbon, in *Proceedings of the NASA-AEC Liquid Metals Corrosion Meeting, Volume I, Lewis Research Center, Cleveland, Ohio, Oct. 2-3, 1963,* USAEC Report NASA-SP-41 (pp. 61-65), National Aeronautics and Space Administration, 1964.

70. L.P. Pepkowitz and J.T. Porter, *The Determination of Carbon in Sodium,* USAEC Report KAPL-1444, Knolls Atomic Power Laboratory, Nov. 28, 1955.

71. W.W. Sabol, D. Dutina, D.E. Rey, and J.L. Simpson, *Sodium Mass Transfer. XIII. The Determination of Total Carbon in Sodium,* USAEC Report GEAP-4540, General Electric Company, June 1964.

72. D.F. Boltz and S.A. Meacham, *Determination of Carbonate Carbon in Sodium Metal,* USAEC Report APDA-166, Atomic Power Development Associates, Inc., Jan. 15, 1965.

73. J.A.J. Walker and E.D. France, *The Determination of Carbonate in Sodium,* British Report TRG-Report-1635, 1968.

74. L.P. Pepkowitz and E.R. Proud, Determination of Hydrogen, *Anal. Chem., 21*: 1000 (1949).

75. J.A. Walker and H. Seed, The Determination of Hydrogen in Sodium, *Analyst, 90*: 19 (1965).

76. D. Dutina and J.L. Simpson, *Sodium Mass Transfer. XVII. The Determination of Hydrogen in Loop Sodium and Cover Gases,* USAEC Report GEAP-4833, General Electric Company, June 1965.

77. S.A. Meacham and E.F. Hill, *The Determination of Hydrogen in Sodium Metal,* USAEC Report APDA-183, Atomic Power Development Associates, Inc., June 1966.

78. B.D. Holt, Determination of Hydrogen in Alkali Metals by Isotope Dilution Method, *Anal. Chem., 31*: 51 (1959).

79. C. Evans and J. Herringron,

Determination of Hydrogen in Sodium by Isotopic Dilution with Tritium, *Anal. Chem.*, *35*: 1907 (1963).

80. G. Naud and J. Sannier, *Analysis of Hydrogen in the Free State or as Hydride in Sodium*, translated from *Bull. Soc. Chim. France*, USAEC Report AEC-tr-6438, Atomic Power Development Associates, Inc.

81. G. Goldberg, *The Rapid Determination of Low Concentrations of Oxygen and Hydrogen in Alkali Metals by a Modified Amalgamation Technique*, USAEC Report ORNL-P-539, Oak Ridge National Laboratory.

82. B.R. Grundy and A.N. Hamer, A Study of Nonmetallic Impurities in Sodium by Amalgamation Coupled with Mass Spectrometry, paper presented at the 10th Conference on Analytical Chemistry in Nuclear Technology, Gatlinburg, Tenn., Sept. 27-29, 1965.

83. R.D. Gardner and W.H. Ashley, *The Gravimetric Determination of Trace Amounts of Hydrogen in Sodium Metal*, USAEC Report LA-3049, Los Alamos Scientific Laboratory, February 1964.

84. R.C. Andrews, K.R. Barker, and R.C. Werner, *Development of Techniques for Measurement of Impurities in Sodium*, Quarterly Progress Report, July - September 1966, USAEC Report MSAR-66-221, Mine Safety Appliances Research Corp., Nov. 9, 1966.

85. R.C. Andrews, S.J. Rogers, R. Tepper, and R.J. Udavcak, *A Critical Review of the Development of Techniques for the Measurement of Impurities in Sodium*. Quarterly Progress Report, April-June 1967, USAEC Report MSAR-67-213, Mine Safety Appliances Research Corp., December 1967.

86. W.E. Winsche and F.T. Miles, *Annual Report, Nuclear Engineering Department*, USAEC Report BNL-50023, Brookhaven National Laboratory, Dec. 31, 31, 1966.

87. H. Farrar IV, *A Description of the Mass Spectrograph*, Atomics International Internal Report, Nov. 17, 1966.

88. Atomics International, *Annual Technical Progress Report, AEC Unclassified Programs, Fiscal Year 1967*, USAEC Report NAA-SR-12492, Atomics International, 1967.

89. C.H. Ward, R.D. Gardner, W.H. Ashley, and A. Zerwekh, *The Titrimetric Determination of Traces of Nitride Nitrogen in Sodium Metal*, USAEC Report LA-2892, Los Alamos Scientific Laboratory, April 1963.

90. E.W. Hobart and R.G. Bjork, Formation of Cyanide in Liquid Sodium, *Nucl. Appl.*, *1*: 490 (1965).

91. C.R.S. Schneifer, Determination of Low-Level Hydrocyanic Acid in Solution Using Gas-Liquid Chromatography, *Diss. Abstr.*, *23*(6): 1898 (1962).

92. J.S. Hanker, A. Gelberg, and B. Witten, Fluorometric and Colorimetric Estimation of Cyanide and Sulfide by Demasking Reactions of Palladium Chelates, *Anal. Chem.*, *30*: 93 (1958).

93. K. Kirtchik, Modified Kjeldahl Determination of Nitrogen in Potassium Metal, *Anal. Chem.*, *37*: 1287 (1965).

94. C.E. Crouthamel, *Applied Gamma-Ray Spectrometry*, Pergamon Press, Inc., London, 1960.

95. R.L. Heath, *Scintillation Spectrometry. Gamma-Ray Spectrum Catalog*, USAEC Report IDO-16880-1 and 2, 2 vols., Phillips Petroleum Co., August 1964.

96. G.D. O'Kelley, *Detection and*

Measurement of Nuclear Radiation, National Academy of Sciences, National Research Council Report, NAS-NS-3105, 1962.

97. J. Korkisch and K.A. Orlandini, *Separation of Traces of Metal Ions from Sodium Matrices,* USAEC Report ANL-7421, Argonne National Laboratory, February 1968.

98. W.W. Sabol and R.W. Lockhart, *Sodium Mass Transfer. VII. Methods for Determining Impurities in Sodium Samples,* USAEC Report GEAP-4178, General Electric Company, September 1963.

99. E.B. Sandell, *Colorimetric Determination of Traces of Metals,* Interscience Publishers, New York, 1959.

100. T.M. Florence, *Estimation of Traces of Nickel in Sodium Metal,* Australian Report AAEC/E-23, February 1958.

101. J.M. Scarborough, C.D. Bingham, and P.F. DeVries, Determination of Trace Metallic Impurities in High Purity Sodium Using Atomic Absorption Spectrometry, *Anal. Chem., 39*: 1394 (1967).

102. J. Rynasiewicz and M.E. Polley, Calcium in High Purity Sodium Salts, Determination of Micro-Amounts by the Oxine-Oxalate Method, *Anal. Chem., 21*: 1398 (1949).

103. D. Dutina, *Determination of Microgram Quantities of Barium in Sodium,* USAEC Report KAPL-1425, Knolls Atomic Power Laboratory, June 1, 1955.

104. R.M. Stevens, *The Barium-Sodium Phase System,* USAEC Report TID-20637, Syracuse University, May 1964.

105. J. Krugers and A.I.M. Keulemans (Eds.), *Practical Instrumental Analysis,* American Elsevier Publishing Company, New York, 1965.

106. Westinghouse Electric Corp., *Examination of the Enrico Fermi Sodium Cold Trap,* USAEC Report WCAP-4321, November 1965.

107. H.E. Perrine, *Collected Methods for Analysis of Sodium Metal,* USAEC Report GEAP-3273, General Electric Company, Oct. 15, 1959.

108. Pratt and Whitney Aircraft, *SNAP-50/SPUR Final Summary Report on Coolants and Working Fluids,* USAEC Report PWAC-491, November 1965.

109. H.L. Hoisch, *Spectrographic Analysis CdS Carrier Precipitation Technique,* Report CTP-661-35-009, Atomics International, Apr. 24, 1967.

111. S. Black *et al.*, Colorimetric Determination of Nonmetals, *Chemical Analysis, Vol. 8,* D.F. Boltz (Ed.), pp. 166-168, Interscience Publishers, New York, 1958.

112. United Kingdom Atomic Energy Authority, Production Group, *Analytical Method for the Absorptiometric Determination of Boron in Sodium Metal,* British Report PG-Report-415, 1963.

113. D. Logie, A New Analytical Separation Technique by Using Ion-Exchange Membranes and Its Application to the Determination of Boron in Sodium Metal, *Chem. Ind. (London), 1957*: 225.

114. E.W. Murbach, *Sampling Blanks for the LMFBR Cladding Program,* USAEC Report NAA-SR-12616, Atomics International, Jan. 30, 1968.

115. C. Luner, A. Cosgarea, Jr., and H.M. Feder, Solubility of Carbon in Sodium, in *Alkali Metal Coolants,* Symposium Proceedings, Vienna, 1966, International Atomic Energy Agency,

Vienna, 1967 (STI/PUB/143).

116. F.A. Scott, *Sampling FFTF Sodium Coolant for Analytical Purposes.* USAEC Report BNWL-491, Battelle - Northwest Laboratory, September 1967.

117. E.F. Madsen, *Sodium Sampling in the Enrico Fermi Atomic Power Plant* USAEC Report APDA-306, Atomic Power Development Associates, Inc., March 1968.

118. K.A. Davis, *Liquid Metal In-Line Impurity Measuring Instruments (Sodium) State-of-the-Art Study,* USAEC Report LMEC-Memo-68-3, Atomics International, Jan. 30, 1968.

119. B. Minushkin, The Liquid Metal Oxygen Meter, in *Proceedings of the Sodium Components Development Program Information Meeting, Chicago, June 16-17, 1965,* USAEC Report CONF-659620, pp. 271-275, Chicago Operations Office.

120. B. Minushkin and M. Kolodney, *Development of a Continuous Electrochemical Meter for Oxygen in Sodium,* USAEC Report UNC-5131, United Nuclear Corp., Dec. 15, 1967.

121. E.F. Hill, Sodium Technology Loop Evacuation of In-Line Instruments and Purification Devices, in *Proceedings of the Sodium Components Development Program Information Meeting, Chicago, June 16-17, 1965,* USAEC Report CONF-650620, pp. 255-270, Chicago Operations Office.

122. Atomic Power Development Associates, Inc., *Evaluation of the Blake Sodium Resistivity Meter,* USAEC Report APDA-149, Oct. 15, 1962.

123. Atomic Power Development Associates, Inc., *Operation of the Sodium Technology Loop for Contamination Meter Evaluations,* USAEC Report APDA-163, Mar. 25, 1964.

124. M. Davis and A. Draycott, Compatibility of Reactor Materials in Flowing Sodium, in *Proceedings of the Second United Nations International Conference on the Peaceful Uses of Atomic Energy, Geneva, 1958,* Vol. 7, pp. 94-110, United Nations, New York, 1958.

125. K.A. Davis, *Detection Device for Hydrogen in Sodium,* USAEC Report NAA-SR-5732, Atomics International, Jan. 15, 1962.

126. H. Strahl, *A Device for Continuous Detection of Hydrogen in Sodium,* USAEC Report NAA-SR-6986, Atomics International, May 31, 1962.

127. United Nuclear Corp., *A Continuous Electrochemical Meter for Measurement of Hydrogen in Sodium,* Progress Report, Oct. 1, 1967-Mar. 31, 1968, USAEC Report UNC-5215, Apr. 30, 1968.

128. United Nuclear Corp., *Carbon Meter for Sodium.* Progress Report, Feb. 21-June 30, 1966, USAEC Report UNC-5160, July 31, 1966.

129. United Nuclear Corp., *Carbon Meter for Sodium,* Quarterly Progress Report, Jan.1-Mar. 3., 1967, USAEC Report UNC-5181, June 30, 1967.

130. J.G. Yevick and A. Amorosi (Eds.), *Fast Reactor Technology: Plant Design,* The M.I.T. Press, Cambridge, Mass., 1966.

131. E.A. Limoncelli, *Use of Helium and Argon as Protective Environments for SNAP-50/SPUR Program,* USAEC Report TIM-824, Pratt and Whitney Aircraft, November 1965.

132. J. Malgiolio, E.A. Limoncelli, and R.E. Cleary, *The Purification and Gas Chromotographic Analysis of Helium,* USAEC Report PWAC-352, Pratt and Whitney Aircraft, June 30, 1961.

133. K.P. Dimick and L.A. Rigali, Principles and Gas Chromatographic Applications of Four Ionization Detectors: Flame, Electron Capture, Cross Section, and Helium, Wilkins Instrument and Research, Inc., Walnut Creek, California, Jan. 24, 1964.

134. T.F. Lyon, *Purification and Analysis of Helium for the Welding Chamber*, Report NASA-CR-54168, National Aeronautics and Space Administration, Cleveland, Lewis Research Center, July 1, 1965.

135. J.E. Harrar (Ed.), *Analytical Chemistry Section Progress Report*, Jan. 1 - Dec. 31, 1965, USAEC Report UCRL-14767, Lawrence Radiation Laboratory.

136. Pratt and Whitney Aircraft, *CANEL Materials Laboratory Manual - Analytical Section*, USAEC Report TIM-936, 1964.

137. M.T. Kelley and C.D. Susano, *Analytical Chemistry Division Annual Progress Report for Period Ending Dec. 31, 1962*, USAEC Report ORNL-3397, Oak Ridge National Laboratory, Feb. 8, 1963.

138. S.K. Dhar, Solubility of Argon in Liquid Sodium, in *Chemical Engineering Division Semiannual Report*, July - December, 1963, USAEC Report ANL-6800, pp. 183-187, Argonne National Laboratory, May 1964.

139. S.K. Dhar, Solubility of Krypton in Liquid Sodium, in *Chemical Engineering Division Semiannual Report*, January - June, 1964, USAEC Report ANL-6900, pp. 125-127, Argonne National Laboratory, August 1964.

140. H. Slotnick, S.M. Kapelner and R.E. Cleary, *The Solubility of Helium in Lithium and Potassium*, USAEC Report PWAC-380, Pratt and Whitney Aircraft, Feb. 24, 1965.

141. C. Mitra, Solubility of Xenon in Liquid Metals, *Diss. Abstr.*, *22*: 100 (1961).

142. L.F. Epstein, *The Solubility of Helium Gas in Liquid Sodium*, USAEC Report KAPL-M-LFE-10, Knolls Atomic Power Laboratory, Oct. 30, 1951.

143. H.W. Savage, E.L. Compere, W.R. Huntley, B. Fleischer, R.E. MacPherson and A. Taboada, *SNAP-8 Corrosion Program Summary Report*, USAEC Report ORNL-3898, p.39, Oak Ridge National Laboratory, December 1965.

144. J.G. Yevick (Ed.), *Fast Reactor Technology*: *Plant Design*, The M.I.T. Press, Cambridge, Mass., 1966.

145. Gmelin Institute, *Gmelin Handbuch der Anorganischen Chemie*, *Natrium*, System-Nummer 21, Verlag Chemie, Weinheim, 1964, 1965, 1966, 1967.

146. A.P. Littlewood, Sodium Hydride, in J.W. Mellor, *A Comprehensive Treatise on Inorganic and Theoretical Chemistry*, Vol. II, Supplement II, pp. 622-627, John Wiley & Sons, New York, 1961.

147. J.W. Mellor, *A Comprehensive Treatise on Inorganic and Theoretical Chemistry*, Vol. II, Longmans, Green & Co., London, 1952.

148. J.W. Mellor, *A Comprehensive Treatise on Inorganic and Theoretical Chemistry*, Vol. II, Supplement II, John Wiley & Sons, New York, 1961.

149. R.E. Kirk and D.F. Othmer (Eds.), *Encyclopedia of Chemical Technology*, Vol. 12, pp. 604 ff., Interscience Publishers, Inc., New York, 1954.

150. M. Sittig, *Sodium. Its Manu-*

facture, Properties, and Uses, Reinhold Publishing Corporation, New York, 1956.

151. U.S. Department of Commerce, National Bureau of Standards, Institute for Applied Technology, *JANAF Thermochemical Tables,* PB-168,370 (August 1965); PB-168,370-1 (August 1966); PB-168,370-2 (August 1967).

152. S.R. Gunn and L.G. Green, The Heats of Formation at 25° of the Crystalline Hydrides and Deuterides and Aqueous Hydroxides of Lithium, Sodium, and Potassium, *J. Amer. Chem. Soc., 80*: 4782 (1958).

153. C.E. Messer, L.G. Fasolino and C.E. Thalmayer, The Heats of Formation of Lithium, Sodium, and Potassium Hydrides, *J. Amer. Chem. Soc., 77*: 4524 (1955).

154. A. Hérold, Dissociation Pressure of Alkali Hydrides, *Compt. Rend., 228*: 686 (1949); *Chem. Abstr. 44*: 24.

155. M.O. Banus, J.J. McSharry and E.A. Sullivan, The Sodium-Sodium Hydride-Hydrogen System at 500-600°C, *J. Amer. Chem. Soc., 77*: 2007 (1955).

156. H.W. Savage, E.L. Compere, R.E. MacPherson, W.R. Huntley and A. Taboada, *SNAP-8 Corrosion Program.* Quarterly Progress Report for Period Ending Feb. 28, 1965, USAEC Report ORNL-3823, Oak Ridge National Laboratory, June 1965.

157. H.W. Savage, E.L. Compere, R.E. MacPherson, W.R. Huntley and A. Taboada, *SNAP-8 Corrosion Program.* Quarterly Progress Report for Period Ending Nov. 30, 1964, USAEC Report ORNL-3784, Oak Ridge National Laboratory, March 1965.

158. C.C. Addison, R.J. Pulham and R.J. Roy, Liquid Metals. Part X. Solutions of Hydrogen in Liquid Sodium, *J. Chem. Soc., 1965* (January): 116.

159. D.W. McClure and G.D. Halsey, Jr., The Solubility of Hydrogen in Liquid Sodium, *J. Phys. Chem., 69*: 3542 (1965).

160. E.L. Compere and J.E. Savolainen, The Chemistry of Hydrogen in Liquid Alkali-Metal Mixtures Useful as Nuclear Reactor Coolants, NaK-78, *Trans. Amer. Nucl. Soc., 8*(1): 18 (1965).

161. D.D. Williams, J.A. Grand and R.R. Miller, *The Solubility of Impurities in Metallic Sodium,* Report NRL-Memo-424, Naval Research Laboratory, Feb. 1, 1955.

162. D.D. Williams, J.A. Grand and R.R. Miller, The Solubility of Sodium Hydride in Sodium, *J. Phys. Chem., 61*: 379 (1957).

163. Atomic Power Development Associates, Inc., *Quarterly Technical Progress Report on AEC-Sponsored Activities,* June 15 - Sept. 15, 1967, USAEC Report APDA-212, p. 11.12.

164. F.A. Kanda, R.C. Faxon and D.V. Keller, The Determination of the Liquid Immiscibility Boundaries of the Lithium-Sodium and Thallium-Selenium Systems by the Liquid Density Method, *Phys. Chem. Liquids, 1*(1): 61 (1968); also Robert C. Faxon, Ph.D. Thesis, Syracuse University (1965).

165. F.A. Kanda, R.C. Faxon and R. Grant, The Use of Liquid Densities as a New Technique for Determining Liquid Immiscibility Phase Boundaries, *Phys. Chem. Liquids, 1*(1): 49 (1968).

166. W.H. Howland and L.F. Epstein, Binary System Sodium-Lithium, in *Handling and Uses of Alkali Metals,* Advances in Chemistry Series 19, pp. 34-41, American Chemical Society, New York, 1957.

167. R.P. Elliott, *Constitution of*

Binary Alloys, First Supplement, McGraw-Hill Book Company, Inc., New York, 1965.

168. O.N. Salmon and D.H. Ahmann, The Lithium-Sodium Liquid Metal System, *J. Phys. Chem. 60*: 13 (1956).

169. M. Hansen and K. Anderko, *Constitution of Binary Alloys,* McGraw-Hill Book Company, Inc., New York, 1958.

170. D.K.C. MacDonald, W.B. Pearson and L.T. Towle, An Investigation of the Sodium-Potassium Equilibrium Diagram, *Can. J. Phys., 34*: 389 (1956); *Chem. Abstr., 50*: 8310.

171. B.R. Orton, B.A. Shaw and G.I. Williams, An X-Ray Structure Investigation of the Liquids of Sodium, Potassium and Sodium-Potassium Alloys, *Acta Met., 8*: 177 (1960).

172. E. Rinck, Freezing Diagrams of Two Alkali Metals. Sodium-Potassium Alloys, *Compt. Rend., 197*: 49 (1933); *Chem. Abstr., 27*: 5705.

173. N.S. Gingrich and R.E. Henderson, The Diffraction of X-Rays by Liquid Alloys of Sodium and Potassium, *J. Chem. Phys., 20:* 1117 (1952).

174. G.L.C.M. Van Rossen Hoogendijk van Bleiswijk, *Z. Anorg. Chem., 73*: 152 (1912).

175. A. Joannis, *Ann. Chim. et Phys., 12*(6): 358 (1887).

176. M. Kawakami, The Heat of Mixing of Metals, *Z. Anorg. Allg. Chem., 167*: 345 (1927); *Sci. Rep. Tohoku Imp. Univ., First Ser., 16*: 915 (1927).

177. R.L. McKisson and L.A. Bromley, Heats of Formation of Sodium-Potassium Alloys, *J. Amer. Chem. Soc., 73*: 314 (1951).

178. E. Rinck, Constitutional Diagram of Alloys Formed of Two Alkali Metals; Sodium-Rubidium Alloys, *Compt. Rend., 197*: 1404 (1933); *Chem Abstr. 28*: 1314.

179. C. Goria, Binary Systems of Alkali Metals. I, *Gazz. Chim. Ital., 65*: 865 (1935); *Chem. Abstr., 30*: 3305.

180. B. Böhm and W. Klemm, Behavior of the Alkali Metals Toward Each Other, *Z. Anorg. Allg. Chem., 243*: 69 (1939); *Chem. Abstr., 34*: 4973.

181. F. Tepper, J. King and J. Greer, Multicomponent Alkali-Metal Alloys, in *The Alkali Metals,* Symposium Proceedings, Nottingham, England, July 19-22, 1966, Special Publication No.22, p. 23, The Chemical Society, London, 1967.

182. E. Rinck, Freezing Diagrams of Alloys of Two Alkali Metals, Sodium-Cesium Alloys, *Compt. Rend., 199*: 1217 (1934); *Chem. Abstr., 29*: 670.

183. C. Goria, Binary Systems of Alkali Metals. I, *Gazz. Chim. Ital., 65*: 1226 (1935); *Chem. Abstr., 30*: 5489.

184. E. Zintl, J. Goubeau and W. Dullenkopf, *Z. Phys. Chem., 154*: 44 (1931).

185. R.L. Eichelberger and R.L. McKisson, *The Solubility of Copper in Sodium,* USAEC Report AI-AEC-12671, Atomics International, May 31, 1968.

186. R.M. Singer and W. Becker, in *Quarterly Progress Report of Work Sponsored by the Fuels and Materials Branch,* Apr. 1 - June 30, 1967, USAEC Report BNL-50065, pp. 12-17, Brookhaven National Laboratory. (Official Use Only)

187. J.R. Humphreys, Jr., Inter-

divisional Document K-3-774, Los Alamos Scientific Laboratory.

188. R.A. Walker, J.N. Pratt and B.W. Mott, The Solubility of Metallic Elements in Liquid Sodium, paper presented at the 1968 AEC Corrosion Symposium, May 6-8, 1968, Battelle Memorial Institute, Columbus, Ohio.

189. G. Kienast and J. Verma, The Behavior of the Alkali Metals Toward Copper, Silver and Gold, *Z. Anorg. Allg. Chem., 310*: 143 (1961).

190. E. Quercigh and G. Bruni, Fusion Diagram of Silver-Sodium Alloys, *Z. Anorg. Chem., 68*: 301 (1910); *Chem. Abstr., 5*: 638.

191. C.H. Mathewson, Sodium-Silver Alloys, *Intern. Z. Metallog., 1*: 51 (1911); *Chem. Abstr., 5*: 2786.

192. W.E. Winsche and F.T. Miles (Eds.), *Nuclear Engineering Department Annual Report,* Dec. 31, 1965, USAEC Report BNL-954, pp. 137 ff. Brookhaven National Laboratory.

193. G.J. Lamprecht, A Study of the Solubility of Metals in Liquid Na, Ph.D. Thesis, University of South Africa, 1966.

194. F.L. Bett and A. Draycott, The Compatibility of Beryllium with Liquid Sodium and NaK in Dynamic Systems, in *Proceedings of the Second United Nations International Conference on the Peaceful Uses of Atomic Energy, Geneva, 1958,* Vol. 7, p.125, Untitled Nations, New York, 1958.

195. J.H. Stang, E.M. Simons, J.A. DeMastry and J.M. Genco, *Compatibility of Liquid and Vapor Alkali Metals with Construction Materials,* Report DMIC-227, Defense Metals Information Center, Apr. 15, 1966.

196. C.H. Mathewson, *Z. Anorg. Chem., 48*: 193 (1906).

197. E. Rinck, Diagram of the Solidification of Calcium-Sodium Alloys, *Compt. Rend., 192*: 1378 (1931); *Chem. Abstr., 25*: 4505.

198. R. Lorenz and R. Winzer, Equilibrium Between Metals and Salts in Fusion Mixtures, XVIII. The Effect of the Addition of Pb and Sb upon the Equilibrium Between Na and Ca and Their Chlorides, *Z. Anorg. Allg. Chem., 183*: 127 (1929); *Chem. Abstr., 24*: 1015.

199. C.B. Jackson (Ed.), *Liquid Metals Handbook. Sodium-NaK Supplement,* USAEC Report TID-5277, Atomic Energy Commission and Bureau of Ships, July 1, 1955.

200. H. Remy, G. Wolfrum and H.W. Haase, Phase Diagram of the Systems Na/Sr and Na/Ba, *Naturwissenschaften, 44*: 534 (1957).

201. F.A. Kanda and D.V. Keller, *Investigation of Specific Volumes of Liquid Metals and Alloys. Phase Equilibria Studies of Alkali-Alkaline Earth Metal Systems,* USAEC Report TID-18619, Syracuse University, May 1963.

202. F.A. Kanda, Syracuse University, personal communication, April 1968.

203. F.A. Kanda and A.J. King, *Phase Equilibria Studies of Systems Involving the Alkali and Alkaline Earth Metals,* USAEC Report TID-5691, Syracuse University, March 1960.

204. F.A. Kanda, R.M. Stevens and D.V. Keller, The Barium-Sodium Equilibrium System, *J. Phys. Chem., 69:* 3867 (1965); also R.M. Stevens, Ph.D. Thesis, Syracuse University, 1964.

205. J.R. Gould, *Solubility of Barium Metal and Barium Oxide in Sodium.* USAEC Report KAPL-1398, Knolls Atomic Power Laboratory, Sept. 1, 1955.

206. W. Häusler, The Activity of Sodium in Molten Sodium-Zinc Alloys at 600°, *Z. Metallk.*, *51*: 95 (1960).

207. C.H. Mathewson, *Z. Anorg. Chem.*, *48*: 195 (1906).

208. E. Zintl, J. Goubeau, and W. Dullenkopf, Metals and Alloys. I. Salt-Like Compounds and Intermetallic Phases of Sodium in Liquid Ammonia, *Z. Phys. Chem.*, *154*: 1 (1931); *Chem. Abstr.*, *25*: 3260.

209. E. Zintl and W. Haucke, Metals and Alloys, XXV. Constitution of the Intermetallic Phases $NaZn_{13}$, KZn_{13}, KCd_{13}, $RbCd_{13}$, and $CsCd_{13}$, *Z. Elektrochem.*, *44*: 104 (1938); also Constitution of the Metallic Phases $NaZn_{13}$, KZn_{13}, and KCd_{13}, *Naturwissenschaften*, *25*: 717 (1937); *Chem. Abstr.*, *32*: 2802.

210. C.A. Kraus and H.F. Kurtz, Reduction of Metals from Their Salts by Means of Other Metals in Liquid Ammonia Solution, *J. Amer. Chem. Soc.*, *37*: 43 (1925); *Chem. Abstr.*, *19*: 787.

211. W.M. Burgess and A. Rose, A Study of the Products Obtained by the Reducing Action of Metals upon Salts in Liquid Ammonia Solution. I. Introduction. II. The Action of Sodium upon Zinc Cyanide, *J. Amer. Chem. Soc.*, *51*: 2127 (1929); *Chem. Abstr.*, *23*: 4157.

212. N.S. Kurnakow and A.N. Kustnetzow, *Z. Anorg. Chem.*, *23*: 455 (1900).

213. N.S. Kurnakow and A.N. Kusnetzow, Sodium Cadmides, *Z. Anorg. Chem.*, *52*: 173 (1907); *Chem. Abstr.*, *1*: 966.

214. C.H. Mathewson, *Z. Anorg. Chem.*, *50*: 180 (1906).

215. S. Allaria, *Atti Reale Accad. Sci. Torino*, *78*: 145 (1942-43).

216. J.R. Weeks and H.A. Davies, Physical and Chemical Properties of Dilute Alloys of Cadmium in Sodium, in *The Alkali Metals*, Symposium Proceedings, Nottingham, England, July 19-22, 1966, Special Publication No. 22, p. 32, The Chemical Society, London, 1967.

217. W. Seith and O. Kubaschewski, The Heats of Formation of Several Alloys, *Z. Elektrochem.*, *43*: 743 (1937); *Chem. Abstr.* *31*: 8478.

218. W. Biltz and C. Haase, Systematic Affinity Principle. XXII. The Heats of Formation of Intermetallic Compounds, *Z. Anorg. Allg. Chem.*, *129*: 141 (1923); *Chem. Abstr.*, *17*: 3273.

219. G.D. Roos, Heat of Fusion and Heat of Formation of Some Metallic Compounds, *Z. Anorg. Allg. Chem.*, *94*: 329 (1916); *Chem. Abstr.* *10*: 1806.

220. N.S. Kurnakow, *Z. Anorg. Chem.*, *23*: 441 (1900).

221. A. Schüller, *Z. Anorg. Chem.*, *40*: 385 (1904).

222. E. Vanstone, Physico-Chemical Study of Mercury-Sodium Alloys or Sodium Amalgams, *Trans. Faraday Soc.*, *7*: 42 (1911); also *Chem. News*, *103*: 181, 198, and 207 (1911); *Chem. Abstr.*, *5*: 2471.

223. W. Klemm and B. Hauschulz, Magnetochemical Investigations. XXXII. Magnetic Measurements on Alkali Metal Amalgams, *Z. Elektrochem.*, *45*: 346 (1939); *Chem. Abstr.*, *33*: 6102.

224. O. Kubaschewski and W. Seith, Heats of Formation of Non-Ferrous Alloys, *Z. Metallk.*, *30*: 7 (1938); *Chem. Abstr.*, *32*: 6600.

225. W. Biltz and F. Meyer, Systematic Affinity Principle. XLVII. Relation of Mercury to a Few Metals, *Z. Anorg. Allg. Chem.*, *176*: 23 (1928); *Chem. Abstr.*, *23*: 755.

226. H. Moissan, *Compt. Rend.*, *114*: 319 (1892).

227. P. Hagenmuller *et al.*, New Binary Compounds of the Alkali Metals with Boron, Silicon, and Germanium, in *The Alkali Metals*, Symposium Proceedings, Nottingham, England, July 19-22, 1966, Special Publication No. 22, p. 207, The Chemical Society, London, 1967.

228. C.H. Mathewson, *Z. Anorg. Chem.*, *48*: 192 (1906).

229. C.T. Heycock and F.H. Neville, *J. Chem. Soc.*, *55*: 668 (1889).

230. W.L. Fink, L.A. Willey, and H.C. Stumpf, Equilibrium Relations in Aluminum-Sodium Alloys of High Purity, *Trans. AIME*, *175*: 364 (1948); *Chem. Abstr.*, *42*: 1862.

231. E.G. Brush, *Aluminum Bearing Alloys in Sodium, Report No. 2 on Evaluation of the Behavior of Aluminum in Sodium*, USAEC Report KAPL-M-EGB-16, Knolls Atomic Power Laboratory, Apr. 6, 1954.

232. E. Scheuer, Solubility of Sodium in Aluminum, *Z. Metallk.*, *27*: 83 (1935); *Chem. Abstr.*, *29*: 7915.

233. C.E. Ransley and H. Neufeld, The Solubility Relationships in the Aluminum-Sodium and Aluminum-Silicon-Sodium Systems, *J. Inst. Metals*, *78*: 25 (1950-51).

234. P. Feschotte and E. Rinck, Solidification Diagram for Na-Ga Alloys, *Compt. Rend.*, *243*: 1525 (1956); *Chem. Abstr.*, *51*: 4245.

235. E. Rinck and P. Feschotte, The Action of Alkali Metals on Gallium, *Compt. Rend.*, *252*: 3592 (1961).

236. E. Rinck and P. Feschotte, Electrical Properties of Sodium-Gallium Alloys, *Compt. Rend.*, *251*: 869 (1960); *Chem. Abstr.*, *55*: 3137.

237. P. Feschotte, Ga-Na and Ga-K Systems, *Ann. Chim. (Paris)*, *6*: 1029 (1961); *Chem. Abstr.*, *57*: 1940.

238. E. Rinck and P. Feschotte, Study of Slight Solubilities in a Molten Metal by Sampling at Constant Temperature in the Liquid Phase: Application to the Ga-Na System, *Compt. Rend.*, *250*: 1489 (1960); *Chem. Abstr.*, *55*: 68.

239. C.T. Heycock and F.H. Neville, *J. Chem. Soc.*, *55*: 676 (1889).

240. E. Zintl and S. Neumayr, Metals and Alloys. XI. Lattice Structure of NaIn and the Deformation of Atoms in Alloys, *Z. Phys. Chem.*, *B 20*: 272 (1933); *Chem. Abstr.*, *27*: 2408.

241. M.F.W. Heberlein, *Trans. Amer. Soc. Metals*, *44*: 545 (1952).

242. H.A. Davies, The Solubility of Indium in Liquid Sodium, *Trans. AIME*, *239*: 928 (1967).

243. G. Grube and A. Schmidt, Electric Conductivity and Phase Diagram of Binary Alloys. XIX. The System Sodium-Thallium, *Z. Elektrochem.*, *42*: 201 (1936); *Chem. Abstr.*, *30*: 5489.

244. O. Kubaschewski, The Thermochemistry of Alloys. IX. The Heat of Formation of an Alloy and the Relation Between the Heat Effect and the Con-

traction of the Volume on Formation of the Alloy, Z. *Elektrochem.*, *47*: 623 (1941); *Chem. Abstr.*, *36*: 4404.

245. W.V. Mässenhausen, The Binary Systems Lanthanum-Sodium and Lanthanum-Calcium, Z. *Metallk.*, *43*: 53 (1952); *Chem. Abstr.*, *46*: 5416.

246. G. Grube and L. Botzenhardt, Alloys of Thorium with Copper, Aluminum, and Sodium, Z. *Elektrochem.*, *48*: 418 (1942); *Chem. Abstr.*, *37*: 5687.

247. H. Pearlman, *Corrosion of Uranium, Thorium, and Uranium Alloys in Sodium and Organics*, USAEC Report NAA-SR-2225, Atomics International, 1957.

248. F. Foote, *Metallurgy Division Progress Report*, Mar. 24 to Mar. 31, 1945, Report CT-2857,

249. J.J. Katz and E. Rabinowitch, *The Chemistry of Uranium*, Chap. 7, p. 177, Division VIII, Vol. 5, National Nuclear Energy Series, McGraw-Hill Book Company, Inc., New York, 1951.

250. T.B. Douglas, A Cryoscopic Study of the Solubility of Uranium in Liquid Sodium at 97.8°, *J. Natl. Bur. Stand.* *52*: 223-226 (1954); *Chem. Abstr.*, *48*: 9158.

251. F.A. Rough and A.A. Bauer, *Constitution of Uranium and Thorium Alloys*, USAEC Report BMI-1300, p. 65, Battelle Memorial Institute, June 2, 1958.

252. E.E. Hoffman, *Compatibility of Dynamic Uranium-Sodium-Type 347 Stainless-Steel System*, Oak Ridge National Laboratory Corrosion Report No. 167, Sept. 16, 1957.

253. F.W. Schonfeld, in *Progress in Nuclear Energy, Metallurgy and Fuels*, Series V, Vol. 2, H.M. Finniston and J.P. Howe (Eds.), p. 579, Pergamon Press, Inc., New York, 1959.

254. C.E. Wicks and F.E. Block, *Thermodynamic Properties of 65 Elements - Their Oxides, Halides, Carbides, and Nitrides*, Bureau of Mines Bulletin 605, 1963.

255. E.W. Guernsey and M.S. Sherman, The Mechanism of the Fixation of Nitrogen as Sodium Cyanide, *J. Amer. Chem. Soc.*, *47*: 1932 (1925).

256. C.C. Addison, M.R. Hobdell, and R.J. Pulham, The Reaction Between Acetylene and Molten Sodium, in *The Alkali Metals*, Symposium Proceedings, Nottingham, England, July 19-22, 1966, Special Publication No. 22, p. 270, The Chemical Society, London, 1967.

257. R.C. Asher and S.A. Wilson, Lamellar Compound of Sodium with Graphite, *Nature (London)*, *181*: 409 (1958).

258. H.L. Recht, G.M. Wolten, and D.E. Gilmartin, The Interaction of Graphite with Sodium Vapour, *J. Inorg. Nucl. Chem.*, *23*: 275 (1961).

259. W.J. Greening and W.A. Davis, *Compatibility of Sodium and Graphite*, USAEC Report NAA-SR-MEMO-1852, Atomics International, 1957. (Internal Distribution Only)

260. M.L. Dzurus, G.H. Hennig, and G.L. Montet, Ternary Lamellar Compounds of Lithium or Sodium with Graphite, in *Proceedings of the 4th Conference on Carbon, Buffalo, N.Y., 1959*, pp. 165-168, Pergamon Press, Inc., New York, 1960.

261. D.C. Gehri and J.B. Ott, *The Solubility of Elemental Carbon in Sodium*, USAEC Report AI-AEC-MEMO-12686, Atomics International, June 19, 1968.

262. F.A. Cafasso, Identification Mechanism(s) of Carbon Transport in Sodium Systems, in *Reactor Development Program Progress Report, January 1968*, USAEC Report ANL-7419, pp. 126-127, Argonne National Laboratory, Feb. 27, 1968.

263. B.W. Mott and G. Long, Atomic Energy Research Establishment, Harwell, personal communication to J.R. Weeks, April 14, 1967.

264. J.G. Gratton, *Solubility of Carbon in Sodium at Elevated Temperatures*, USAEC Report KAPL-1807, Knolls Atomic Power Laboratory, June 30, 1957.

265. J. Wing and J.D. Varley, *Reactor Development Program Progress Report, April 1964*, USAEC Report ANL-6886, p. 18, Argonne National Laboratory, May 1964.

266. Argonne National Laboratory, *Reactor Development Program Progress Report, July 1964*, USAEC Report ANL-6923, p. 32, Aug. 20, 1964.

267. Argonne National Laboratory, *Chemical Engineering Division Research Highlights*, May 1965-April 1966, USAEC Report ANL-7175, p. 143.

268. Argonne National Laboratory, *Reactor Development Program Progress Report, May 1967*, USAEC Report ANL-7342, p. 68.

269. Argonne National Laboratory, *Chemical Engineering Division Research Highlights*, May 1966-April 1967, USAEC Report 7350, p. 60.

270. R.C. Andrews, R.H. Hiltz, L.H. Kirschler, S.J. Rodgers, and F. Tepper, *Effect of High-Temperature Sodium on Austenitic and Ferritic Steels. Topical Report No. 4. Results of Mechanical Properties Tests of 316 SS Specimens in 1200°F Sodium Contaminated with Carbon*, USAEC Report MSAR-65-194, p. 88, MSA Research Corp., December 1965.

271. F.A. Cafasso, Studies of the Colloidal Behavior of Carbon-Bearing Species in Sodium, in *Reactor Development Program Progress Report, December 1967*, USAEC Report ANL-7403, p. 124, Argonne National Laboratory, Jan. 31, 1968.

272. R. Davies, in Discussion, p. 179, of C. Luner, A. Cosgarea, Jr., and H.M. Feder, Solubility of Carbon in Sodium, in *Alkali Metal Coolants*, Symposium Proceedings, Vienna, 1966, International Atomic Energy Agency, Vienna, 1967 (STI/PUB/143).

273. F. Tepper and J. Greer, *Factors Affecting the Compatibility of Liquid Cesium with Containment Materials*, Report AFML-TR-64-327, MSA Research Corp., September 1964.

274. H. Moissan, *Bull. Soc. Chim.*, *27*: 1204 (1902); also *Compt. Rend.* *134*: 1083 (1902).

275. H. Nowotny and E. Scheil, A Ternary Compound in the System Aluminum-Silicon-Sodium, *Metallforschung*, *2*: 76 (1947); *Chem. Abstr.*, *42*: 3635.

276. E. Hohmann, Silicides and Germanides of the Alkali Metals, *Z. Anorg. Chem.*, *257*: 113 (1948); *Chem. Abstr.*, *43*: 5321.

277. R. Schafer and W. Klemm, The Behavior of the Alkali Metals Toward Semimetals. IX. Further Contribution to the Knowledge of the Silicides and Germanides of the Alkali Metals, *Z. Anorg. Allg. Chem.*, *312*: 214 (1961).

278. L.M. Dennis and N.A. Skow, Germanium. XXIX. Germanium Monohydride, *J. Amer. Chem. Soc.*, *52*: 2369 (1930); *Chem. Abstr.*, *24*: 3451.

279. C.A. Kraus and E.S. Carney, Compounds of Ge and H. Reactions and Derivatives. I. Preparation of Monogermane. II. Sodium Tri-hydrogermanides, *J. Amer. Chem. Soc.*, *56*: 765 (1934); *Chem. Abstr.*, *28*: 3019.

280. W. Hume-Rothery, The System: Sodium-Tin, *J. Chem. Soc., 1928*: 947; *Chem. Abstr., 22*: 2696.

281. E. Zintl and A. Harder, Metals and Alloys. XXI. Stoichiometry of Binary Sodium Compounds, *Z. Phys. Chem., B 34*: 238 (1936); *Chem. Abstr., 31*: 1338.

282. W. Biltz and W. Holverscheit, The Systematic Affinity Principle. XXX. The Heats of Formation of Intermetallic Compounds. VI. Tin Alloys, *Z. Anorg. Allg. Chem., 140*: 261 (1924); *Chem. Abstr., 19*, 925.

283. R.L. McKisson and L.A. Bromley, The Heats of Formation of Sodium-Tin Alloys, *Trans. AIME, 194*: 33 (1952).

284. G.R. Barber, L. Brewer, L.A. Bromley, and R.L. McKisson, *Application of the High-Temperature Calorimeter to the Determination of the Heats of Formation of Na-Sn and Li-Sn Alloys*, USAEC Report AECD-2294, University of California Radiation Laboratory, July 1948.

285. W. Biltz, The Heats of Formation of Intermetallic Compounds, *Z. Metallk., 29*: 73 (1937); *Chem. Abstr., 31*: 6543.

286. O. Kubaschewski and F.E. Wittig, The Heat of Formation of Magnesium Telluride, *Z. Elektrochem., 47*: 433 (1941).

287. O. Kubaschewski, The Energetics of Alloy Formation, *Z. Elektrochem., 48*: 646 (1942); *Chem. Abstr., 37*: 4349.

288. G. Tammann, *Z. Phys. Chem., 3*: 446, 448 (1889).

289. H.A. Davies, Brookhaven National Laboratory, personal communication from J.R. Weeks, March 1968.

290. C.T. Heycock and F.H. Neville, *J. Chem. Soc., 57*: 380 (1890).

291. N.L. Pokrovsky and N.D. Galanina, Properties of Metallic Solutions. IV. Surface Tension of Tin and Tin-Sodium Alloys, *Zh. Fiz. Khim., 23*: 324 (1949); *Chem. Abstr., 43*: 6023.

292. C.H. Mathewson, *Z. Anorg. Chem., 50*: 172 (1906).

293. G. Calingaert and W.J. Boesch, Correction to the Freezing Point Diagram of Lead-Sodium Alloys, *J. Amer. Chem. Soc., 45*: 1901 (1923); *Chem. Abstr., 17*: 3473.

294. I.T. Krohn, R.C. Werner, and H. Shapiro, The Compound Na_9Pb_4, *J. Amer. Chem. Soc., 77*: 2110 (1955).

295. D.P. Shoemaker, N.E. Weston, and J. Rathler, On the Dubious Existence of a Second Na_4Pb Phase ($Na_{31}Pb_8$), *J. Amer. Chem. Soc., 77*: 4226 (1955).

296. E. Zintl and A. Harder, Metals and Alloys. II. Polyplumbides, Polystannides and Their Transition into Metal Phases, *Z. Phys. Chem., 154*: 58 (1931); *Chem. Abstr., 25*: 3261.

297. E.S. Makarov and Z.V. Popova, *Izv. Akad. Nauk SSSR Otd. Khim. Nauk, 1951*: 377.

298. C.A. Kraus and J.A. Ridderhof, Heats of Solution and Heats of Reaction in Liquid Ammonia, *J. Amer. Chem. Soc., 56*: 79 (1934); *Chem. Abstr., 28*: 1257.

299. G. Falkenhagen and W. Hofmann, Influence of High Cooling Rates on Solidification and Structure of Binary Alloys, *Z. Metallk., 43*: 69 (1952). *Chem. Abstr., 46*: 5507.

300. Sidney Siegel, R.L. Carter, F.E. Bowman, and B.R. Hayward, Basic Technology of the Sodium Graphite Reactor, in *Proceedings of the International*

Conference on the Peaceful Uses of Atomic Energy, Geneva, 1955, Vol. 9, p. 321, United Nations, New York, 1956.

301. R.L. Eichelberger, Recent Information on Moderator Sheath Corrosion in Liquid Sodium, in *Proceedings of the French-American Conference on Graphite Reactors, Upton, N.Y., Nov. 12-15, 1957*, USAEC Report BNL-489, pp. 168-173, Brookhaven National Laboratory.

302. T.L. Mackay, Oxidation of Zirconium and Zirconium Alloys in Liquid Sodium, *J. Elektrochem. Soc., 110*: 960 (1963).

303. R.L. Carter, R.L. Eichelberger, and Sidney Siegel, Recent Developments in the Technology of Sodium-Graphite Reactor Materials, *Proceedings of the Second United Nations International Conference on the Peaceful Uses of Atomic Energy, Geneva, 1958*, Vol. 7, p. 72, United Nations, New York, 1958.

304. R.L. Eichelberger, R.L. McKisson, and B.G. Johnson, *Solubility Studies of Refractory Metals and Alloys in Potassium and Lithium*, Report AI-68-110, Atomics International, 1968.

305. L. Zehnder, *Wied. Ann., 52*: 56 (1894).

306. Dennis and Browne, *Z. Anorg. Allg. Chem., 40*: 93 (1904).

307. M. Funaoka and E. Iwanaga, *Alkali Azides*, Japanese Patent 3475 to Asahi Glass Company, June 15, 1954; *Chem. Abstr., 49*: 7203.

308. F.A. Cafasso, Characterization of Nitrogen - Bearing Species in Sodium Systems, in *Reactor Development Program Progress Report*, November 1967, USAEC Report ANL-7399, p. 137, Argonne National Laboratory, Dec. 28, 1967.

309. J.J. Gill and J.C. Bokros, *Nitriding of Type 304 Stainless Steel in a Sodium-Nitrogen System*, USAEC Report NAA-SR-6162, Atomics International, May 30, 1961.

310. E.G. Brush and C.R. Rodd, *Preliminary Experiments on the Nitriding of Reactor Materials in Sodium*, USAEC Report KAPL-M-EGB-21, Knolls Atomic Power Laboratory, Sept. 22, 1955.

311. R.C. Andrews and F. Tepper, Mechanical Properties of Materials in Sodium, in *Proceedings of the Sodium Components Development Program Information Meeting, Chicago, June 16-17, 1965*, USAEC Report CONF-650620, p. 1, Chicago Operations Office.

312. J.R. Distefano and E.E. Hoffman, *Corrosion Mechanisms in Refractory Metal-Alkali Metal Systems*, USAEC Report ORNL-3424, Oak Ridge National Laboratory, Sept. 16, 1963.

313. G. Brauer and E. Zintl, Metals and Alloys. XXIII. Phosphides, Arsenides, Antimonides, and Bismuthides of Li, Na, and K, *Z. Phys. Chem., B 37*: 323, 342 (1937); *Chem. Abstr., 32*: 443.

314. M.P. Morozova, G.A. Bol'shakova, and N.L. Lukinykh, Enthalpy of Formation of Compounds of Sodium with Elements of the Main Subgroup of Group V, *Zh. Obshch. Khim., 29*: 3144 (1959); *Chem. Abstr., 54*: 12763.

315. D.J. Peterson and T.J. Logan, Preparation and Methylation of Alkali Metal Phosphides, *J. Inorg. Nucl. Chem., 28*: 53 (1966).

316. C. Legoux, The Decomposition of Alkali Phosphides by the Action of Heat, *Bull. Soc. Chim. Fr., 7*: 545 (1940); *Chem. Abstr.*, 36: 3448.

317. P. Royen, W. Zschaage, and A. Wutschel, *Angew. Chem., 67*: 75 (1955).

318. C.H. Mathewson, *Z. Anorg. Chem., 50*: 192 (1906).

319. E. Zintl and W. Dullenkopf, Metals and Alloys. III. Polyantimonides, Polybismuthides and Their Transformation into Alloys, *Z. Phys. Chem., B 16*: 183 (1932); *Chem. Abstr., 26*: 2952.

320. F. Weibke and O. Kubaschewski, Thermochemie der Legierungen, p. 282, J.W. Edwards Company, Ann Arbor, Mich., 1949 (Berlin, 1943).

321. C.A. Kraus, The Properties of the Elements in the Electronegative Condition, *Trans. Amer. Electrochem. Soc., 45*: 175 (1924); *Chem. Abstr., 18*: 2273.

322. C.H. Mathewson, *Z. Anorg. Chem., 50*: 187 (1906).

323. A.K. Fischer, S.A. Johnson, and S.E. Wovel, Liquid-Vapour Phase Diagram and Thermodynamics of the Sodium-Bismuth System, *J. Phys. Chem., 71*: 1465 (1967).

324. S. Greenberg, W.E. Ruther, and H.A. Levin, Corrosion of Vanadium-Base Alloys in Sodium at 550°C to 750°C, in *Alkali Metal Coolants,* Symposium Proceedings, Vienna, 1966, p. 63, International Atomic Energy Agency, Vienna, 1967 (STI/PUB/143).

325. L. Champeix, R. Darras, and J. Sannier, Corrosion du Vanadium et de ses Alliages dans le Sodium Liquide, in *Alkali Metal Coolants,* Symposium Proceedings, Vienna, 1966, p. 45, International Atomic Energy Agency, Vienna, 1967 (STI/PUB/143).

326. J.W. Evans and A. Thorley, *Corrosion of Niobium and Vanadium in Liquid Sodium,* British Report IGR-TN/C-1019, 1958.

327. T.A. Kovacina and R.R. Miller, *The Solubility of Columbium-1% Zirconium in Sodium by Activation Analysis,* Report NRL-6051, Naval Research Laboratory, Mar. 20, 1964.

328. J.A. Grand *et al.*, The Solubility of Tantalum and Cobalt in Sodium by Activation Analysis, *J. Phys. Chem., 63*: 1192 (1959).

329. D.F. Anthrop, *The Solubilities of Transition Metals in Liquid Alkali and Alkaline Earth Metals, Lanthanum and Cerium: A Critical Review of the Literature,* USAEC Report UCRL-50315, Lawrence Radiation Laboratory, Sept. 20, 1967.

330. R. Bouaziz, G. Papin, and A.P. Rollet, The Oxide of Sodium and the Binary System Na_2O-NaOH, *Compt. Rend., 262*: 1051 (1966).

331. T.P. Whaley and J. Kleinberg, A Contribution to the Chemistry of the Alkali Metal "Ozonates", *J. Amer. Chem. Soc., 73*: 79 (1951).

332. G.P. Nikol'skii, Z.A. Bagdasar'yan, and I.A. Kezarnovskii, Ozonides of Na, Rb, and Cs, *Dokl. Akad. Nauk SSSR, 77*: 69 (1951).

333. O.N. Salmon and T.J. Cashman, Jr., *The Solubility of Sodium Monoxide in Liquid Sodium,* USAEC Report KAPL-1653, Knolls Atomic Power Laboratory, Nov. 30, 1956.

334. S.L. Walters, *The Effects of Adding Oxygen to Sodium Flowing in a Stainless Steel System.* Technical Report VI, USAEC file No. NP-1955, Mine Safety Appliances Co., Sept. 1, 1950.

335. A.D. Bogard and D.D. Williams, *Solubility of Sodium Monoxide and of Sodium Hydroxide in Metallic Sodium,*

Report NRL-3865, Naval Research Laboratory, Sept. 26, 1951.

336. J.D. Noden and K.Q. Bagley, *The Solubility of Oxygen in Sodium and Sodium-Potassium Alloy,* British Report RDB(C)-TN-80, July 20, 1954.

337. W. Jahns and G. Weidmann, The Determination of Low Oxygen Concentrations in Sodium, *Nukleonik, 1*: 189 (1959).

338. A.W. Thorley, in K.T. Claxton, Review of Solubility Data for the Liquid Sodium-Oxygen System, *J. Nucl. Energy, 19*: 849 (1965).

339. S. Dorner, *Solubility of Oxygen in Sodium,* Report EURFNR-179P, U.S.-Euratom Fast Reactor Exchange Program, Apr. 25, 1966.

340. D.B. Hall, R.H. Perkins, and V.J. Rutkauskas, Measurement of Impurities and Development of Quality Control Techniques for High-Temperature Sodium Coolant Systems, in *Quarterly Status Report on the Advanced Plutonium Fuels Program,* Apr. 1-June 30, 1967, USAEC Report LA-3745, Los Alamos Scientific Laboratory, Aug. 30, 1967.

341. C.R.F. Smith, *The Determination of Oxygen in Sodium - A Critical Review of Analytical Methods,* USAEC Report NAA-SR-Memo-2061, Atomics International.

342. K.T. Claxton, Contribution on the Solubility of Oxygen in Liquid Sodium, *J. Nucl. Energy, 21*: 351 (1967).

343. R.L. Eichelberger, *The Solubility of Oxygen in Liquid Sodium: A Recommended Expression,* USAEC Report AI-AEC-12685, Atomics International, Nov. 1, 1968.

344. T.F. Prach, Determination of Oxygen in Sodium, in *Annual Progress Report of Work Sponsored by the Fuels and Materials Branch,* Jan. 1 - Dec. 31, 1967, USAEC Report BNL-50092, p. 45, Brookhaven National Laboratory, March 1968.

345. V.I. Subbotin, P.L. Kirillov, and F.A. Kozlov, Purification of Sodium from Oxygen and the Control of the Content of Oxygen in Sodium, *Teplofiz. Vyso. Temp., Akad. Nauk SSSR, 3* (1): 154-163 (1965); *Chem. Abstr., 62*: 15799 g.

346. T.F. Kassner and D.L. Smith, *Calculations on the Kinetics of Oxygen Solution in Tantalum and Niobium in a Liquid - Sodium Environment,* USAEC Report ANL-7335, Argonne National Laboratory, September 1967.

347. E.J. Kohlmeyer and H. Brinkman, Sodium Sulfide, Na_2S_2, and Its Behavior in the Liquid State, *Z. Anorg. Chem., 299*: 182 (1959).

348. O. Erametsa and K. Karlsson, Crystal Chemistry of Some Sodium Polysulfides, *Acta Polytech. Scand., 1961*(15); 18: *Chem. Abstr., 56*: 2066.

349. T.G. Pearson and P.L. Robinson, The Polysulfides of the Alkali Metals. I. Sodium (i), *J. Chem. Soc., 1930*: 1473; *Chem. Abstr., 24*: 4724.

350. M. Hansen, *Der Aufbau der Zweistofflegierungen,* Edwards Bros. Inc., Ann Arbor, Mich., 1943 (Julius Springer, Berlin, 1936).

351. C.H. Mathewson, The Selenides of Sodium, *J. Amer. Chem. Soc., 29*: 867 (1907); *Chem. Abstr., 2*: 235.

352. F.D. Rossini *et al.* (Eds.), *Selected Values of Chemical Thermodynamic Properties,* National Bureau of Standards, Circular No. 500, Superintendent of Documents, U.S. Government Printing Office, Washington, 1952.

353. P.G. Maslov, Thermodynamic Properties of Sodium Compounds in the Solid Phase, *Zh. Fiz. Khim., 33:* 1461 (1959); *Chem. Abstr., 54*: 9480.

354. H.D. Mulder and F.C. Schmidt, Heats of Solution and Reaction in Liquid Ammonia VIII, *J. Amer. Chem. Soc., 73*: 5575 (1951); *Chem. Abstr., 46*: 2389.

355. G. Pellini and E. Quercigh, Tellurides of Sodium, *Atti Reale Accad. Lincei, 19* (2): 350 (1910); *Chem. Abstr., 5*: 1567.

356. C.A. Kraus and S.W. Glass, Liquid Mixtures of Tellurium and Sodium Telluride. II. Phase Diagram of the System Te-Na_2Te, *J. Phys. Chem., 33*: 995 (1929); *Chem. Abstr., 23*: 5375.

357. Atomics International, *Quarterly Technical Progress Report, AEC Unclassified Programs,* January-March 1968, USAEC Report AI-AEC-12680.

358. R.L. McKisson, R.L. Eichelberger, R.C. Dahleen, J.M. Scarborough, and G.R. Argue, *Solubility Studies of Ultra-Pure Transition Elements in Ultra-Pure Alkali Metals,* Report NASA-CR-610, North American Aviation, Inc., October 1966.

359. M.A. Bredig, J.W. Johnson, and W.T. Smith, Jr., Miscibility of Liquid Metals with Salts. I. The Sodium-Sodium Halide Systems, *J. Amer. Chem. Soc., 77*: 307 (1955).

360. L. Stockem, *Z. Angew. Chem., 17*: 431 (1904).

361. R.A. Baus, A.D. Bogard, J.A. Grand, L.B. Lockhart, Jr., R.R. Miller, and D.D. Williams, The Solubility of Structural Materials in Sodium, *Proceedings of the International Conference on the Peaceful Uses of Atomic Energy, Geneva, 1955,* Vol. 9, p. 356, United Nations, New York, 1956.

362. A.D. Bogard, *The Solubility of Iron in Sodium Metal, Sodium-Sodium Oxide, and Sodium-Sodium Oxide-Sodium Hydroxide,* Report NRL-4131, Naval Research Laboratory, Mar. 9, 1953.

363. S.J. Rodgers, J.W. Mausteller, and E.F. Batutis, *Iron and Nickel Concentrations in Sodium,* USAEC file No. NP-5247, Mine Safety Appliances Co., June 30, 1954.

364. L.F. Epstein, Preliminary Studies on the Solubility of Iron in Liquid Sodium, *Science, 112*: 426 (1950).

365. J.R. Weeks (Comp.), *Annual Progress Report of Work Sponsored by the Fuels and Materials Branch,* Jan.1-Dec. 31, 1967, USAEC Report 50092, Brookhaven National Laboratory, March 1968.

366. Atomics International, *Quarterly Technical Progress Report., October - December, 1967,* USAEC Report AEC-12638, pp. 166 and 167.

367. P.G. Drugas and L.R. Kelman, *Equipment and Procedures for Studying the Equilibrium Solubility of Iron in NaK,* USAEC Report ANL-5359, Argonne National Laboratory, Sept. 4, 1953.

368. T.A. Kovacina and R.R. Miller, The Solubility of Nickel in Sodium by a Tracer Technique, *Nucl. Sci. Eng., 10*: 1963 (1961).

369. A.W. Thorley and C. Tyzack, Corrosion Behavior of Steels and Nickel Alloys in High-Temperature Sodium, in *Alkali Metal Coolants,* Symposium Proceedings, Vienna, 1966, p. 97, International Atomic Energy Agency, Vienna, 1967 (STI/PUB/143).

370. J.H. DeVan, Corrosion of Iron and Nickel-Base Alloys in High-Temperature Sodium and NaK, in Alkali Metal Coolants, Symposium Proceedings, Vienna, 1966, p. 643, International Atomic Energy Agency, Vienna, 1967 (STI/PUB/143).

371. C.P. Nash, F.M. Boyden, and L.D. Whittig, Intermetallic Compounds

of Alkali Metals with Platinum. A Novel Preparation of a Colloidal Platinum Hydrogenation Catalyst, *J. Amer. Chem. Soc.*, *82*: 6203 (1960).

372. C.C. Addison *et al.*, The Liquid Metals as Reaction Media, in *The Alkali Metals*, Symposium Proceedings, Nottingham, England, July 19-22, 1966, Special Publication No. 22, p. 290, The Chemical Society, London, 1967.

373. C.C. Addison, Liquid Sodium, *Endeavour*, *26*(98): 91 (1967).

374. H.M. Feder, Chemistry in Liquid Metal Solvents, *Annual Priestley Lectures*, *39*: 111-130 (1965).

375. J.A. Ford, *Literature Review of Sodium-Water Reactions*, USAEC Report APDA-167, Atomic Power Development Associates, Inc., Mar. 15, 1965.

376. H. Rompp, *Chemie der Metalle*, Franck'sche Verlag, Stuttgart, 1949.

377. L. Corrsin, H. Steinmetz, and B. Marano, *Sodium-Water Reaction Rate Studies*, USAEC Report NDA-84-19, Nuclear Development Corp. of America, May 15, 1959.

378. A.J. Marino, Letter, in *Metal Progr.*, *72*: 116 (1957).

379. G. Naud, *Contribution to the Study of Hydrogenated and Oxygenated Impurities in Liquid Sodium*, USAEC Report AEC-TR-6582, translated from French Report CEA-R-2583, 1964.

380. Nuclear Development Corp. of America, *Chemical Considerations in the Sodium-Cooled, D_2O-Moderated Reactor (SDR)*, USAEC Report NDA-84-6, Apr. 30, 1958,

381. M. Kilpatrick, L.L. Baker, Jr., and C.D. McKinney, Jr., Studies of Fast Reactions Which Evolve Gases. The Reaction of Sodium-Potassium Alloy with Water in the Presence and Absence of Oxygen, *J. Phys. Chem.*, *57*: 385 (1953).

382. D.D. Williams, *A Study of the Sodium-Hydrogen-Oxygen System*, Report NRL-MEMO-33, Naval Research Laboratory, June 1952.

383. C.C. Addison and J.A. Manning, The Reaction of Water Vapor with Liquid Sodium, Sodium Peroxide, Sodium Monoxide and Sodium Hydride, Vapor Pressures in the Sodium Hydroxide-Water System, *J. Chem. Soc.*, *1964* (December): 4887.

384. W.B. Woollen, D. Scott, and F.R. Dell, *Sodium-Steam Reaction Experiments*, British Report AERE-CE/R-2158, 1956.

385. P.B. Longton, *Alkali Metal-Gas Reactions. Part X. The Influence of Hydrogen on the Reaction of Sodium with Oxygen*, British Report IGR-TN/C-536, April 1957.

386. J.R. Humphreys, Jr., Sodium-Air Reactions as They Pertain to Reactor Safety and Containment, in *Proceedings of the Second International Conference on the Peaceful Uses of Atomic Energy, Geneva, 1958*, Vol. 11, p. 177, United Nations, New York, 1958.

387. C.O. Nelson and D.B. Nelson, *Sodium-Air Reaction Experiments*, USAEC Report KAPL-639, Knolls Atomic Power Laboratory, Jan.1, 1952.

388. J.D. Gracie and J.J. Droher, *A Study of Sodium Fires*, USAEC Report NAA-SR-4383, Atomics International, Oct. 15, 1960.

389. D.D. Williams, J.A. Grand, and R.R. Miller, Determination of the Solubility of Oxygen Bearing Impurities in Na, K and Their Alloys, *J. Phys. Chem.*, *63*: 68 (1959).

390. E.C. King and C.A. Wedge, Jr., *Reaction of NaK and H_2O.* Technical Report VII, USAEC file No. NP-1956, Mine Safety Appliances Co., Nov. 1, 1950.

391. E.C. King, *The Reaction of NaK and H_2O,* USAEC file No. NP-3334, Mine Safety Appliances Co., Sept. 7, 1951.

392. USAEC Health and Safety Information, *Explosions Involving Metallic Potassium or NaK,* Series No. 251, March 13, 1967.

393. M.A. Salmon, *Effects of Tube Leaks in Sodium-Heated Steam Generators,* USAEC Report NAA-SR-8140, Atomic Atomics International, Apr. 15, 1963.

394. J. Jortner, Energy Levels of Bound Electrons in Liquid Ammonia, *J. Chem. Phys., 30*: 839 (1959).

395. E. Becker, R.H. Lindquist, and B.J. Adler, Model for Metal Ammonia Solutions, *J. Chem. Phys., 25*: 971 (1956).

396. T.P. Das, Structure and Properties of Metal Ammonia Solutions, in I. Prigogine (Ed.), *Advances in Chemical Physics,* Vol. 9, p. 303, Interscience Publishers, New York, 1966.

397. F. Griengl, F. Steyskal, and K. Steyskal, Conductivities and the Solubility Relations in the Systems, Na-K-NH_3 and Na-Li-NH_3, *Monatsh., 63*: 394-426 (1933).

398. W.L. Jolly, Metal-Ammonia Solutions, in F.A. Cotton (Ed.), *Progress in Inorganic Chemistry,* Vol. I, pp. 239 and 240, Interscience Publishers, New York, 1959.

399. H.W. Alter and P.A. McManus, *Sodium Mass Transfer. III. The Application of Liquid NH_3 as a Sodium Leaching Agent,* USAEC Report GEAP-4006, General Electric Company, April 1962.

400. M. Skossarewsky and N. Tchitchinadze, Solubility of Caustic Soda in NH_3, *J. Chim. Phys., 14*: 153 (1916)

401. W.M. Burgess and H.L. Kahler, Study of Heterogenous Catalysis in Liquid NH_3 Solutions. I, *J. Amer. Chem. Soc., 60*: 189 (1938).

402. C.A. Kraus and F.C. Schmidt, Heats of Solution and Heats of Reaction in Liquid Ammonia. III, *J. Amer. Chem. Soc., 56*: 2297 (1934).

403. E.J. Hart (Ed.), *Solvated Electron,* Proceedings of Solvated Electron Symposium, Atlantic City, 1965, American Chemical Society, Washington, 1965.

404. G.W. Watt, Reactions of Organic and Organometallic Substances with Solutions of Metals in Liquid Ammonia, *Chem. Rev., 46*: 317 (1950).

405. G.W. Watt, Reactions of Inorganic Substances with Solutions of Metals in Liquid Ammonia, *Chem. Rev., 46*: 289 (1950).

406. L. Paoloni, Solutions of Alkali Metals in Liquid Ammonia, *Gazz. Chim. Ital., 90*: 1682 (1960); also *91*: 121, 412, 518, 529, 787, and 1063 (1961).

407. S.R. Gunn and L.G. Green, Heats of Solution of Alkali Metals in Liquid Ammonia at 25°, *J. Chem. Phys., 36*: 368 (1962).

408. T.R. Tuttle, Jr., *et al.*, Heats of Solution of Alkali Metals in Ammonia, *J. Chem. Phys., 45*: 2206 (1966).

409. P.R. Marshall, Activities in Alkali - Ammonia Solutions, *J. Chem. Eng. Data, 7*: 393 (1962).

410. G. Lepoutre and M.J. Sienko (Eds.), *Metal Ammonia Solutions: Physicochemical Properties,* W.A. Benjamin, New York, 1964.

411. W.L. Jolly, Methods for Estimating Thermodynamic Quantities of Species in Liquid Ammonia, *J. Phys. Chem., 58*: 250 (1954).

412. V.M. Sinclair, R.A. Davies, and J.L. Drummond, Reaction of Carbon Monoxide with Sodium, in *The Alkali Metals,* Symposium Proceedings, Nottingham, England, July 19-26, 1966, Special Publication No. 22, p. 260, The Chemical Society, London, 1967.

413. F. Lenze and L. Metz, The Explosibility of Systems of Base Metals and Halogen Compounds, *Chem. Ztg., 56*: 921 (1932).

414. R.M. Bowie, Color and Intensity of the Chemiluminescence of Solid Na, *J. Phys. Chem., 35*: 2964 (1931).

415. H.N. Gilbert, Some Unique Properties of Sodium and Potassium, *Chem. Eng. News, 26*: 2604 (1948).

416. H.C. Miller, *Hexasodium Hexacarbonyl,* U.S. Patent No. 2,858, 194, to E.I. du Pont de Nemours & Company, Oct. 28, 1958.

417. H.N. Gilbert, *Sodium Carbide and Acetylene,* U.S. Patent No. 2,642,347, to E.I. du Pont de Nemours & Company, June 16, 1953.

418. H. Haupt, German Patent 286,461.

419. H.W. Nicolai, Na Amalgam as an Industrial Raw Material, *Chim. Ind., 73*: 1149 (1955).

420. Atomic Power Development Associates, *Quarterly Technical Progress Report on AEC - Sponsored Activities,* October - December, 1965, USAEC Report APDA-182, p. 11.10.

421. Atomic Power Development Associates, *Quarterly Technical Progress Report on AEC - Sponsored Activities,* Mar. 15 - June 15, 1967, USAEC Report APDA-206, p. 11.25.

422. H. Ornig Processes for the Carbonization of Steels in Melts, *Atompraxis, 6*(4/5): 129 (1960).

423. Argonne National Laboratory, *Reactor Development Program Progress Report,* December, 1965, USAEC Report ANL-7132, p. 49, Jan. 25, 1966.

424. Argonne National Laboratory, *Reactor Development Program Progress Report,* September, 1967, USAEC Report ANL-7382, p. 125, Oct. 31, 1967.

425. C.J. Smithells *et al.*, High Temperature Phenomena of Tungsten Filaments, *Trans. Faraday Soc.,* advance copy, 1921.

426. V.S. Lyashenko and B.A. Nevzorov, The Mechanism of Carbon Transfer in Liquid Sodium, in *Corrosion of Reactor Materials,* Symposium Proceedings, Salzburg, Austria, June 1962, Vol. II, p. 373, International Atomic Energy Agency, Vienna, 1962 (STI/PUB/59). (In Russian.) For English translation, see USAEC Report AEC-tr-5408.

427. A. Glassner, *The Thermochemical Properties of the Oxides, Fluorides, and Chlorides to 2500°K,* USAEC Report ANL-5750, Argonne National Laboratory, 1957.

428. J.R. Weeks and C.J. Klamut, Liquid Metal Corrosion Mechanisms, *Corrosion of Reactor Materials,* Symposium Proceedings, Salzburg, Austria, June 1962, Vol. I, p. 105, International Atomic Energy Agency, Vienna, 1962 (STI/PUB/59).

429. L.F. Epstein and C.E. Weber, Problems in the Use of Molten Sodium as a Heat Transfer Fluid, Part II, in *Nuclear Science and Technology,* USAEC Report TID-2501 [Del.] (1957), pp.

455-520, 1957.

430. D.T. Livey and P. Murray, *The Surface Energies of Solid Oxides and Carbides,* British Report AERE-M/R-1846, Jan. 24, 1956.

431. J.R. Weeks, C.J. Klamut, and D.H. Gurinsky, Corrosion by the Alkali Metals, in *Alkali Metal Coolants,* Symposium Proceedings, Vienna, 1967, p. 3, International Atomic Energy Agency, Vienna, 1967 (STI/PUB/143).

432. W.T. Chandler and N.J. Hoffman, The Role of Oxygen in Attack of Refractory Metals by Alkali Metals in R.I. Jaffe (Ed.), *Refractory Metals and Alloys III: Applied Aspects,* p. 509, Gordon & Breach, Science Publishers, Inc., New York, 1966.

433. G.W. Horsley, The Corrosion of Iron by Oxygen-Contaminated Sodium, *J. Iron Steel Inst., 182:* 43 (1956).

434. C.C. Addison, M.G. Barker, and R.J. Pulham, Reactions of Liquid Sodium with Transition - Metal Oxides. Part I. The Dioxides of Mo, W, and U, *J. Chem. Soc., 1965* (August): 4483.

435. C.C. Addison and M.G. Barker, Reduction of Chromium Trioxide to a Ternary Oxide of Chromium IV, *J. Chem. Soc., 1965* (October); 5534.

436. C.C. Addison *et al.*, The Reactions of Liquid Sodium and Liquid Potassium with Niobium Pentoxide, in *The Alkali Metals,* Symposium Proceedings, Nottingham, England, July 19-22, 1966, Special Publication No. 22, p. 460, The Chemical Society, London 1967.

437. M.J. Sienko, Solid State Studies of Alkali Metals in Transition - Metal Oxides, in *The Alkali Metals,* Symposium Proceedings, Nottingham, England, July 19-22, 1966, Special Publication No. 22, p. 429, The Chemical Society, London, 1967.

438. H. Kessler, A. Hatterer, and A. Hérold, Action of Alkali Metal Vapours on the Trioxides of Molybdenum and Tungsten, in *The Alkali Metals,* Symposium Proceedings, Nottingham, England, July 19-22, 1966, Special Publication No. 22, p. 465, The Chemical Society, London, 1967.

439. R. Hoppe, On Ternary Oxides of Alkali Metals "Rich in Cations", in *The Alkali Metals,* Symposium Proceedings, Nottingham, England, July 19-22, 1966, Special Publication No. 22, p. 452, The Chemical Society, London, 1967.

440. P. Hagenmuller *et al.*, Comparative Study of Methods of Preparation of Ternary Oxides of Potassium with Elements in the +4 Oxidation State, in *The Alkali Metals,* Symposium Proceedings, Nottingham, England, July 19-22, 1966, Special Publication No. 22, p. 483, The Chemical Society, London, 1967.

441. R.L. Loftness, W.C. Ruebsamen, and T.A. Coultas, *The Corrosion of Refractory Materials in Sodium,* USAEC Report NAA-SR-126, Atomics International, Nov. 20, 1951.

442. W.H. Cook, *Corrosion Resistance of Various Ceramics and Cermets to Liquid Metals,* USAEC Report ORNL-2391, Oak Ridge National Laboratory, June 15, 1960.

443. L.R. Kelman, *Effect of Na-K Alloy on Various Materials at Elevated Temperatures,* USAEC Report CT-3726, Argonne National Laboratory, Dec. 1, 1946.

444. *Corrosion of Reactor Materials,* Symposium Proceedings, Salzburg, Austria, June 1962, Vols. I and II, International Atomic Energy Agency, Vienna, 1962 (STI/PUB/59).

445. *Proceedings of the NASA-AEC Liquid-Metals Corrosion Meeting,* Vol. I, Lewis Research Center, Cleveland, Ohio, Oct. 2-3, 1963, Report NASA-SP-41, National Aeronautics and Space Administration, 1964.

446. *Proceedings of the Third International Conference on the Peaceful Uses of Atomic Energy, Geneva, 1964,* United Nations, New York, 1965.

447. *AEC-NASA Liquid Metals Information Meeting, Gatlinburg, Tenn., Apr. 21-23, 1965,* USAEC Report CONF-650411, Oak Ridge National Laboratory.

448. *The Alkali Metals,* Symposium Proceedings, Nottingham, England, July 19-22, 1966, Special Publication No. 22, The Chemical Society, London, 1967.

449. *Alkali Metal Coolants,* Symposium Proceedings, Vienna, 1966, International Atomic Energy Agency, Vienna, 1967 (STI/PUB/143).

450. J.M. Williams, The Oxidation of Refractory Metals in Liquid Sodium, in *AEC-NASA Liquid Metals Information Meeting, Gatlinburg, Tenn., Apr. 21-23, 1965,* USAEC Report CONF-650411, pp. 57-60, Oak Ridge National Laboratory.

451. R.L. McKisson, R.L. Eichelberger, and J.B. Ott, *The Construction and Operation of a Sodium Purification Apparatus,* USAEC Report NAA-SR-12444, Atomics International, July 15, 1967.

452. L.F. Epstein and J. Nigriny, *The Thermodynamics of Reducibility of Fission Product Oxides by Sodium and Other Elements,* USAEC Report AECD-3709, Knolls Atomic Power Laboratory, Apr. 27, 1948.

453. R.T. Pepper, J.R. Stubbles, and C.R. Tottle, The Constitution of the Sodium-Rich Region of the Sodium-Uranium-Oxygen System, *Appl. Mater. Res., 3*(4): 203 (1964).

454. R. Ward (Ed.), *Nonstoichiometric Compounds,* Advances in Chemistry Series 39, American Chemical Society, Washington, 1963.

455. *Nuclear Reactor Chemistry, Second Conference, Gatlinburg, Tenn., Oct. 10-12, 1961,* USAEC Report TID-7622, Oak Ridge National Laboratory.

456. D.L. Keller, *Progress Relating to Civilian Applications During October - December, 1967,* USAEC Report BMI-1826, Battelle Memorial Institute, Jan. 1, 1968.

457. F.P. Glasser, The Lithium and Sodium Silicates, in *The Alkali Metals,* Symposium Proceedings, Nottingham, England, July 19-22, 1966, Special Publication No. 22, p. 474, The Chemical Society, London, 1967.

458. B.A. Nevzorov, Discussion Following V.S. Lyashenko and B.A. Nevzorov, The Mechanism of Carbon Transfer in Sodium, in *Corrosion of Reactor Materials,* Symposium Proceedings, Salzburg, Austria, June 1962, Vol. II, p. 373, International Atomic Energy Agency, Vienna, 1962 (STI/PUB/59).

459. C.E. Weber and L.F. Epstein, Problems in the Use of Molten Sodium as a Heat Transfer Fluid, Part I, in *Nuclear Science and Technology,* USAEC Report TID-2501 [Del.], pp. 291-316, 1957.

460. O. Flint, *Carbon Transport in Liquid Sodium,* British Report AERE-M-1522L, January 1965.

461. L.F. Epstein, *Notes on Liquid-Metal Studies in France and Great Britain,* Report NASA-TM-X-884, General Electric Company, June 1963.

462. E.K. Storms, *The Refractory Carbides,* Academic Press, Inc., New York, 1967.

463. Mine Safety Appliances Research Corp., *Effect of High-Temperature Sodium on Austenitic and Ferritic Steels. Mechanical Properties of Materials*, USAEC Report MSAR-66-71, Apr. 25, 1966.

464. E.G. Brush and R.F. Koenig, Low-Cost Materials for Sodium Heat Transfer Systems, in Chemical Engineering Progress Symposium Series, No. 20, p. 59, American Institute of Chemical Engineers, New York, 1957.

465. S.W.K. Shaw and A.G. Quarrel, The Formation of Carbides in Low - Carbon Chromium-Vanadium Steels at 700°C, *J. Iron Steel Inst.*, *185*: 10 (1957).

466. C.S. Campbell and C. Tyzack, A Preliminary Model for the Carburization of Stainless Steel at High Temperatures in Sodium Containing Carbon at Unit Activity, in *Alkali Metal Coolants*, Symposium Proceedings, Vienna, 1966, p. 159, International Atomic Energy Agency, Vienna, 1967 (STI/PUB/143).

467. R.C. Andrews and K.R. Barker, *Effect of High-Temperature Sodium on Austenitic and Ferritic Steels. Physical Properties of Materials*. Topical Report No. 3. Results of Physical Property Tests of 2¼ Cr-1 Mo Steel Specimens in Sodium with High and Low Oxygen, Air, and Helium Environments at 1100°F, USAEC Report MSAR-64-81, Mine Safety Appliances Research Corp., July 1964.

468. B.R.T. Frost, The Carbides of Uranium, *J. Nucl. Mater.*, *10*(4); 265 (1963).

469. R.L. McKisson, G. Ervin, Jr., E.W. Murbach, and R.L. Eichelberger, *Literature Review and Evaluation of Factors Affecting the Chemical Stability of Carbide Fuels for the LMFBR*, Report AI-66-TDR-197, Atomics International, 1966.

470. B.A. Webb, *Carburization of Austenitic Stainless Steel by Uranium Carbides in Sodium Systems*, USAEC Report NAA-SR-6246, Atomics International, May 31, 1963,

471. P.E. Elkins, *Compatibility of Uranium Carbide Fuels with Cladding Materials*, USAEC Report NAA-SR-7502, Atomics International, Aug. 1, 1964.

472. E.K. Storms and E.J. Huber, Jr., The Heat of Formation of Uranium Carbide, *J. Nucl. Mater.*, *23*: 19 (1967).

473. The Roessler and Hasslacher Chemical Co., Inc., *Sodium*, Niagara Falls, N.Y., 1931.

474. R.L. McKisson and K.E. Horton, *The Behavior of Tetralin in Liquid Sodium*, USAEC Report NAA-SR-1771, Atomics International, Feb. 1, 1957.

475. B. Fetkenheur, The Action of Sodium Amalgam on Carbon Tetrachloride, *Z. Anorg. Allg. Chem.*, *117*: 281 (1921); *Chem. Abstr. 16*: 1192.

476. H. Staudinger, *Z. Elektrochem.*, *31*: 549 (1925).

477. J. Cueilleron, Explosion Reduction by Shock of Halides by the Alkali Metals, *Bull. Soc. Chim.*, *12*: 88 (1945); *Chem. Abstr.*, *40*: 4309.

478. V. Neustadter, Methylethylacetaldehyde, *Monatsh.*, *27*: 879 (1906); *Chem. Abstr.*, *1*: 325.

479. S.C. Furman, *Metal-Water Reactions. V. The Kinetics of Metal-Water Reactions - Low-Pressure Studies*, USAEC Report GEAP-3208, General Electric Company, July 31, 1959.

480. E.A. Shaede and D.C. Walker, The Reaction Between Alkali Metals and Water, in *The Alkali Metals*, Sym-

posium Proceedings, Nottingham, England, July 19-22, 1966, Special Publication No. 22, p. 277, The Chemical Society, London, 1967.

481. J.V. Cathcart, L.L. Hall, and G.P. Smith, Oxidation Characteristics of the Alkali Metals. I. Oxidation Rate of Sodium Between -79 and 48°C, *Acta Met.*, *5*: 245 (1957).

482. N.B. Pilling and R.E. Bedworth, Oxidation of Metals at High Temperatures, *J. Inst. Metals*, *29*: 529 (1923); *Chem. Abstr.*, *17*: 1941.

483. N. Cabrera and N.F. Mott, Theory of Oxidation of Metals, *Repts. on Progress in Physics*, *12*: 163-184 (1949).

484. J. Besson and P. Touzain, Cinétique de l'Oxydation du Sodium Liquide par l'Oxygene Sec, *Compt. Rend.*, *258*: 3720 (1964).

485. A. Hatterer and M. Thevenin, Influence of Water Content of Oxygen on the Kinetics of Sodium and Potassium Oxidation, in *The Alkali Metals*, Symposium Proceedings, Nottingham, England, July 19-22, 1966, Special Publication No. 22, p. 167, The Chemical Society, London, 1967.

486. F.E. Bowman and D.D. Cubicciotti, Use of Zirconium in Liquid Sodium Systems, *A. I. Ch. E. (Amer. Inst. Chem. Eng.) J.*, *2*: 173 (1956).

487. B.A. Nevzorov, The Nature of Oxygen in Liquid Sodium, in *Corrosion of Reactor Materials*, Symposium Proceedings, Salzburg, Austria, June 1962, Vol. II, p. 271, International Atomic Energy Agency, Vienna, 1962 (STI/PUB/59). (In Russian.) For English translation, see USAEC Report AEC-tr-5412.

488. Mine Safety Appliances Research Corp., *Development of Techniques for Measurement of Impurities in Sodium.* Quarterly Progress Report, October - December, 1966, USAEC Report MSAR-67-18, Feb. 7, 1967.

489. L.F. Epstein, Static and Dynamic Corrosion and Mass Transfer in Liquid Metal Systems, Chemical Engineering Progress Symposium Series, No. 20, p. 67, American Institute of Chemical Engineers, New York, 1957.

490. S.S. Blecherman, G.F. Schenck, and R.E. Cleary, Solubility Studies in Alkali Metals, in *AEC-NASA Liquid Metals Information Meeting, Gatlinburg, Tenn., Apr. 21-23, 1965*, USAEC Report CONF-650411, pp. 48-53, Oak Ridge National Laboratory.

491. A.P. Litman, Interactions in the Niobium-Oxygen-Potassium System, *AEC-NASA Liquid Metals Information Meeting, Gatlinburg, Tenn., Apr. 21-23, 1965*, USAEC Report CONF-650411, pp. 61-62, Oak Ridge National Laboratory.

492. C. Tyzack, Application of Sodium Chemistry in Fast Reactors, in *The Alkali Metals*, Symposium Proceedings, Nottingham, England, July 19-22, 1966, Special Publication No. 22, p. 236, The Chemical Society, London, 1967.

493. C.W. Hickam, Jr., *Corrosion Product of the Tantalum-Interstitial Oxygen-Potassium System at 1800°F (1255°K)*, Report NASA-TN-D-4213, National Aeronautics and Space Administration, Cleveland, Lewis Research Center, 1967.

494. C.M. Scheuermann and C.A. Barrett, *Compatibility of Columbium and Tantalum Tubing Alloys with Refluxing Potassium*, Report NASA-TN-D-3429, National Aeronautics and Space Administration, May 1966.

495. R.E. Cleary, S.S. Blecherman,

and J.E. Corliss, *Solubility of Refractory Metals in Lithium and Potassium*, USAEC Report TIM-850, Pratt and Whitney Aircraft, November 1965.

496. J.W. Mausteller and E.F. Batutis, *Effect of Oxygen on Mass Transport of Stainless-Steel Components in Sodium*, USAEC file No. NP-5583, Mine Safety Appliances Co., Mar. 17, 1955.

497. E.F. Batutis, J.W. Mausteller, and C.A. Palladino, *Nitrogen Containing 2% Oxygen as a Sodium System Cover Gas*, USAEC file No. NP-5935, Mine Safety Appliances Co., Apr. 10, 1956.

498. E.F. Batutis, C.A. Palladino, R. Gagne, and J.W. Mausteller, *A Study of Nitrogen as a Cover Gas in Sodium Systems*, USAEC file No. NP-6178, Mine Safety Appliances Co., Dec. 7, 1956.

499. L. Baker, Jr., and A.D. Tevebaugh, Sodium-Air Reaction Calculations, in *Chemical Engineering Division Semiannual Report*, January-June 1965, USAEC Report ANL-7055, pp. 208-211, Argonne National Laboratory, October 1965.

500. R.S. Young, *Sodium Components Development Program. Mass-Transfer Investigations in Liquid-Metal Systems.* Quarterly Progress Report No. 1, March-May 1967, USAEC Report GEAP-5508, pp. 5-13, General Electric Company, June 1967.

501. I. Johnson, J.W. Reishus, and C. Luner, Mass Spectrometric Studies, in *Chemical Engineering Division Semiannual Report*, January-June 1965, USAEC Report ANL-7055, pp. 85-86, Argonne National Laboratory, October 1965.

502. C. Luner and K. Anderson, Liquid-Liquid Extraction Studies, in *Chemical Engineering Division Semi-Annual Report*, January-June 1965, USAEC Report ANL-7055, pp. 86-87, Argonne National Laboratory, October 1965.

Index